PROCEEDINGS — Volume 1

SECOND CANADIAN SYMPOSIUM ON REMOTE SENSING

DEUXIÈME SYMPOSIUM CANADIEN SUR LA TÉLÉDÉTECTION

University of Guelph, Guelph, Ontario, Canada.
April 29 — May 1, 1974.

Theme: The Applications of Remote Sensing and Benefits to Canada.

Sponsored by
Canada Centre for Remote Sensing, Dept. EMR
The Ontario Ministry of Natural Resources
The Ontario Association for Remote Sensing
The Canadian Aeronautics and Space Institute
The Canadian Institute of Forestry
The Canadian Institute of Surveying

PROCEEDINGS — Volume 1

SECOND CANADIAN SYMPOSIUM ON REMOTE SENSING

DEUXIÈME SYMPOSIUM CANADIEN SUR LA TÉLÉDÉTECTION

University of Guelph, Guelph, Ontario, Canada.
April 29 — May 1, 1974.

Theme: The Applications of Remote Sensing and Benefits to Canada.

Sponsored by
Canada Centre for Remote Sensing, Dept. EMR
The Ontario Ministry of Natural Resources
The Ontario Association for Remote Sensing
The Canadian Aeronautics and Space Institute
The Canadian Institute of Forestry
The Canadian Institute of Surveying

Published by The Second Canadian Symposium on Remote Sensing
for the Canadian Remote Sensing Society
Suite 406, 77 Metcalfe St., Ottawa

Copies are available from the Canadian Remote Sensing Society
Price $50 (2 volumes)

Edited and prepared by
G.E. Thompson
Pubic Relations and Information Services
Department of Energy, Mines and Resources
Ottawa

AUGUST 1974

Lithographed in Canada by
CAMPBELL PRINTING

FROM THE GENERAL CHAIRMAN
OF THE SECOND CANADIAN SYMPOSIUM ON REMOTE SENSING

Serving as General Chairman for the Second Canadian Symposium on Remote Sensing was like leading an orchestra, from inside the base drum. I came out stunned, and with little idea of the general effect. People were kind enough to say that it went very well, and I can only accept their opinions with grateful relief.

The attendance, students included, was about 400; just enough to make the Symposium a financial success and plenty to make a happy crowd. Much of our advance publicity refused to cross the postal strike picket lines and only the brave were willing to risk air travel at that time, or we might have been swamped. There is no question that remote sensing is now a vital force in linking the activities of a very large and diverse group of Canadian scientists.

It was a great personal pleasure to serve so many of these scientists by bringing them together at the University of Guelph. I know that you will join me in thanking the wonderful workers who made such a meeting possible.

What a thrill to be able to say "Good luck to the Third Canadian Symposium on Remote Sensing!"--from a safe seat out in the audience!

Stanley H. Collins,
School of Engineering,
University of Guelph.

C O N T E N T S

VOLUME 1

WHERE IS REMOTE SENSING FROM SATELLITES GOING?

Charles H. Smith
Assistant Deputy Minister (Science & Technology)
Department of Energy, Mines & Resources
Ottawa, Ontario, Canada

Ladies and Gentlemen:

As we undergo the current difficulties of moving people and mail across the land surface of Canada, we must marvel again at the efficient satellites which move through outer space, transmitting continual observational data on the Canadian landmass to you and your colleagues.

The life history of these earth-observing satellite systems is indeed short. Only seven years ago the Science Council stated, quote, "Resource survey by satellite is a subject of increasing interest. Although no activity on a significant scale has as yet been undertaken, informal discussions have been held with U.S. authorities on the subject of Canadian participation in the earth resources observation satellite (EROS) project". Remote sensing of the earth caught the public eye less than two years ago when, on July 23, 1972, the United States launched ERTS-1. At your first Symposium in February, 1972, Canadian experience was limited to airborne instrumentation, and remote sensing satellites were still a thing of the future - albeit the near future. Now, with ERTS orbiting overhead, the sky is no longer the limit for you; and sometimes, when I look over the proposals emanating from your offices, I can't help wondering if that phrase applies not only to your sensors, but also to your budgetary requirements!

Since earth observational satellites have such a brief history, my remarks this morning will be limited to the present state of Canada's space program, and some comments on where it is heading.

Remote Sensing from satellites came as a surprise to many government administrators. They began by trying to "classify the problem" as lawyers are prone to do, knowing that until the problem is properly classified it is not possible to make the proper decisions to deal with it. One can debate whether remote sensing from space is a space science or one of the solid-earth sciences... Is it really a science, or a technology? - Is it a new technology or simply another form of aerial photography? Is it an experimental research program or an operational program? It arose from the development of space and military surveillance, so should it be managed by the military, or by a space agency? It observes the land, so should it be managed by an environmental agency? - An agricultural agency? - or a resource agency?

Decisions on all these points are necessary to understand the extent to which the remote sensing program should relate to the rules of a space policy, a science policy, an industrial policy, a resource policy, international policies, and the many other national policy frameworks. They govern decisions on where a centre for remote sensing should be located in government structures, i.e. who funds it, who should manage it, etc. I think the government of Canada made a wise decision in deciding to set up the Canada Centre for Remote Sensing as a single federal entity, guided by the Interagency Committee on remote sensing at the federal level and the Canadian Advisory Committee on Remote Sensing at the national level, and attached to a Resource Department concerned with a number of national mapping programs of which remote sensing is a new addition.

Canada's interests in space programs relate primarily to the potential contributions they may make toward economic, social or other national goals. In the late fifties our space interest related to upper atmospheric and ionospheric research of a pure nature. This led to the Alouette - ISIS Program of the Defence Research Board and the NRC Rocket Research Program. In 1966-67, the government decided that more emphasis should be placed on practical applications and the Alouette group turned toward the idea of operational communications satellites. The communications group spun off the Canadian Telesat Corporation which launched ANIK. Now the Department of Communications Research Centre is involved with Canadian industry in the development of a Communications Technology Satellite (CTS). Because of this historical background, Canada's present space policies and programs are largely dominated by communications considerations. Although Communications Satellites and Earth-Observing Satellites have much in common, they also have significant differences in their state of development toward an operational mode, in the hardware, in the user groups, and in other ways, and it remains to be seen whether policies for space communications systems will serve well the development of earth observing systems for Canadian needs.

Canada does not have its own satellite launch facilities, and we plan to continue to rely on foreign launching services. The question often arises as to whether we intend to construct an earth resources satellite for launch by the United States. There are three reasons against this idea at the moment.

1. The estimated cost would be of the order of $60 million, for a 2-3 year life. Much more needs to be done to enlist the support of users and to document benefits before this expenditure can be justified.

2. At present Canada has no sensors to place in a Canadian satellite that are different from those planned for the U.S. program.

3. The policy of NASA has been to provide access to the ERTS program on the basis of no transfer of funds across the international border. Every indication is this policy will continue. We are extremely fortunate to be able to take advantage of this opportunity.

Our strategy in satellite remote sensing in Canada has been to develop a federal facility to collect and disseminate the ERTS data on a national basis, and to emphasize the use of the data for various resource and environmental purposes rather than the development of space hardware. We are, of course, interested in technology related to receiving stations, data processing and sensors. But we are saying, in effect, that if the information is of no use, then we can't be bothered with the space hardware, and, of course, that is what this Symposium is all about. The titles of your papers demonstrate the wide range of possible applications you are examining - ecology, environmental impact, water quality, forest management, crop identification, snow conditions, topographic mapping, terrain classification, tornado damage, landslides, ice reconnaissance, and many more.

The conclusions of many of your papers indicate exciting uses or potential uses for ERTS imagery in these areas. Your responsibility is to (a) convince your professional colleagues of the importance of the imagery (obtain technical endorsement) and then (b) convince your organizations of its importance in their operations (obtain program endorsement). This is the area of concern now - is the information of sufficient value to the program sponsor that he will buy it from his limited funds, or will it have to be heavily subsidized to be used? Our federal policy up to now has been to subsidize the system while it is still in the experimental stage. You will note that cost-benefit analyses and other reviews are now underway to justify the future of the national program. I am convinced these analyses will support the continuance of the program - but the level of activity still hangs in the balance. Users are scattered across many government agencies - both provincial and federal, as well as in the resource industry and universities. Until the verdict is in, there can be little hope or justification to establish a viable

ongoing program on a commercial basis, as has been done in the communications sector. Your Symposium has an important role to play in rendering this verdict.

In regard to the future of remote sensing satellites, we look forward to participating in NASA's ERTS-2 and possibly ERTS-3 programs. We understand these will be followed by the EOS series which will have higher resolution and more bands. Oceanographic satellites capable of measuring ocean temperature, colour and sea state are on the way and Canada will wish to participate in these programs. By the early 80's we shall be in the age of the space shuttle, permanent space stations, and a host of new unmanned applications and scientific satellites. Canadians must prepare themselves to adapt to and benefit from this new era.

Canada must also remain alert for opportunities to participate in international programs and be prepared to contribute her part insofar as she is able. We are playing an active role in the U.N. Committees on Outer Space and planning for the use of ERTS imagery in the lesser developed areas of the world. The current proposal of the FAO to consider a regional data acquisition and processing centre in Africa is one which we heartily support.

In regard to airborne remote sensing activities in Canada, plans are a little more firm. The Department of Energy, Mines and Resources is receiving proposals from a number of private Canadian companies to operate the four aircraft belonging to the Canada Centre for Remote Sensing. In the next few years we expect that the chosen company will take over these aircraft as well as adding some of its own and begin offering world-wide commercial services in remote airborne sensing and interpretation. The Canada Centre for Remote Sensing will continue on as an R&D and a coordinating organization, and as the federal focus for future remote sensing satellite operations.

In the early 1980's, if and when the Canadian Forces long range patrol aircraft come on stream, we expect that they too will be producing a lot of remote sensing data in the Arctic and over the ocean for analysis by the civilian sector.

Finally, what of the Canadian Symposium on Remote Sensing ten years from now? If one makes a linear projection of the growth in national activity and interest to date, via the first two Symposia and several meetings of the Canadian Advisory Committee on Remote Sensing, one can expect a much larger interest than to-day. Your plans to develop a Canadian Remote Sensing Society show you are preparing further for this growth. I expect that in the 80's the glamour and the benefits of remote sensing will be well entrenched in our Canadian landmass information programs. Whether this comes about, however, depends heavily on the outcome of your sessions over the next few days on "The applications of remote sensing and benefits to Canada", and the extent to which your conclusions are projected and accepted by the Canadian public. Please accept my congratulations to the organizers of this timely Symposium, and my best wishes for its success.

THE IMPACT OF REMOTE SENSING ON THE DEVELOPING WORLD

John A. Howard
Senior Officer (Remote Sensing)
Food and Agriculture Organization of
The United Nations, Rome Italy.

Chairman, Ladies and Gentlemen,

It is an honour to be invited to address this learned Canadian gathering and to meet friends and colleagues from Canada, the United States and other countries. In my address, I wish to direct your attention for a short while to the present and future impact of remote sensing on the developing countries and the ways by which these countries may be assisted.

Let us begin with a thumbnail sketch of the global scenario in which remote sensing is developing. This is a scenario where Man's plundering of Nature's resources is threatening him with increasing problems of pollution, an accelerating rate of depletion of mineral resources - not only oil - and declining reserves of essential food materials and forest products. A world in which, in little more than a century and a half, the world population has grown from an estimated 1000 million people to about 3700 million, and unless there is widespread famine, pestilence or civil strife, the population is likely to reach 7000 million by 2000 A.D. and in the following five years is likely to increase by a further 1000 million. Recently Dr. Arnold Toynbee, the well-known historian, expressed the opinion that even many developed countires will be living shortly in a permanent siege economy having a materialistic life at least as austere as during the two World Wars.

Possibly this is too gloomy a scenario and that the impact of the adverse social, economic and ecological factors will not be so devastating on the developing world; but, it must be borne in mind that an increasing number of developing countries in the dry tropics and semi-tropics are faced with problems related not only to the population explosion and a very low per capita income - often under $300 a year - but to what may emerge as a major climatic change. Some climatologists (e.g. Professor Lamb, U.K.; Dr. Bryson, U.S.A.) fear that the catastrophic drought in "French speaking Africa" may last at least 30 years and is due to a shift southwards of the winds of the circumpolar vortex. Long periods of regional droughts have occurred on previous occasions, but then the human population was much smaller than it is today. The Sahelien drought in northern Africa has already engulfed part of Ethopia and now threatens neighbouring countries including parts of the Sudan, Nigeria, Kenya, Tanzania and the Somali Republic. At similar latitudes elsewhere drought is occuring in India and has threatened Mexico.

Dr. Henry Kissinger, in an address to the United Nations General Assembly only two weeks ago, sees the global dilemma as a challenge to all mankind and that "we must come to terms with the fact of our interdependence". As he pointed out: "For the first time in history, mankind has the technical possibility to escape the scourges that used to be considered inevitable..... For the first time in history, it is technically within our grasp to relate the resources of this planet to man's needs..... The global economy must achieve a balance between food production and population growth and must restore the capacity to meet food emergencies". He urged that an international group of experts, working in the association with the United Nations, undertake immediately a comprehensive survey of the Earth's non-renewable and renewable resources and the development of a global early warning system. This, I feel is of major interest to most of us working in the field of remote sensing.

Remote sensing - past and present

It is within this global scenario portraying pessimism and a challenge to man's technological competence that we must examine the past and present impact of remote sensing on the developing world. This is a world in which the GNP's of the countries have been mainly derived from the productivity of the soil. A world in which agriculture, including fisheries and forestry, plays the major key-role to the well being of the people. A world, therefore, in which the applications of remote sensing may be significantly more important than to the technologically advanced and urbanized countries.

As long ago as 1922, remote sensing. as represented by aerial photography, was used in land-use studies and for simple photogrammetric mapping (i.e. Irrawadi survey, Burma). However, it was only some years after World War II, that aerial photography was widely used in the developing countries and then its main objective was to provide planimetric and occasionally topographic maps from black-and-white panchromatic photographs. As today, the forester, geologist and soils photo-interpreter had to be content with using aerial photographs taken specifically for planimetric mapping and, with few exceptions, infrared black-and-white photography was not used in the developing countries. The impact of remote sensing at this stage can be viewed as providing a national awareness of a country's physiography and, aided by ground surveys, information on regional geology, soils, forestry and land-use. The indigenous people played little or no technical role in these developments.

As we know, colour aerial photography and photointerpretation and thematic mapping from panchromatic colour photographs have only gained popularity in the last decade; but this has given impetus to development in many countries with a low per capitem. The first large-scale colour aerial photographic project was probably the coverage of Malawi in 1966. Somewhat surprisingly, even today, infrared colour photography is only occasionally used and black-and-white panchromatic photography remains the most popular. Reasons for this include the continued reliance on black-and-white photography for mapping, an increasing awareness of the developing countries of the need to control and operate their own aerial photographic surveys, the lack of expertise in the developing countries to undertake colour photography and often the relative high cost under contract of infrared small-scale colour photography. The latter type of photography may necessitate moving high-ceiling aircraft and photographic equipment several thousand miles - an expensive operation.

Parallel with the emergence of colour photography and the wider use of black-and-white photographs for thematic mapping as distinct from planimetric and topographic mapping, regional (e.g. CIAF, Columbia) and national (e.g. Dehra Dun, India) photogrammetric and photo-interpretation training and operational centres are developing. These centres are usually started with direct assistance from the developed countries or through the United Nations or its agencies (e.g. F.A.O.). Brazil and a few other developing countries have now developed a very high level of skill, which is capable of being extended beyond remote sensing; but most countries urgently need assistance in training their nationals.

Non-photographic remote sensing techniques are also having an impact on some developing countries. Thermal scanning has been used to a limited extent in mineral exploration (e.g. Egypt) and water resource studies (e.g. Lebanon). As we know, side-looking radar (SLAR), with its cloud penetrating ability, was used successfully in the 1960's for the planimetric mapping of the Panama Republic and this has been followed in the 1970's by the Brazilian RADAM project to map extensive cloud covered areas of the Amazon basin and by several major projects in other areas of the world (e.g. Indonesia, Papua-New Guniea, Nicaragua). The serious cloud problem existing in some regions is indicated by the fact that only 50% of South America had been covered by satellite imagery with less than 30% cloud cover imagery within the first 18 months of the launching of ERTS-1 and only 38% of the continent was covered with two ERTS passes. The coverage is much better for Africa and Asia.

Satellite sensing probably offers the developing countries an economically viable technique second only to aerial photography; but at present, its application to the study of natural resources seems comparable to aerial photography in the 1930's. The low resolution imagery obtained by meteorological satellites precludes their general application to the study of the Earth's resources. ERTS imagery, on the other hand, with a resolution of about 70 metres is proving increasingly useful to developing countries for the purpose of providing small-scale regional maps of areas not previously mapped or inadequately mapped and for the purpose of up-dating old maps or correcting errors on existing maps. For example, F.A.O. having 59 remote sensing investigations in 45 countries has found ERTS imagery useful in investigations related to ground water (Ethiopia), land-use (Indonesia), vegetation (Sudan) and the World Soil Map (Africa), and is rapidly expanding its ERTS activities.

Remote sensing - in the future

Let us now consider briefly the future impact of remote sensing on the developing world. To many of us, remote sensing continuously provides a challenge against the unknown; but, new to the scenario, is the urgent need in the future to apply remote sensing to global problems and the need, even at the expense of accuracy, to update rapidly national data on the Earth's resources. Satellite sensing is seen as the only practicable means of providing this information.

Recent investigations related to ERTS-1 imagery have indicated the practicability of thematic mapping at a scale of 1:250,000 for agriculture, forestry, geology, hydrology, land-use and soils; and, with improved optical techniques and recently developed numerical techniques, larger scale mapping (e.g. 1:100,000) may be possible. Also ERTS investigations indicate the feasibility of aerial monitoring of areas free from long periods of cloud cover and that satellite information can be used in regional crop forecasting, which is now urgently needed. Satellite imagery has been used to identify several crops, land-use categories and to measure accurately crop acreages. The measurement of crop condition is far more difficult but can be made operational by incorporating large-scale aerial photographic under-flights in the sampling design.

Whereas, in the past, developing countries have received direct assistance in the form of remote sensing undertaken by expatriate commercial companies, the request for indirect assistance in the form of technological advice and the supply of equipment will increase in the future. Many countries need help in the training of their nationals in remote sensing either through short courses or through the establishment of regional training centres. This is an aspect of overseas aid, to which you may wish to give greater attention in the future.

In a recent F.A.O. study of the need for a global satellite information system (SIS) for natural resources, it was concluded that the trend is towards a global network of national and regional satellite data receiving stations; and that,under UN auspices, one or more central offices of satellite information (COSI) will be needed. If the national/ regional stations process the data and disseminate processed data, the cost of establishing a central office of satellite information should be less than one million dollars - a modest figure. However regional stations will cost much more.

As Canada was the first country, outside the United States, to establish an ERTS data receiving and processing facility, Canadian experience would be valuable to fact finding missions for choosing suitable sites for receiving stations in the developing countries and, even more important, in advising on and assisting with the establishment of regional stations. A start might be made by a feasibility study in "French speaking" Africa. This would serve as a prototype and would fulfill an important and much needed monitoring role for this drought-stricken region which includes the Sahel. It should be borne in mind that it may take two years to make a station fully operational from the time the project is activated.

LA TELEDETECTION ET LES PAYS EN VOIE DE DEVELOPPEMENT

John A. Howard
Agent principal (Télédétection)
Organisation des Nations-Unies pour
l'Alimentation et l'Agriculture
Les Nations-Unie, Rome, Italie.

Monsieur le Président, Mesdames et Messieurs,

C'est pour moi un honneur que de m'adresser au présent auditoire de Canadiens érudits et de recontrer des amis et collègues du Canada, des Etats-Unis et d'autres pays. Au cours de cette conférence, j'ai l'intention d'attirer quelque peu votre attention sur l'impact présent et futur de la télédétection sur les pays en voie de développement et sur les moyens à prendre pour les aider.

Pour commencer, dressons un bref aperçu de la situation globale dans laquelle se développe la télédétection. A l'heure actuelle, le pillage qu'exerce l'homme envers les ressources de la nature est en train de se tourner contre lui: accroissement des problèmes de pollution, rythme d'épuisement sans cesse accru des ressources minérales (et il ne s'agit pas seulement du pétrole), ainsi que baisse des réserves de denrées ailmentaires essentielles et des produits forestiers. C'est un monde où, en un peu plus de cent ciquante ans, la population est passée d'un milliard d'habitants à environ trois milliards sept cent millions, et où, à moins d'une famine universelle, d'une grande épidémie ou d'une guerre civile, la population atteindra sept milliards vers l'an 20000, et s'accroîtra d'un autre milliard dans les cinq années qui suivront. Récemment, le Dr. Arnold Toynbee, l'illustre historien, a exprimé l'opinion que même de nombreux pays riches vivront, à court terme, dans une "économie d'occupation" permanente, subissant une vie matérielle au moins aussi austère que pendant les deux grandes guerres mondiales.

Il est possible que ce scénario soit trop sombre et que l'impact des facteurs sociaux, économiques et écologiques adverses ne soient pas si dévastateurs dans le monde en voie de développement; cependant, il faut garder à l'esprit qu'un nombre croissant de pays en voie de développement situés sous les tropiques et dans les zones arides font face à un revenu par habitant très bas, souvent moins de $300 par année, mais encore à ce qui peut être un changement climatique majeur. Certains climatologues comme le professeur Lamb du Royaume-Uni et le Dr. Bryson des Etats-Unis d'Amérique, craignent que la sécheresse qui sévit actuellement en Afrique francophone et qui est causée par un renversement vers le sud des vents du vortex circompolaires ne dure au moins 20 ans. Il s'est déjà produit de longues périodes de sécheresse régionale, mais la population d'alors était beaucoup moins nombreuse qu'elle ne l'est aujourd'hui. La sécheresse du Sahel, en Afrique du Nord, a déjà commencé à s'étendre sur une partie de l'Ethiopie et menace maintenant les pays voisins dont certaines régions du Soudan, du Nigéria, de la Tanzanie et de la République de Somalie. Le même phénomène se produit ailleurs, à des latitudes semblables, notamment en Inde, et menace le Mexique.

Lors d'une conférence qu'il a faite à l'Assemblée générale des Nations-Unies il y a deux semaines, M. Henry Kissinger considérait le dilemme global comme un défi lancé à l'humanité entière, et était d'avis que "nous devons admettre le fait de notre interdépendance". Comme il l'a souligné: "Pour la première fois de son histoire, l'humanité a la possibilité technique d'échapper aux fléaux qu'on avait toujours considérés comme inévitables..... Pour la première fois dans l'histoire, nous pouvons techniquement assujettir les ressources de cette plantète aux besoins d l'homme ..... L'économie globale doit parvenir à un état d'équilibre entre la production de denrées ailmentaires et l'accroissement de la population, et coit faire renaître la capacité de faire face à des situations d'urgence dans le domaine de l'alimentation". Il a insisté pour qu'un groupe international d'experts, travaillant de concert avec les Nations-Unies, entreprenne immédiatement l'étude complète des ressources renouvelables et non renouvelables de la terre, et le développement d'un système global de pré-alerte. C'est, à mon avis, d'un intérêt primordial pour la plupart d'entre nous qui travaillons dans le domaine de la télédétection.

Télédétection - passé et présent

C'est donc dans le cadre de cette situation d'ensemble qui dépeint un certain pessimisme

et présente un défi à la compétence technologique de l'homme que nous devons examiner l'influence passée et présente de la télédétection sur les pays en voie de développement. C'est un monde où le PNB provient principalement de la productivité du sol. Un monde où l'agriculture, y compris les pêches et l'exploitation forestière, joue le rôle clé pour le bien-être des populations. Un monde, donc, où les applications de la télédétection peuvent être vraiment plus importantes qu'elles ne le sont pour les pays technologiquement avancés et urbanisés.

Déjà en 1922, le télédétection, sous forme de photographie aérienne, était utilisée dans les études relatives à l'utilisation des sols, et pour la cartographie photogrammétrique (i.e. les levés d'Irrawaddi, Birmanie). Cependant, ce ne fut que quelques années après la Seconde guerre mondiale que la photographie aérienne fut utilisée sur une grande échelle dans les pays en voie de développement, et, à ce moment là, elle avait pour objectif principal de fournir des cartes planimétriques et, quelquefois, topographiques, à partir de photos panchromatiques en noir et blanc. Aujourd'hui le géologue, le garde-forestier et l'interprète des photos des sols doivent se satisfaire de photos aériennes prises exclusivement pour faire des cartes planimétriques; de plus, à quelques exceptions près, la photographie infrarouge en noir et blanc n'était pas utilisée dans les pays en voie de développement. A ce stage, on peut considérer l'impact de la télédétection comme un instrument d'éveil national à la physiographie d'un pays, appuyé par des levés et des renseignements sur la géologie, les sols, l'exploitation forestière et l'utilisation des sols des régions.

Comme nous le savons tous, la popularité de la photographie aérienne, de la photo-interprétation et de la cartographie à partir de photos panchromatiques en couleurs n'est venue que pendant la dernière décennie; toutefois, ce phénomène a apporté un nouvel essor au développement dans nombre de pays au revenu par habitant peu élevé. Le premier projet de photographie aérienne de couleurs à grande échelle fut probablement celui du territoire de Malowi en 1966. Il est quelque peu surprenant de constater que même aujourd'hui la photographie de couleurs n'est utilisée qu'à l'occasion et que la photographie panchromatique en noir et blanc reste la plus populaire. La confiance en la photographie noir et blanc pour la cartographie provient d'un accroissement de l'éveil des pays en voie de développement quant au besoin de contrôler et d'effectuer leurs propres levés aériens, de leur manque d'experts en photo de couleurs. et, souvent, du coût relativement élevé des contrats de photographie infrarouge de couleurs à petite échelle. Ce dernier type de photographie peut nécessiter le déplacement, sur plusieurs milliers de milles, d'aéronefs pouvant voler à grande altitude, ainsi que d'équipement photographique, ce qui représente des opérations fort coûteuses.

Parallèlement à l'arrivée de la photographie de couleurs et à l'extension de l'emploi de photos noir et blanc pour la cartographie thématique, par opposition à la cartographie planimétrique et topographique, il se développe de centres régionaux (la CIAF en Colombie) et nationaux (Dehra Dun en Inde) d'exploitation et de formation relatifs à la photogrammétrie et à la photo-interprétation, Habituellement, ces centres profitent au départ de l'aide directe des pays développés, des Nations-Unies ou de ses agences, notamment de la F.A.O. Le Brésil et quelques autres pays en voie de développement possèdent maintenant un niveau élevé de compétence, en mesure de s'étendre au-delà de la télédétection.

Les techniques de télédétection non photographique sont aussi utilisées dans certains pays en voie de développement. La détection thermique a servi jusqu'à un certain point dans l'exploration visant à découvrir des minéraux, en Egypte entre autres, ainsi que pour des études sur les ressources en eau, par exemple au Liban. Comme vous le savez, la radar à balayage latéral, qui a la propriété de pouvoir traverser les nuages, a été utilisé avec succès au cours des années 1960 pour faire la cartographie planimétrique de la Répubique de Panama, entreprise qui a été suivie, au cours des années 1970, par la projet brésilien RADAM qui avait pour but de cartographier les régions fortement nuageuses dans le bassin de l'Amazone, et par plusieurs autres projets importants dans d'autres régions du monde, par exemple en Indonésie, dans la Papouasie en Nouvelle-Guinée et au Nicaragua. La gravité du problème des nuages existant dans certaines régions nous est indiquée par le fait qu'après 18 mois le satellite ERTS-1 n'avait pu relever que 50% de l'Amérique du Sud des conditions de nébusolité inférieure à 30%, et que seulement 38% du continent était visible après deux passages. La couverture est bien meilleure pour ce qui est de l'Afrique et de l'Asie.

La détection par satellite offre probablement aux pays en voie de développement une technique viable du point de vue économique, qui n'est surclassée que par la photographie aérienne à l'heure actuelle, on peut comparer son application à l'étude des ressources naturelles à la photographie aérienne des années 1930. A cause de leur faible résolution, les satellites météorologiques

ne peuvent servir à l'étude des ressources naturelles. Au contraire, les images de l'ERTS, dont la résolution est d'environ 70 mètres, le rendent de plus en plus utile aux pays en voie de développement pour l'obtention des cartes régionales à petite échelle de lieux qui ne sont pas encore cartographiés ou qui le sont d'une façon imprécise, et pour la mise à jour de vieilles cartes ou la correction d'erreurs sur des cartes qui existent déjà. Par exemple, la F.A.O. qui a entrepris 59 programmes de recherche par télédétection dans 45 pays, trouve les images de l'ERTS utiles dans des recherches relatives aux eaux souterraines en Ethiopie, à l'utilisation des sols en Indonésie, à la végétation au Soudan et à la carte mondiale des sols en Afrique, et accroît rapidement sa participation aux activités de l'ERTS.

La télédétection dans l'avenir

Maintenant, voyons brièvement quel sera le rôle de la télédétection dans les pays en voie de développement dans l'avenir. Pour un grand nombre parmi nous, la télédétection représente un défi continuel à l'inconnu; mais un nouveau fait s'est ajouté au tableau: le besoin urgent, désormais, d'appliquer la télédétection à des problèmes globaux, et celui de mettre rapidement à jour, au risque d'y perdre un peu d'exactitude, les données nationales sur les ressources. Il semble que le seul moyen d'y parvenir soit la détection par satellite.

Des recherches récentes relatives aux images fournies par l'ERTS-1 ont indiqué qu'il était possible de faire de la cartographie thématique à l'échelle de 1/250,000 pour l'agriculture, l'exploitation forestière, la géologie, l'hydrologie, l'utilisation des sols et les sols; de même, il sera possible de faire de la cartographie à une plus grande échelle, par exemple à 1/100,000, grâce à des techniques optiques améliorées et au récent développement des techniques numériques. De plus, grâce à l'ERTS, nous savons qu'il est possible d'exercer une surveillance aérienne dans les régions exemptes de nuages pendant de longues périodes, et de faire des prévisions sur les cultures régionales au moyen des informations transmises par l'ERTS, ce qui est devenu une urgence. En effet, on a utilisé les images fournies par l'ERTS pour identifier plusieurs cultures et les catégories d'utilisation des sols, et pour mesurer avec précision les superficies ensemencées. Il est beaucoup plus difficile d'estimer la condition des cultures, mais il est possible d'y parvenir en procédantpar échantillonnage à l'aide de photographies aériennes à grande échelle.

Tandis que dans le passé les pays en voie de développement recevaient une aide directe sous forme de travaux de télédétection effectués par des sociétes commerciales venues de l'étranger, il y aura à l'avenir un accroissement de la demande pour une aide indirecte sous forme de consultation technologique et de fourniture d'équipement. Nombre de pays ont besoin d'aide pour former des citoyens à la télédétection, soit par l'intermédiaire de cours intensifs, soit par l'établissement de centres régionaux de formation. Cet aspect de la question relève de l'aide à l'étranger, à quoi vous voudrez peut-être consacrer plus de temps à l'avenir.

Dans une étude récente sur la nécessité d'établir un système global d'information par satellite (SIS) sur les ressources, la F.A.O. concluait que la tendance est à la création d'un réseau global de stations nationales et régionales de réception des données provenant de satellites, et qu'il serait nécessaire d'établir, sous les auspices des Nations-Unies, un ou plusieurs centres de diffusion de l'information provenant de satellites (CDIS). Si les stations nationales et régionales traitent les données et les diffusent, il devrait en coûter moins d'un million de dollars, ce qui est peu, pour établir un centre de données provenant de satellites. Cependant, il en coûtera beaucoup plus pour les stations régionales.

Le Canada a été, outre les Etats-Unies, le premier pays à établir des installations de réception et de traitement des données ERTS, et, à ce titre, l'expérience canadienne aurait une grande valeur pour les missions de recherche en vue de choisir des sites appropriés pour les stations de réception dans les pays en voie de développement et, encore plus important, pour les aider à établir des stations régionales et les conseiller dans ce domaine. Le tout pourrait commencer par une étude des possibilités en Afrique francophone. Cette étude servirait de prototype et remplirait un rôle de surveillance important et très nécessaire pour cette région, frappée par la sécheresse, qui comprend le Sahel. Il ne faut toutefois pas oublier qu'il faut deux ans pour rendre une station complètement opérationnelle à partir de la mise-en-oeuvre du projet.

NASA'S VIEW OF THE APPLICATIONS FOR REMOTE SENSING

By

PITT G. THOME

This paper presented at the Second Canadian Symposium on Remote Sensing, University of Guelph, Guelph, Ontario, April 29 - May 1, 1974.

NASA'S VIEW OF THE APPLICATIONS FOR REMOTE SENSING

Pitt G. Thome,
NASA

Since most of us here today come from relatively affluent nations, it is very hard to fully comprehend the changes that are taking place in this very limited world of ours--changes that are of such magnitude that they are affecting our political, social, and physical environment on a global scale. The undesirable manifestations of these changes take the form of resource depletion, inflation, environmental poisoning, overcrowding, and inadequate food supply. The concommittant growth in the world's population and the increasing affluence of more and more of its people have begun to cause localized imbalances in the supply and demand equation. These imbalances are beginning to strain the world economy and the political and social institutions that were established in an era when it was possible for many nations to solve their problems independent of or with a minimum of cooperation from other countries.

We have not, as yet, reached the point where the earth is unable to sustain its total population--but we have reached the point where dislocations between population, food supply, natural resources and affluence are causing severe stress in many parts of the world. Such stress cannot be relieved by a small group of nations or by any nation acting alone. Accidents of climate, geography, soils, and geology and the achievement of technological maturity that have endowed some nations must not be used as weapons to promote strictly national interest at the expense of less endowed countries. Our problems are worldwide by nature and can only be solved by nations acting in concert to their mutual benefit.

Someone once said "necessity is the mother of invention." As it has happened so often in the past, a new technological development has appeared at a time in history when the need is becomming urgent--the capability for remotely surveying the earth's resources from a satellite. A remote sensing satellite by its very nature is global in extent and has the potential for aiding immeasurably in the addressing of world wide resource and environmental problems.

However, in addressing the use of remotely sensed data, it is only natural that the first emphasis was placed on attempting to use the data to solve local problems--problems that we face everyday--problems that were most upon the minds of the investigators analyzing the usefulness of this new type of data. For example, soon after the first data were available from ERTS, it was found that it could be very useful for updating maps. (Figure 1) Numerous rivers, highways, coastlines, and islands were found to be either mislocated on the most up-to-date maps or their described geometric shape were grossly in error.

The ERTS data was also quickly found to be of use in delineating different categories of land use. (Figure 2) In the United States the data has been found to be of great utility in developing state-wide land use maps and making timely updates as changes occur. In fact, ERTS-type data may be the only practical data source for such maps.

However, as the areas of interest decrease to the size of large cities, the usefulness of ERTS data becomes limited since higher resolution is required for the type of land use planning required within cities.

Another application that shows promise, especially I understand in Canada, is the monitoring of ice conditions on navigatable waters. (Figure 3) In northern regions, ERTS can be used to locate leads through the ice that can be used for shipping. In these regions, viewing through the usually overcast weather is somewhat counterbalanced by more frequent orbital coverage. Identification of ice from ERTS is excellent, even multi-year ice can be distinguished from new ice.

Another of the features that is readily identifiable on the ERTS imagery is the disruption of the vegetation, the surface terrain and the pollution of the streams due to the presence of strip mines. Previously, because of the wide extent of strip mines in many states, it has been impractical to identify and monitor the effects they are having on the environment and the progress the owners are making in complying with the laws requiring reclamation of strip mine areas. Figure 4 indicates the rapidity with which an analysis was completed for a strip mining district in the State of Maryland. The total number of strip mines listed were derived from the ERTS data and is considered by the state officials to be more accurate and up to date than their latest data from normal sources.

These four applications that I have summarized are just a few examples of the many promising applications of ERTS data for assisting in solving critical local problems or problems associated with small regions. These applications are very important and must be developed; however, I would hope as we learn more about the methods and techniques for extracting useful information from satellite data, that more investigators would begin to focus their efforts on applying this expertise to solving critical world wide resource and environmental problems, the solution of which may be heavily dependent on the use of remotely-sensed data. Let me give you a few examples.

Bad as the oil shortage was earlier this year in some countries, it is not as serious as the food shortage in many countries of Asia, Africa and South America, for here the availability of food is often the difference between life and death, rather than whether one has to go on a weight reduction program or not. In all probability, the energy shortage will be overcome in a relatively few years, but the outlook for solving the world wide food problem is more sanguine for in the final analysis it is a population problem which means it would be intractable, human nature being what it is. Therefore, as a result of expanding and shifting world markets and ever increasing population pressures, there is widespread need in not only increasing the available agricultural acreage which is severely limited and increasing the yield, but also in obtaining a more accurate and timely prediction of the world wide production of important agricultural crops so that some internationally coordinated decisions regarding planting and harvesting could be made to maximize the availability of food supply throughout the world.

Since some countries such as Canada and the United States have the most efficient agricultural production capability in the world, we are increasingly being called upon to assist in supplying feed and grain to those countries that are not so fortunate in terms of climate, soil and technology. Recent observation warns that coincident crop disasters can occur around the world and it is these events which must be anticipated as effectively as techniques and resources permit. In the United States, two of the last corn crops have experienced near failures. At the

same time, the Russian winter wheat crop was just emerging from an open winter with a high potential for frost kill in early spring. Probability theory assigns a low risk to simultaneous occurrence of unlikely independent events but it also specifies a finite possibility that such events will coincide. Given a long enough outlook to the future it is only a question of when. Any forewarning of such a coincidence will aid plans for softening its impact.

Up to the present time, agricultural inventoring has required a tremendous effort on the part of on-the-ground enumerators and have presented a formidable data compliation task. Now satellite remote sensing systems, which can survey large areas of land throughout the world and provide data on a repetitive and consistent basis, can do much to alleviate these problems. A crop inventory utilizing remote sensing technology appears to offer great potential for upgrading existing information gathering capabilities and for contributing to a long-range solution of the food supply problem.

The results of studies conducted to date for crops such as wheat, corn and soybeans indicate that the data from ERTS will make the existing sampling methods more efficient and provide more timely and accurate estimates of crop acreage. For example, in Kansas, estimates of wheat acreage made from ERTS data were 99% accurate. Similar results were obtained in Holt County, Nebraska, utilizing data from successive passes of the satellite. Figure 5 is a classification map of 81 square miles of Holt County, in which the individual data points had been classified automatically by a computer, given a distinctive color and displayed on film. The use of data from two satellite passes allowed the computer to classify the seven crop types with higher accuracy.

With further research, especially in the development of signature extension techniques, the modelling of the factors affecting yield and the development of sampling strategies, it is believed that accurate and more timely production predictions could be achieved for the more important crops.

Another application of remote sensing data that has the potential for increasing the production of the world's food supply, is improving the productivity of range lands. Range lands are of more than passing interest to those of us who live in large urban areas since it is an important source of our meat supply. The efficient utilization of range land for the production of meat is directly related to range management decisions which in turn are based on knowledge of range conditions at the time.

For example, the beef industry of the Great Plains region of the United States which produces 40% of the nation's beef, a 23 billion dollar operation, is extremely vulnerable to adverse seasonal or climate conditions. Currently, only gross information based on climatology reports and limited observations are available to determine range conditions. The beef output of this area is contingent on the decisions made by the farm and ranch owners of the region. Some 170 million acres of western range land are managed in the United States by a relatively small number of range managers. On the average, approximately 700,000 acres are handled by one manager who requires timely information on regional range forage conditions to support sound management decisions.

An important indicator of range land forage conditions is the biomass content. Several investigators found they could achieve good estimates of the biomass content utilizing ERTS data. One of the investigators showed that radiance measurements in two of the bands were correlated at the 93% level with biomass and vegetative moisture content. Another of the investigators was able to establish a procedure to visually analyze color enhanced ERTS imagery and map broad vegetative communities and broad

classes of annual forage production in the arid southwest.

In summary, we are finding that ERTS provides a means of acquiring information critical to efficient management of our range lands that heretofore has been too costly to acquire and hence unavailable.

I would like to turn next to the subject of water and its availability. As the population and standard of living of the world increases, man requires more and more water for support of his industrial and agricultural activities. Present management practices permit man to economically extract his water supply from less than .01% of the total water amount in the earth/atmosphere system. It is, therefore, apparent that water must be managed with increasing efficiency and the quantity and quality of water conserved wherever possible.

To become more efficient in the utilization of available water supplies and to find new sources of water, a system that can observe and monitor large areas of the world on a repetitive basis is a necessity. Because of the strong contrast between water and surrounding surfaces when viewed in the near infrared, accurate global estimates of the actual area covered by surface water can be made for the first time with ERTS data. By knowing the kinds of water bodies indicative of various physiographic areas, indices of the volume of water available in a particular region can be obtained. By locating surface water area in relation to urban centers, irrigated areas, and industrial development, plans can be made for future water resources development. Some of the practical applications of this data identified by ERTS investigators include the location of underground water through rock type identification, flood analysis, water management, glacier monitoring, and snow cover mapping.

An example of the location of new underground water supplies by rock-type identification is given in Figure 6. Potential perched sandstone aquifers, outlined in black in the lower central portion of this figure, were identified for the first time on digitally enhanced ERTS imagery based on recognized structural relationships. The one area on the far right that has been drilled was successful and is expected to provide ground water to ranchers in the area. Since this successful drilling, the investigator has been deluged by other ranchers to assist them in locating promising sites to drill for water.

In the western United States, snowmelt provides a major portion of the water runoff which is used for several purposes, including hydroelectric power generation, irrigation, human consumption industrial uses and recreation. Because this snow cover and the glaciers are often located in relatively inaccessible regions, the satellite provides an obvious and beautiful tool for measuring the snow cover and rate of melt. Snow line altitudes can be observed to within plus or minus 60 meters under good conditions, snow cover area can be observed to within a few percent and knowing snow cover the water runoff can be determined empirically. Figure 7 dramatically demonstrates how easy it is to observe the change in the aerial extent of the snow cover during the period of four satellite passes. By monitoring the buildup of snow in the winter it is possible to estimate quite accurately the total amount of water that will run off in the spring, and by monitoring the melt in the early spring a better estimate of the runoff rate can be obtained. Such a technique using satellite data is currently being used in the pacific northwest to provide for a more effective management of reservoir storage and river flow for irrigation, human and industrial uses. Such techniques should have application in many areas of the world.

As everybody is becoming increasingly aware of, the world wide supply of oil

and many other strategic minerals is rapidly falling behind the increasing demand.

To help alleviate this situation, I believe new sources for some of these minerals can be found through a better understanding of the earth's geology.

The major contribution of ERTS in geology to date is its exceptional ability to detect new linear features exposed at the earth's surface.

Those linears which prove to be of structural origin, mainly crustal fractures, will as they are mapped and verified provide a new level in understanding the tectonic framework for continental evolution, mineral emplacement, petroleum localization and potential hazards to man's activities.

To date, no fully verified discoveries of mineral deposits made directly through ERTS data have been reported, but rumors about finds continue to reach NASA geologists. Nevertheless it is now becoming obvious that ERTS has pinpointed many new characteristics of the geologic components of the earth's surface which, as our understanding increases, should eventually lead to real documented payoffs.

However, a note of warning. Very recently one of our investigators analyzed multispectral data from Skylab over an area that he previously had analyzed using ERTS data. There appeared to be very little correlation between the linears identified from the ERTS data and those identified from the Skylab data. The reason for this is believed to be due to the difference in the angle of the sun; the ERTS imagery of course was taken at approximately 9:30 in the morning local sun time, while the Skylab data was taken in the afternoon.

More research is required to fully understand these differences; however, it may mean that to more fully map geological features from orbit, data may have to be collected at various sun angles.

Another puzzlement was turned up by an investigator studying the Anadarko Basin in Oklahoma, a known reservoir of gas and oil deposits. (Figure 8) The investigator found on this picture small hazy areas in the center of the picture which correlated with known oil deposits. However, when the ground truth was collected he found that these hazy areas were associated with very sandy soils. The correlation of sandy soils in this region with oil deposits has not been proven. For instance , known oil deposits in the most south/central portion of this picture exhibit no such manifestation on this imagery.

Here again it is evident that more research is required to properly interpret tonal variations and the patterns observed on ERTS type imagery in terms of geological features.

There are many more potential applications of remote sensing data that are under study and are showing great promise. However, in the interest of time, I will refer you to the many interesting papers to be given at this symposium.

During the first year and a half after the launch of ERTS-1, the majority of the investigations that were conducted using the satellite data were exploratory in nature to determine what information could be extracted from the data for a wide range of applications. Some of the information has proved to be of immediate use without any additional development and hence is today being used routinely in addressing resource management problems. However, most of the applications require additional development to perfect the techniques and procedures for extracting useful information from the data and for integrating this information into existing or new information systems.

To accelerate this development, NASA is defining relatively larger scale quasi/operational demonstration projects

called Applications System Verification Test or ASVT's for short. An ASVT will involve NASA and the federal or state agency with the operational authority working closely together to develop and demonstrate the techniques and procedures for applying ERTS data to an important resource management problem. For instance, we are in the process of defining and implementing ASVT's in the areas of agriculture, water resources and land use.

In order to undertake these ASVT's and to develop other applications to the point that they can become operational, a near continuous supply of remote sensed data must be available. The ERTS-1 spacecraft has been operating for over 21 months, well beyond its design life. Early next year if ERTS-1 is no longer returning useful data, ERTS-B will be launched to continue supplying multispectral data. ERTS-B will be identical to ERTS-1 and is the last of the approved ERTS spacecraft.

However, there is a strong need in many application areas for a thermal infrared channel on the multispectral scanner, and for a continuing collection of data beyond ERTS-B. Therefore, NASA is studying the requirements for an ERTS-C for launch in late 1977 or early 1978. In addition to adding the thermal channel, other design changes are being studied; for instance installing 2 multispectral scanners to increase the swath width and hence provide coverage more often than once every 18 days.

NASA also has under active study a more advanced satellite called the Earth Observatory Satellite or EOS which will carry a scanner with perhaps more channels and have a resolution capability of 30-60 meters. In addition, it may carry a pointable scanner for applications that require even higher resolution but over very limited areas such as for urban land use management. The EOS will not be ready before 1979.

I should reemphasize that at the present time ERTS-B is the last of the approved earth resources satellites. However, NASA believes that there is a need for additional satellites similar to ERTS-C and EOS designs.

In closing, I would like to state that I believe the world wide benefits that will acrue from earth resources survey satellites in the years to come will be enormous. History repeatly tells us that we always underestimate the impact of a new technology in the long run. But to achieve this potential, will require the hard work, the dedication and visionary leadership of people like you.

REVISION OF VIRGINIA MAPS: LAKE ANNA RESERVOIR

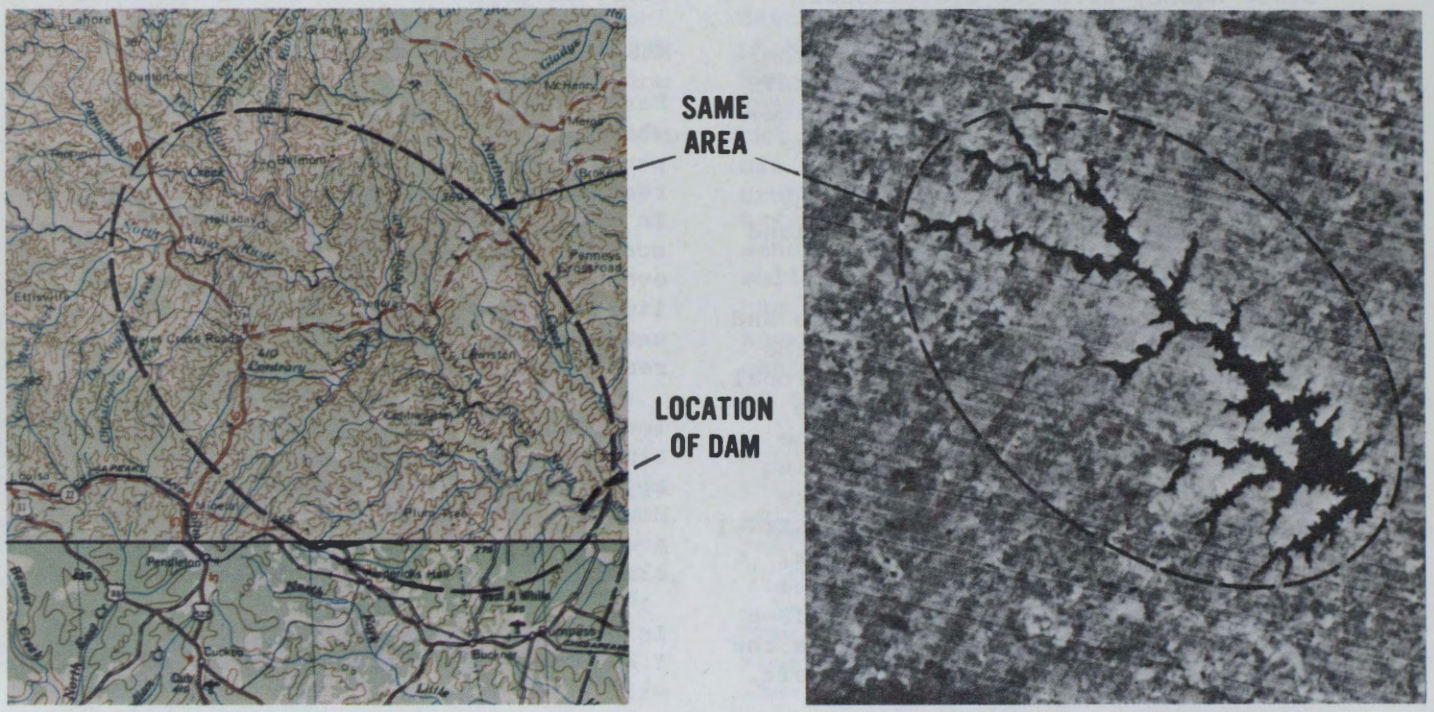

SCALE 1:250,00
AS REVISED 1969

ERTS 1 IMAGERY
OCTOBER 11, 1972

Figure 1

REGIONAL ECOLOGICAL MAP NEW JERSEY

Let's protect our earth

NEW JERSEY DEPARTMENT OF ENVIRONMENTAL PROTECTION

Ecozones are defined as regional areas characterized by homogenous interrelationships of soils, landforms, vegetation, geology, drainage, and land use. Because of their regional areal size (at least 200 square miles) and uniform characteristics, ecozones should logically be recognized as integral regional planning units. Within New Jersey, certain ecozones contain critical environmental resources worthy of special protection and regulation: Coastal Zone (coastal bays and wetlands); Pine Barrens (unique forest associations and extensive aquifer zone); Agricultural Belt (prime agricultural land); Highlands and Kittatinny Mountain (relatively undisturbed forest areas). A small scale, synoptic view is required for the recognition and delineation of regionally similar land areas. Earth Resources Technology Satellite (ERTS) imagery is ideally suited for this purpose because each image covers approximately 10,000 square miles. Portions of only three ERTS-1 images were required to prepare this mosaic base on which the ecozones of New Jersey have been mapped.

LEGEND

- **A COASTAL ZONE: coastal lands, wetlands and water directly affected by coastal processes**
- **B PINE BARRENS: contiguous forest cover with low intensity land use**
- **C LAKEWOOD: forested area with mixed residential and commerical land use**
- **D VINELAND: mixed agriculture and forest**
- **E AGRICULTURAL BELT: extensive farmland with small woodlots and some urban development**
- **F URBAN AND INDUSTRIAL ZONE: areas of intensive land use**
- **G PIEDMONT PLAIN: mixed cropland and urban land with scattered forested traprock ridges**
- **H HUNTERDON PLATEAU: curvilinear forested ridges and cleared valleys**
- **I UPPER DELAWARE RIDGE AND TERRACE: rolling terrain with forest and agricultural use**
- **J KITTATINNY MOUNTAIN: steep series of forested ridges with low intensity land use**
- **K KITTATINNY VALLEY: rolling topography with forested ridges, cleared valleys (agricultural use), and numerous small lakes**
- **L HIGHLANDS: rugged, partially forested area with numerous lakes**
- **M WASHINGTON: level valley (rural land use) enclosed by Highlands Ecozone**
- **N PASSAIC BASIN/WACHUNG MOUNTAINS: forest cover and urban land use in a level river basin ringed by forested traprock ridges**
- **O RIDGEWOOD: urban land use and forest cover**

Scale in Miles

0 10 20 30 40

Earth Satellite Corporation
1747 Pennsylvania Ave., N.W.
Washington, D.C. 20006

This photomap produced from a NASA ERTS-1 mosaic of MSS [illegible]

Figure 2

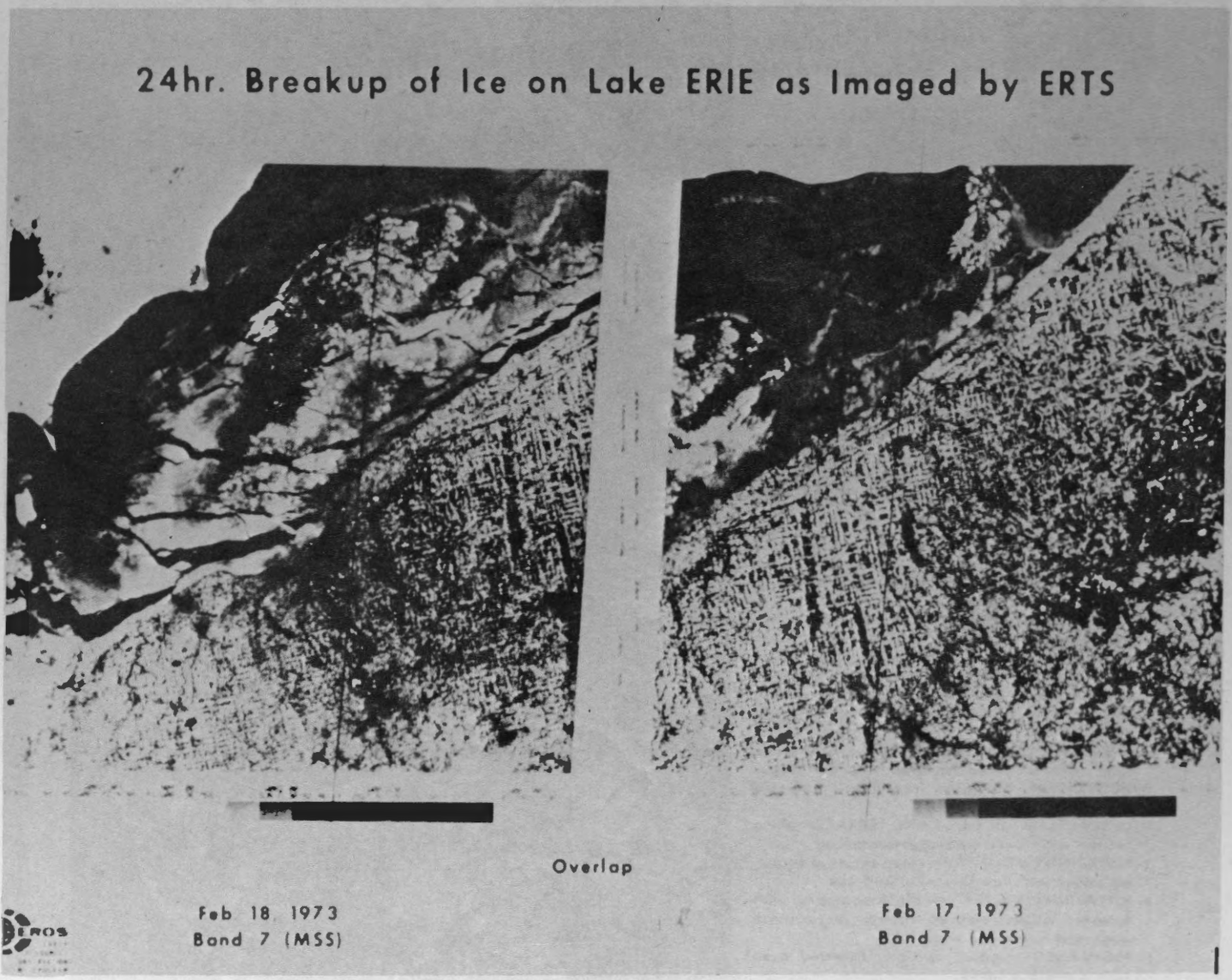
24hr. Breakup of Ice on Lake ERIE as Imaged by ERTS
Overlap
Feb 18 1973
Band 7 (MSS)
Feb 17 1973
Band 7 (MSS)

Figure 3

- 377,929 Acres, Surveyed and Analyzed in 8 Man-Hours
- 140 Mines, 3109 Acres, Surveyed by ERTS, - Only 58 Mines, 568 Acres, Surveyed Routinely by the State of Maryland (1972)
- 5—10% of Area Disturbed by Mining
- Total Number of Strip Mines

Size (Acres)	Number
0 - 11.3	68
11.4 - 22.6	39
22.7 - 33.9	11
34.0 - 45.2	3
45.3 - 56.5	4
56.6 - 67.8	3
67.9 - 79.1	5
79.2 - 90.4	3
90.5 - 101.7	1
101.8 - 124.3	1
158.2 - 169.5	1
271.2 - 282.5	1

Figure 4

COMPUTER IDENTIFICATION OF CROPS

DIGITAL CLASSIFICATION OF ERTS 1 IMAGERY HOLT COUNTY, NEBRASKA, AUGUST 1972

RED: FIELD CORN
YELLOW: POP CORN
ORANGE: SUNFLOWER
L. GREEN: ALFALFA AND GRASS
D. GREEN: PASTURE
BLUE: GRAIN SORGHUMS
PURPLE: ALFALFA
BROWN: BARE SOIL

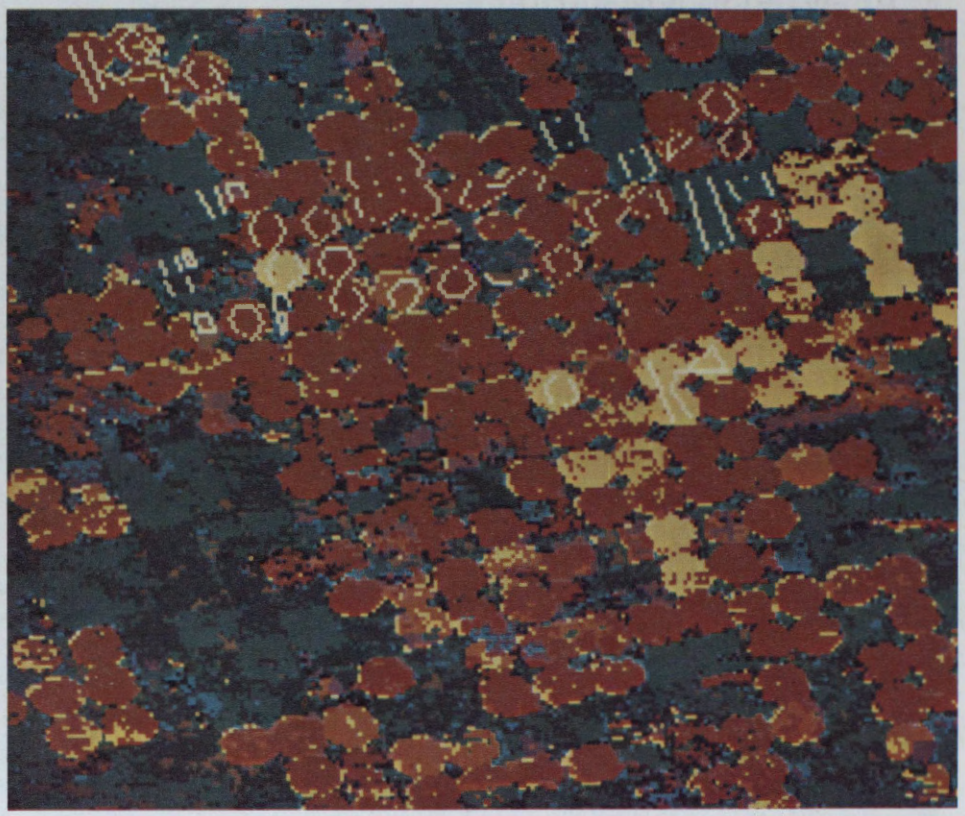

NASA ER74-1614 (3)
2-11-74

Figure 5

LOCATION OF GROUNDWATER IN NORTHERN ARIZONA

COMPUTER ENHANCED SANDSTONE LENSES WITHIN THE KAIBAB LIMESTONE PERMITTED SUCCESSFUL DRILLING OF PERCHED WATER TABLES FOR STOCK WATERING

NASA ER74-1611(3)
2-12-74

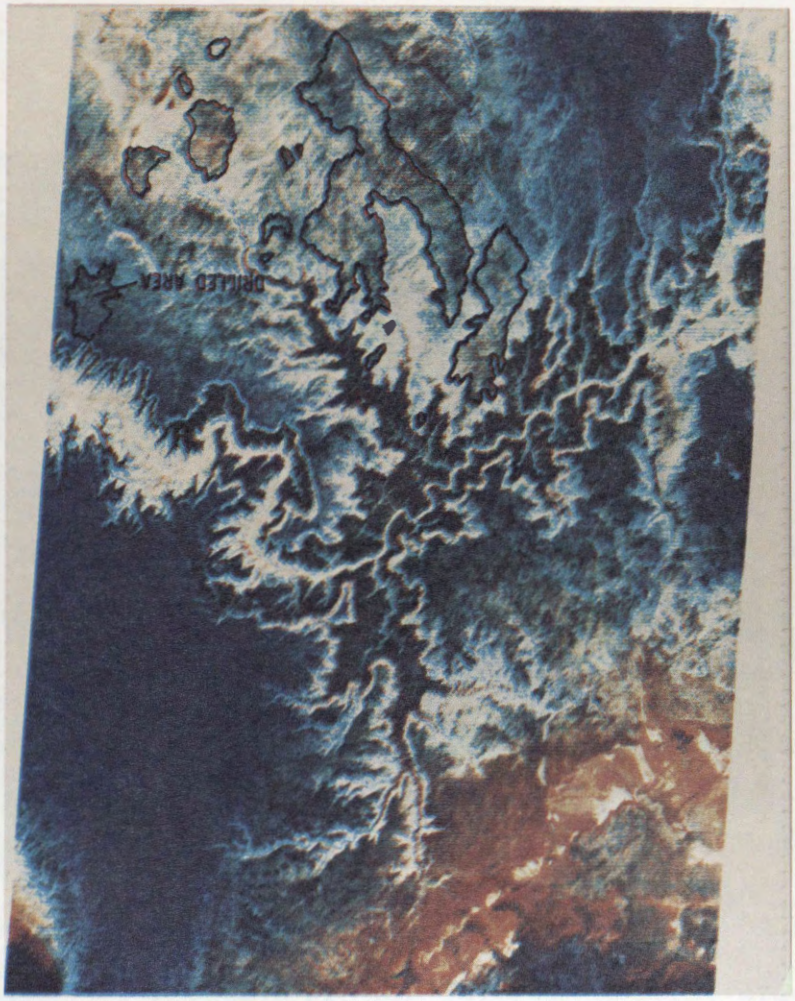

Figure 6

NASA HQ ER74-15586 (2)
2-6-74

Figure 7

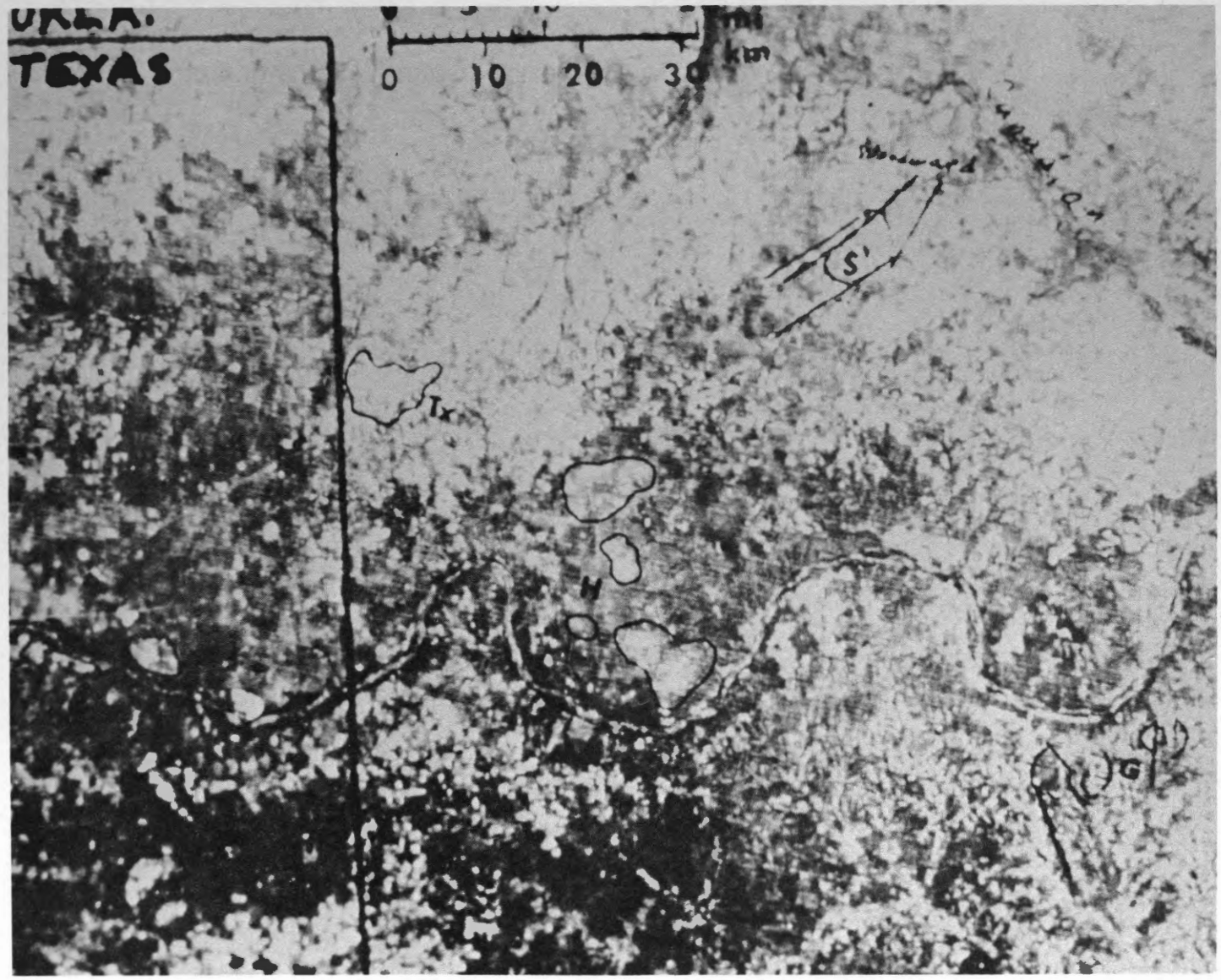

Figure 8

CASE STUDIES OF CANADIAN BENEFITS OF REMOTE SENSING

By

DONALD J. CLOUGH
J.C. HENEIN
A.K. MCQUILLAN

This paper presented at the Second Canadian Symposium on Remote Sensing, University of Guelph, Guelph, Ontario, April 29 - May 1, 1974.

CASE STUDIES OF CANADIAN BENEFITS OF REMOTE SENSING

Donald J. Clough*, J. C. Henein**, A. K. McQuillan**.

*Professor and Chairman, Department of Management Sciences, Faculty of Engineering, University of Waterloo, Waterloo, Canada.

**Program Planning and Evaluation Unit, Canada Centre for Remote Sensing, Department of Energy, Mines and Resources, Ottawa, Canada.

ABSTRACT

The Canada Centre for Remote Sensing is carrying out a benefit-cost analysis of satellite and airborne remote sensing applications in Canada. A case study approach has been adopted whereby economic, environmental, and social benefits of remote sensing to specific areas of application are evaluated. This paper presents a discussion of some of the general socio-economic considerations and a preliminary report of current studies. Results of a sea ice case study are summarized and preliminary considerations of streamflow forecasting and northern resource development are given.

INTRODUCTION

At the First Canadian Symposium on Remote Sensing in 1972, we presented a pre-program benefit-cost analysis of potential satellite and airborne remote sensing applications in Canada[1] That analysis was based on an extrapolation of U.S. estimates to Canada, and the plausibility of the estimates was subject to debate[2].

In the 1972 report we estimated that it would take about 15 years to develop an infrastructure and to provide the necessary learning time to realize the full potential benefits of remote sensing, assuming that the level of CCRS activity remained about the same during that period. We estimated that the full potential gross benefits of some 45 different applications would gradually build up to a level between $25 million and $250 million per year, depending on one's pessimism or optimism about the experts' opinions.

Our ongoing studies of the benefits and costs of remote sensing have led us to the conclusion that the original estimates were far too conservative. For example, our recent study of remote sensing applications to sea ice[3], which is summarized briefly in this paper, indicated that gross benefits of feasible systems could grow from about $4 million in 1975 to about $40 million in 1980, and between $100 and $150 million in 1990. This is the surprising result - a single application that was not covered at all in earlier cost-benefit reports will probably generate gross benefits of the same order of magnitude as the previously estimated total for 45 applications, with benefit-cost ratios of about 10 to 1.

We are undoubtedly on a steep technological learning curve and will probably have to revise our estimates of benefits upward again and again as new applications are invented.

This paper presents a discussion of some of the general socio-economic considerations, as a kind of philosophical background, followed by a preliminary report of some tentative findings of our current studies. Full reports will be forthcoming in the CCRS Technical Report Series.

2 GENERAL SOCIO-ECONOMIC CONSIDERATIONS

2.1 National Systems and Infrastructures

The Canada Centre for Remote Sensing (CCRS) forms the hub of a growing National Program in Remote Sensing, involving federal and provincial agencies, universities, regional associations and private enterprises. The Program involves an extensive and

complex infrastructure of physical systems and human organizations dispersed across the country. It has strong links with similar infrastructures in other countries, particularly in the United States.

The physical systems include those centralized in the CCRS for purposes of control and economies of scale, those centralized in other government agencies for similar purposes of control and economies of scale related to their own missions (e.g., Atmospheric Environment Service satellite and airborne remote sensing for weather and sea ice monitoring), and those centralized in private enterprises for commercial purposes[4]. The physical systems also include many that are decentralized in a variety of organizations for purposes of local accessibility and efficiency(e.g., university laboratories, regional and specialized interpretation facilities).

The human organizations include the centralized service organization of the CCRS, the Inter Agency Committee on Remote Sensing (IACRS), the Canadian Advisory Committee on Remote Sensing (CACRS), a multitude of groups in various divisions of federal and provincial government departments, university groups, provincial centres, specialized interpretation centres, coordinating committees and task forces in and out of government, "invisible colleges" in various disciplines, and an informal "matrix organization" of project teams of people from government, industry and university sectors, private enterprises including instrument companies, computer companies and air survey firms, and various linkages to provide liaison with similar organizations in other countries.

Indeed, there has occurred a rapid evolution of a global fraternity in remote sensing. Formal and informal communication links have been forged, and the continuing evolution will help to unify mankind in his approach to controlling the environment and the earth's resources for the common welfare of all people.

The intangible benefits that have already been generated by the creation of the infrastructure cannot be measured in the conventional terms of economic theory. The intangible future benefits of further development of the infrastructure cannot be measured in conventional terms. However, there is no doubt that remote sensing will ultimately supplement or replace many of the traditional ground-based observational and monitoring activities presently employed in Canada, and will provide new opportunities to observe natural phenomena that are economically out of reach at the present time.

The national infrastructure of systems and organizations is a political reality. The CCRS forms only a part of the infrastructure, but an important part. Without the CCRS in its promotional and coordinating role, the infrastructure would not exist, in its present form, in Canada.

Any cost-benefit analysis of Canadian remote sensing applications or evaluation of CCRS as part of the larger national infrastructure must take into account the richness of present and future opportunities that exist because the infrastructure exists.

2.2 Information, Knowledge, Education and Time Lags

An output of remote sensing - whether it be an image,a table of numbers,or a report of qualitative factors - is information. When it is abosrbed by a human mind it becomes knowledge. It passes in time from person to person. It accumulates and expands. It reinforces other knowledge and is synthesized for problem-solving and design.

The phenomena of human information processing and knowledge accumulation are "non-conservative" phenomena. They are different from "conservative" phenomena of physics (e.g., conservation of mass and energy), and the "conservative" phenomena described by the equilibrium theory of economics. Knowledge grows.

An output of remote sensing becomes an information input - one of many kinds of inputs - to a variety of users. The users may be scientists, teachers, managers, legislators, artists and ordinary citizens. They may need the information to generate further knowledge, to teach, to design systems, to manage resources, to make and enforce

laws, to produce aesthetic models of the earth, and to obtain aesthetic enjoyment.

Consider the scientist. He receives outputs of remote sensing as inputs to his own research. He transforms these inputs to new outputs, including sceintific papers that may be useful to other scientists and special reports that may be useful to engineers, teachers and managers. The scientist enters a process in which the original remote sensing information is diffused throughout the scientific community. But it is a "non-conservative" diffusion process in which the information is synthesized, augmented, amplified, transformed, aggregated and mulled over at each stage of the diffusion process.

The individual scientist does not exist in a vacuum but in a community. The individual bit of information does not exist in a vacuum but in a rich field of other information and a context of human language, thought, mathematics and theory. The non-conservative diffusion process takes time, and the history of science shows that one must be patient with the time lags between scientific thought and tangible economic benefits.

Consider the teacher. He receives outputs of remote sensing as inputs to his own teaching program. He synthesizes these remote sensing inputs to obtain new perspectives of the earth. He exposes the new perspectives to his pupils. For example, a real picture of the earth obtained by the ERTS satellite reveals to the human mind a richness of detail and a multitude of surprises that no ordinary map can convey. Scientists are surprised; pupils in school are equally surprised. The processes of learning and enquiry are enhanced by the surprising aspects of nature that the pupil sees when the teacher takes him by the hand and leads him to the spacecraft's window on the earth.

Consider the manager. He receives outputs of remote sensing as inputs to his decision-making processes, but these inputs are usually pre-digested by engineers, applied scientists and other specialist interpreter-analysts. The manager needs information about the systems he has to regulate. He needs information to design new control rules ("goals", "policy") and information feedback to control systems ("operations").

Management....goals....policy.... operations. The words convey a sense of bigness - big institutions, government, complex operations, advanced management techniques. But the words apply to any scale of management, big or little. A small farmer, for example, is a manager of crops. He may use remote sensing inputs that have been processed and reduced to meaningful terms by specialists in a government service agency. However, before he is able to use such information effectively he may have to educate himself about the use of the information and he may have to become part of a larger infrastructure of users (e.g.,a cooperative grouping to facilitate irrigation or harvesting). The educational process takes time.

Some economic effects of remote sensing may be direct and immediate. But some may be indirect and may require years of gestation time. The short-run effects of remote sensing inputs to certain resource management decisions may be direct, observable, and measurable in tangible economic terms. But the long-run chain-reaction effects of remote sensing inputs on science, education, legislation, art, social justice, and the quality of everyday life are obviously indirect, difficult to observe, and generally difficult to measure in economic terms.

It would be wrong to base a cost-benefit analysis of remote sensing and evaluation of specific agencies solely on the tangible economic effects of, say, a perceived subset of resource management decisions, or to give undue weight to such "tangibles". The "intangible" effects of scientific research and development, education, and other uses of remote sensing must also be assigned some weight in the analysis and evaluation. The time lags, non-conservative accumulations of knowledge, and potentials for future human development have to be taken into account.

2.3 Common Property Resources and Role of Government

As discussed in 2.2, the main outputs of remote sensing activities are information outputs. Some of these outputs are designed to satisfy a specific consumer (e.g., airborne remote sensing for a particular scientist's project). Other outputs are designed to satisfy a variety of consumers (e.g., ERTS satellite images distributed by National Air Photo Library (NAPL) to the general public). In either case, most information is stored by the CCRS and NAPL and is sooner or later publicly available to any consumer.

In the terminology of economics, the publicly available information outputs are common property resources. They are common property resources because, as a matter of public policy, they represent valuable information about the world which cannot be reduced to individual ownership. The information itself may not enter into the market exchange process, though certain information transmission media may be priced and bought and sold in the marketplace (e.g., duplicate films or tapes which carry the publicly available information). The main information produced by the CCRS is, like the air we breathe, a common property resource.

One of the roles of government is to regulate the accessibility and use of common property resources such as air, water and certain kinds of information. This role involves the prevention of exclusive private ownership, access or control over certain resources, so that they may be maintained as common property resources.

Remote sensing information outputs produced by the CCRS, as common property resources, may be consumed by one person or by many. Consumption by one person does not impair another person's ability to consume the same outputs. The output information by itself, unconsumed, does not possess intrinsic economic value. It possesses value only as it is consumed by someone. The total value increases as the number of consumers of the same information increases.

Now consider arbitrary pricing by the CCRS as a branch of government, whatever the purpose might be (e.g., to prove the existence of a "real demand" or to obtain "cost recovery"). Suppose the CCRS sets an arbitrary price for the common property resource, and sells the resource (or access to its media) in the marketplace. In this case, the quality of consumption depends, in turn, on "ability to pay", which depends on consumers' disposable incomes. If the consumers include government and university scientists, corporate managers and ordinary citizens, they may have unequal ability to pay, hence unequal willingness to pay.

Any government decision to establish a price at too high a level will have the discriminatory effect of restricting consumption or making the common property resource inaccessible to certain classes of consumer. On the other hand, prices that are set too low may not succeed in either "proving demand" or recovering a high proportion of government costs. In either case, the arbitrary price that some people are evidently "willing to pay" may be, by itself, a poor measure of the long-run social benefits of the common property resource.

Now consider government "make or buy" policies. Suppose the decision is to "buy" the services of an outside contractor organization to produce remote sensing information that the government wants to supply as a common property resource. In this case, the government would have to ensure that the information is not reduced to individual ownership by the contractor, but remains in the public domain as an accessible (reasonably priced) common property resource.

Common property resources....the role of government....pricing actions.... make or buy actions. Whatever the circumstances, any cost-benefit analysis of remote sensing must take into account the government's underlying position concerning CCRS outputs as common property resources, and weigh prices and benefits accordingly.

2.4 Experimental vs Operational Systems

The development of operational remote sensing information-communication systems has been evolutionary. A sub-

stantial transition period is required to develop new technology and organizational modes, and to progress from experimental to "quasi-operational", then to "fully operational" systems.

For example, the Canadian ERTS satellite program has been gradually evolving from an experimental phase to a "quasi-operational" phase, providing useful information almost routinely through a variety of organizational arrangements and communication channels, to private and public users alike. As planned, at some future time it will undoubtedly evolve into a more comprehensive "fully operational" management information system to serve resource managers and environmental control agencies on a routine basis.

ERTS-1 is providing certain "one-shot" benefits related to the observation of static phenomena such as geological features. A fully operational future system would be designed to provide ongoing benefits related to the repetitive monitoring of dynamic phenomena such as seasonal agricultural changes and urban growth.

Figure 1 shows a schematic time-series of both the "one-shot" benefits of the ERTS experimental satellites and the ongoing benefits of the future operational satellites. The "one-shot" benefits, based on prior decisions and sunk costs, would be left out of any benefit-cost analysis of future alternative operational systems.

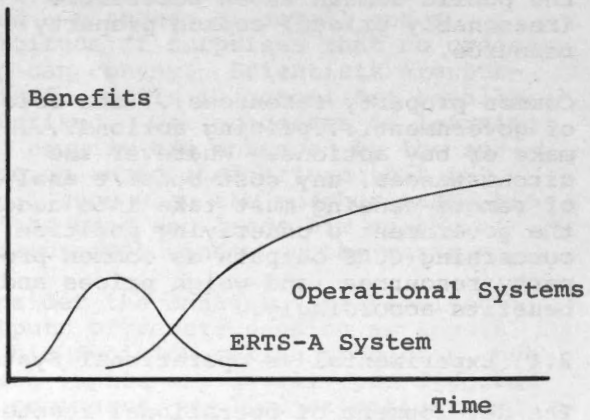

Figure 1

The CCRS is presently engaged in studies of potential benefits and costs of postulated future quasi-operational and fully operational systems, as a basis for program planning. The studies include satellite and airborne remote sensing and a variety of applications, as described in Section 2.

2.5 Structure of Decision Processes

The chain of effects of an experimental remote sensing project can be simplified by dividing it into stages as follows:

- -Data acquisition
- -Data processing
- -Data interpretation by scientist
- -Scientific information output
- -DELAY for diffusion of knowledge
- -DELAY for organization and management systems development
- -Future manager's actions based on remote sensing
- -DELAY for effects of manager's actions
- -Posterior measurement of effects in cost/benefit terms.

The delays in this chain may be of the order of years or decades.

By way of comparison, the chain of effects of an operational remote sensing system can be simplified as follows:

- -Data acquisition
- -Data processing
- -Data interpretation by manager's technical staff
- -Manager's actions based on remote sensing
- -DELAY for effects of manager's action
- -Effects of manager's actions
- -Posterior measurement of effects in cost/benefit terms.

The delays in this chain may be of the order of hours, days or months. In extreme cases, such as disaster monitoring, the operational system must operate in "real time" with very fast response and short delays.

An a priori cost-benefit analysis attempts to forecast what the ultimate effects will be in physical terms, and in economic terms. The technological and economic forecasting is difficult. The following major problems arise:

1. Forecasting the characteristics of future management decision processes entailing an operational system, in diverse fields of application (agriculture,mining, etc.).

2. Forecasting the delays and the ultimate physical effects.

3. Making value judgements about the economic efficiency of applications by user agencies.

The value judgements of discipline experts are required before any economic cost-benefit analysis can proceed.

2.6 Context of Economic Theory and Modelling

Economics deals with the subject of individual and collective human welfare. Economic values are the values held by human beings, whether those values be expressed as the monetary values of the marketplace, the preferences displayed by the choices people make and the votes they cast, or the values imputed as "shadow prices" by an economist using a particular mathematical model of economic behaviour.

Social, political, technological and economic variables, and the human values associated with these variables, are all within the domain of economic modelling and analysis. However, while the present state-of-the-art of economics allows us to model and analyze some relations among some variables, usually based on the simplifying assumptions of general equilibrium theory, it does not permit us to model the more complex, dynamic and non-equilibrium relationships. Nor does the state-of-the-art permit us empirically to transform all human values onto a common scale of measurement, particularly the monetary scale of the marketplace.

Economic modelling and analysis is useful for many purposes. But it is limited. Let us make this caveat clearly evident: at the present state-of-the-art, economic modelling and analysis have only limited usefulness in the quantitative analysis of the benefits of remote sensing, although they may be qualitatively useful.

At a technical level, economics includes models of the production and the consumption of goods and services, and models of investment for future production and consumption. These models are conceptually useful if not readily applicable to accurate quantitative analysis. The models are normative and most are based on the assumption that both producers and consumers attempt to maximize their own welfares independently. (A defined economic man, or rational man is assumed as the basis for the normative models of economic behaviour.)

Consider production and consumption. The CCRS and other members of the remote sensing infrastructure are involved directly in the production of remotely sensed data and derived information. Each is both a consumer of inputs and a producer of outputs, and each enters into a complex chain of inter-industry inputs and outputs. The outputs of remote sensing information become the inputs to other economic production activities. The benefits and costs of remote sensing may therefore be measured in terms of its indirect chain of effects on such economic production activities.

Consider remote sensing as an investment. Investment means that certain outputs produced this year are not consumed this year but are stored in some form to be employed as input factors of production in future years. For example, labour and material inputs may be consumed this year to produce remote sensing output products, (e.g., imagery, tapes). The products may be stored in the archives of the National Air Photo Library (NAPL) and may then be employed in future years as input factors of future production, to yield many kinds of new output products or services. In the simplest terms, resource inputs today are invested to obtain the means of producing output products in the future.

Remote sensing investment includes research and development. R and D itself may be viewed as a production process in which manpower and other input resources are used to produce outputs of information, in the form of published papers, reports, images on film, legal patents, etc., which may be consumed in future years as

inputs to various production processes (including other R and D).

Remote sensing investment includes education. Education has been viewed as a process in which information inputs consumed by a person today are stored and used productively in the future when the person is employed as an input factor of production. Thus, education resource inputs today are invested to obtain the means of producing output products and services (including information) in future years.

Production....consumption....investment. In principle they can be described in terms of economic models. In practice, however, economic modelling is not easy and in some cases it seems impossible. Normal market-pricing mechanisms do not exist as a basis for valuation ("pricing") of all inputs and outputs, and arbitrarily defined proxy measures of value may not be acceptable to all economists. The CCRS, one of the producers, is a government agency operating under certain rules of subsidy, and is not supposed to maximize its own welfare. Scientists, one class of consumer, also operate under certain subsidy rules and are not supposed to maximize their own welfares (at least in a profit maximization sense). In these circumstances it is difficult to specify plausible economic models. There exist no strong tests of "validity", but only the weaker tests of "acceptability" by professional experts.

Welfare economics poses particularly difficult problems for economic analysts and decision-makers alike. Welfare economics is that branch of economic theory which deals with the policy recommendations that economists make. These policy recommendations affect the allocation of resources - that is, the distribution of inputs to producers and outputs to ultimate consumers - and thus affect the welfares of citizens.

Cost-benefit analysis is essentially a tool of welfare economics - albeit a primitive tool. Three major problems arise, as follows: (1) Almost any policy decision will affect the real income of some people - hence the distribution of income - and this in turn will affect demands for goods and the equilibrium solutions of the general theory. (2) Data of sufficient accuracy, precision and "coverage" are exceedingly costly to obtain, and impossible to obtain in many cases. (3) The difference between private and social welfare costs and returns (benefits) is essentially determined as a matter of public policy, outside the domain of state-of-the-art economic models. Policies that provide benefits for one sector of society may provide disbenefits (external diseconomies) for another sector, and the judgement to shift these benefits is a political (not economic) judgement.

In spite of the lack of theoretical underpinnings to deal with all factors, and the lack of data and other forms of supporting empirical evidence, some cost-benefit analyses have to be made and some value judgements made, as a partial basis for public policies which govern the further development of the infrastructure and the economic application of remote sensing.

3 SOME RESULTS OF CASE STUDIES OF REMOTE SENSING BENEFITS

3.1 Introduction

Remote sensing information can provide an important input to a number of operational systems. Large annual benefits can result when the phenomena being monitored are dynamic in nature and require constant surveillance. Several operational systems are possible which can result in large economic benefits. Among those operational systems which are most attractive are the following: ice reconnaissance and forecasting, hydrologic forecasting, and crop yield monitoring and forecasting. Remote sensing can also have an input in many environmental monitoring systems.

A second area where remote sensing can provide large economic and environmental benefits results from the build up of a historical data bank of information which is useful in the planning phase of many projects.

This section summarizes results of a sea ice case study. It also gives preliminary considerations of streamflow forecasting and northern resource development case studies.

3.2 Remote Sensing of Sea Ice

Remote sensing provides an input into an operational system for sea ice surveillance and forecasting. Currently observers on aircraft aided by some remote sensing techniques, (i.e., cameras, ground mapping radar and laser profilometers) provide valuable information for shipping and some exploration activities. The rapid expansion of these activities and the high cost of exploration and transportation in ice-infested waters make it desireable to make more operational use of existing satellite capabilities if possible. Also, it is desirable to provide an all weather reconnaissance capability and to establish better data relay methods as part of the operational system to bring high quality, reliable, timely ice reconnaissance information to those operating in these waters. ERTS and NOAA satellite imagery made available to a ship's captain on a real time basis combined with weather forecasts and the captain's knowledge of current local weather conditions could increase ships' operating efficiencies in these waters [3].

Current satellite imagery can provide a broad coverage when cloud cover conditions permit (i.e. about 30% of the time). ERTS coverage of the Arctic is on the average 5 to 6 consecutive days out of 18. ERTS imagery provides a broad coverage to show ice conditions in an area of 10,000 square miles and provides sufficient detail to permit the ship's captain to manoeuvre his ship amongst ice pans or along leads or to decide if straight survey lines can be run in certain areas. It therefore provides both tactical and strategic information. The very high resolution radiometer of NOAA2 and 3 provides twice daily coverage of the Arctic and although, with one kilometer resolution it does not give the detail of ERTS imagery, it shows areas that are ice free and provides strategic information for the ship's captain.

Table 1 indicates the gross economic benefits that would result from sea ice surveillance systems. Three scenario's are indicated. Scenario A involves rapid transmission (within about two hours of passage of the satellite) of ERTS and NOAA imagery to the user (i.e. the ship's captain). It involves rapid facsimile transmission of the imagery to Ice Forecasting Central so that the information may be included in their daily ice forecast charts. Data relay currently could be by HF radio or experimental satellite and in future by more appropriate communication satellites. Scenario B involves the addition of microwave imaging sensors to existing operational ice reconnaissance aircraft providing all weather reconnaissance capability and Scenario C involves the same basic elements described in A and B with extended airborne and satellite remote sensing coverage. It also involves the use of airborne ice thickness measuring devices.

The incremental costs required to achieve the incremental benefits shown in all cases give a benefit-cost ratio of at least 10:1.

In addition to the benefits shown for operational ice reconnaissance, there are substantial benefits which can result from a better data bank on ice conditions in ice-infested waters which can be obtained by satellite and aircraft remote sensing over several years. For example, scheduling of many activities such as laying pipelines off ice, offshore drilling in the open water season, or construction of artifical islands in the open water season requires a good knowledge of freeze-up and break-up conditions. Design of ships, offshore drilling rigs, and offshore oil storage vessels depend on ice conditions and millions of dollars in savings can result from improved statistics on pressure ridge heights and frequencies and iceberg population and velocities [3].

3.3 Streamflow Forecasting

A second operational system for which remote sensing can provide important input data is streamflow forecasting.

One of the basic problems in water management is to forecast accurately waterflow volumes. Such forecasts are of vital importance in hydroelectric power generation, irrigation, flood control, water supply, navigation and recreation. Although the applications of remote sensing are still largely

in a research phase, it is already certain that these techniques will contribute to improved measurements of the amount of water in storage as snow, of precipitation and extent, of evaporation and evapotranspiration, and of the rate at which water is released during snow melt.

We have taken a very preliminary look at benefits to hydropower generation through better snow survey. It is clear that snow water equivalent is the key parameter here although extent of snow cover can also be important. Benefits would come from reservoir drawdown and refill and from improved use of secondary energy. Snow water equivalent measurements are useful both in the seasonal runoff volume forecasts and in the short term runoff forecasts and it is believed could increase power generation in some cases by more than 1%. Snow cover data is most useful for forecasting runoff after the melt season is well underway. Satellite imagery (ERTS and NOAA) can give information on snow line elevation in mountanous areas. In flat prairie regions, once snow melt begins and snow cover becomes patchy, areal extent will give an indication of how much snow is left to melt. This can be particularly valuable for flood control purposes. Although snow thickness and water equivalent cannot as yet be determined from satellite data, under certain conditions visible band reflectance seems to be related to snow depth.[5]

Preliminary estimates indicate gross annual benefits from improved streamflow of several million dollars if appropriate remote sensing techniques were available. For example, it has been estimated that each 1% improvement in in-flow forecast to the reservoir behind Bennett Dam on the Peace River would result in $1 million per year increase in revenue through improved operating efficiencies for that generating station alone.[6] More research work needs to be done with ERTS and NOAA to determine how well these can be used to determine snow line elevation in forested areas and to determine ground wetness and snow ripeness before benefits can be estimated properly for existing systems.

Similar information on snow cover is necessary for flood control. A more quantitative knowledge of the amount of water still to be released from snowmelt can be the deciding factor in taking steps to move people, livestock and other moveable objects. In the St. John River flood of 1973 for example, more than $1 million damage to moveable objects resulted. It is reasonable that a 20% reduction in such damages could result from a more precise knowledge of how much water was still to be released. More precise data would increase the confidence in flood predictions and affect a decision to take action or not.

3.4 Northern Resource Development

There are about 2.8 million square miles lying north of that part of Canada mapped by the Canada Land Inventory. There is a great lack of bio-physical and environmental baseline data. It is probable that in this vast relatively unpopulated northland with its fragile environment and containing the majority of Canada's mineral and petroleum reserves remote sensing will have its major benefits. ERTS is providing us now with both seasonal and yearly information on lakes and rivers, ice and snow conditions, vegetation and so forth. This baseline data is vital for current and future development projects. These development projects tend to be very expensive. Planning has gone on with a lack of physical resource data and poor decisions have resulted within some cases, serious economic, environmental or social cost. One example of this might be the Peace River Dam project which resulted in very negative effects on the Athabasca delta. The Beaufort Sea environmental study and the intensive environmental studies being carried out on the pipeline projects indicate the growing public concern about northern development. Future development projects may be held up through lack of baseline data resulting in a large economic loss to Canada. Satellite data collected over several years will provide a good deal of baseline information for these future projects.

In an effort to assess the economic benefits of having better information, we have been researching engineering

projects which have been carried out in the north. We have been trying to determine where poor decisions may have resulted from lack of information which remote sensing could provide. In some cases dams have been over-designed or improperly designed at a loss of several hundred thousand dollars. In other cases transportation routes have been poorly located resulting in excessive maintenance costs.

A poorly designed transportation route can result not only in higher initial construction costs but also higher maintenance and cost of transport. A pipeline costs about $1 million per mile. Located on bad terrain, swamp, or muskeg, costs can be more than one quarter million dollars more per mile. Routing of highways over hard bedrock and crops where blasting is necessary can add more than $100,000 per mile, while building in muskeg or permafrost regions can increase dollar costs per mile by several tens of thousands. Locating scarce gravel deposits in the north can save $50,000 per mile of haul distance. It can reduce the possibility of "making do" with inferior construction materials. There are many examples of roads having to be rebuilt because poor materials were used. Better routing can reduce the number of bridges which may cost $2 million each or the number of culverts which can cost from $10,000 to one quarter million dollars.

ERTS imagery is part of a package of information desireable for optimum route selection. It helps in choosing initial route possibilities and is particularly valuable for the long routes in the north where many alternate route possibilities exist. It is useful for identifying gross terrain features that provide a general appreciation and overview of regional landscape conditions. Aerial photography at several scales is also necessary.

The use of ERTS imagery can reduce the time required in deciding on the best route and increase the level of confidence that an optimum route has been selected before beginning expensive field surveys. Had several years of ERTS imagery been available prior to the MacKenzie pipeline study it might have reduced the $50 million already spent on environmental and engineering studies and perhaps helped in selecting better,more representative areas for detailed environmental study. Water is a chief enemy of all transportation routes in the north and although satellite imagery suffers from lack of resolution, it does provide a great deal of information on drainage systems, sediment load, and flooding.

Much of northern construction must be done in the winter,so knowledge of snow conditions is important for scheduling. For example, if the MacKenzie Valley pipeline is to be built in three winters it is desireable to know how many working days can be expected integrated over that three year period in order to have the optimum number of spreads. If eight spreads rather than nine can build the line and meet the schedule,possibly $20 million in equipment for the extra crew could be saved. Historical data on snow conditions obtained from satellite data over several years can therefore have a large economic value in similar projects in the future.

We have not as yet attempted to total the benefits possible from applications of remote sensing to such engineering projects in the north but indications are that they will be large both from an economic and environmental point of view.

The accelerating development of the north has brought a need for a multi-disciplinary inventory of northern resources which is required for land use planning and zoning, engineering and construction, and wildlife and forest land management. The problems are time and cost. A detailed study such as carried out in Quebec for the James Bay project would cost $50 to $60 million for northern Canada and possibly take 20 years. A less ideal inventory could be carried out at about one fifth of this cost in 3 to 4 years using ERTS imagery together with existing conventional aerial photography. This could satisfy some of the urgent planning needs and provide a framework for a detailed inventory on selected areas where development projects are to take place. From a cost-benefit viewpoint time is the important parameter here.

3.5 Discussion

The continuing benefit/cost studies should provide a sound basis for recommendations of future remote sensing systems and applications in Canada. In the next several months it is planned to investigate case studies of remote sensing applications to environmental monitoring, urban and rural land use, water resource management, agriculture, forestry, mineral resource development, and oceanography.

REFERENCES

1. Clough, Donald J., "Preliminary Benefit/Cost Analysis of Canadian Satellite/Aircraft Remote Sensing Applications" in Proceedings of the First Canadian Symposium on Remote Sensing, Ottawa, Feb. 1972, p. 3-28.

2. Interplan Corporation, Review and Appraisal: Cost-Benefit Analysis of Earth Resources Survey Satellite Systems, Santa Barbara, 1971. (This is a report of a study commissioned by NASA (70 16R) published in March 1971. It cites ten other major studies.)

3. McQuillan, A.K. and Donald J. Clough, "Benefits of Remote Sensing of Sea Ice", Research Report 73-3 Canada Centre for Remote Sensing, Ottawa, January, 1974.

4. For example, the CCRS study report "A Study of the Research and Development Needs for Airborne Sensing Systems Within the Department of Environment" by R.A. Boorne, Philip A. Lapp Limited, Ottawa, May 30, 1973, provides detailed information about available physical facilities, including those of government agencies such as CCRS, NAE, GSC, AES, private enterprises such as instrument and computer companies, 13 air survey companies, and other facilities.

5. Wiesnet, D.R., "The Role of Satellites in Snow and Ice Measurements". Interdisciplinary Symposium on Advanced Techniques in the Study of Snow and Ice Resources, Monterey, California, December 1973.

6. Sampson, F., "Peace River Project with Specific Reference to Reservoir Filling and Runoff Forecasts". Proceedings 29th Annual Meeting, Western Snow Conference, Spokane, April 1961.

TABLE 1

SOURCE OF BENEFITS	SCENARIO	1975	1977	1980	1990
Arctic Seismic Surveys [a]	A	1.0	1.0	1.0	1.0
	B		2.5	2.5	2.5
	C	-	-	-	-
Arctic Shipping Inbound [b, c]	A	2.4-3.0	4.4-5.5	6.4-8.0	6.4-8.0
	B		3.7-4.0	5.3-5.9	5.3-5.9
	C			9.0-10.2	9.0-10.2
Arctic Shipping Outbound [d]	A	-	-	-	-
	B	-	-	-	-
	C	-	-	-	64-100
Offshore Drilling and Production [c]	A	-	0.5	1.8	3.6
	B	-	-	-	-
	C	-	-	1.8	3.6
St.Lawrence Shipping [c, e]	A	-	-	-	-
	B	-	4.0	4.0	4.0
	C	-	-	8.0	8.0

AGGREGATE BENEFITS	SCENARIO	1975	1977	1980	1990
	A	3.4-4.0	5.9-7.0	9.2-10.8	11.0-12.6
	B		10.2-10.5	11.8-12.4	11.8-12.4
	C			18.8-20.0	84.6-121.8
TOTALS		3-4	16-18	40-43	107-147

(a) Arctic seismic surveys include both marine and on-ice surveys. These economic benefits result from increased productivity because of better ice reconnaissance.

(b) The number of ships is estimated to increase from 150 at present to 400 by 1980. Benefits result from increases in productive times of a ship under Arctic charter including those due to better long range planning. It is conservatively assumed that the inbound Arctic shipping remains constant from 1980-1990.

(c) The benefits for 1980 attributed to Scenario C would occur only if these systems were developed by that time.

(d) Substantial Arctic shipping outbound is expected to occur in the 1980's. Although all of the benefits for outbound shipping in 1990 have been attributed to Scenario C as it is expected that complex surveillance systems will exist at that time, some of these benefits could be obtained from Scenarios A and B. These benefits would result if one million barrels of oil were shipped daily from Ellesmere Island, six million tons of liquified gas annually from Devon Island and five million tons of iron ore from Baffin Island, and are derived from reduced ship delay times and decreased insurance rates.

(e) It is conservatively assumed that the number of ship movements in the Gulf, which is currently about 3000 each winter,remains constant through 1990.

REGIONAL ECOLOGY AND ENVIRONMENTAL STUDIES USING ERTS DATA

By

ALLAN FALCONER

This paper presented at the Second Canadian Symposium on Remote Sensing, University of Guelph, Guelph, Ontario, April 29 - May 1, 1974.

REGIONAL ECOLOGY AND ENVIRONMENTAL STUDIES USING ERTS DATA

by
Allan Falconer
Department of Geography, University of Guelph

Regional ecology is the integrated study of organisms and their environment on a regional scale. ERTS data may easily be used to view regions which are many square miles in extent, thus the data are applicable to organisms which are of appropriate scale - for example, large mammals, migrating birds, and plant communities of large extent such as forests. Movement of the organisms cannot be recorded directly by ERTS but change in the environmental conditions is recorded and can be applied in regional ecological studies. The example presented here is of the changing environmental conditions of the Beaufort Sea during a period in the early summer of 1973.

Environmental impact studies using ERTS data must also be concerned with impact at the appropriate scale. An important dimension to this, however is the requirement that environmental conditions over an appropriate area must be recorded before the environment begins to respond to the changes being imposed upon it. The impact of these changes may then be appropriately assessed. Alberta's Tar Sands region provides the examples for both the recording and the assessment of environmental conditions. The records generated can also be appropriately presented as decision maps providing a compact and complete basis for decisions about environmental management.

These types of evaluation can be conducted on a provincial scale to aid on the planning and monitoring of conservation areas, urban growth and parkland.

The Beaufort Sea is a major wildlife refuge and, because of its extent, the details of wildlife movements are not well documented. It is therefore difficult to provide any amount of work on the ecology of the whole region because the major wildlife visitors to this region are migrating birds including geese, ducks and some swans. To study these in relation to their environment requires detailed local study of behaviour during the nesting and moulting seasons, and regional studies of their behaviour as they enter and leave the region each year. Detailed behaviour studies exist from the work of individual observers and shore-based study groups over a few decades. Much of this work relates directly to local study during the nesting and moulting season. Records of movement of birds at other times are, in most cases restricted to the observations of individuals, and shore-based groups. The value of these observations cannot be denied and yet the effectiveness of such a data base must be realistically evaluated by considering the range of vision of a shore based individual and comparing this to the hundreds of miles over which the Beaufort Sea extends.

The ecologist seeking to relate the behaviour of the organism to environmental conditions thus has a very limited data base on which to establish behaviour patterns particularly during periods of major movements of birds. Until recently environmental conditions were also recorded on a similar basis with very few observing stations to provide measurements of climatic conditions. The available information about ice conditions was also very limited. Thus regional data on either the paths of movement of the migrating flocks of birds or the environmental conditions was very limited. ERTS clearly provides a means of greatly improving the record of environmental conditions. The power of ERTS data in this regard is well illustrated by data from the Beaufort Sea for the months of May, June and July 1973 (these illustrations are not included in the text for reasons of space and cost).

Over land areas data collection for environmental studies is less difficult than over areas such as the Beaufort Sea. Detailed studies over large areas however, require considerable numbers of personnel and frequently this proves to be expensive. One such region where an environmental study has recently been completed (Alberta Environment 1973) is the Athabasca Tar Sands, an area of some 11,340 square miles in north-eastern Alberta. It is clear from the study that much basic research is required in the assessment of the impact of development in the Tar Sands region. The research is required in all aspects of the physical, biological and human environments.

Some development of the Athabasca Tar Sands is already underway and further development is imminent. A record of environmental conditions provided by ERTS is available for several occasions during 1973. Many of the individual topics studied by the report can be seen in complete juxtaposition in the ERTS data. The 1:1,000,000 photographic prints of this have been examined and from season to season important environmental parameters can readily be viewed. The fact that one ERTS frame almost completely displays the region of interest is a useful coincidence. Figure 1 is an annotated view of the area using an image recorded on January 3rd 1973. This image with a low sun angle and snow cover provides a very clear differentiation between major features although the topographic enhancement resulting from the low sun angle is sometimes confusing as it produces inverted hillshading by having the light source in the south-east rather than the north-west as is the cartographic norm.

Items reported in the environmental study can be viewed in surprising detail from the ERTS image. Boundaries of muskeg areas can be rapidly and accurately drawn on a regional scale from the ERTS images. Many of the regional divisions of the physical environment are easily drawn in this way. Forest areas can easily be delineated and major landform regions (sand dunes, drumlins etc.) are clearly visible. The January 3rd image carries additional information about the extent of the dust or smoke or condensation area around the operating Tar Sands plant and so apparently underlines the comments in the environmental study which claim, "Natural conditions can create ice fogs but they are generally mild compared with those caused by the discharge of large quantities of water vapour to a localised atmosphere. A tar sands plant emits enormous volumes of water vapour especially from the hot liquid tailings".

Decision Maps - there is a distressing tendency in the interpretation of remote sensing data to claim that everything is revealed by the data. This is clearly not the case and boundaries between drainage basins (watersheds) are an excellent example of this. Unless one is provided with a map which shows watersheds it is indeed difficult to determine their location in the field and often it is difficult to determine the perimeter of a drainage basin by any method at all. Surface water is a major resource in the tar sands and a requirement of the processing plant presently in operation. By superimposing drainage basin boundaries onto the ERTS image the relationships between the various areas can easily be viewed in relation to the region pattern of water movement. By superimposing the boundaries of the leases the total picture of water, leaseholdings and major ecological regions can be immediately viewed. Figure 2 provides an example of this. The value of this use of ERTS to regional planning and management of the environment is very great.

If ERTS data are assembled for larger areas similar decision maps can be created for whole provinces or major resource or planning areas. By adopting this system information is reduced to a highly efficient and compact form for use by planners.

Acknowledgements - the author is indebted to L.G.L. Environmental Research Associates Ltd. (Edmonton, Toronto) who supported this study.

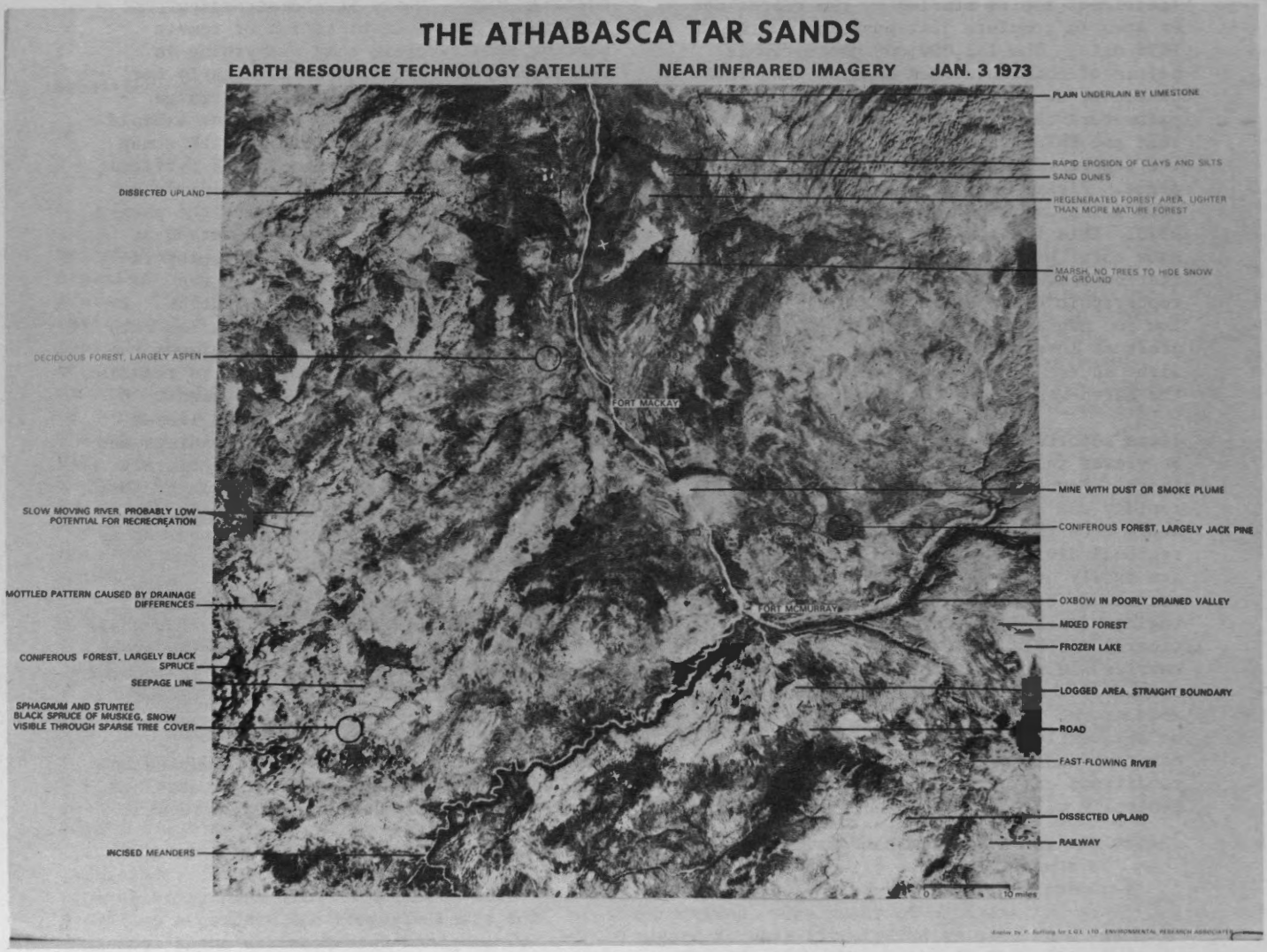

Figure 1. An annotated ERTS image of the Athabasca Tar Sands.

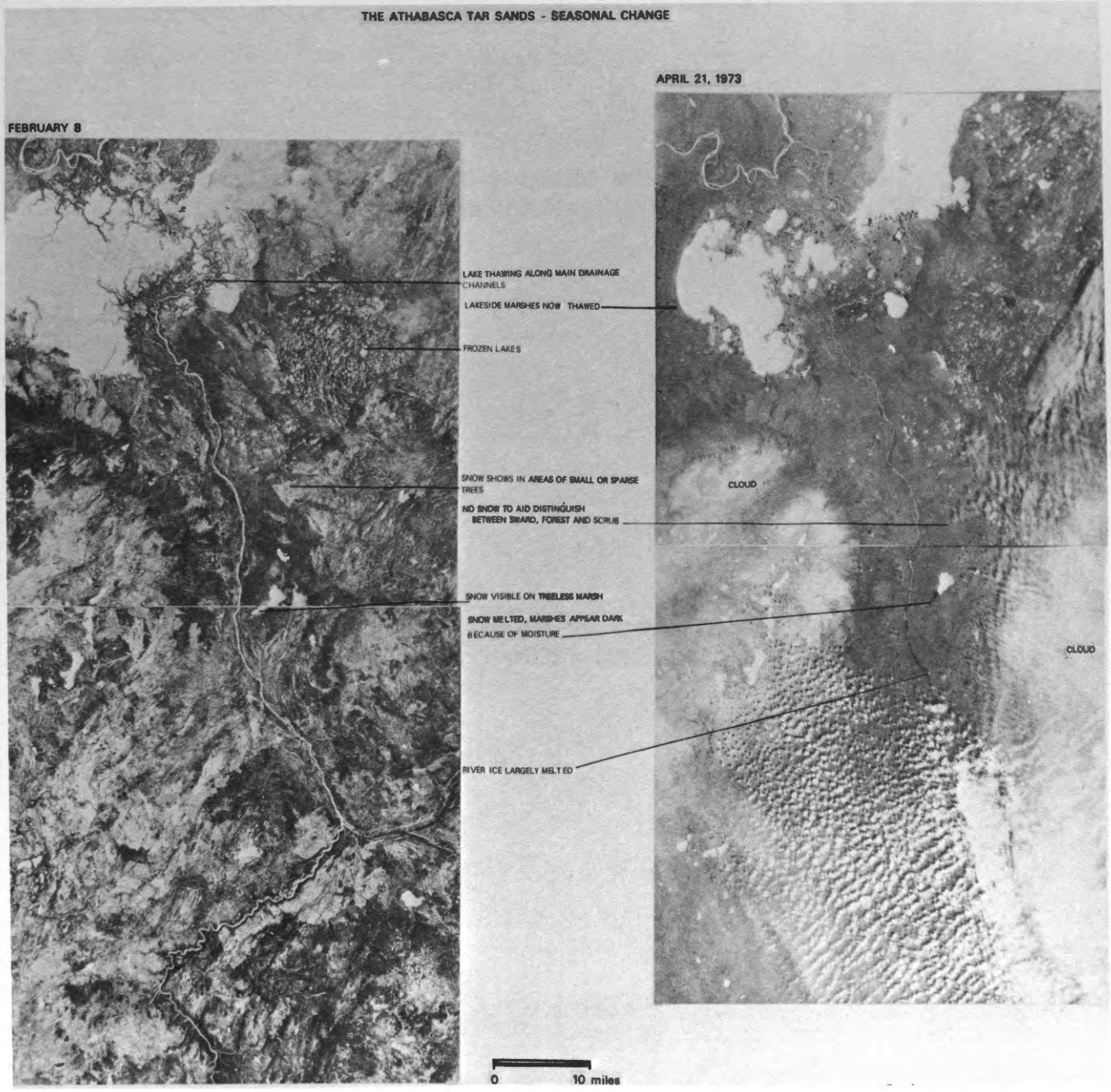

Figure 2. Athabasca Tar Sands change with time.

TEMPORAL ANALYSES OF ERTS-1 IMAGES FOR FOREST AND TUNDRA AND THEIR SIGNIFICANCE IN VISUAL INTERPRETATION OF GEOLOGY

By

HAROLD D. MOORE
ALAN F. GREGORY

This paper presented at the Second Canadian Symposium on Remote Sensing, University of Guelph, Guelph, Ontario, April 29 - May 1, 1974.

TEMPORAL ANALYSES OF ERTS-I IMAGES FOR FOREST AND TUNDRA AND THEIR SIGNIFICANCE IN VISUAL IN VISUAL INTERPRETATION OF GEOLOGY

Harold D. Moore and Alan F. Gregory
Gregory Geoscience Ltd., 1750 Courtwood Crescent, Ottawa, K2C 2B5

ABSTRACT

The geological significance of temporal changes recorded by ERTS-1 was investigated for a forested environment in New Brunswick and a tundra environment near Bathurst Inlet, N.W.T. Sets of images representing an annual cycle of seasons were analyzed for each area.

Specific characteristics of the terrain (e.g. vegetation, drainage, texture, linears and topography) were interpreted selectively to recognize seasonal changes in observables. Diverse geologic features were found to be enhanced, during appropriate seasons, by: shadows from low sun, residual snow in shaded areas, meltwater in subsidiary drainage and preferential growth of vegetation.

In this study, geologic interpretation of tundra areas proceeded faster than for forested areas; however, the quantity of derived information was not necessarily limited by forest cover. In both areas, there was a marked increase in the total amount of geologic information that could be derived by temporal analysis of a seasonal sequence of images compared to analysis of a single image for any season. A composite of the separate seasonal interpretations provides a fuller geologic interpretation.

We conclude that temporal analysis of ERTS images can provide important new information to assist geologic mapping at scales of about 1/250,000 or smaller. While specific costs have not been identified in this study, it appears that the small cost of initial temporal analysis should be more than offset by the consequent saving in field time and attendant expenses.

INTRODUCTION

Terrestrial Canada has a wide variety of seasonal conditions which are faithfully recorded every 18 days by ERTS-1 at a scale of 1 to 1 million. Canadian terrain is even more varied than the seasons. In particular, the geology ranges from Precambrian rocks over 2.5 billion years old through unconsolidated Pleistocene sediments to Recent alluvium.

ERTS-1 has now recorded nearly two full cycles of the seasons since the satellite was launched in late July, 1972. In view of the availability of such temporal data, Gregory Geoscience Limited initiated a program to assess, by means of visual interpretation, the physical and spectral changes associated with geologic observables and their significance in geological mapping. With such a great variety of seasonal and surficial conditions in Canada, it is probable that the conclusions drawn from this study may have to be modified for use in different parts of the country, as well as elsewhere in the world. However, this study should comprise a useful model for similar studies of other types of terrain.

METHOD OF INTERPRETATION

The premise on which this study was based is that natural features on the surface of the Earth are enhanced by changing illumination through the year and by temporal characteristics of associated soils, vegetation, moisture, snow, etc.(1,2,3). In other words, it is feasible to observe the "unchanging" lithosphere from many different points of view and, thus, to obtain a fuller understanding of the lithosphere at the particular scale of observation. For ERTS data this appears to be not only feasible but cost effective also.

This premise was tested with three sets

of nearly cloud-free imagery representing the major seasonal contrasts. These were selected from a much larger volume of data. After preliminary study, Band 6 (700-800nm) was chosen as the optimum single band for displaying data about rocks, snow, water and vegetation. Visual interpretation of Band 6 images was focused sequentially on different types of observables (lineaments, drainage, vegetation, etc.) for each season (3). The seasonal results were then compiled into composite interpretations of bedrock and surficial geology.

CHOICE OF AREAS

Two different types of terrain were studied and compared. One of the areas, Bathurst Inlet, N.W.T., is in the Canadian Arctic beyond the treeline and is subject to extreme climatic changes. The other area, St. John River valley, N.B., is in southeastern Canada and has large tracts of forest with intervening areas of settlement and urban developments. This latter area also has less dramatic changes in climate.

Bathurst Inlet, N.W.T.:

Bathurst Inlet lies on the Arctic coast of Canada at the latitude of the Arctic Circle. The area was chosen as representative of a tundra environment because of the availability of good sequential ERTS imagery and recent mapping of bedrock and surficial geology.

The topography of the area is quite rugged with elevations ranging from sea level to over 650 metres (2100 feet) and with local relief as great as 500 metres (4,5). A folded basin of Proterozoic sedimentary rocks lies unconformably on steeply-dipping Archean basement, which comprises gneisses, granites, metavolcanic and metasedimentary rocks (4,5,6). Gabbro sills have been extensively emplaced along the unconformity. Numerous diabase dykes, with a common strike of N25^{o}W, are found in the western part of the area. Several fault sets cut the area, the most prominent being the northwesterly-striking Bathurst fault zone with vertical relief on the scarp of as much as 330 metres.

The Pleistocene features are quite varied with extensive areas of hummocky moraine, long eskers (up to 120km) and broad deposits of marine and lake clays. The Mackenzie Uplands comprise bedrock with a thin and discontinuous veneer of boulder-till. The well-drained surface supports only scattered tussocks of grass, patches of lichen and occasional marshy tundra. These uplands also include extensive deposits of lacustrine clays. The Coronation Gulf lowlands paralleling Bathurst Inlet comprise clay-till and bedrock which are largely covered by marine silts and clays. This surface, like the clays on the Mackenzie Uplands, is poorly drained and is covered by a relatively luxurious growth of vegetation (8). Grasses, sedge tussocks, marshy tundra and flowering plants are abundant. Woody shrubs are common, especially on the west side of Bathurst Inlet. Three sets of images were analyzed, each representing a different season. The early winter image (Oct.9/72) was obtained when the ground was covered by a thin layer of snow which served to suppress terrain noise (varied reflectances) from rocks, soil, vegetation and water. The spring image (May 30/73) portrays residual snow and ice and melt water on the terrain. The early summer image (June 18/73) shows new growth of vegetation although lake ice is still present. Separate seasonal interpretations were completed and then compiled into composite interpretations of bedrock and surficial geology (see figures 1 & 2). There is a great variation in the type and amount of geological information that can be interpreted from ERTS data for each season. The composite provides more information than any one seasonal interpretation and thus provides a fuller understanding of the geology, as may be seen by comparison with published maps (figure 3). There are a number of discrepancies between interpretation and published map which require further investigation.

Discussion of Results

Structural Geology: The most obvious geologic observables on ERTS images are lineaments related to structure(2). The number of lineaments observed vary from season to season because of temporal aspects of illumination and enhancement. The form, attitude, size and foliation of formations are well displayed, as are folds, faults, fractures, shears and joints (figure 1). In particular, the composite interpretation produced by temporal analysis provides more information than any one seasonal interpretation. The major structural features are identified in all interpretations but more subtle features may be seen on only one or two images. Of the three seasonal interpretations, the spring (May 30) image has the greatest amount of information; however, this image required a longer time to interpret and was more difficult to analyze than the October image. When compared with the geological map, the composite interpretation shows that much of the structural information on the map is represented on the interpretation. Hence such an interpretation can provide a quick useful framework for carrying out geologic mapping. Further, there are many lineaments and structural features on the images that were not shown on the geological maps and which may ultimately prove to have geologic significance. Thus we conclude that selected ERTS images can comprise an excellent basis for mapping structure and that a temporal study provides additional information at little extra cost.

Surficial Geology: The temporal changes in amount of information about glacial deposits are even more dramatic than those for bedrock structure. Hummocky moraine and eskers are best seen on the winter image with the light snow cover and low angle of illumination. On the other hand, the spectral data of the summer image reveals highly reflective areas that are interpreted as abundant vegetation on deposits of lacustrine and marine clays (1,8). Comparison of the separate seasonal interpretations and the composite shows that any one of the seasonal interpretations is incomplete with respect to the actual distribution of glacial deposits (figure 3) while the composite compares favourably with the existing maps (7,8). We conclude that without temporal analysis, much information about glacial deposits may be overlooked.

Lithology and Stratigraphy: The classification of rocks and soils requires close inspection. Hence only supplementary information can be obtained by visual interpretation of ERTS data. While lithologies cannot ordinarily be classified from such data, major units can often be recognized and their stratigraphic continuity and thickness may be determined. Sometimes broad rock classes can be inferred within reasonable limits (1). In this study, the intersection of river valleys and rock foliation in the Proterozoic rocks strongly suggests a flat-dipping basin of thin-bedded sedimentary rocks, probably sandstones and shale. At an adjacent locality (1), several areas of low reflectance correlate with large outcrops of gabbro. Hence we conclude that visual interpretation of ERTS data provides temporal, textural and spectral data that can assist in classifying rocks and soils.

St. John River Valley, N.B.:

The St. John River valley lies in southeastern New Brunswick at a latitude of about 46^{o}N. The area was chosen as representative of a forest environment with moderate climatic changes and a variety of rock types. The study area includes three major geological regions (6, 9, 10): the Caledonian Highlands comprising Precambrian crystalline rocks along the coast of the Bay of Fundy; the St. Croix Highlands composed of metamorphosed lower Paleozoic sedimentary rocks along the west side of the area; and the large undeformed central basin of non-marine Carboniferous sediments. Elevations range from sea level to 454m (1500 feet) with local relief as great as 330m (1000 ft.) in the Precambrian to about 50m in the flat lying

sediments. Several large northeasterly-striking faults transect the area. There is surprisingly little evidence of glaciation; bedrock is deeply weathered and mantled with a thick residual soil with local sandy till (11). Much of the area is heavily forested with abundant spruce, balsam and pine intermixed with yellow birch and maple. The consequences of human activities are obvious on the ERTS images with urban areas, settlements, transportation networks, cultivated land and cut-over areas being particularly prominent.

Three sets of images were interpreted to obtain information relative to the season of late summer (Aug. 12/72), early winter (Nov. 28/72) and spring (Apr. 21/73). The latter image also shows flood conditions in the St. John River valley. The same procedures were used to produce separate seasonal interpretations and a composite (fig. 4) as for the Bathurst Inlet study.

Discussion of Results:

Structural Geology: The three major geological regions are clearly visible on each of the seasonal interpretations (figure 4) with the greatest detail being shown on the composite. The same types of structural features are observed in each season; the only real difference between the seasonal images being the quantity of information that can be derived. As can be seen from figure 4, the early winter image (Nov. 28/72) provides the greatest amount of detail because of the low sun inclination (20°) and the pseudo-radar effect. The composite structural interpretation contains only a small amount of additional information.

Numerous lithological boundaries can be identified and these compare favourably with mapped boundaries (compare figures 3c & 4). Most of the interpreted boundaries are at the contact between sedimentary rocks and igneous or metamorphic complexes and along unconformities. Many internal stratigraphic features show up within the sedimentary sequences. As in the case of the Bathurst Inlet study, few specific lithologic data were obtained although extent of formations and textural differences between formations (e.g. igneous vs. sedimentary) can be seen.

Two circular features (A & B, fig. 4) were interpreted. "A" was visible in all seasons and was found to correlate with a granitic stock (10). "B" was visible only on the April image and its origin is presently unknown.

Surficial Geology: Interpretation of spectral and textural patterns related to the surficial soils is greatly hindered by the heavy growth and the disturbances related to the activities of man (the so-called anthropogenic factors). The amount of information derived was insufficient to warrant a set of seasonal interpretive maps concerned with surficial geology although other disciplines will find much useful information. Glacial fluting was interpreted in several areas and a direction of glaciation identified (fig. 4) which agrees with published information. Although they are not indicated on these figures, several deposits of glacial outwash were also identified. To a first approximation, the pattern of cultivated land seems to define the major belts of marine clays, presumably because these have the highest agricultural potential. While this observation is not likely to be useful in assessing the surficial geology, it may be of use to investigators concerned with other aspects of the scene.

SEASONAL ENHANCEMENTS OF GEOLOGICAL FEATURES

Seasonal enhancement of observables on the surface of the Earth is the main reason that a temporal analysis of ERTS imagery provides new geological information in addition to that interpreted from a scene for one season. In the course of the studies reported here, six types of enhancement were identified and used:

1. Terrain noise suppression - A thin cover of snow suppresses noise (varied

reflectances) from grasses and low vegetation, soils, rocks and water(1). It thus precludes or greatly limits spectral discrimination. However, the uniformly reflective surface enhances topographic and textural patterns which have geological and geomorphological significance. Deeper snow obscures terrain details and may introduce drift patterns. Terrain noise suppression was found to be very useful for outlining geologic structure in the tundra. It also serves to enhance anthropogenic factors in forested regions because of the strong contrast between white snow and dark forest. Thus such features as power lines, transportation networks, cut-over areas, cultivated land and urban development may be more clearly defined than on images for snow-free seasons.

2. Shadow enhancement - Low inclination of the sun accentuates textural and topographic patterns with shadowing analogous to that observed with side-looking radar (1,2,3). For both high and low latitudes in Canada, shadow enhancement is a very important means of interpreting geological structure. Textures and topography need only have low relief, for example hummocky ground moraine, eskers, and drumlins with relief less than 30 metres are readily interpreted under favourable conditions. The solar inclinations involved in the studies reported here were 25° for Bathurst Inlet and 20° for New Brunswick, however inclinations as low as 3° have been used in other interpretations. Current evidence suggests that there is a preferred orientation for enhancement of features relative to solar azimuth (2, 12).

At first glance, the shadowing on images of the tundra appear to present finer detail than on images of forested regions. However, it is not yet clear whether this results from differences in textures and topography of the surface or from a lower contrast because of the forest cover or, as is most probable, a combination of these factors.

3. Residual snow enhancement - The last snow from winter commonly remains in the shadow of topographic features and depressions sheltered from direct sunlight. The high contrast between white snow and the terrain serves to enhance textural and topographic patterns. Although it is not the most obvious type of enhancement, residual snow and ice provided the greatest amount of structural information in the tundra environment. However, it was of lesser importance in the forested regions, presumably because the forest cover precludes selective enhancement of terrain features but possibly also because images were not obtained with the proper timing to represent this effect. Residual snow and ice persist for a relatively short period of time, hence images should be selected to optimize this enhancement.

4. Melt-water enhancement - Spring freshets resulting from melting snow fill the drainage system and serve to outline joints, faults, fractures and other major and minor topographic linears. The high contast between the black (low reflectance) of water on Band 6 and the terrain is an effective enhancement, particularly on the tundra. Here the permafrost causes all the water to drain off on the surface and the lack of tall vegetation makes it possible to record the whole drainage system.

5. Vegetative enhancement - As is well known from photogeology, preferential growth of vegetation may enhance geological features, particularly under marginal conditions of growth. This type of enhancement was most apparent in our study of the tundra where harsh climate, low precipitation and relatively poor soils localize the growth of vegetation. In the Bathurst Inlet study, abundant vegetation appears to be restricted to lacustrine and marine clays. Further validation of this observation is required.

6. Anthropogenic enhancement - This tertiary effect results from modification of the terrain and vegetation by man to meet his needs for cultivation, exploitation and habitation. The

seasonal aspects result from solar illumination, defoliation, snow and moisture which enhance the contrast between man-made features and the natural environment. In the New Brunswick study, the current major areas of cultivation and settlement are closely associated with deposits of marine clays. One of the major zones of cultivation also outlines a zone of Mississippian sedimentary rocks on which marine clays were deposited. Hence it appears that this type of enhancement may serve to outline areas of contrast without leading specifically to the recognition of geological reasons for their existence.

CONCLUSIONS

1. Immediate benefits can be achieved by simple interpretation of ERTS images. Where the formations are reasonably well exposed, the images may comprise useful quasi-geological maps. The derived information can provide valuable assistance to geological mapping at all scales, but especially those smaller than 1/250,000. In particular, regional structure and some information about gross stratigraphy and lithology can be derived in a matter of a few hours or days. However the level of detail and the type of information will only partly satisfy the requirements for a geological map.

2. Major structural features are commonly recognizable on ERTS images with many structural details apparent where overburden is thin. ERTS images commonly record more structural information than is presented on most geological maps. While the significance of such lineaments is not always apparent, their available record makes it feasible to undertake future analyses when the need arises.

3. Temporal analyses of a set of seasonal images and compilation of a composite interpretation can provide more geological information than analysis of a single image for either tundra or forest environments. However, the tundra seems more suited to temporal analysis because of a lack of tall vegetation and because of dramatic seasonal changes.

4. Seasonal enhancements are a valuable aid to identifying a variety of geologic features. During appropriate seasons, terrain noise suppression and enhancement by shadows, residual snow, meltwater and preferential growth of vegetation all proved useful. Especially in the tundra, these enhancements produce high contrast observables that are amenable to automated processing. In addition, anthropogenic enhancement resulting from the activities of man was also observed.

5. In the tundra, maximum structural information was obtained using residual snow enhancement while in forested areas, shadow enhancement was most useful for this purpose. In both areas, shadow enhancement with terrain noise suppression proved most useful for rapid interpretation of structure. On the other hand, spectral discrimination, which may help to identify materials, is facilitated by the high sun angles of summer imagery.

6. Temporal analysis is an important technique for mapping surficial deposits on the tundra because of the seasonal differences in the types of material that can be identified.

7. Date of image acquisition is important with respect to seasonal enhancement; hence a search through several years of data may be required to select the best images.

8. Selected ERTS images are certain to be cost effective for any regional geologic mapping because of the low cost per unit area (e.g. 13,000 sq. miles in 4 bands and 2 colour composites for $10) and the relatively short time required for visual interpretation.

REFERENCES

1. Gregory, A.F. (1973): "Preliminary Assessment of Geological Applications of ERTS-1 Imagery for Selected Areas of the Canadian Arctic", Symposium on Significant Results obtained from the Earth Resources Technology Satellite-1", vol. 1, pp. 329-343.

2. Gregory, A.F. & Moore, H.D. (1973): "Recent Advances in Geologic Applications of Remote Sensing from Space", 24th Congress of International Astronautical Fed., Baku, U.S.S.R.; proceedings in press as "Astronautical Research, 1973".

3. Moore, H.D. & Gregory, A.F. (1973): "A Study of Temporal Changes Recorded by ERTS and their Geological Significance", Third ERTS Symposium, NASA (Dec. 10-14); abstracts available, proceedings in press.

4. Fraser, J.A. (1964): "Geological Notes on Northeastern District of Mackenzie", Paper 63-40, Geological Survey of Canada.

5. Tremblay, L.P. (1968): "Preliminary Account of the Goulburn Group, N.W.T., Canada", Paper 67-8, Geological Survey of Canada.

6. Douglas, R.J.W. (1968): "Geological Map of Canada, 1/5 million", Map #1250A, Geological Survey of Canada.

7. Prest, V.K., Grant, D.R. & Rampton, V.N. (1967) "Glacial Map of Canada, 1/5 million", Map #1253A, Geological Survey of Canada.

8. Bird, J.B. & Bird, M.B. (1961): "Bathurst Inlet, N.W.T.", Memoir #7, Geographical Branch, Dept. of Energy, Mines & Resources.

9. Alcock, F.J. (1939): "New Brunswick-Gaspé Sheet", Map #259A, Geological Survey of Canada.

10. Mackenzie, G.S. (1951): (a) "Westfield; Kings, Queens, St. John and Charlotte Counties, N.B.", Paper 51-15, Geological Survey of Canada.
(b) "Hampstead; Queens, Kings and Sunbury Counties, N.B." Paper 51-19, Geological Survey of Canada.

11. Prest, V.K. (1968): "Quaternary Geology of Canada", Economic Geology Report #1 (fifth edition), p.679.

12. Wise, D.U. (1968): "Regional and Sub-continental Sized Fracture Systems Detectable by Topographic Shadow Techniques" in "Proceedings of the Conference on Research in Tectonics", Paper 68-52, Geological Survey of Canada, pp. 175-198.

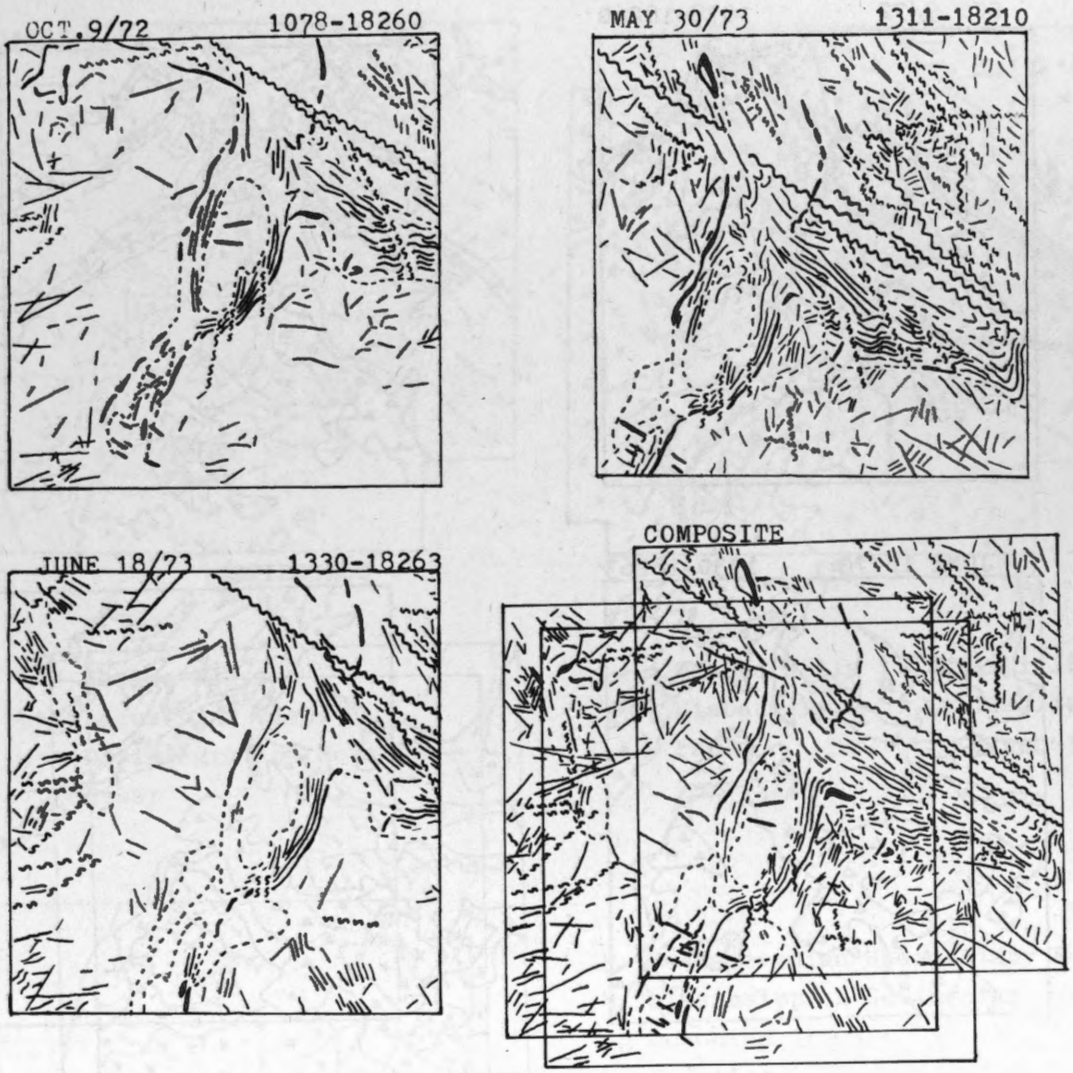

Figure 1. Seasonal and Composite interpretations (bedrock) for Bathurst Inlet N.W.T.

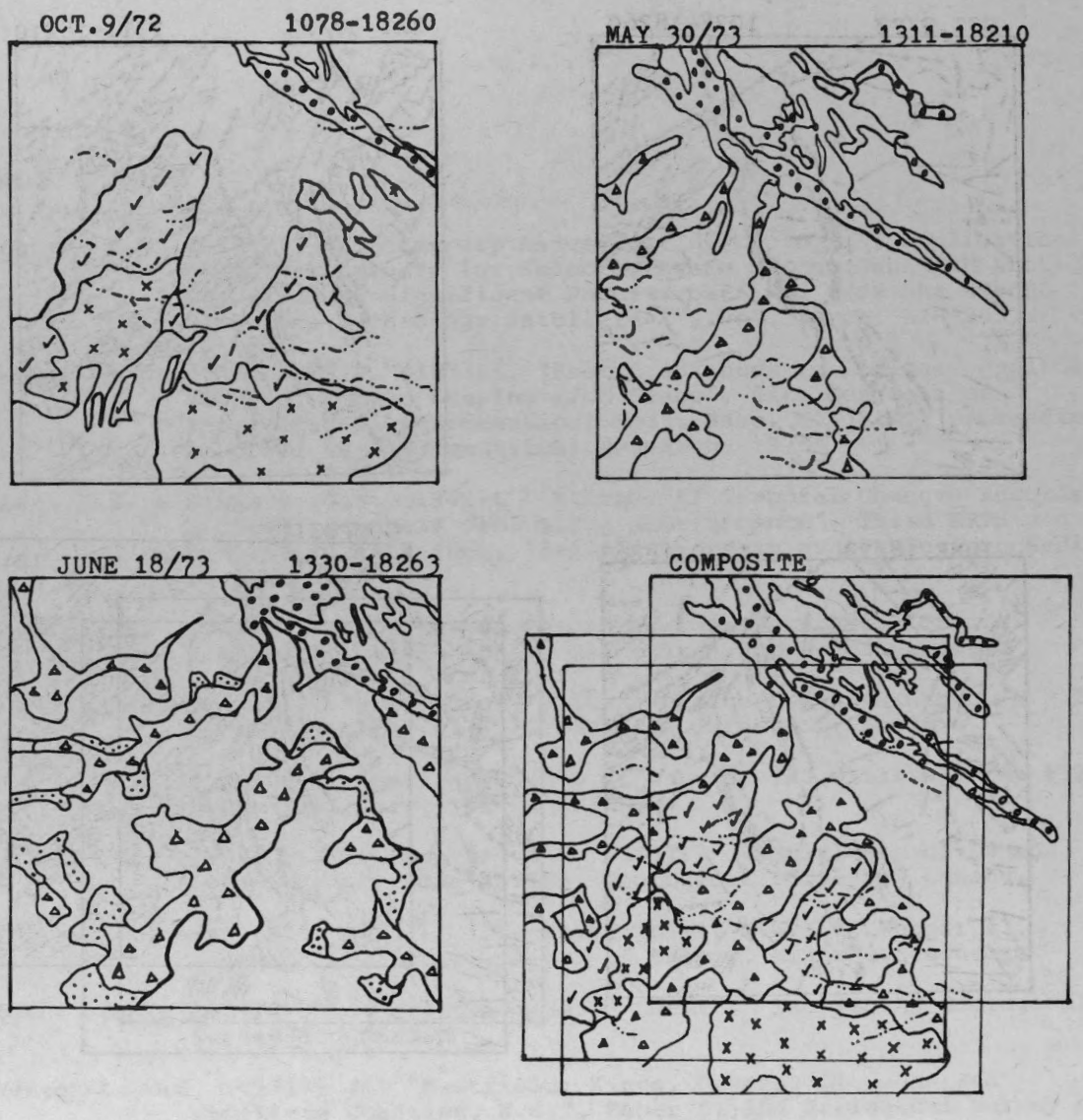

Figure 2. Seasonal and composite interpretations (Glacial) for Bathurst Inlet N.W.T.

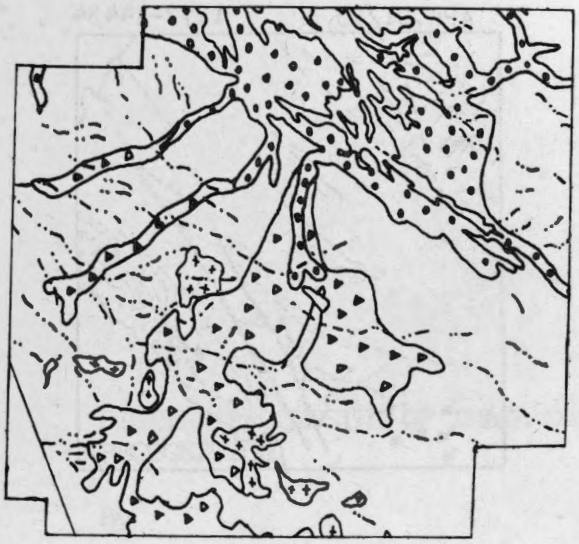

(A)

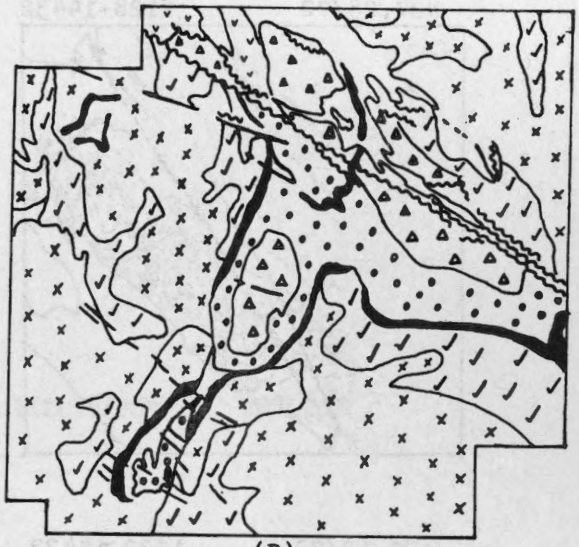

(B)

°₀°₀° Marine Clays
▲△▲△▲ Lacustrine Clays
ˣ×ˣ×ˣ Disintegration Moraine
Esker

Gabbro Sills
Diabase Dyke
Fault
°₀°₀° Quartzite
▲△▲△▲ Argillite
ˣ×ˣ×ˣ Granites
✓✓✓ Greenstone

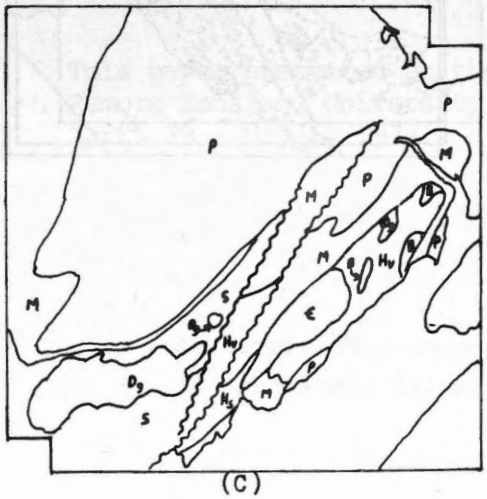

(C)

P Pennsylvanian Sedimentary Rocks
M Mississippian Sedimentary Rocks
Dg Devonian Granite
S Silurian Sediments and Volcanics
€ Cambrian
Hv Hadrynian Volcanics
B Hadrynian Gabbro
Fault

Figure 3. "Ground truth" maps (A) Bathurst Inlet Glacial (B) Bathurst Inlet Bedrock (C) Saint John N.B. Bedrock.

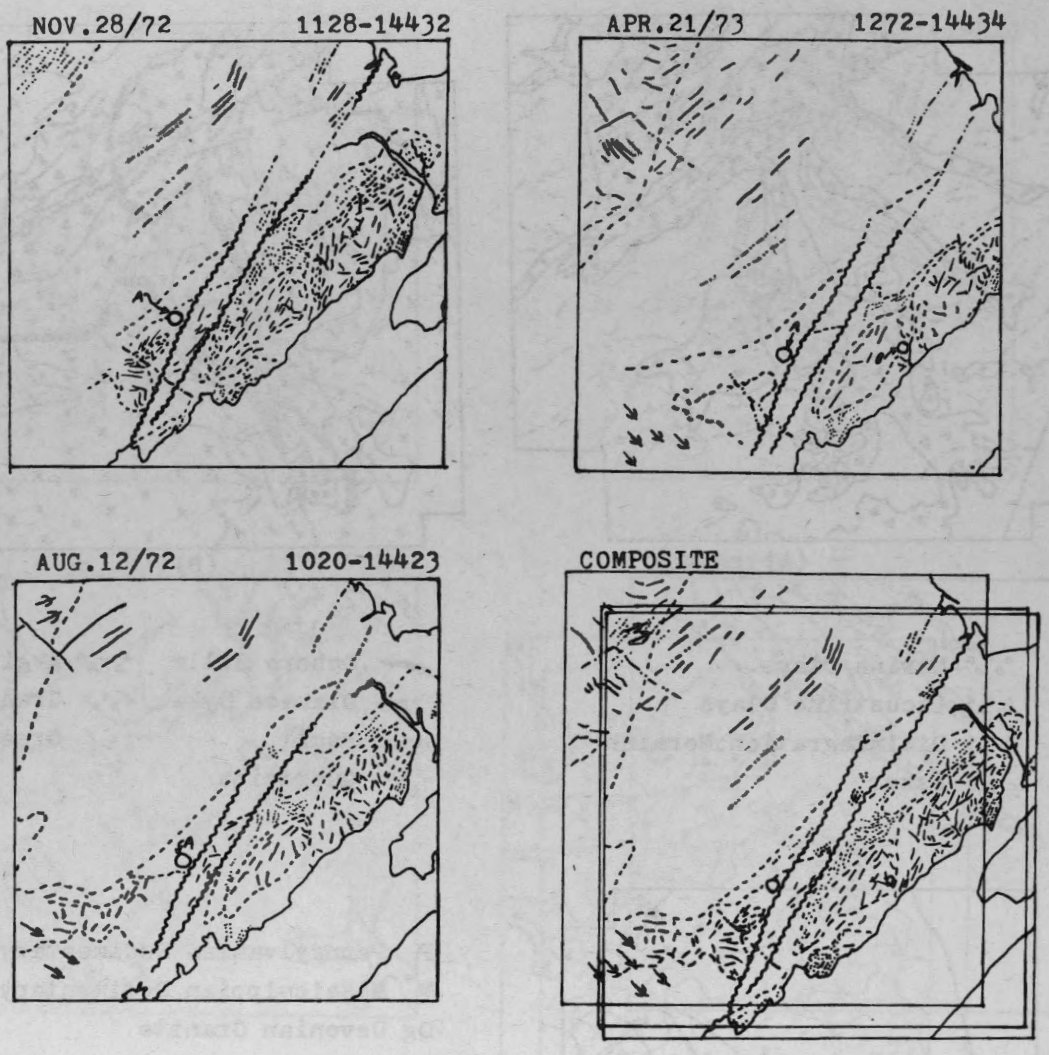

Figure 4. Seasonal and composite interpretations for Saint John River area.

DIGITAL PROCESSING OF IMAGE DATA FOR AUTOMATIC TERRAIN RECOGNITION

By

DIETER STEINER
BOB DOWHAL
HOWARD TURNER
VIGGO HELTH
MICHAEL KIRBY
JOHN CRAWFORD

This paper presented at the Second Canadian Symposium on Remote Sensing, University of Guelph, Guelph, Ontario, April 29 - May 1, 1974.

DIGITAL PROCESSING OF IMAGE DATA FOR AUTOMATIC TERRAIN RECOGNITION*

Dieter Steiner, Bob Dowhal**,
Howard Turner***, Viggo Helth****,
Michael Kirby*** and
John Crawford***

Department of Geography
Faculty of Environmental Studies
University of Waterloo

ABSTRACT

This paper reports on selected aspects of more recent work carried out within a project dealing with the establishment of a digital image data processing capability. The objective is the development of techniques for the automatic or semi-automatic extraction of data on ground features and parameters. The topics covered include image data accessing, noise removal, geometrical image registration, the matching of map to image data, multispectral pattern recognition, spatial analysis and shadow analysis for the purpose of deriving building parameters in urban areas.

INTRODUCTION

For some years the first author of this paper, together with a group of students and assistants, has been engaged in the development of a capability for the digital processing of remote sensing image data at the University of Waterloo. Until last year, the study concentrated on digitized photographs. Since then work has also started on the processing of digital ERTS data. The main objective is an investigation into the feasibility of extracting automatically or semi-automatically data on terrain features and ground parameters from remote sensing images. A first account was presented at the First Canadian Symposium on Remote Sensing in 1972 (see Steiner, 1972). The software development until fall 1973 is reviewed in a progress report by Steiner et al. (1973). This present paper summarizes some selected aspects of the most recent work. The financial support provided by the National Research Council of Canada is gratefully acknowledged.

1. SOURCES OF IMAGE DATA

Multispectral and multitemporal black-and-white aerial photographs at scales of 1:4000 and 1:30,000 were acquired with a cluster of Hasselblad 70 mm cameras over an agricultural test area situated between Guelph and Elora, Ontario, during the summer of 1971 (for details see Steiner, 1972). Vertical photos of a physical urban area model were taken on the ground last year. Selected frames of both types of photography have been digitized on an Optronics drum scanner with spatial resolutions between 50 and 200 micrometers and with 256 gray levels. More recently, we have obtained selected digital ERTS MSS data on computer-compatible tape from the Canada Centre for Remote Sensing in Ottawa. The data on the original ERTS tapes have been converted to an IBM 360/OS compatible format. Also, the multispectral bands have been separated and each has been stored as a file of scan line records (see Fig.1).

---

* Research supported by grants A 7501, E 3127 and C 0867 from the National Research Council of Canada.

** Undergraduate student in Computer Science.

*** Graduate students in Geography.

**** Research assistant, now with Chr.Rovsing A/S, Herlev, Denmark.

2. IMAGE DATA ACCESSING

Working with large volumes of digital image data requires that selected portions (windows) can be accessed for the practical implementation of image processing operations. This is particularly important for the ERTS data where one frame comprises more than 8 million pixels. Because of the large amount of storage required to hold such windows, a paging scheme has been implemented. The desired image window is divided into 4K-page blocks and maintained as direct access file. Individual image points, defined by their window coordinates, are found by converting their position in the window to a page address and a relative position within that page. Accessing is optimized by the implementation of page-buffer swapping (compare with Fig.2): Three buffers are used to hold the three most recently accessed pages. If a request for a new page is made the lowest priority page is replaced by this new page.

3. NOISE REMOVAL FROM ERTS DATA

All bands of the ERTS imagery were found to contain varying degrees of scan line noise. The noise produces more or less consistent patterns of increased intensity values along certain scan lines. For example, in band 5 every sixth scan line shows an increase of about 2 gray levels for all its pixels (see Fig.1). The same scan lines exhibit increased values in band 7, but the noise function seems to be more random.

Several simple noise removal techniques were combined in an attempt to create a general noise removal program. Noisy scan line patterns are located by visual inspection of the image printout. If the noise is systematic throughout a line, a constant is subtracted from the gray values of that line (see Fig.1e). The correction constant is supplied by the user or obtained from the difference of the marginal totals of the noisy line and a neighbouring line. If the noise is random throughout a line, each pixel on the line is assigned the average gray value of a small neighbourhood about that pixel.

The above technique fails if the noisy scan lines do not follow a consistent pattern or if two scan lines with random noise are contiguous. More complex and expensive noise removal techniques were not applied because of the large sizes of the image windows used in our various research studies. However, some of this research is concerned with Fourier analysis (see section 7.2), in which case the scan line noise effect on the transform can be detected and the values in the Fourier coefficient array associated with it can be removed from consideration.

4. GEOMETRICAL IMAGE REGISTRATION

For spectral difference enhancement of multispectral and/or multitemporal pattern recognition on a point-by-point basis corresponding pictures must be registered. In the case of digitized photography the main sources of misregistration are (a) the lack of control when mounting individual frames on the drum scanner for digitization, which leads to translational and rotational errors, and (b) differences between photos taken at different times, resulting not only in translation and rotation but in scale changes as well. There are obviously additional sources of errors, most of which lead to nonlinear distortions. However, for the present study, they were regarded as being negligible, and the registration scheme described below attempted to correct for the gross errors caused by the two main factors by linear transformations involving translation, orthogonal rotation and scaling.

4.1 Locating Control Points

A geometrical picture transformation is based on the coordinates of corresponding points identified in all the images to be registered. Such control points were identified visually on the original transparencies, their location with respect to the frame edges was determined with a measuring magnifier and then transferred as best as possible to digital printouts of the images in question to derive their row and column position. Working directly

with the digital printouts proved to be too uncertain because of lack of contrast and resolution. This relatively crude procedure lead to quite satisfactory results (see below). Improvements are possible, however. Also, the technique is rather cumbersome. For future work it is suggested that one of the following methods should be tried: (a) Prepare a photographically reduced version of the digital printouts and transfer control points from the original photos to the printouts by overlaying the two in an instrument such as the Bausch and Lomb Transferscope; (b) Prick holes at the control point locations in the original transparencies before digitization and let the computer locate the zero density values caused by these holes in the digital picture.

4.2 Formulating the Geometrical Transformation

Taking one picture as a master the parameters for a linear transformation which matches another picture to the master can be derived from the row and column position of the control points. Let x(i,M) (i=1,...,n) be the row coordinates and y(i,M) (i=1,...,n) the column coordinates of n control points in the master picture and, correspondingly, x(i,R) and y(i,R) (i=1,...,n) the row and column coordinates, respectively, of the same points in the picture to be registered. It is convenient to treat translation, rotation and scaling separately. For each a least squares solution can be derived. The following is a summary.

Translation:

$$x'(i,R)(t) = x(i,R) + t(x)$$
$$y'(i,R)(t) = y(i,R) + t(y)$$
$$(i=1,\ldots,n),$$

where x'(i,R)(t) and y'(i,R)(t) are the new coordinates after translation and t(x) and t(y) are the translation constants in the x- and y-direction, respectively. These constants are given by:

$$t(x) = xbar(M) - xbar(R)$$
$$t(y) = ybar(M) - ybar(R) ,$$

i.e., the least squares translation in x and y is simply equal to the difference between the control point coordinate averages.

Orthogonal rotation:

$$x'(i,R)(r) = x^*(i,R)\cos\theta - y^*(i,R)\sin\theta$$
$$y'(i,R)(r) = x^*(i,R)\sin\theta + y^*(i,R)\cos\theta$$
$$(i=1,\ldots,n),$$

where $x^*(i,R) = x(i,R) - xbar(R)$ and $y^*(i,R) = y(i,R) - ybar(R)$ and θ = rotation angle. The least squares rotation angle is given by

$$\theta = \arctan[(A - B)/(C + D + E + F)] ,$$

where

$$A = n\ sum(i)[y(i,M)\ x'(i,R)(t)]$$
$$B = n\ sum(i)[x(i,M)\ y'(i,R)(t)]$$
$$C = n\ sum(i)[x(i,M)\ x'(i,R)(t)]$$
$$D = n\ sum(i)[y(i,M)\ y'(i,R)(t)]$$
$$E = (sum(i)[x(i,M)])^{**}2$$
$$F = (sum(i)[y(i,M)])^{**}2 .$$

Scaling:

$$x'(i,R)(s) = s\ x'(i,R)(r)$$
$$y'(i,R)(s) = s\ y'(i,R)(r)$$
$$(i=1,\ldots,n),$$

where s = scaling factor (assumed to be equal in x and y). Formulated this way, however, requires that the rotation be carried out prior to scaling. It is possible to derive the scaling parameters from the control point coordinates before rotation by considering the distances (d(i,j)) between pairs of control points in the master image and the corresponding points in the image to be registered. The scaling operation can the be expressed as

$$d'(i,j,R) = s\ d(i,j,R) ,$$

and the scaling factor is given by

$$s = (sum(i=1,n-1)\ sum(j=i+1,n)[d(i,j,M)\ d(i,j,R)]) / (sum(i=1,n-1)\ sum(j=i+1,n)[d(i,j,R)^{**}2]) .$$

4.3 Implementing the Geometrical Correction

Once the geometrical correction parameters have been calculated with respect to a master image they can be applied to actually transform the images to be registered. The difficulty is that the geometrically corrected pixel locations of an input picture will not generally correspond to the elements of an output matrix, i.e., the coordinates of individual pixels after transformation will not in general coincide with integer row and column positions in an output array matching the master image. It would be possible to assign tonal values to the output pixels by interpolation. This solution is, however, not very attractive mainly

for two reasons: (a) It is very time-consuming, and (b) high frequency information may get lost.

For the present study we therefore opted for a procedure which is similar to the point shift approach described by Will et al., 1970. It involves the segmentation of an image into regions and shifting all pixels within a region by the same number of rows and columns. Neighbouring regions differ in terms of the row or column shift by one unit. The segmentation is done in such a way that the locational errors caused by the fact that, within a region, the amount of shift is a constant do not exceed one half pixel. This procedure obviously leads to discontinuities at region boundaries in the output picture, but the original image information is preserved within regions. A difference between the method chosen here and the one described by Will et al. (1970) is that we employ a forward instead of a backward transformation. A forward transformation looks at the pixels in the input image, calculates their new position according to the geometrical correction to be applied and assigns to them the best fitting pixel location in the output array. A backward transformation on the other hand takes the pixel locations in the output array, calculates for them the inverse geometrical transformation and superimposes the result onto the input picture, whereupon tonal values are assigned to the output pixels on the basis of a nearest neighbour rule. An advantage of the forward transformation is that the input picture can be read and corrected record by record; the results are stored in an output array which is in core memory. A disadvantage is that holes will appear in the output picture unless some additional operation is carried out. How this problem can be solved will be reported elsewhere.

The procedure followed in this investigation can be understood as one which calculates in the input picture the position of isolines of (r+1/2) pixels row shift and (c+1/2) pixels column shift where r and c are integer numbers. One must determine for each row of the input picture where the lines cross and which pixels lie between two subsequent isolines (see Fig.3). For example, all pixels whose centre points are located between the +3 1/2 and +4 1/2 row shift isolines will be assigned a row shift of +4.

4.4 An Example

Photographic frames at a scale of 1:30,000 covering approximately the same area were selected from the multispectral-multitemporal set of aerial photographs mentioned in section 1 and digitized with 200 micrometer resolution. The task then consisted in bringing a total of 11 different frames to a match. 5 control points were located within the common area on every frame using the method described in section 4.1. A program called GECOPA (for "Geometric Correction Parameters") was used to calculate a least squares registering transformation for each picture except the fifth one, which had been selected as a master.

The residual errors in the transformed control point locations were also determined. Theoretically, if nonlinear distortions are absent from the images and the location of control points could be determined exactly, a perfect match should result, neglecting for the moment the fact that the new point locations will be rounded off to integer pixel positions. In reality it was found that 85% of the control points had residual errors in x and y that were smaller than 1 pixel. The remaining errors exceeded 1 pixel, but no error was larger than 2 pixels. This result is quite good, considering the relative crudeness of the control procedure.

The actual transformations were then carried out using a program called GEPICO ("Geometric Picture Correction"). As indicated above the amounts of rotation and scale change in this experiment were quite small. However, to demonstrate the capability of the correction program results from applying large amounts of rotation and scale change to a small image section are shown in Figs.4 and 5.

5. MATCHING MAP TO ERTS DATA

A geometrical correction of images can of course, also be applied in an absolute sense, i.e. one can try to match the geometry of an image to ground control points, practically to a map with a given projection. The resulting product has then a map-like quality and direct image-map comparisons are possible. This idea has been implemented in both the Canadian and the American ERTS precision processing systems. However, whatever the reasons may be, it seems that the production of precision processed ERTS images has been largely discontinued. For the American case it has been reported that precision processing degrades the image quality, since it involves a rescanning of a previously produced bulk image (Colvocoresses and McEwen, 1973). In any event, the question can be asked whether the gain in geometrical accuracy justifies an expensive picture correcting operation, and whether it would not make more sense to do an inverse operation, i.e., distorting map data to match the geometry of ERTS data in either pictorial or digital form. Map features are largely of a linear nature and can easily be digitized and transformed. A superimposition of map grids, boundaries of admininstrative units, etc. on ERTS data can then aid the visual interpretation or a digital analysis and facilitate a comparison with already existing information.

A geometric map transformation can be based on two sources of information (compare with Hieber et al., 1973):

a) Satellite orbital and attitude data such as altitude, location, track direction, roll, pitch and yaw;

b) Comparison of control points located on both the map and ERTS imagery (or digital printouts).

Ideally, one might wish to make use of both types of data. However, in the absence of data of type (a) one must resort to approach (b) exclusively. Moreover regardless of the question of availability of satellite data, it would be desirable to have a procedure which can be easily applied by the average user. We have therefore started to investigate approach (b), and we expect that satisfactory results can be obtained with relatively simple transformations.

So far, we have carried out some preliminary experiments using ERTS frame E-1353-15471 (Windsor-Detroit area in upper part of picture). Twenty control points were located on both the ERTS image and a 1:250,000 map based on the UTM projection in an area around the shoreline of Kent, Lambton and Essex Counties, including Pelee Island. These points are scattered over an area covering about one third of the total ERTS frame. First, an attempt was made to gather some information about the precision with which such points can be located on the image and the map. To this end the coordinates of every point were measured 10 times on a map digitizer with a resolution of 0.01". The following results were obtained with regard to standard deviations in x and y [s(x) and s(y)] as well as combined standard distance (s(d) = sqrt[s(x)**2 + s(y)**2]):

	s(x)	s(y)	s(d)
ERTS image	0.010"	0.006"	0.012"
Map	0.006"	0.005"	0.008"

As expected, the standard deviations for the map points are smaller than those for the image points. This can be attributed to the fact that it is easier to locate points on the map where features are clearly defined. Better results could probably be obtained if a digitizer with a higher resolution were used or if the measurements were carried out on an enlarged image.

The second part of this preliminary experiment consisted of calculating a least squares linear transformation to match the map to the image points. First, correction parameters were calculated by using the previously mentioned program GECOPA. The accuracy of the match can be expected to be rather limited in this case because the program is restricted to the formulation of an orthogonal rotation only. The average residual error was about 0.02" (0.01" corresponding to about 4 1/2 pixels), the maximum error 0.06". A second calculation was based on a program for a general multiple linear regression,

thus allowing an oblique rotation. In this case, the average residual error was about 0.01", the maximum error 0.04". Future work will concentrate on the question of the adequacy of linear fits and the size of area for which such fits can possibly be obtained. Non-linear transformations will be tried if necessary.

For the matching of map data to digital ERTS data we face again the problem of locating points on digital printouts. The problem is compounded in this case by the fact that apparently the beginning and the end of digital data acquired on tape do not generally coincide with the edges of the corresponding picture. A good solution would seem to be to overlay a square grid on the digital data and then to produce both a printout on the high-speed printer and a photographic record on a film recorder (personal communication by Michael Hord, EarthSat, Washington, D.C.). The full gray tone capability of the photographic record allows to locate control points. Corresponding pixel locations on the digital printout can then be found by interpolation between grid lines.

6. MULTISPECTRAL PATTERN RECOGNITION

Various discriminant analysis programs have been set up for the purpose of automatic classification of terrain features on the basis of multi-variate training sample data. They range from deterministic (or distribution-free) techniques, such as distance-to-centroids and nearest neighbour analysis, to statistical techniques involving maximum likelihood decisions based on normal distributions (linear and quadratic). For details the reader is refered to the report by Steiner et al. (1973). So far, a number of experiments have been carried out on the digitized multispectral photographic data and on multispectral scanner data from ERTS. An example each is given in the following:

a) A quadratic discriminant analysis (normal maximum likelihood technique) was applied to a training set of digital four-band photographic data obtained over the agricultural area mentioned in section 1 in June 1971. An evaluation of the classification accuracy in the training data set is given in Table 1.

b) A linear discriminant analysis (normal maximum likelihood technique) applied to ERTS MSS training set data for the Detroit-Windsor area (July 13, 1973) lead to the following percent classification accuracies: Woodland 80, agricultural land 68, manufacturing industry 88, extractive industry 88, residential 68, highways 90, marshland 88 and water 92.

We should remember the fact, of course, that estimates of classification accuracy based on the reclassification of training samples is usually optimistic. A more reliable estimate must be based on the application of training sample derived discriminant functions to independent samples. One difficulty in this context, at least in the case of ERTS data, is the reliability with which image data can be related to ground truth. The importance of a capability for matching map to image data (see section 5) becomes apparent.

A major problem in multispectral pattern recognition applied to ERTS data seems to be the similarity in spectral responses of urban and agricultural areas over longer time periods within a year (compare with Ellefsen et al., 1973). It is possible that this problem can be overcome by resorting to multi-temporal and, particularly, to spatial information (see next section).

7. SPATIAL ANALYSIS

So far most of the automatic pattern recognition research in remote sensing has been based on multispectral data. Moreover, decision-making has been largely confined to a point-by-point approach. This leads to simple techniques in terms of computer implementation. However, this approach completely neglects the fact that a spatial autocorrelation exists (i.e., if the identity of a pixel has been recognized, it is probable that the neighbouring pixels will belong to the same class) and also that in conventional photo interpretation a human interpreter relies heavily on

spatial patterns and textures. The situation can be remedied with respect to the first point by aggregating multispectral data over areas and then following a per-field decision process (see, for example, Fu, 1971). Much remains to be researched with respect to textural analysis, however, although there have been some attempts to find a numerical description for textures and use this data as input to subsequent pattern recognition.

For the present project a number of computer programs have been developed which allow to derive data on spatial textures by either operating in the original spatial domain or in a transform domain. For the latter approach the Fourier transform, which analyses a picture in terms of component sinewave frequencies, and the Hadamard transform, which decomposes pictorial data into square waves, look promising. So far we have devoted some time to experimenting with spatial gradient extraction and analysis and with Fourier analysis as briefly described in the following.

7.1 Spatial Gradient Analysis

Gradient analysis based on a local operation in the spatial domain has been performed on digital ERTS data. The algorithm used (Prewitt, 1970) calculates the slope between neighboring pixel cells using a two dimensional gradient filter. The processing technique enhances the edges in the original picture matrix. Line segments (i.e. roads, shorelines, rivers, field boundaries) are extracted by thresholding the high gradient values (see Fig.6). A statistical analysis can then be performed on the enhanced image. Calculations can be made describing the frequency of edge values, length of line segments, direction and changes of direction of line segments, and the spatial differences of edge characteristics. One would expect to find long dendritic edge patterns in mountainous areas, dense short perpendicular patterns in cities and agricultural areas and random patterns in forested areas and other areas with a more natural vegetation. This work has just gotten underway and it is too early to draw any conclusions at this stage.

7.2 Fourier Analysis

A spatial frequency analysis by means of the Fourier transform can be carried out in two ways to produce input variables for a subsequent classification:

a) Transforms are calculated separately for individual defined regions. The transform coefficients can then be used to derive further measures which tell whether there are any dominant frequencies or directions present (see, for example, Hornung and Smith, 1973). A program based on the Fast Fourier Transform algorithm has been implemented, but again the work along these lines is in a preliminary stage. One lesson learned thus far is that the discrete nature of digital pictures means that resulting Fourier transforms have some pecularities with which a researcher should be familiar before he tries to analyse transforms derived from remote sensing imagery. As a preliminary step therefore we are experimenting with various artificial patterns to gain some experience in this direction.

b) One overall transform is calculated for a whole image. By carrying out filtering operations in the Fourier domain and subsequent inverse transformations one can generate a number of derived images with a content that is limited in terms of frequencies or directions or both. An example of an edge-enhanced image obtained by high-pass filtering in shown in Fig.7.

8. SHADOW ANALYSIS TO DERIVE BUILDING PARAMETERS IN URBAN AREAS

This section gives a brief account of a research study examining the feasibility of analysing shadows for the purpose of deriving the heights, ground areas and volumes of buildings in urban areas by automatic or semi-automatic means. There are a number of reasons why one would want to tackle this problem. The most important ones are the following:

a) Three-dimensional data on urban areas can find a variety of useful applications, including physical studies (micrometeorology, lighting conditions, heating volumes), morphological studies (delimitation of Central Business District, three-dimensional computer plans, height indices) and population and transportation studies (estimation of population density and traffic generation); b) Data of this kind are either not available or, if they exist, they are often incomplete or not directly organized for computer processing (tax assessment rolls) or confidential (architectural plans). c) Other methods of acquiring the data (ground surveys, photogrammetric measurements) are time-consuming and cumbersome.

8.1 Theoretical Basis

Well defined geometrical relationships exist between buildings and their shadows. Consider the diagram shown in Fig.8. It can be seen that there are basically three ways in which one can determine the height of an object (h) at image scale on a single image, assuming that the focal length f, the principal point P and the no-shadow point N are known:

a) From radial distortion (t):
$h = f\ t\ /\ (p + t)$;

b) From shadow length (s):
$h = f\ s\ /\ n = s \tan(a)$,
where a = solar altitude;

c) From distance between corresponding object and shadow points (u):
$h = f\ u\ /\ v$.

The first two relationships are, of course, well known. For computer processing, (a) requires the detection of a building edge (a radial edge from the point of view of perspective projection) and the end points (top and foot point) of this edge. The difficulty is that this method depends on a radial distortion which is sufficiently large to be measured. This excludes the possibility of using it for the central portion of an image. Procedure (b) requires the detection of the building shadow, or rather of the edge of a shadow, and its end points. Solution (c) is less known. Here we must be able to find the end point of a shadow edge and the corresponding building point. Both (b) and (c) should be feasible and should be applicable anywhere in a photograph except in the area of the no-shadow point. However, it is possible to choose the field of view and the solar altitude such that this point is located outside the frame of the picture. The detection of shadows by computer should be straightforward and possible with simple density slicing. Once a binary shadow image has been derived, the determination of shadow edges and corners is possible. However, because of the geometry (radial distortion) of the aerial photograph, it is not possible to determine building heights at every point on the photograph by using either (b) or (c), but with a combination height can be obtained at all locations on the photographs.

If the shadow outline can be followed and the coordinates of the corners of the shadows be found, then calculating the ground area of the building is simply a matter of calculating the distance between two pairs of rectangular coordinates and multiplying the distances together.

8.2 Analysis of a Physical Model

To develop the necessary computer techniques this study has concentrated so far on the analysis of photographs taken of a physical model which simulates simple and somewhat ideal conditions. The special problems associated with more complex and more realistic situations (for example, shadows falling on neighbouring buildings) will be explored later. A small physical model of a city was built last year by mounting wooden blocks simulating buildings of rectangular shapes and varying heights on a board. The model was photographed with a Hasselblad 70 mm camera in full sunlight from two positions (to obtain stereo coverage, see Fig.9) and the photos were digitized with 25 micrometer resolution and 8-bit gray level accuracy.

Since it was difficult to orient the camera in a vertical direction precisely a computer program obtained from the Photogrammetry Section of the National Research Council of Canada is being used to determine the orientation parameters from control points. The shadow analysis procedure worked out thus far proceeds as follows:

Digital printouts of selected picture windows serve to determine the gray level range of shadows. The photo can then be density-sliced and the resulting binary picture is stored as a LOGICAL*1 array (see Fig.10).

Shadows are located using a systematic sampling procedure. The gray level of every n-th pixel is looked up. If a shadow pixel is found the program backtracks until the edge of the shadow has been found. The outline of a shadow is determined by means of a border following algorithm proposed by Rosenfeld (1969). Starting from an initial border pixel it decides on the location of the next border pixel in counter-clockwise direction by looking at the configuration of object and non-object pixels within a 3-by-3 neighbourhood. The coordinates of the border pixels are stored. A modified version of a curve detection algorithm by Ledley et al. (1968) is then used to locate shadow corners. It consists of comparing the directions of a leading and a trailing vector along the border (see Fig.11). A shadow is then fully described and building parameters can be derived as indicated previously.

REFERENCES

Colvocoresses, A.P. and R.B.McEwen, 1973: Progress in cartography, EROS program. Paper NASA Symp. on Significant Results Obtained from ERTS-1, Goddard Spaceflight Center, Greenbelt, Md., 17 pp. (US Geol. Survey, McLean, Va.).

Ellefsen, R., P.H.Swain and J.R.Wray, 1973: Urban land-use mapping by machine processing of ERTS-1 multispectral data: A San Francisco Bay area example. Conf. on Machine Processing of Remotely Sensed Data: 2a-7 - 2a-22, IEEE Headquarters, 345 47th St., New York.

Fu, K.S., 1971: On the application of pattern recognition techniques to remote sensing problems. Techn. Rep. EE 71-13, 91 pp., School of El. Engin., Purdue Univ., Lafayette, Ind.

Hieber, R.H., W.A.Malila and A.P.McCleer, 1973: Correlation of ERTS MSS data and earth coordinate systems. Conf. on Machine Processing of Remotely Sensed Data: 2b-1 - 2b-13, IEEE Headquarters, 345 47th St., New York.

Hornung, R.J. and J.A.Smith, 1973: Application of Fourier analysis to multispectral/spatial recognition. Proc. Symp. on Management and Utilization of Remote Sensing Data: 268-283, Amer. Soc. of Photogramm., Falls Church Va.

Ledley, R.S., M.Legator and J.B.Wilson, 1968: Automatic determination of mitotic index. In "Pictorial Pattern Recognition" (ed. by G.C.Cheng et al.): 99-103, Thompson, Washington, D.C.

Prewitt, J.M.S., 1970: Object enhancement and extraction. In "Picture Processing and Psychopictoris" (ed. by B.S.Lipkin and A.Rosenfeld): 75-149, Academic Press, New York.

Rosenfeld, A., 1969: Picture processing by computer. 196 pp., Academic Press, New York.

Steiner, D., 1972: Multispectral-multitemporal photography and automatic terrain recognition. Proc. 1st Canad. Symp. on Remote Sensing, vol.2: 601-609, Dept. of Energy, Mines and Resources, Ottawa.

Steiner, D., V.Helth and H.Turner, 1973: Digital image processing for the automatic mapping of terrain cover types and ground parameters. Progr. Rep., 41 pp., Dept. of Geogr., Univ. of Waterloo, Waterloo, Ont.

Will, P., R.Bakis and M.A.Wesley, 1970: On an all-digital approach to Earth Resources Satellite image processing. IBM Research RC 3027, 135 pp., IBM T.J.Watson Research Center, Yorktown Heights, N.Y.

Table 1

Evaluation of an 8-class multiband data training sample in terms of percent classification accuracy obtained with quadratic discriminant analysis

	SG	CO	FO	IP	RP	RO	FA	GR	Number of pixels
Small grains (SG)	49.5	0.0	0.0	14.4	35.2	0.9	0.0	0.0	216
Corn (CO)	0.0	99.5	0.0	0.0	0.0	0.0	0.0	0.5	216
Forest (FO)	6.0	0.0	88.9	2.3	2.8	0.0	0.0	0.0	217
Improved pasture (IP)	0.0	0.0	0.0	92.4	1.3	6.2	0.0	0.0	224
Rough pasture (RP)	2.8	0.0	15.9	8.4	65.4	6.5	0.9	0.0	214
Roads (RO)	13.2	0.5	0.0	20.5	6.3	54.2	1.0	4.2	190
Farm yards/bldgs. (FA)	7.2	5.8	1.4	1.4	1.4	20.3	58.0	4.4	69
Gravel pits (GR)	0.0	0.0	0.0	4.8	0.0	1.9	4.3	89.0	210

Total number of pixels = 1556
Overall accuracy: 76.6% (1192 out of 1556 pixels classified correctly)

The table should be read as follows: Of 216 pixels belonging to small grain fields, 49.5% were assigned to small grains, 14.4% to improved pasture, 35.2% to rough pasture, and 0.9% to roads, etc.

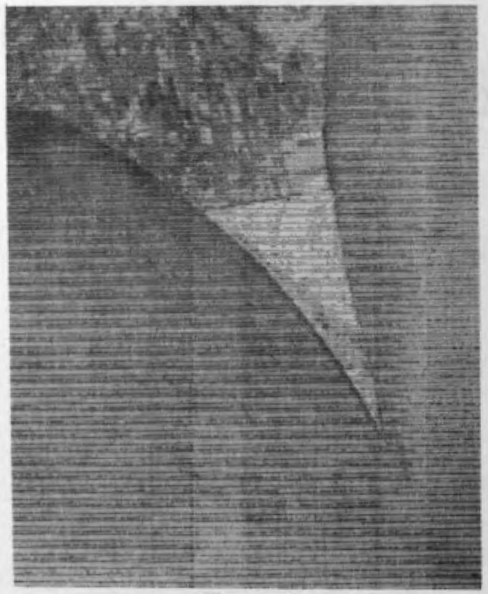

A

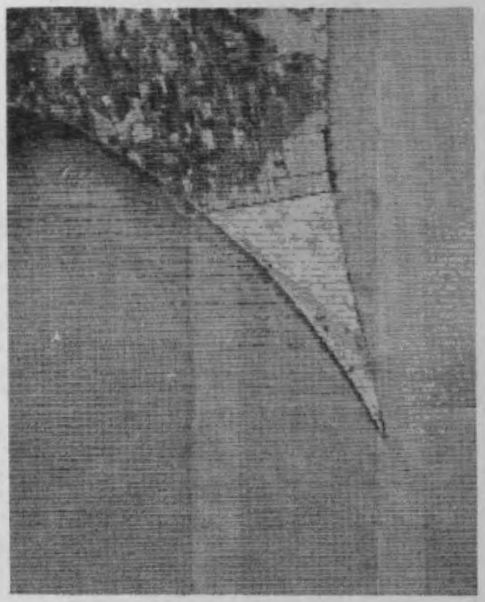

B

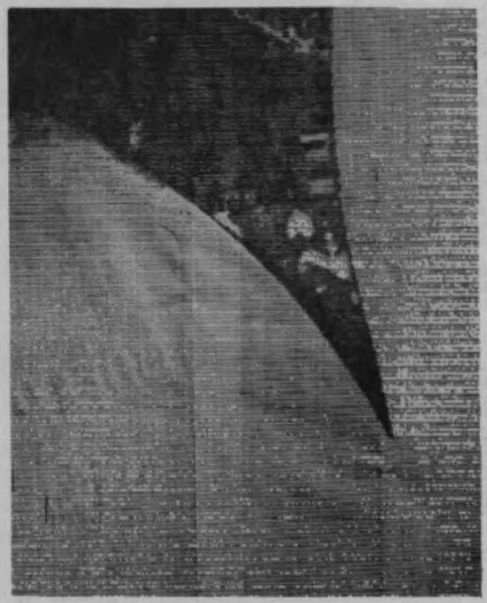

C

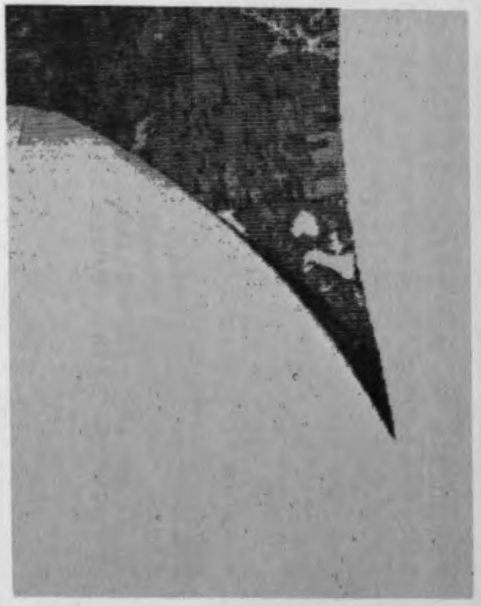

D

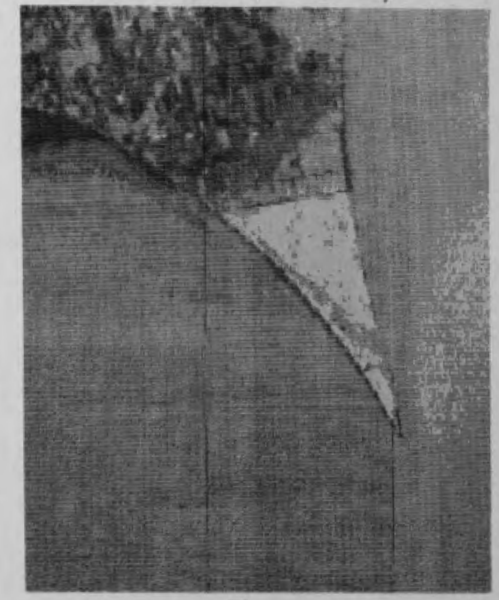

E

Fig.1
Digital printouts of a small part of ERTS frame E-1353-15471 (July 13, 1973), showing Point Pelee (S.Ontario). a) Raw data of band 4; b) id., band 5; c) id., band 6; d) id., band 7; e) band 5 after scan line noise removal.

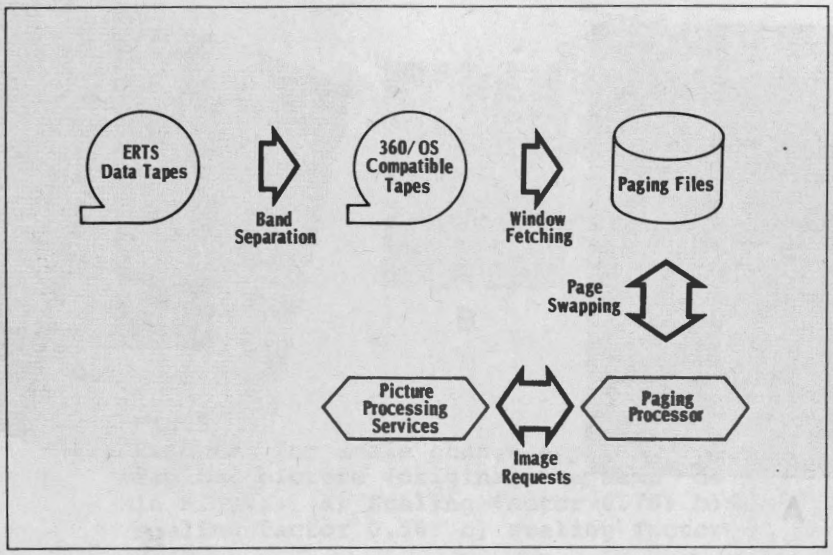

Fig.2
Flow diagram for the ERTS digital data conversion and accessing procedure.

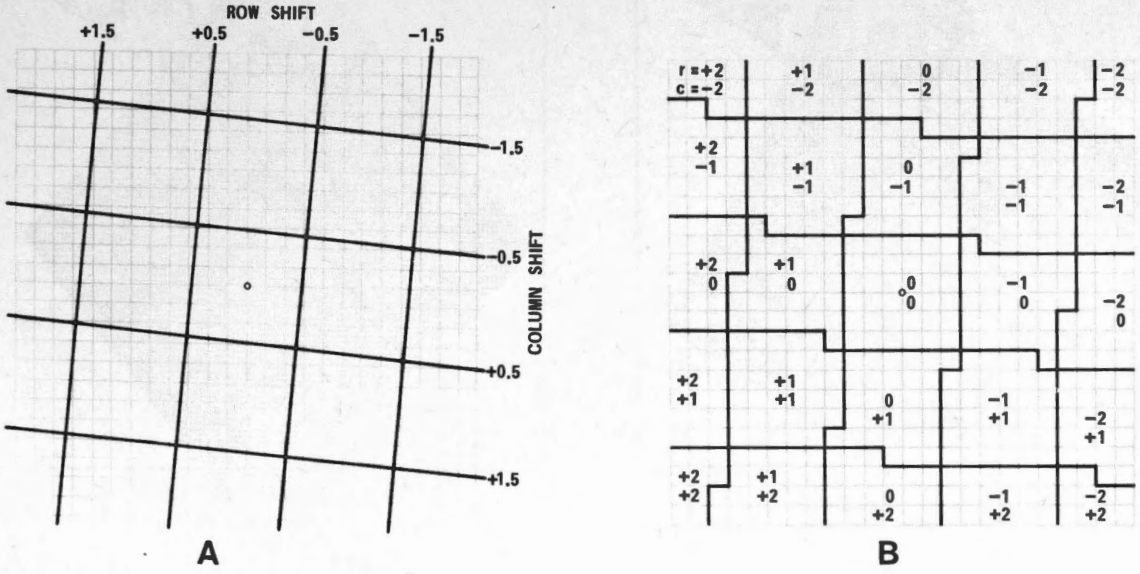

Fig.3
Subdivision of a digital image into regions of equal row and column shift for geometrical registration. a) Overlay of shift isolines on the picture matrix; b) segmentation of picture matrix into regions of equal shift.

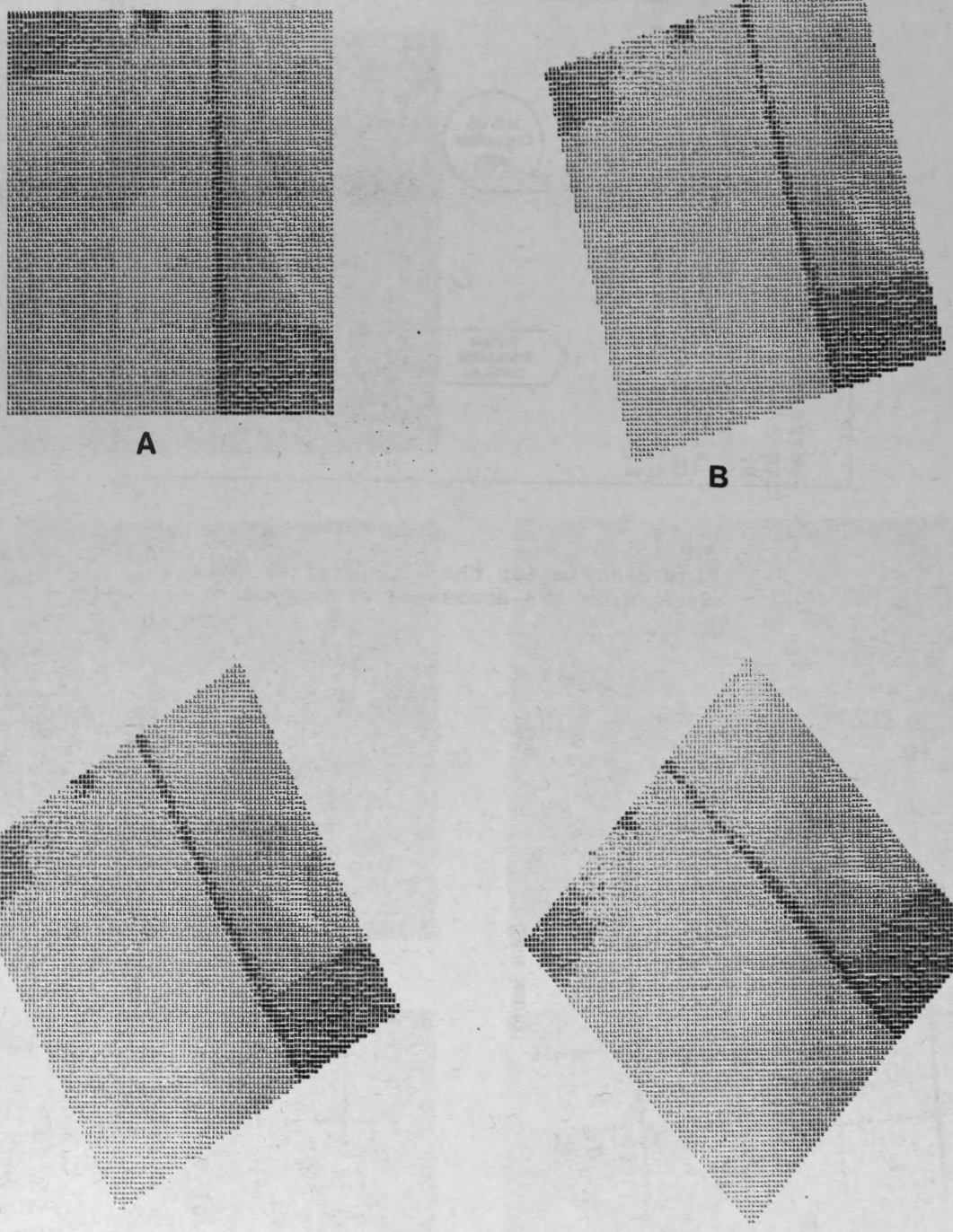

Fig.4
Example for the rotation of a digital picture (part of an aerial photograph showing fields and a road): a) Original picture; b) rotation angle 15 deg.; c) rotation angle 30 deg.; d) rotation angle 45 deg.

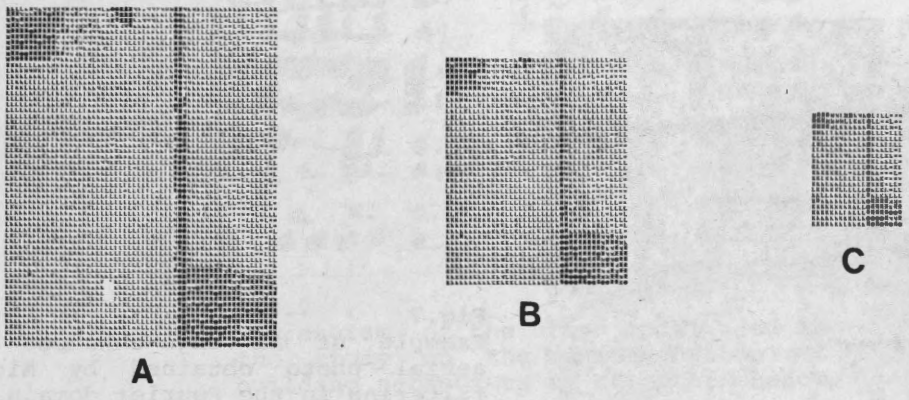

Fig.5
Example for scale change applied to a digital picture (original the same as in Fig.4): a) Scaling factor 0.75; b) scaling factor 0.50; c) scaling factor 0.25.

Fig.6
Edge enhancement by spatial gradient filtering applied to the ERTS window shown in Fig.1 after removal of scan line noise: a) Band 5; b) band 6.

Fig.7
Example of an edge-enhanced 70 mm aerial photo obtained by high-pass filtering in the Fourier domain. High values (dark tone) are associated with field boundaries, roads, farm buildings and gravel pits.

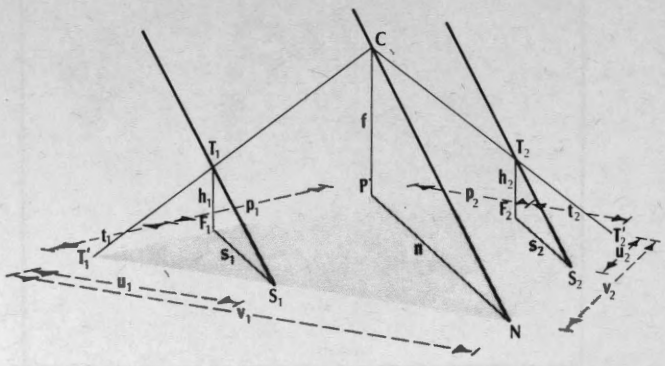

Fig.8
Geometrical relationships between objects, their radial distortion and their shadows. C = projection centre; P = principal point (assumed to coincide with the nadir); T = top point of a building edge; F = foot point of a building edge; T' = T projected into image plane; f = focal length of camera; h = building height; p = distance of F from P; N = no-shadow point; n = distance of N from P; s = shadow length; S = end point of cast shadow; u = distance between T' and S; v = distance of T' from N; thick lines = rays of light.

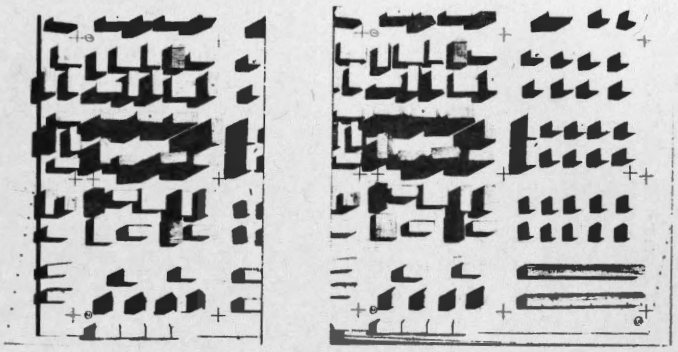

Fig.9
Stereogram of the urban model used in the study on the determination of building parameters by computer shadow analysis.

Fig.10
Example of a density-sliced picture of part of the urban model. The dark areas are shadows cast by buildings.

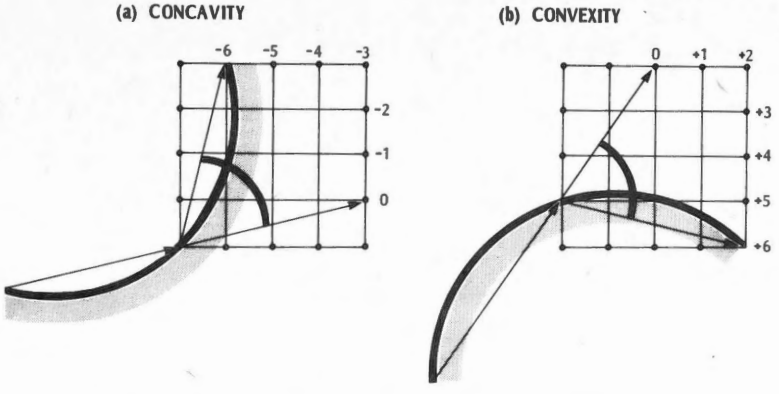

Fig.11
Curve detection procedure based on the comparison of a leading and a trailing vector (after Ledley et al., 1968).

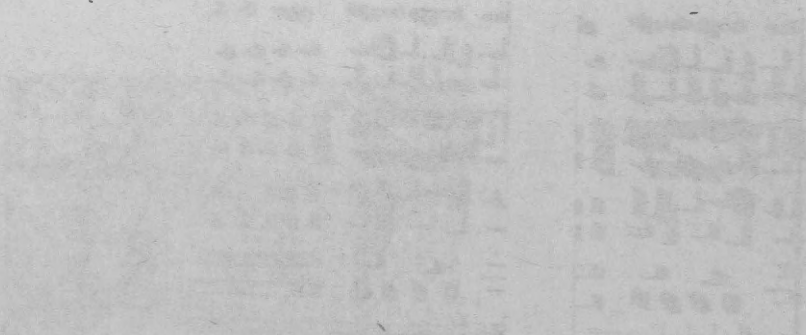

WATER QUALITY OF LAKES OF SOUTHERN ONTARIO FROM ERTS-1

By

JOHN C. MUNDAY JR.

This paper presented at the Second Canadian Symposium on Remote Sensing, University of Guelph, Guelph, Ontario, April 29 - May 1, 1974.

WATER QUALITY OF LAKES OF SOUTHERN ONTARIO FROM ERTS-1

John C. Munday Jr.
Department of Geography
University of Toronto
Erindale College
Clarkson, Ontario

ABSTRACT

Relative water quality of water bodies in southern Ontario is investigated using ERTS-1 data. Image densities are reduced to scene radiances N_i (of band i), transformed by $x = N_4/(N_4 + N_5 + N_6)$ and $y = N_5/(N_4 + N_5 + N_6)$, and plotted on an x,y chromaticity diagram. Water points fall near $x + y = 0.9$; cloud-corrected y_c is chosen as a water quality index, with high values indicating sediment loading, low values clear water, and very low values (probably) chlorophyll a loading. y_c vs. time may be useful in long-term monitoring of lake water quality and site selection for surface investigation.

INTRODUCTION

Water suffers many types of modifications, from natural causes and from man. Those caused by man are large in variety, and continually proliferating, as new substances are developed and become potential pollutants. Pollutants are dispersed to hitherto pristine bodies of water, and interfere with natural changes. Natural changes have assumed increasing importance in recent years; a lack of natural baseline data, and insufficient understanding of natural dynamic relationships, have impaired attempts to determine man's impact on water quality, and to set environmental protection standards.

Water quality can be measured in as many ways as there are types of modification. Moreover, water's multiple uses provide each user with a distinct viewpoint and need. Four broad categories can be used to classify the various user viewpoints and needs: public health, eutrophication, non-nutrient chemical pollution and sediment loading.

Public health needs are satisfied only by contact sampling and laboratory counting of total coliform, fecal coliform, and more recently, fecal streptococcus. Remote sensing is useless for bacterial counting, but it may provide data about dispersion from points of bacterial input.

The degree of eutrophication in a body of water can be assessed by a variety of methods. Remote sensing can be used profitably for six basic indicators of the trophic state: water transparency, water color, chlorophyll, algal blooms, aquatic vegetation, and suspended solids (Wezernak and Polcyn, 1972; Wezernak, 1974). To remotely discriminate several of these indicators simultaneously, multispectal scanner data with several channels of narrow bandwidth are required (see Wezernak, 1974).

The problem of chemical pollution is formidable because of the large number of pollutants, and requires contact sampling and laboratory analysis. Remote sensing is of assistance only in case of water discoloration, or secondary effects such as vegetation change.

Suspended sediment levels, traditionally measured by laboratory analysis of water samples, are now being frequently measured by remote broad band sensors. Measurement of the suspended sediment profile, as well as surface levels, appears possible (Mairs, 1970; Hickman et al., 1972; Stortz and Sydor, 1974); profile measurement would be of special benefit in dredging problems and in the analysis of chemical exchange between water and bottom sediments.

The utility of remote sensing for water quality measurement is thus mixed, and strongly dependent on the category of interest. It is clear that simultaneous measurement of several water quality variables requires several narrow-band channels of remote sensing data. For high measurement accuracy, conditions specific to individual water bodies and the dates of remote sensing coverage have to be known and used as input data during data processing. Such considerations are a discouragement to water quality surveys by routine remote sensing over wide areas, in that the principal, inherent advantages of remote sensing are constrained.

The ERTS-1 multispectral scanner has three channels, MSS 4, 5, and 6, which can provide water quality data. MSS 7, because of the high near-infrared absorptivity of water, images only those water conditions with a superficial aspect, such as very high surface sediment levels, floating plants, and intense algal blooms. Since such features are also

sensed by MSS 6, the MSS 7 record is for this application redundant.

With just three useful bands, with wide bandwidths, the water quality data which can be obtained with ERTS-1 are limited. Only variables amenable to wide-band sensing can be pursued, including suspended sediment, large-volume dumps of discoloring pollutants, and biological discoloration. Although numerous investigators have collected surface data for many variables during ERTS-1 passes, the limitations inherent in three wide bands allows few independent correlations between the surface variables and the ERTS-1 data. In response to this situation, one can develop a scalar index based on remote sensing data which usefully correlates with a composite of surface data. Wezernak (1974) has developed for aerial multispectral scanner data a scalar 'trophic index' having high correlation with sufface data. A similar development can be sought with ERTS-1 data.

The large area covered in a single ERTS-1 frame precludes frame-wide simultaneous surface truth efforts with any frequency. This limitation is important in the case of widely scattered small water bodies, as in Ontario and elsewhere in Canada. ERTS-1 data have been used thus far for study of a small number of water bodies, for each of which extensive surface data could be collected. If the number of water bodies under study is allowed to become large, surface data collection for many of them will have to be omitted.

The goal in this study is an ERTS-1 index of water quality which, despite serious hindrance from the constraints discussed above, can function usefully over a large number of widely-scattered water bodies and over long times. The index developed appears to be useful in monitoring water quality changes, and thus indicating water bodies for which surface data collection might be desirable. The regional focus in this preliminary work has been water bodies in ERTS-1 images of southern Ontario.

METHODS

ERTS-1 Data

MSS 9-in photographic transparencies were obtained as listed in Table 1. The utility of EROS Data Center imagery was limited by excessive cloud cover (actual cover was greater than source-listed cover). NAPL imagery was largely unusable because of unreliable radiometry; an effort to develop a radiometric scale from internal image data for NAPL images 7 and 8 was only partially successful (see Results).

Densitometry and Radiometry

Diffuse image densities were measured with a Sargent-Welch Densichron 1 densitometer with a 1 mm diameter blackened aperture. NASA suggests a 3 mm aperture to eliminate image development and MTF problems (EDUH, p. F-11); the smaller aperture was necessary to allow measurement in small water bodies (for CCTs the smallest usable ponds are reportedly 1 acre; for images here, 1 mm aperture at a scale 1:1M permits measurement of lakes > 1 km in diameter.) Densities were converted to radiances using radiance calibration factors (see EDUH, p. 3/6) and step wedge densities.

Radiance Analysis

Earlier work indicates that total water radiance in MSS 4, 5, and 6 varies with the distribution of radiance over these bands. Particularly, high total radiance occurs for partial to complete cloud cover (and air pollution), and high concentrations of suspended sediment, both of which have characteristic spectral signatures. The ratio transformation $x = N_4/\Sigma N_i$, $y = N_5/\Sigma N_i$, $z = N_6/\Sigma N_i$ and $x + y + z = 1$, where N_i is radiance of band i, removes the influence of total radiance, leaving only spectral information. The two dimensions x and y are analogous to chromaticity coordinates for human color vision. They are convenient for plotting on a chromaticity diagram. Partial cloud cover can be identified as a decrease of spectral saturation, and graphically corrected to obtain the cloud-free water hue. Chromaticities here were computed by a 100-card FORTRAN program (IBM 370; copies available) using the sensitometric equation, and image densities and radiance calibration factors as input. For a more complete discussion of these methods see Munday (1974) (see also Results, and Discussion).

RESULTS

The distribution of chromaticities for various features in image 1 is shown in Figure 1. A white point C is defined by opaque cloud chromaticities. Woodland and agricultural fields plot to the z-side of C due to high MSS 6 reflectance. Water bodies plot to the x-side of C due to high MSS 4 reflectance. Thin cloud cover shifts all target hues toward C.

Various water bodies in southern Ontario plot are shown in Figure 1. Only a small selection of the 200 image points investigated for Lake Ontario and Lake Erie is shown. For smaller lakes, the number of differentiable image points was small; thus, their loci of chromaticities in

Figure 1 are perhaps less representative than loci for Lake Ontario and Lake Erie. With each lake, the image points were selected to encompass the full range of conditions discernible by visual image inspection.

The Lake Scugog chromaticities are significantly cloud-shifted. The cloud identifications are definitive, as thin cloud boundaries crossed land-water interfaces.

For all water bodies as a group, the chromaticities free of cloud influence fall in a linear region parallel to and limited by $z = 0.1$. This finding held true for all images investigated, with only minor variations in the magnitude of the limiting z-value. Only a few image points, which obviously involve extremely high concentrations of suspended sediment, have shown a white shift free of cloud influence, and these are localized at high N_5/N_4 ratios. On the locus $z = 0.1$, $x + y = 0.9$; thus, MSS 6 contributes cloud information but not water hue information; consequently, a scalar index is defined for water quality, either x or y. Because of MSS 5's widespread appeal in delineating suspending patterns, y is chosen for the index.

Water hues are cloud-corrected by graphical extension of the line CP (P is the point of interest) to $z = 0.1$; the intersection defines a high-saturation, cloud-corrected y-value denoted y_c. From Figure 1 were obtained maximum and minimum y_c values for all lakes represented. The y_c ranges with midpoints are shown in Figure 2. The range for Lake Ontario is large; near-shore suspended sediment produces high y_c values, and mid-lake clear water produces low y_c values. The Georgian Bay has the lowest y_c values (and the lowest total radiance).

For a lake water quality monitoring program, y_c values can be obtained from a sequence of ERTS-1 passes and plotted versus time. Figure 3 shows the results which were obtained from the coverage listed in Table 1. The number of water bodies and image dates used in Figure 3 is small and hardly represents a sample large enough for definitive conclusions (especially so because of the lack of field data). The small number is due to excessive cloud cover, unreliable radiometry, and ERTS-1 orbit drift. NAPL image radiometry was generally unusable. An attempt was made to obtain useful results from NAPL images 7 and 8 (which are successive-day passes). A set of maximum and minimum densities was obtained from cloud (or snow) and clear-water areas, and a scale of radiometric calibration factors was arbitrarily established using the chosen set of densities as end points. The resulting chromaticity diagrams showed the general features described earlier, but anomalous features were frequent; even lake points found on both images (due to successive-day sidelap) did not always yield strongly similar chromaticities. The results indicate that NAPL relative radiometry is unreliable within single pass images as well as over successive passes.

For the EROS Data Center imagery, there was variation in the general range of y_c values from date to date. This variation may be caused by environmental processes, or by sensor drift and image production processes. All y_c values were normalized by bringing the lowest y_c value for Lake Ontario to a constant value equal to that for image 1. Hence, the ordinate of Figure 3 is a normalized y_c denoted y_n.

Lake Ontario (O), Lake Erie (E), Toronto Bay (T), and Hamilton Harbour (H) show generally constant midpoint values of y_n. The Niagara River above Niagara Falls (R) and the New York power reservoir below Niagara FAlls (Y) show large drops of y_n in June 1973 as compared to earlier, reaching nearly the low y_n values of the Georgian Bay (G). Unfortunately, the small data base does not allow tracing y_n through time for any other water body.

DISCUSSION

Two important considerations with regard to the utility of y_n are the significance of y_n as a water quality index, and the long-term accuracy of results with respect to ERTS-1 data production and atmospheric haze.

The significance of y_n is partially known at present. y_n increases with suspended sediment concentration, as shown by high y_n for obvious river plumes and near-shore turbidity, and low y_n for deep off-shore waters. How y_n varies with chl *a* (chlorophyll *a*) concentrations and plankton biomass must presently be hypothesized, in view of the lack of surface truth in this study, and the lack (to date) of quantitative correlation of chl *a* with MSS radiances in the literature. The reflectance data of Clarke, Ewing, and Lorenzen (1970) show that reflectance between 500 and 650 nm increases with chl *a*, and that the increase is greater over 500-600 nm (corresponding to MSS 4) than over 600-650 nm (corresponding to MSS 5). Szekielda and Curran (1973) noticed qualitatively that chlorophyll loading was more visible in MSS 4 than in MSS 5. Thus, N_5/N_4 and y_n should decrease with chl *a*. For extremely high levels of phytoplankton, or for floating plants, MSS 6 as well as MSS 4 radiance should increase relative to MSS 5 radiance. The results on a chromaticity diagram should be a y_n decrease with moderate levels of chl *a*, and at very high levels, a z-shift (with a white component) of the (uncorrected and unnormalized) y value, which upon white correction and

normalization should produce a very low, perhaps negative value of y_n.

In sum, high y_n ($\sim$ 0.28) indicates sediment loading, low y_n ($\sim$ 0.2) indicates relatively clear water, and very low y_n (<0.2) should indicate high chl *a* levels. Bowker *et al.* (1973) found some correlation of suspended sediment and chl *a* in the Chesapeake Bay; if high suspended sediment concentrations and chl *a* concentrations occur simultaneously, y_n will indicate clear water, but this eventuality can be discriminated from truly clear water by its high total radiance. If thin cloud cover, high suspended sediment concentrations, and high chl *a* concentrations occur simultaneously, the ERTS-1 data will be ambiguous.

Other influences on y_n need to be investigated. For example, shallow water could have a variety of influences depending on bottom spectral reflectivity. Bowker *et al.* (1973) and Klemas *et al.* (1974) have noticed variations of MSS response with bathymetry even in very turbid water.

As y_n values for small lakes probably reflect lake-specific conditions, the absolute value of y_n can be interpreted only if surface data are available. A lake water quality monitoring program, for a large number of lakes over a large area, could not hope to frequently arrange surface data collection for all the lakes of interest. Consequently, a modest goal must be accepted in the utilization of y_n versus time. A useful approach is to utilize such charts as in Figure 3 to establish when important changes are occurring. Some anomalous and seasonal variations in y_n will be expected in all lakes of interest, as ERTS-1 continues to collect data. But these variations will be distinguishable from long-term trends and sudden extreme changes in some of the lakes of interest. ERTS-1 in this approach is to function as a lake water quality change-detector.

Useful long-term results will depend on the radiometric accuracy of ERTS-1 data. Analysis of CCT data would in this regard be superior to image analysis. However, there are distinct advantages in using images. First, very cloudy ERTS-1 data will usually be avoided by investigators using CCTs, yet cloudy data may have little or non-existent cloud cover over some of the water bodies of interest. For a small number of points, image densitomery then allows rapid measurement of y_n. Second, the long-term utility of y_n depends on knowledge of background variations for all lakes of interest, and the background variations are best ascertained from a maximum number of y_n values; the expense in getting a large number may be prohibitive with CCT analysis, but tolerable with images. Third, many users will not have CCT capability; with image analysis they will be able to conduct useful ERTS-1 monitoring of their regions of interest.

The effect of atmospheric scattering on the results has not been considered here. This problem must be investigated in future study.

SUMMARY

An ERTS-1 chromaticity analysis for water bodies in several southern Ontario images shows that water quality can be summarized by a scalar variable y_n. Sediment loading produces high values of y_n, clear water produces low values, and high chlorophyll *a* loading (should) produce very low values. Graphs of y_n versus time may be useful in long-term monitoring of lake water quality, especially in the case of remote water bodies in uninhabited areas, for which surface data are lacking.

ACKNOWLEDGEMENTS

I thank the Canada Centre for Inland Waters, Burlington, Ontario, for contract support of this study (Department of Supply & Services, Federal Government, Ottawa: 01GRKW111-2-1073, 0GR2-0522). M. Riendeau prepared Figure 1. B. Stiff prepared the typescript.

REFERENCES

1. Bowker, D.E., P. Fleischer, T.A. Gosink, W.J. Hanna, and J. Ludwick. 1973. Correlation of ERTS multispectral imagery with suspended matter and chlorophyll in lower Chesapeak Bay. Proc. Symp. Significant Results obtained from ERTS-1, March 1973, NASA Goddard, Greenbelt, Maryland, publ. SP-327, p. 1291-1297.

2. Clarke, G. L., G. C. Ewing, and C. J. Lorenzen. 1970. Spectra of backscattered light from the sea obtained from aircraft as a measure of chlorophyll concentration. Science 167: 1119-1121.

3. ERTS Data Users Handbook. NASA Goddard, Greenbelt, Maryland.

4. Hickman, G. D., J. E. Hogg, and A. H. Ghovanlou. 1972. Pulsed neon laser bathymetric studies using simulated Delaware Bay waters. Sparcom Inc., Alexandria, Virginia, Techn. Rep. No. 1, 79 p.

5. Klemas, V., M. Otley, W. Philpot, C. Wethe, and R. Rogers. 1974. Correlation of coastal water turbidity and circulation with ERTS-1 and Skylab imagery. Proc. 9th Intl. Symp. Remote Sensing of Environment, Env. Res. Inst. Michigan, Ann Arbor, in press.

6. Mairs, R. L. 1970. Oceanographic interpretation of Apollo photos. Photogram. Eng. 36(10): 1045-1058.

7. Munday, J. C., Jr. 1974. Lake Ontario water mass delineation from ERTS-1. Proc. 9th Intl. Symp. Remote Sensing of Environment. Env. Res. Inst. Michigan, Ann Arbor, in press.

8. Stortz, K., and M. Sydor. 1974. Remote sensing of Lake Superior. Proc. 9th Intl. Symp. Remote Sensing of Environment, Env. Res. Inst. Michigan, Ann Arbor, in Press.

9. Szedielda, K., and R. J. Curran. 1973. Chlorophyll structure in the ocean. Proc. Symp. ERTS-1, September 1972, NASA Goddard, Greenbelt, Maryland, p. 139-141.

10. Wezernak, C. T., and F. C. Polcyn. 1972. Eutrophication assessment using remote sensing techniques. Proc. 8th Intl. Symp. Remote Sensing of Environment, Env. Res. Inst. Michigan, Ann Arbor, p. 541-551.

11. Wezernak, C. T. 1974. The use of remote sensing in limnological studies. Proc. 9th Intl. Symp. Remote Sensing of Environment, Env. Res. Inst. Michigan, Ann Arbor, in press.

TABLE I

INSPECTED ERTS - 1 COVERAGE OF WESTERN LAKE ONTARIO (N43°30'/W79°00')

FROM 21 AUGUST 1972 TO 1 JULY 1973

No.	Date	Image Id.	% Cloud	Bands	Source
1	21 Aug 72	81029-153455N0	0	4,5,6,7	NASA Goddard*
2	01 Nov 72	81101-153545N0	60	4,5,6,7	EROS Data Center, Sioux Falls
3	01 Nov 72	E1101-153515-1	30	4,5,6,7	NAPL, Ottawa**
4	20 Nov 72	E1120-154115-1	30	4,5,6,7	NAPL, Ottawa**
5	07 Dec 72	81137-153555N0	50	4,5,6,7	EROS Data Center, Sioux Falls
6	17 Feb 73	81209-153615N0	0	4,5,6,7	EROS Data Center, Sioux Falls
7	12 Apr 73	E1263-153555-0	10	4,5,6	NAPL, Ottawa**
8	13 Apr 73	E1264-154135-0	0	4,5,6	NAPL, Ottawa**
9	29 Apr 73	E1280-153036-0	30	4,5,6	NAPL, Ottawa**
10	18 May 73	81299-153605N0	60	4,5,6,7	EROS Data Center, Sioux Falls
11	05 Jun 73	81317-153545N0	30	4,5,6,7	EROS Data Center, Sioux Falls
12	23 Jun 73	81334-15353N0	60	4,5,6,7	EROS Data Center, Sioux Falls

* Image 1 kindly supplied by N. Ursel, P. Eng., Mississauga, Ontario

** Images 3, 4, 7, 8, and 9 kindly loaned by P. Howarth, Department of Geography, McMaster University, Hamilton, Ontario.

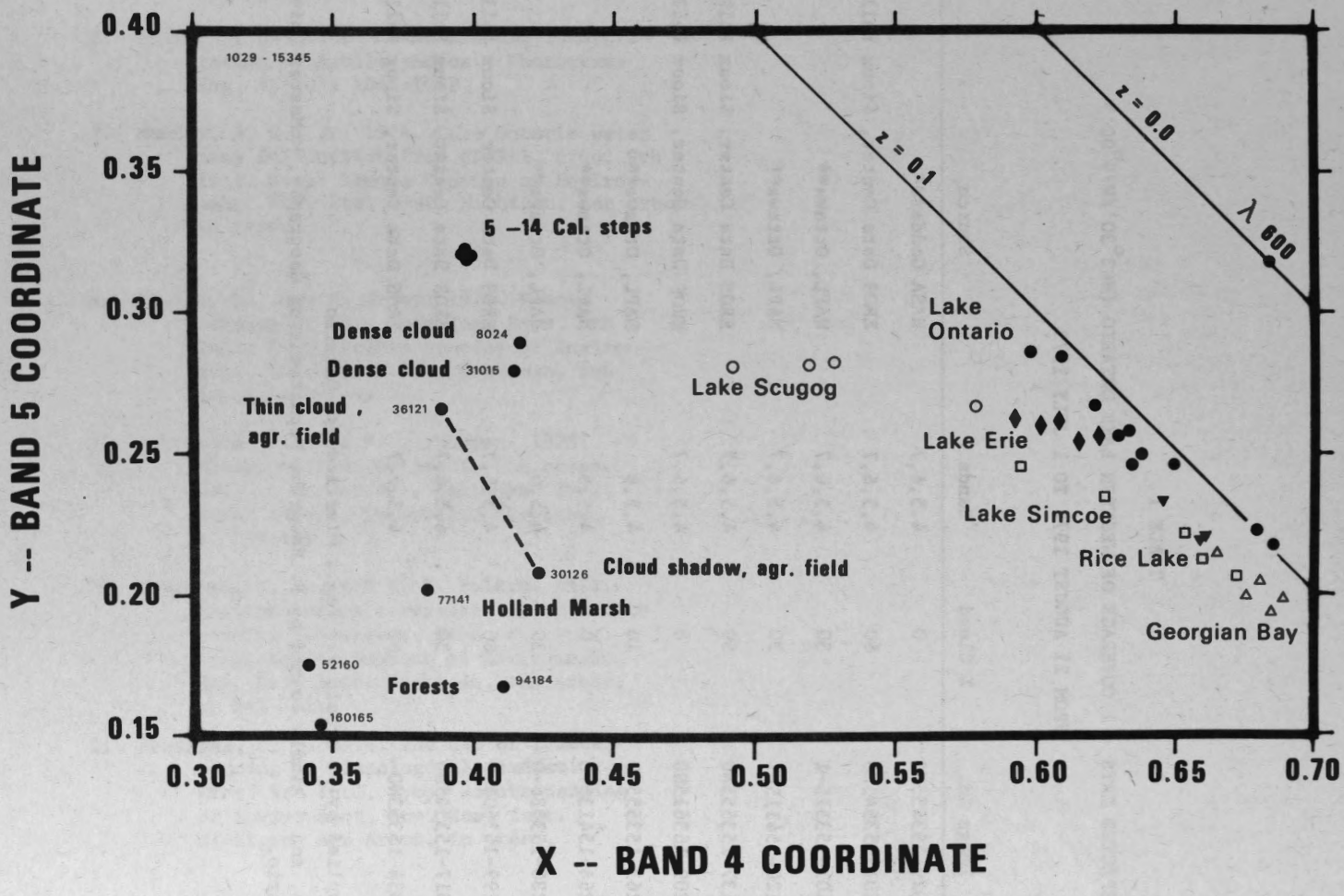

Figure 1. Chromaticity Diagram for Selected Points in southern Ontario. Image 1029-15345 (21 August 1972). Locus representing z = 0.1 placed on high-saturation side of typical (x,y) values. Image densities measured with Sargent-Welch Densichron.

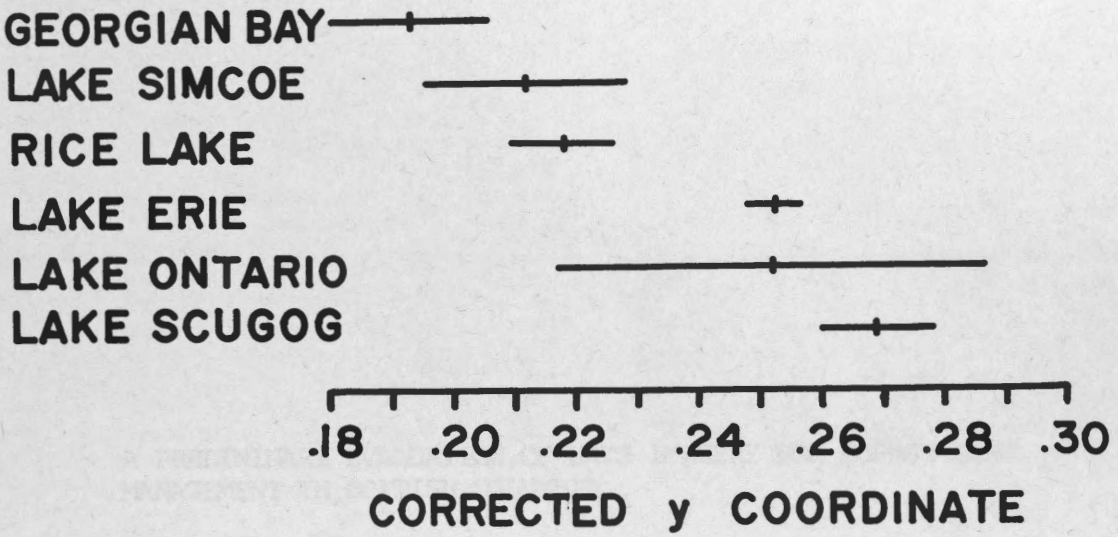

Figure 2. Y Chromaticity Values for Southern Ontario Water Bodies Cloud Corrected to High Saturation Locus. Image 1029-15345 (21 August 1972). Vertical separation for ease of interpretation. Y range and mean shown.

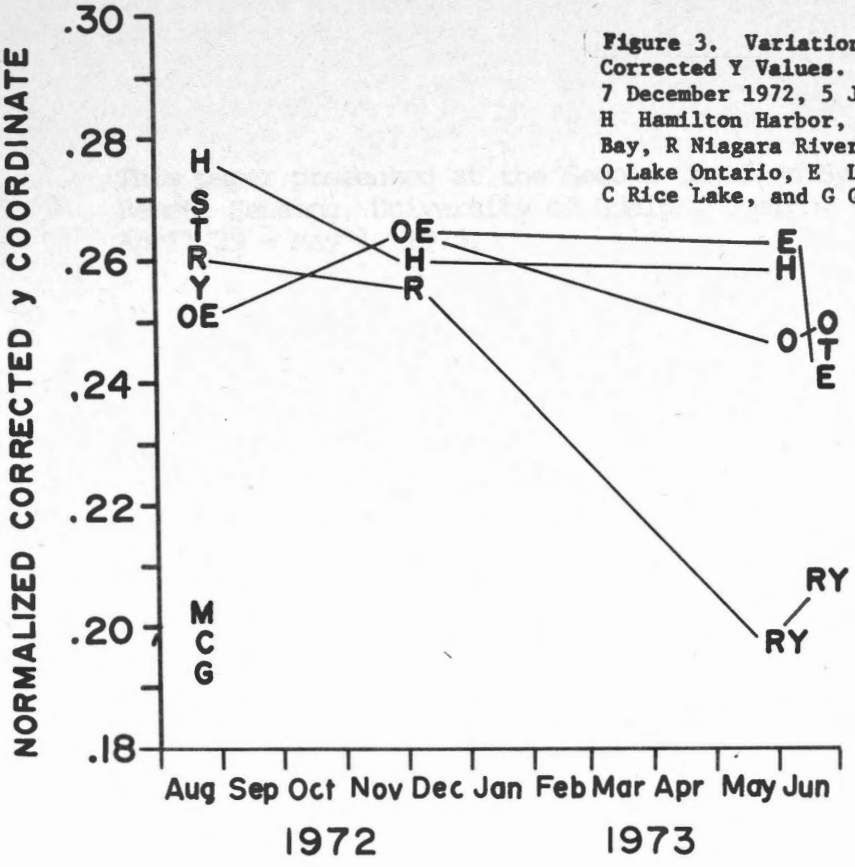

Figure 3. Variation with Time of Normalized Mean Corrected Y Values. Image dates 21 August 1972, 7 December 1972, 5 June 1973, and 23 June 1973. H Hamilton Harbor, S Lake Scugog, T Toronto Bay, R Niagara River, Y New York power reservoir, O Lake Ontario, E Lake Erie, M Lake Simcoe, C Rice Lake, and G Georgian Bay.

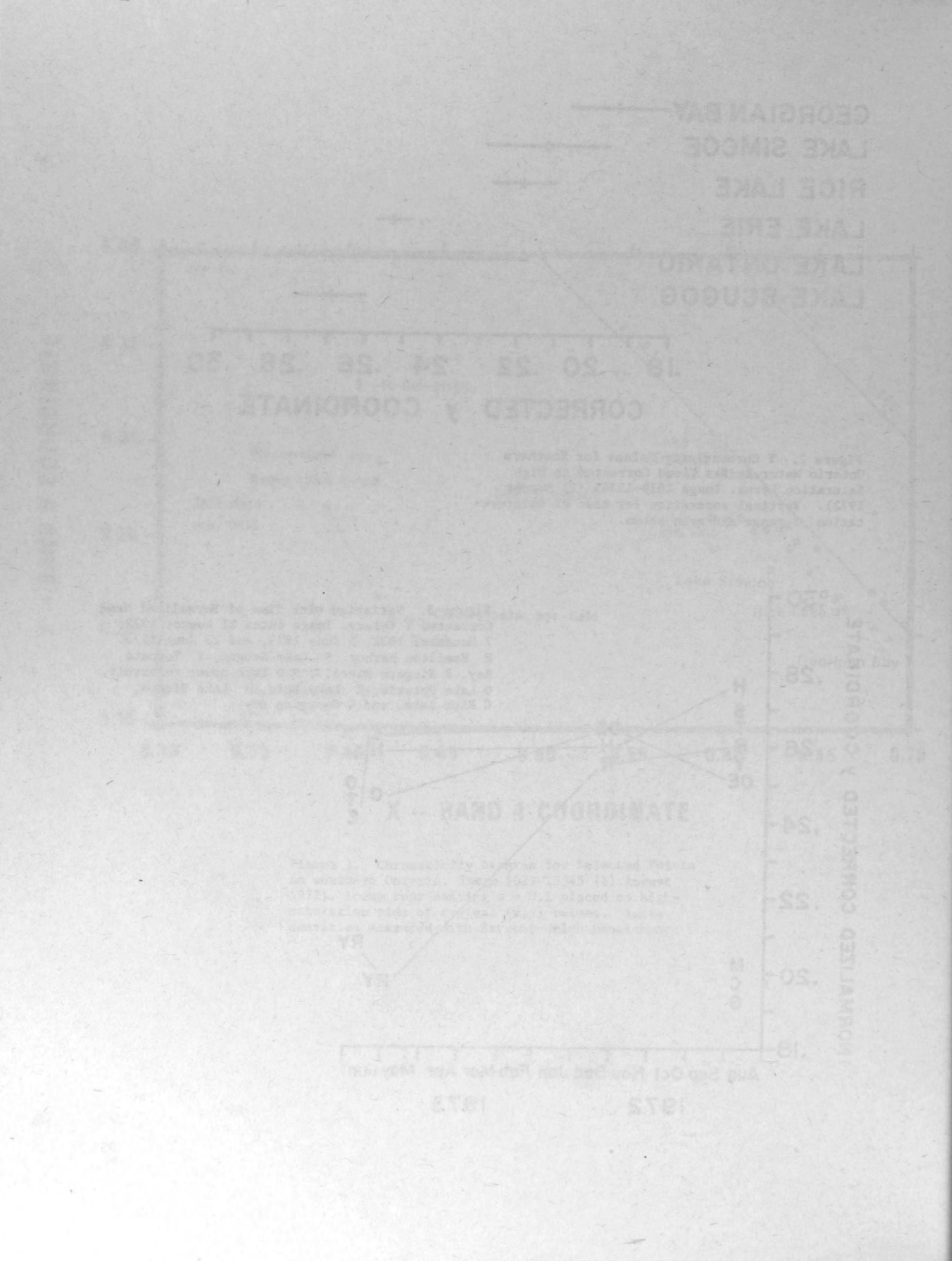

A PRELIMINARY EVALUATION OF ERTS IMAGERY FOR FOREST LAND MANAGEMENT IN BRITISH COLUMBIA

By

Y. JIM LEE
E.T. OSWALD
J.W.E. HARRIS

This paper presented at the Second Canadian Symposium on Remote Sensing, University of Guelph, Guelph, Ontario, April 29 - May 1, 1974.

A PRELIMINARY EVALUATION OF ERTS IMAGERY FOR FOREST LAND MANAGEMENT IN BRITISH COLUMBIA

Y. Jim Lee, E.T. Oswald and J.W.E. Harris,
Research Scientists,
Department of the Environment,
Canadian Forestry Service,
Pacific Forest Research Centre,
506 West Burnside Road,
Victoria, B.C., V8Z 1M5

ABSTRACT

Visual evaluation of ERTS data, comparing imagery from each MSS band and color composite with small-scale, high altitude photography and conventional scale, low-level photography, has suggested how satellite imagery may be useful for examining various features in the forest environment and for monitoring changes in it. ERTS imagery provides an overview of entire management units and surrounding areas that should be useful to the forest manager. Features studied, all distinguishable to some extent, included vegetation types, roads, railroads, power lines, logging, lakes and streams. Grassland was easily distinguished from forested areas, but difficulty was encountered in separating coniferous species. Recognized also were age patterns that aided conifer species identification through knowledge of successional trends and policy of cutting operations. Tree damage, caused by a variety of pests, was readily interpreted from very small-scale photographs and, in some instances, could be delineated on ERTS imagery. Enhancement of some features may be possible. Thus the value of satellite imagery, which provides a routinely available, easily examined permanent record, is favorably indicated. The encouraging results at this point suggest that subsequent satellites will be of still greater assistance to forest managers.

RÉSUMÉ

L'évaluation visuelle des données fournies par ERTS, en comparant les images et les couleurs de chaque bande MSS avec photographies à petite échelle et prises à haute altitude, et d'autres photos à échelle conventionnelle et prises à basse altitude, permet de voir comment les images provenant de satellites peuvent être utiles pour examiner les divers aspects de l'environnement Forestier et pour juger des changements qui s'y produisent. Les images de l'ERTS fournissent une vue d'ensemble d'unités entières d'aménagement et secteurs voisins, fait qui devrait être utile à l'aménagement forestier. Les détails étudiés, tous distincts jusqu'à un certain point incluaient les types de végétation, les chemins, les chemins de fer, les lignes de transmission de pouvoir électrique, les coupes de bois, les lacs et les cours d'eau. Les prairies se distinguaient facilement des forêts mais il était difficile d'identifier les espèces de Conifères, bien que les groupes d'âges fussent reconnaissables et aidassent à identifier les espèces à partir de la connaissance des successions d'associations et des politiques de coupes. Les dommages aux arbres, causés par divers ravageurs, étaient immédiatement interprétés via des photos à très petite échelle et, parfois, leurs limites pouvaient être dessinées sur les images ERTS. La plus grande netteté de quelques particularités peut être possible. Ainsi, la valeur des images obtenues par satellites, qui constituent des données disponibles routinièrement, permanentes et facilement examinables, est grande. Les résultats encourageants obtenus à ce jour laissent croire que les satellites subséquents aideront encore plus les aménagistes forestiers.

INTRODUCTION

Forest land management in British Columbia involves a large variety of extensive biogeoclimatic types, and the development of suitable management techniques is a continuing process. ERTS offers a new and unique periodic overview of forest lands and could facilitate the economical collection of much useful data. Several studies are presently underway in the province to evaluate the usefulness of ERTS for collecting information on such management activities as logging, and on natural phenomena such as forest type classification and tree damage. The results of these studies are described here.

MANAGEMENT ACTIVITIES

Evaluation of ERTS data by several interpretive techniques has suggested how ERTS imagery may be used for examining various features in forest management operations. The Greater Victoria Watershed and surrounding areas was selected as a test site because of the variety of activities taking place in it. The area included more than 13,760 hectares of forest, of which 76% was productive timber land, and contained several lakes and dams connected by water pipe lines. The forested area consisted of immature conifers (51%), mature conifers (41%) and hardwoods (8%). Clear-cut patch logging in blocks of up to 20 hectares, was practised within the mature stands. There was an extensive road system, 2 railway lines and a power line, the latter having a right-of-way at least 30 meters wide. Log booms were anchored in Sooke Basin and Victoria Inner Harbor.

Ground truth for comparison with ERTS imagery was based on high-level (scale 1:120,000) and low-level 70mm (scale range from 1:500 to 1:2,000) color photography, as well as forest cover maps and field visits. ERTS imagery from the 4 bands recorded by the multispectral scanner was obtained on July 30, 1972, September 4, 1972, and August 12, 1973.

The following results were obtained by three interpretation techniques, namely, visual comparison of black and white and color composite images produced by the Canada Centre for Remote Sensing and the National Air Photo Library, Ottawa, and diazo (Ryerson, 1973) and color additive viewer enhancement of black and white images.

Visual Evaluation

The choice of MSS band for interpretation purposes depended on the items being studied. Band 5 (Figure 1) was best for identifying most features, and Band 4 was next. Bands 6 and 7 were suitable only for identifying lakes; those as small as 1.2 hectares could be identified (a Figure 2). Vegetation on composite bands 4,5,6 could be broadly delineated into 4 classes: mature conifers (b Figure 1), immature conifers (c Figure 1), regeneration or logged areas (d Figure 1) and hardwoods (color composite). Water pipe lines were not noticeable (e Figure 1). Only the larger dams could be identified (f Figure 1). Logged areas could be clearly identified (i Figure 1), and the progress of logging was evidenced by comparing uncut areas (g Figure 1) with cut areas (h Figure 3) in 1972 and 1973 imagery, respectively. In the former, the recently cut areas (i Figure 1) were lighter in tone, owing to fresh slash and exposure of mineral soil, than those (j Figure 1) cut and burned earlier, which had burned slash and some vegetation. The patch-like nature of some logging was also evident (k Figure 1 and m Figure 3). Log booms could be observed (n Figures 1 and 3). The logging road network (q Figure 1) (12.2 metres wide) and highways (r Figure 1) could be seen clearly where they crossed forested areas but not where they passed through clear-cuts. Highways in urban areas became indiscernible (s Figure 1) owing to lack of contrast. Railway lines (t Figure 1) were similar to but less obvious than highways. Power lines (u Figure 1) were very easy to identify, as they ran in straight lines through wooded areas and had right-of-ways over 30 metres wide.

Diazo Enhancement

Twelve color transparencies were made using red, blue and green diazo films for the 4 bands of ERTS frame 1385-18365 obtained in 1973. From these transparencies, a rating table (Table 1) for composites of different colors from different bands (overlay technique) was prepared for the detection of different features. The 6 rating classes were: excellent (E=5), good (G=4), medium (M=3), fair (F=2), poor (P=1) and not visible (N=0). A perfect composite would score 12 x 5 = 60 points. Table 1 was arranged in order of increasing total points, with a range of 3 to 35 and an average of 17.6. In general, a composite good for detail of road identification was not good for identification of vegetation or lakes.

Detailed analyses for the detection of different features are summarized in Table 2.

Color Additive Viewer Enhancement

The color additive viewer (Spectral Data Corporation) produced similar results to the diazo process except that the light intensity illuminating each band and the scale of each image could be adjusted so that imagery taken from different orbits could be superimposed to enhance the observation of a dynamic event over time, such as logged areas in red color (Figure 7). Once the size of 1 or 2 logged areas is determined by actual measurement in the field, the size of the remaining logged areas can be estimated from the imagery. Similarly, forested areas can also be broadly delineated into hardwoods and conifers (mature, immature and regeneration). The size of these areas can also be estimated and mapped.

PLANT COMMUNITIES

The possibility of recognizing and delineating forest plant communities on ERTS-1 imagery was investigated over a transect, approximately 400 km long and 50 km wide, extending across the interior of British Columbia (51° -52.5° N Lat., 120° - 124° W Long.). The broad vegetation types of this area were delineated by Rowe (1972) and Krajina (1969). Both recognized five vegetation types, although their criteria and definitions differed; consequently, the boundaries were not the same.

Two sets of ERTS imagery (May 14, 1973 and August 12, 1973) were available for analysis. High altitude color (approximate scale 1:130,000) and 70mm low-level color and panchromatic (1:2,000, 1:4,000, 1:24,000 and 1:48,000) aerial photographs were obtained for parts of the transect to aid plant community recognition. Forest cover maps were available for age and height determinations. A limited amount of field cruising was performed before the ERTS imagery became available. The image interpretations were mainly simple enhancement techniques.

Non-forested land could be readily distinguished from forested land on ERTS imagery. Bands 4 and 5 were both suitable, although band 5 (Figure 4) had greater contrasts than band 4. Non-forested land appeared in white to light gray, in contrast to forested land in darker gray.

Within the non-forested land, certain features could be distinguished. Wet meadows produced a similar signature to grassland on bands 4 and 5 but could be recognized on bands 6 and 7 because their tones remained light on these bands, while grassland produced medium gray tones. Also, bodies of water prominent on bands 6 and 7 were often associated with the meadows. Perpetual snow fields could be distinguished by their topographic position, drainage pattern, seasonal fluctuations of boundaries and subtle tone differences on bands 6 and 7. Recently cutover forested land often had tones similar to grassland but the former could be discerned by its straight boundaries and sharp contrast with the forest background. Urban development proved to be the most difficult to separate from grassland but sometimes, at least for large developments, urban areas produced a somewhat mottled appearance on bands 4 and 5 due to vegetated areas, and had some degree of boundary regularity with discernible highways, railroads and power lines converging to and/or passing through. Cottage and rural dwellings could rarely be distinguished from forest clearings.

The forested areas produced certain distinguishable patterns, but these were generally less prominent than features in the non-forested regions. Generally, the boundaries of the Biogeoclimatic Zones of Krajina (1969) or Forest Regions of Rowe (1972) could not be precisely defined, although this was not surprising since the boundaries were most often diffuse, and stand histories and conditions had greater influence than species on image signatures. The Interior Western Hemlock and Interior Douglas Fir Biogeoclimatic Zones (Figure 5) constituted most of the dark portion noticeable in the upper right corner of the summer band 5 image (Figure 4). Mountainous topography, mostly along the bottom of the images in Figure 4, and other areas above 1200 m supported the Subalpine Engelmann Spruce - Subalpine Fir Biogeoclimatic Zone. The remainder of the area covered by the sample images consisted of the Cariboo Aspen - Lodgepole Pine - Douglas Fir Biogeoclimatic Zone, since Krajina does not recognize the grassland along the Fraser River as a separate entity.

Broad age class, and therefore usually height class, differences could be detected. The medium gray tones, especially discernible on the summer band 5 image, consisted of nearly pure stands of lodgepole pine less than 100 years old and less than 25 m tall. Within this area, younger stands were slightly lighter gray than older stands. The dark tones in the vicinity of the Fraser - Chilcotin Rivers junction (Figure 5) were stands 150 or more years old and mostly over 30 m in height consisting of various mixtures of lodgepole pine and Douglas-fir. Old growth Engelmann spruce - subalpine fir stands produced similar dark tones but the dendritic drainage pattern and snow coverage revealed mountainous topography which provided the habitat for these species. Old growth stands in the Interior Douglas-Fir and Western Hemlock Zones also produced dark tones, but consisted of various mixtures of lodgepole pine, Douglas-fir, western hemlock, western red cedar, Engelmann spruce and subalpine fir. Age differences could, however, be recognized in these two zones as well, as revealed in Figure 6, which is an enlargement of the upper right hand portion of Figures 4 and 5. Several stand ages, produced by forest fires or forest harvesting, could be recognized by differences in gray tones. Younger stands arising from restocked cutovers and natural reforestation following fires consisted of lodgepole pine, while old stands (dark tones) were mixtures of coniferous species; however, a few dark toned stands consisted of nearly pure old-growth lodgepole pine.

Poor quality sites often produced light tones, even though the trees were over 150 years old, if the stands consisted of sparse and short trees. Conversely, high quality sites produced darker tones at an earlier stand age than medium or low quality sites. These features produced some of the tone differences in Figure 6, but they could not be separated from normal growth stands by ERTS imagery alone.

Hardwoods, e.g. aspen, could not be recognized, even by comparing spring and summer imagery, possibly because of the lack of stands of adequate size or purity--aspen usually occurred in small groves intermingled with conifers. Also, differences in processing quality of the images made comparisons difficult. Future images and image enhancement techniques may reveal more clearly some aspen stands, as well as other features.

PEST DAMAGE

One event of considerable concern to the forest manager is tree damage caused by pests. This damage, visible as discoloration resulting from defoliation or mortality, is normally assessed by ground and aerial surveys which form the basis for possible salvage and control efforts.

When the areas involved are more extensive than can be sampled efficiently from the ground, an overview is often sought from the air. This usually has taken the form of sketch-mapping from small aircraft, but when more precise details are needed, various remote sensing techniques, producing accurate, permanent records suitable for intensive study, have been used effectively.

Color aerial photography, used occasionally in forest pest surveys at scales up to about 1:60,000, has two major disadvantages which discourage its use in surveys that do not require the detail such scales provide: 1) a large number of photographs, and therefore a large interpretation effort, is required to cover infestations which often are spread over extensive areas; 2) a specific survey is required in each instance, with the entire costs chargeable to that single use, and such surveys are more expensive than sketch-mapping.

Smaller scale photographic capabilities, which could overcome some of the difficulties just described, are now becoming available to forest managers, and it is important to determine whether or not significant tree damage information can be obtained from such imagery. Harris (1972) reported high-level, small-scale color photography could play a useful part in pest surveys, and there was further opportunity to test small-scale photography (about 1:100,000) and also ERTS imagery (1:1,000,000) in 1972 and 1973.

Color photographs at scales ranging from 1:500 to 1:140,000 were taken of a variety of pest infestations in British Columbia, including western spruce budworm, *Choristoneura occidentalis*; western blackheaded budworm, *Acleris gloverana*; western hemlock looper, *Lambdina fiscellaria lugubrosa*; western false hemlock looper, *Nepytia freemani*; Douglas fir tussock moth, *Orgyia pseudotsugata*; larch casebearer, *Coleophora laricella*; forest tent caterpillar, *Malacosoma disstria*; and mountain pine beetle, *Dendroctonus ponderosae*. Damage caused by adverse winter conditions and sulfur fumes were also examined.

The ability to discern tree damage from the photographs depended on the intensity of tree discoloration, the size of the discolored area, and the contrast of the area with the surrounding forest. The intensity of discoloration depended upon the degree of damage to individual trees, and the proportion of damaged trees present.

Pest damage visible from the air during observation flights was discernible on most of the above color photography. Generally, difficulties were encountered only with the smallest scales, where patches of damage (usually consisting of only a few trees), and those with light defoliation or poor contrast, were difficult or impossible to see.

On ERTS imagery, however, pest damage was visible only where it appeared most distinctly. The best example was the extensive damage caused by the western spruce budworm in the Pemberton area of British Columbia, where fairly distinct reddening of the foliage occurred over large areas (Figure 8). ERTS imagery at peak defoliation during 1972 and 1973 showed some damaged areas clearly on band 5, and even more clearly on the standard color composites available from the National Air Photo Library, Ottawa, which were of bands 4,5,6; 4,5,7 and 5,6,7 (Figures 9 and 10). Similar results were obtained using a color additive viewer. Damaged areas can be enhanced by combining bands 5 and 6 with green and red filters, respectively, and also with those plus band 4 with a blue filter.

Most other identified current pest damage was not discernible on the ERTS imagery because the patches were too small or did not contrast clearly with surrounding stands. Table 3

gives some examples.

The results show that small-scale high-altitude photography could supplement conventional aerial pest observations by providing a convenient, permanent record of conditions over large areas. Larger scale photographs provided more individual tree data but the handling effort could be formidable. Small-scale photography could play an active part in locating damaged areas and serve as a basis for sampling with more intensive surveys. ERTS imagery provided information concerning extensive damage which could be of assistance in guiding additional surveys.

LITERATURE CITED

Harris, John W. E. 1972. High-level photography for forest insect damage surveillance in British Columbia. Proc. First Canadian Symposium on Remote Sensing, Ottawa, February 1972, Vol. 1: 145-148.

Krajina, V. J. 1969. Ecology of forest trees in British Columbia. Ecology of Western North America 2: 1-147. Botany Dept., Univ. British Columbia, Vancouver, B. C.

Rowe, J. S. 1972. Forest Regions of Canada. Dept. of Environ. C.F.S. Publ. No. 1300. 172 pp.

Ryerson, R. A. 1973. Diazo composites; an inexpensive tool for ERTS imagery analysis. CCRS, Ottawa. Techn. Note 73-5.

TABLE 1. Rating [1] table for the detection of different features on ERTS imagery using diazo color enhancement.

No.	Bands and Colors red (R), blue (B) green (G)	Lakes	Hard-woods	Conifers 3 classes	Water pipe lines	Dams	Logged Areas	Logged & burned areas	Log Booms	Logging Roads	High-Ways	Rail-ways	Power Lines	Total Points
1	6G7B	1	1	1	0	0	0	0	0	0	0	0	0	3
2	6R7B	3	1	1	0	0	0	0	0	0	0	0	0	5
3	6B7R	4	2	0	0	0	0	0	0	0	0	0	0	6
4	6G7R	5	1	1	0	0	0	0	0	0	0	0	0	7
5	6R7G	5	1	1	0	0	0	0	0	0	0	0	0	7
6	4B5R	1	0	0	0	1	0	1	1	0	2	0	2	8
7	4G5R	1	0	0	0	1	1	1	1	1	1	0	2	9
8	4G5B	1	0	0	0	1	4	2	0	0	1	0	1	10
9	4R5G6B	2	1	1	1	1	1	1	0	0	1	0	1	10
10	4R5B	1	0	0	0	1	4	1	1	0	1	0	1	10
11	5B6G	2	5	2	0	0	1	0	1	0	0	0	0	11
12	4B6R	4	5	2	0	0	0	0	0	0	0	0	0	11
13	4B7G	5	5	1	0	0	0	0	0	0	0	0	0	11
14	6B7R	5	5	2	0	0	0	0	0	0	0	0	0	12
15	5B6G7R	3	4	2	0	0	1	1	1	0	0	0	0	12
16	4R6B	1	5	3	0	0	2	1	0	0	0	0	0	12
17	4R6G	4	5	1	0	0	1	1	0	0	0	0	0	12
18	5B6R	2	5	2	0	1	1	1	1	0	0	0	0	13
19	4R5G7B	4	0	1	1	1	1	1	0	0	1	0	4	14
20	4B6G	5	5	5	0	0	0	0	0	0	0	0	0	15
21	5G6B	1	1	1	0	1	4	3	1	0	1	0	3	16
22	4G6R	4	5	1	0	1	1	1	0	0	0	0	0	16
23	4G5B6R	2	5	0	0	2	4	2	1	0	0	0	0	16
24	5B7G	5	4	3	0	0	2	1	1	0	0	0	1	17
25	5B6R7G	5	5	5	0	0	1	0	1	0	0	0	0	17
26	4G7B	4	5	1	0	0	4	3	0	0	0	0	0	17
27	4G6B	2	5	2	0	0	5	2	0	0	0	0	1	17
28	5B7R	5	5	3	0	0	2	1	1	0	0	0	1	18
29	4R5B6G	2	5	2	0	0	3	4	1	0	0	0	1	18
30	5R6B	2	5	3	0	0	4	4	1	0	0	0	0	19
31	4G5R6B	2	5	1	0	2	4	1	1	0	1	0	2	19
32	4B5R6G	4	5	2	0	1	1	3	1	0	1	0	1	19
33	4B5G	1	0	0	0	3	1	0	2	0	4	4	4	19
34	5G7B	2	4	2	0	1	4	3	1	0	1	1	1	20
35	4B7R	5	5	5	0	0	3	2	0	0	0	0	0	20
36	4B5G6R	1	4	1	0	3	2	2	3	0	2	0	2	20
37	4R7G	5	5	1	0	0	5	5	0	0	0	0	0	21
38	5R6G	2	5	3	0	3	4	2	1	0	1	0	1	22
39	4R7B	5	5	4	0	0	4	4	0	0	0	0	0	22
40	5G6R7B	5	4	2	0	1	4	4	1	0	1	0	1	23
41	5G6B7R	4	5	5	0	1	4	3	0	0	0	0	1	23
42	4G5B7R	3	5	3	0	1	5	5	0	0	0	0	1	23
43	5R7B	5	5	2	1	1	4	3	1	0	1	0	1	24
44	5R6G7B	4	5	4	0	3	3	2	1	0	1	0	1	24
45	5G6R	3	5	3	1	3	2	2	1	1	2	0	2	25
46	4G7R	5	5	5	0	0	5	5	0	0	0	0	0	25
47	4R5B7G	5	5	5	0	0	4	5	2	0	0	0	0	26
48	5G7R	5	5	4	1	1	2	5	2	0	1	0	1	27
49	5R6B7G	5	5	5	0	1	5	5	1	0	0	0	0	27
50	5R7G	5	5	4	0	1	5	3	1	0	2	0	2	28
51	4G5R7B	3	5	4	0	2	4	3	1	1	2	1	3	29
52	4R5G	2	0	0	2	4	3	3	4	1	4	1	5	29
53	4B5R7G	5	5	5	2	2	3	4	3	0	1	0	1	31
54	4B5G7R	3	5	5	3	3	3	5	4	0	2	1	1	35

[1] Each composite was rated initially according to 6 classes: excellent (E=5), good (G=4), medium (M=3), fair (F=2), poor (P=1) and not visible (N=0). A perfect composite would score 12 x 5 = 60 points.

Table 2. Analyses for the detection of different features using diazo color enhancement

No.	Features	Essential bands and color to provide the best rating	Number of composites out of 54 that provide the best view
1	Lakes	6R, 7R, 7G, or 7B with 4R or 5R	19 excellent
2	Hardwoods	5R with 4 and 6 or 4 and 7 or 6B with 7R	35 excellent
3	Conifers	5R, 5G or 5B in composite of 3 bands	9 excellent
4	Water Pipe Lines	4B5G7R	1 medium
5	Dams	4R5G	1 good
6	Logged areas	4G6B, 4R7G, 4G5B7R, 4G7R, 5R6B7G or 5R7G	6 excellent
7	Logged and burned areas	4R7G, 4G5B7R, 4G7R, 4R5B7G, 5G7R, 5R6B7G or 4B5G7R	7 excellent
8	Log booms	4R5G or 4B5G7R	2 good
9	Logging roads	4G5R, 5G6R, 4G5R7B or 4R5G	4 poor
10	Highways	4B5G or 4R5G	2 good
11	Railways	4B5G	1 good
12	Power lines	4R5G	1 excellent

Table 3. Status of pest damage on ERTS imagery, British Columbia, 1972-73

Location	Date	Image no.	Band combinations examined[1]	Pest[2]	Visibility	Size of infested area (hectares)	Contrast[3]
Pemberton	4/9/72	1043 18364	456;567	wsb	Yes	60-800	VG. Large areas with similar types.
				wsb	No	60-800	P. Light defol.
				mpb	No	up to 8	P
	12/8/73	1385 18362	457;567	wsb	Yes	200-2000	VG. Large areas with similar types.
				wsb	No	60-800	P
				mpb	No	up to 8	P
Hope-Princeton Highway	16/9/73	1420 18303	457;567	wsb	Yes	40-200	F
Fraser Canyon	29/7/72	1006 18304	567	wsb	Yes (poor)	60-250	F
				wsb	No	60-800	P
				mpb	No	up to 8	P
	16/9/73	1420 18300	457;567	wsb	Yes	60-250	G
				wsb	No	60-800	P
				mpb	No	up to 8	P
Okanagan Lake	10/8/73	1383 18250	567	mpb	Yes (barely)	16	G
				mpb	No	up to 360	P
				fhl	No	10-280	P. Mixed agriculture
				Dftm	No	0.5-20	P
Adams Lake	10/8/73	1383 18243	457;567	mpb	Yes (barely)	16	G
				mpb	No	up to 20	P
				fhl	?	16	P. Rocky, open stand; mixed agric. sites
				whl	?	200-600	G
N. Vancouver Island	2/8/72	1010 18534	457	fd & wbb	Yes	400	G
				wbb	No	extensive	P. Most of susceptible type affected

[1] MSS bands combined. [2] wbb, western blackheaded budworm; wsb, western spruce budworm; mpb, mountain pine beetle; fhl, false hemlock looper; Dftm, Douglas fir tussock moth; whl, western hemlock looper; fd, fume damage. [3] N-none, P-poor, F-fair, G-good, VG-very good.

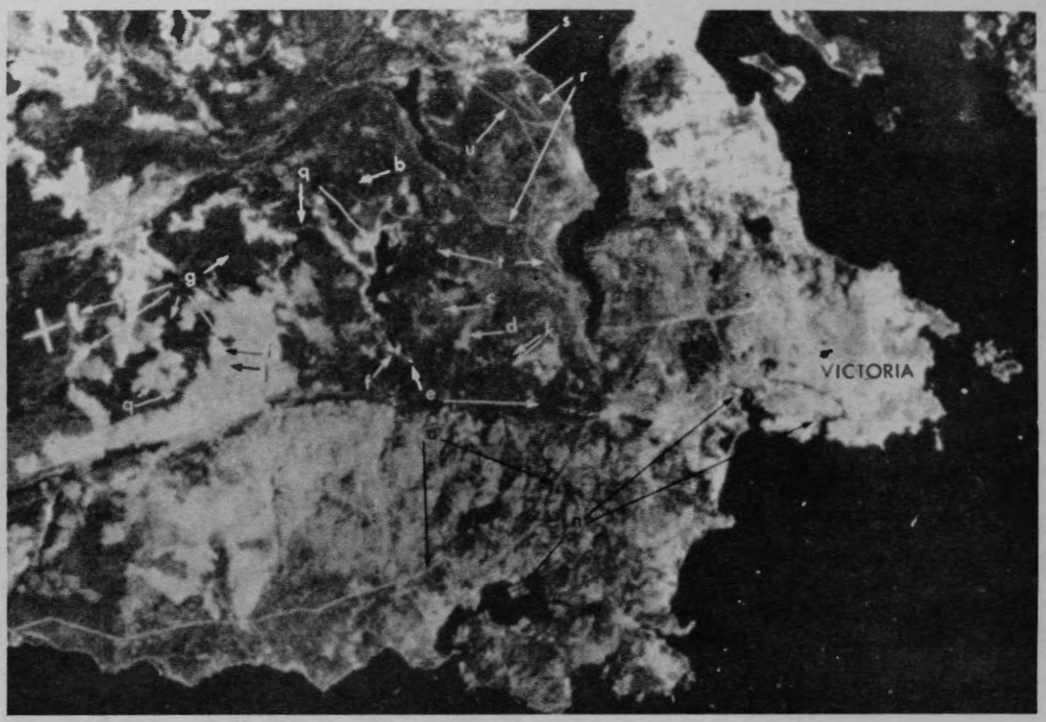

Figure 1. An enlargement of ERTS-1 imagery from frame 1043-18370 MSS-5 (September 4, 1972), showing Greater Victoria Watershed Forest.

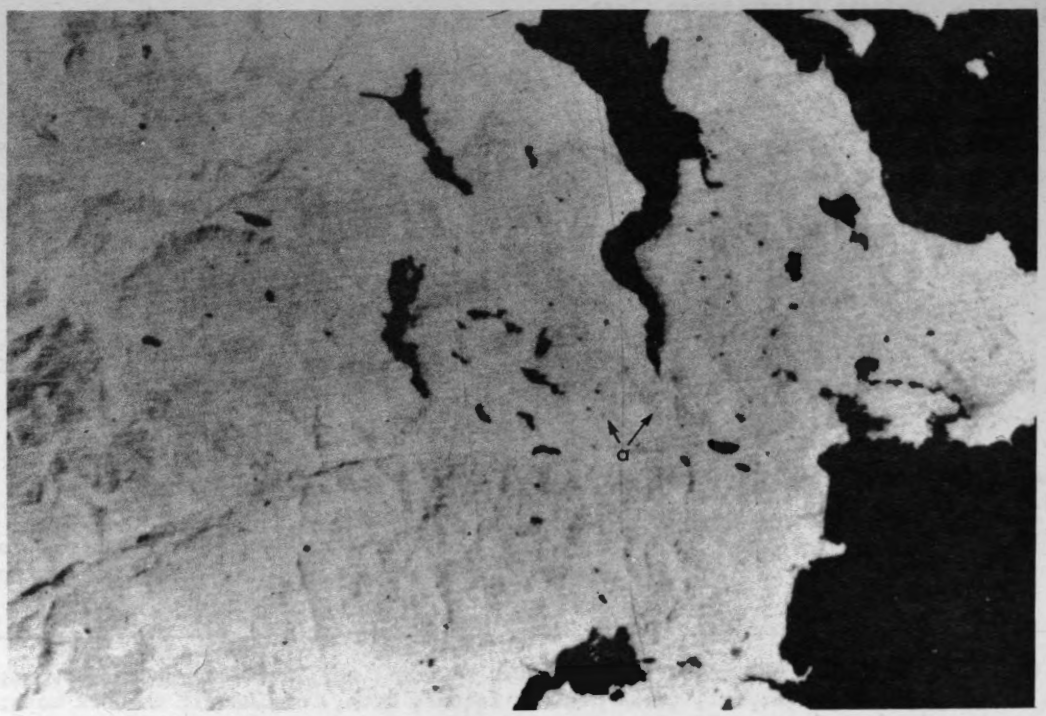

Figure 2. An enlargement of ERTS-1 imagery from frame 1043-18370 MSS-7 (September 4, 1972), showing Greater Victoria Watershed Forest.

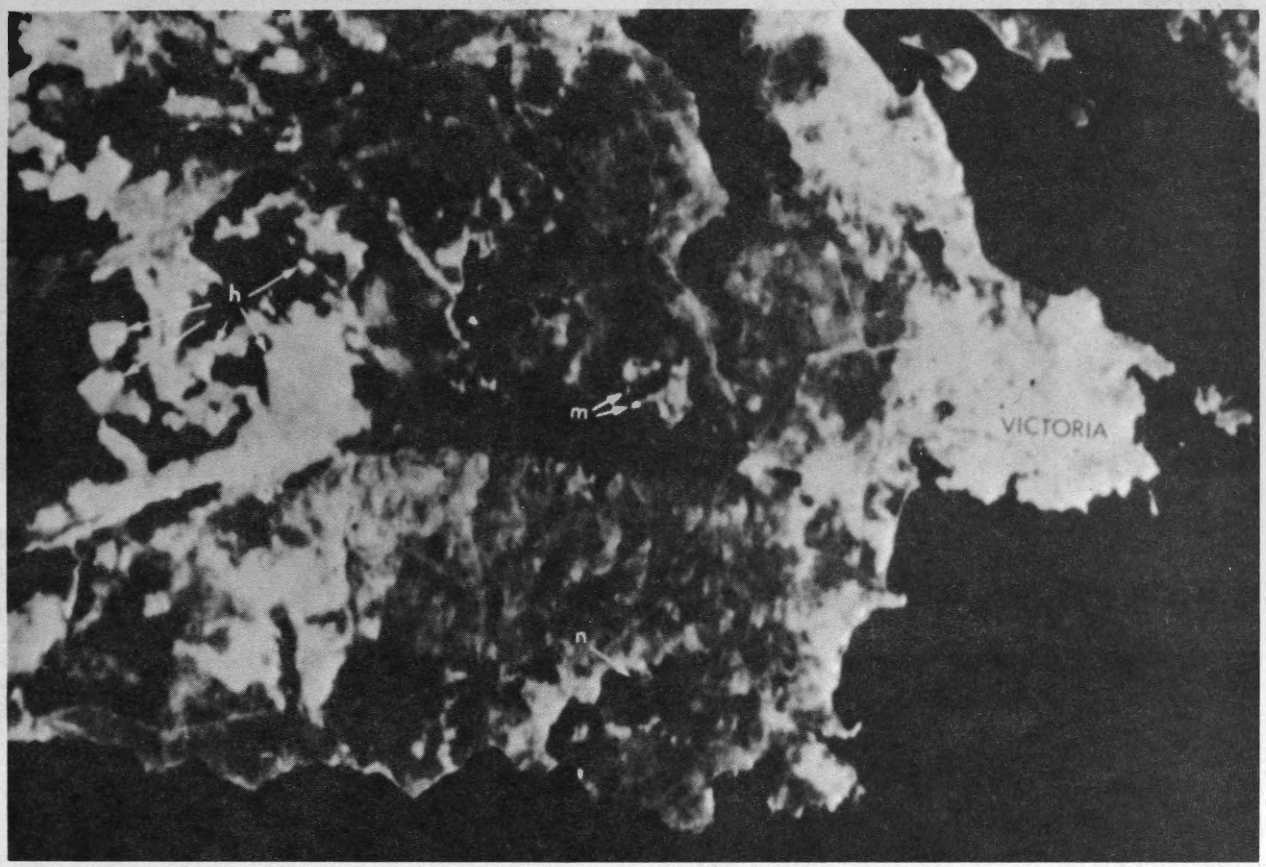

Figure 3. An enlargement of ERTS-1 imagery from frame 1385-18365 MSS-5 (August 12, 1973), showing Greater Victoria Watershed Forest.

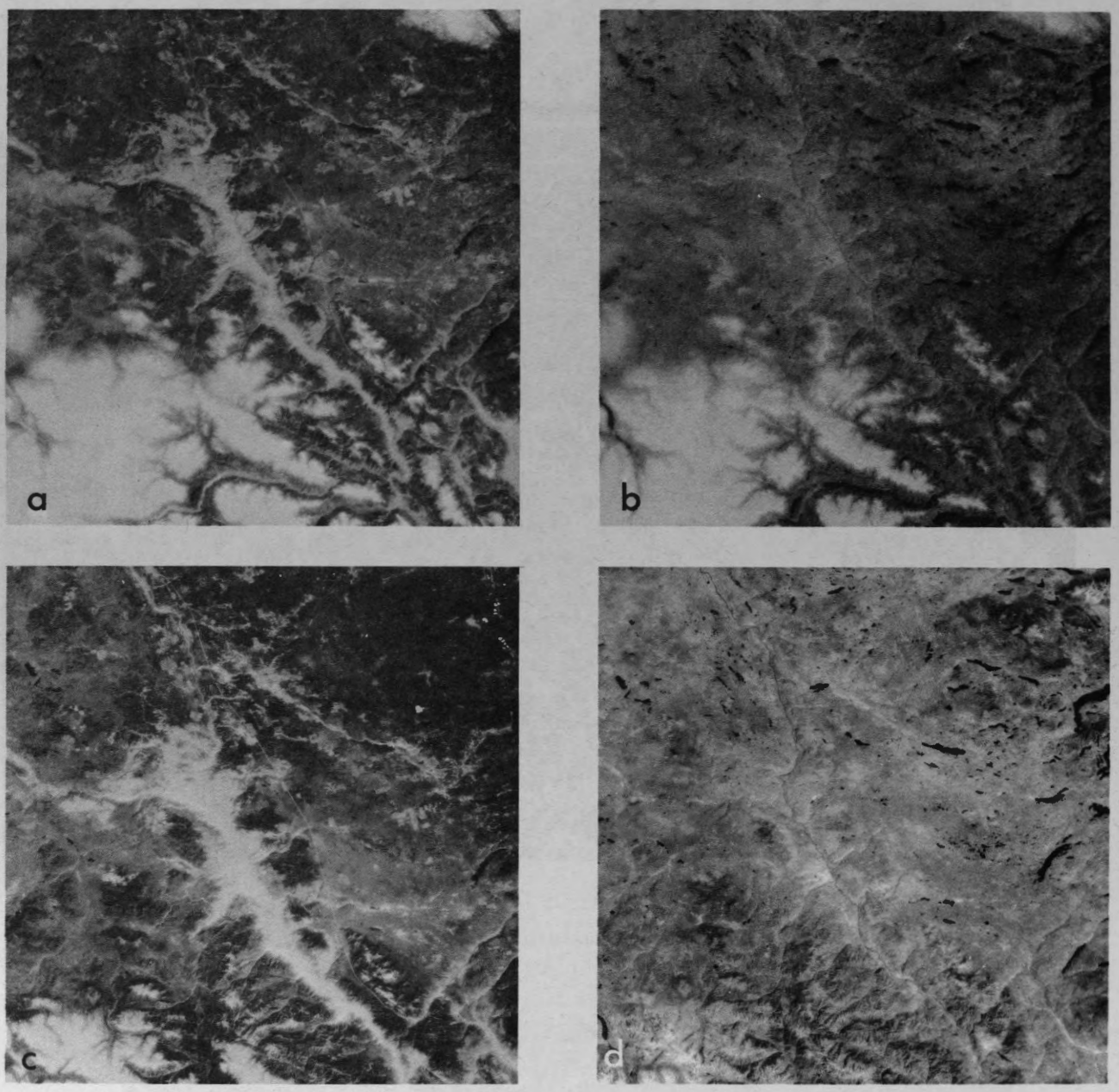

Figure 4. ERTS imagery of a portion of the vegetation interpretation evaluation transect across the interior of British Columbia; a and b are bands 5 and 6, respectively, of frame 1295-18371 (May 14, 1973), c and d are bands 5 and 6, respectively, of frame 1385-18360 (August 12, 1973).

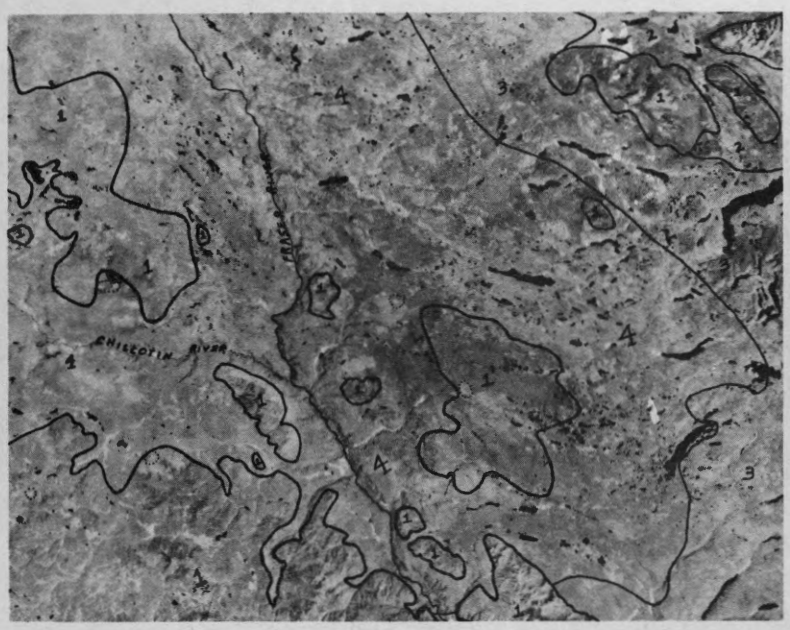

Figure 5. ERTS frame 1385-18360 MSS-7 indicating Biogeoclimatic Zones of Krajina (1969) and forest harvesting operations conducted during summer of 1973. 1--Subalpine Engelmann Spruce-Subalpine Fir Zones, 2--Interior Western Hemlock Zone, 3--Interior Douglas Fir Zone, and 4--Cariboo Aspen-Lodgepole Pine-Douglas Fir Zone. Areas of recent harvesting operations are indicated by dotted lines. These features may be compared on Figure 4.

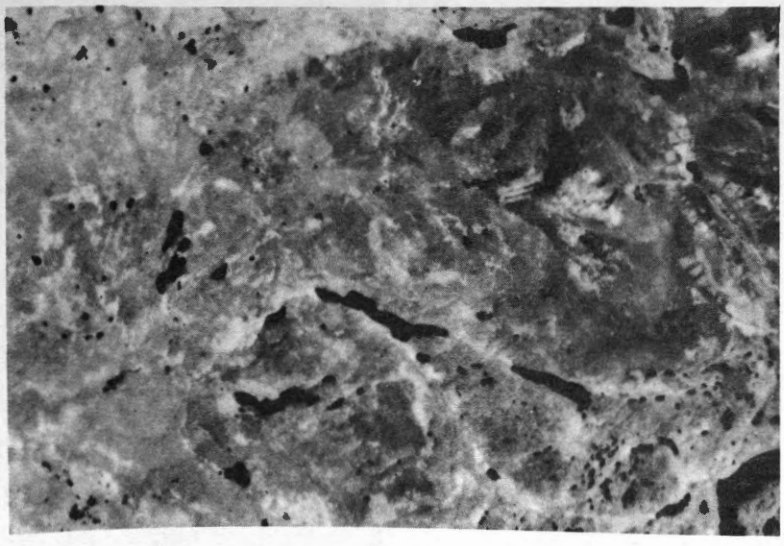

Figure 6. Enlarged upper right hand corner of ERTS 1385-18360 MSS-7. Lighter gray patches are young stands, comprised mostly of lodgepole pine, while darker gray ones, comprised of mixed coniferous species, are older.

Figure 7. Color additive viewer enhancement of logged areas (in red color, see arrows), using ERTS frame 1043-18370 MSS-5 (Sept. 4, 1972) with red filter superimposed on frame 1385-18365 MSS-5 (Aug. 12, 1973) with green filter.

Figure 8. Low altitude photograph of representative defoliated area taken from Beaver aircraft using Kodak C.P.S. 70 mm film.

Figure 9. ERTS image 1385-18362, bands MSS 5,6,7 (August 12, 1973), of Lillooet River Valley, B.C., showing western spruce budworm defoliation. Location shown in Figure 8 indicated by arrow.

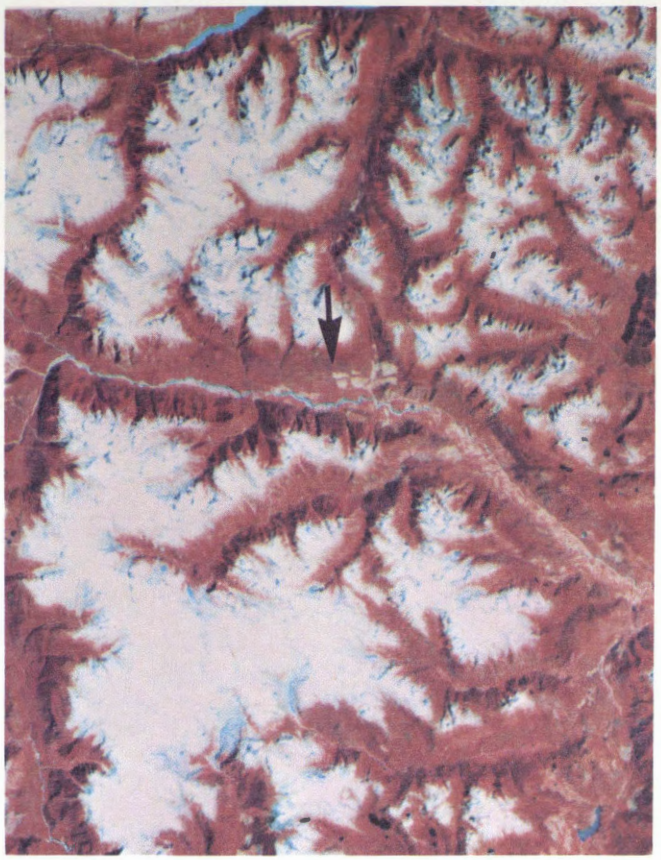

Figure 10. ERTS image 1385-18362, same as Figure 9 except color composite is of bands 4,5,7.

CANADIAN INITIATIVES IN SENSOR DEVELOPMENT

By

PHILIP A. LAPP

This paper presented at the Second Canadian Symposium on Remote Sensing, University of Guelph, Guelph, Ontario, April 29 - May 1, 1974.

CANADIAN INITIATIVES IN SENSOR DEVELOPMENT

Philip A. Lapp
CCRS Working Group on Sensors

ABSTRACT

Some new and sophisticated remote sensing devices are beginning to emerge from development programs in the Canadian government, industry and the universities. Supported by the Canada Centre for Remote Sensing of the Department of Energy, Mines and Resources, and in some instances by the Department of the Environment, the programs range from exploratory development to operational systems. They include instruments designed to operate at fixed positions on the ground as well as complete systems for mounting on aircraft and space platforms.

Specific Canadian sensing systems will be described including laser fluorometer devices for detecting oil slicks and effluents on water, ice thickness radar systems and special electro-optical remote sensors for detecting vegetation stresses, chlorophyll and ocean colour from aircraft and satellites. Probable future developments in remote sensing also will be explored.

1. INTRODUCTION

Canadian scientists and engineers have every reason to take pride in their contributions to the development of remote sensing systems now in use. Up until recently, most have been directed at military applications, but since 1970 the Canada Centre for Remote Sensing has sponsored a program to cultivate existing centres of excellence and develop new sensors to meet the needs of a rapidly expanding non-military remote sensing activity.

The modern era began during the second world war which spurred new developments in photogrammetry and related research and development conducted by the National Research Council. Immediately following the war, geophysical activities picked up in Canada and the late 1940's and early 1950's saw the development of a number of successful sensor systems. PSC Applied Research was one of the more active companies in the country at that time with an airborne magnetometer, the airborne profile recorder, automatic dodging equipment for image enhancement and several new devices in the airborne navigation field such as the Ground Speed Interception Computer and the Rho-Theta Computer for the Canadian military.

The military continued to provide the impetus for sensor development. The Dopplar radar and associated navigation system is an example. Pioneered by the then Defense Research Telecommunications Establishment (now the Communications Research Centre) and developed by Canadian Marconi, it is in active military and civilian service in several countries. The late 1950's was a period when Canada got into more sophisticated weapons development - motivated by the CF-105 Arrow program, cancelled in 1959. During that period, advances in photoconductive infrared detectors of high detectivity led to developments in still-classified military surveillance, guidance, fuzing and countermeasures systems in Canada. More important, however, was that they laid the groundwork for Canada's entry into the space era of the 1960's and 1970's. Companies like RCA Limited and Spar Aerospace Products Limited (then the SPAR Division of the de Havilland Aircraft of Canada Limited) cut their teeth on these early military sensor programs and formed technical teams that made the major Canadian industrial

contributions to the Alouette and ISIS satellite series, Anik and now CTS.

Following the recommendations contained in Science Council of Canada Report No. 1, A Space Program for Canada, in July 1967, wherein there was recognized a need to create an agency for coordinating and funding of a Canadian research program on resource satellites, an interdepartmental committee on Resource Satellites and Remote Airborne Sensing was formed in the fall of 1969. It recommended, among many other things, the creation of the Canada Centre for Remote Sensing (CCRS), that Canada participate in the ERTS program, establish an airborne sensing program and initiate a sensor R and D program. These recommendations were approved by cabinet, and a Sensor Working Group was established early in 1970.

The first action of the Group was to develop a "Request for Proposal" which would lead to initial study and development contracts on remote sensing devices and techniques. It was sent to 64 potential bidders, 53 of whom submitted proposals. Eleven contracts were placed in the year 1970-71. To date, the Working Group has supported a total of 17 programs with an annual budget of approximately $200,000 for the first three years, dropping to $100,000 for last year and the present. Initially, industry and university shared about equal portions of the budget, but more recently, the industrial component has dropped to approximately 30%. By March, 1974, the total expenditure from inception had been just under three quarters of a million dollars.

CCRS is not the only organization funding sensor programs in Canada. The Department of the Environment, Department of Communications and the Department of National Defense all have on-going programs of their own, as does industry - for example, Barringer Research.

The CCRS - funded programs have had to meet certain criteria. They must be:

1. Innovative and technologically sound,
2. Relevant to Canadian needs,
3. Undertaken by organizations capable of carrying the sensor to the field prototype stage,
4. Capable of achieving a market that would be attractive to industry, and
5. Capable of being developed within the financial resources of CCRS.

A number of programs funded initially did not survive these tests in subsequent years and therefore were dropped. The initial ones were selected on the basis of excellence, innovation and relevance.

The sensors to be described have not all been supported by CCRS, others have been included that are relevant to civilian remote sensing needs. The list is far from complete, and omits most geophysical instruments and meteorological sensors. For others that are relevant, and that have been omitted, the writer apologizes as either being unaware of their existence or equipped with insufficient details. The descriptions are directed at the user, and thus do not cover technical details of interest to the instrument developer.

The sensors fall under three main headings: Spectrometers and Multispectral Imaging Systems which are general sensors not necessarily directed at any specific application, Remote Probing with Lasers covering systems usually associated with air and water quality measurements and Special Purpose Sensors developed with very specific applications in mind. Finally, there is some speculation on future developments - the stimuli in Canada for new sensors, the opportunities to exploit them and an appeal to treat the sensor as a component of a remote sensing system, bearing in mind the requirements for data storage and processing, and the ultimate needs of the interpreter.

2. SPECTROMETERS AND MULTISPECTRAL IMAGING SYSTEMS

Detectivity, speed of response, spectral and spatial resolution are the four most important parameters in any general purpose instrument used to measure reflected and scattered radiation in the optical region of the electromagnetic spectrum. The four are not usually mutually exclusive in any particular instrument, but technology now is moving rapidly toward new instruments capable of maximizing all of them simultaneously, limited only by the information rate capacity or bandwidth of the associated electronics, detector noise limitations and the blur circles of the receiving optics. While certain aspects of the Canadian program are progressing in this direction, specific sensors have been developed which maximize or enhance one or two of the four parameters, in some cases at the expense of the others. Six such systems have emerged in Canada over the past few years.

2.1 Scanning Interference Filter Photometer

Developed by Shepherd, Miller and Koehler at York University, and supported by CCRS, the photometer is a rugged, compact instrument capable of studying four different spectral intervals simultaneously, each up to about 600 A in extent at a resolution of 15A. The photometer makes use of the passband shift of an interference filter with changes in incidence angle in 15 discrete steps created by stepping a mask between the filter and a photomultiplier detector. The patterns on the mask permit light to enter the detector successively from fifteen different angles of incidence resulting in a stepped spectral scan. The region of the spectrum is determined by the passband of the interference filter, and obviously must be within the spectral response band of the detector. The instrument has a 15° field-of-view, and a spectral scan requires 3 seconds.

The photometer also can operate in the multiplex mode. That is, it has the ability to observe <u>all</u> the relevant spectral elements <u>simultaneously</u> rather than one-at-a-time. The spectral mask is replaced by a multiplex mask and a Hadamard transform is applied to the 15-step output to retrieve the spectrum. Observing all spectral elements together improves the signal-to-noise ratio for detector-noise-limited cases.

The instrument has been flown in the CCRS DC-3 aircraft, and measurements were made over several lakes in southern Ontario. Figure 1 is a view showing the four-channel sensor on the right with a Lambert diffusing screen as a backdrop. The screen is used to measure incident solar radiation on the scene to be observed in order to determine the albedo. On the left are the power supply, control electronics and FM instrumentation tape recorder used in the aircraft installation.

Applications include the field of botany where the presence of chlorophyl can be detected because it is a good reflector in the near infrared, water quality measurements where the presence of algae and phytoplankton can be determined by changes in water colour, ocean depth measurements and water temperature mapping and where more detailed spectral information is required than that afforded by aerial cameras and line scanners. The relatively low spatial resolution of the instrument is advantageous in situations where total "biomass" measurements are wanted.

2.2 Multichannel Silicon Diode Spectrometer

This instrument, developed by Prof. G. A. H. Walker, University of British Columbia and supported by the DOE, Marine Sciences Directorate, Pacific Region, was developed particularly for the measurement of sea colour, but will have a number of other applications and so can be classified as a general purpose sensor. It makes use of a 256 silicon photodiode linear array illuminated by light reflected from a grating. The spectral response of the instrument covers 4000 to 8000A so that each diode corresponds to about 16A. The exact response depends on the gratings, but the diodes are sensitive over the range 3500 to 11,000A.

The diode outputs are scanned sequentially at a rate determined by an external clock. The output signal can be digitized and averaged over repeated scans of the array to give added sensitivity. The entrance optics consist of a standard Nikon 35 mm. camera lens, and the field-of-view is approximately 1 milliradian. Figure 2 is a view of the instrument with the cover removed. It is a rugged, compact sensor using no moving parts designed for aircraft installations.

While designed as a device to assess water productivity through chlorophyl content, it could be used in many other applications where rapid spectral measurements are wanted. Also, because of its narrow field-of-view, it could serve as a receiver in a laser induced fluorescence system of a type that will be described in a later section.

2.3 Wide Angle Michelson Interferometer

Supported by CCRS, this sensor is being developed by Shepherd and Gault at York University to measure reflection spectra from an aircraft or spacecraft platform. It produces a circular interference fringe pattern by means of a beamsplitter and two reflectors. The intensity of the central fringe is monitored photoelectronically as one reflector is scanned along the optic axis. The resulting intensity record is called an "interferogram" and can be Fourier transformed to yield the desired spectrum. The spectral resolution obtained is proportional to the length of the scan. Such an instrument collects far more light than a conventional slit spectrometer of comparable size and resolution, and therefore can measure spectra much more rapidly.

The special feature of this Michelson is the method of scanning by means of a gas cell which translates the reflector in one arm of the interferometer in accordance with the change in cell pressure. The motion of the reflector, and the change in refractive index of the gas through which the light beam passes, both cause the instrument to scan. The chief advantage of the gas scanning method is that the Michelson can be "field compensated" and accept a much larger solid angle than a conventional Michelson. The field-of-view with field compensation is 7° in diameter. With Freon - 115 as the scanning gas, a resolving power of about 1000 can be achieved at 5000A. The detector is sensitive to the spectral range 3000 to 10,800A.

Figure 3 is a photograph of the instrument which now has undergone successful flight tests. The cylindrical housing at the right rear is the main Michelson body. The detector housing projects vertically from the main body in front of which is a He-Ne laser reference source. On the left is the gas handling unit and electrical controls.

In its present state, the instrument has been fitted with a scanning mirror to compensate for aircraft motion during the scan period of 3 seconds (shown in Figure 3). The mirror "freezes" the image during the scan, permitting a spectrum to be obtained for a fixed area of the terrain the size of which is determined by the field-of-view and aircraft altitude. The next step is to take advantage of the wide field and place a two-dimensional array in place of the single-element detector. When the path difference is scanned, each detector in the array produces a separate interferogram. Thus, the image is dissected, and a separate spectrum can be computed for each section of the image. In this way, it is possible to combine good spatial and spectral resolution in a single instrument, but obviously a high-speed special purpose minicomputer is needed to handle the data rates required. As a first step, a 100 x 100 element solid-state self-scanned array will be tested in the laboratory.

2.4 Image Intensifier Scanning Spectrometer

The project, supported by CCRS, was motivated by the investigator's interest in using the Fraunhofer line depth technique for the detection of luminescence. The instrument, developed by Jeffers at York

University, is built around a grating spectrograph with a dispersion of 60A./mm. A single-stage electrostatically-focussed image intensifier (ITT Model F-4708) is mounted at the focus of the spectrograph. A transverse magnetic field is applied by two deflecting coils mounted around the image intensifier. With the centre of the appropriate absorption line coinciding with the exit slit pressed against the output fibre optic faceplate of the intensifier, a square wave modulated transverse magnetic field chops the spectrum between the absorption line and the adjacent continuum. The output of a photomultiplier tube placed at the exit slit then is a measure of line depth. An alternative scanning mode is achieved by applying a linear ramp voltage to the deflection coils and thus scanning the spectrum past the exit slit.

The instrument has been flown and used to detect the luminescence from Rhodamine B dye. In general, it can be used for the rapid recording of reflection spectra. Of considerable importance, however, is that this program has gained valuable Canadian experience in the use of image intensifiers and has led to the purchase and application of a 500-channel SSR optical multichannel analyser. The 500 silicon photodiodes are 25 microns wide on a 12.5 x 0.5 m.m. format, and an image intensifier stage is employed ahead of the diode array. Each photodiode is subdivided into two halves (top and bottom). The top half is generally reserved for viewing the background, the bottom half is used for the signal measurement.

The spectrum to be detected is focussed onto a fibre optic faceplate on which is deposited an S-20 photocathode.

The released photoelectrons are accelerated to a few KV and focussed on to the silicon diode array. The target is scanned in 33 msec. executing a closely-spaced sawtooth pattern of 500 cycles across the spectrum. The digital output is directed to either of two 500 word, 21 bit memories (memory A for the bottom half, B for the top half). These memories may be used to store the result of a single scan, or may be used to signal average over many scans, thus greatly improving the signal-to-noise ratio. The electronics provide for B-A subtraction so as to remove the background electronically before displaying the desired signal. Each channel may be read digitally on a panel display, directed to an auxilliary plotter, displayed on an oscilloscope or stored on a tape printer for further computer analyses. The laboratory setup containing these components of the system is shown in Figure 4.

The general advantages of the system are its very high sensitivity in the region 3500-8000A., simultaneous detection in 500 channels, and its ability to be gated for pulse durations in the range 10 nsec - 2msec. This capability permits it to be used in laser ranging applications. It can readily receive the short pulse, high repetition rate signal from a laser and its sensitivity will permit the recording of Raman scattering under this sort of illumination. This application will be described in a later section.

Before leaving the applications of the linear array, it should be mentioned that CCRS may be involved at some future time in the development of a multispectral scanner. Such arrays make it possible to construct one with no moving parts using push-broom scanning. This is a term that describes the technique of using the forward motion of the vehicle (aircraft or spacecraft) to sweep a linear array of detectors oriented perpendicular to the ground track across a scene being imaged. The array must be sampled at the appropriate rate so that contiguous lines are produced. In this way, the photon flux from the scene is allowed to be integrated during the time required for the instantaneous field-of-view to advance the dimension of one resolution element on the ground. There is a considerable improvement in signal-to-noise ratio over mechanical scanners which permit only much shorter integration times for the same resolution. For comparable performance, size and weight can be reduced significantly. In future, silicon photodiode arrays will give way to charge-coupled devices with perhaps as many as 12,000 detectors per array or more. The data rates

associated with such multispectral scanners will be prodigious, and a high degree of sophistication will be contained in the associated digital logic and storage systems. Canada needs to gain background and experience in such technology.

2.5 Multispectral Camera System

Supported by CCRS and developed by Spar Aerospace Products Limited, it uses an image dissector tube which is a type of photomultiplier where the optical image, focussed on a photocathode, can be scanned or sampled elementally. The image causes photoemission of electrons proportional to light intensity which are accelerated toward an aperture behind which is a photomultiplier. The size and shape of the aperture depends on the required resolution and the type of scan employed.

Used in a television mode, its aperture of 0.001 - inch diameter provides a resolution of 1000 TV lines per inch (20 lines/mm). The camera uses an ITT F-4052 tube with an S-20 response (3000-7000A). A wedge interference filter is placed in front of the system so that in one direction, y, the wavelength can be varied; and in the perpendicular direction, x, the camera can be line-scanned. When mounted in an aircraft, the line-scanning can be synchronized with the aircraft velocity so that a continuous strip of the terrain can be recorded similar to a conventional line-scanner. The wavelength then can be easily altered by varying "y" across the wedge interference filter. Thus, the multispectral camera can produce high resolution imagery at readily selected wavelengths within the range of the filter and the response of the tube. Figure 5 is a photograph of the system.

It is a general purpose instrument that can be used for a wide variety of applications where it is critical that it be rugged (no moving parts), have high spatial resolution - up to 40 lines/mm. with 0.0005" aperture, have a large number of spectral channels that can be selected and programmed remotely, have a small spectral bandpass (100-350A.) and/or have a wide dynamic range (10^4). The system has been flight tested and has produced imagery of correct quality using the Daedalus tape recorder in the CCRS DC-3 aircraft. It is available for operational use.

2.6 Semiconductor Infrared Photography (SCIRP)

Supported by CCRS and the Forest Fire Research Institute, DOE, the SCIRP program has been conducted by Dr. W. Pinson at McMaster University. The objective is to develop a simple and inexpensive method of infrared photography. At infrared wavelengths, ordinary film will fog because of natural ambient thermal radiation. Fogging times (and thus storage life) depend on wavelength sensitivity and ambient temperature which become shorter at longer wavelengths and at higher temperatures. SCIRP overcomes the problem by introducing the image-forming substance only at the time of exposure.

Two types of processes are being investigated - contact sensitized and electrically controlled. In the contact-sensitized technique, two separate parts of the photographic process, each incapable of recording an image separately, are brought into contact during exposure (typically a semiconductor and an electrolyte). However, because a separate semiconductor film must be used for each exposure, it is more expensive than the electrically-controlled technique. In this type of process, the capability of recording an image exists only during the time an electric field is applied to the system and current flows through it. The photoelectric gain can be several tens for this process, thus making it more sensitive than the contact-sensitized processes where the gain is less than unity.

Both methods are based on electrode reactions which transform the distribution of radiation intensity on the semiconductor surface into a current density or potential distribution, and as a final stage, into a distribution of a substance which is precipitated from an electrolyte solution to form a photographic image.

A lead sulphide film camera, electrically sensitized, has been used

to record controlled fires. Current efforts are being devoted to increasing the speed of the PbS film and improve its thermal resolution using a charge injection method. Applications include forest fire detection, the steel industry, forensic science and situations where thermal photographs are needed. The related technology can be applied to the flotation process where semiconductor minerals are involved, and even to the extraction of oil from tar sands.

3. REMOTE PROBING WITH LASERS

Two major classes of remote sensing devices utilize the laser as a source of radiation to stimulate a response from the target. The first group induces fluorescence, and thus they are call fluorosensers; the second generates back scattering in the medium through which the laser beam passes, and operates much like a conventional radar but at optical frequencies - called a LIDAR (Light Detection and Ranging).

3.1 Fluorosensors

Two types of fluorosensors have been developed in Canada - one using a continuous wave (CW) laser sponsored and developed by the Inland Waters Directorate, DOE, and the other using a pulsed laser supported by CCRS, and developed at the University of Toronto Institute for Aerospace Studies. Both operate on the principle that various substances fluoresce when excited by radiation of a suitable wavelength. Of particular interest are crude oil or bunker C, fluorescent dyes such as rhodamine, chlorophyl in algae and seaweed, and effluent from pulp mills and chemical plants.

3.1.1 CW Fluorosensor - Developed by Kruus, Davis and Gross of DOE, this instrument uses a He-Cd CW laser with a 15 mw. output at 4416A. The receiver is an 8" Schmidt Cassegrain focussing the return radiation through optical filters onto a photomultiplier. The filters block laser light and background, passing only in the fluorescence band of interest. Figure 6 is a photograph of the system.

The instrument has been flown on several occasions and has successfully detected oil slicks, rhodamine dye and lignon sulphonates from pulp mills. Because of the relatively low power of the CW laser, it can only be operated at night at relatively low altitude (in the order of 500 feet). For this reason, its most likely application would be as a fixed monitor viewing a lake or a stream, suspended perhaps from a bridge or embankment where it could creat an alarm when pollutant concentrations exceed some preset value. It is compact, rugged and cheap - the cost of components is less than $10,000.

3.1.2 Pulsed Fluorosensor - Developed by Measures, UTIAS, and Bristow, CCRS, the system uses a pulsed nitrogen laser operating in the ultraviolet at 3371 A. It emits short, powerful pulses of 100 kw. for a duration of 10 nsecs. with a maximum pulse rate of 100 per sec. The receiver is an 8" Newtonian telescope - photomultiplier system. The fluorosensor, weighing about 450 lbs., has been installed in a CCRS DC-3 aircraft and has completed flight tests successfully. Figure 7 is a photograph of the system set up at a field site.

Laboratory studies on such materials as crude oils, refined petroleum products, fish oils, rock and mineral samples have shown that their fluorescence spectra have limited use as a means of identification and discrimination because of spectral overlap and the difficulties associated with measuring and calibrating the relative magnitude of fluorescence return signals. An alternative procedure for improving the identification potential has been investigated using the fluorescence decay characteristics. It was discovered that each of the materials investigated had a more or less unique fluorescence lifetime - emission wavelength characteristic. Such fluorescence decay spectra are far less susceptible to uncertainties than is the amplitude of the signal. The program on decay spectra now is entering an intensive investigation stage.

3.2 Lidar

Back-scattered radiation from a high-power laser can reveal a lot about the properties and species of the medium through which the laser beam passes. The information is based on Rayleigh scattering of light by molecules and very small particles, Mie scattering by aerosols and Raman scattering by certain molecular components in the medium. Carswell at York University has developed an atmospheric and marine lidar system in a program supported by CCRS.

3.2.1. Atmospheric Lidar - The instrument shown in Figure 8, consists of a Q-switched ruby laser capable of providing up to 150 megawatts at the fundamental wavelength of 6943 A. in an 18 nsec. pulse. The system is water-cooled and provides pulse repetition rates of 10 per minute. The system also contains a second harmonic generator to provide radiation at 3472 A. The receiver includes four channels to permit simultaneous analysis of four backscatter signals capable of providing complete polarization measurements; the data can be recorded in digital form on magnetic tape. The unit is installed in its own mobile truck laboratory and incorporates precise motor-driven horizontal and vertical steering controls for aerosol and plume tracking. It is being used by air pollution agencies and utilities concerned with air quality management.

3.2.2 Marine Lidar - Figure 9 is a view of the marine lidar developed by Carswell and Sizgoric. The argon laser shown on the right works in the cavity-dumped mode. The output pulse is controlled by means of an intra-cavity acousto-optic diffraction cell that operates to switch out very short pulses. This unit at 4880 and 5140 A. delivers peak powers of up to 75 watts and pulse repetition frequencies variable from CW to 10 MHz, with pulse widths variable from 10 nsecs. to 1 msec. Average power in the cavity-dumped mode of up to about 1 watt at these wavelengths is available. The unit will operate on seven other Argon lines in the blue-green spectral range at lower power outputs.

The receiver is a 25 cm diameter Newtonian telescope with variable field stop and processing optics which include a 10 A. bandpass filter and a quarter-wave plate and linear polarizer for analysis of the scattered signal. A very high speed 5-stage photomultiplier is used as the detector. The output is fed through a preamplifier to a scope or to a "boxcar" signal averager and recording system.

Seen in Figure 9 are the 45 degree mounted mirrors for downward direction of the transmitter and receiver beams. These are mounted on an extendable member which protrudes over the side of the tank (for lab use) or the vessel (for shipborne measurements). The system has been tested in indoor-tanks and on board a ship in Lake Erie to check out the instrument, and to determine its useful operating range. When combined with the optical multichannel analyzer described in Section 2.4, it will be used to measure Raman scattering and thus identify certain molecular species in the water. For this reason, the marine lidar could become an important water quality sensor.

3.2.3 Bathymetric Lidar - In relatively clear and shallow waters such as are found over some parts of the Arctic north slope, an aircraft - mounted lidar, operating as a visible light radar, might be capable of performing bathymetric measurements of sufficient quality to be used for hydrographic survey purposes. It would be a logical extension of the aerial hydrography program now being planned by the Marine Sciences Directorate, Pacific Region, DOE. The most appropriate laser should emit in the blue-green window, and a likely candidate would be a frequency-doubled neodynium laser operating at 5300 A. We may expect to see such a development within the next year or two.

4. SPECIAL PURPOSE SENSORS

There are a number of Canadian sensor development programs that have been directed at very specific applications, some supported by CCRS, others by various government agencies and

private industry. Four such applications will be described: ice and snow, soil moisture determination, forestry and atmospheric analysis.

4.1 Ice and Snow

A number of sensor developments have been directed at problems associated with Canada's arctic. There still does not exist an operational sensor that can measure the thickness of sea ice from an aircraft - this problem has been the subject of several developments. Other ice and snow sensors will be described in what is to follow.

4.1.1 Holographic Ice Surveying System (HISS) - The HISS radar, developed by Iizuka, University of Toronto and supported by CCRS, is designed to measure ice thicknesses up to four metres. Shown in Figure 10 it consists of three major parts - transmitter and receiving antenna arrays seen slung under the helicopter on the beam assembly, a receiver-transmitter unit and a special-purpose computer both located inside the vehicle. In contrast with conventional radars, HISS measures the spatial distribution of the scattered waves from the top and bottom sides of the ice, and from this determines the ice thickness.

Earlier tests in 1972 off the arctic coast near Tuktoyaktuk will be repeated in the near future at an arctic location where the salinity is more predictable. Meanwhile, the equipment has been tested successfully on fresh water ice in Lake Ontario and in an experimental setup at the the University of Toronto.

4.1.2 Wideband Radar - Under development by Page and Chudobiak at the Communications Research Centre, DOC, a new wideband radar technique is being explored for measuring ice thickness, initially fresh water ice. Figure 11 shows an experimental version of a very high resolution radar undergoing final checkout on a sled on the Ottawa River in February, 1974. It uses a small horn suspended at the side of the sled. In March, this radar was tested extensively in airborne trials over Lake Ontario and the St. Lawrence and Ottawa Rivers. It operated reliably and showed itself capable of producing continuous profiles of ice thickness to an accuracy in the order of 1 cm. A modified version will be fabricated for use over sea ice.

4.1.3 Microwave Radiometer - The radiometer is a very sensitive passive receiver which takes advantage of the fact that all bodies radiate electromagnetic energy, the intensity of which depends on the frequency, the absolute temperature, the electrical properties of the materials contained in the body, and the nature of the boundaries or surfaces. Water is a medium-strength radiator, metallic structures such as ships are weak radiators, while pack ice, icebergs, wakes and land are strong radiators.

Adey et al of the Communications Research Centre has developed a UHF radiometer that can be operated in four bands in the range 400-2300 MHz. It uses two antennas - a log-periodic and a horn with beamwidths of 50° and 40° respectively. The equipment has been flown on a number of occasions in an aircraft and in a helicopter.

Flight tests carried out in 1971 near Resolute, N.W.T. showed that the radiometer can give a qualitative statement about ice thickness and ice condition. Flights the following year over the Strait of Belle Isle and over Hudson Strait recorded signatures of ships, icebergs, pack ice, rocky and lichen-covered areas and fresh water lakes and streams. They revealed that there is a clear distinction between icebergs and ships, icebergs can be detected against a water background, the radiometer signal from open pack ice in a given area correlates with the fractional ice cover and the intensity of the radiation from water at the lower UHF frequencies is sensitive to the degree of salinity. Because of its abilities to operate in darkness, microwave radiometry is highly relevant to the arctic. For this reason, further work should be carried out to learn how such techniques can be fully exploited in operational surveillance systems.

4.1.4 Gamma Ray Spectrometer - Developed by Gasty and Holman of the Geological Survey of Canada, this instrument was developed to measure the water equivalent of snow pack.

Natural gamma radiation emitted by potassium, uranium and thorium is attenvated by the water content in snow layers over top of such elements. The sensor consists of twelve 9" x 4" sodium iodide crystals held at a constant temperature. When gamma rays impinge, the crystals put out pulses which are fed via an amplifier to a 128-channel analyzer. Appropriate portions of the gamma ray spectrum can be selected. Background calibration flights with no snow cover are necessary for comparison with flights in the presence of snow.

4.2 Soil Moisture Determination

In response to requests from the CCRS Working Group on Agriculture, a study was initiated with Barringer Research on the potential of electromagnetic techniques for the remote sensing of soil moisture. The quantity of interest is the amount of free water in the upper few feet of the earth's crust not held under tension, so that it is available for vegetation. The first phase of the study concluded that within the frequency range from 100 MHz to 20 GHz there is a relaxation phenomenon directly related to water content, although the nature of this relaxation and the bonding are not well understood. Subsequently, it was concluded that the spectral region from 100 MHz to 2 GHz was the most suitable for the remote sensing of soil moisture. The next phase involves laboratory measurements of various soil types in this frequency range, followed by in situ measurements which, if successful, could lead to the design and development of a multifrequency airborne radar system. Communications Research Centre and the Geological Survey of Canada are collaborating with CCRS on this project.

4.3 Forestry Radar Altimeter

At the request of the Forest Management Institute, DOE, Westby at the Radio and Electrical Engineering Division of NRC has developed a special type of radar altimeter for use in large-scale (low altitude) photography for forest inventory work. Photography at lower altitudes, however, presents a special problem of accurately determining the flying height of the aircraft above the ground. This is required before useful photo measurements can be made.

The forestry radar altimeter operates at a frequency that penetrates foliage and so is not affected by intervening vegetation between the aircraft and the terrain. The instrument error is ±1% of flying height, and this accuracy is maintained when flying over slopes up to 30°. The minimum height over forests is 200 feet, and the effective beam width is approximately 1.7°. Further work on the equipment will extend the range to 10,000 feet altitude, and reduce the maximum error to 1/3 of 1%.

4.4 Correlation Gas Analyzer (GASPEC)

Developed by Barringer Research and supported by CCRS, this instrument is designed to detect the presence of combustion gases associated with forest fires - the gas selected was carbon monoxide. A non-dispersive gas analyzer, it is designed to detect the decrease in energy in the incoming radiation due to the presence of an absorbing target gas. The instrument uses a reference call containing nitrogen or a non-absorbing gas in the region of interest, and a sample gas cell containing carbon monoxide. Ground chopping is used based on the work of an earlier CCRS contract. The incoming 4600 A. radiation is so chopped and passes, via a beam splitter, through both arms of the instrument to a double-element detector. When no target gas is present, the instrument is balanced and no signal is observed. When target gas drifts into the path of the instrument, a signal is observed proportional to the amount of gas present. A reference lamp is used to balance any variations in the respective gains of the two channels. A photograph of GASPEC appears in Figure 12.

The instrument has been fully laboratory and environmentally tested, and meets its intended specifications. Also, it has had an initial flight test under extreme atmospheric conditions and has been field operated from a truck. Further field testing as a CO detector is desirable, and there is interest by users to apply the instrument to other gases such as HCl, SO_2, NO_2, etc.

Barringer Research has developed a number of proprietary instruments for atmospheric analysis including the COSPEC correlation spectrometer for detecting SO_2, NO_2 and other gases, and the CO Pollution Experiment (COPE), a Michelson correlation interferometer which CCRS is flying in their Falcon aircraft over US and Canadian cities for NASA. The company also has developed a wide range of its own geophysical instruments.

5. FUTURE DEVELOPMENTS

Without doubt, future developments in Canadian sensors will be determined by government policy, plans and programs - mainly at the federal level, but also by an increasing extent at the provincial level. Policy and plans will create the stimuli, programs the opportunities.

The greatest stimuli of all has been the formation and on-going presence of the Canada Centre for Remote Sensing and its Working Group on Sensors. The Oceans policy announced by the Minister of State for Science and Technology, the energy crisis and the resulting focus on Canada's arctic and the accelerating need for conducting environmental baseline studies before developing remote Canada will all provide further stimulus for new and better sensors.

At the provincial level, there is increasing emphasis on land use planning - particularly as major energy projects get launched. Environmental and resource management techniques will grow in sophistication as the provinces begin to flex their technological muscle and new provincial remote sensing interpretation centres gain in strength and stature. Such changes can be anticipated as a result of a recent and growing interest on the part of the provinces in developing individual provincial science policies.

As policies and plans merge into programs, it becomes possible to foresee very specific applications for new sensors. Such an opportunity could develop from the long range patrol aircraft program (LRPA) now being pursued by the Department of National Defence. There could be a major civilian role for such an aircraft, and with it an opportunity for new sensor developments. Other programs will merge from the implementation of the Oceans policy, and there could well be a resource satellite in Canada's future.

Sooner or later, however, the true benefits from remote sensing must be forthcoming. Increased investment in this field, including new sensors, can only result from anticipated adequate rate of return. Thus it is critically important to monitor and document present remote sensing programs if we are to collect the necessary evidence for future investment.

Finally, for the sake of future remote sensorists, the sensor must increasingly be thought of as being part of a complete system, and not as a separate entity in its own right. The requirements for data storage and processing have become the main thrust of most new remote sensing systems, particularly those utilizing large detector arrays. The most important entity in the system, however, is the interpreter. He is the hub around which the entire system rotates. Let us in future, therefore, not stray from him as we have occasionally in the past, but become part of the system so that we may pursue the needs of the user as he perceives them.

6. ACKNOWLEDGEMENTS

The writer acknowledges the support received from the Canada Centre for Remote Sensing and many of the persons responsible for the sensor developments described in this paper. Their help in providing background material, photographs and slides is deeply appreciated.

7. REFERENCES

The descriptive material contained in this paper was derived from one or more of the following references:

1. Canadian Aeronautics and Space Journal, October, 1968 p. 315

2. Canadian Aeronautics and Space Journal, December, 1971

3. Canadian Aeronautics and Space Journal, December, 1972

4. Canadian Aeronautics and Space Journal, December, 1973

5. MacDowall and Lapp, Sensor Development, An Overview of Recent Canadian Experience, 10th Annual Meeting, American Astronautical Society, Dallas, Texas, June 1973.

6. Thompson, Advanced Solid State Sensor System for Remote Sensing from Satellite, Proceedings of the Symposium on Management and Utilization of Remote Sensing Data, American Society of Photogrammetry, Sioux Falls, North Dakota, October-November, 1973.

7. CASI Aerospace Electronics Symposium, Victoria, B. C. February, 1974.

Figure 1 Scanning Interference Filter Photometer

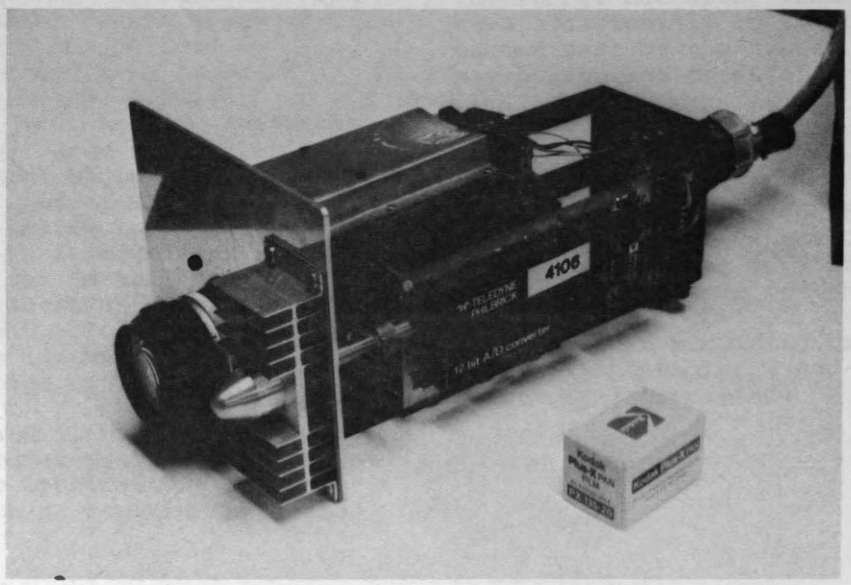

Figure 2 Multichannel Silicon Diode Spectrometer

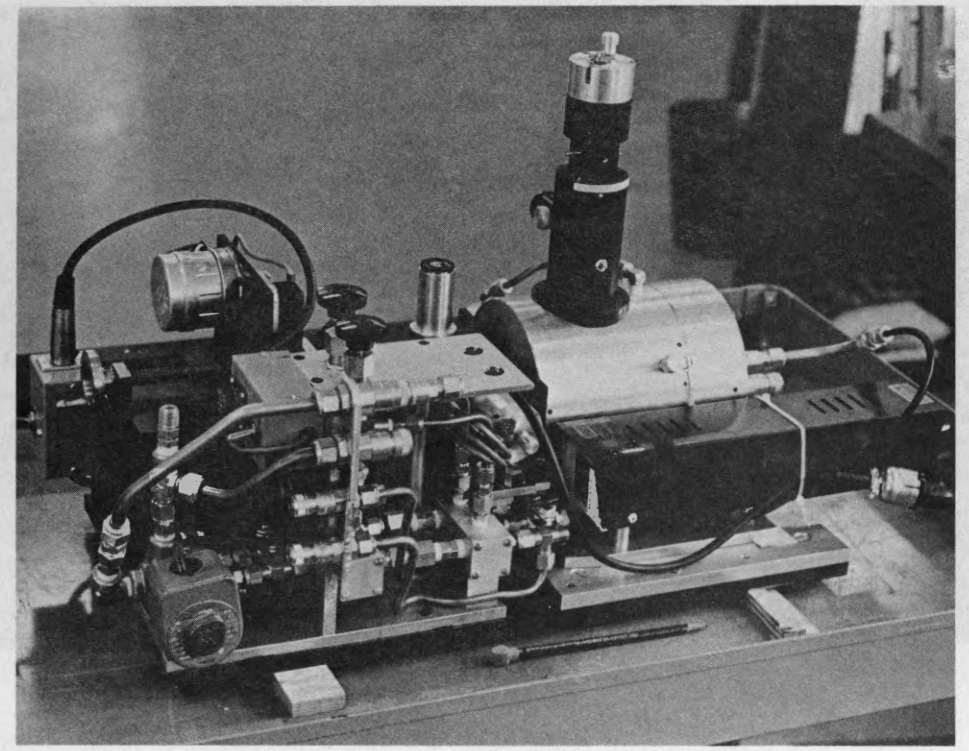

Figure 3 Wide Angle Michelson Interferometer

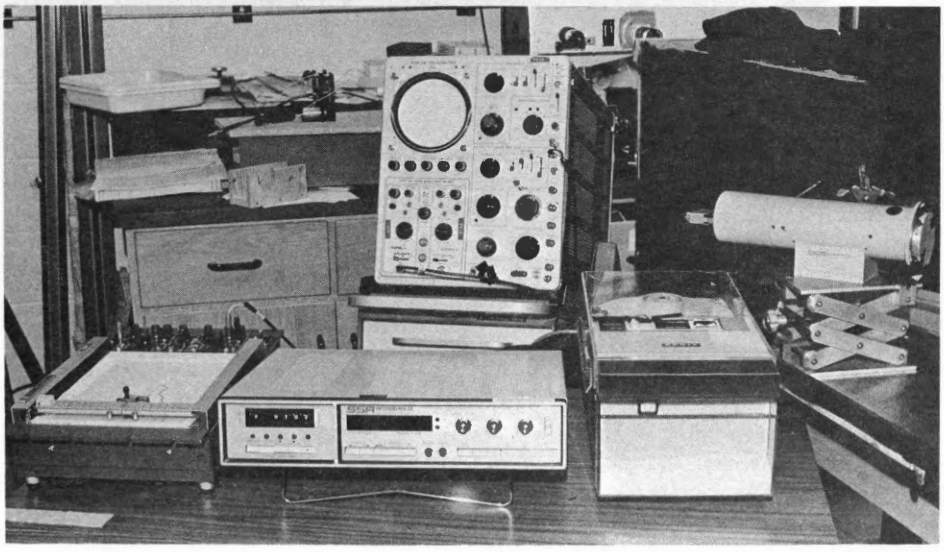

Figure 4 Optical Multichannel Analyser System

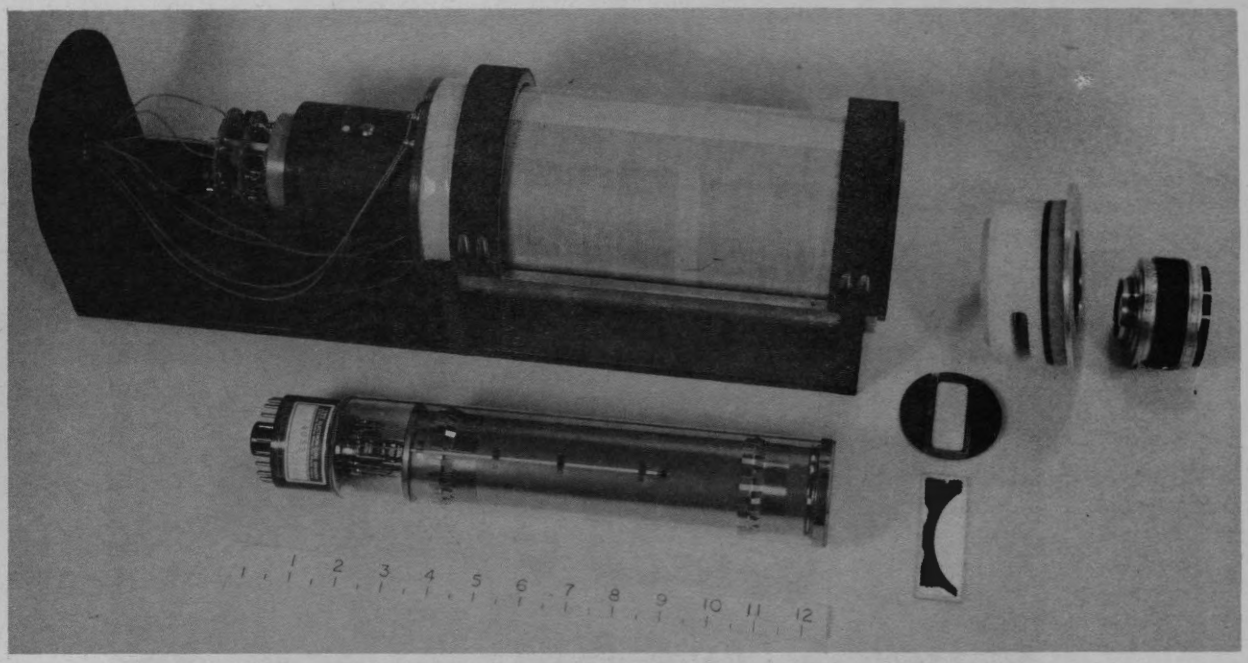

Figure 5 Spar Multispectral Camera System

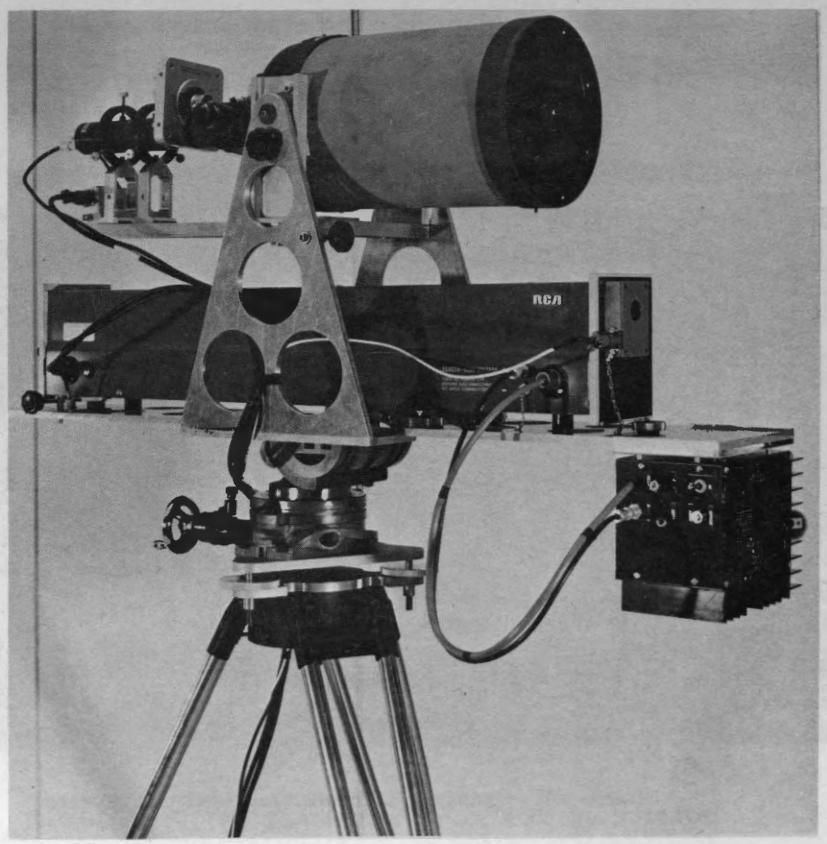

Figure 6 CW Laser Fluorosensor

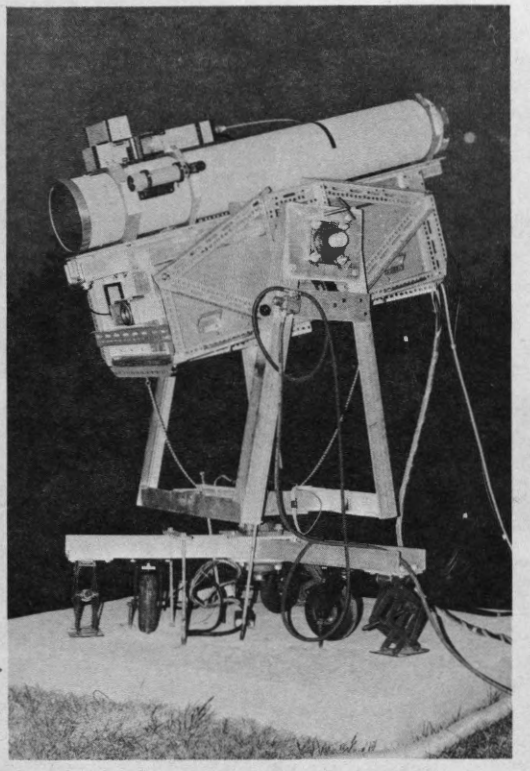

Figure 7 Utias Pulsed Laser Fluorosensor System

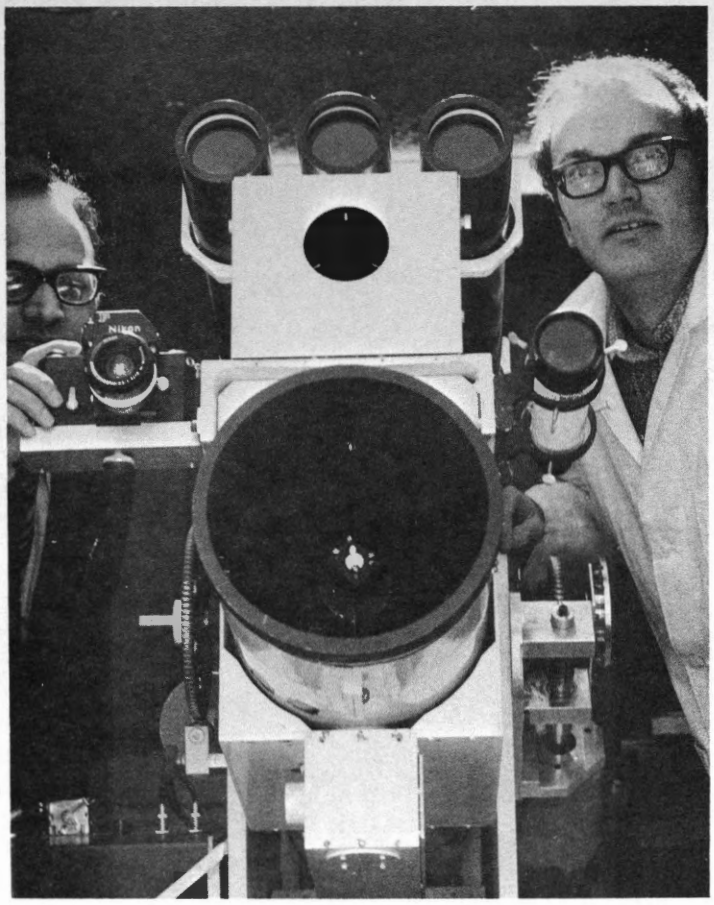

Figure 8 York University Mobile Atmospheric Lidar

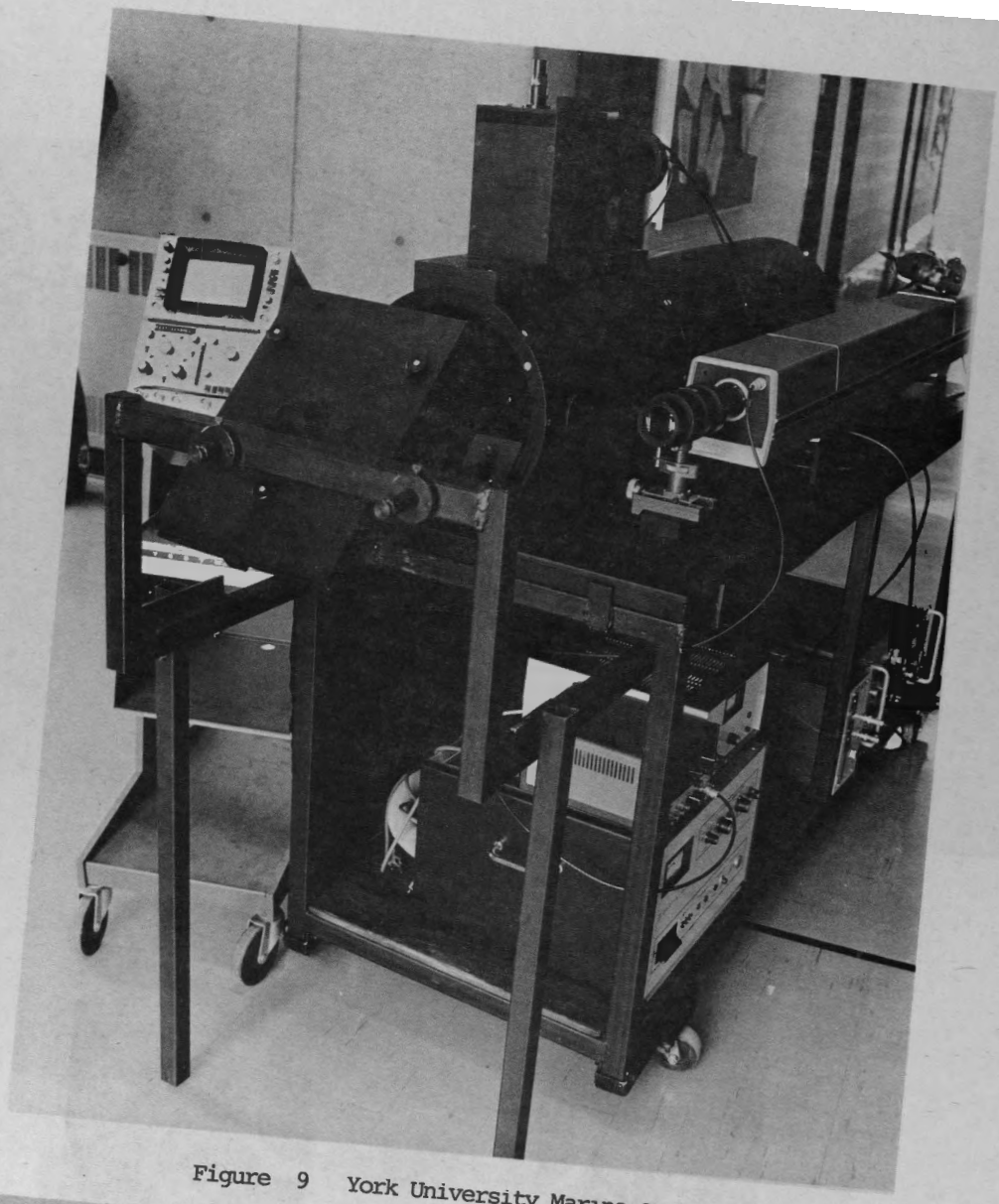

Figure 9 York University Marine Lidar

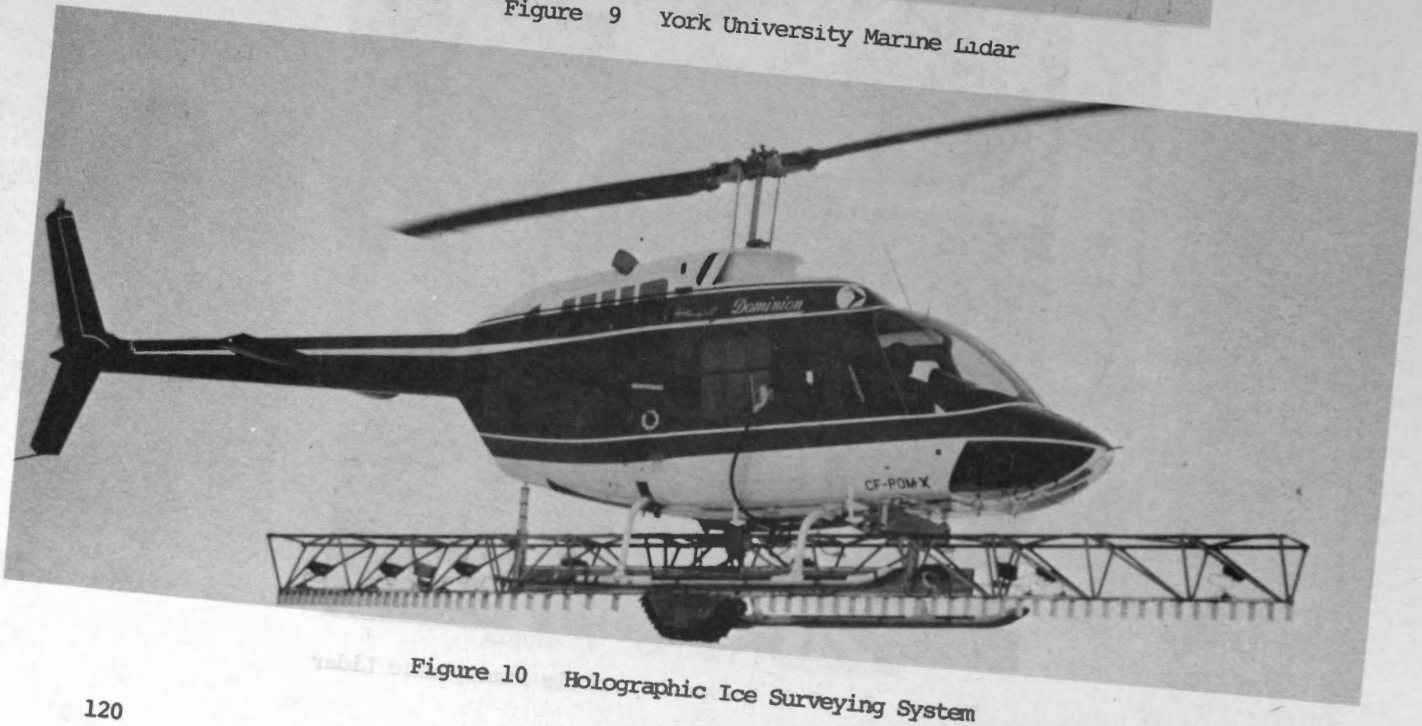

Figure 10 Holographic Ice Surveying System

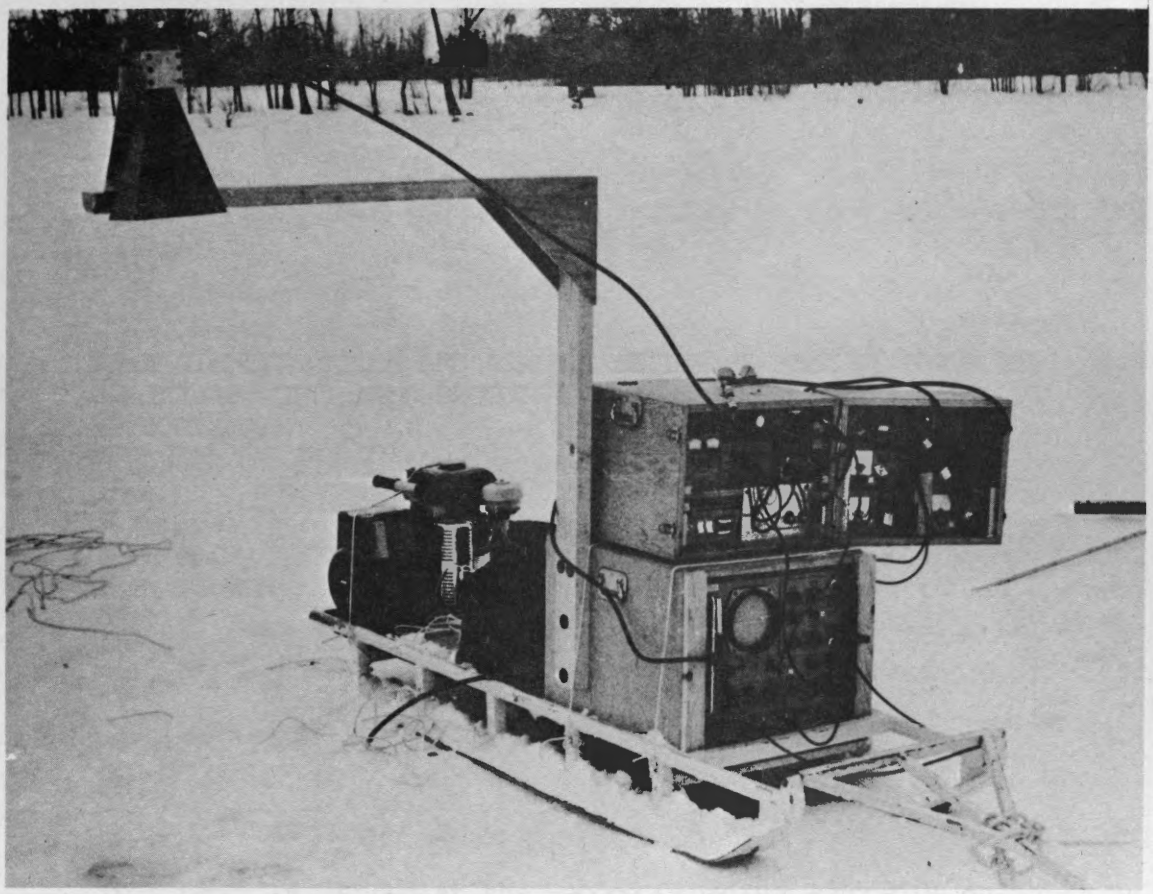

Figure 11 Wideband Ice Thickness Radar

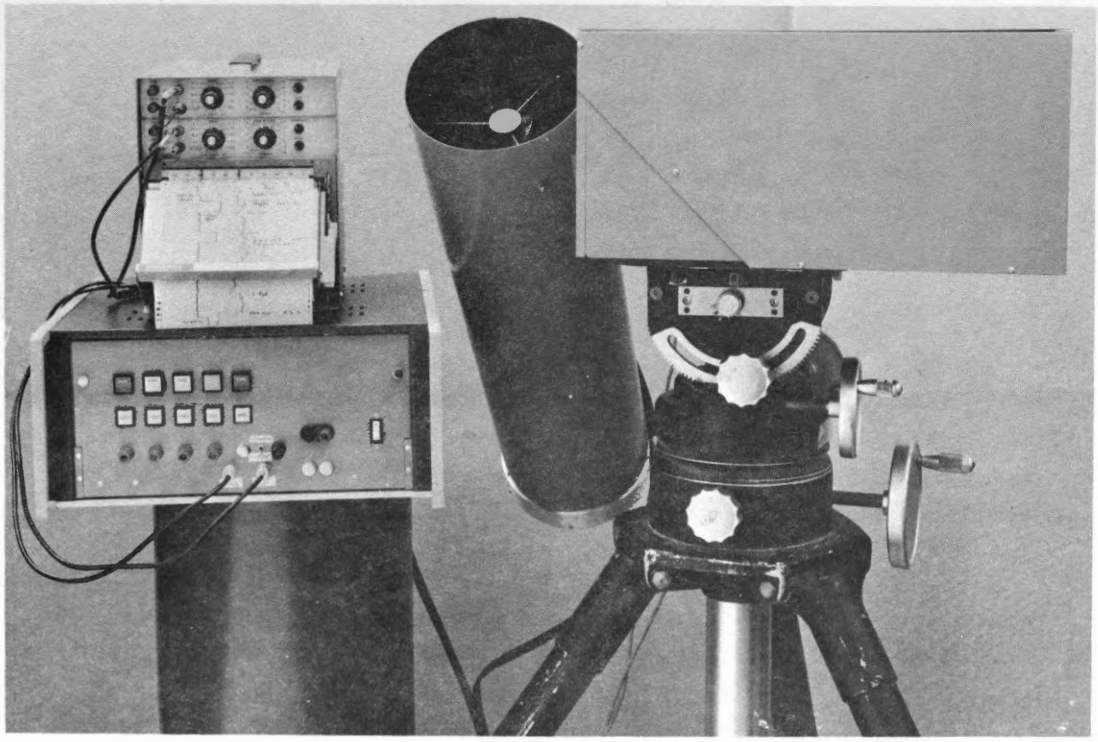

Figure 12 Barringer Correlation Gas Analyzer (Gaspec)

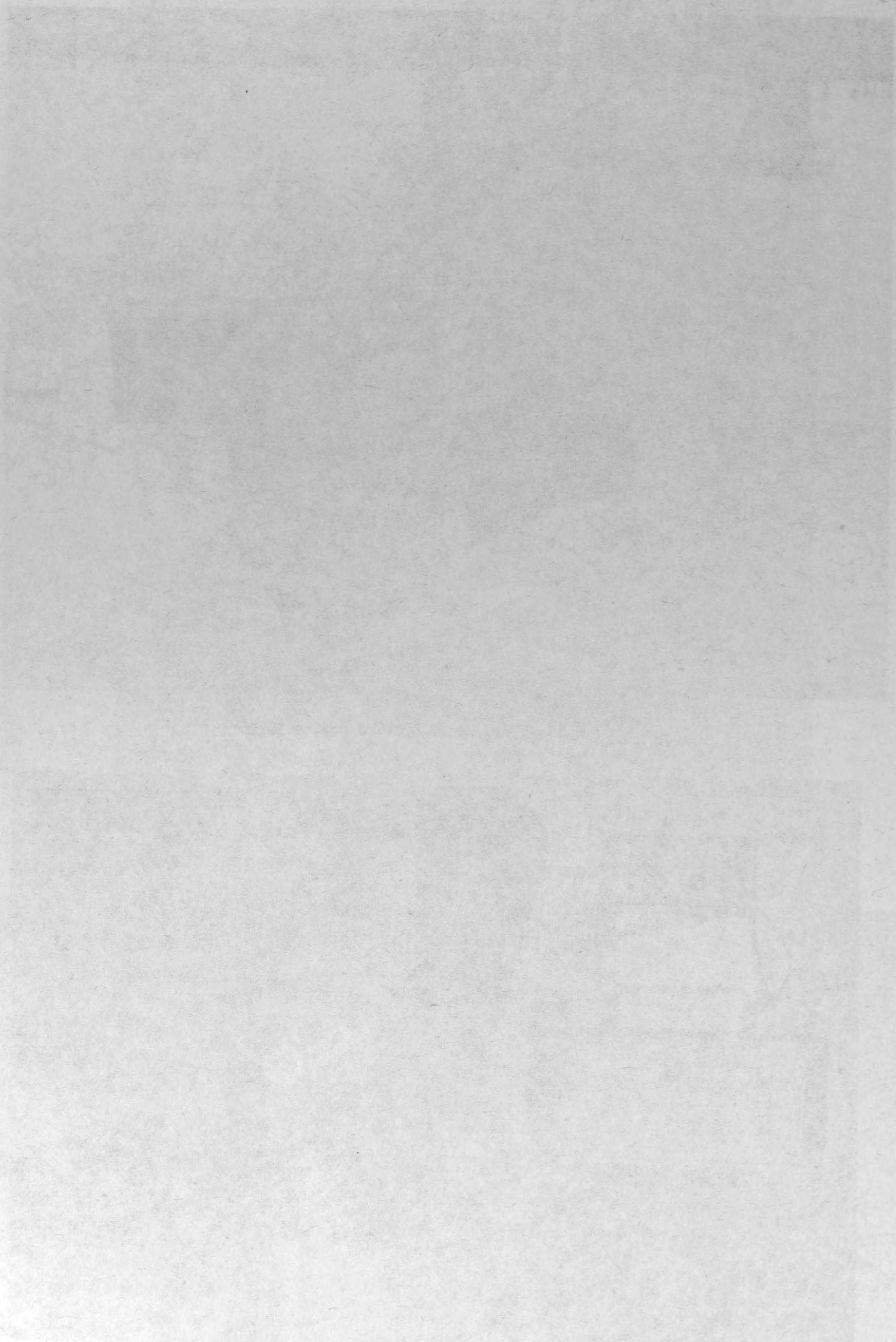

CROP IDENTIFICATION AND ACREAGE ESTIMATES FROM AIRBORNE AND SATELLITE MULTI-BAND PHOTOGRAPHY OF NORTHEASTERN SASKATCHEWAN

By

A.R. MACK
K.E. BOWREN

This paper presented at the Second Canadian Symposium on Remote Sensing, University of Guelph, Guelph, Ontario, April 29 - May 1, 1974.

CROP IDENTIFICATION AND ACREAGE ESTIMATES FROM AIRBORNE AND SATELLITE MULTI-BAND PHOTOGRAPHY OF NORTHEASTERN SASKATCHEWAN

A.R. Mack[1] and K.E. Bowren[2]

ABSTRACT

Using a simple six-step grey scale criterion, numeric values were assigned to the grey-level densities on black and white photographs taken in August 1972 with infrared and red radiation bands. The grey-level densities were calibrated to known crops or other features determined from data taken on the ground from training sites. A classification "key" was developed from the calibrated grey-scale values for the two spectral bands. Using the classification "key", > 90% of the cereal crops-harvested, cereal crops not-harvested, rapeseed, and fallowland were identified on areas adjacent to the training site. It was not possible to distinguish between wheat and barley in this study using August photography. Nearby sites were used to "verify" the criterion.

A high proportion of the fields was identified similarly (i.e., > 90%) on satellite (ERTS-1) black and white photographs of the infrared and red bands (Band #7, 0.8-1.1 μ; Band #5, 0.6-0.7 μ). At least two of the four spectral bands of ERTS-1 were required to establish a suitable "key" for adequate identification - an infrared band and a visible, e.g., red. In general, the green spectral reflection band appeared to be similar to the red band for most of the fields except for a few of the fallow and grassland. However, further studies are required to evaluate the place of the green band in crop identification. The transference of known physiographic features onto ERTS imagery from topographic survey maps and high-altitude air photographs enlarged to a comparable scale facilitated positioning, e.g., legal description, water courses, main roads, etc. Acreage estimates of crops and fallowland were made on both satellite imagery and airborne using calibrated grid overlays.

By comparing the values of unknown fields to those calibrated with known features on the same photograph, variation in exposure, photographic development, and reproduction are eliminated.

INTRODUCTION

The possibility of identifying agricultural crops and vegetative conditions from small-scale photography has been reported previously (Draeger, 1971). In general, infrared sensitive film, either color or black and white, is used because of the high reflection of infrared (.7 to 2.5 μ) radiation from healthy green plants and the wide variation under different conditions of plant stress and stage of maturity. Infrared reflection, thus may be used as a sensitive indicator of poor crop vigor due to disease, insect damage, nutritional problems, etc. For crop identification, the sensitivity of I.R. reflection to stage of maturity is used to separate crops and fields differing in their maturity at time of measurement. Healthy vegetation is a high absorber of red radiation (e.g., .62 to .68 μ) and the absorption decreases with a decrease in chlorophyll activity. Thus, in contrast to I.R. radiation, the reflection of red may increase under conditions of poor vigor or advancing maturity. Consequently, quantitative measurements of the reflection from crops of these two bands can be used to discriminate between vegetative conditions or crops at different stages of maturity. The green radiation band is used to supplement information from the red band.

---

[1] Soil Research Institute, Research Branch, Agriculture Canada, Ottawa, Ontario K1A 0C6 Contribution No. 487.

[2] Melfort Research Station, Research Branch, Agriculture Canada, Melfort, Saskatchewan.

Lauer (1971), Pittinger (1971), Weigand, Lauer et al. (1971) among others have shown how sample ground sites may be established to calibrate imagery and develop identification "keys" for the entire area represented by the "training" sites and tested against "verification" or control sites, before estimating acreages.

This study was undertaken in 1972 in cooperation with the Canada Centre for Remote Sensing (Dept. of Energy, Mines and Resources) to evaluate the feasibility of using black and white airborne photography and satellite imagery for manual identification of field crops, delineation of field boundaries, and estimation of crop acreage. An area was selected in a dominantly annual cropping farm management system within the Moderately Cold Subhumid Climatic region of the north-eastern agricultural region of Saskatchewan dominated by Black Chernozemic soils.

PROCEDURE

Site Location

In 1972 an area on Chernozemic soils near Melfort, Saskatchewan was selected within a Moderately Cold Subhumid Soil Climatic region. The cropping system of the area included the production of cereal crops, mainly wheat and barley, an oilseed crop (rapeseed), and summer-fallow with some acreage in grassland, bushland, creeks and streams, oats, flax and sweet clover.

Several ground sites were established in the area as training areas to provide data from which to develop a key for crop identification and to serve as "verification" sites for the developed "keys". The following sites were located: Test Site A: A 6x1 mile east-west training site was located within a 6x2 mile area extending westward from a point three miles south of Melfort. Test Site B: A 6x1 mile east-west training-verification site within a 6x2 mile area extending westward from a point 1 mile south of Melfort. Test Site C: A 4x6 mile block extending northward from the town of Melfort.

Ground Observation Data

On July 13 and 14, 1972, ground observational data were taken on all fields bordering the main east-west roads (i.e., on the north and on the south sides) in Sites A and B, and along all north-south roads within Site C. Type of crop, height, stage of growth and crop density were recorded on each of the fields. However, due to weather conditions airborne imagery was not taken by the Airborne Data Division, Canada Centre for Remote Sensing, until August 26, 1972.

Airborne Data

Airborne photography was acquired using a CF-100 equipped with multi-camera package consisting of one RC 10 Super Wide-angle camera and four 70-mm cameras. The cameras were equipped with film-filter combinations to provide visual color, infrared color and black and white photographs of the infrared, red and green spectral radiation bands (Table 1).

The photography was taken at two altitudes (17,000 and 37,000 ft. ASL) to provide a range in coverage and scale. The multi-band 70-mm cameras photographed a centre strip within that covered by the RC 10 camera (Table 2).

An illustration of the tonal variation among the fields for a 2-square mile block from black and white infra-red and red radiation band airborne photograph is presented in Figs. 1C and 1D.

Numeric values were assigned to the grey values of fields using an arbitrary six-step grey scale ranging from zero to represent low reflection as shown by dark grey on the photos to a value of five to represent high reflection as shown by a light grey tones. Black and white photos of the infrared, red and green bands were used. This numeric scale is analagous to that of the Munsell color system. Photographic Density Ranges are available which provide suitable number of density steps within a satisfactory range of values from approximately > .90 (dark) to .05 (light).

A classification "key" was developed by calibrating the numeric values with fields identified from the ground based observation data. Visual identification was also made on the color aerochrome to verify the identifications made on the black and white photograph prints. All identification was done on prints enlarged to a scale around 1:50,000 from the high altitude photography (1:126,700) or on prints at a scale of approximately 1:50,000 (Table 2). The fields were coded as follows: Rapeseed (4), cereal crops (1 for wheat and 3 for barley), grassland (12) and fallowland (black - 15; recent tillage - 15, trash - 17, weedy - 18).

TABLE 1

The camera package-types of airborne camers and film-filter combinations

	Type of Camera[a]	Focal Length	Width of Film Inch	Film Type	Filter	Radiation Band Imaged Microns
1	Wild RC 10 SWA	230 mm	9 x 9	Aerocolor 2445	NAV	Visual .4 - .7
2	Vinten 547	70 mm	3 x 3	Aerographic IR 2424	89B	I.R. (B.W.) .7 - .9
3	Vinten 547	70 mm	3 x 3	Double X Aerographic 2405	25A	Red (B.W.) .58 - .70
4	Vinten 547	70 mm	3 x 3	Double X Aerographic 2405	W12 + 58	Green (B.W.) .50 - .58
5	Vinten 547	70 mm	3 x 3	Aerochrome IR 2443	W12	I.R. (Color) .7 - .9

[a] CCRS Task No. 72-21.

TABLE 2

Scale of photography for each aircraft altitude and satellite imagery

Altitude (ft. ASL)	Original scale[a]		Scale of selected enlargements used		Ground Coverage[b]	
	RC 10	Vinten	RC 10	Vinten	230 mm RC 10	70 mm Vinten
					miles*	
17,000	1:58,230	1:63,000	1:52,500	1:63,000	7.5	2.2
37,000	1:126,700	1:144,800	1:50,000	1:54,000[c]	18.0	4.5
ERTS-1	1:1,000,000		1:250,000 1:50,000			

* 1 kilometer = .621 miles [a] 1 inch = 1 mile is 1:63,360

[b] miles across frame [c] Color I.R.: 1:50,000

Satellite data

The first data from ERTS-1 was obtained on August 23, 1972 (Frame No. 1031-17265). Photographs of imagery at scales of 1:1,000,000, 1:250,000 and 1:50,000 were obtained from a negative transparency produced at a scale 1:1,000,000 which had been enlarged from a 70-mm positive transparency produced from computer high-density tape by an Electron Beam Imager Recorder at the Canada Centre for Remote Sensing, Dept. of Energy, Mines and Resources, Ottawa. An illustration of the red and the infrared bands at scales of 1:250,000 and 1:50,000 are presented (Fig. 1A-B and 1E-F, respectively). A transferscope was used to transfer field boundaries from airborne imagery (enlarged from 1:144,800 to 1:50,000) to ERTS-1 imagery at a scale of 1:50,000 for Site A. The field boundaries were visually transferred for Sites B and C.

Numeric values from 0 to 5 were assigned according to the density of grey (0 dark and 5 light) on the "infrared" and red photos of Site A at a scale of 1:50,000. A classification key was established and calibrated to ground observation data. Using the "key", the remaining fields in Sites A and B were identified.

Acreage Estimates

Following identification of all fields in Site A, acreages of the 3 major classes of fields (cereals, rapeseed and fallow) were determined by grid counts from an overlay using the enlargement of the color I.R. 70-mm print (Scale 1:54,000, taken at 1:144,000). A small desk model line-digitizer was also used for area measurement. Acreage estimates were made on the ERTS-1 Black and White Infrared photo enlarged to a scale of 1:50,000 after identification of the entire site.

RESULTS

1. Crop Identification from Airborne Photography

The numeric values assigned to levels of grey density on airborne multi-spectral photography (black and white, red and infrared) showed that a number of classes of crops could be identified (Site A). It was observed that wheat could not be readily separated from barley (Table 3). From the photographs for the infrared radiation, the major classes that could be distinguished were: cereals, rapeseed and bushland, and fallow. From the photographs for the red radiation, the harvested cereals could be separated from non-harvested cereal fields. A classification key was developed using the infrared for the initial classification and refining it with the aid of red radiation data (Table 4). The ratios of I.R./Red values were studied but they appeared to be of little value.

The proportion of fields which were correctly and incorrectly identified is presented (Table 5). For example, of the twelve fields of cereals (headed), ten were correctly classified, one assigned erroneously to fallow, and one to grassland. All the rapeseed and fallow fieldswere correctly classified. However, of the total seven fields classified as fallow only six of them were actually fallow. Consequently acreage estimates based on this identification could result in somewhat high fallow estimates and low cereal estimates. Of the 25 fields tested in Site C, 23 were correctly identified, two were wrongly assigned.

A study of the stages of growth that the cereal crops had reached by July 13 and of the grey values for the cereal crops by late August showed that, except for a few fields of late crops the grey levels were inversely related to stage of growth (Fig. 2). By July 13, the late crops mentioned were < 26 cm in height compared to the general crop height of > 60 cm.

TABLE 3

Numeric grey scale values on airborne photography for ground identified fields along north and south of road in Site A grouped according to kind of crop

	Crop code	Grey scale values Black and White I.R.	Red	Green
Wheat-Headed	1H	3	1-4	2
Ripe-Cut	1C	3	5	3-4
Barley-Headed	3H	2-3	3-4	3
Ripe-Cut	3C	3	5	3-4
Rapeseed Napus	4	3.5-4	1-2	3-3.5
Campestris	5	3-4	3-4	4
Rye-Cut	8	3	5	4
Grassland	12	2	2	4
Bush-Bushland	14	5	1	2
Fallow-Black	15/16/17	1	1-3	1-2
-Weedy	18	1	1-2	1

H Headed near maturity (Standing)

C Harvested fields (i.e., cut)

B.W. Range: 5 represents low absorption, i.e., high reflection or light grey on photo.

0 represents high absorption, i.e., low reflection or dark grey on photo.

TABLE 4

Key for identification of fields developed from Ground Identified Fields in Site A using multi-band airborne photography.

Grey-scale values B.W. Photos			Crop identification	Crop code
I.R.	Red	Green		
4-5	1-2	2-3	Bush (Bushland)	(14)
3-4	3-4	4	Rapeseed - Campestris	(5)
3.5-4	1-2	3-3.5	Napus	(4)
3	5	4	Rye	(8)
3	5	3-4	Barley-Cut	(3C)
3	5	3-4	Wheat-Cut	(1C)
3	1-4	2-3	Wheat-Headed	(1H)
2-3	3-4	3	Barley-Headed	(3H)
2	2	2	Grassland	(12)
1	1-3	1-3	Fallow: Black/Trash	(15/17)
0-1	0-1	1-2	Fallow: Green Weeds	(18)

2. Crop Identification from Satellite Imagery

ERTS-1 imagery enlarged to a scale of 1:50,000 showed marked contrast in grey values among fields of cereals, rapeseed and fallowland (Table 6). Transferring field boundary lines from air photography enlarged from 1:126,700 to 1:50,000 provided sharp delineation of boundaries on the ERTS-1 imagery and enabled ready identification of field location (Fig. 1E and 1F). From the grey values a key was developed to assist in the classification of the "unknown" fields (Table 7). Infrared radiation values were used for the initial classification and refinements were based on red radiation values. Thus, rapeseed, cereals (cut/not harvested), and fallowland are readily classified from the calibrated data. The key was then used for Block C using imagery without the designated field coding (Table 8). The results showed that of the six cereal fields which were cut, the photoidentifier correctly identified all six. The nine cereal fields not harvested (Head) were correctly identified, but the photo identifier erroneously assigned one grass field and one fallow field to cereal crops.

TABLE 5

Identification test results for Site C using Classification Key developed from Airborne Photography of Site A

		Crop code	Ground Observed Identification					Total Seen by P.I.	Error committed
			Cereals Cut	Cereals Head	Rape-seed	Grass-land	Fallow		
Photo Identification	Cereals-Cut	1-3C						0	0
	Cereals-Head	1-3H		10				10	
	Rapeseed	4,5			7			7	
	Grassland	10-14		1				1	1
	Fallow	15-18		1			6	7	1
	Total fields		0	12	7	0	6	25	
	Error omitted by P.I.			2		0			

Total percentage correct identification 23/25 = 92%

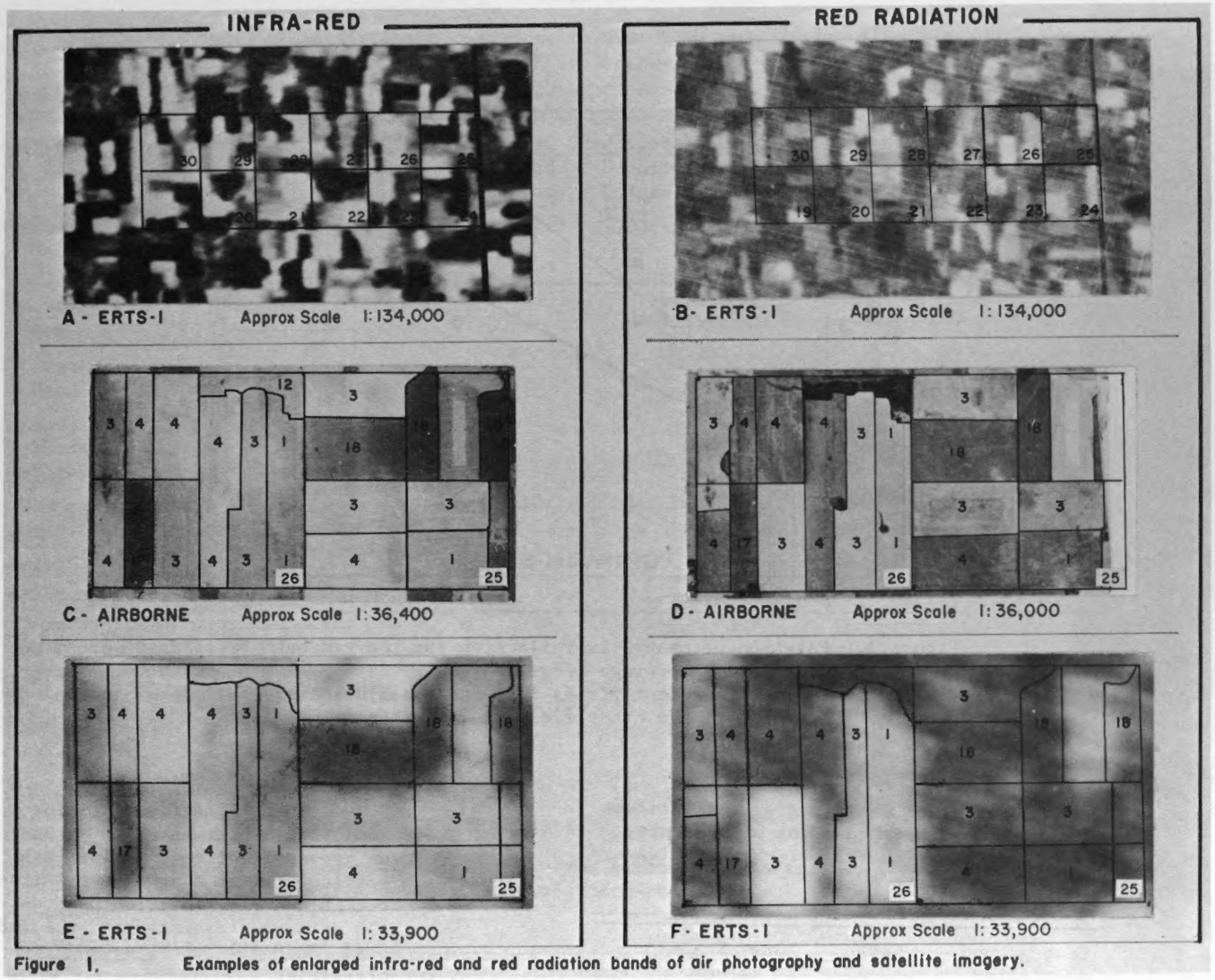

Figure 1 Examples of enlarged infrared and red radiation bands of air photography and satellite imagery.

The nine rapeseed fields were correctly identified. One fallow field was identified as grassland. It was not possible to separate the wheat and barley fields with a high level of certainty. It was possible however, to identify the headed cereals from the harvested cereals and easy to distinguish rapeseed from the cereals. Without knowledge of virgin land or bushland along streams, some confusion could occur between rapeseed and bushland. Thus, of the 44 fields only three were erroneously identified giving a 93% correct identification.

3. Acreage Estimates from Airborne and Satellite Imagery

Estimates of acreage for the three main classes of fields (cereals, rapeseed and fallow) from airborne and satellite imagery for Site A are reasonably similar for data obtained by: (1) grid overlay on I.R. Color (Airborne); (2) Mini-computer line digitizer on I.R. Color and (3) a grid overlay on ERTS-1 infrared imagery near a scale of 1:50,000 (Table 9).

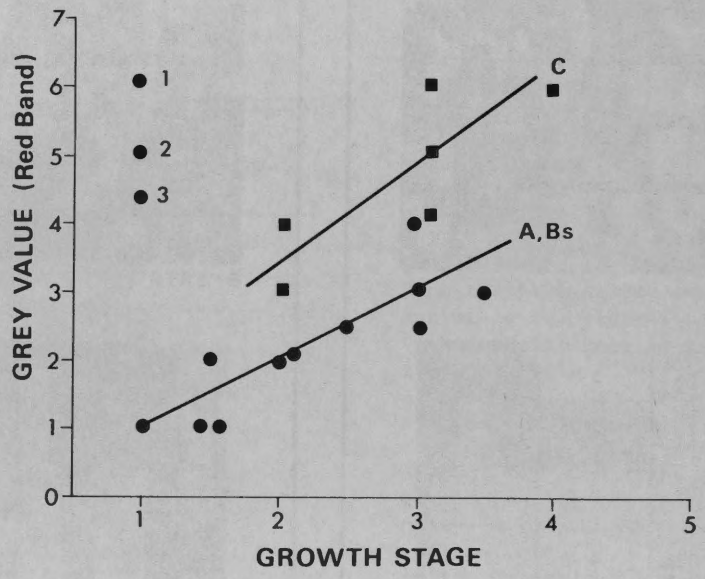

Figure 2. Relation of change in reflection for the red band by cereals (August 26) to stage of growth (July 13) for Site A. Points 1, 2, 3 represent fields 8-12 inches in height (July 13) compared to the other fields > 24 inches.

TABLE 6

Visual density grey-scale values established using a Kodak grey scale on ERTS black-white imagery in Site A

Crop ground identified	Code	Grey Scale Values	
		I.R.	Red
Wheat-Headed Cut	1H	2	1-2
	1C	4-5	4
Barley-Headed Cut	3H	1-3	2
	3C	4-5	4
Rye	8	1-5	4
Rapeseed-Napus Campestris	4	4-5	1-2
	5	3-4	1-4
Native Grassland	10	2	2
Grass	12	2	1
Bush/Bushland	14	4-5	0-1
Fallow fields	15-18	1	1

TABLE 7

Key of identification of fields from ERTS black-white photos based on ground identified fields in a portion of Site A using the infra-red (B and #7) radiation band as the primary classifier and the red band (Band #5) as the secondary classifier.

Grey-Scale Value on ERTS photo		Crop identification	Crop code
I.R. #7	Red #5		
4-5	0-1	Bush/Bushland	14
4-5	1-2	Rapeseed - Napus	4
3-4	1-4	Rapeseed - Campestris	5
4-5	4	Barley, Wheat-Cut	1C, 3C
2-5	2	Barley-Headed	3H
2-.4	1-2	Wheat-Headed	1H
2	1-2	Grassland	10/12
1	1	Fallow	15-18

TABLE 8

Identification test results from ERTS imagery for Site B as established from ERTS imagery in Site A

Crop	Crop code	Ground Observed Identification						Total seen by Photo Identifier	Error committed
		Cereals		Rapeseed		Bushland			
		Cut	Head	Napus	Camp.	Grass-land	Fallow-land		
Cereals - Cut	1-3	6						6	
Cereals - Head	1-3		9			1	1	11	
Rapeseed - Napus	4			8				8	
Rapeseed - Camp.	5				1			1	
Bushland Grassland	10 12					3		3	
Fallowland	15-18					1	13	14	1
Total fields in Site		6	9	8	1	5	14	44	
Error omitted by Photo Identifier		0	0	0	0	2	1		3

Total percentage correct identification $\frac{41}{44}$ = 93%

TABLE 9

Acreage estimates of several crops from airborne and satellite imagery (Black-White) for Site A using color infra-red and black-white, infra-red, respectively.

	Site A - Melfort south (12 sq. mile area) Area			Ratio:	
	Airborne I.R. (Color) Grid	Digitizer[a]	ERTS I.R. (B.W.)	Airborne I.R. (Color)	ERTS I.R. (B.W.)
	ac		ac		
Cereals	3350	3430	3312	.4362	.4313
Rapeseed	1805	1791	1700	.2350	.2213
Total Crop	5155	5133	5012		
Fallow	1738	1704	1615	.2263	.2102
Total	6893	6837	6627		

[a] Hewlett Packard Digitizer 9864A used in conjunction with H-P 9820A Calculator Mini-Computer - Courtesy L. Philpotts, Economics Branch. Time 3 1/2 hours.

DISCUSSION AND CONCLUSIONS

The results show that preliminary identification of such imagery may be conducted without sophisticated instrumentation. Initially, identification and acreage may be obtained using basically two radiation bands, one infrared and a red band (#6 or 7 and #5 - ERTS-1) enlarged to standard topo-survey map (1:50,000) supplemented by an overlay of small-scale airborne photography (e.g., 1:126,000) enlarged to comparable satellite scale. The inclusion of training sites containing fields identified from ground-based data is used to calibrate the airborne photography and satellite imagery from which a classification "key" is readily developed. Following verification of the key, fields within the imagery were identified to an accuracy > 90%. The calibration aspect of using a sample area of ground data within the area of unknown fields to be identified, precludes major source of error from photographic variation due to exposure and processing. The use of a simple numeric scale of six-steps in this study was sufficient to adequately identify the major groups of fields. It is doubtful if much greater number of steps would have appreciably increased the per cent fields correctly identified due to the range in density within each class (e.g., cereal-headed). The use of I.R. Color did assist to verify some of the identification made. It is, however, more difficult to assign numerical value to colored fields. Where densitometers are available, numeric grey-scale values may be read directly. In this study grey values varying from dark to light were arbitrarily scaled from 0 to 5 to correspond to low and high reflectance from the fields for each respective radiation band of both satellite and airborne black and white photographs.

Acreage estimates may readily be made using a grid overlay calibrated to the scale of the photography. However, a small desk-top mini-computer, if available for digitization of boundaries, greatly simplified area measurements. Precision of acreage estimates would be improved if the boundaries of the permanent and non-arable features were first transferred onto the satellite imagery from the airborne photography. This is particularly important where field boundaries are irregular, topography is rolling, bushland is of irregular areas, or if fields are $\leq$ 40 acres in size.

In this study rapeseed fields were readily identified from cereal crops because of their earlier stage of maturity. It was not possible to distinguish between the cereal crops (wheat, barley) as their maturity stages were rather close to each other.

Cereal fields which were cut were, readily identified from cereals not harvested and from rapeseed when both bands (I.R. and Red) were used. There was a tendency to classify on the air photographs some of the cereal fields as fallowland, and on the satellite imagery, some of the fallowland as cereals. Thus, acreage estimates would tend to be somewhat lower on air photos and higher on satellite imagery. Rapeseed radiation was somewhat confused with bushland reflection. However, if the location of the permanent bush features were known the fields could be excluded prior to identification.

ACKNOWLEDGEMENTS

The authors recognize the assistance of Drs. Nuttal and Waddington, Melfort Research Station and staff of the Plant Products Division, Agriculture Canada, Saskatoon, for ground observation data, Mr. G. Harder for processing of the data, the Graphics Unit and Mr. R. Lafrance for the illustrations, and Mr. L. Philpotts for many helpful suggestions.

REFERENCES

(1) Draeger, C. William. 1971. "The Use of Small Scale Aerial Photography in a Regional Agricultural Survey". Proc. Inter. Workshop on Earth Regources Survey Systems. May 3-4, 1971. Vol. II.

(2) Draeger, W.C. Agriculture Applications of ERTS-1 Data 1973. Symposium on Significant Results Obtained from the Earth Resources Technology Satellite-1. Vol. I. Technical Presentation Section App. 197-204. Paper A24. Sci. and Tech. Inform. Office National Aeronautics and Space Administration, Washington, D.C. NASA SP-327.

(3) Lauer, D.T. Testing Multi-Band and Multi-Date Photography for Crop Identification. Proc. Inter. Workshop on Earth Resources Survey Systems. May 3-4, 1971. Vol. II. Superintendent of Documents US Government Printing Office DC 20402.

(4) Pettiger, Lawrence. 1971. "Field data collection - an essential element in remote sensing applications". Proc. Inter. Workshop on Earth Resource Survey Systems. May 3-4. Vol. II.

(5) Weigand, C.L., R.W. Leamer, D.A. Weber, and A.H. Gerbermann. 1971. Multi-base and multi-emulsion space photos for crops and soils. Photogrammetric Engin. Feb. 147-156.

RESULTS OF COVER-TYPE CLASSIFICATION BY MAXIMUM LIKELIHOOD AND PARALLELEPIPED METHODS

By

DAVID GOODENOUGH
SEYMOUR SHLIEN

This paper presented at the Second Canadian Symposium on Remote Sensing, University of Guelph, Guelph, Ontario, April 29 - May 1, 1974.

RESULTS OF COVER-TYPE CLASSIFICATION BY MAXIMUM LIKELIHOOD AND PARALLELEPIPED METHODS

David Goodenough and Seymour Shlien
Canada Centre for Remote Sensing
2464 Sheffield Road
Ottawa, Ontario, Canada.

ABSTRACT

This paper describes the results of automatic ground cover classification utilizing the spectral intensities of ERTS-1 images. The methodology used for the interactive software classifier has been described in the preceding paper (Shlien and Goodenough, 1974). The classifier was used to distinguish crops and different types of vegetation and water in Manitoba and Ontario. The results are presented in the form of colour photographs showing regions before and after classification. The effects of ratioing and radiometric calibrations on the classifications are also visually presented. The accuracies of the classification are discussed. The lowest classification accuracies occurred with crop identification.

INTRODUCTION

In order to map and monitor Canadian resources by means of satellite imagery by, for example, ERTS-1, it is necessary to develop methods for automatic and rapid interpretation of the large volume of data generated. This paper describes the results of classifications for three areas by classification methods and with three preprocessing modes. The mathematical background for this paper was presented in a previous paper, Shlien and Goodenough, (1974), hereinafter referred to as Paper I.

The development of automatic classification methods follows three phases: (1) selection of the ground-cover classes to be distinguished; (2) selection of the features to discriminate the different classes; (3) selection of a scheme for deciding class membership. We chose, on the basis of available ground-truth information, three test sites, two near Winnipeg, Manitoba, and a third one centred on Thunder Bay, Ontario. Feature selection was restricted to the four spectral bands of the multispectral scanner (MSS) on board ERTS-1. Spatial and textural information were not included in this analysis. The decision scheme we chose for class discrimination was the Maximum Likelihood Decision Rule (MLDR) which minimizes the classification error provided the probability distributions associated with each of the classes are known exactly (Van Trees, 1968). Although this latter assumption is not strictly true for MSS imagery, the MLDR was favoured since it is a well established decision scheme.

As described in Paper I, the authors supplied the MLDR under two assumptions: (1) the spectral intensities were uniformly distributed within four-dimensional, rectangular parallelepiped; (2) the spectral intensities were distributed as Gaussian random variables. From the training data for each class one determines under the first assumption the minimum and maximum intensity values in each MSS band. These values define the parallelepiped in four-dimensional space. In the case of overlap between the classes, observed pixels with intensities in the overlap region are assigned to the class with the smallest volume; that is, the class with the maximum likelihood. Under the Gaussian assumption it is necessary to compute the logarithm of the likelihood of observing a pixel with intensity vector (i_1, i_2, i_3, i_4) for a given class with means (m_1, m_2, m_3, m_4) by equation 2 in Paper I. The pixel is assigned to the class with the maximum likelihood, provided this likelihood is above a predetermined threshold value. The threshold value is chosen to maximize the number of correct decisions.

PREPROCESSING CORRECTIONS

Before applying the two classifiers one may manipulate the image data to

enhance the accuracy achievable. We compared three possible manipulations or preprocessing modes: (1) no corrections to the raw ERTS-1 data; (2) application of radiometric corrections; (3) ratioing. The first mode requires the least computing time and the last mode, the most. The uneven response of the sensors in the multispectral scanner (Paper I; Strome and Vishnubatla, 1973) produces banding in the image. This paper answers quantatively the question of how much effect this banding has on classification accuracy.

The banding in an image results from differences in the relative gains of the various sensors with respect to each other. There are also changes in the absolute sensitivities of the photomultiplier tubes for bands 4, 5, and 6 and solid state detectors for band 7.

Many astronomical investigators (e.g. Hardie, 1962; Goodenough, 1969) have found for photomultiplier tubes that their relative spectral sensitivities are more constant than their absolute sensitivities. Atmospheric effects also contribute to variations in intensities observed by ERTS. The three most dominant factors affecting atmospheric extinction are: (1) molecular absorption bands; (2) molecular scattering; and (3) haze, which is almost a gray absorber. The wavelength dependence of extinction has been well determined by Abbott (1929) and Hiltner (1956). Changes in band intensities caused by spectrally gray variations in extinction can be overcome by utilizing the ratio of the intensity in one band with respect to another (Hardie, 1962).

A preliminary study of the advantages of ratioing for classification accuracy was carried out for three cloud-free scenes with little topographic relief. It had already been demonstrated (Goodenough, 1974) that ratioing for scenes with areas of high relief (with extensive shadows) or with clouds would increase classification accuracy. However, for cloud-free scenes with low relief the results for a classification with feature space axes of 4/5, 5/6, and 6/7 were disappointing. The intensity information in these scenes was significant and needed to be incorporated in the feature space. The shorter wavelength bands, 4 and 5, are more effected by the atmosphere than the infrared bands. We, therefore, examined feature spaces with axes (4/5, 5/6, 6, 7) or (4/5, 5/6, 6/7, 7) or (4/5, 5/6, 6/7, 6). Sequential forward feature selection was used to select that combination yielding the greatest divergence between classes (Goodenough and Shlien, 1974); namely, (4/5, 5/6, 6, 7) with all intensities linearized and radiometrically corrected. This feature space was used for all of the subsequent "ratio" classifications described in this paper.

TEST SITE RESULTS

(A) Thunder Bay, Ontario

Our first test site was an area centred on Thunder Bay, Ontario (Figure 1). The ERTS-1 frame E-1037-16192 used for this investigation was imaged on August 29, 1972. Ground-truth information was based on high and low altitude airborne imagery obtained for summer and winter and a recent land-use map (Ryerson, 1973). The following ground-cover classes were chosen as being compatible with the multispectral scanner data:

(1) Lake Superior - (blue) - water with a clear, uniform appearance;
(2) Urban - (green) - includes quarries, residential, industrial, and transportation networks;
(3) Softwoods - (red) - includes Black Spruce and Tamarack;
(4) River - (light blue) - includes the Dog River and inland, shallow lakes;
(5) Shore Water - (pink) - includes heavily sedimented water directly offshore from the city;
(6) Hardwoods and Mixed Forests- (yellow) - includes Trembling Aspen, Maple, Yellow Birch, and, unavoidably a few softwoods.

Classifications by the "parallelepiped" method are shown in Figure 2 for the three preprocessing modes, raw data (top panel), radiometrically corrected data (middle panel), and ratioing (bottom panel). Figure 3 is a similar presentation for the "Gaussian" method. The striping in the "shore water" classes for the raw data mode in Figures 2 and 3 results from banding in the original ERTS data. This banding in the classified portions of

Figure 2 and 3 is almost eliminated for radiometrically corrected data (middle panels) and ratioed data (bottom panels).

The decision regions for raw data, Gaussian classifications are shown projected onto MSS bands 6 and 7 in Figure 4. Radiometrically correcting the data reduces the overlap between ellipsoids of concentration, as demonstrated in Figure 5. The ratioed intensities are scaled to cover the gray-scale range available. By adjusting this scale factor one alters the relative importance of colour information, as represented by the ratioed data, with respect to intensity information. Scale factors are adjusted to produce the greatest divergences between classes. For example, the first feature Y for the ratioed mode was computed by the equation:

$$Y=(I4/I5)\cdot S$$

where I4 is the linearized and radiometrically corrected intensity for MSS band 4; I5 is the linearized and radiometrically corrected intensity for MSS band 5; and S is the scale factor. In this case S was set equal to 15.0.

A projection plot of decision regions for ratioed data for band 6 versus the ratio 4/5 is shown in Figure 6. Changes in the volumes of these four-dimensional ellipsoids of concentration by each of the preprocessing modes impacts on the results of the classifications, as can be seen from the confusion matrices given in Tables I, 2 and 3. These confusion matrices were derived by comparison of the training data with the classifications resulting from the classifiers. The average classification accuracies obtained by the "parallelepiped" method and the "Gaussian" method for the three preprocessing modes are summarized in Table 4. Classification accuracy is increased significantly if one utilizes radiometrically corrected data with a "Gaussian" classifier. Although Table 4 does not suggest any accuracy improvements are achieved by the use of ratioed data for this scene, we found by comparison with ground-truth information that the ratioed mode did permit greater overall accuracies to be achieved. Confusion matrices based on original training data can give only a partial indication of classification success. One must also look at the changes in the areal distributions of the themes for each preprocessing mode and classifier. In Table 5 we list the class areas for the 141 km^2 scene for each classifier and preprocessing mode. Note the substantial reduction in unclassified area (black) as one moves from uncorrected data to ratioed data. This effect is more noticeable on this frame than for our next two test sites because scanner sensor variation was much worse for this frame. Comparison with ground-truth data indicated this reduction in unclassified area was correct and that the most accurate results were obtained for the "Gaussian" classifier with ratioing as the preprocessing mode.

(B) Vegetation Region - Winnipeg, Manitoba

The second test site was a vegetation area southeast of Winnipeg, Manitoba (Figure 7). Ground-truth information for the ERTS-1 frame E-1007-16531 was provided by Thie (1973). The ground-cover classes chosen for this study were: (1) water - (blue); (2) Jack Pines - (green); (3) Black Spruce - (red); (4) Sedges - (light blue); (5) Trembling Aspen - (pink); (6) Community Pasture - (yellow); (7) Tamarack - (gray). The colour codes correspond to the classifications by "Gaussian" method and the "parallelepiped" method shown in Figures 8 and 9, respectively. The panels in these figures are arranged in order from top to bottom by processing mode: no corrections, radiometrically corrected data, and ratioed data. The distributions of classes remain fairly constant for the "Gaussian" classifier, but vary widely for the "parallelepiped" classifier for the three preprocessing modes. The distributions of Jack Pines, Black Spruce, and Tamarack are markedly different in the two pictures. Figure 8 (Gaussian) is the correct classification based on a comparison with ground-truth.

Insight into the differences between Figures 8 and 9 can be gained from

examination of the quantitative results. The Gaussian decision regions for uncorrected intensities are shown projected onto MSS bands 6 and 5 in Figure 10. Overlap occurs between classes 2(Jack Pines), 3(Black Spruce), and 7(Tamarack). With radiometrically corrected data the overlap between the decision regions for these three classes is reduced (Figure 11). Ratioing, as shown in Figure 12, reduces this overlap still further. The confusion matrices for the two classifiers and three preprocessing modes are given in Tables 6,, 7, and 8. The "parallelepiped" classifier is not able to classify "Black Spruce" accurately, but instead produces considerable confusion with "Tamarack". The "Gaussian" method produces a higher average classification accuracy for all preprocessing modes, as is evident from Table 9. There is no significant increase in accuracy by the use ratioing or radiometrically corrected data according to the confusion matrices and the results listed in Table 9. This is due to the fact that the radiometric errors are smaller than the scatter in intensities for the classes, unlike the situation found for the Thunder Bay test site.

Theme areas (Table 10) are approximately constant for the "Gaussian" classifier no matter which preprocessing mode is used. If we add together the percentage areas for Black Spruce, Jack Pines, and Tamarack, we find a total percentage of about 65% for the "parallelepiped" classifier and about 59% for the "Gaussian" classifier for each preprocessing mode. The large differences in theme areas between the two classifiers and their considerable differences in Figures 7 and 8 results from the extensive confusion between Black Spruce, Jack Pines and Tamarack for the "parallelepiped" classifier. Direct comparison with ground-truth leads us to conclude that the "Gaussian" classification is the more correct one, for all classes with the ratioing mode yielding slightly higher accuracy.

(C) Agricultural Region - Winnipeg, Manitoba

Classification of an agricultural area southeast of Winnipeg, Manitoba (Figure 13) was carried out using data from the ERTS-1 frame E-1007-16531. Ground-truth information was from a study of the area by Woo (1973). The agricultural classes Woo chose, and we used, were: (1) fallow (blue); (2) wheat (green); (3) grain stubble (red); (4) corn (light blue); (5) rapeseed (pink); (6) sunflower (yellow); (7) grainfield (grey). Colour-coded classifications for the "Gaussian" classifier and the "parallelepiped" classifier are given in Figures 14 and 15 respectively. The preprocessing order of the panels is the same as before. One sees extensive differences in the areal distributions of the crops for the two classification methods. Examination of the projection plots of the decision regions for uncorrected data (Figure 16), radiometrically corrected imagery (Figure 17), and ratioed data (Figure 18) reveals the considerable overlap between the decision regions. This is confirmed in the confusion matrices for the three preprocessing modes (Tables 11,12 and 13.

In each of the confusion matrices the four classes, grain, corn, sunflower, and grainfield, are heavily confused. The spectral means in the four bands differ by less than 1 part in 64 for grain (stubble), sunflower and grainfields. The corn class has means similar to the other three classes, but in addition, the corn class shows greater variation in infrared reflectivity than the other classes. The large overlapping scatter in spectral intensities for four of the classes makes detection of improvements in classification accuracy for different preprocessing modes impossible solely on the basis of confusion matrices, as one can see from Table 14.

Computation of theme areas (Table 15) over a large region and comparison of the resulting classifications with ground-truth can reveal which combination of classifier and preprocessing mode is most accurate. For this test site it was found that the "Gaussian" classifier with ratioed data produced the most accurate thematic map. The average accuracy achieved for the "Gaussian" classifier with ratioed imagery was 71%. Subsequent analysis by the authors of the ground-truth data (Woo, 1973) revealed a number of misidentifications of crops as a result of the difficulty in categorizing some crops by their

winter stubble. One should note the classification consistency in Table 15 for the "Gaussian" classifier for each preprocessing mode. For some purposes, the reduction by 6% (1900 acres) in an unclassified region may not be worth the added computational cost required for classification with ratioed data instead of uncorrected data.

CONCLUSIONS

Three test sites were mapped thematically by two classification methods (parallelepiped and Gaussian), both of which incorporated the Maximum Likelihood Decision Ruel, (MLDR) and for three preprocessing modes. The preprocessing modes involved the use of uncorrected data, or radiometrically corrected data, or ratioed imagery. Classification based only on the ratios of MSS bands 4/5, 5/6, and 6/7 proved ineffective. Sequential forward feature selection indicated a feature space made up of axes 4/5, 5/6, 6, and 7 for classification of these test sites would provide the greatest divergence between classes, and hence, the highest accuracy.

The results obtained imply the following conclusions:

1. Classification with the MLDR, with the assumption that the intensities are Gaussian random variables was the most accurate method of the two methods examined.

2. Radiometrically corrected data produced classifications with less confusion between classes based on training site computations.

3. For each test site, ratioed data yielded better classifications in the sense of higher accuracies when compared with ground-truth data available.

4. The highest accuracies achieved, averaged over the themes investigated, were: (a) Thunder Bay, Ontario - 98%; (b) Vegetation area - 94%; (c) agricultural area - 71%.

REFERENCES

Abbott, G. E., 1929, The Sun, P. 297 (New York; Appleton and Co.).

Goodenough, D., 1969, Six Colour Photometry of Galactic Clusters, Doctoral Thesis, University of Toronto.

Goodenough, D., and Shlien, S., 1974, "Automatic Classification Methodology", Aerospace Electronics Symposium - CASI, Victoria, British Columbia.

Goodenough, D., 1974, in preparation.

Hardie, R. H., 1962, "Photoelectric Reductions", in Astronomical Techniques, ed. Hiltner, (Chicago: University of Chicago Press).

Hiltner, W.A., 1956, Ap. J. Suppl., 2, 389.

Ryerson, R. A., 1973, private communication.

Shlien, S., and Goodenough, D., 1974, "A Quantitative Method for Determining the Information Content of ERTS Imagery for Terrain Classification", Second Canadian Symposium on Remote Sensing, Guelph, Ontario.

Thie, Jean, 1973, private communication.

Van Trees, H. L., 1968, Detection Estimation and Modulation Theory, Part 1, (New York: Wiley).

Woo, V., 1973, "Red River Crop Study", Technical Report, Manitoba Remote Sensing Office.

TABLE I

THUNDER BAY CLASSIFICATION

(NO CORRECTIONS)

CONFUSION MATRIX-PARALLELEPIPED

Chosen Class/True Class	Lake Superior	Urban	Softwoods	River	Shore Water	Hardwoods
No Class	0	0	0	0	0	0
Lake Superior	100	0	0	33	0	0
Urban	0	100	0	0	0	0
Softwoods	0	0	100	3	0	0
River	0	0	0	64	0	0
Shore Water	0	0	0	0	100	0
Hardwoods	0	0	0	0	0	100

CONFUSION MATRIX-GAUSSIAN

Chosen Class/True Class	Lake Superior	Urban	Softwoods	River	Shore Water	Hardwoods
No Class	0	1	0	0	0	0
Lake Superior	98	0	0	10	0	0
Urban	0	99	0	0	0	0
Softwoods	0	0	100	3	0	0
River	2	0	0	87	0	0
Shore Water	0	0	0	0	100	0
Hardwoods	0	0	0	0	0	100

AVERAGE SAMPLE SIZE = 450 ACRES PER CLASS

TABLE 2

THUNDER BAY CLASSIFICATION

(RADIOMETRIC CORRECTIONS)

CONFUSION MATRIX-PARALLELEPIPED

Chosen Class/True Class	Lake Superior	Urban	Softwoods	River	Shore Water	Hardwoods
No Class	0	0	0	0	0	0
Lake Superior	100	0	0	13	0	0
Urban	0	100	0	0	0	0
Softwoods	0	0	100	3	0	0
River	0	0	0	84	0	0
Shore Water	0	0	0	0	100	0
Hardwoods	0	0	0	0	0	100

CONFUSION MATRIX-GAUSSIAN

Chosen Class/True Class	Lake Superior	Urban	Softwoods	River	Shore Water	Hardwoods
No Class	0	2	0	0	0	0
Lake Superior	99	0	0	3	0	0
Urban	0	98	0	0	0	0
Softwoods	0	0	100	3	0	0
River	1	0	0	94	0	0
Shore Water	0	0	0	0	100	0
Hardwoods	0	0	0	0	0	100

AVERAGE SAMPLE SIZE = 450 ACRES PER CLASS.

TABLE 3

THUNDER BAY CLASSIFICATION

(RATIOING)

CONFUSION MATRIX-PARALLELEPIPED

Chosen Class/True Class	Lake Superior	Urban	Softwoods	River	Shore Water	Hardwoods
No Class	0	0	0	0	0	0
Lake Superior	100	0	0	7	0	0
Urban	0	100	0	0	0	0
Softwoods	0	0	100	3	0	0
River	0	0	0	83	0	0
Shore Water	0	0	0	7	100	0
Hardwoods	0	0	0	0	0	100

CONFUSION MATRIX-GAUSSIAN

Chosen Class/True Class	Lake Superior	Urban	Softwoods	River	Shore Water	Hardwoods
No Class	1	1	0	0	0	0
Lake Superior	98	0	0	3	0	0
Urban	0	99	0	0	0	0
Softwoods	0	0	100	3	0	0
River	1	0	0	94	0	0
Shore Water	0	0	0	0	100	0
Hardwoods	0	0	0	0	0	100

AVERAGE SAMPLE SIZE = 450 ACRES PER CLASS.

TABLE 4

THUNDER BAY

-AVERAGE CLASSIFICATION ACCURACIES-

CLASSIFIER	PREPROCESSING MODE		
	NO CORRECTIONS	RADIOMETRICALLY CORRECTED	RATIOED
PARALLELEPIPED	94%	97%	97%
GAUSSIAN	97%	98.5%	98.5%

TABLE 5

THUNDER BAY CLASSIFICATION

THEME AREAS

A. Parallelepiped

Class/Method	No Corrections	Radiometric Corrections	Ratioing
Blank	32%	21%	18%
Lake Superior	18	17	17
Urban	23	25	24
Softwoods	11	15	15
River	2	3	4
Shore Water	4	4	7
Hardwoods	10	15	15

B. Gaussian

Class/Method	No Corrections	Radiometric Corrections	Ratioing
Blank	32%	17%	11%
Lake Superior	15	15	14
Urban	24	30	31
Softwoods	9	13	14
River	2	6	6
Shore Water	7	5	5
Hardwoods	12	13	19

TOTAL CLASSIFIED AREA = 31,500 ACRES

TABLE 6

WINNIPEG, MANITOBA

-VEGETATION REGION-

(NO CORRECTIONS)

CONFUSION MATRIX-PARALLELEPIPED

Chosen Class/True Class	Water	Jack Pines	Black Spruce	Sedges	Trembling Aspen	Community Pasture	Tamarack
Blank	0	0	0	0	0	0	0
Water	100	0	0	0	0	0	0
Jack Pines	0	52	0	0	0	0	0
Black Spruce	0	42	35	0	0	0	0
Sedges	0	3	0	100	0	0	0
Trembling Aspen	0	0	1	0	100	0	0
Community Pasture	0	0	0	0	0	100	0
Tamarack	0	3	64	0	0	0	100

CONFUSION MATRIX-GAUSSIAN

Chosen Class/True Class	Water	Jack Pines	Black Spruce	Sedges	Trembling Aspen	Community Pasture	Tamarack
Blank	0	0	1	0	1	1	1
Water	100	0	0	0	0	0	0
Jack Pines	0	87	6	0	0	0	0
Black Spruce	0	10	78	0	0	0	10
Sedges	0	3	0	100	0	0	0
Trembling Aspen	0	0	1	0	99	0	0
Community Pasture	0	0	0	0	0	99	0
Tamarack	0	0	14	0	0	0	90

AVERAGE SAMPLE SIZE = 430 acres PER CLASS.

TABLE 7

WINNIPEG, MANITOBA

-VEGETATION REGION-

(RADIOMETRIC CORRECTIONS)

CONFUSION MATRIX-PARALLELEPIPED

Chosen Class/True Class	Water	Jack Pines	Black Spruce	Sedges	Trembling Aspen	Community Pasture	Tamarack
Blank	0	0	0	0	0	0	0
Water	100	0	0	0	0	0	0
Jack Pines	0	96	37	0	0	0	0
Black Spruce	0	0	3	0	0	0	0
Sedges	0	3	0	100	0	0	0
Trembling Aspen	0	0	1	0	100	0	0
Community Pasture	0	0	0	0	0	100	0
Tamarack	0	1	59	0	0	0	100

CONFUSION MATRIX-GAUSSIAN

Chosen Class/True Class	Water	Jack Pines	Black Spruce	Sedges	Trembling Aspen	Community Pasture	Tamarack
Blank	0	0	1	0	0	1	0
Water	100	0	0	0	0	0	0
Jack Pines	0	91	6	0	0	0	0
Black Spruce	0	7	81	0	0	0	11
Sedges	0	3	0	100	0	0	0
Trembling Aspen	0	0	1	0	100	0	0
Community Pasture	0	0	0	0	0	99	0
Tamarack	0	0	11	0	0	0	89

AVERAGE SAMPLE SIZE = 430 ACRES PER CLASS.

TABLE 8

WINNIPEG, MANITOBA

-VEGETATION REGIONS-

(RATIOING)

CONFUSION MATRIX-PARALLELEPIPED

Chosen Class/True Class	Water	Jack Pines	Black Spruce	Sedges	Trembling Aspen	Community Pasture	Tamarack
Blank	0	0	0	0	0	0	0
Water	100	0	0	0	0	0	0
Jack Pines	0	95	33	0	0	0	0
Black Spruce	0	0	6	0	0	0	0
Sedges	0	5	0	100	0	0	0
Trembling Aspen	0	0	2	0	100	0	0
Community Pasture	0	0	0	0	0	100	0
Tamarack	0	0	59	0	0	0	100

CONFUSION MATRIX-GAUSSIAN

Chosen Class/True Class	Water	Jack Pines	Black Spruce	Sedges	Trembling Aspen	Community Pasture	Tamarack
Blank	0	0	1	0	1	0	1
Water	100	0	0	0	0	0	0
Jack Pines	0	92	4	0	0	0	0
Black Spruce	0	5	80	0	0	0	10
Sedges	0	3	0	100	0	0	0
Trembling Aspen	0	0	0	0	99	0	0
Community Pasture	0	0	0	0	0	100	0
Tamarack	0	0	14	0	0	0	90

AVERAGE SAMPLE SIZE = 430 ACRES PER CLASS.

TABLE 9

WINNIPEG, MANITOBA

-VEGETATION REGION-

AVERAGE CLASSIFICATION ACCURACY

CLASSIFIER	PREPROCESSING MODE		
	UNCORRECTED	RADIOMETRICALLY CORRECTED	RATIOED
PARALLELEPIPED	84±2.84%	86%	86%
GAUSSIAN	93%	94%	94%

TABLE 10

WINNIPEG, MANITOBA

-VEGETATION CLASSIFICATION-

THEME AREAS

A. PARALLELEPIPED

Class/Method	No Corrections	Radiometric Corrections	Ratioing
Blank	9%	13%	0.3%
Water	0	0	0
Jack Pines	1	12	10
Black Spruce	10	2	2
Sedges	6	5	7
Trembling Aspen	13	14	15
Community Pasture	4	3	13
Tamarack	57	49	53

B. GAUSSIAN

Class/Method	No Corrections	Radiometric Corrections	Ratioing
Blank	26%	28%	27%
Water	0	0	0
Jack Pines	5	4	4
Black Spruce	28	31	28
Sedges	5	5	5
Trembling Aspen	10	10	10
Community Pasture	0.2	0.5	0.5
Tamarack	25	22	27

TOTAL CLASSIFIED AREA = 31,500 ACRES

TABLE 11

WINNIPEG, MANITOBA

-AGRICULTURAL REGION-

(NO CORRECTIONS)

CONFUSION MATRIX-PARALLELEPIPED

Chosen Class/True Class	Fallow	Wheat	Grain	Corn	Rapeseed	Sunflower	Grainfield
Blank	0	0	0	0	0	0	0
Fallow	100	0	0	0	0	0	0
Wheat	0	99	3	4	0	0	3
Grain	0	0	39	0	0	0	21
Corn	0	0	0	38	0	0	15
Rapeseed	0	0	0	0	100	0	1
Sunflower	0	1	59	57	0	100	50
Grainfield	0	0	0	0	0	0	10

CONFUSION MATRIX-GAUSSIAN

Chosen Class/True Class	Fallow	Wheat	Grain	Corn	Rapeseed	Sunflower	Grainfield
Blank	0	0	3	0	0	0	1
Fallow	100	0	0	0	0	0	0
Wheat	0	99	1	3	0	2	3
Grain	0	1	43	3	0	5	15
Corn	0	0	0	60	0	18	12
Rapeseed	0	0	0	0	100	0	1
Sunflower	0	0	49	25	0	75	31
Grainfield	0	0	5	9	0	0	38

AVERAGE SAMPLE SIZE=109 ACRES PER CLASS

TABLE 12

WINNIPEG, MANITOBA

-AGRICULTURAL REGION-

(RADIOMETRIC CORRECTIONS)

CONFUSION MATRIX-PARALLELEPIPED

Chosen Class / True Class	Fallow	Wheat	Grain	Corn	Rapeseed	Sunflower	Grainfield
Blank	0	0	0	0	0	0	0
Fallow	100	0	0	0	0	0	0
Wheat	0	100	3	3	0	7	5
Grain	0	0	41	0	0	0	21
Corn	0	0	56	73	0	58	48
Rapeseed	0	0	0	0	100	0	0
Sunflower	0	0	0	24	0	35	15
Grainfield	0	0	0	0	0	0	12

CONFUSION MATRIX-GAUSSIAN

Chosen Class / True Class	Fallow	Wheat	Grain	Corn	Rapeseed	Sunflower	Grainfield
Blank	0	0	3	0	0	0	0
Fallow	100	0	0	0	0	0	0
Wheat	0	99	1	2	0	4	2
Grain	0	1	39	0	0	12	23
Corn	0	0	1	55	0	16	12
Rapeseed	0	0	0	0	100	0	0
Sunflower	0	0	44	35	0	67	27
Grainfield	0	0	13	8	0	2	36

AVERAGE SAMPLE SIZE = 109 ACRES PER CLASS

TABLE 13

WINNIPEG, MANITOBA

-AGRICULTURAL REGION-

(RATIOING)

CONFUSION MATRIX-PARALLELEPIPED

Chosen Class/True Class	Fallow	Wheat	Grain	Corn	Rapeseed	Sunflower	Grainfield
Blank	0	0	0	0	0	0	0
Fallow	100	0	0	0	0	0	0
Wheat	0	100	3	0	0	7	6
Grain	0	0	30	1	0	0	15
Corn	0	0	0	34	0	0	7
Rapeseed	0	0	0	0	100	0	1
Sunflower	0	0	67	65	0	93	68
Grainfield	0	0	0	0	0	0	4

CONFUSION MATRIX-GAUSSIAN

Chosen Class/True Class	Fallow	Wheat	Grain	Corn	Rapeseed	Sunflower	Grainfield
Blank	0	0	1	0	0	0	0
Fallow	100	0	0	0	0	0	0
Wheat	0	99	1	2	0	5	3
Grain	0	1	31	0	0	7	20
Corn	0	0	3	55	0	7	13
Rapeseed	0	0	0	0	100	0	0
Sunflower	0	0	50	39	0	77	30
Grainfield	0	0	14	3	0	4	34

AVERAGE SAMPLE SIZE = 109 ACRES PER CLASS.

TABLE 14

-AGRICULTURAL REGION-

AVERAGE CLASSIFICATION ACCURACY

CLASSIFIER	PREPROCESSING MODE		
	UNCORRECTED	RADIOMETRICALLY CORRECTED	RATIOED
PARALLELEPIPED	69%	66%	66%
GAUSSIAN	74%	71%	71%

TABLE 15

WINNIPEG, MANITOBA

-AGRICULTURAL CLASSIFICATION-

THEME AREAS

A. PARALLELEPIPED

Class/Method	No Corrections	Radiometric Corrections	Ratioing
Blank	22%	14%	13%
Fallow	9	9	9
Wheat	29	31	30
Grain	15	25	23
Corn	3	13	4
Rapeseed	2	2	2
Sunflower	17	3	17
Grainfield	2	3	0.4

B. GAUSSIAN

Class/Method	No Corrections	Radiometric Corrections	Ratioing
Blank	14%	11%	8%
Fallow	13	13	14
Wheat	21	20	25
Grain	13	14	11
Corn	8	6	6
Rapeseed	3	3	3
Sunflower	8	9	10
Grainfield	20	23	23

TOTAL CLASSIFIED AREA = 31,500 ACRES

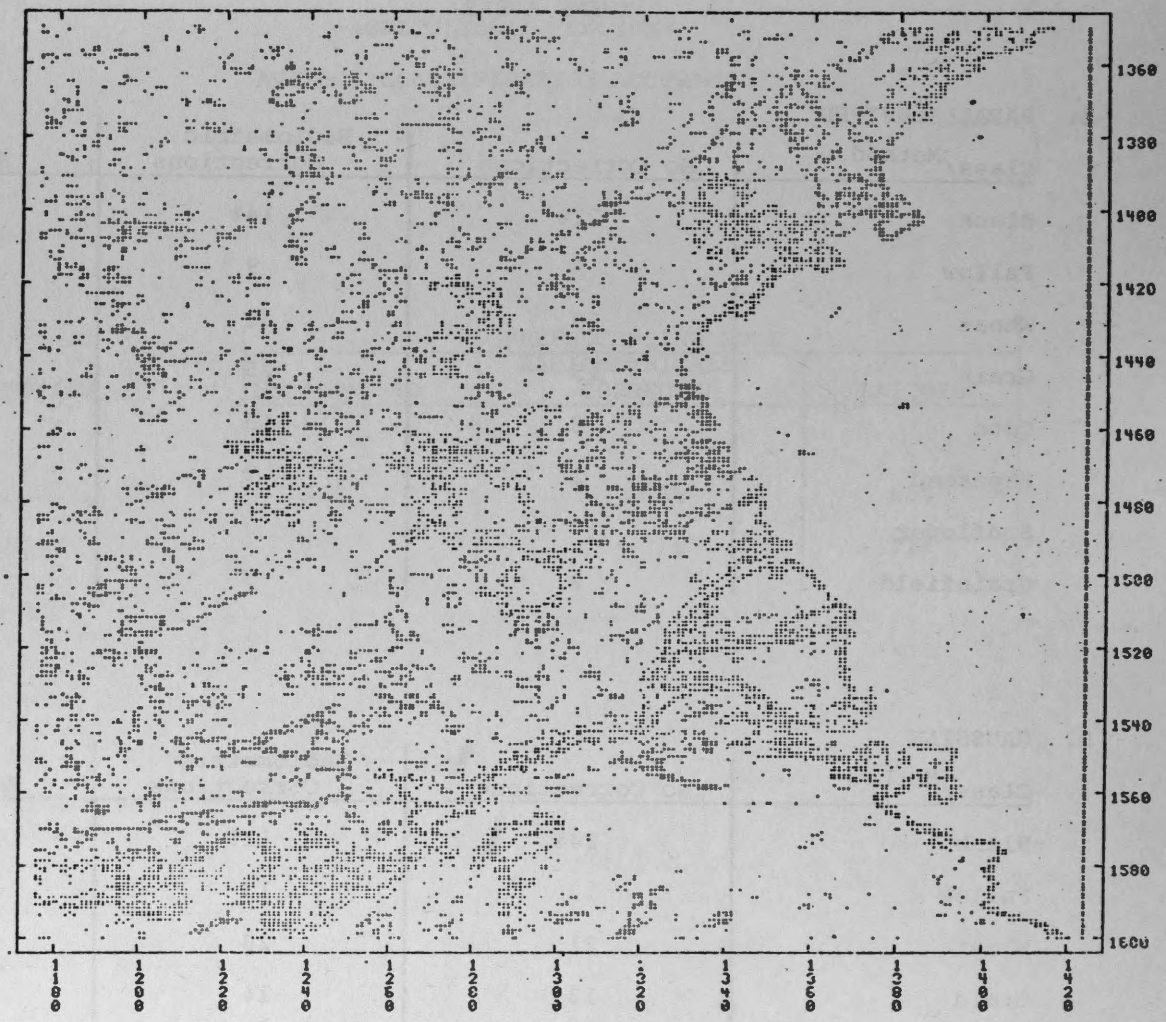

Figure 1

The Thunder Bay, Ontario, region (38 km by 29 km) as seen in the ERTS-1 frame E-1037-16192. The plotted points denote areas of rapidly varying spectral signature. The large, white area on the right of the figure is a portion of Lake Superior.

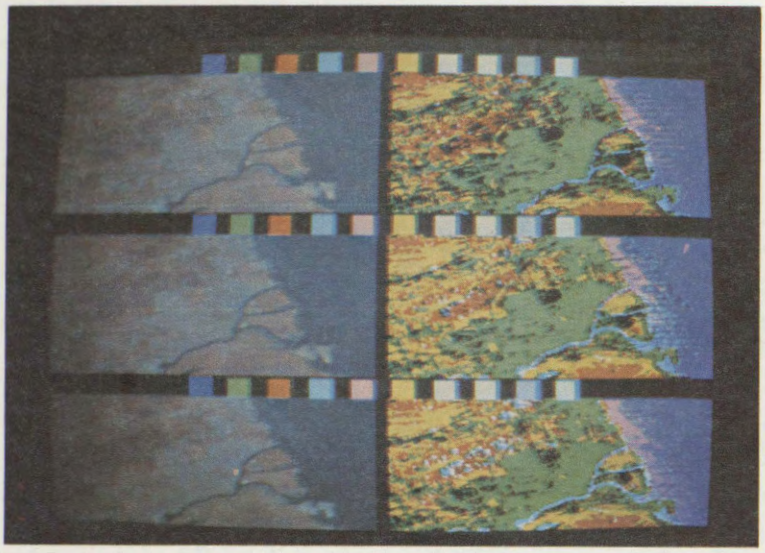

Figure 2

Classifications by the "parallelepiped" method are shown on the right-hand portion of this photograph. The same Thunder Bay, Ontario scene is shown before classification on the left side of this figure. Each panel shows an area of 31,500 acres. The top panel is classification with no corrections applied to the data. Radiometrically corrected data were used for the classification shown in the middle panel. Classification with ratioed data appears in the bottom panel. The class colour codes are: (1) blue - Lake Superior; (2) green - Urban; (3) red - Softwoods; (4) light blue - River; (5) pink - Shore Water; (6) yellow - Hardwoods and Mixed Forests. Radiometric corrections can be seen to reduce greatly the striping in the Shore Water theme (pink). The unclassified regions (black) are considerably reduced with the ratioed imagery.

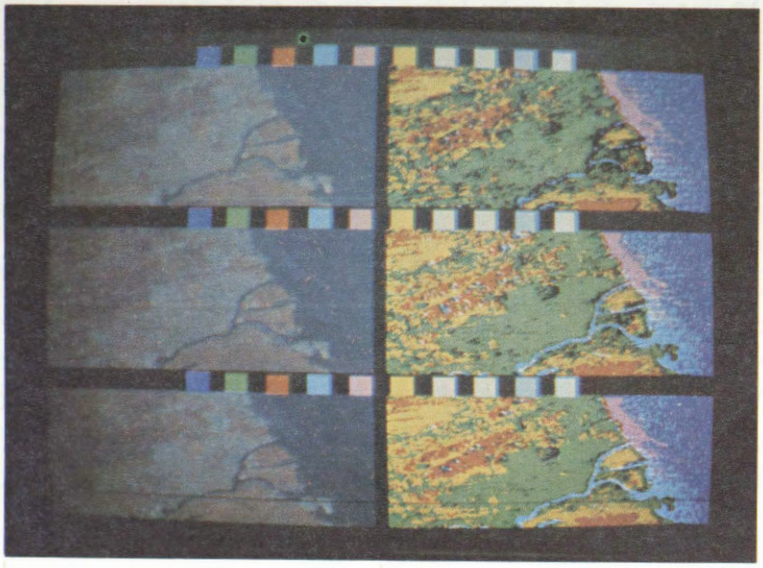

Figure 3

Classifications by the "Gaussian" method for the same Thunder Bay, Ontario scene shown in Figure 2. The classifications are ordered from top to bottom by preprocessing mode: no corrections, radiometric corrections, and ratioed data. Improvements are noted in classification when one uses radiometrically corrected data (middle panel) which eliminates the banding resulting from differences in sensor gains. Comparison of Figures 2 and 3 reveals to us the sharp and correct reduction in unclassified area (black) for the "Gaussian" classifier with ratioing (bottom panel).

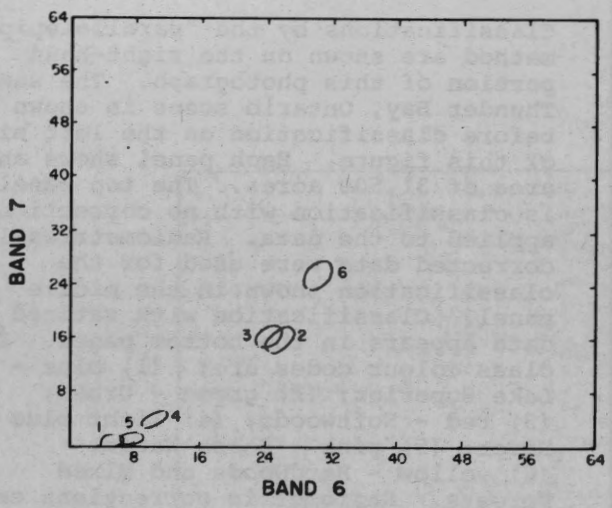

Figure 4

The projection plot for uncorrected bands 6 and 7 for frame E-1037-16192 (Thunder Bay, Ontario) is shown with the following classes: (1) Lake Superior; (2) Urban; (3) Softwoods; (4) River; (5) Shore Water; (6) Hardwoods - mixed. The intensities are assumed here to be distributed as Gaussian random variables.

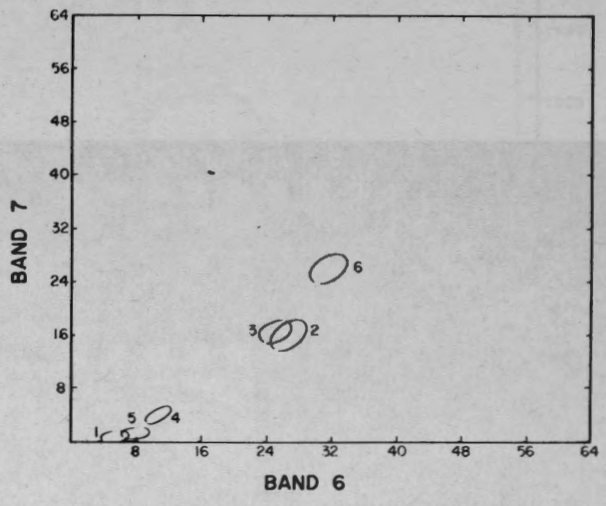

Figure 5

Projection plot for Thunder Bay, Ontario (frame E-1037-16192) for the radiometrically corrected MSS bands 6 and 7 showing the following ellipsoids of concentration: (1) Lake Superior; (2) Urban; (3) Softwoods; (4) River; (5) Shore Water; (6) Hardwoods - mixed.

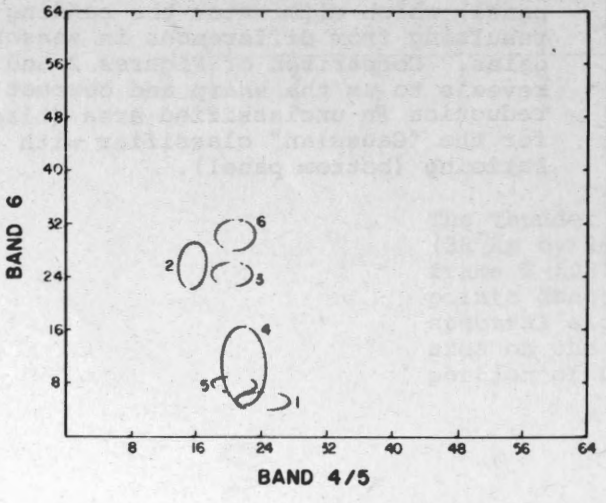

Figure 6

This projection plot gives the decision regions for the radiometrically corrected band 6 versus the ratio of bands 4/5, The Thunder Bay, Ontario classes shown are: (1) Lake Superior; (2) Urban; (3) Softwoods; (4) River; (5) Shore Water; (6) Hardwoods - mixed.

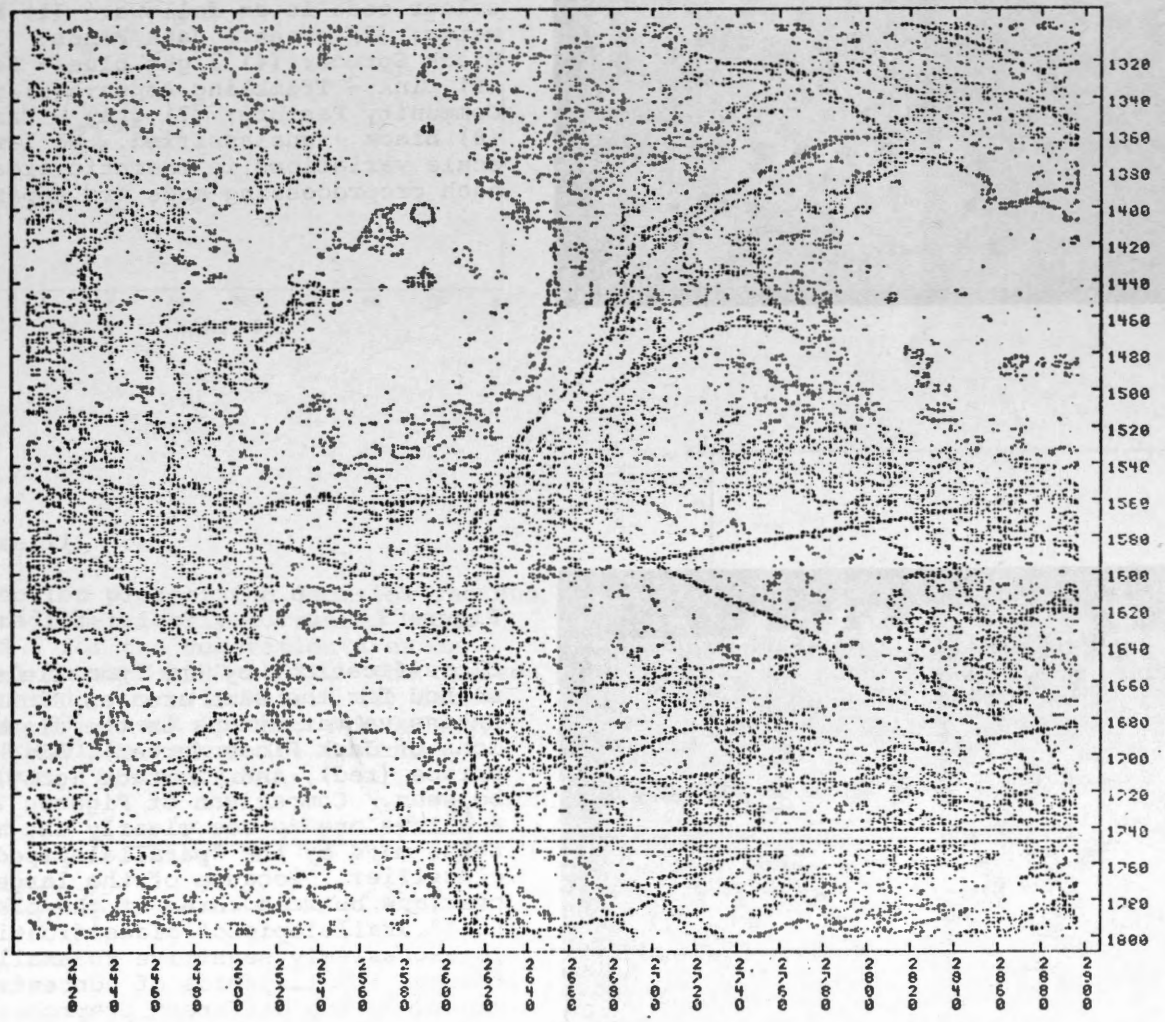

Figure 7

The vegetation area southeast of Winnipeg, Manitoba, is shown in this diagram (38 km by 29 km) which shows points of rapidly varying spectral signature as seen on the ERTS-1 frame E-1007-16531.

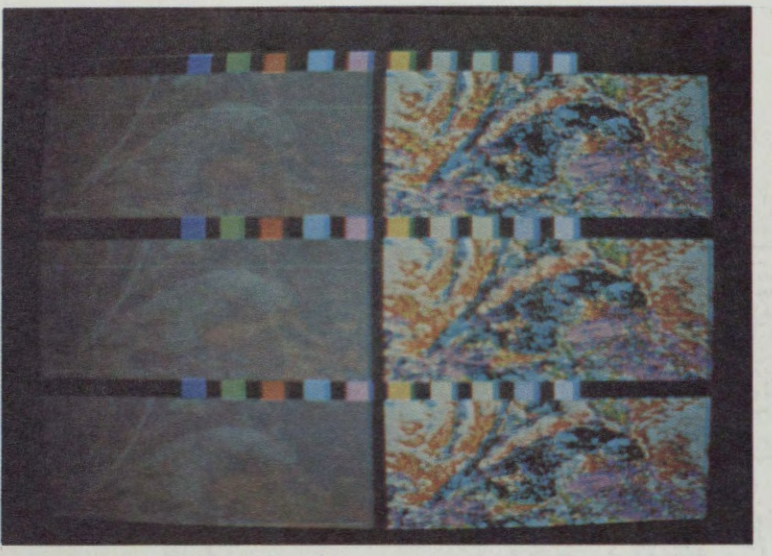

Figure 8

This is a photograph of classifications by the "Gaussian" method for a vegetation region in southeastern Manitoba as seen on ERTS-1 frame E-1007-16531. The panels are in the same order as used previously for Figure 2. The colour code is as follows: (1) blue - water; (2) green - Jack Pines; (3) red - Black Spruce; (4) light blue - Sedges; (5) pink - Trembling Aspen; (6) yellow - Community Pasture; (7) gray - Tamarack; (8) black - unclassified. No large scale variations in thematic areas with each preprocessing mode are apparent.

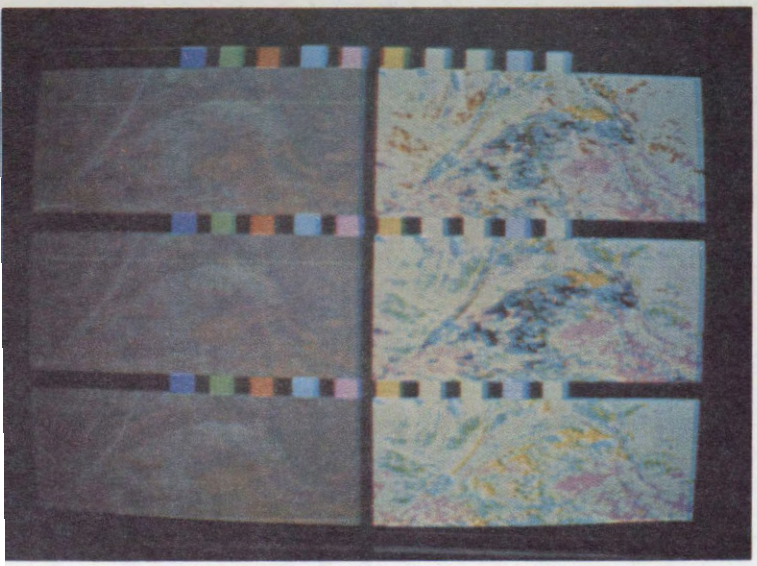

Figure 9

Classifications by the "parallelepiped" method for the same area as Figure 8. Extensive variations in the distributions of Jack Pines (green), Black Spruce (red), and Tamarack (gray) can be seen. Comparison of Figures 7 and 8 allows one to see clearly the mistakes made by the "parallelepiped" classifier. Because of the large overlaps between three of the classes, the "parallelepiped" classification is excessively sensitive to small changes in ellipsoids of concentration caused by the different preprocessing modes.

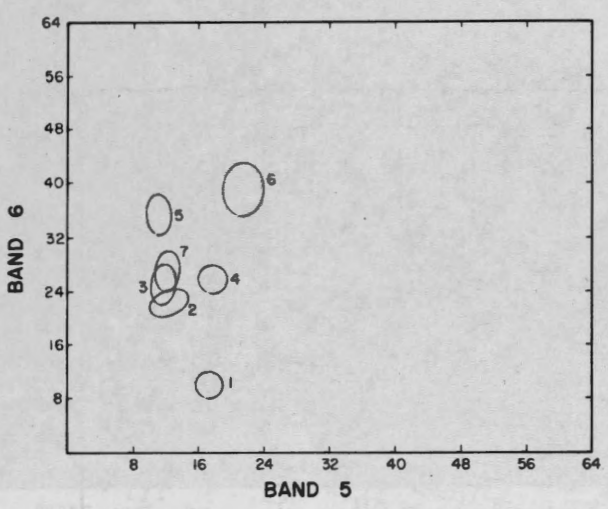

Figure 10

This figure shows the decision regions for uncorrected bands 6 and 5 for the vegetation area on ERTS-1 frame E-1007-16531. The classes are: (1) Water; (2) Jack Pines; (3) Black Spruce; (4) Sedges; (5) Trembling Aspen; (6) Community Pasture; (7) Tamarack.

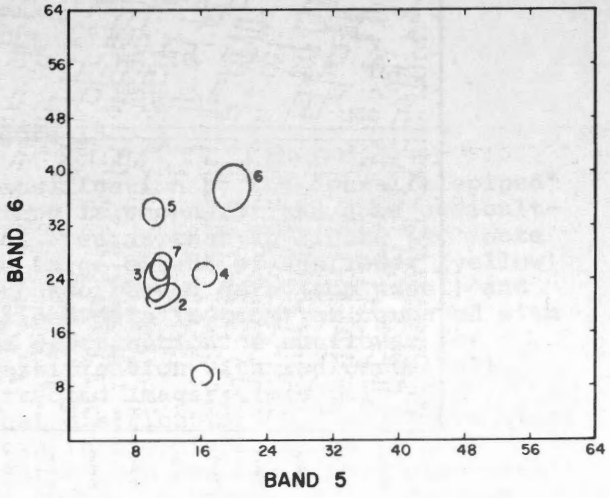

Figure 11

Projection plot of the decision regions for radiometrically corrected bands 6 and 5 for the vegetation area on ERTS-1 frame E-1007-16531. The classes indicated are: (1) Water; (2) Jack Pines; (3) Black Spruce; (4) Sedges; (5) Trembling Aspen; (6) Community Pasture; (7) Tamarack.

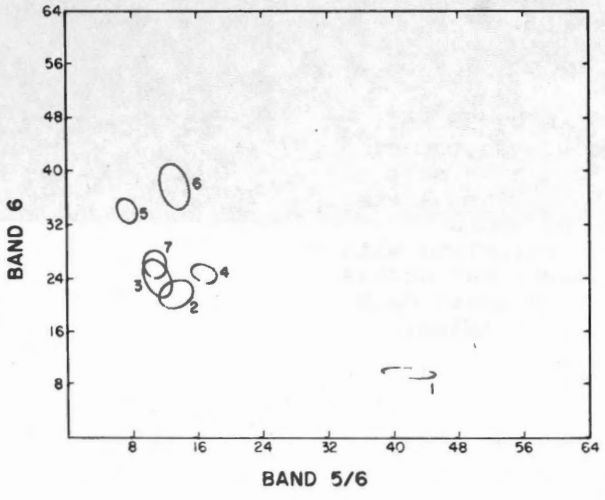

Figure 12

Projection plot for vegetation area near Winnipeg, Manitoba (E-1007-16531) for band 6 versus the band ratio 5/6. The decision regions shown are: (1) Water; (2) Jack Pines; (3) Black Spruce; (4) Sedges; (5) Trembling Aspen; (6) Community Pasture; (7) Tamarack.

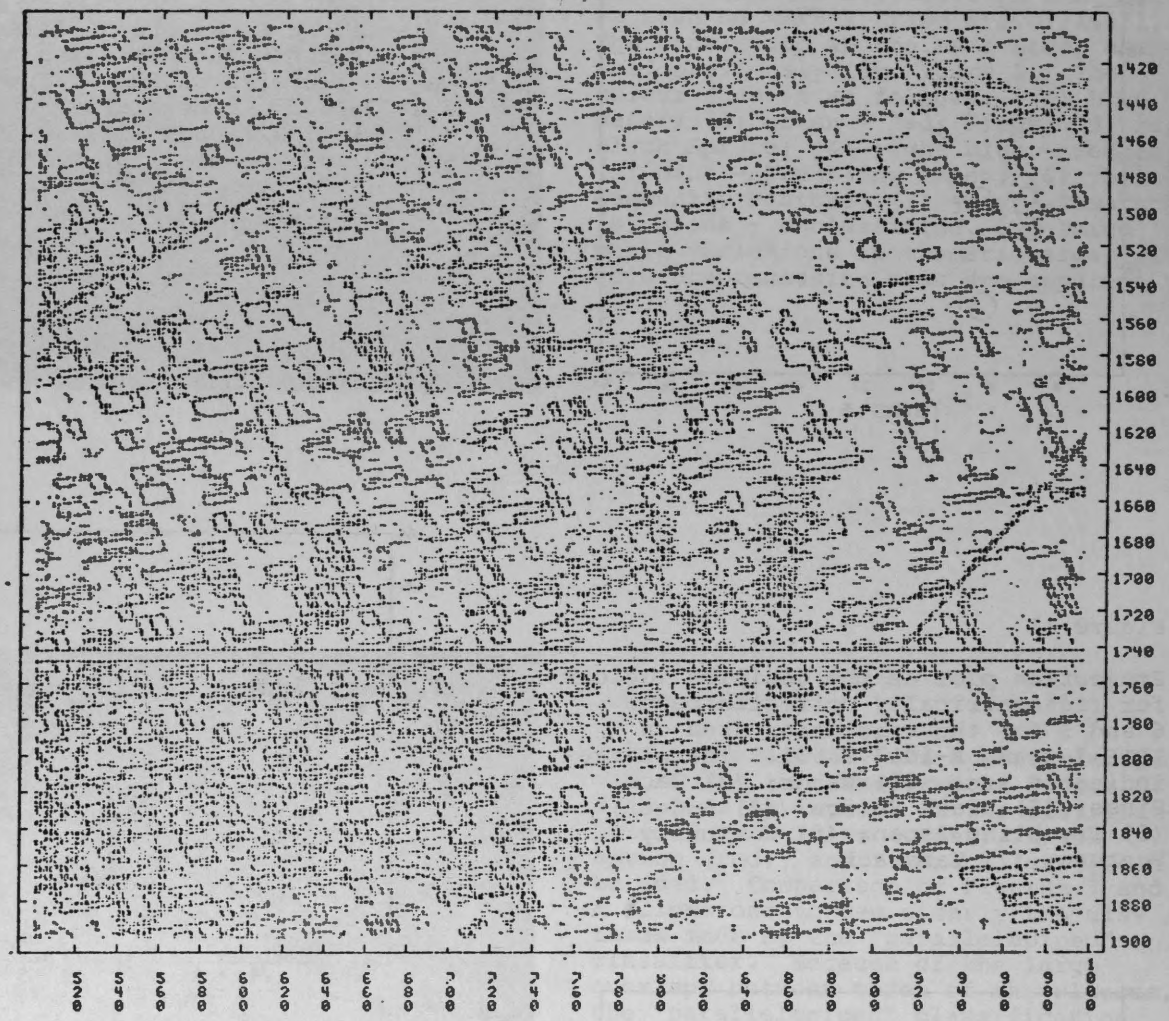

Figure 13

This diagram shows a 38 km by 29 km agricultural region located southwest of Winnipeg, Manitoba, as shown on the ERTS-1 frame E-1007-16531. The plotted points indicate regions of rapid spectral variation which correlate with field boundaries. The white bar across the frame at line 1740 represents data lost during satellite transmission.

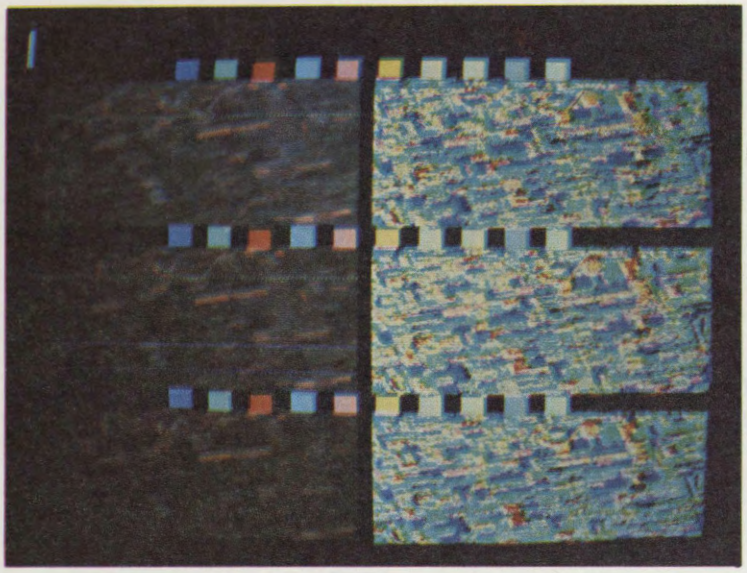

Figure 14

This photograph of an agricultural area near Winnipeg, Manitoba shows classifications by the "Gaussian" method for three preprocessing modes: no corrections (top); radiometric corrections (middle); ratioed data (bottom). The class colour codes are: (1) blue - fallow; (2) green - wheat; (3) red - grain stubble; (4) light blue - corn; (5) pink - rapeseed; (6) yellow - sunflower; (7) grey - grainfield; (8) black - unclassified. Radiometric corrections remove most of the banding in the rapeseed (pink) classification. The use of ratioed data produces a more distinct classification as can be seen by the crisp field delineations and the correct reduction in unclassified area.

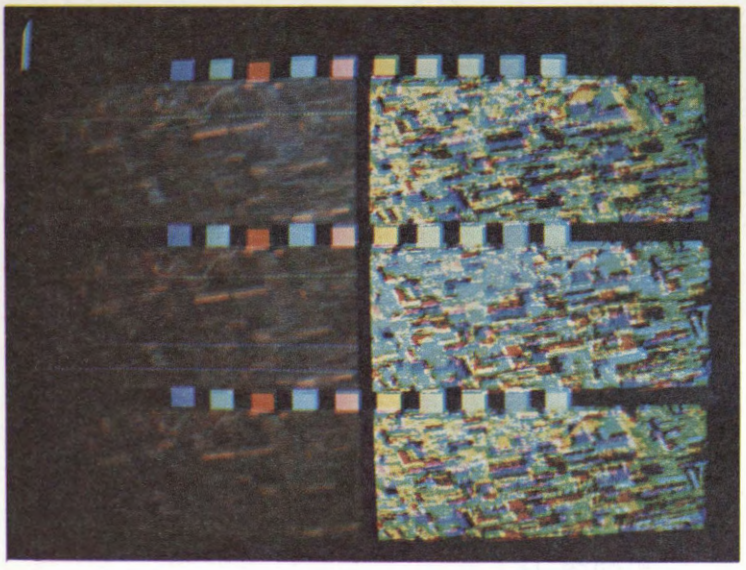

Figure 15

Classification by the "parallelepiped" method is shown for the same agricultural area as that in Figure 14. Note the large extent of sunflower (yellow) for uncorrected data (top panel) and ratioed data (bottom) as compared with the distribution of sunflower for classification with radiometrically corrected imagery (middle). The areal distribution of corn (light blue) shown in the middle panel is much greater than for the other preprocessing modes. A comparison of Figures 14 and 15 reveals extensive misclassification of grain stubble (red) and grainfields (gray) by the "parallelepiped" classifier. The "Gaussian" classifier provides also a more accurate identification of fallow field (blue) distribution than the "parallelepiped" classifier.

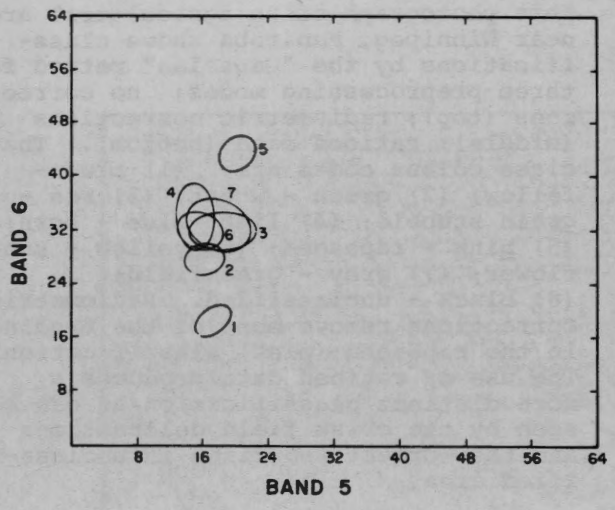

Figure 16

The decision regions for the agricultural area are projected onto uncorrected bands (5, 6) for ERTS frame E-1007-16531. The classes shown are: (1) Fallow; (2) Wheat; (3) Grain Stubble; (4) Corn; (5) Rapeseed; (6) Sunflower; (7) Grainfield.

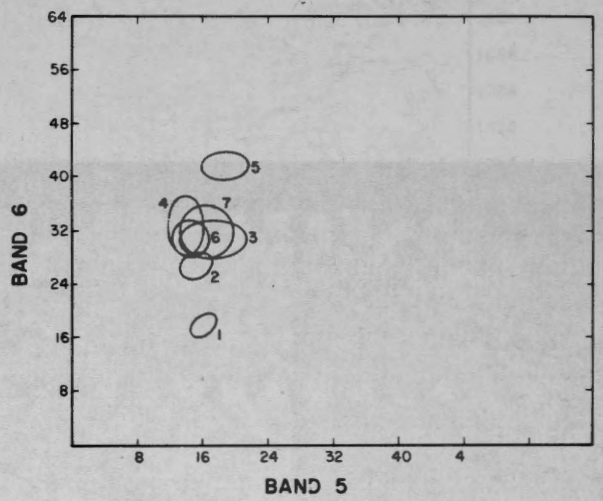

Figure 17

Projection plot of radiometrically corrected bands (5, 6) for the agricultural area of ERTS frame E-1007-16531 showing the following regions: (1) Fallow; (2) Wheat; (3) Grain Stubble; (4) Corn; (5) Rapeseed; (6) Sunflower; (7) Grainfield.

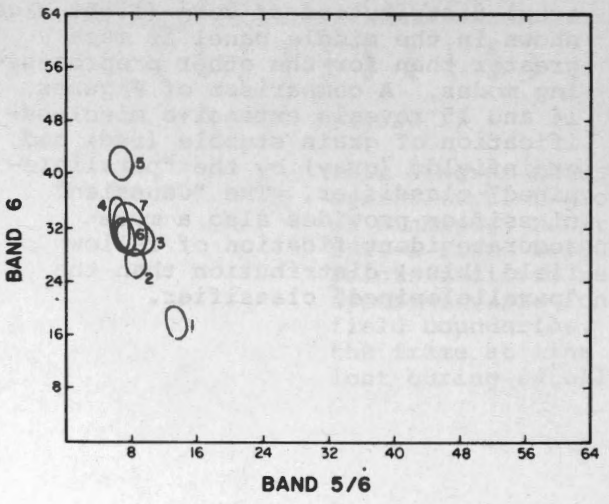

Figure 18

This diagram shows the decision regions for the projection plot for ERTS frame E-1007-16531 for radiometrically corrected band 6 versus the ratio of bands 5/6 for the agricultural classes: (1) Fallow; (2) Wheat; (3) Grain Stubble; (4) Corn; (5) Rapeseed; (6) Sunflower; (7) Grainfield.

THE USE OF COMPOSITE MINIMUM BRIGHTNESS CHARTS IN THE MAPPING AND INTERPRETATION OF SNOW IN QUEBEC-LABRADOR

By

J.T. PARRY
B.J. GREY

This paper presented at the Second Canadian Symposium on Remote Sensing, University of Guelph, Guelph, Ontario, April 29 - May 1, 1974.

THE USE OF COMPOSITE MINIMUM BRIGHTNESS CHARTS IN THE MAPPING AND INTERPRETATION OF SNOW IN QUEBEC-LABRADOR

J. T. Parry and B. J. Grey,
Terrain Evaluation Project,
Department of Geography,
McGill University, Montreal.

SUMMARY

This study is concerned with the interpretation of snow conditions using five-day composite minimum brightness charts (CMB) which are computer products derived from digitized and rectified satellite video data. The usefulness of CMB charts is tested in the study of the areal extent and temporal variation of the snow cover over the Quebec-Labrador peninsula during the period early March to late July, 1972. Using a Densichron densitometer and a grid overlay, the spatial distribution of brightness values was analysed, and each C. M. B. chart was reformated into a map of approximately five hundred and fifty reflection values. Relationships were established between reflection values and both snow depth and recent snow occurrence, and the physiographic influences were identified. The data were used to follow temporal changes in the areal extent of the snow cover, and an attempt was made to use the data as an indicator of snow conditions.

INTRODUCTION

The new technology of satellite remote sensing provides both synoptic and repeat coverage of areas of interest, two factors which are of fundamental importance in the monitoring of snow conditions on a sub-continental scale. Regional snow cover is very difficult to assess in sub-arctic areas because of the sparsity of climatic data from the relatively small number of recording stations and the problems of interpolating snow course measurements from specific sites to distant and dissimilar sites. The potential of satellite imagery for snow surveys has been appreciated for just over a decade and there have been several studies involving specific applications of snow cover data provided by orbiting spacecraft (Tarble, 1963; Barnes and Bowley, 1968; McClain and Baker, 1969; Itten, 1970; Barnes et al., 1973). An excellent review of the potential of satellites in all aspects of hydrology is in Ferguson et al., 1969.

Purpose of The Study

Regional patterns of snow accumulation and melt are of obvious interest to both the climatologist and the hydrologist. The migration of the transient snow line during the melt period is of particular significance especially when examined at a sub-continental scale. In this study, regional snow patterns in Quebec-Labrador were examined using ESSA-9 composite minimum brightness (CMB) charts for the period March-July, 1972, which included the time of maximum snow cover and continued into the final stages of the melt. The specific problems investigated were (1) the relation between CMB chart brightness and snow depth; (2) the relation between CMB chart brightness and snow increments and deficits; (3) the effect of physiographic background on CMB chart brightness; (4) the use of the charts in monitoring the transient snow line; and (5) the use of CMB charts in snow pattern recognition.

Snow and Physiographic Conditions in Quebec-Labrador

The peninsula of Quebec-Labrador north of the 50-degree parallel spans 12 degrees of latitude and 25 degrees of longitude, and the total area examined in this study is 500,000 square miles (1,300,000 square kilometers). The total annual snowfall of any area depends on two factors - the intrinsic snowiness of the winter climate and the duration of the winter period. Quebec-Labrador has both a long winter and a snowy winter climate. Approximately two-thirds of the peninsula receives more than 100 inches (250 cms) annual snowfall, with more than 200 inches (500 cms) on the higher southeastern margin and the central Mecatina Plateau, (Hare, 1950). The duration of the winter period in Quebec-Labrador is basically controlled by latitude; the number of days with snow lying decreases from north to south, but this trend is modified by topographic effects. The central portion of the peninsula is appreciably higher toward its southern margin, and the ameliorating effects of a southerly latitude are countered by the topographic influence.

The whole area lies within the Canadian Shield, but there is considerable topographic variation including mountains, plateaux and plains. The physiographic sub-divisions adopted in this study are basically those of Bostock (1964, 1970), incorporating an earlier scheme of Hare (1959), which identifies vegetation zones (Fig. 1). The most extensive and significant topographic units are the plateaux which cover almost all of the study area, fringed in many sections by the hilly or mountainous units, and to the south of Ungava Bay and in southern James Bay by lowland units. Vegetation provides the second major element in the scheme of physiographic sub-division for Quebec-Labrador (Fig. 1). The vegetation has a direct influence on both snow accumulation and melt patterns and is of particular significance in this study because of the effect of cover type and density on the surface reflection (Fig. 3 and Morrison, 1964). The three basic cover types - tundra, woodland, and forest - form broadly parallel, latitudinal zones across the peninsula. The pattern of physiographic regions of Quebec-Labrador shown in Figure 1 is fairly complex and for the purposes of this study it was necessary to generalise the detail into a simple matrix-cartogram as presented in Figure 2. Each of the grid squares covers approximately 900 square miles (2330 square kilometers), and as a result of this generalisation process, twenty regional units were created, each internally homogenous in terms of topography and vegetation.

INTERPRETATION PROCEDURES

The imagery used in this study is a product of the ESSA 9 camera system operating in the visible wavelengths. A brief description of the processing of this imagery is given below, and additional details are given in Bristor (1968) and McLain and Baker (1969). The imagery is a meso-scale product with a resolution of 34 miles (55 kilometers) and a relative brightness scale of 16 steps. The composite minimum brightness (CMB) charts are the product of further processing, involving spatial averaging of the full resolution brightness data for each mesoscale resolution cell, and then compositing these average values over a selected period of days by saving only the minimum value for each resolution cell. Thus, clouds are only retained when they are present for every day of the compositing period. The optimum number of days for the compositing period has to be long enough for effective cloud filtering, but short enough to minimise time changes in snow boundaries and conditions. Five day CMB charts were used in this study (Fig. 5).

To obtain precise data on surface brightness a Welch Densichron reflection densitometer was used in the standard mode with a 0.062 inch (1.57 mm) aperture and amber filter. In order to obtain brightness data for exactly the same geographical position for a time series of CMB charts, a transparent stereographic overlay grid was prepared at the chart scale (inset Fig. 5). The grid provided exactly the same matrix as the cartogram of physiographic units, and this was found to be convenient for storing the data and facilitated the direct comparison of snow conditions in each of the physiographic units over the study period. Each chart produced an average of 550 data values. There was modification of the actual brightness values as a result of using the overlay grid. The values referred to in the study are the modified ones, and Figure 4 is the correction curve relating these to actual chart brightness.

For the purpose of this study, specific snow data in the form of daily measurements of snowfall and snow depth were required and these were provided for 22 meteorological stations. The distribution of these stations is far from ideal, exacerbated by the complexity of snow accumulation. The inadequacy of the snow data must be borne in mind when considering the results of the CMB chart analysis.

Interpretation Problems

(1) Gaps in the chart sequence (Fig. 6) making the establishment of trends difficult at certain stages.
(2) Incomplete cloud filtering in five day period due to inherent cloudiness of Quebec-Labrador in spring.
(3) Difficulty in reconciling minimum composite parameters with real daily meteorological data.
(4) Contamination of the image by fiducial and boundary marks.
(5) Lack of internal consistency from chart to chart (McClain 1973). External calibration was found satisfactory with the ocean grey tones, but deviations found in ice-cap measurements over Greenland could be due to either processing and/or system changes or actual surface luminance changes.

ANALYSES AND DISCUSSION

In the following pages the potential of CMB charts for monitoring snow conditions at a sub-continental scale is investigated by examining some of the basic questions that the climatologist, the hydrologist, and the military planner would pose with regard to snow depth, the variations in snow patterns

related to physiographic factors, and the migration of the transient snow line during the melt period.

CMB Chart Brightness and Snow Depth

One of the most obvious uses of the CMB chart is as a small scale map of the regional snow distribution, and it is tempting to expect some relation between chart brightness and snow depth. At its crudest this could be a simple differentiation between snow and no-snow areas, and at a more sophisticated level a correlation between brightness and mean snow depth could be sought. To test whether any such relationship did in fact exist, a scattergram was constructed in which the snow depths recorded at the 17 meteorological stations in Quebec-Labrador were plotted against the percent reflection for the corresponding grid square on the CMB chart. The snow depth figures were the minimum values for each CMB chart period, since these seemed to offer the best prospects of correlating with the minimum brightness values. As shown in Figure 8 there is considerable variation in the reflection values associated with any particular snow depth; however, when the data are considered in terms of the physiographic regions, there appear to be four major groupings with considerable overlap of the lower values.

The data point clusters correspond in general terms with the vegetation zones described in the previous section with some overlap resulting from the regional differences in snowfall amounts. The Tundra cluster with maximum snow depths of 15 inches (40 cms) has the highest mean reflection value (4.9%) which is to be expected; however, there is quite a wide range in the reflection values associated with any particular snow depth. The Tundra/Woodland Edge cluster with maximum snow depths up to 30 inches (75 cms) has a lower mean reflection of 3.35% and a wide scatter of values for particular snow depths which can be explained in part by the different physiographic conditions for the stations in this zone. The Woodland cluster, which includes the coastal tundra areas, exhibits a somewhat lower mean reflection value (3.09%). Snow depth maxima for this group range between 40 and 60 inches (100–150 cms), and there is a very marked scatter of the reflection values, particularly for the greater snow depths, which probably results from the wide variation in canopy closure occurring in this zone. At lesser snow depths the scatter of reflection values is considerably reduced, and there is some evidence of a trend in the scatter plot. The Forest cluster, with snow depth maxima the same as the Woodland group, has the lowest mean reflection value (1.81%). For the greater snow depths there is a very broad spread of reflection values producing two sub-groups in the scatter plot. The smaller of these is to some extent anomalous since it is the product of a period of prolonged snowfall during the melt period when the tree canopies were probably blanketed in snow, thus dramatically increasing the regional reflection values at a time when the actual snow depths were well below the seasonal maxima.

Viewing the scatter plot as a whole, it is clear that there is no simple direct relationship between reflection and snow depth. However, the plot emphasises the important influence which cover type exerts on the reflection values, and indicates that the relationships differ appreciably from one vegetation zone to the next. In addition, there are indications that a distinction should be made between the accumulation and the melt phases, and it would appear that consistent relationships between snow depth and reflection are only likely to occur during the latter period.

CMB Chart Brightness and Snow Increments and Deficits

It is clear that variations in the CMB chart reflection values prior to the melt period are related to factors other than snow depth, and in order to investigate this problem further, data plots were constructed for each of the grid squares in which meteorological stations reporting daily snow conditions were located. In each plot the daily snowfall amounts and changes in snow depth as given in the station data are recorded together with the reflection values as measured on the CMB charts. A representative group of these data plots is presented in Figure 9 for each of the main physiographic regions of Quebec-Labrador.

It can be seen that all of the data plots exhibit a similar pattern of reflection values during the CMB chart periods 5 to 12. There are two peaks (charts 7 and 9) separated by a trough (chart 8). In each case the meteorological data indicated that the peaks were associated with fresh snowfalls which occurred at various times during the chart period. Comparing the data from one station with another it would appear that the brightness peaks can be related to the number of fresh snowfalls occurring during the chart period. The most dramatic effects were experienced when a fresh snowfall occurred on each day of a particular five day period, even when the total snow depth for the same period showed an actual decrease. Brightness

peaks were also associated with situations where fresh snowfalls occurred on the majority of days of a particular chart period. However, fresh snowfalls for one or two day periods did not generally produce a peak in the reflection values, and this is understandable when it is remembered that the charts record the minimum brightness for each five day period. Nevertheless, a fresh snowfall at the end of a particular chart period often affected the succeeding chart since it raised the brightness base for the next five day period.

The data plots in Figure 9 show a general decrease in reflection values between the peaks, and this may occur even when the snow depths as recorded at the meteorological stations remain constant. The explanation for this apparent anomaly can be found in the changes occurring within the snow pack as a result of sublimation. Mckay (1970) has shown that in the ageing process there is a reduction in the number of crystal surfaces and a corresponding decrease in the albedo, which is particularly noticeable in the first few days after a fresh snowfall (Fig. 7).

During the melt period there is a fairly steady decline in reflection values and this can be related to the decreasing snow depth. However, even during this stage it is possible for a major snow storm of four or five days duration to interrupt the downward trend in reflection values. The final stages of the melt are marked by a flattening of the reflection curves as the extent of the snow-free areas within a particular grid square increase in size and the physiography comes to dominate the reflection values.

CMB Chart Brightness and Physiographic Regions

The rationale for the regional physiographic subdivision of Quebec-Labrador was presented in the previous section using the two criteria of topography and vegetation type. It can be argued that the relationship between the reflection values for an individual grid square in a particular physiographic region and the snow data for a meteorological station within that grid square can be extended to apply to the whole physiographic region in which the grid square occurs. To test this argument the mean reflection values for each physiographic region for each chart period were plotted in a composite graph. As shown in Figure 10 there is a general consistency in the relative ordinate position of the physiographic regions from one chart period to the next illustrating the control exerted by the vegetation type at all stages of the snow cover period. The regional values in the Tundra Zone are generally brighter than those in the Woodland, which in turn are brighter than those in the Forest Zone.

There are some variations from the general trends, and these appear to be related to particular meteorological conditions for the chart period. For example, during the period covered by chart 7 there was a severe snow storm which affected the eastern section of Quebec-Labrador thereby increasing the general level of reflection values for the Woodland Zone, so that for this chart period they are comparable to values in the Tundra Zone. In general, however, there are consistent differences in the regional values for the different vegetation zones, and these become very well-marked during the intermediate snow stage and the initial melt period. A generally snow-free situation occurs first in the Forest Zone (chart 12), and then it progresses through the Woodland to the Tundra Zone (charts 15 and 19). The meteorological data indicate that a mean reflection value of 1% or less corresponds to a more or less snow-free situation throughout the Forest and Woodland Zones, whereas for the Tundra Zone this critical value is somewhat lower.

The regional differences in brightness can be demonstrated even more effectively by examining the reflection values for specific CMB charts. A selection of diagrams illustrating the range of reflection values and the means for each physiographic region under different snow conditions is presented in Figure 11. The physiographic regions have been grouped according to vegetation zone, and the general consistency in the relative brightness of each group is apparent at all stages of the snow cover with the exception of the final melt period. The differences between the vegetation zones are most marked after periods of extensive snow, as in charts 1, 7 and 9. The contrasts are somewhat subdued during the intervening periods (charts 5 and 9), but even then the Tundra regions are generally brighter than the Woodland, which in turn are brighter than the Forest. During the melt period, minimum reflection levels are first attained in the Forest Zone and then spread northward through the Woodland Zone and finally into the Tundra (charts 12 and 15).

CMB Chart Brightness and the Transient Snow Line

One of the most important phenological events of the spring and summer months in Quebec-Labrador is the northerly retreat of the snow

line, and it is apparent that the CMB charts provide a means of monitoring this retreat and mapping the changing pattern of snow cover during the melt period. Although the concept of tracing the migration of the snow line with successive CMB charts is simple enough, there are various problems that must be overcome before this can be put into practice. In the first instance, it is necessary to establish the brightness level that corresponds to a snow-free condition for a particular region. The minimum brightness levels for the different regions do vary as a function of the physiography, and before these levels can be used in a predictive manner the absence of snow in the area has to be confirmed from the meteorological station data. The problems of relating the daily snow measurements of the stations to the CMB chart reflection values which are five day minima has already been mentioned, and it seems probable that some slight lack of synchronism is inevitable. The relatively small number of stations in Quebec-Labrador made it impossible to map precise snow limits, and all that could be done was to interpolate the isolines of zero and one inch (2.54 cms) snow depth on various CMB cartograms for the latter part of the snow cover period. It must be remembered that these interpolated snow isolines do not accurately portray the snow limit for a particular period. Indeed, it is very probable that the CMB charts provide a more accurate delineation. The isolines are presented simply for comparison purposes to demonstrate that the snow lines on the CMB charts do correspond with what is known about the ground conditions from the meteorological data.

The results are presented in Figure 12. For CMB chart 12 (May 19-23) it can be seen that the northern edge of the shaded zone (representing areas with reflection values of 1% or less) falls between the zero and one inch isolines and,therefore, must correspond very closely with the actual snow line. In the succeeding cartogram (number 15, June 13-17), the northern edge of the area with 0.9% reflection values or less falls between the zero and one inch isolines. The northern limit of the area with reflection values of 0.8% and less shows good correspondence with the zero isoline . There has been a general retreat of the snow line since chart 12, and the critical reflection values for differentiating snow trace and no-snow areas have changed as the regional luminance decreases. On chart 19 (July 13-17) the northern edge of areas with 0.8% reflection or less corresponds in a general way with the zero isoline and the cartogram indicates that significant areas of snow remain only in the far northern sectors of the peninsula. In the final cartogram (number 21 July 23-27), 99% of the reflection values for the area as a whole are at the 0.7% level. Higher reflection values occur only in the Sugluk Plateau, the Labrador Highlands, and the higher parts of the Mecatina and Larch Plateaux where it is probable that remnant snow areas may still remain.

It can be appreciated from these results that it would be invalid to take a single reflection value, for example 1%, as a criterion for determining whether an area was snow-free. The decrease in reflection values associated with the snow line from 1% to 0.7% between chart periods 12 and 21 is of very great significance in making a correct interpretation of the charts. The explanation for this decrease can be found in the reduced albedo of the snow surface during the melt phase (as illustrated in Figure 7) and the gradual emergence of surface features as the snow cover thins and becomes discontinuous.

Frequency-density Analysis of CMB Chart Brightness

In pattern recognition studies, frequency-density analysis is commonly used as a technique for identifying particular types of spatial distribution which have special significance. The CMB charts provide a suitable data base for frequency-density analysis, and there are possibilities for the development of an automatic or semi-automatic system for the recognition of particular regional snow conditions, such as fresh snow, initial melt, advanced melt, and so on. For this type of analysis the first requirement is the preparation of models or training sets which match the various snow conditions.

The models used in this study are simple histograms of reflection values for selected CMB charts of the whole of Quebec-Labrador. The resulting frequency-density distributions for some typical snow conditions are illustrated in Figure 13. The frequency distribution of reflection values after a prolonged snowfall is shown in histogram 1. It is a right-skewed, normal distribution with a modal class of 7.5 to 8.0% , in marked contrast to the pattern in histogram 5, which is the frequency distribution after a period of almost a month without extensive fresh snowfall. The mean reflection is therefore considerably less than in histogram 5, and the distribution is left-skewed, as a result of the reduced albedo of the snow and its redistribution by wind. The effect of wind is significant in all the physiographic regions - it removes the snow from the tree crowns in the Forest and Woodland Zones and

sweeps the ridge tops clear of snow in the Tundra Zone.

Histograms 7, 8, and 9 cover consecutive five day periods and illustrate a typical winter sequence. In histogram 7, the effect of fresh snowfall on the intermediate conditions of histogram 5 can be seen. There is a general increase in reflection values with a shift of the modal class from 1.5 - 2.0% to 6.5 - 7.0%. No snow occurred during the succeeding five day period, and so histogram 8 shows an intermediate snow situation with a reduction in the total range of reflection values, and a marked shift in the modal class from 6.5 - 7.0% to 1.5 - 2.0%. In the following period, there was a fresh snowfall over part of the area, resulting in a bimodal frequency distribution (histogram 9) with the concentration of values in the 6.5 - 7.5% reflection classes resulting from the fresh snow, and the concentration in the 1.5 - 2.5% range representing the intermediate snow conditions of the other areas.

Typical melt patterns are depicted in histograms 12 and 15. In the former, which represents an early stage of melt, the frequency distribution is markedly leptokurtic with a strong left skew. The range of values is still quite appreciable, but the great majority are less than 3%, and the modal class (1.0 - 1.5%) contains nearly half the total number of readings. At the time of histogram 15, snow melt was well-advanced throughout the area. The distribution is extremely leptokurtic and left-skewed with 97% of the values falling between 0.5 and 1.5% reflection and a total range of only 2.5%.

The statistical analysis of the frequency distribution of reflection values would appear to offer a useful tool in the interpretation of snow conditions. A distribution with high values and a moderate right skew represents a fresh snowfall over the greater part of the area, whereas a bimodal distribution indicates that the snowfall was restricted to particular parts of the region. With the same range of values and a left skew, the snow conditions can be interpreted as intermediate, which implies settling, redistribution, ageing, and compaction. A strongly unimodal, left-skew distribution indicates that the melt stage has been reached, and the subsequent shift of the modal class toward lower values reflects the progressive expansion of the snow-free areas. With the development of additional training sets, and the use of a microdensitometer and a series of computer programs, it should be possible to provide an evaluation of snow conditions in Quebec-Labrador throughout the winter period within a few minutes of receipt of the CMB charts.

CONCLUSIONS

In many respects the CMB chart is a unique product of remote sensing, and the results obtained in this study support the view that these charts are a useful tool in the analysis of snow conditions on a sub-continental scale. The CMB chart is a sophisticated type of satellite imagery requiring some adjustment in the interpreter's outlook to fully appreciate the implications of the concept of temporal averaging, and before attempting to work with this type of imagery, the interpreter should be aware of the various steps in the processing and the parameters controlling the rendition of the grey tones. The experiences in this investigation with regard to the usefulness of CMB charts in analysing snow conditions in Quebec-Labrador can be summarised as follows.

- Clouds are not entirely filtered in the five day compositing period; however, the amount of residual cloud appearing in the CMB chart is very limited, and, in general, areas of snow can be readily differentiated by virtue of their more uniform appearance and higher reflection values;
- No simple and direct relationship between CMB chart reflection values and snow depth was discernible except during the melt stages when a distinction could be made between snow-free areas, snow-trace areas, with depths of less than one inch (2-3 cms), and snow-covered areas, with depths of several inches or more;
- Extensive fresh snowfalls were generally identifiable, particularly when the snowfall period spread over several days; intermediate snow conditions with redistribution by wind in the Tundra Zone and settling of canopy snow in the Woodland and Forest Zones were also recognizable;
- Terrain factors, particularly the vegetation cover type, have a significant effect on the reflection values for a given area, and in similar snow conditions, physiographic regions of the same type will generate comparable brightness levels on CMB charts;
- The migration of the transient snow-line can be monitored relatively easily on CMB charts once the brightness levels corresponding to a snow-free condition have been established. The snow-line can be located very much more accurately by interpretation of the brightness levels on CMB charts than by interpolation of daily station records;
- Different snow conditions give rise to different frequency-density distributions of brightness data, which can be used as signatures in the routine analysis of CMB charts over an extended time period.

ACKNOWLEDGEMENTS

This study is part of a wider investigation of surface conditions and their interpretation from aircraft and spacecraft imagery being undertaken by the Terrain Evaluation Project at McGill University. The research was supported by the Defence Research Board of Canada Contract SP2. 7090153, Serial 2SP2-0076, and the Department of Indian Affairs and Northern Development (McGill University Research Committee Grant). The authors wish to acknowledge the assistance of the U.S. Department of Commerce, National Oceanic and Atmospheric Administration for supplying ESSA 9 CMB charts and the Atmospheric Environment Service of Environment Canada for providing meteorological data.

REFERENCES

Barnes, J.C. and C.J. Bowley, 1968, Snow cover distribution as mapped from satellite photography, Water Resources Research, Vol. 4:2, pp. 257-272.

Barnes, J.C. et al., 1973, Use of satellite data for mapping snow cover in the western United States, Proc. Symp. on Management and Utilization of Remote Sensing Data, pp. 166-176.

Bostock, H.S., 1964, A provisional physiographic map of Canada, Paper 64-35, Geol. Surv. Canada, 24 pp.

Bostock, H.S., 1970, Physiographic Regions of Canada, Map 1254 A, Geol. Surv. Canada.

Bristor, C.L., 1968, Computer processing of satellite pictures, ESSA Tech. Mem. NESCTM-6, U.S. Dept. of Commerce, 11 pp.

Ferguson, H.L. et al., 1969, Applications of satellite photographs to hydrology in Canada, N.R.C. Hydrology Symp. No. 7, pp. 311-343.

Hare, F.K., 1950, The climate of the eastern Canadian arctic and sub-arctic and its influence on accessibility, Unpubl. D. és A. thesis, Université de Montréal, Vol. 1, 255 pp.

Hare, F.K., 1959, A photo-reconnaissance survey of Labrador-Ungava, Memoir 6, Geographical Branch, Dept. Mines and Tech. Surveys, 83 pp.

Itten, K., 1970, The determination of snowlines from weather satellite pictures, Berichte des III Int. Symp. für Photo interpretation, pp. 455-466.

McClain, E.P., 1973, Quantitative use of satellite vidicon data for delimiting sea ice conditions, Arctic, Vol.26:1, pp. 44-57.

McClain, E.P. and D.R. Baker, 1969, Experimental large-scale snow and ice mapping with composite minimum brightness charts, ESSA Tech. Mem. NESCTM-12, U.S. Dept. of Commerce, 19 pp.

McKay, G.A., 1970, Section II Precipitation, in Handbook on the Principles of Hydrology (ed) D.M. Gray, CNC/IHD, Ottawa, p. 28.

Morrison, A., 1964, Relation between albedo and air photographic tone in Canadian sub-arctic regions, Can. Geog., Vol. 8, pp. 72-84.

Parry, J.T. and B.J. Grey, 1974, The mapping and interpretation of snow conditions in Quebec-Labrador using ESSA 9 composite minimum brightness charts, Contract Report SP2.7090153, Serial 2SP2-0076, Defence Research Board of Canada, 33 pp.

Tarble, R.D., 1963, Aerial distributions of snow as determined from satellite photographs, Publ. No. 65, I.A.S.H., pp. 372-375.

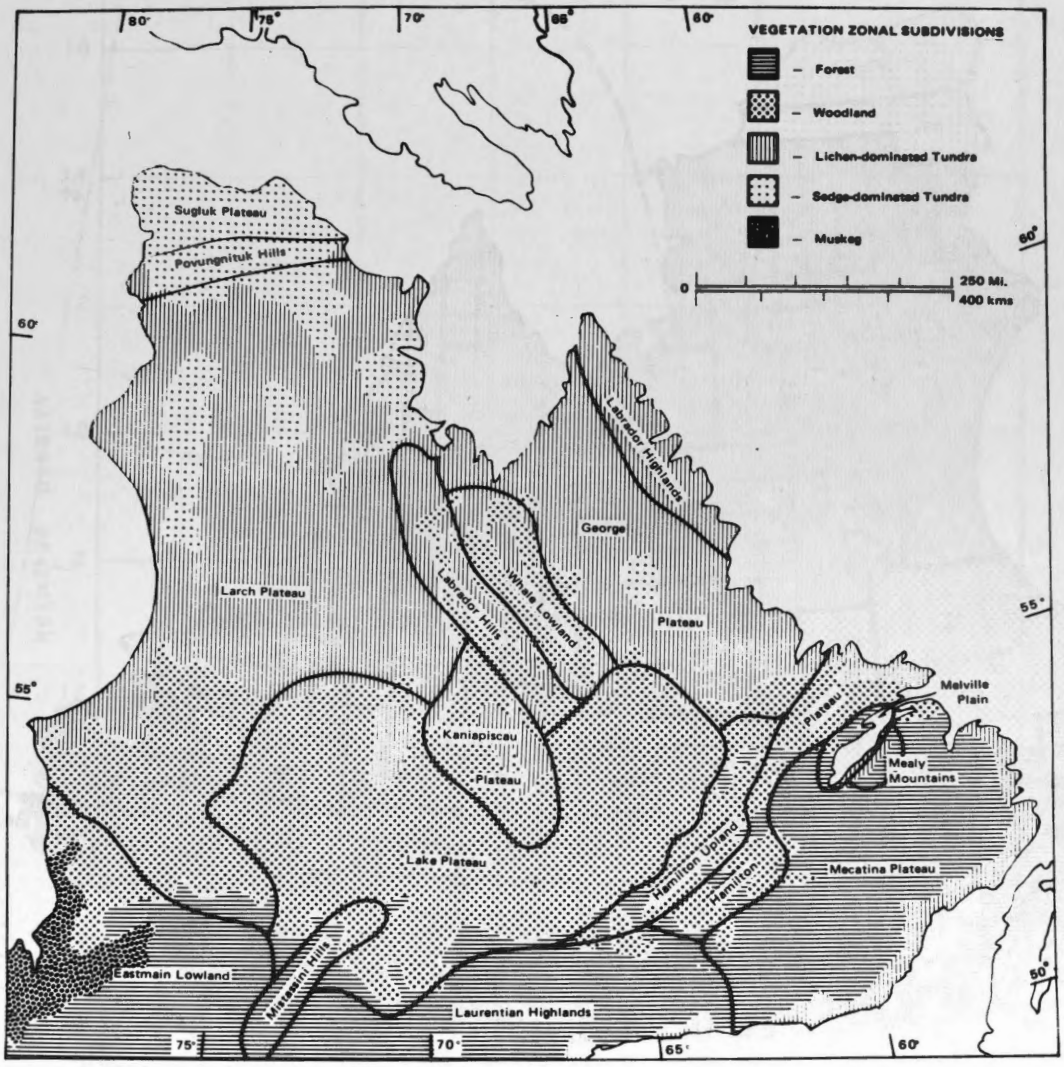

Figure 1. Physiographic regions of Quebec-Labrador (adapted from Hare 1959 and Bostock 1970).

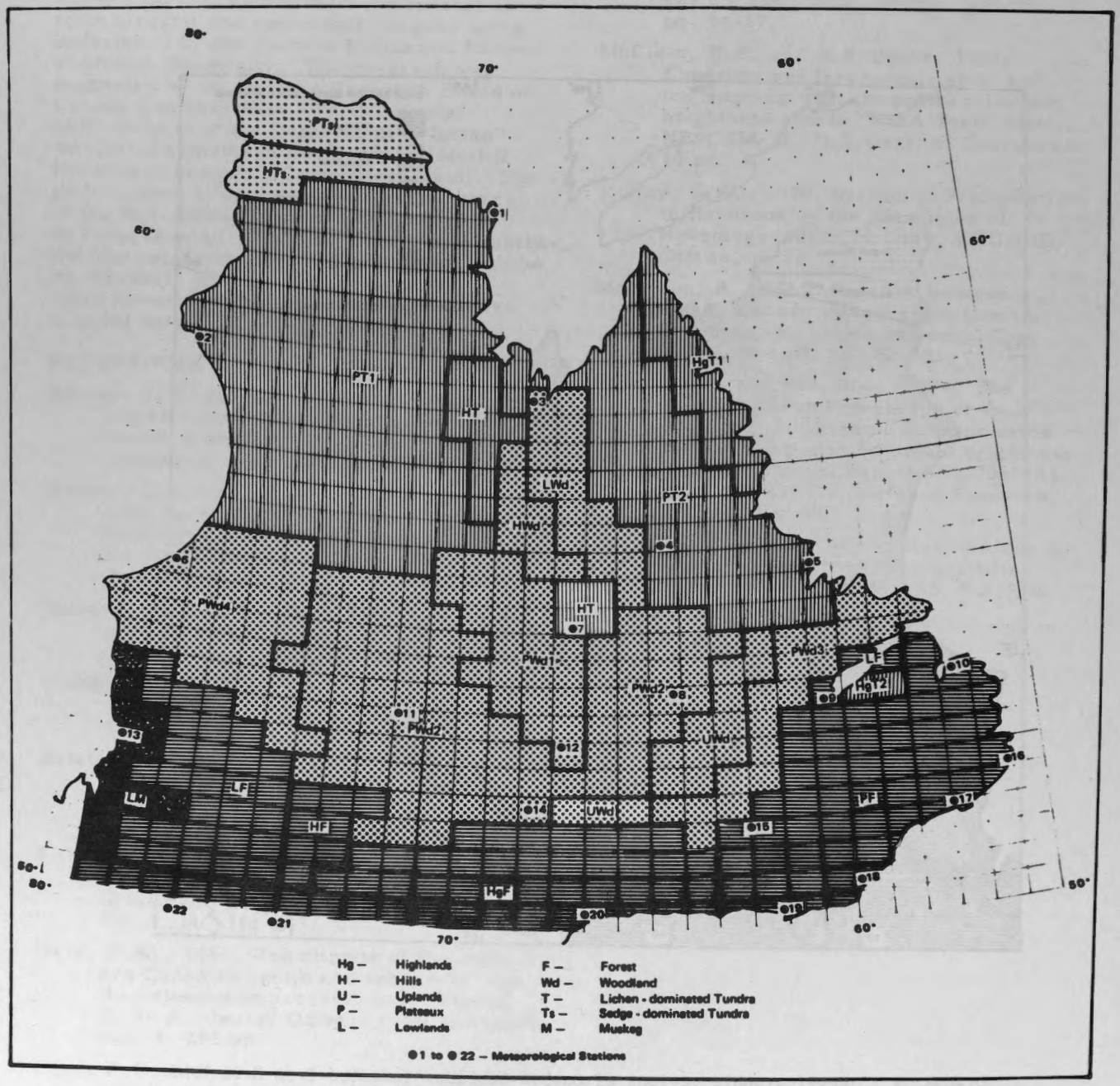

Figure 2. Matrix-cartogram of the physiographic regions of Quebec-Labrador.

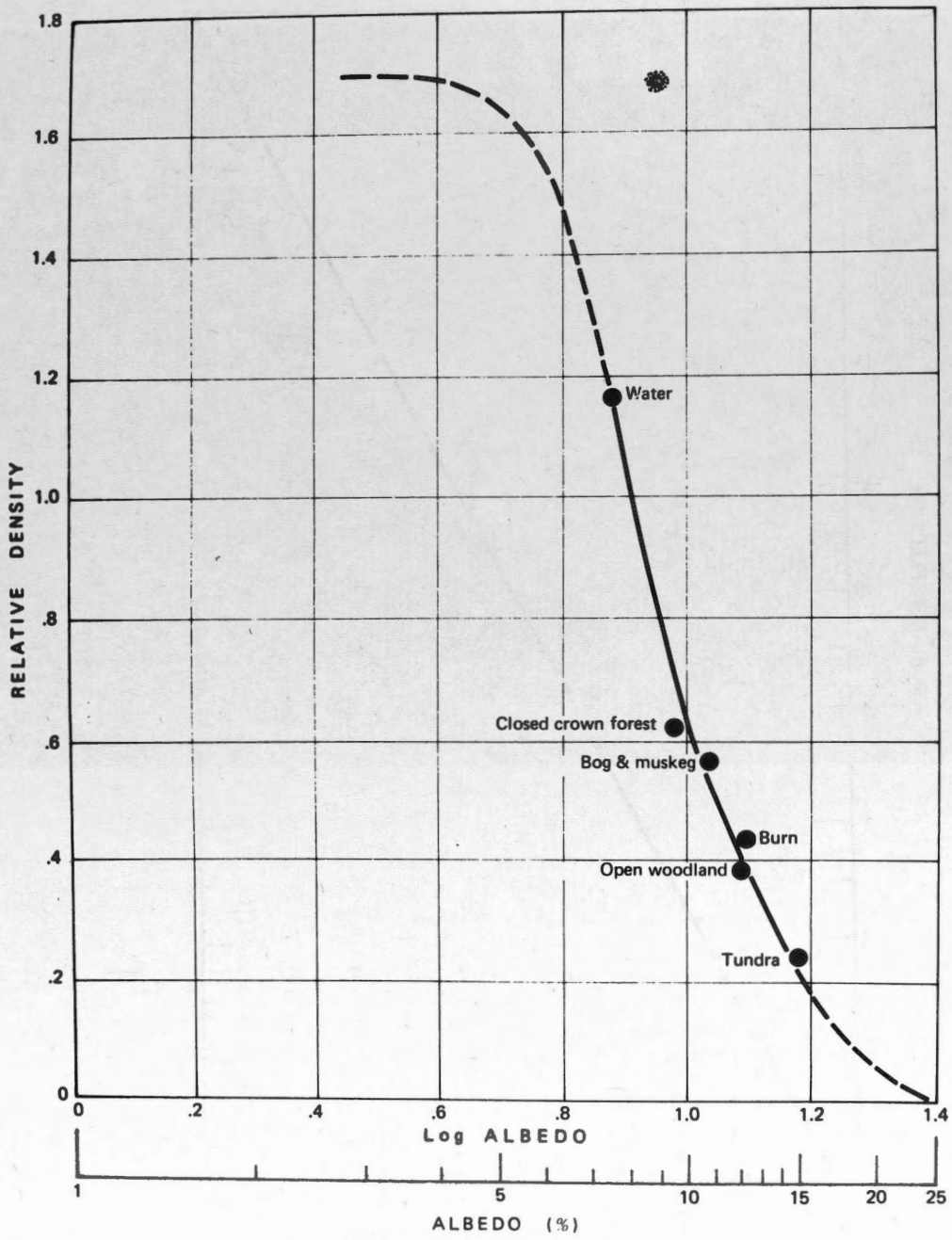

Figure 3. Generalized relations between albedo and photographic tone for cover types in Quebec-Labrador (after Morrison 1964).

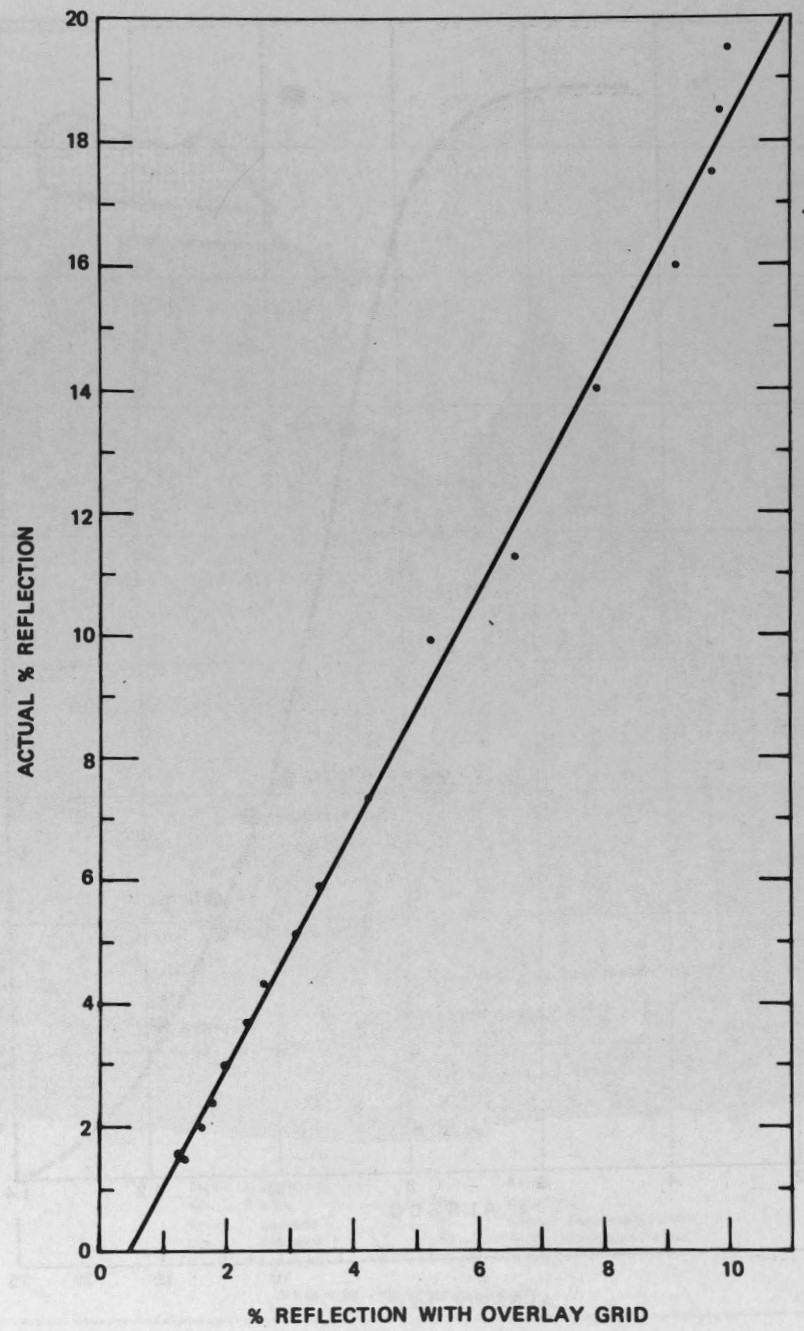

Figure 4. Relationship between actual CMB chart reflection values and modified values measured with overlay grid.

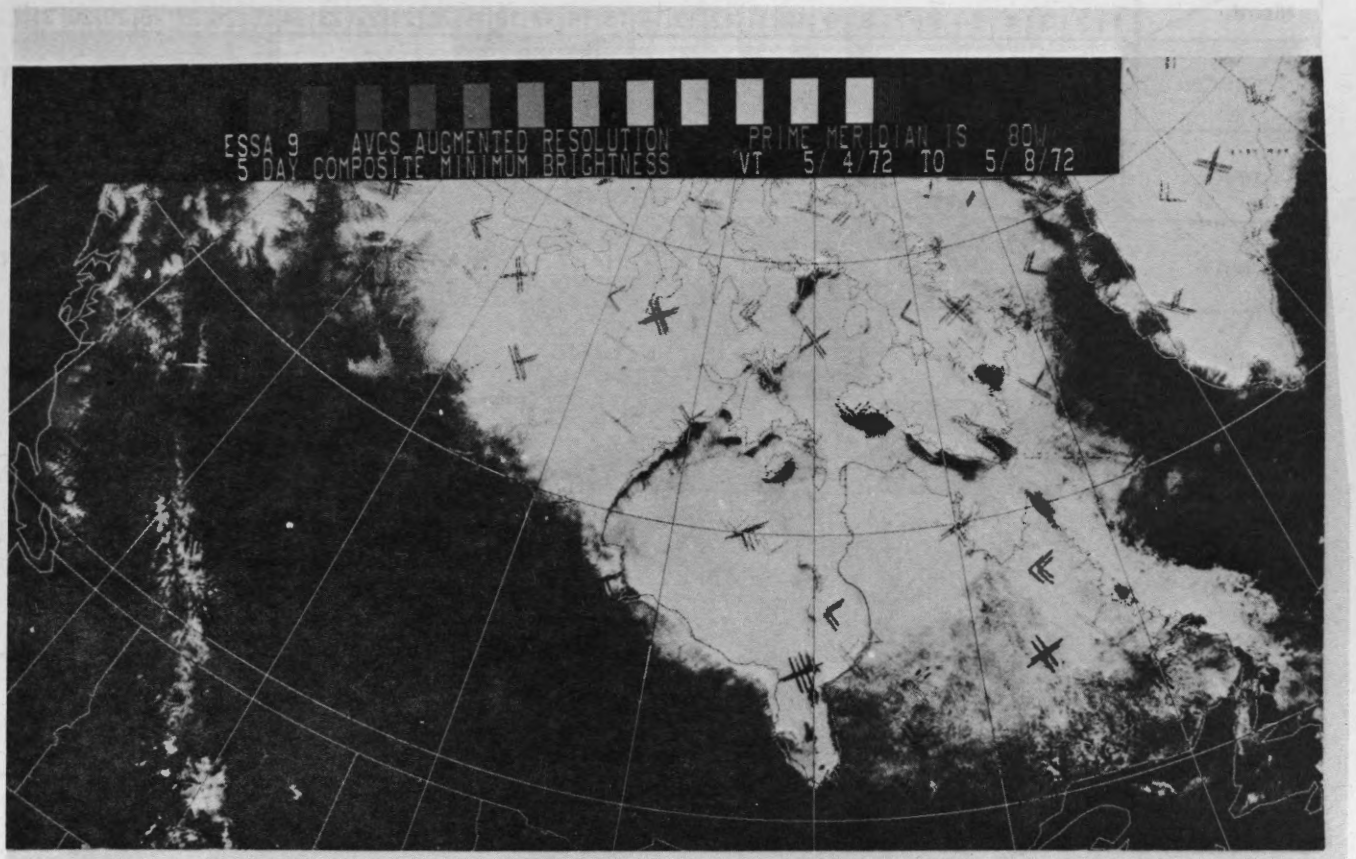

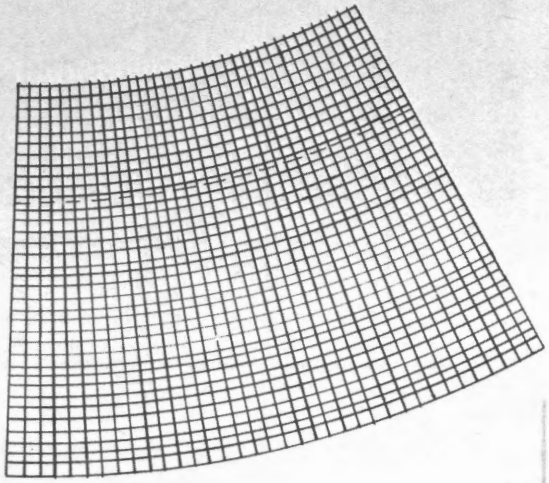

Figure 5. ESSA 9 5-day CMB chart and overlay grid for Quebec-Labrador.

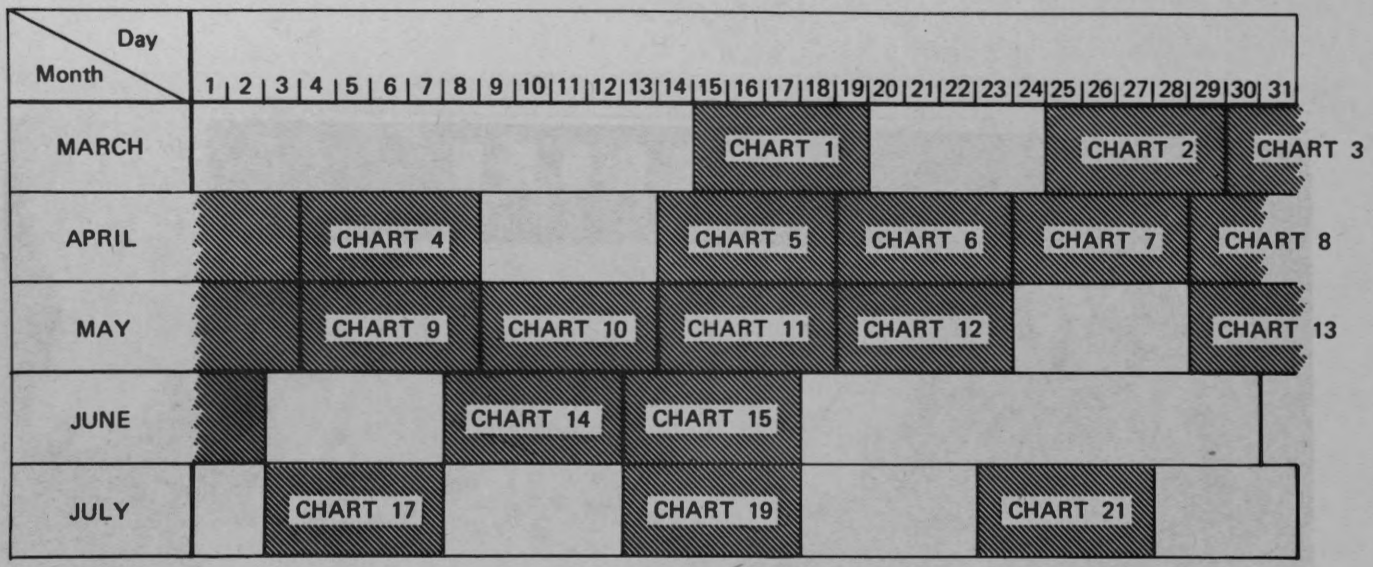

Figure 6. CMB chart calendar.

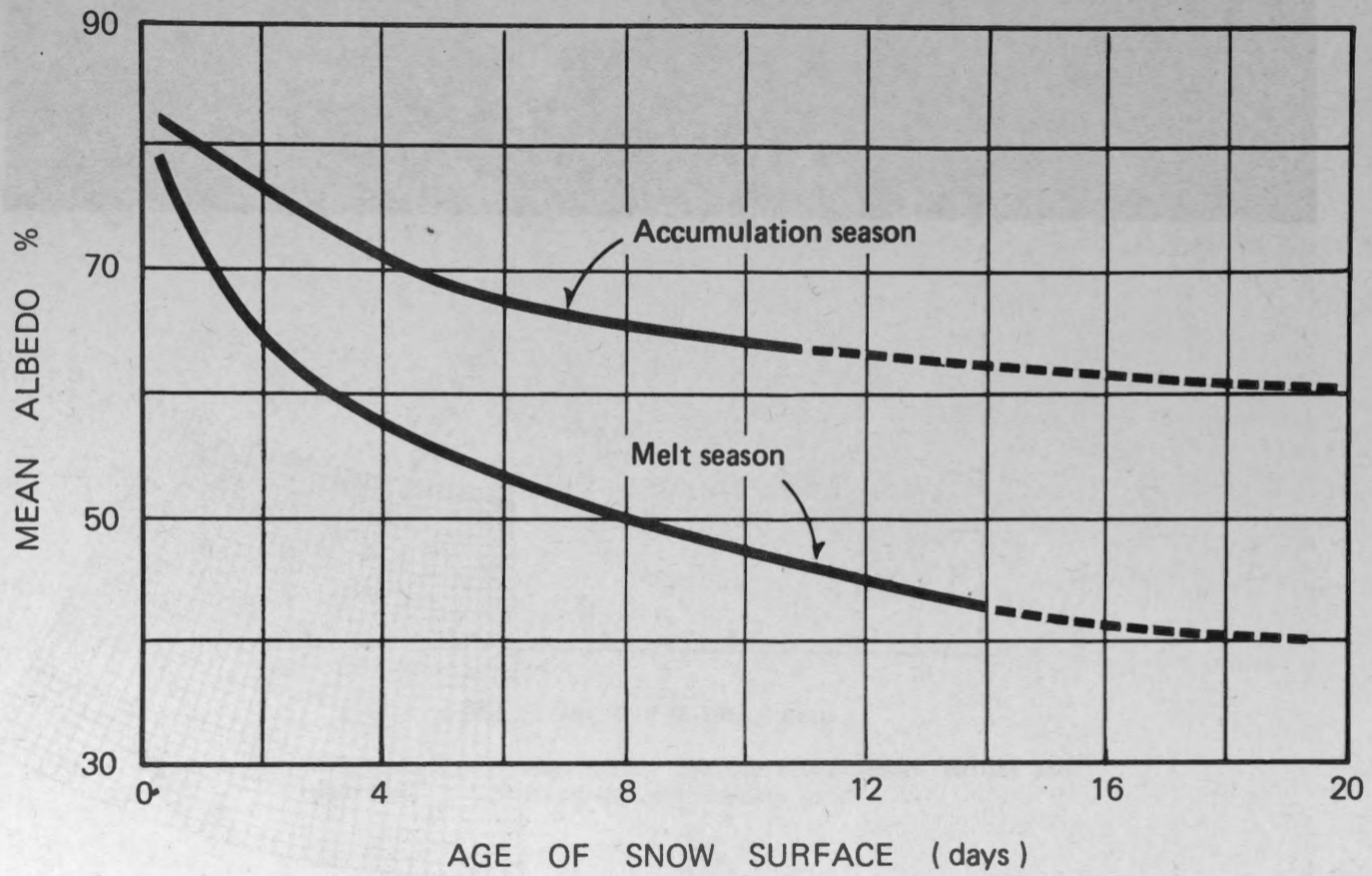

Figure 7. Variation in the albedo of snow with time (after McKay 1970).

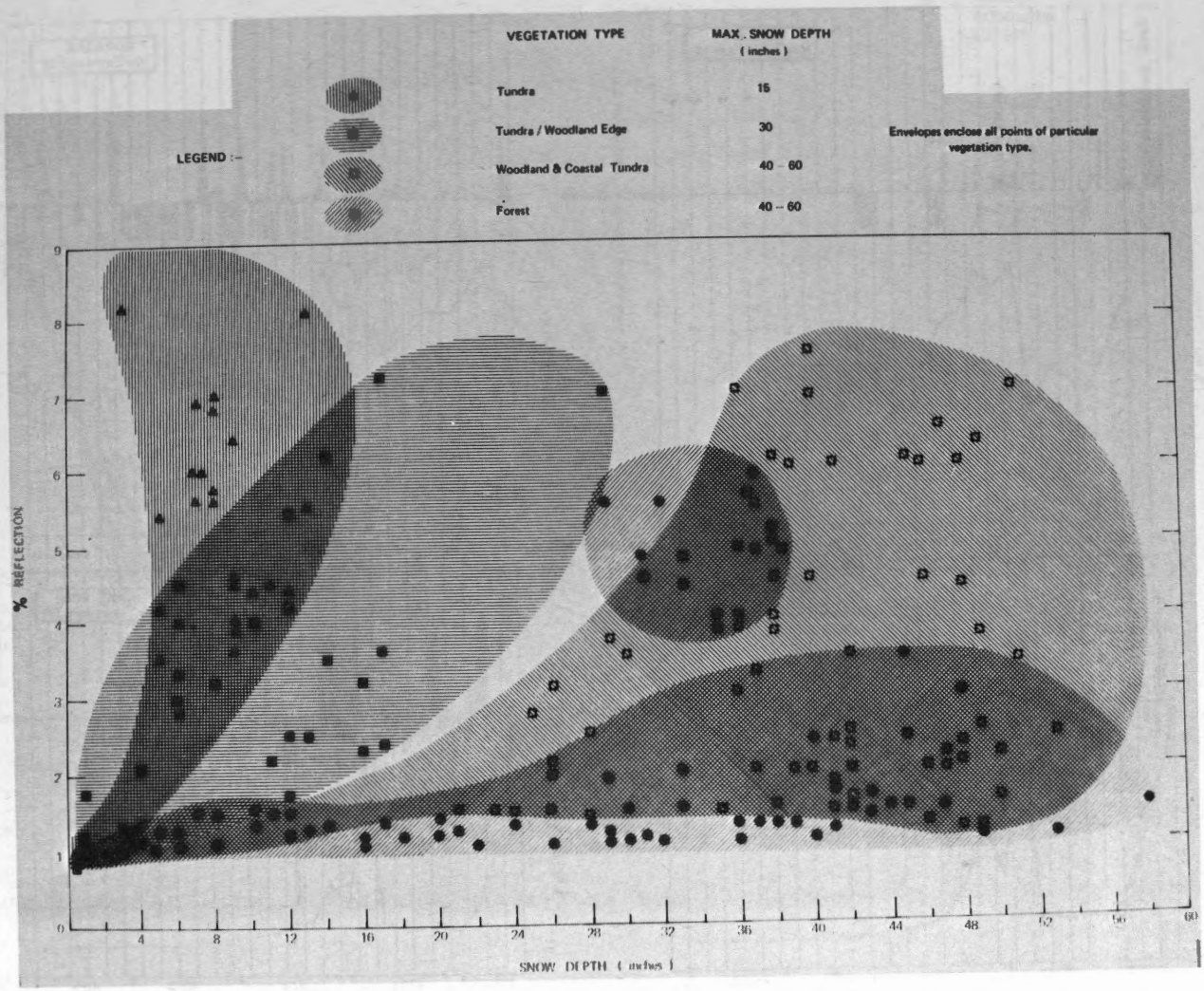

Figure 8. Scatter plot of snow depth and CMB chart reflection values for meteorological stations in Quebec-Labrador.

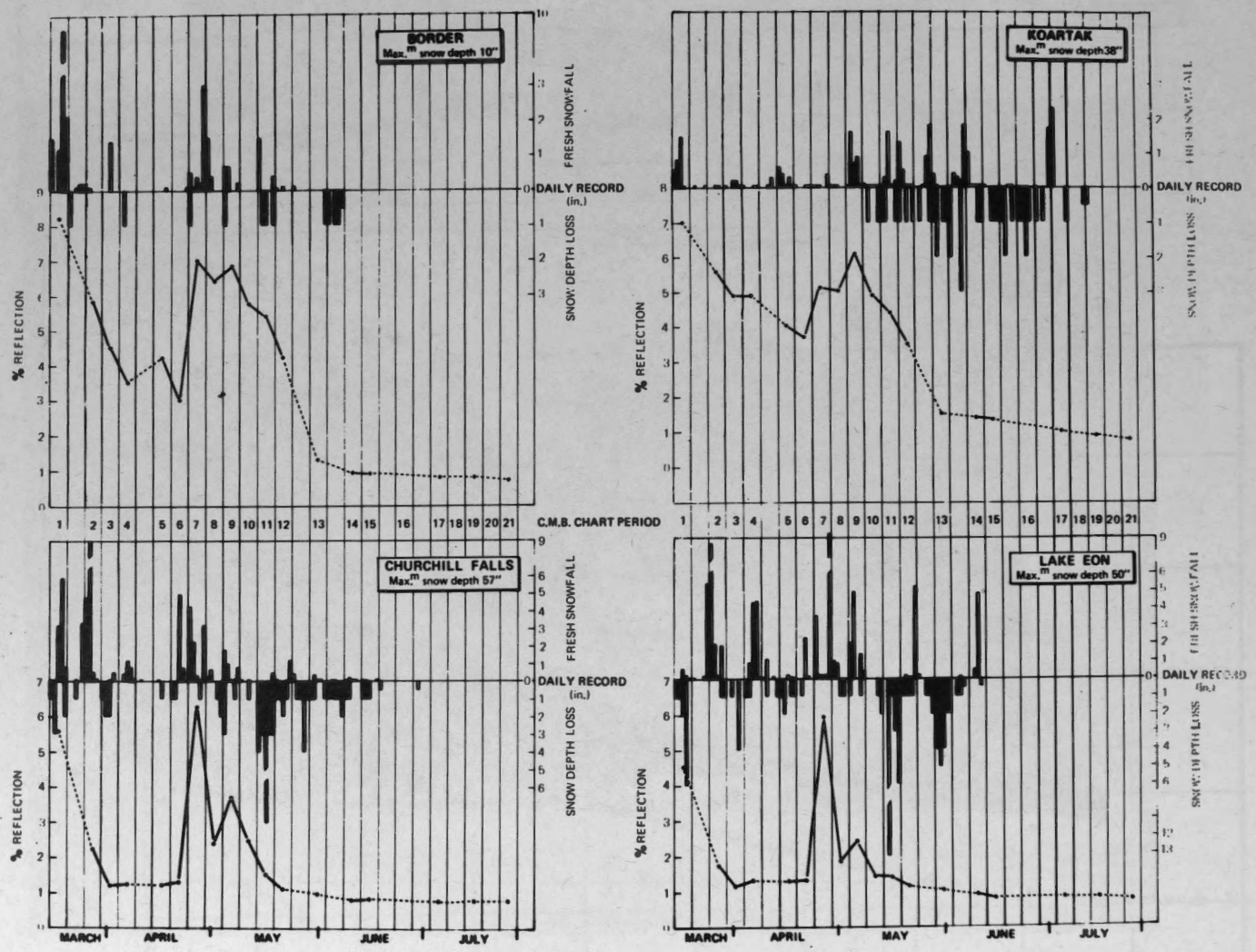

Figure 9. Data plots of daily snow conditions and CMB chart reflection values for selected stations in Quebec-Labrador.

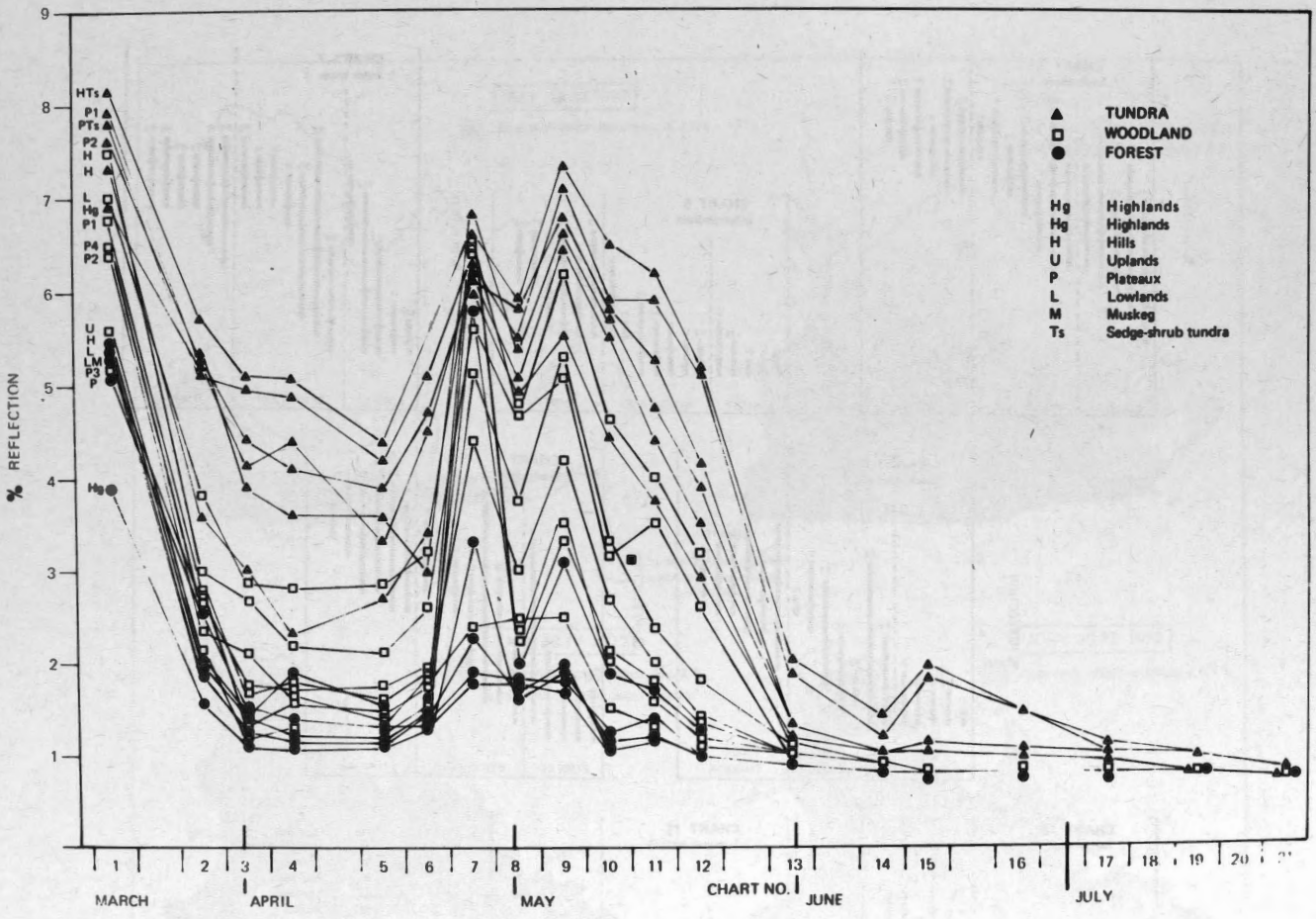

Figure 10. Regional mean reflection values for the study period.

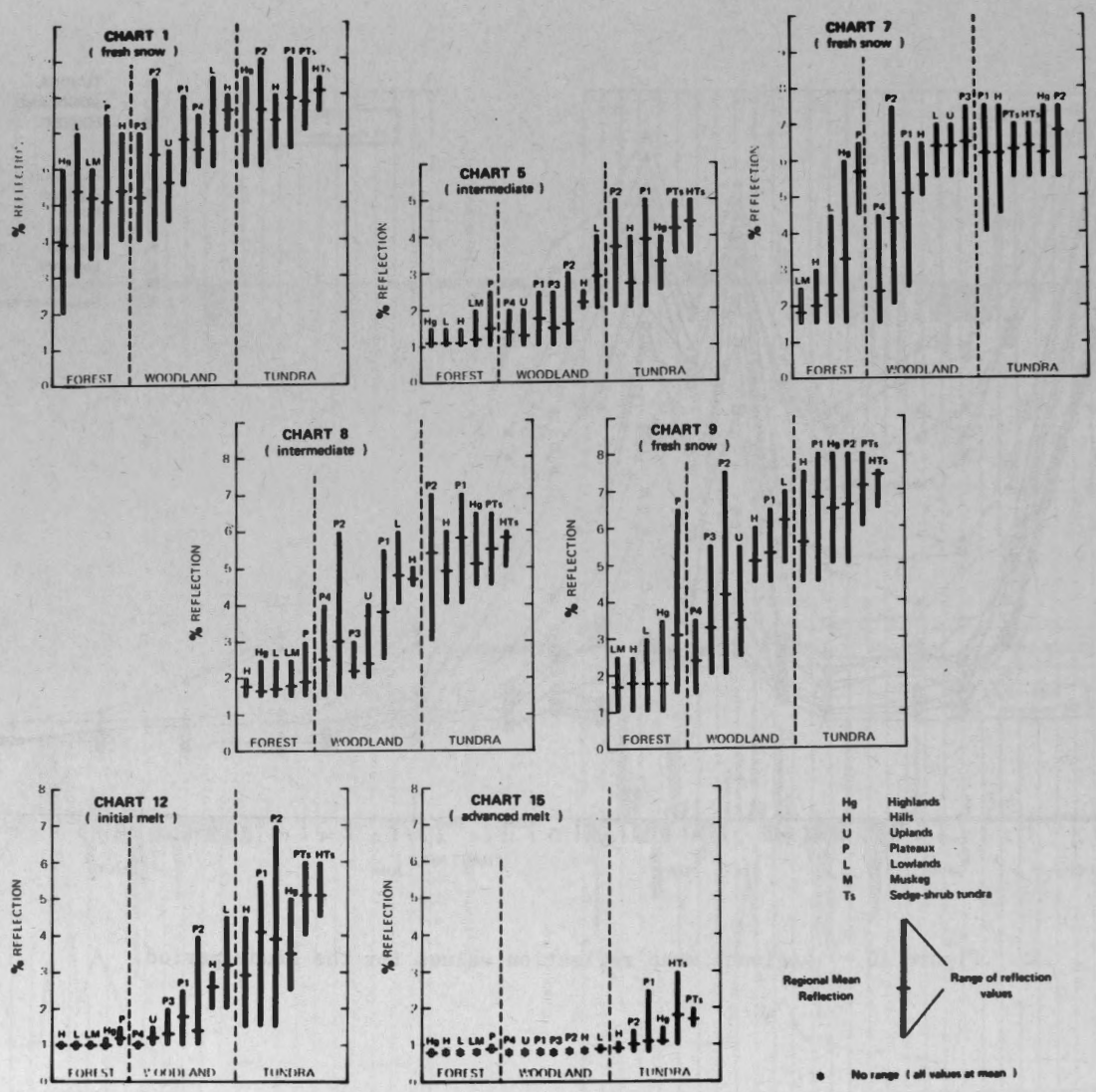

Figure 11. Range of CMB chart reflection values for the different physiographic regions of Quebec-Labrador at selected stages of the snow cover period.

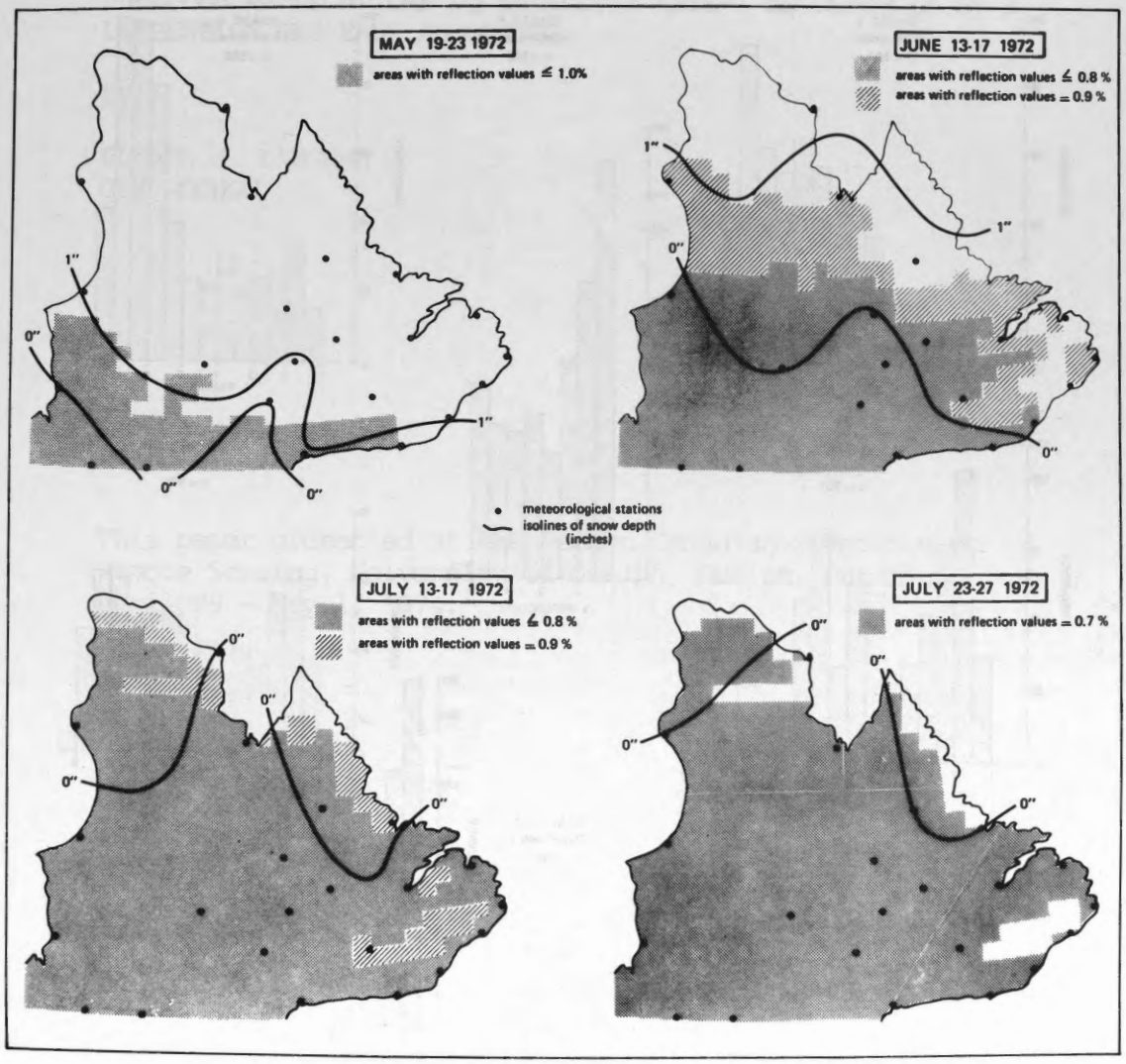

Figure 12. Relation between the transient snow line and CMB chart reflection values during the melt period.

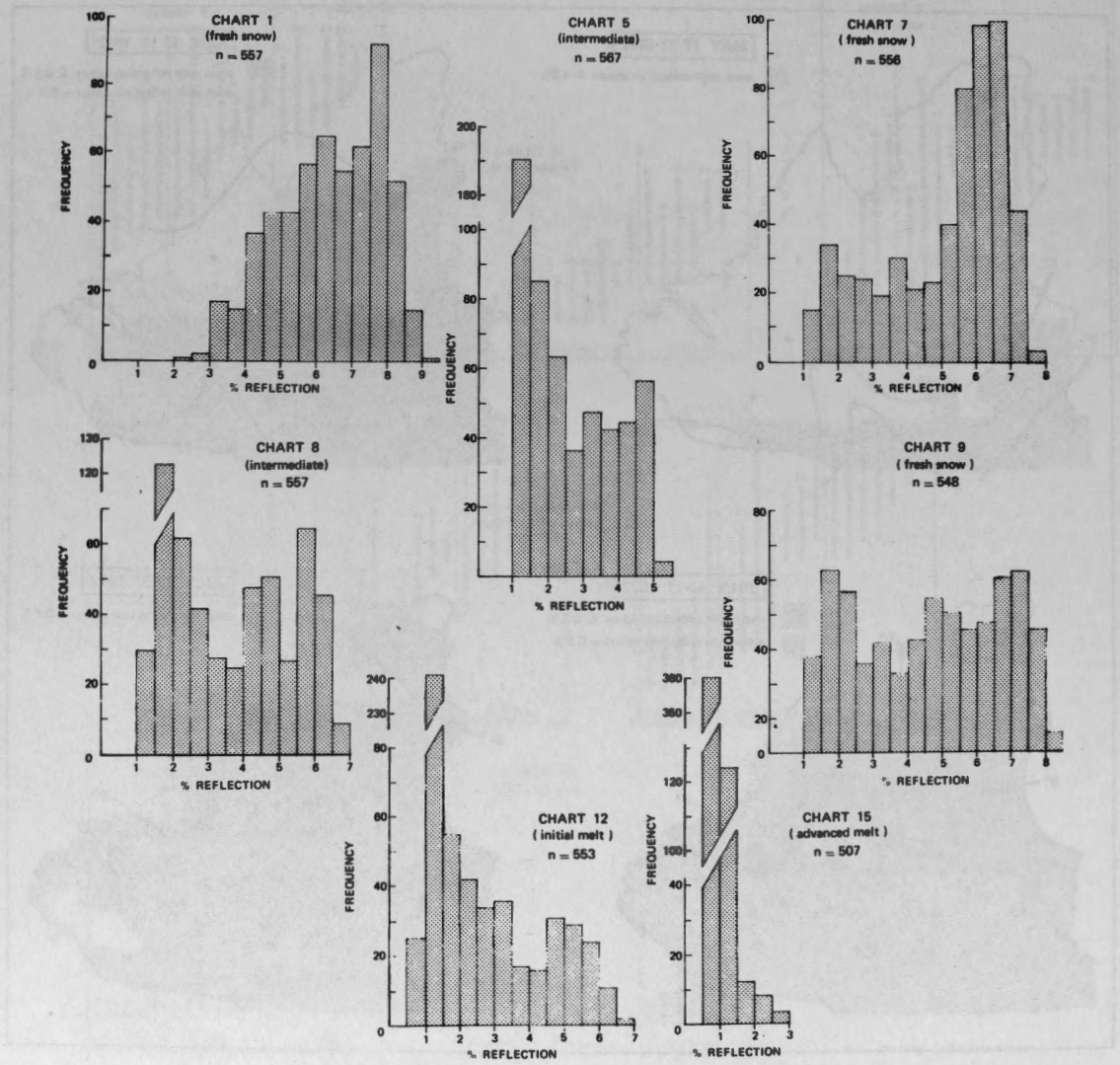

Figure 13. Frequency-density distributions for different snow conditions in Quebec-Labrador.

QUELQUES APPLICATIONS DU SATELLITE ERTS-1 AU CONTROLE ET A LA GESTION DES EAUX AU QUEBEC

By

EDWARD J. LANGHAM
GUY ROCHON

This paper presented at the Second Canadian Symposium on Remote Sensing, University of Guelph, Guelph, Ontario, April 29 - May 1, 1974.

QUELQUES APPLICATIONS DU SATELLITE ERTS-1 AU CONTROLE ET A LA GESTION DES EAUX AU QUEBEC

Edward J. Langham, INRS-Eau, Univ. du Québec.
Guy Rochon, CENTREAU, Université Laval.

- L'importance de la ressource eau.

La richesse en eau, du Canada en général et du Québec en particulier, est un concept si répandu que souvent il frise le folklore. 290,000 milles carrés environ de territoire canadien couvert par de l'eau douce, 13.6% du territoire au Québec, plus d'un milliard de dollars de production hydro-électrique, la voie d'eau intérieure la plus importante au monde, et bien d'autres statistiques semblables nous ont trop souvent portés à considérer cette ressource renouvelable comme inépuisable et inaltérable.

Une nouvelle conscience se développe progressivement dans notre société: la dégradation du milieu hydrique par les eaux d'égout, et par les différentes formes d'utilisation de l'eau que nous favorisons sans égard au milieu naturel ont déjà entraîné chez nous des conséquences néfastes quelquefois à partir desquelles nous comprenons mieux les disponibilités hydriques du milieu géographique, ses limitations et la vulnérabilité de la ressource.

On se dirige donc immanquablement vers un plus grand contrôle, et à la limite, à une gestion globale de la ressource eau par nos gouvernements. Or cette gestion implique une connaissance approfondie du cycle de l'eau et des effets des différentes formes d'utilisation de l'eau sur le cycle de celle-ci ainsi qu'une surveillance étroite des nappes d'eau de surface comme d'un contrôle des utilisations.

Territoire	SUPERFICIE			
	Terre milles carrés	% de la superficie totale	Eau douce milles carrés	% de la superficie totale
Canada	3,560,000	91.8	291,000	8.2
Québec	523,000	86.4	71,000	13.6

Superficie et territoires occupés par l'eau douce au Canada et au Québec.

- Le rôle particulier de la télédétection.

Compte tenu de l'immense étendue du territoire à considérer, de la multiplicité des utilisateurs de l'eau, souvent avec des vocations différentes ou contradictoires, de la complexité des échanges entre les substances et organismes véhiculés par l'eau et le milieu environnant, il semble évident que l'on devra utiliser des techniques de mesure beaucoup plus en rapport avec l'envergure des problèmes considérés.

Dans cette optique la télédétection est appelée à jouer un rôle de premier plan dans la mise en place de mécanismes de gestion appropriés, en raison des avantages inhérents à l'utilisation de plates-formes aériennes et spatiales. Si jusqu'à maintenant ces nouvelles techniques de mesure à distance ont été en général peu utilisées au Canada et à peu près pas au Québec, ce n'est pas à notre avis en raison de la valeur des données qui nous sont accessibles grâce aux capteurs disponibles au Canada, mais plutôt à la forme de gestion de ces données. Nous devons trouver ou appliquer, si elles existent déjà, des méthodes d'analyse et de présentation des données permettant de transférer efficacement ces informations aux agents chargés de la planification et de l'aménagement de la ressource[1]. C'est en ayant à l'esprit cet objectif de combler le fossé entre les utilisateurs, d'une part, et le réservoir de données accessibles par télédétection que nous avons entrepris l'analyse des données du satellite ERTS-1. D'abord parce que les méthodes d'analyse numérique des informations nous semblent celles qui seront privilégiées dans un avenir rapproché, par rapport aux méthodes conventionnelles de photo-interprétation, surtout si l'on considère la prochaine génération de satellites d'observation des ressources où la résolution spatiale approchera celle obtenue par photographie à haute altitude. De plus, on peut espérer que la méthodologie ainsi développée puisse être utilisée à court terme et avec beaucoup plus de puissance, à partir de scanners multispectraux transportés par avion.

Voici donc quelques résultats de nos travaux s'inscrivant dans ce cadre.

---

[1] BROONER, W.G. and D.A. NICHOLS: Considerations and Techniques for Incorporating Remote Sensed Imagery into Land Resource Management Process, Remote Sensing of Earth Resources, Vol. I, Space Inst., Univ. of Tennessee, 1972.

- Quelques résultats de nos travaux.

Avant d'aborder précisément ces résultats, voyons d'abord quelle méthodologie nous avons suivie.

- Méthodologie

Choix de la forme d'emmagasinement des données

Les données de ERTS, telles que livrées par le Centre canadien de télédection, peuvent être emmagasinées soit sur pellicule photographique, sous forme d'image, soit sur ruban magnétique. Deux raisons principales nous ont conduits à n'utiliser que des rubans magnétiques :
1) la résolution du scanner, de l'ordre de 80 mètres, étant déjà tout juste suffisante pour l'étude des lacs de moyenne ou faible étendues, les images photographiques à des échelles inférieures ou égales au millionième ne permettent donc pas d'utiliser au maximum cette résolution.
2) La pellicule photographique introduit un bruit supplémentaire, bruit dont le niveau de base constitue déjà un problème dans l'étude de l'eau.

Les données de base

Outre les quelque 300 images photographiques qui nous ont servi de référence, nos analyses ont donc été effectuées principalement à partir des sept rubans magnétiques contenant chacun une image dans les quatre bandes spectrales. Ces images ont été recueillies entre le 30 juillet 1972 et le 7 juillet 1973 (1007-15105, 1007-15112, 1059-14591, 1062-15170, 1311-15001, 1349-15114) et couvrent la vallée du Saint-Laurent, depuis Kingston jusqu'au Saguenay. Quant aux mesures de contrôle au sol, nous nous sommes servis principalement des données sur la qualité de l'eau de 147 lacs du Québec compilées par le ministère des Richesses naturelles et des données sur le Saint-Laurent mesurées depuis quelques années par le Centre de recherches sur l'eau de l'université Laval.

Traitement des données

A partir d'un ordinateur IBM 370/158, des programmes écrits en assembler et en PL/1 permettent de:
1) transformer les données de 6 à 8 bits et de les conserver dans un nouveau format ce qui permet d'augmenter la précision du lissage.
2) d'éliminer les erreurs de gains ou de déplacements entre les capteurs d'une même bande spectrale à partir des équations suivantes:

Pour le gain $b_k = Cb_j$

$$\text{où} \quad :C = \sqrt{\frac{P_k^{\,2} - Q_k}{P_j^{\,2} - Q_j}}$$

Pour le déplacement: $a_k = C(a_j - P_j) + P_k$

où : a : déplacement du capteur

b : gain du capteur

j et k: indice identifiant le capteur considéré (de 1 à 6)

P : moyenne des valeurs de réflectance

Q : moyenne des carrés de réflectance

3) d'effectuer des opérations mathématiques sur ces données.
4) d'imprimer les résultats sous différentes formes.

Etude des lacs

L'objectif de cette étude était de démontrer la possibilité d'utilisation du satellite ERTS pour la surveillance de l'évolution des lacs. Au Québec on en compte plus d'un million et il est bien évident que dans de telles conditions il n'est pas possible d'en suivre l'évolution par des mesures au sol. Si bien qu'une évaluation même grossière de l'eutrophisation des lacs par satellite serait une contribution importante à l'état de nos connaissances dans ce domaine. C'est également vrai dans le cas de nappes d'eau de grande étendue où les mesures ponctuelles par échantillonnage permettent difficilement de tracer une vue d'ensemble des caractéristiques globales du lac et encore moins d'en évaluer la dynamique.

L'approche la plus rationnelle pour établir la capacité du satellite à identifier les éléments chimiques et leurs concentrations, dissous ou en suspension dans l'eau est évidemment de mesurer *in situ* les concentrations de ces éléments et leurs propriétés optiques et d'en dégager des relations empiriques à partir d'un modèle théorique. Dans une première étape cependant, et en raison des contraintes techniques et financières qu'une telle étude exige, nous avons tenté d'établir des corrélations entre les caractéristiques

de l'eau (couleur, turbidité, concentrations de solides en suspension, etc.) et la réflectance de l'eau telle que mesurée par le satellite. La procédure était la suivante:
1) Il est d'abord nécessaire d'identifier les parties du territoire recouvertes d'eau. Pour ce faire une lecture est effectuée pour chaque point de l'image dans la bande MSS7 (0.8 à 1.1 μ), là où la réflectance de l'eau est minimale. Cette propriété de l'eau pour ces longueurs d'onde permet de différencier très nettement les parties du territoire suivant qu'elles sont recouvertes d'eau ou non. A partir de l'histogramme des valeurs de la réflectance de cette bande, on choisit donc un niveau correspondant aux nappes d'eau et excluant les terres.

Pour des valeurs calculées en 6 bits (0 à 63) ce niveau se situe à 2 généralement, alors que la réflectance du sol se situe à des niveaux supérieurs à 10. En choisissant des seuils entre 3 et 9 on peut donc inclure à volonté une plus ou moins grande étendue des rives des nappes d'eau ou des marécages.

Ce seuil choisi, on ne conserve en mémoire que les points de l'image où les valeurs de réflectance dans la bande MSS7 y sont inférieures ou égales.
2) Générer une image à l'échelle approximative du cent vingt millième en imprimant, à l'aide d'une imprimante standard couplée à l'ordinateur, des caractères alphanumériques formant une échelle de gris reliée au niveau d'énergie des pixels considérés. Chaque caractère, à cette échelle, représente 42 pixels (6 lignes par 7 colonnes). Cette étape permet d'identifier les nappes d'eau sans être obligé d'imprimer toutes les données à l'échelle maximum, ce qui nécessiterait environ 6,000 pages d'impression pour les quatre bandes.
3) Localiser sur cette image les lacs où une analyse sera exécutée.
4) Imprimer en 8 bits et à l'échelle maximum (~ 1 : 20,000) les portions d'images contenant ces lacs, après correction des gains et déplacements des capteurs.
5) Localiser sur ces nouvelles images des points particuliers où une mesure de la réflectance sera comparée aux mesures effectuées à partir des stations d'échantillonnage au sol.
6) Imprimer les résultats de ces analyses.
Cette procédure fastidieuse serait évidemment grandement améliorée par un traitement des données en mode conversasionnel entre l'analyste et l'ordinateur, par le biais d'une console vidéo d'entrée-sortie.

La figure 1 montre comment se situe la réflectance de l'eau dans les bandes MSS5 pour quelques nappes d'eau étudiées. Les conclusions que l'on peut tirer de ces analyses peuvent être résumées comme suit:
1) Il est absolument essentiel de procéder au lissage des images en éliminant les variations de gains et de déplacements des capteurs et d'effectuer ces calculs en 7 ou 8 bits.
2) Un filtrage spatial réduisant les variations de réflectance de haute fréquence serait également très avantageux.
3) Pour des lacs oligotrophes comme la plupart de ceux que nous avons considérés dans cette étude, les faibles variations de réflectance ne permettent pas de relier ces données aux mesures *in situ*.
4) L'effet d'atténuation de la lumière dans l'eau étant dû principalement à l'absorption par les substances dissoutes et le scattering sur les particules en suspension on peut espérer différencier ces deux contributions dans les cas où les concentrations de solides en suspension sont importantes. On remarque en effet à la figure 1 que pour une nappe d'eau donnée on peut tracer une droite dont la pente est voisine de l'unité. Nous estimons que cette pente est directement reliée à l'absorption (la "couleur" de l'eau) tandis que sa longueur serait une mesure indirecte de la concentration de solides en suspension (scattering).

Une autre hypothèse peut être formulée à partir de cette figure. On peut en effet supposer que le point de rencontre des droites tracées à partir des différentes masses d'eau considérées représente la contribution résiduelle, d'une part de la réflexion de la lumière par la surface de l'eau et, d'autre part, de la diffusion moléculaire dans l'atmosphère. On peut donc supposer que les valeurs a et b indiquées à la figure 2 sont une mesure de ces deux contributions dans les bandes MSS4 et MSS5.

Finalement ces quelques résultats fragmentaires accumulés portent à croire qu'il ne sera peut-être pas trop difficile de relier les données d'une image à une autre, pour des orbites différentes. La figure 3 montre que la position relative des lacs est à peu près constante d'une image à l'autre, en l'absence de modifications des caractéristiques des lacs. Il suffirait donc de soustraire les quantités c et d des valeurs respectives de réflectance dans les bandes MSS4 et MSS5 pour pouvoir suivre l'évolution temporelle des caractéristiques des lacs.

Ces résultats et conclusions préliminaires ne permettent certes pas de confirmer catégoriquement les hypothèses avancées. Ils permettent toutefois de situer plus précisément les limites et les potentialités d'une étude systématique et continue de millions de lacs couvrant le territoire canadien.

Le développement d'une méthodologie s'inspirant de ces quelques résultats pourrait peut-être servir de base à un contrôle continu des caractéristiques globales des lacs, ce qui constituerait en soi un immense progrès par rapport à la situation actuelle.

- Etude du Saint-Laurent

Corrélations avec la qualité de l'eau.

Utilisant les données numériques de la réflectance pour des points de l'image correspondant aux stations d'échantillonnage de la qualité de l'eau, nous avons systématiquement comparé ces valeurs aux résultats des analyses de l'eau. Bien qu'il n'y ait pas eu de correspondance de date, pour ces deux séries de données, et qu'au surplus la localisation des stations soit très imprécise nous avons obtenu des équations de régression confirmant l'allure des courbes tracées précédemment. Les équations peuvent se ramener sous la forme suivante:

$$C_1 P = C_2 - (MSS4-MSS5)$$

où : C_1 et C_2 : constantes

P : valeur du paramètre considéré

MSS4 : réflectance de l'eau dans cette bande

MSS5 : réflectance de l'eau dans cette bande

Pour $\frac{\partial P}{\partial MSS4} = Cte$ et $\frac{\partial P}{\partial MSS5} = Cte$,

ce qui se vérifie dans nos analyses des données, on retrouve en effet la relation linéaire illustrée précédemment entre les valeurs de la réflectance dans ces deux bandes spectrales, soit: $MSS4 = MSS5 + C_3$

Les paramètres considérés étaient la fluorescence naturelle, la dureté et la conductivité. Les coefficients de corrélation variaient autour de 0.35, ce qui est assez faible mais qui peut s'expliquer par le fait qu'il n'existe pas de lien direct entre la réflectance de l'eau et ces paramètres. C'est par le biais d'une forte corrélation entre ces paramètres et la turbidité que l'on en perçoit l'influence. Malheureusement pour l'image considérée dans cette étude (1044-15170) nous ne possédions que très peu de données ponctuelles sur la turbidité et c'est pourquoi nous n'avons pu comparer ce paramètre à la réflectance de l'eau.

Hydrodynamique

Nous avons tenté de montrer le potentiel de ERTS à l'étude hydrodynamique du Saint-Laurent. L'histogramme de la figure 4 montre que, dans certains cas du moins, il est possible de différencier nettement deux types d'eau suivant leurs caractéristiques spectrales. On peut donc espérer pouvoir tracer le front de mélange de ces eaux lorsqu'elles se rencontrent et possiblement définir leur profil de diffusion. Les figures 5 et 6 ont été obtenues pour des dates assez voisines, la première par l'analyse des données de ERTS, la seconde par des relevés par bateau. On peut constater une similitude dans la localisation du front de mélange, similitude que l'on pourrait sans doute constater pour d'autres portions plus étroites du Saint-Laurent avec des méthodes d'analyse numérique des données plus sophistiquées.

Dans l'estuaire moyen du Saint-Laurent, soit dans la région aval de Québec, deux séries d'images (1007-15113 et 1349-15114) révèlent des "pattern" dans l'eau assez saisissants mais que nous n'avons point encore étudiés au moyen d'un modèle hydrodynamique.

Classification semi-automatique de l'utilisation du sol.

La connaissance de l'utilisation du sol et sa dynamique sont essentielles à la gestion de l'eau si l'on veut relier l'utilisation du territoire aux caractéristiques des eaux drainées.

D'autre part, on peut dans certains cas améliorer la prévision des débits des rivières dans un modèle hydrologique par la mesure de certains paramètres reliés à l'utilisation du sol (type de couverture végétale et superficie, localisation des nappes d'eau, des marécages, etc.). Dans cette optique, il nous est apparu intéressant d'illustrer la puissance des techniques d'analyse statistique appliquées à l'identification de l'utilisation du sol d'une portion du territoire de la vallée du Saint-Laurent.

Les facilités techniques et les programmes-ordinateur d'une firme américaine ont donc été utilisées pour traiter une image que

nous a fournie le Goddard Space Flight Center. Cette image couvre à peu près le territoire compris dans l'image 1007-15104.

A l'aide de cartes d'utilisation du sol au cinquante millième, une série de zones de contrôle ("training set") furent sélectionnées et localisées exactement sur l'image de ERTS, chaque zone correspondant à une couverture du sol connue. Au moins 100 pixels composaient chacun de ces territoires de référence. L'analyse canonique des données a permis alors d'identifier dans le reste de l'image les territoires qui avaient la même distribution spectrale que les zones de contrôle.

La figure 7, obtenue suivant cette méthode, montre la couverture forestière le long du Saint-Laurent, entre Montréal et Trois-Rivières. Plusieurs autres classes ont été obtenues de la même manière: les grandes cultures, les cultures maraîchères (le tabac principalement), les marécages et l'urbanisation intensive. Si l'on considère qu'une dizaine d'heures-hommes de travail ont permis d'obtenir ces résultats, et ce en dépit de notre inexpérience comme opérateurs, on comprendra facilement que ce type d'analyse présente un potentiel énorme en regard des besoins mentionnés précédemment.

- Conclusions

En s'inspirant de la conception du rôle de la télédétection par satellite dans la gestion des eaux, esquissée au début de ce texte, nous avons pu déjà montrer quelques exemples du potentiel de cette technologie. Ceci malgré le fait que l'imagerie étudiée et les données de contrôle au sol étaient fort limitées et qu'au surplus nos méthodes d'analyse des données ne tiraient pas pleinement profit de toutes les informations contenues dans ces images. Il apparaît donc assuré que le développement d'une telle méthodologie puisse servir d'instrument privilégié dans le contrôle et plus globalement dans la gestion des eaux.

Dans la perspective du lancement, d'ici quelques années, de satellites géostationnaires ou sur orbites multiples beaucoup plus puissants en ce qui concerne la résolution spatiale et spectrale, ce qui risque avant tout de manquer, au Québec particulièrement, c'est le savoir-faire et les facilités techniques permettant d'exploiter efficacement ces données au profit de la collectivité. C'est en voulant faire face à ce défi que nous avons entrepris ces travaux. L'envergure des besoins sous ce rapport nous force cependant à croire qu'une amélioration sensible de la position du Québec dans ce domaine ne peut être envisagée sans qu'un organisme régional d'analyse et d'interprétation des données recueillies par télédétection soit créé et qu'un soutien financier lui soit accordé, comme aux différents groupes oeuvrant déjà dans ce domaine, par les différents paliers de gouvernement.

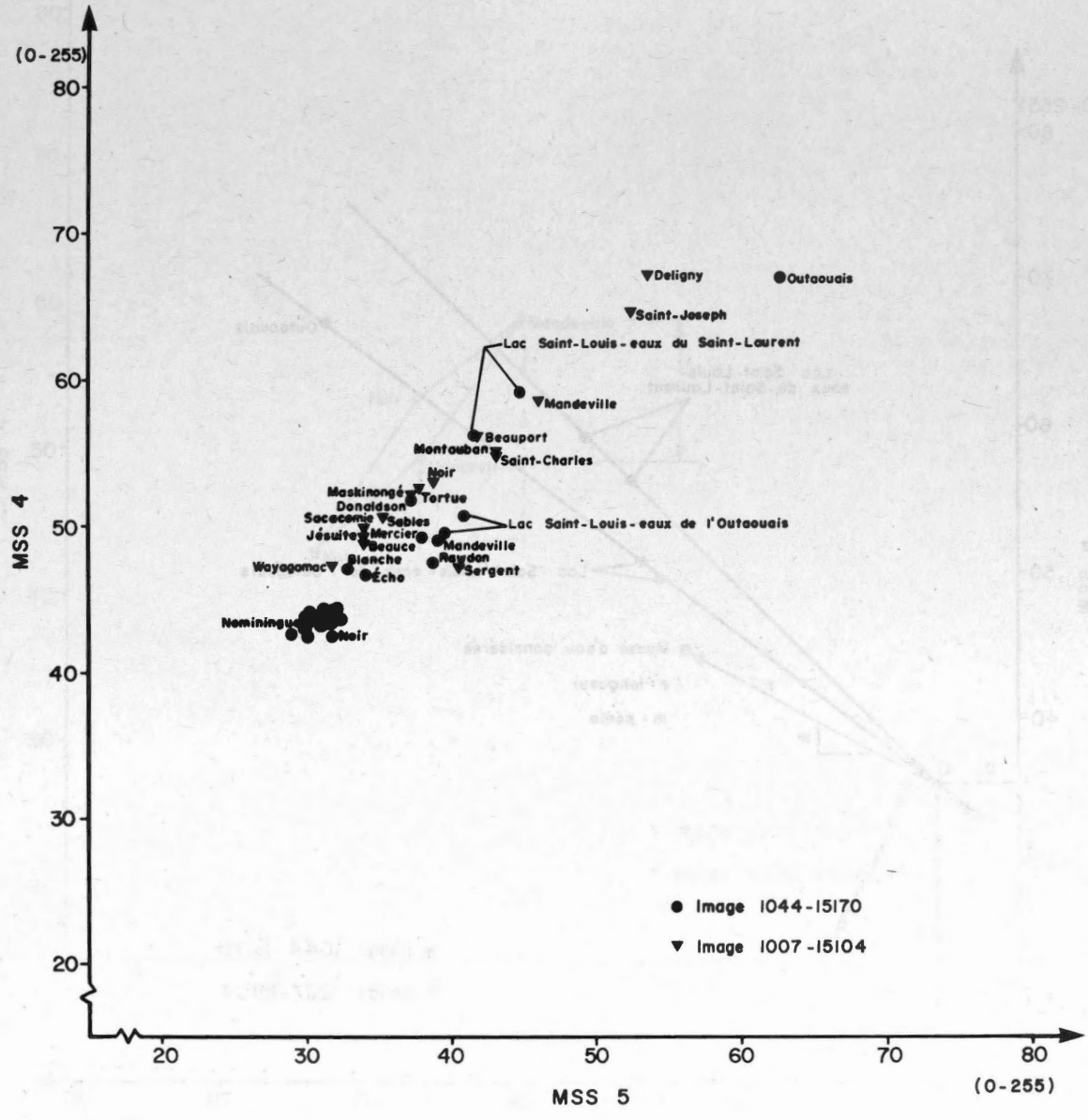

Figure 1

RÉFLECTANCE DE QUELQUES LACS DANS LES BANDES MSS 4 ET MSS 5

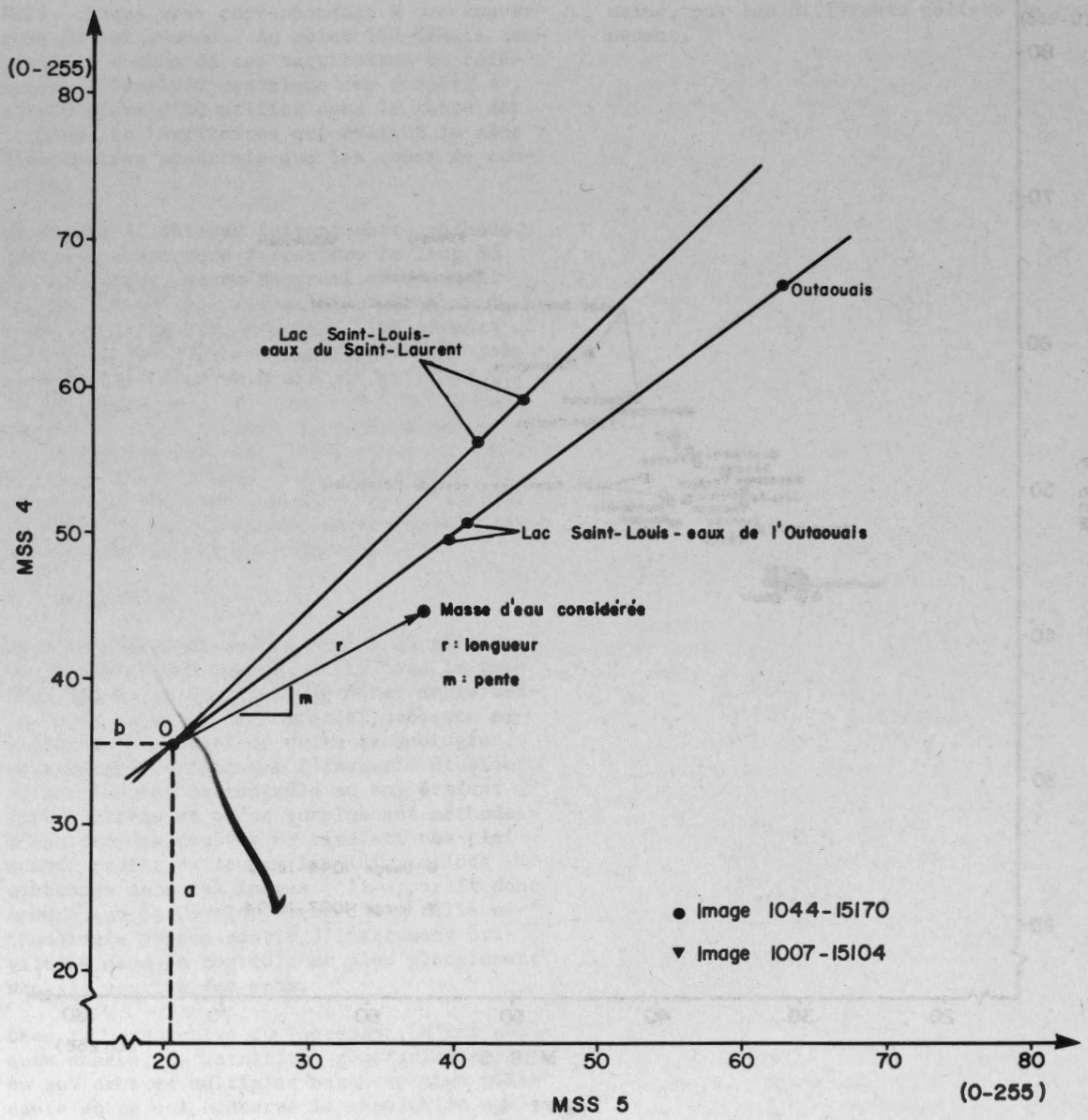
(0-255)
80
70
60
50
40
30
20
MSS 4
Lac Saint-Louis-
eaux du Saint-Laurent
Outaouais
Lac Saint-Louis - eaux de l'Outaouais
Masse d'eau considérée
r : longueur
m : pente
r
m
b
0
a
● Image 1044-15170
▼ Image 1007-15104
20
30
40
50
60
70
80
(0-255)
MSS 5

Figure 2

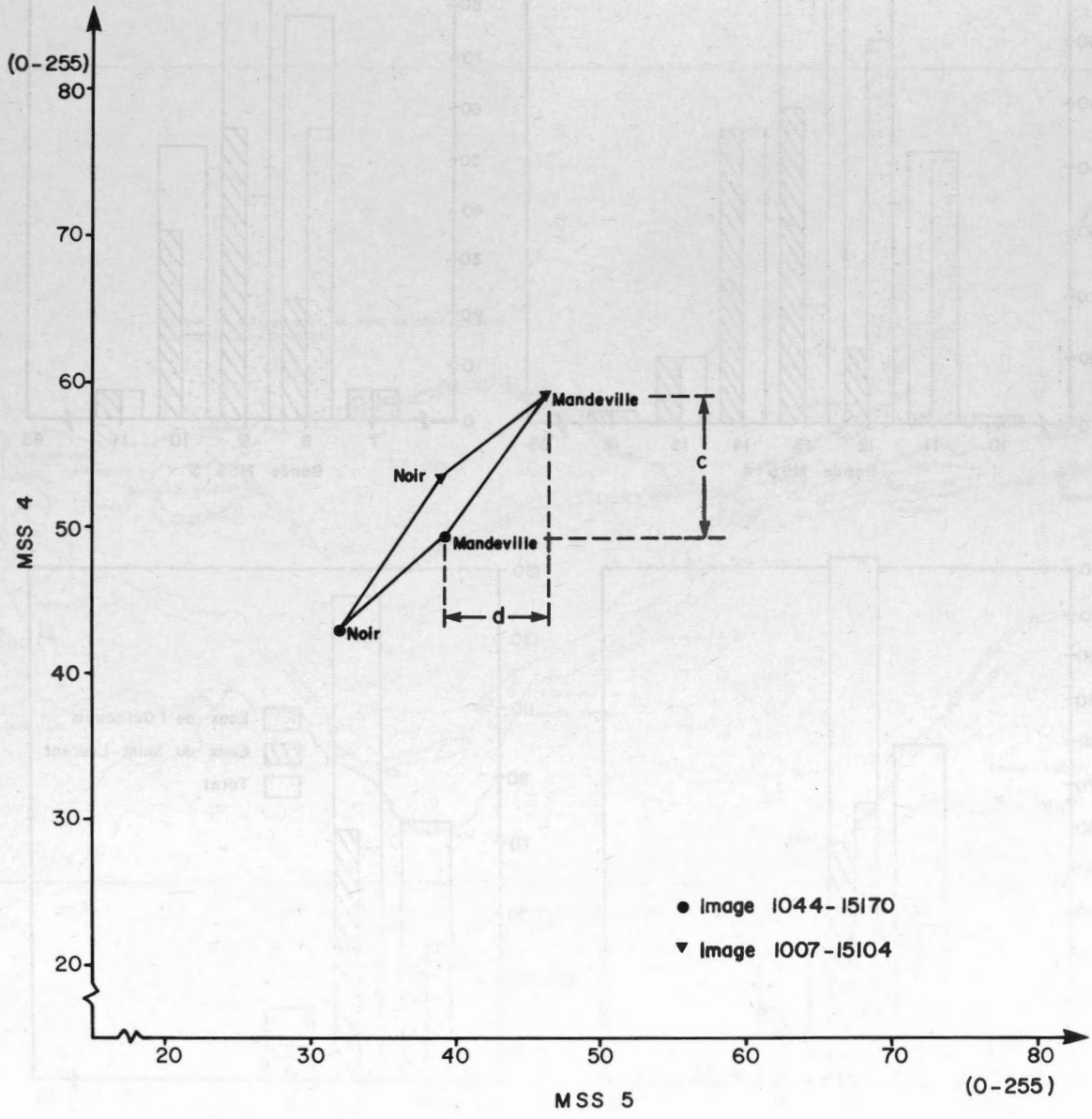
(0-255)
80
70
60
50
40
30
20
MSS 4
Mandeville
Noir
Mandeville
Noir
C
d
● Image 1044-15170
▼ Image 1007-15104
20
30
40
50
60
70
80
(0-255)
MSS 5

Figure 3

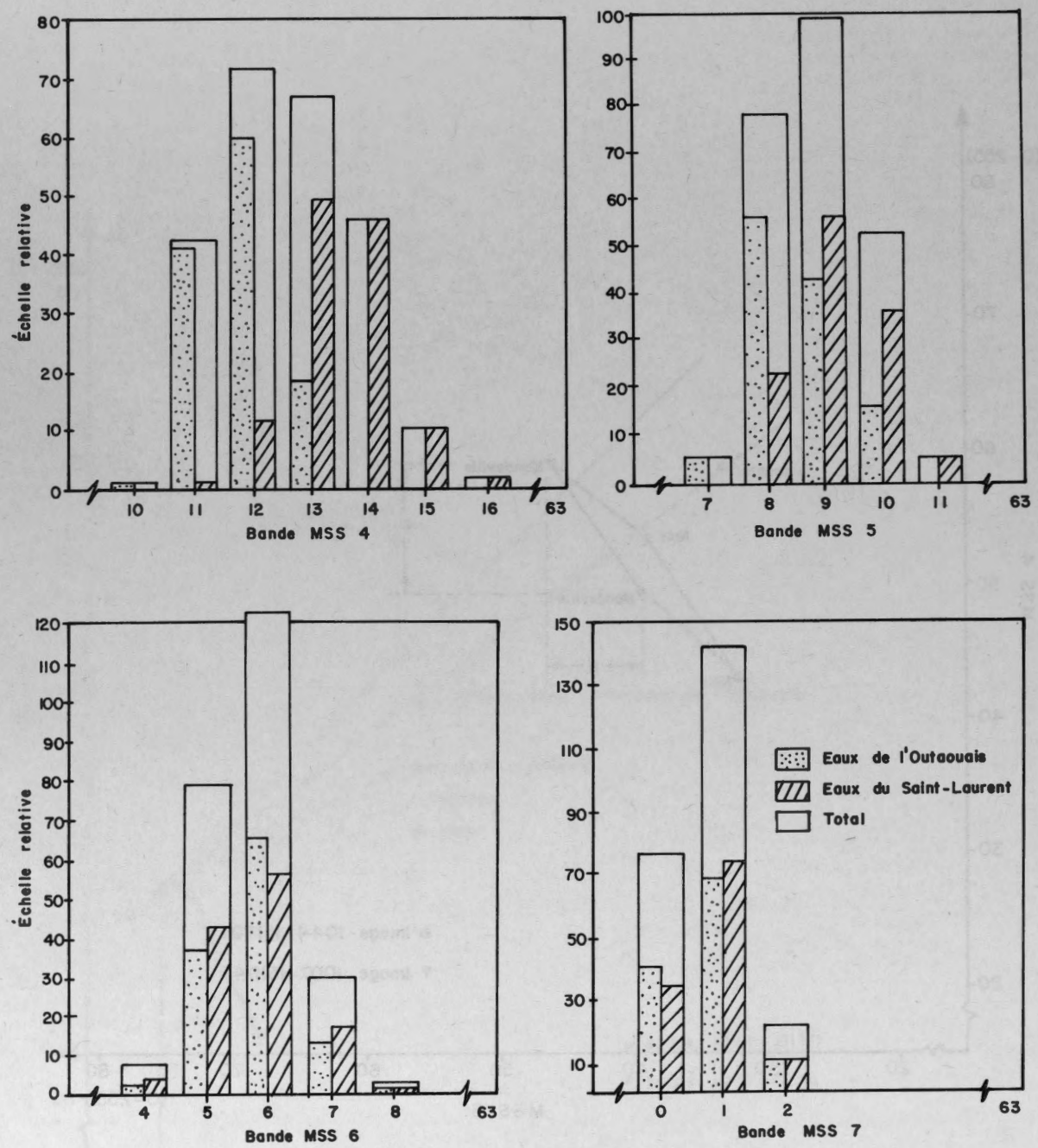

Fig. 4 - HISTOGRAMMES DE LA RÉFLECTANCE , LAC SAINT-LOUIS - IMAGE 1044-15170

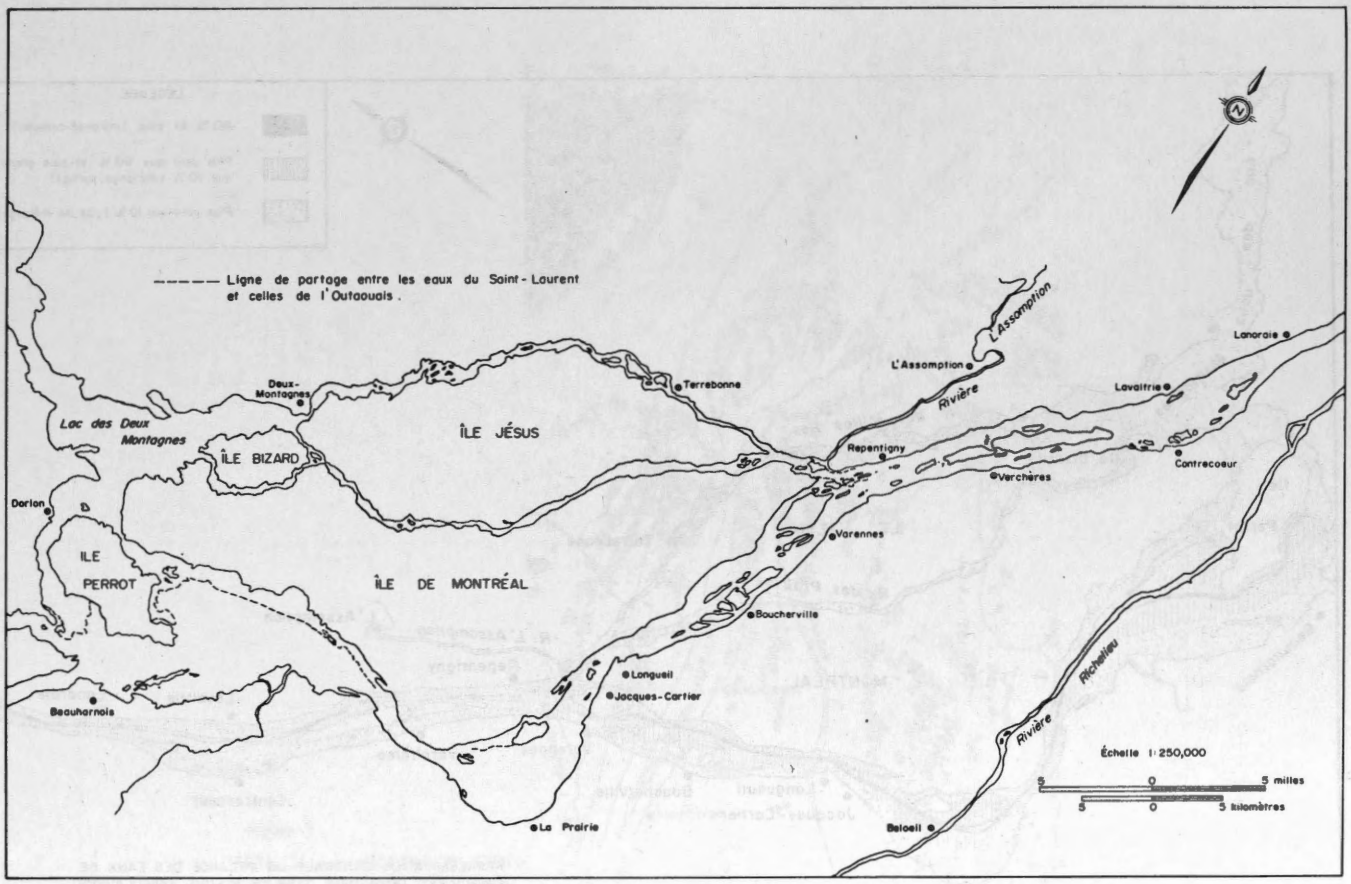

FRONT DE MÉLANGE DES EAUX DE L'OUTAOUAIS ET DU SAINT-LAURENT (ERTS)

FIGURE 5

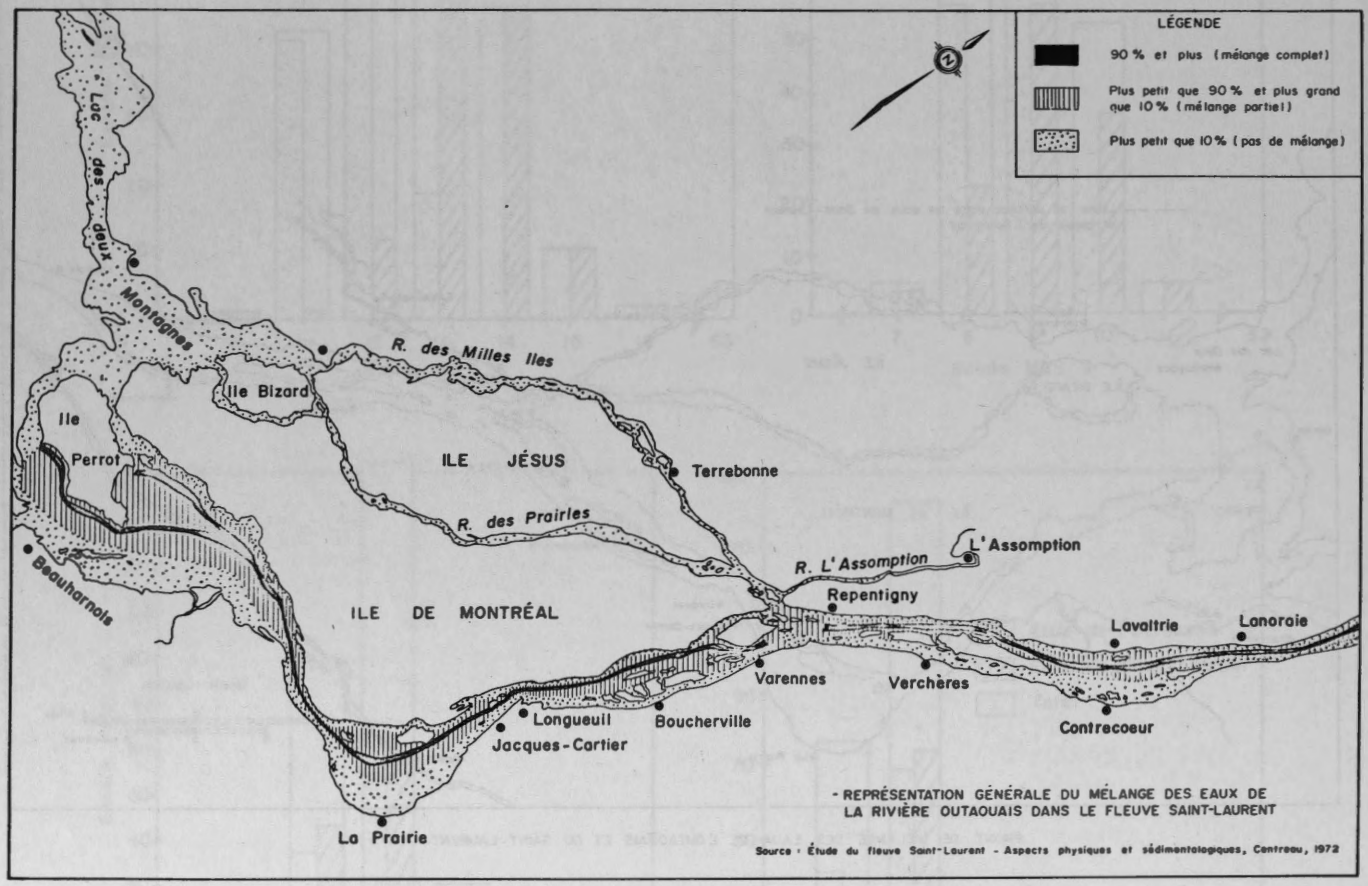
LÉGENDE
90 % et plus (mélange complet)
Plus petit que 90 % et plus grand que 10 % (mélange partiel)
Plus petit que 10 % (pas de mélange)
Lac des deux Montagnes
R. des Milles Iles
Ile Bizard
Ile Perrot
ILE JÉSUS
Terrebonne
R. des Prairies
R. L'Assomption
L'Assomption
Repentigny
Beauharnois
ILE DE MONTRÉAL
Lavaltrie
Lanoraie
Varennes
Verchères
Longueuil
Jacques-Cartier
Boucherville
Contrecoeur
La Prairie
- REPRÉSENTATION GÉNÉRALE DU MÉLANGE DES EAUX DE LA RIVIÈRE OUTAOUAIS DANS LE FLEUVE SAINT-LAURENT
Source : Étude du fleuve Saint-Laurent - Aspects physiques et sédimentologiques, Centreau, 1972

FIGURE 6

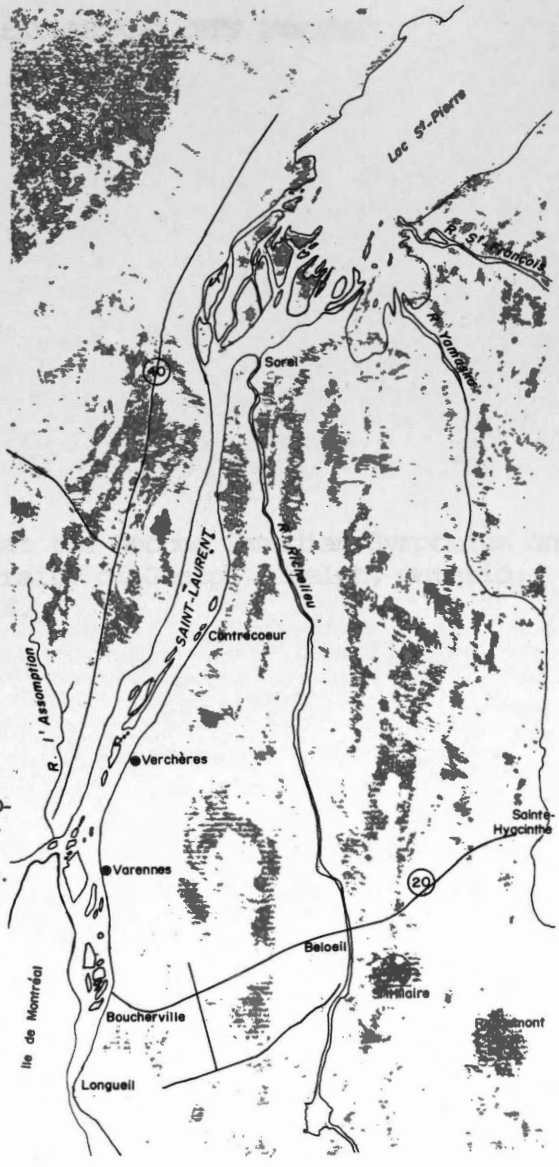

Figure 7

CARTE DE LA VÉGÉTATION ARBORESCENTE DRESSÉE AUTOMATIQUEMENT PAR ANALYSE CANONIQUE DES DONNÉES DE ERTS.

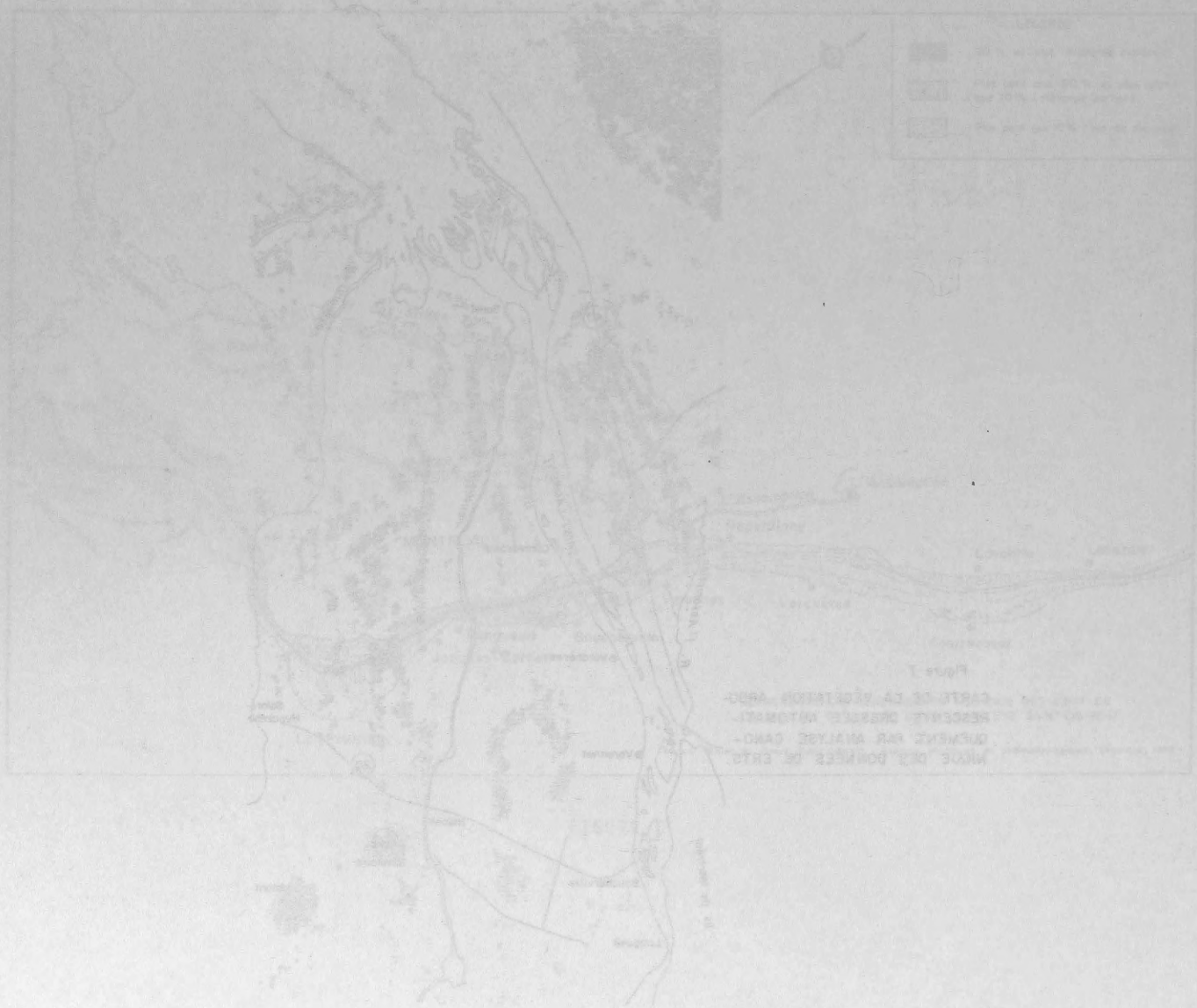

MAPPING ACTIVITIES: SKYLAB AND ERTS IMAGERY

By

DR. R.A. STEWART
E.A. FLEMING

This paper presented at the Second Canadian Symposium on Remote Sensing, University of Guelph, Guelph, Ontario, April 29 - May 1, 1974.

MAPPING ACTIVITIES: SKYLAB AND ERTS IMAGERY

Dr. R.A. Stewart and E.A. Fleming
Topographical Survey Directorate,
Surveys and Mapping Branch,
Department of Energy, Mines and Resources,
Ottawa, Ontario.

I SKYLAB

1. Introduction

In February, 1971, NASA solicited international participation in the proposed SKYLAB earth sensing experimentation. We in the Surveys and Mapping Branch, Department of Energy, Mines and Resources, saw this as our first opportunity to acquire satellite imagery at relatively large scale, with high resolution, high metric quality and of a selected area of Canada. In April, 1971, R.A. Stewart submitted to NASA a detailed proposal for investigation of SKYLAB imagery for mapping purposes.

Confirmation that our proposal had been approved was received in October, 1971. The manned mission was scheduled for launch in late 1972 (later postponed to early 1973).

Earth sensing was only one part of the multi-purpose mission. Bio-medical studies of man over protracted periods in a zero-gravity environment, engineering experiments, sun observations, and several other types of experiments were allotted most of the mission time. Since the space vehicle had to be rotated so that the sensors were pointing down at local vertical each time an earth sensing "pass" was recorded, the number and duration of these "passes" were limited.

2. Projected Investigations

The original request for SKYLAB EREP (Earth Resources Experimental Package) data covered a 100-mile wide swath from Toronto to Quebec City. This particular area was chosen primarily because it had the most complete coverate by 1:25,000 mapping - for subsequent ground truthing work. The subject area also had a wide variation in types of topography, ground cover classifications, and incidentally, a large proportion of the population of Canada. The 100-mile width was dictated by the coverage capability of the primary (S-190A) camera system on board SKYLAB. The requested coverage was subsequently extended southwest to begin at Windsor.

Imagery and attendant data were requested from four of the six sensors in the EREP system. These four were (a) the 6-chamber (6 lens-emulsion combinations) multi-spectral metric camera system, (b) the long focal length high resolution camera, (c) the 13-band multi-spectral scanner, and (d) the infrared spectrometer. These instruments are designated the S-190A, S-190B, S-192, and S-191 systems respectively. The other two sensors were the S-193 radiometer/scatterometer/altimeter and the S-194 L-band radiometer. Data from the latter two sensors were not required or requested for this project.

Only a few basic specifications for the S-190A and S-190B systems are given here. Detailed specifications for all 6 sensors are available in printed form. The S-190A system is comprised of 6 lens-emulsion combinations. The emulsions used were 2 panchromatic X black and white, two infrared black and white, 1 "Aerial" colour, and 1 infrared colour. The S-190A lens focal length was 6 inches, format of 70 mm by 70 mm, which provided an original image scale of 1:2,800,000, and the terrain coverage is approximately 100 by 100 statute miles. The S-190B is a single camera with focal length of 18

inches, 4½" x 4½" format, which provided an original image scale of approximately 1:940,000 and a terrain coverage of approximately 80 x 80 statute miles. The S-190B was loaded with either Pan X or aerial colour film for the various earth sensing "takes".

The Topographical Survey Directorate, Surveys and Mapping Branch, Department of Energy, Mines and Resources, will conduct experiments to determine the usefulness of the metric camera imagery for new and revision line mapping, photomapping and mapping photo-interpretation - as required for the various national mapping series. Co-investigators in the Surveying Engineering Department, University of New Brunswick, The Department of Photogrammetry, Laval University, and the Canada Centre for Remote Sensing will conduct specified investigations within this total project proposal. UNB will investigate the applicability of these types of satellite photography to the establishment of photogrammetric control points for mapping. Laval will determine the efficiency of using satellite photography to control and position strips, or a block if possible, of conventional aerial photography. The Canada Centre for Remote Sensing will assess the multi-spectral scanner and infrared spectrometer data for development of interpretation techniques and classification of terrain cover features.

The investigations outlined above must still be described in the future tense because the requested imagery and data have just begun to arrive from NASA and are being reproduced for the approved investigators. Acquisition of these data was conditional on the agreement with NASA that approved investigators receive the imagery first - so that they may get on with their proposed investigations. In addition, these investigators may not release any of their findings without prior approval of NASA. The results of the investigations belong first to NASA, in exchange for receipt of the requested data. NASA reserves the right to release all findings to the public domain.

However, NASA has agreed that the National Air Photo Library, Ottawa, may sell reproductions of SKYLAB imagery of Canada to any and all interested Canadian concerns. Master copies of the imagery received to date will be deposited in the National Air Photo Library by about May 15, and they will accept orders for reproductions from that date.

Since all expected data has not yet been received from NASA, the actual magnitude and scope of the proposed investigations cannot yet be fully ascertained. The actual experimentation will depend upon the ultimate quantity, quality and coverage of the received data. It appears that one approved proposal has already had to be cancelled because of the unavailability of requested coverage. This proposal was made by the Photogrammetry Section, Ontario Department of Transportation and Communications, and was to consist of a study of SKYLAB imagery for the purpose of plotting transportation routes - both highways and water courses.

3. SKYLAB Missions and Data Received

The satellite was designed to fly in a near-circular orbit at an altitude of approximately 270 statute miles. The inclination to the equator was 50°, and thus it only over-flew a relatively narrow band of southern Canada. (In fact, the satellite is still orbiting, but now unmanned.) SKYLAB I, the unmanned workshop, was launched on May 14, 1973. On May 25, the first team of 3 astronauts was sent up to start the SKYLAB II manned mission. This mission was terminated on June 22, 1973. The second manned mission, designated SKYLAB III, began on July 28 and terminated on September 25. Finally, the third manned mission, with the third team of three astronauts, began on November 10, 1973 and terminated on February 8, 1974.

At the beginning, the prospect of acquiring our full requested pass, from Windsor to Quebec City, looked very good. Our pass was scheduled for May 19, early in the first manned mission.

However, as you may recall, during the SKYLAB I launch, a large solar panel deployed and ripped off, severely damaging the space station's solar heat shield. That occurance ultimately eliminated the possibility of acquiring our requested pass during the first manned mission. During the second manned mission - SKYLAB III - problems were encountered with the gyro stabilizers, and this curtailed the number of earth sensing attempts, However, on September 9, the first pass was taken over the requested project area. It was only minimally successful because of cloud conditions. Several attempts were subsequently made to acquire data over eastern Canada.

During SKYLAB III, a total of 7 earth sensing passes were recorded over eastern Canada, and 2 along the Canada-U.S. border south of Winnipeg. Three of these passes produced short series of good images, the others were largely cloud covered. One of the good passes covers southern New Brunswick and northern Nova Scotia, the other two show a stretch of the southern edge of Manitoba. The other passes produced the occasional good view of the Windsor-Detroit and Toronto areas. Where the terrain can be seen, however, some excellent images of high quality were obtained.

A small amount of additional coverage from the third manned mission (SKYLAB IV) was scheduled, but no information has yet been received on the results of any attempts. One must keep in mind that some 145 principal investigators from around the world are continually badgering NASA for their requested data. A total of about 40,000 frames of photography and 228,000 feet of magnetic tape were expended in acquiring the requested data.

In summary, although the imagery and data received (and expected) is somewhat less than we had hoped for, we have received samples of sufficient size to permit some of the investigations to proceed. A preliminary quick-look at the imagery on hand indicates that some very useful and interesting findings can be expected.

II ERTS IMAGERY FOR MAPPING PURPOSES

Since the operational specifications and performance characteristics of ERTS are now well known to the remote sensing fraternity, no attempt need be made here to describe them.

1. Usefulness of ERTS Imagery

Several uses of ERTS imagery have been explored in relation to map production requirements in the Surveys and Mapping Branch, Department of Energy, Mines and Resources.

(a) Revision

(i) Off-Shore Islands - Because of the recent dramatic increase in interest and activity in the Arctic Islands, principally due to oil and gas developments, the need for revision of the existing 1:250,000 scale series of maps and for new 1:50,000 scale coverage is becoming increasingly more evident. Efficient and safe air and sea navigation and pilotage require the accurate positioning of the myriad of small off-shore islands. ERTS imagery is becoming a valuable tool in the positioning and orientation of these often remote off-shore islands. Although the absolute geometric accuracies of features on ERTS imagery are quite variable, and generally inadequate for standard 1:250,000 scale mapping, these images are nevertheless extremely useful when no ground control exists and when conventional aerial photography cannot bridge the water gaps between islands. The 110 x 110 statute mile coverage of an ERTS image usually bridges the gap quite nicely. The cost of establishing ground control points on all of the large number of small, isolated off-shore islands would be prohibitive.

It has been found that revision of such features as the major roads, reservoirs and transmission lines that appear on 1:250,000 maps, or the smaller scale aeronautical charts, can be made with adequate accuracy from ERTS imagery in many cases.

The technique used is to enlarge the imagery to the map scale either optically or photographically (or in combination) and transfer the feature to the map base by local fit of common detail between the image and the map.

(ii) Reservoirs - The reservoir formed behind the Kettle Rapids dam provided a test area to evaluate the accuracy of transfer of water features to 1:250,000 mapping. Although revision had been done on the 1:50,000 map sheets using larger scale aerial photography, the 1:250,000 map sheet was not yet revised. Two revision outlines for the reservoir at this scale were therefore prepared. One was derived from the 1:50,000 maps, and the second was derived from a Band 6 ERTS image of the reservoir obtained a year after the revision photography. The outline of the reservoir was transferred to the map base using an enlargement of the ERTS image under the base and making local fits to adjoining map detail. The enlargement scale was only approximate since in this case an "initial" image was used. Local fitting was aided by the abundance of small lakes in the vicinity of the reservoir.

The two outlines so obtained differed very little. There are some differences that can be attributed to errors in positioning islands, and other differences that might reflect a difference in water level between the two coverages a year apart. The outline obtained from the ERTS image is not inconsistent with the 1:250,000 map accuracy requirements.

(iii) Roads - The location of roads in remote areas is difficult to determine accurately from anything less than vertical photographic coverage that can be linked to surrounding detail. Only the most general of plans ever exist for these roads; they are adapted to the terrain as they are constructed.

The road to Tungsten in the Yukon was one such road whose location was only approximate on the published 1:250,000 map. The road was visible through part of its length on an ERTS precision image. It had also been photographed at a scale of 1:12,000 for revision purposes.

The road location determined from ERTS coincided over the greater part of its length with that derived from the large scale aerial photography, but there was one section of the road that deviated in position by 1500 m. Since the ERTS image was unambiguous about the road location, the large scale photos were re-examined. It was found that in this particular section there was very little mapped detail which could be used to position the large scale photography accurately and errors in azimuth had crept into the plot resulting in a misplacement of the road.

Although the broader view of ERTS in this instance resulted in a more accurate road position, such is not always the case. The new highway to link Ottawa and Montreal runs through predominantly rural land, and although the roadway under construction can be seen on the ERTS image, positioning it accurately is made difficult by the lack of well-defined adjoining features. Normal aerial photography that clearly shows all the secondary roads can be positioned much more accurately with respect to mapped detail.

(iv) Transmission Lines - Power developments such as the one at Churchill Falls in Labrador result in transmission lines being erected across hundreds of miles of uninhabited territory. Such a transmission line could well be almost the only man-made feature on an entire 1:250,000 map sheet. Where vegetation is cleared for the erection of these lines, their location can often be established accurately on ERTS imagery. Although the cut lines are often visible on band 5 summer imagery, snow in the winter makes the line visible on any band.

(b) Photomapping

The use of the ERTS image as a photomap base imposes a requirement in the imagery for planimetric reliability and image definition suitable for the scale of map selected.

The planimetric accuracy of the image varies with the type of correction applied to the image as it is generated and those generated by CCRS fall into three groupings in this respect:

Initial or Quick-Look imagery	±5000m skew
Imagery with earth rotation correction	±1000-1500m
Precision imagery	RMS 300-700m

Tests with precision imagery have shown that both accuracy and image quality did not warrant the use of scales larger than 1:500,000 for a photomap product.

Because the ERTS orbital path is diagonal to the conventional map sheet boundaries, a single-image format sheet with the sheet boundaries conforming to the image boundaries offers a number of advantages, but has the drawback of resulting in redundant coverage due to the high overlap between orbital paths.

Various test sheets have been made, both on conventional sheet formats and on image formats, but lack of adequate imagery and lack of any expressed need preclude any extensive photomapping program proceding at this time.

(c) Relief Shading

Portrayal of the character of the ground by means of relief shading is an integral part of the World Aeronautical Chart Series. At a scale of 1:1,000,000 contours are not effective for this purpose, although they are the basis from which the person doing relief shading works. He must supplement his information of the topography, with aerial photography. When working at a scale of 1:1,000,000 this involves looking at hundreds of photos. It has been found that ERTS images, particularly winter ones with snow on the ground can be very helpful in picking out the minor topographic features which give character to the ground - the fault lines, the folds, the ridges - which contours fail to portray. It is additionally helpful in that the scale of the ERTS image matches that of the maps being compiled.

2. The Limitations of ERTS as a Mapping Tool

Although the possibility of using ERTS imagery for 1:250,000 revision mapping has been demonstrated, it must be borne in mind that ERTS was not designed as a map-maker's tool. The very multi-spectral aspect of the sensor which is of value to the resource scientist, works to the detriment of the map-maker. To have water areas well-defined on a band 6 or 7 image, but to have to refer to a band 4 or 5 image in order to see the roads adds a compilation that the map-maker does not face when he works with the broader spectrum recorded by aerial photography.

Colour composites theoretically overcome this disadvantage, but only with the accompanying added cost of colour, and since a four times enlargement of the ERTS image is required to utilize the data on 1:250,000 maps, any lack of registration of the bands in a colour composite is quite apparent. In general, it is more satisfactory to work with the black and white band which portrays the feature the best.

The multi-spectral aspect of ERTS creates a similar problem for the photomapping uses of the imagery. Any one band does not give a complete picture of the terrain.

Two bands can be combined in black and white, and by careful balancing of exposures, the water features of a band 6 image can be combined with the culture and vegetation of a band 5 image. Similarly colour can be used to combine the information content of 3 bands, although the colour of the resulting image bears no relation to natural colour. The colour can be arbitrarily set for any <u>one</u> image.

Thus, a photomap produced from a <u>single</u> ERTS image, either in colour or black and white is practical. But producing a photomap of a standard map sheet requires the mosaicing of a number of images, and in making mosaics in either black and white or colour compromises must be made with respect to content.

For a black and white product, each band must be mosaiced separately for a uniform presentation of the ground features. For colour, the lack of a colour standard, the seasonal differences, the changes in atmospheric conditions and the variations in sensor output present expensive colour matching problems. In the preparation of a 1:1,000,000 colour mosaic of Iran, the EARTHSAT Corporation took three months to colour match 20 images using dye transfer techniques, and a match was achieved only at the expense of compressing the colour scale.

THE STATISTICS OF ERTS MSS IMAGERY

By

IAN K. CRAIN

This paper presented at the Second Canadian Symposium on Remote Sensing, University of Guelph, Guelph, Ontario, April 29 - May 1, 1974.

THE STATISTICS OF ERTS MSS IMAGERY

Ian K. Crain
Applications Division
Methodology Section
Canada Centre for Remote Sensing
Department of Energy, Mines and Resources
Ottawa, Ontario

INTRODUCTION

Much effort in remote sensing methodology is being expended on the design and implementation of algorithms for automatic classification of ERTS multispectral scanner imagery. There are two major alternative approaches to this problem of algorithm selection, namely, 'ad hoc' selection and 'data oriented' selection. The former is basically a try-it-and-see philosophy where the selection criteria are often such things as, ease of computer programming, simplicity of mathematical form or fast computation time. In 'data oriented' selection, the nature (usually statistical) of the data is examined and the algorithm selected or designed to fit the particular needs of the type of data.

Both methods have merits and defects which can be argued at great length. However, if one is to apply data oriented algorithm selection to ERTS imagery, then it is necessary to thoroughly analyze the statistical nature of the imagery over large regions. This then, is the objective of this paper, and it is hoped that the statistics compiled will be a constructive aid to algorithm selection for ERTS imagery analysis.

SCOPE OF THE STATISTICAL STUDY

There is, of course, an endless series of 'statistics' that should be compiled for an ERTS image. This study has chosen a limited subset of these which are of a basic nature and directly provide useful information about the imagery. The statistics measured are: 1) marginal density functions of image grey levels in each band. This provides information concerning the effective dynamic range of the image, the nature of the density function which best describes the spectral data, and allows the placing of limits on the number of possible themes which the various standard classification schemes can achieve, 2) various conditional probability densities within and between spectral bands, these provide information on the physical texture and non-independence of pixels within a band and the non-independence of spectral bands respectively. The observations on probability densities are supported by studies of the observed correlation coefficients within and between bands and by two-dimensional histograms. These statistics give indications of the "region of influence" of a pixel and would be beneficial in the design of textural identification algorithms. 3) Run length statistics. The distribution of the length of 'runs' (consecutive identical pixels) is important for consideration of problems of ERTS image data compression and transmission.

THE STUDY AREA

It is important in a statistical study that a relatively large sample be obtained. In this study a portion of an ERTS frame containing about 80,000 pixels was chosen, in an area of predominently agricultural land-use in Saskatchewan. Intentionally, there were no significant bodies of water in the area. The data are derived from ERTS frame No. 103117265 which dates from Aug. 1972. Figure 1 shows the study area.

An agricultural area was chosen because of the current high interest in automatic crop identification in Canada. Work is on-going on producing equivalent statistics for agricultural areas in different regions, forested areas, urban areas, tundra and high arctic scenes.

It is worthy of note that the statis-

tical properties of image, in general, will not have any of the commonly assumed 'ideal' properties, such as homogeneity, ergodicity, stationarity, isotropy. This does not prevent the taking of statistical measures, but it does emphasize the need for care in interpreting such observations.

MARGINAL DENSITY FUNCTIONS

Figures 2 through 5 show frequency histograms of the grey-levels recorded on each of the four ERTS MSS bands in the study area. (Note: this paper uses the notation 1, 2, 3, 4 for the MSS bands rather than the NASA-ERTS notation of 4, 5, 6, 7).

Means and standard deviations of each of the bands in the study area are given in Table I.

The following observations may be made concerning these distributions:

1) The effective dynamic range in bands 1 and 2 is extremely small, there being only significant counts over a range of about 15 levels. The range for bands 3 and 4 is larger (about 25) but still only represents a small portion of the available 64 levels.

2) All the histograms are highly right-skewed and could not be represented by normal distributions. Bands 1 and 2 could be closely approximated by gamma distributions.

3) Bands 3 and 4 exhibit strongly bi-modal distributions, further ruling out normality. The physical origin of this bimodality is unknown.

TABLE 1

Means and Standard Derivations of Marginal Distribution in Study Area

Band	Mean	Stan.Dev.
1	18.1	1.98
2	18.7	3.45
3	26.6	6.01
4	16.7	6.12

Figure 6 shows the histograms of the spectral signatures of three fields within the study area, which were at this time bearing three different crops. The overall marginal densities for study area are shown at the bottom for comparison. The three crops are probably relatively easy to separate on a spectral basis; summer fallow being identified by very low reflectance in band 4, wheat by high levels in band 3 and barley by its high reflectance in band 2. It is clear however that some overlap exists between wheat and barley, so that on a spectral basis alone, these two crops will not always be completely separable.

Important also, is the fact that these three crops cover almost the entire range of the overall marginal densities. This implies that the separation of a large number of crops on the basis of spectral signatures alone will be very difficult.

Theoretical calculations (of the author) based on these observations, would place the maximum number of discernible classes in such an image in the vicinity of five or six. There is not room to elaborate on this aspect here, but it is included to give another example of the potential usefulness of the statistical analysis of images.

IN-BAND STATISTICS

This section examines the statistical relationship between pixels in a given spectral band. It is clear that image pixels will, of necessity, be highly correlated with their neighbours. The manner in which this correlation decreases with increasing distance from a reference pixel is an indication of image texture and should be useful in designing textural measures. In agricultural areas, for instance, the correlation decrease with distance will reflect the size of the fields. The variables correlated therefore are U_i, the value of the pixel; and $V_{i,n}$ the value of the pixels displaced a distance n from U_i. The sample includes all i within the study area. Figure 7 shows the correlation coefficient fall-off curves for bands 1 through 4.

All four curves fall off rather slowly and, indeed, significant correlation

coefficients were observed at 50 to 100 pixels from the reference pixel, a distance of 5 km or more. The fall-off pattern in each band is similar, the higher bands showing lower correlation coefficients for the same distance. This indicates that, in this study area, bands 3 and 4 carry more information than 1 and 2. (This was also evident in the greater width of the marginal density.)

Figures 8,9,10 show the two-dimensional histogram for U_i vs $V_{i,n}$ for n = 1, 5 and 10 for band 1. As n increases, the highly elongated distribution pattern becomes increasingly circular, showing the decreasing correlation.

It is expected that the rather slow and almost linear fall-off in the range of 1-5 pixels will be typical of large-field agricultural areas. By comparison, the dotted line superimposed on band 2 of Figure 7 shows the fall-off curve for a mixed forest area in Northern Ontario. The steeper decline is evident and not unexpected.

Further research in this area is in progress, but this preliminary work would indicate that the correlation coefficient curve may be useful in designing measures of regional texture.

INTER-BAND STATISTICS

The four spectral bands of ERTS MSS imagery are by necessity correlated with each other. The highest correlation is found between bands 3 and 4 and the lowest between bands 2 and 4. Band 1 and 2 are highly correlated.

Table 2 shows the correlation coefficients between the bands for the study area.

INTERBAND CORRELATION COEFFICIENTS IN STUDY AREA

TABLE 2

BAND	1	2	3	4
1	1.0	-	-	-
2	.77	1.0	-	-
3	.52	.26	1.0	-
4	.40	.11	.96	1.0

These correlations do not depend strongly on image texture or geometry and so will be relatively invariant from image to image. Table 3 shows the coefficients for a smaller region in the vicinity of the study area, and the consistancy of the correlation coefficients is evident.

INTERBAND CORRELATION COEFFICIENTS FOR A SMALLER AREA

TABLE 3

BAND	1	2	3	4
1	1.0	-	-	-
2	.81	1.0	-	-
3	.56	.31	1.0	-
4	.45	.17	.97	1.0

Figure 11 shows the two dimensional histogram of band 1 vs band 3 for the study area. The high correlation between the bands is evident. Histograms between other bands are similar. It is important to note the large amount of empty space in the histograms. This has obvious implications for spectral classification because of the relatively large width of overlap of the spectral signatures of various cover types as previously noted.

RUN LENGTH STATISTICS

It is clear from the foregoing statistics that much of the information in an ERTS image is redundant, there being such a high correlation between adjacent pixels and between bands. It should therefore, be possible to make use of this redundancy to store the image information in a compressed form, or to transmit the image with fewer bits of information.

It is well known that some reduction in storage can be gained by using run length encoding instead of storing the value of each individual pixel (e.g. Haskell et al, 1972). A series of identical consecutive pixels constitutes a 'run'. If the runs tend to be long and occur frequently, then there would be an obvious advantage to coding the grey-level of the run, and the length of the run (two items) rather than all

the individual pixels in the run. The number of items necessary to record all the information in an image is therefore twice the number of runs (including runs of unit length). If many of the runs are long, so that these are less than half as many runs as pixels, then a gain in storage is obtained. Figure 12 shows histograms of run lengths for the four bands in the study area. (The indicated grey-level resolution, RES, is relative to the nominal 64 level resolution which is set equal to 1). In all bands, the total number of runs is more than half the number of pixels, meaning that run length encoding actually increases the storage requirements. If, however, the data is compressed to 32 from 64 grey-levels, (RES=2) cutting in two the grey-level resolution, then the compression ratios improve considerably. (The compression ratio is the ratio of the number of items necessary to reconstruct the image divided by the total number of pixels in the image.) This loss in grey-level resolution is less than the normal loss experienced in the photographic process, so if the end-product desired is a print, then this loss is quite tolerable. Table 4 shows the compression ratios for various grey-level resolutions and bands for the study area.

COMPRESSION RATIOS FOR RUN LENGTH ENCODING

TABLE 4

GREY-LEVEL RESOLUTION	BAND 1	BAND 2	BAND 3	BAND 4
1	1.02	1.26	1.47	1.47
2	.33	.53	.84	.83
3	.31	.37	.57	.54
5	.16	.21	.34	.30

Obviously, enormous savings in storage and transmission time can be obtained if a low grey-level resolution is tolerable. This has obvious implications for the transmission of low quality facsimile imagery.

CONCLUDING REMARKS

A basic understanding of the nature of the data is always important in designing data analysis methodologies. The knowledge of the data structure provides criteria for choosing between alternate 'standard' algorithms and a basis for new algorithm design.

With ERTS MSS data (and other multispectral scanner data) there is a high non-independence within the data. It is clear, therefore, that algorithms must be designed that maximize the use of the independent information, while minimizing the processing of redundant information. It is hoped that the quantitative information presented here will be of assistance in this area of study.

REFERENCE

Haskell, B. G.,

Mounts, P. W. and Candy, J. C.,

1972,Interframe coding of video telephone pictures,

Proc. IEEE,v. 60, No. 7, p. 792 - 800

ACKNOWLEDGEMENTS

I would like to thank Drs. Fred Peet and Alec Mack for providing the spectral signature information for some crops in the study area.

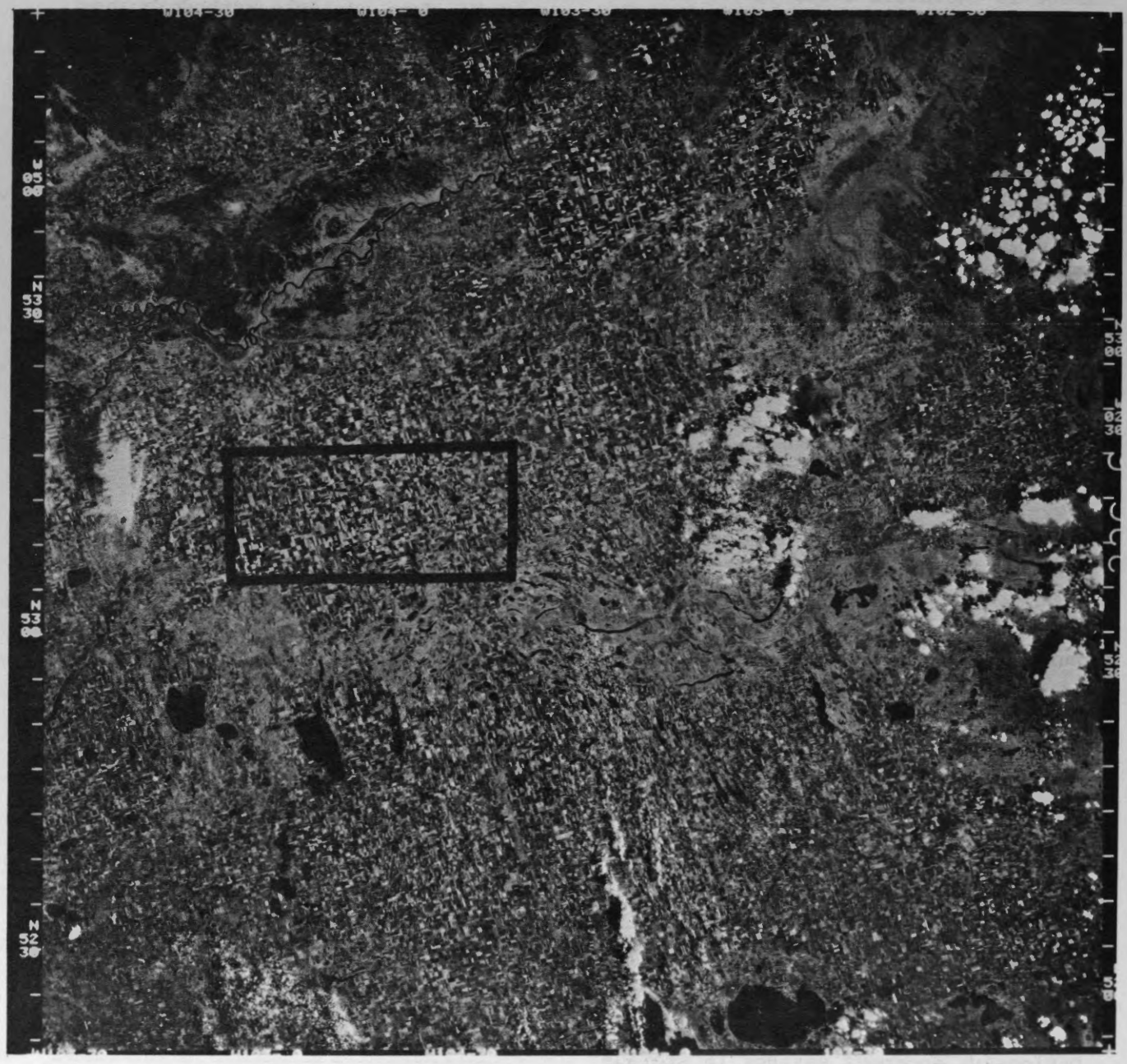

Figure 1 The study area

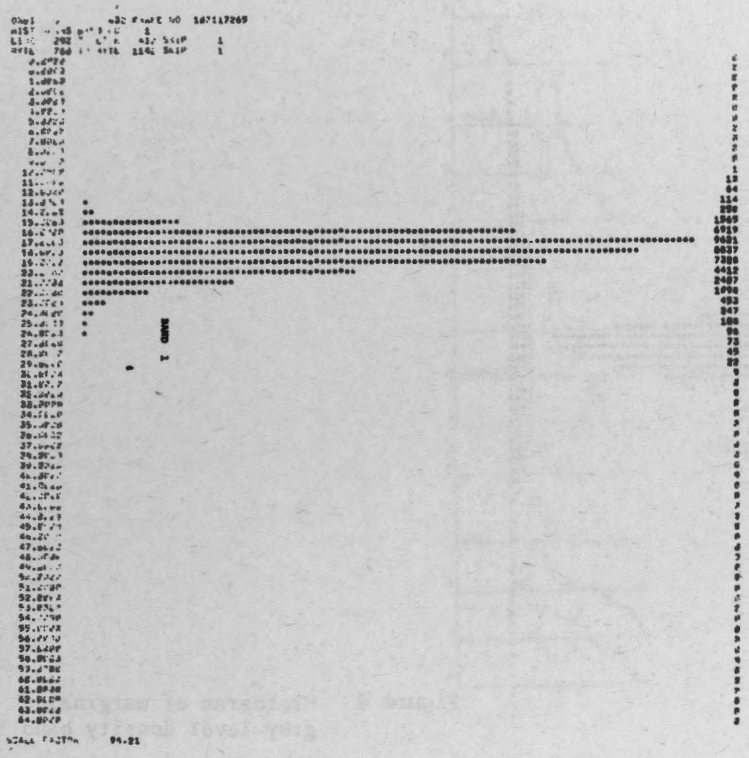

Figure 2 Histogram of marginal grey-level density band 1

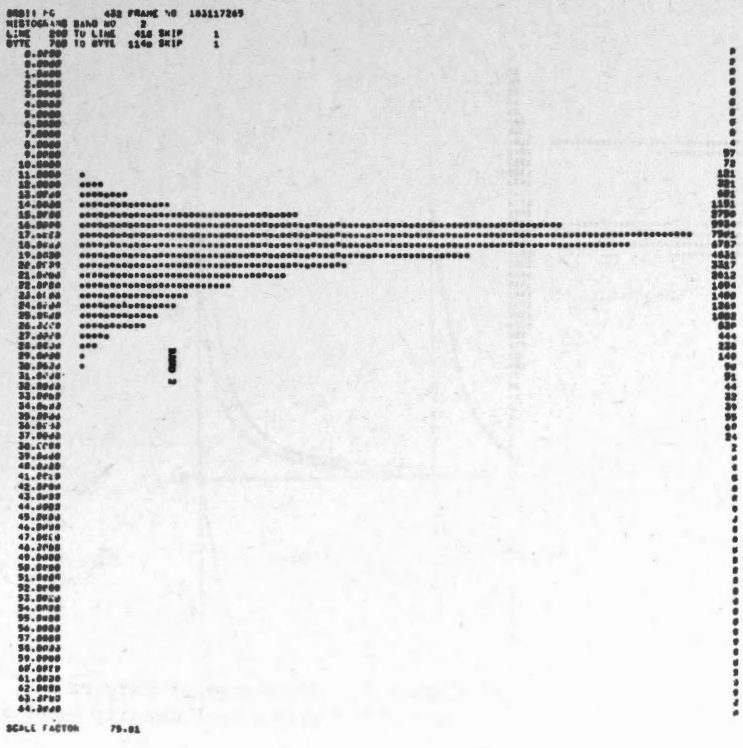

Figure 3 Histogram of marginal grey-level density band 2

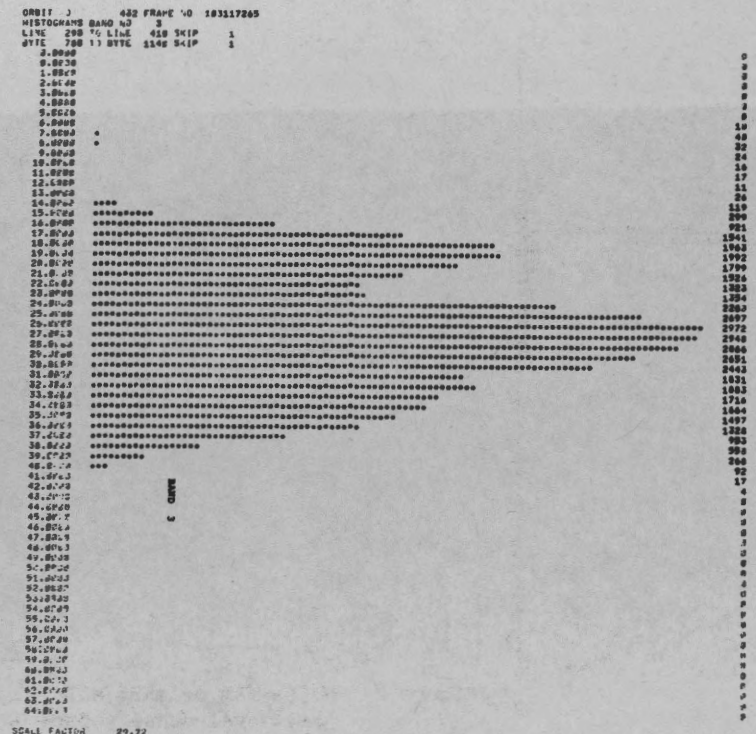

Figure 4 Histogram of marginal grey-level density band 3

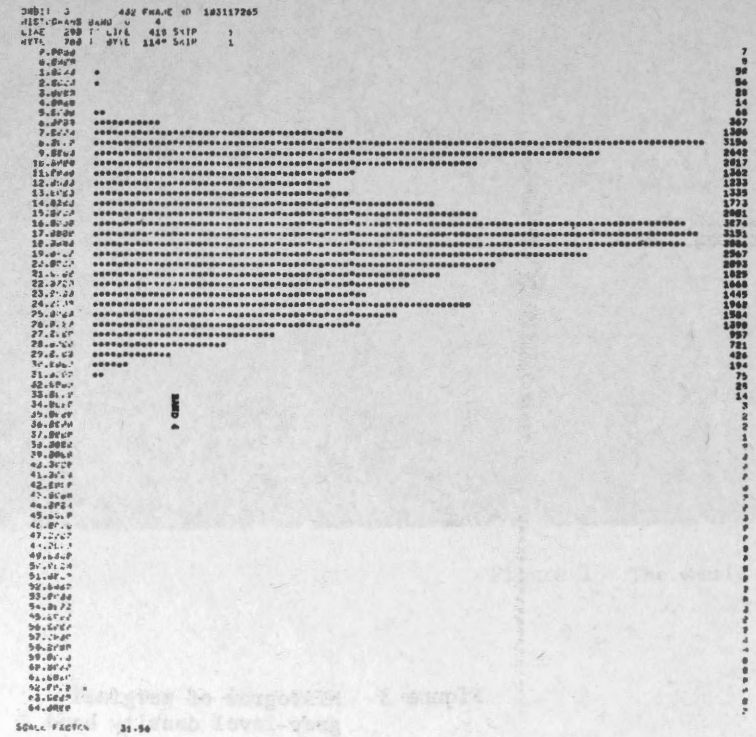

Figure 5 Histogram of marginal grey-level density band 3

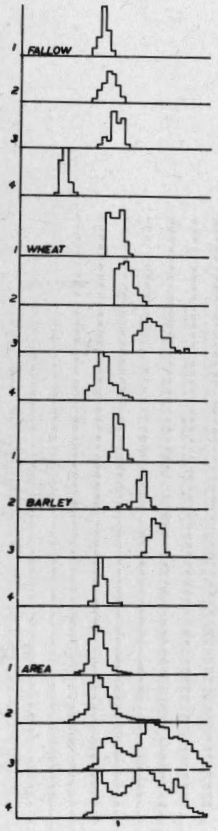

Figure 6 Spectral signatures of several crops in the study area

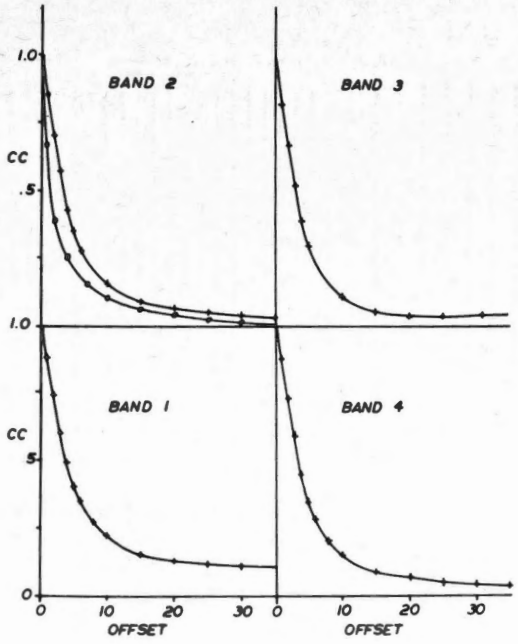

Figure 7 Correlation coefficient drop-off curves for the study area

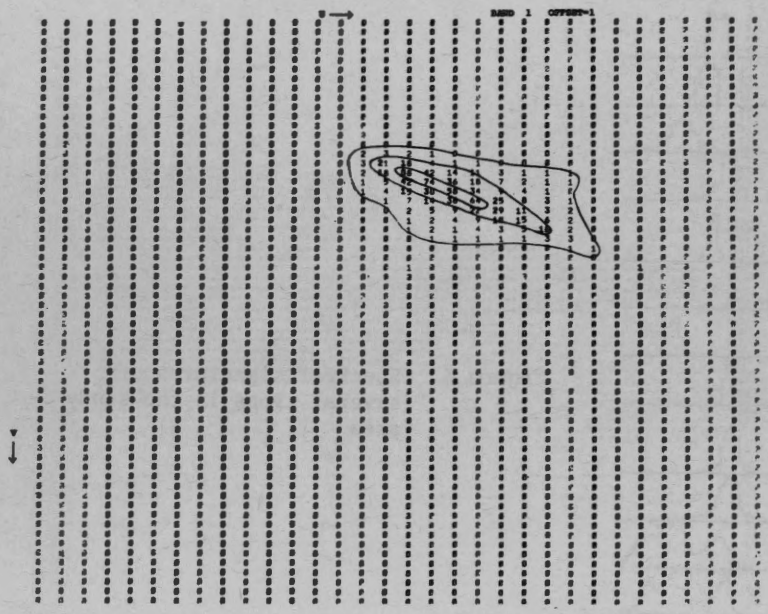

Figure 8 2-dimensional histogram showing in-band correlation for a pixel offset of 1

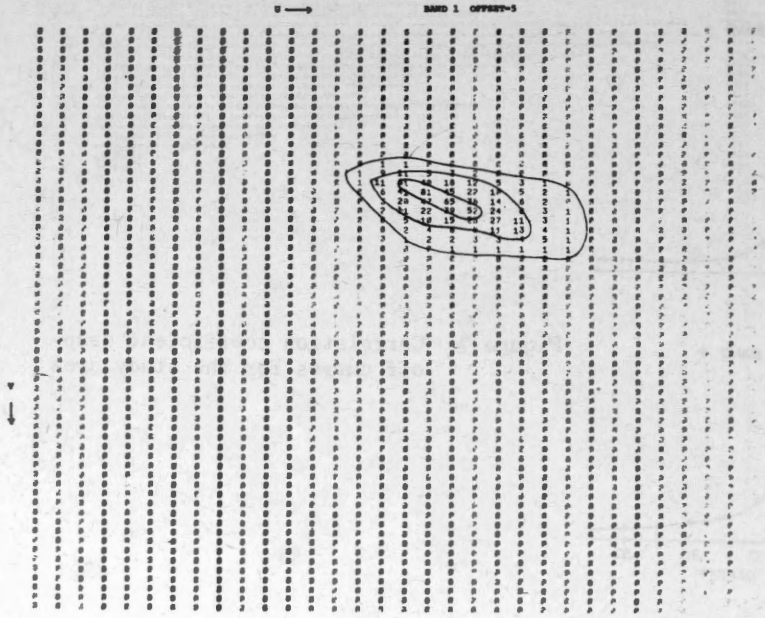

Figure 9 2-dimensional histogram showing in-band correlation for a pixel offset of 5

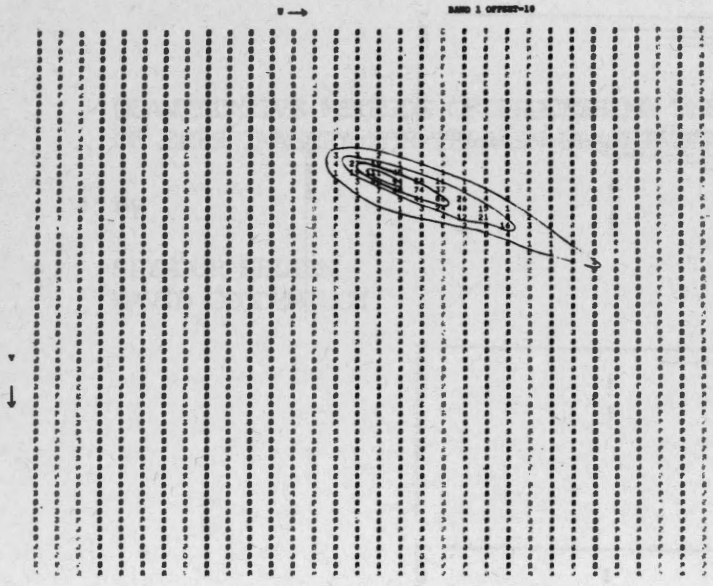

Figure 10 2-dimensional histogram showing in-band correlation for a pixel offset of 10

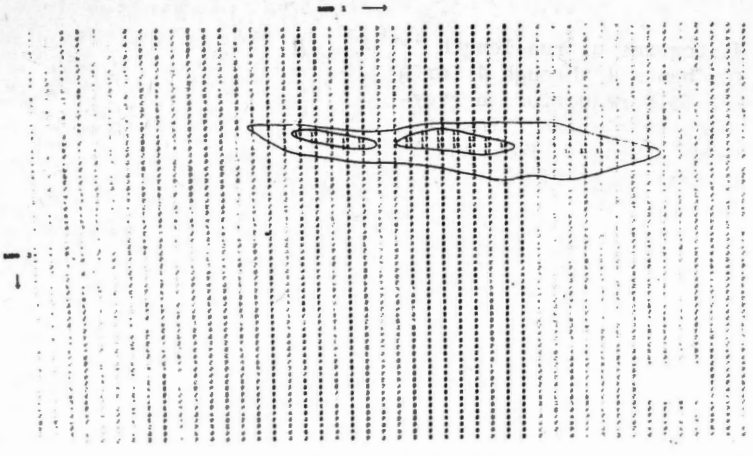

Figure 11 2-dimensional of band 1 vs band 3

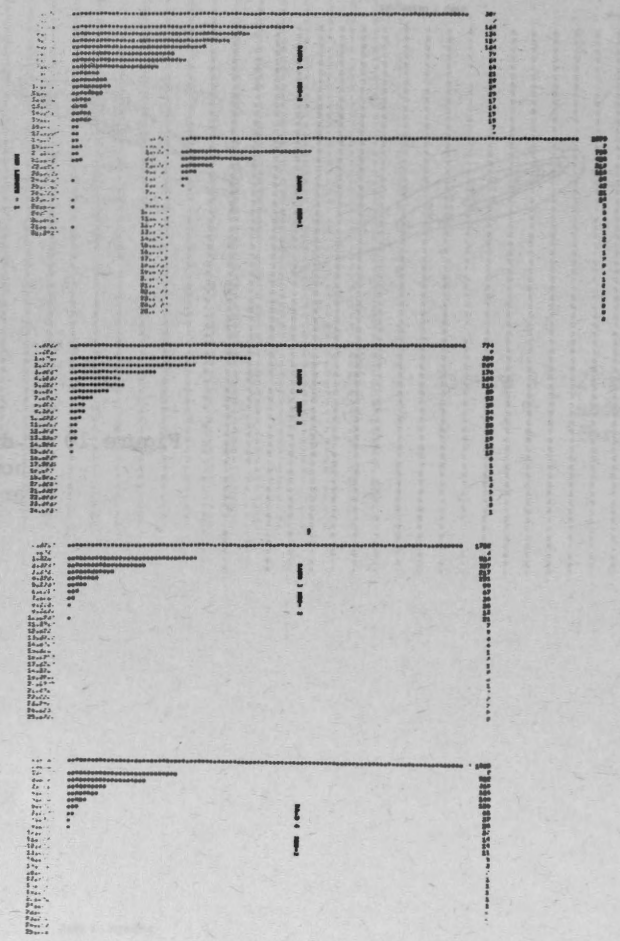

Figure 12 Histograms of run-length for bands 1 through 4 for a two-fold reduction in grey-level resolution. Insert shows histogram for band 1 at full resolution.

QUANTITATIVE METHODS OF PROCESSING THE INFORMATION CONTENT OF ERTS IMAGERY FOR TERRAIN CLASSIFICATION

By

SEYMOUR SHLIEN
DAVID GOODENOUGH

This paper presented at the Second Canadian Symposium on Remote Sensing, University of Guelph, Guelph, Ontario, April 29 - May 1, 1974.

QUANTITATIVE METHODS OF PROCESSING THE INFORMATION CONTENT OF ERTS IMAGERY FOR TERRAIN CLASSIFICATION

Seymour Shlien and David Goodenough
Canada Centre for Remote Sensing
Department of Energy, Mines and Resources
Ottawa, Canada K1A OR4

ABSTRACT

Automated interpretation of ERTS images utilizing pixel by pixel spectral classifiers is discussed. The quadratic discriminant was found to be a most suitable method since it is based on the statistical parameters of the intensity distribution. To expedite the processing time of classifying an ERTS image, the use of look up tables are suggested. A method of implementing look up tables on a medium sized computer is indicated.

Removable radiometric errors in the image introduce striping and cause many misclassifications. The errors originate from the unequal radiometric responses of the sensors in any one band. By compensating for these responses most of these errors can be eliminated.

Thirty-five images were analyzed to determine how the sensor responses have been drifting over the first 15 months of operation of ERTS-A. The sensor responses were characterized by relative gain and zero offset parameters which were determined from the scenic content of the image using Strome and Vishnubhatla's (1973) method. It was found that in general the sensor parameters were stable within a frame but that considerable variations occurred over longer periods.

The sensors in band 7 were found to be most stable while the sensors in band 6 showed the greatest variation in their responses. These results show the necessity of redetermining the sensor parameters on any new image.

INTRODUCTION

Since the launch of ERTS-A, large quantities of high resolution images of the earth have been made available in machine readable form. Quantitative interpretation of this data and the automatic generation of ground cover type maps is becoming increasingly popular. The human interpreter is still far ahead of the computer since he can easily extract and use spatial, textural, contextual, a priori information as well as spectral information. However the trained analyst would find the job of estimating the areal extent of the different ground cover types very tedious.

Many new methods of automatic interpretation using the latest developments in pattern recognition and statistical decision making are being tested on ERTS and airborne imagery. For example an iterative method of detecting closed field boundaries in agricultural areas has been developed by Kettig and Landgrebe (1973). Unfortunately many of these methods require much computer processing time and are not yet economic on a production basis.

In this report we shall limit ourselves to pixel by pixel spectral classifiers. Though these classifiers cannot use spatial and textural information they are at least rapid and have yielded many encouraging results. The next section reviews various types of spectral classifiers. The main advantages of using the quadratic discriminant or otherwise known as the maximum likelihood classifier with multivariate normal assumption is brought forth. A scheme of speeding up this classifier so that an entire ERTS frame can be processed at a reasonable cost is discussed in the third section.

Unless the image is corrected for radiometric errors due to sensor miscalibrations the classified image will

contain many errors and have a noisy appearance. An intensive investigation conducted on the sensor responses and how they have changed as a function of time is described in the fourth and fifth section.

PIXEL BY PIXEL CLASSIFIERS

The observations or features that are used to classify a given pixel are the spectral reflectances in the four Multispectral Scanner (MSS) bands 4, 5, 6 and 7. The intensities are digitized into 64 grey levels in each band so that in principle 16 million different intensity vectors can occur. The spectral classifier may be viewed as a mapping F of the intensity vectors

$X=(x_1, x_2, x_3, x_4)$ into

classes K_i (i= 1, 2, ..., n).

$$F(x_1, x_2, x_3, x_4) = K_i \qquad (1)$$

How this mapping is created determines the nature and name of the classifier.

The mapping may be determined with or without the interaction of the analyst. In the first method, unsupervised learning, the statistical distribution of the data is estimated, and classes are associated with clusters. The final theme map produced may have little relevance to the ground cover types one wants to distinguish. In the second approach, supervised learning, the interpreter furnishes the computer with several training sets. On the basis of the statistics of these samples, the best mapping is determined. The discussion in this report will be limited to the second method.

Given a set of intensity vectors from various training classes there are several ways of building the mapping F. The direct method consists of using the actual training vectors to define the mapping. Given an intensity vector from an unknown class, the classifier searches the training fields for an identical vector. If such a vector is found the classifier assigns the unknown vector to the class corresponding to this vector. The method does not guarantee that the mapping F is single valued. If the same intensity vector is found in two or more training classes no decision could be made. Furthermore the training set must contain all the possible intensity vectors in the classes.

The next method which is the simplest one to implement on a computer, uses the minimum and maximum intensity values in each band of the training class to define a four dimensional rectangular parallelepiped in intensity space. If an overlapping region occurs, the region is assigned to the rectangular parallelpiped with the least volume. The method is not very efficient since it is sensitive to extreme points and does not properly take into account the statistical properties of the data, in particular the high correlation between bands.

More sophisticated methods partition the intensity space on the basis of the statistical distribution of the intensities. There are several classes of these methods such as minimum distance rule (Wacker and Landgrebe, 1972), linear discriminants (Steiner, Baumberger, Maurer, 1969) and the maximum likelihood decision rule (Fukunaga, 1972). In the latter rule, the probabilities of observing a given intensity vector are computed for all the possible classes. The intensity vector is then assigned to the class with the largest probability. Nonparametric or parametric methods are used to estimate the probabilities.

In the latter method, it is invariably assumed that the intensities follow a multivariate normal distribution. The decision rule reduces to the evaluation of n quadratic discriminants L(1), L(2),...,L(n) given by equation (2).

$$\begin{aligned} L(i) = &-\tfrac{1}{2} y_1 Q^i_{11} y_1 \qquad (2)\\ &- y_1 Q^i_{12} y_2 - \tfrac{1}{2} y_2 Q^i_{22} y_2 \\ &- y_1 Q^i_{13} y_3 - y_2 Q^i_{23} y_3 - \tfrac{1}{2} y_3 Q^i_{33} y_3 \\ &- y_1 Q^i_{14} y_4 - y_2 Q^i_{24} y_4 - y_3 Q^i_{34} y_4 - \tfrac{1}{2} y_4 Q^i_{44} y_4 \\ &- \ln(4^{-2} C^{i\,\frac{1}{2}}) \end{aligned}$$

where Q^i is the inverse covariance

matrix, $|C^i|$ is the determinant of the covariance matrix for class i and (y_1, y_2, y_3, y_4) is the intensity vector shifted about the class mean. The intensity vector is then assigned to the class j with the largest L(j) provided that L(j) is above a user selected threshold. Otherwise no decision is made.

The quadratic discriminant was found to give the best results (Goodenough and Shlien, 1974). Unfortunately, the method is slow since 200 multiplications must be performed per intensity vector for a 10 theme classification.

A PRACTICAL METHOD OF CLASSIFYING A COMPLETE ERTS IMAGE USING LOOK UP TABLES

On our present PDP-10 computer, we can classify about 100 intensity vectors a second using the quadratic discriminants (2) for 10 classes. In order to classify a complete ERTS frame consisting of 7 million pixels, 70 kiloseconds or approximately a full day of processing time would be required.

Since most of the processing time is spent evaluating a function $F(x_1, x_2, x_3, x_4)$, much time could be saved by storing this function in a table. This way it is not necessary to repeat the lengthy calculations if the same intensity vector is encountered. If an ERTS frame consists of only several thousand distinct intensity vectors, the computational time could be reduced by much as 100 fold. In fact an analysis of several ERTS images has shown that the number of distinct intensity vectors is in the range of 2 to 5 thousands.

Three ERTS frames were chosen in this study. The first frame (E1366-18271) was in the vicinity of Yellowknife and was covered mostly by vegetation and burns. The air was fairly hazy due to smoke produced by several active forest fires. The second frame (E1384-18295) was located at the Rocky Mountain Trench. The area was covered with vegetation, bare rock, and snow. The last frame (E1396-17560) covered the Lethbridge area. The area consisted of many agricultural fields both irrigated and non-irrigated. Four dimensional histograms were computed from a sample of 20000 pixels scattered over the first quarter of each frame.

From these histograms the minimum number of intensity vectors to cover various percentages of the image were determined and plotted in Figure 1. Assuming that the samples are reflective of the actual images, it is apparent that the first 50 percent of the pixels in the image consist of mostly 300 distinct intensity vectors.

In implementing such a method, it is necessary to find a practical and efficient method of storing the look up table. There are two desirable specifications: (1) the address of any given intensity vector is known immediately, and (2) the look up table should be as compact as possible. Unfortunately these specifications are mutually conflicting and there must always be a tradeoff. If one is only concerned with the first specification, then the best scheme is as follows. Convert the intensity vector into a scalar by multiplying the first component by 2^{18}, the second component by 2^{12}, and third by 2^6 and the last by 2^0 and adding the results. (These operations can be done instantly using byte manipulation routines.) The resulting number is used as the address of the word in the computer containing the classification of this vector. To apply this method one needs a computer with 16 million addressable locations. In contrast if one does not have this amount of memory space then one is forced to employ the following scheme. Create two one-dimensional data arrays, one containing the distinct vectors and the other containing the classification corresponding to each of the distinct vectors. If the word length of the computer is 30 bits or greater, the two arrays could be combined into one by using the first 24 bits to contain the vector and the remaining bits to contain the classification. To classify any given vector, search through the entire table until one finds the vector, then read off the classification contained in the appropriate location. If the vector was not classified yet, then classify it using the maximum likelihood rule and put the answer in the proper location. This method is rather slow since most of the time is spent looking for the vector.

On the computing system at the Canada Centre for Remote Sensing, we were forced to use the second approach.

To speed up the actual searching the intensity vectors were first sorted in an initial pass. Since bands 5 and 6 appear to be the least correlated (Figure 2) the intensity vectors were sorted according to these bands and another array was introduced to point to the positions of the intensities with the specified intensities in bands 5 and 6. The intensities in this group were then searched sequentially. With this scheme,classification was carried out five times faster than with no look up tables.

Further work is in progress to speed up the searching procedure. Many techniques have been developed in the field of sorting and searching (Knuth, 1973). The relative speeds of the different methods depend upon the nature of the data and the relative time of various instruction on the computer. For example if arithmetic operations are faster than memory access, savings in time could be realized by transforming the intensities to principal components (Taylor; 1973, 1974) and compacting the information content in the intensity vectors.

COMPENSATION FOR SENSOR RESPONSES ON THE MSS

Despite all the sophisticated classification schemes one may use, many misclassifications will occur unless radiometric errors in the image are corrected. Errors are introduced because the Multispectral Scanner (MSS) utilizes six sensors to generate an image in any one band. These sensors scan a swath of six lines in a single sweep. The scan rate and the angular velocity of the satellite have been preset such that each time the next swath begins the first sensor is positioned exactly one scan line beyond the line scanned by the sixth sensor in the previous swath. The spectral intensities are sampled about 3200 times along one line and are digitized into 64 grey levels. A logarithmic transformation is applied to the first three spectral bands before digitization to obtain improved separation of intensity levels in the in the intensity range of greatest importance to remote sensing.

The sensors on board the Multispectral Scanner are photomultiplier tubes for bands 4, 5 and 6, and solid state detectors for band 7. These sensors are unfortunately susceptible to drift owing to their sensitivities to operating temperature (Gard, 1974). As a result, the radiometric responses of the six sensors for each band are no longer equal. This means that an intensity measured as 10 units in one sensor may be measured as 7 units on another sensor. The net result is a striping appearance of the image which is not only a nuisance to the photo-interpreter but also a serious source of error in the generation of automated theme detection and classification.

Since in automated classification, a spectral change in one intensity unit may change the classification of a given pixel, accurate spectral information is very important. This is particularly true in the study of the water quality of lakes. If nothing is done to compensate for the different sensor responses, the intensity distributions of any ground cover class is more dispersed, there is greater overlap between the spectral response of the different classes, and more misclassification occur. Theme classification maps produced on our Multispectral Analyzer Display (Goodenough, Shlien, Smith, Davis, Edel, Fawcett and Wayne, 1974) had a noisy and striped appearance.

Fortunately there are several methods available to remove this striping. One method, developed by Strome and Vishnubhatla (1973), uses only the scenic data in the image and in many cases succeeds dramatically in improving the appearance of the image and reducing the misclassification. The method works as follows. In the first pass the parameters of the sensor responses are estimated and a look up table to equalize the sensor responses is produced. In the second pass the data is transformed using this table. The method assumes that the response of one sensor in any band relative to any other sensor in the same band follows a linear relation. Thus if x_n and x_m are the spectral intensities recorded by sensors n and m respectively, for the same area, then x_m can be transformed to x_n by equation (3).

$$x_n = a + bx_m \qquad (3)$$

where a and b are suitable constants. In spite of the logaritmic transformations applied to the intensities of the first three bands, this assumption appears valid for all the sensors. As an illustration of this relation a correlation plot is shown in Figure 3 of the intensity levels recorded by sensors 1 and 2 band 6 for a pair of adjacent scan lines. To emphasize the difference between the sensor responses, the ordinate scale is the actual difference of intensities recorded by sensor 1 and sensor 2 band 6, for the same pixel number (horizontal coordinate) in the pair of lines. (A random number uniformly distributed between plus and minus 0.5 was added for cosmetic purposes to this difference.) The pair of scan lines did not sweep over the same area, but since the lines were contiguous the intensitites in the two lines were highly correlated. Though sensor responses differ by as much as several units depending on the actual ground intensity, a linear transformation appears to be sufficient to equalize the responses.

On the basis of this assumption, sensor responses were equalized using the following formula

$$\gamma_n = a_m + b_m x_n \qquad (4)$$

where x_n is the observed intensity for any pixel in line n, γ_n is the corrected intensity, and a_m and b_m are estimated parameters for sensor m, m = 1,2,...6. The parameters a_m and b_m could only be determined relative to a chosen sensor. Sensor 2 was chosen throughout this analysis since it was found to be generally stable for all bands. Thus γ_n will denote the intensity that sensor 2 would have observed if it had covered the specific area. a_2 and b_2 always have the value 0 and 1.

Throughout this report the parameters a_m and b_m shall be called relative gain and zero offset. In actual fact b_m is the relative gain of sensor 2 with respect to sensor m (or relative attenuation of sensor m with respect to sensor 2) and a_m is the offset that must be added to sensor m so that its zero level will correspond to sensor 2. The terms are unfortunately misleading, when we say the "relative gain" of sensor 1 has decreased we actually mean that the gain of sensor 1 with respect to sensor 2 has increased. These parameters were chosen since they can be used directly in equation (4) to transform the intensity measured by sensor m to the intensity that would have been measured by sensor 2.

The coefficients a_m and b_m were determined on the basis of the statistical distribution of x_n. Assuming that the banding structure in the image is instrumental and not due to highly organized structure of vegetation and water features, then the statistical distribution of the intensities on the average should not depend on the scan line number. Due to shifts induced by the sensor biases, and scale expansions or contractions caused by different gains, the observed distributions of x_n does depend upon the sensor and hence the line number. To remove the banding the coefficients a_m and b_m are adjusted so that the distribution of γ_n for all sensors is the same.

Having only two parameters at ones disposal to equalize a particular distribution, it is sufficient to simply use the mean and the variance to describe the distributions. Beside being key parameters of a statistical distribution, the mean and variance are especially convenient to use since they are automatically computed by the MSS.

Strome and Vishnubhatla (1973) determine a_m and b_m from

$$b_m = \frac{(\mathrm{var}(x_2))^{\frac{1}{2}}}{(\mathrm{var}(x_m))^{\frac{1}{2}}} \qquad (3)$$

and $a_m = x_2 - b_m x_m$

where $\mathrm{var}(x_j)$ denotes variance observed by sensor j and (x_j) the mean of x observed by sensor j.

Error bounds of sensor parameters a_m and b_m are very difficult to determine

analytically. The high correlation of pixel intensities in both the vertical and horizontal directions strongly affects the accuracy to which the means and variances can be estimated. This correlation depends on the spatial structure of the imaged areas. For best accuracy the image should be highly correlated in the vertical direction (between scans) but uncorrelated in the horizontal direction (between pixels). The ideal image should have mostly vertical linear boundaries between ground cover types. Error bounds were therefore determined empirically as a function of the number of swaths that were averaged. It was found that in most cases 20 swaths was sufficient to gain 1 per cent accuracy.

The effectiveness of this method to eliminate the striping in the images was tested both visually and quantitatively. Quantitative methods estimated the spatial power spectrum using the one dimensional fourier transform in the vertical direction (Appendix A). If striping is present in the image the power spectrum would contain peaks corresponding to 6, 3, and 2 line periodicities. This is very visible in the spectrum shown in Figure 4a. Incorporation of radiometric corrections removed these peaks (Figure 4b).

The information content of the images before and after the incorporation of radiometric corrections was also examined. In Figure 5 the marginal discrete probability functions of the intensities in each of the four bands were plotted before the application of radiometric corrections. In Figure 6 the same functions were plotted after applying these corrections. The sensor miscalibration generally introduces more scatter in the distributions. Without corrections, a sharp peak in band 4 becomes a double peak and small bumps in the function in band 6 become washed out. Data samples were taken from an area covered by small lakes and vegetation.

SENSOR STABILITY

Sensor parameters were determined from 35 images spaced over the first 15 months of the satellite's existence. The parameters were estimated using Strome and Vishnubhatla's (1973) method using sensor 2 in each band as the base.

To study the short term stability characteristics of the sensors, moving averages of the sensor mean recorded intensities and variances, using either 5 or 10 swaths, were computed over the beginning quarter of some selected images. The relative gain and zero offset were then determined by substituting these statistics into equation (3). In most cases, the sensor parameters were stable over the section analyzed. A typical example for the sensors in band 6 is shown in Figure 7. Some exceptions were found, for example, in Figure 8, sensor 1, showed unusual variation while the oscillations of the other sensors were probably within the statistical uncertainty. (A five swath average was used in Figure 8 in contrast to a 10 swath average in order to obtain higher resolution.) No cause for this drift could be found from a visual examination of the image.

To study the long term stability characteristics of the sensors, accurate estimates of sensor parameters using the first 100 swaths were made for 35 frames. These estimates are listed in Table 1 and plotted in Figures 9-18 as a function of the number of days from the launch of ERTS. Save for a few exceptions the relative gains were stable within three percent and the zero offsets were stable within about an intensity unit. In general the gains of the sensors were within 10 percent of each other and the zero offsets were within 2 units. At low intensity levels the zero offsets introduce the most radiometric error while at high intensity levels the relative gains predominate. The relative gains and zero offsets act constructively to increase the error or act destructively to minimize the error. For example in band 6, sensor 1 has a relative gain below unity and a zero offset below zero, both working in the same direction to increase the radiometric error.

The stability characteristics vary markedly from band to band. The sensors in band 7 seem to be the most stable with time. On the other hand, the sensors in band 6 have the most drift. Long term trends are apparent in several cases. The relative gain of sensor 1 band 6 has gone down by 10

percent over a period of 500 days. In band 4 sensor 3 shows a slight negative drift in relative gain while sensor 5 shows a slight positive drift. Sensor 6 band 7 also shows a negative drift in relative gain. Small long term trends were also seen for the zero offsets. For example the zero offset of sensor 5 band 4 drifted up by 1 unit while the relative gain did not change.

CONCLUSIONS

Methodology related to the automated classification of ground cover types in ERTS images was examined. Particular emphasis was placed on pixel by pixel spectral classifiers which could economically classify an entire ERTS frame. The main conclusions were:

1. The quadratic discriminant or maximum likelihood classifier under the multivariate normal assumptions is one of the best pixel by pixel spectral classifier.

2. In order to economically classify an entire ERTS frame the quadratic discriminant should be used in conjunction with lookup tables.

3. The number of distinct intensity vectors composed of the 4 band pixel intensities lies in the range of 2 to 5 thousand for an ERTS image.

4. Radiometric miscalibrations of the sensors on the Multispectral Scanner introduce striping in the image and misclassification errors.

6. If compensation is made for the different sensor responses, this striping can be removed and the number of misclassifications can be reduced.

6. Sensor parameters were generally stable in the short term (within a frame).

7. Considerable drift in the sensor parameters were found in the long term.

8. The amount of drift varied with different sensors, however, drift was minimal for most sensors in band 7 and extreme for a few sensors in band 6.

9. Long term trends were detected for some of the sensors. In particular sensor 1 band 6 showed a 10 percent increase in gain relative to sensor 2 over a period of 500 days. The zero offset of sensor 5 band 4 drifted up by one unit.

10. Most of the time, the relative gains of the sensors were within 10 per cent of each other. The zero offsets were within 2 units of each other under normal periods.

ADDED NOTE

After the presentation of this paper at the 2nd Canadian Symposium on Remote Sensing, Dr. Guy Rochon pointed out that in some MSS tapes where the spectral intensities become truncated at level 63, inaccurate estimates of a_m and b_m would be obtained. This error could be eliminated by computing the means and variances of the sensor intensities not exceeding level 62. Though this method was not applied here; we instead did not include any results from tapes where this effect was important.

ACKNOWLEDGEMENTS

We would like to thank Dr. Sarma Vishnubhatla for making available his programs and giving us assistance. Also we would like to thank Mr. John Adams for his help on ground interpretation for some ERTS frames.

REFERENCES

Capon, J.,R. J. Greenfield, and R. J. Kolker (1967). Multidimensional maximum likelihood processing of a large aperture seismic array. Proc. IEEE 55 192-211.

Fukunaga, K. (1972). Introduction to Statistical Pattern Recognition. Academic Press.

Gard, W. (1974). Personal communication.

Goodenough, D. and S. Shlien, (1974). Results of cover-type classification by maximum likelihood and parallelepiped methods. Proceedings of the Second Canadian Symposium on Remote Sensing.

Goodenough, D., S. Shlien, A. Smith, N. Davis, H. Edel, R. Fawcett and G. Wayne. (1974). The Multispectral Analyzer Display (MAD) User's Manual. Canada Centre for Remote Sensing Technical Report.

Kettig, R. L. and D. A. Landgrebe. (1973). Automatic Boundary Finding and Sample Classification of Remotely Sense Multispectral Data. LARS Information Note 041773, Purdue University.

Knuth, D. E. (1973). The Art of Computer Programming Vol. 3 Sorting and Searching. Addison-Wesley.

Steiner, D., K. Baumberger, and H. Maurer, (1969). Computer processing and classification of multivariate information from remote sensing imagery. Proc. of 6th Int. Symposium on Remote Sensing of Environment, Vol. 2 895-907. Univ. of Michigan, Ann Arbor.

Strome, M. and S. Vishnubhatla (1973). A system for improving the radiometric corrections for ERTS-1 MSS data. Proceedings XXIV International Astronautical Congress, Baku, USSR

Taylor, M. M. (1973). Principal components colour display of ERTS imagery. Proceedings of the Third ERTS Symposium Dec. 10-14, 1973. Washington, D. C.

Taylor, M. M. (1974). Principal components colour display of ERTS imagery. Proceedings of the Second Canadian Symposium on Remote Sensing.

Wacker, A. G. and D. A. Landgrebe. Minimum distance classification in remote sensing (1972). Proc. 1st Canadian Symposium on Remote Sensing. Vol. 2 577-592.

Welch, P. D. (1967). The use of fast fourier transform for the estimation of power spectra: a method based on time averaging over short, modified periodgrams. IEEE Trans Audio Electroacoust. Vol. AU-15 pp. 70-73.

APPENDIX

Striping in images can be measured quantitatively by spectral analysis. The miscalibration of the six sensors in any one band introduces a 6 line fundamental periodicity going in the vertical direction of the image. Higher harmonics, two and three line periodicities, are also introduced and may exceed the fundamental considerably.

Power spectrum estimates were computed using block averaging technique. (Capon, Greenfield, and Kolker, 1967; Welch, 1967). At any specific horizontal coordinate in the image the fourier spatial spectrum of the intensities in the vertical direction was computed using the fast fourier transform. The fourier spectrum was multiplied by its complex conjugate to obtain the power spectrum. In order to reduce the variance of the power estimates, twenty estimates were made using different horizontal coordinates, and averaged. A mathematical description of the method is given below.

Let $x_{m,n}$ be the intensity level at pixel m and line n. Define

$$w^k = \exp(2\pi ik/120) \qquad \text{(A-1)}$$

Then the fourier spectrum f(k,m) was computed using equation (A-2)

$$f(k,m) = \frac{1}{120} \sum_{n=1}^{120} x_{m,n} w^{kn} \qquad \text{(A-2)}$$

for pixel locations m=100 ,200...,2000.

The power spectrum was determined using equation (A-3)

$$P(k) = \frac{1}{20} \sum_{m=100,100}^{2000} f(k,m) f^{*}(k,m) \qquad \text{(A-3)}$$

where "*" denotes the complex conjugate.

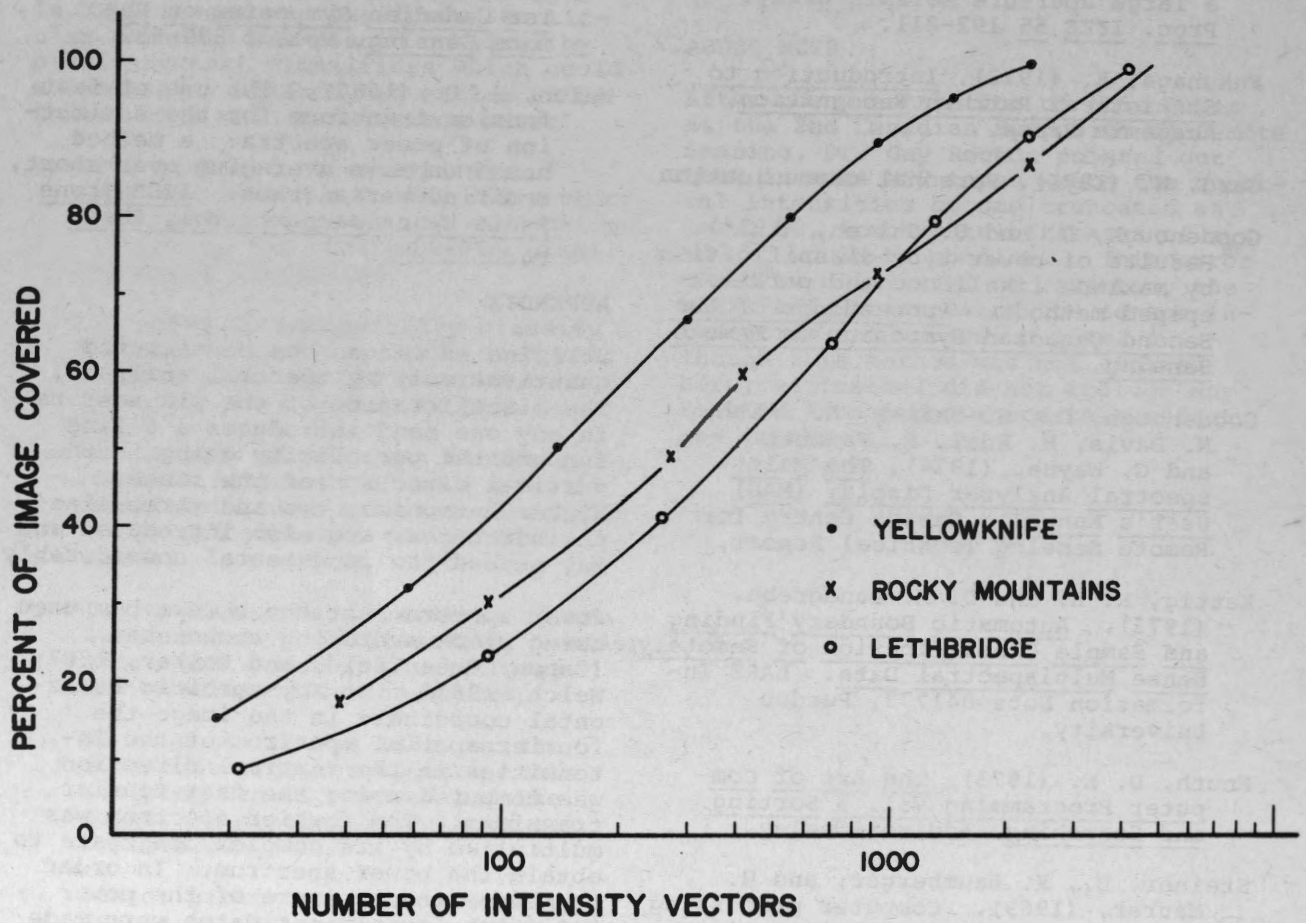

Figure 1. Maximum percent of ERTS image covered versus the number of distinct intensity vectors formed from the intensities in bands 4, 5, 6 and 7. The top quarter of the following frames were used: 1)E1366-18271 (Yellowknife); 2)E1384-18295 (Rocky Mountain Trench); 3)E1396-17560 (Lethbridge).

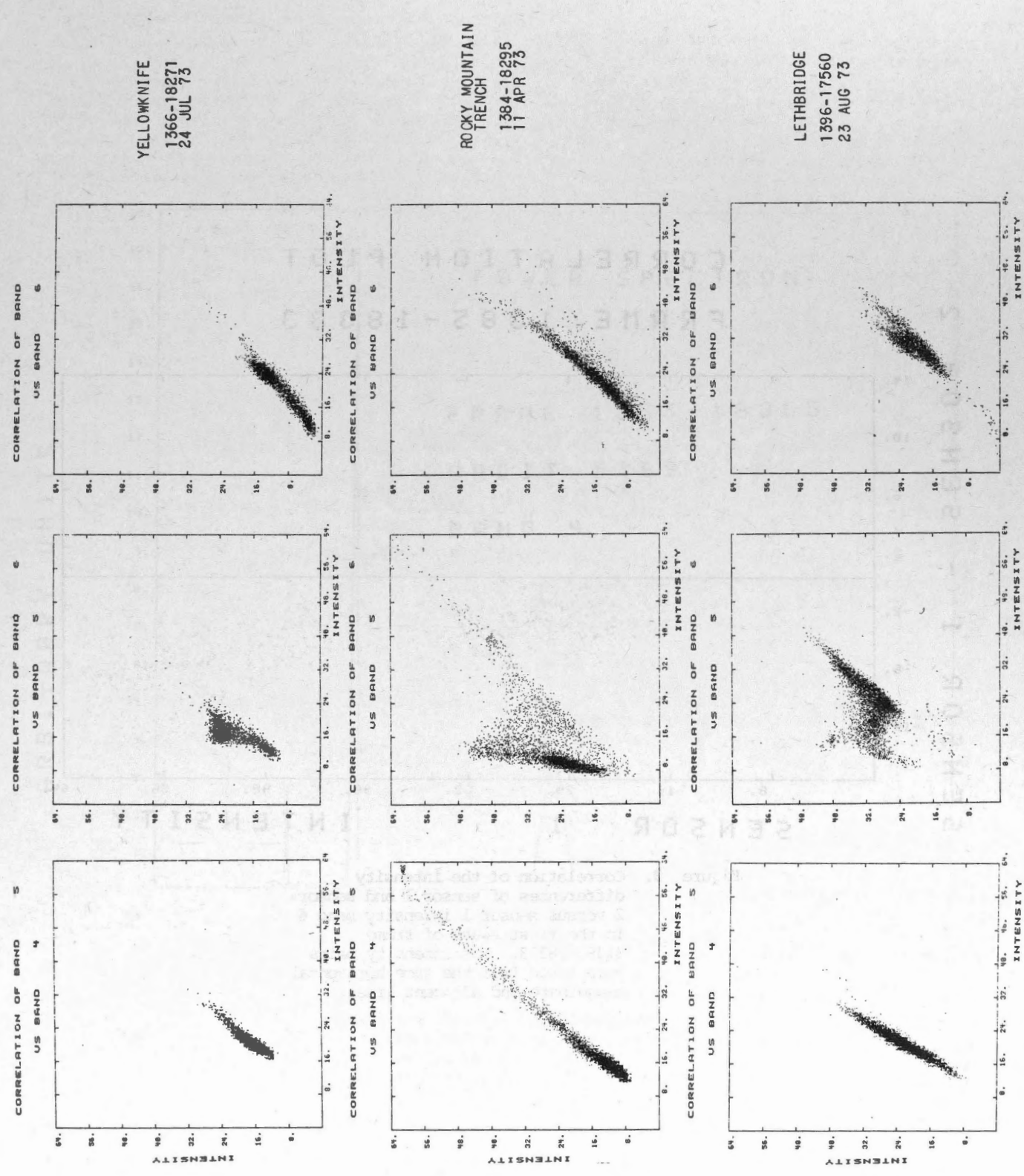

Figure 2. Correlation plots of the intensities for adjacent pairs of bands determined from the top quarter of three frames. Random numbers uniformly distributed between ±0.5 intensity units were added for cosmetic purposes.

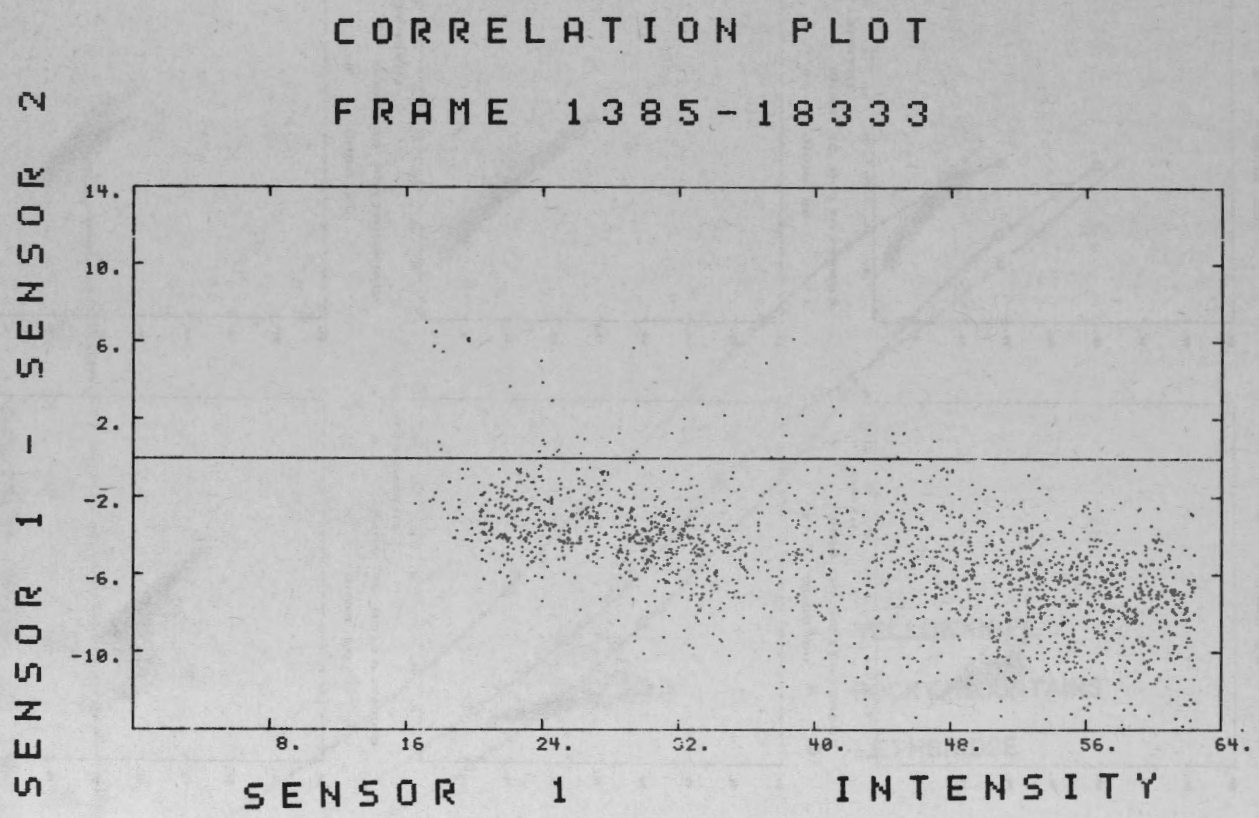

Figure 3. Correlation of the intensity differences of sensor 1 and sensor 2 versus sensor 1 intensity band 6 in the first swath of frame E1385-18333. The intensity pairs were taken from the same horizontal coordinate and adjacent lines.

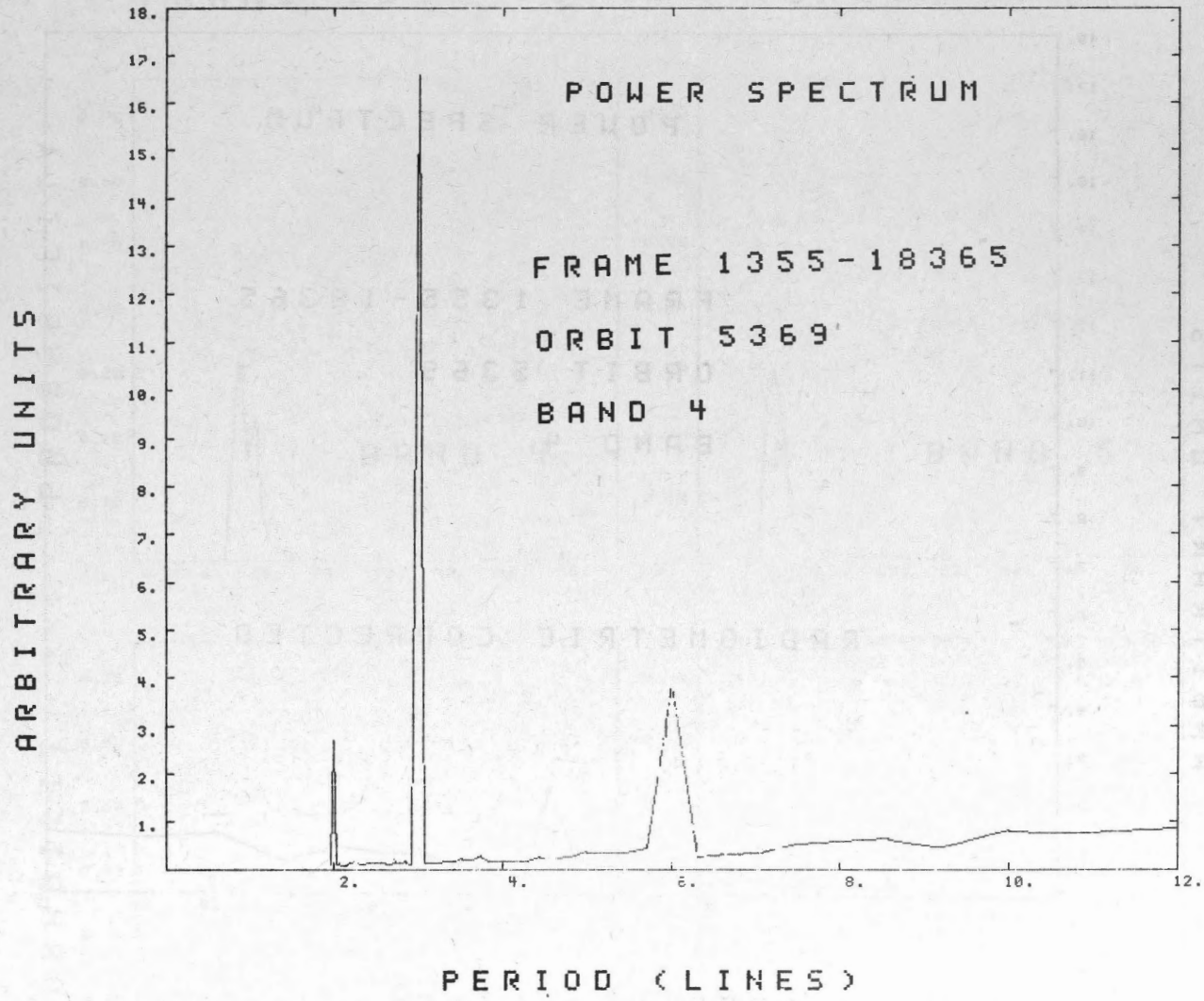

Figure 4 a Spatial one dimensional vertical intensity power spectrum versus period (number of lines) with no radiometric corrections.

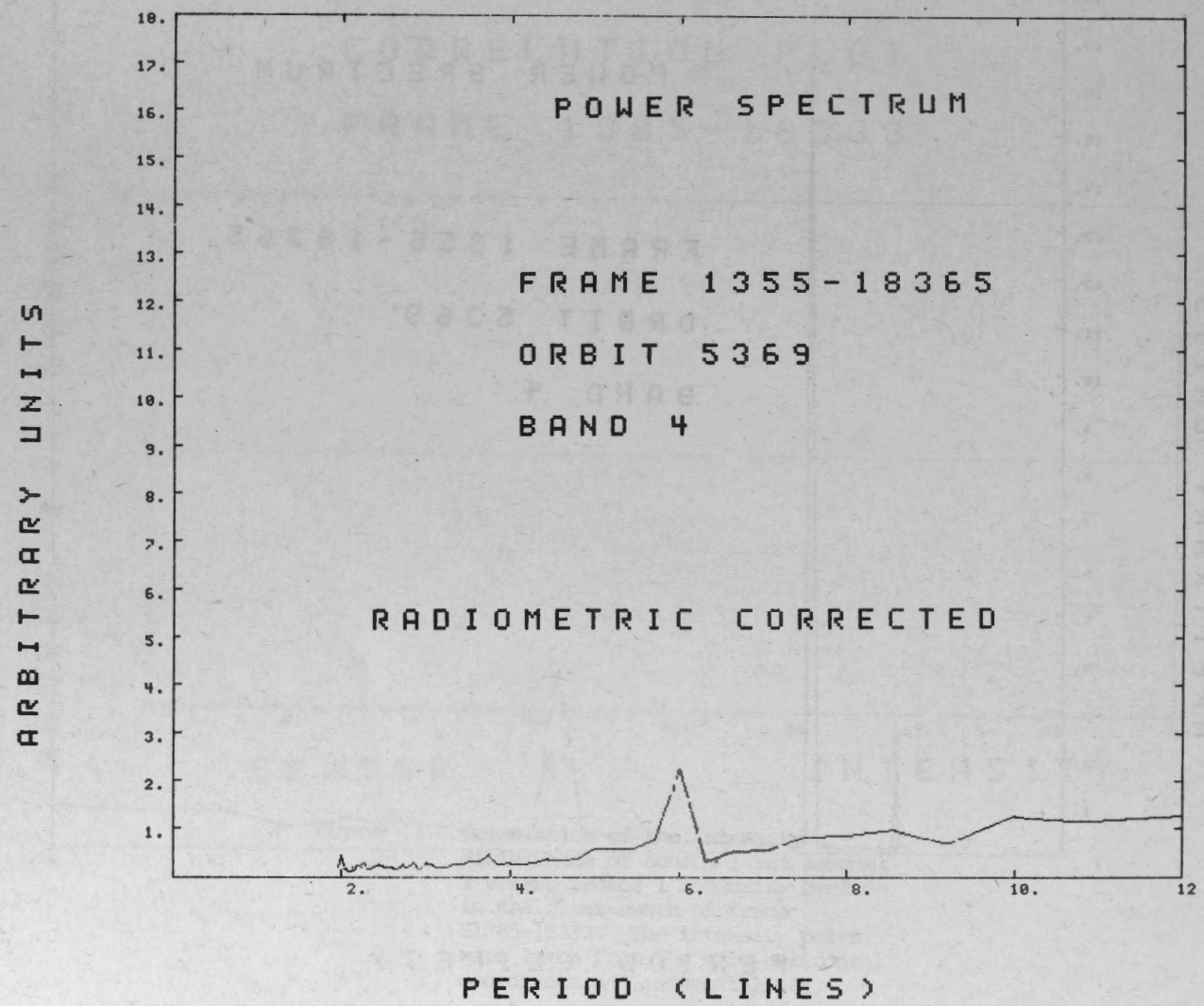

Figure 4 b Spatial one dimensional vertical intensity power spectrum versus period(number of lines). Radiometric corrections were applied to the same portion of the frame in Figure 4 a.

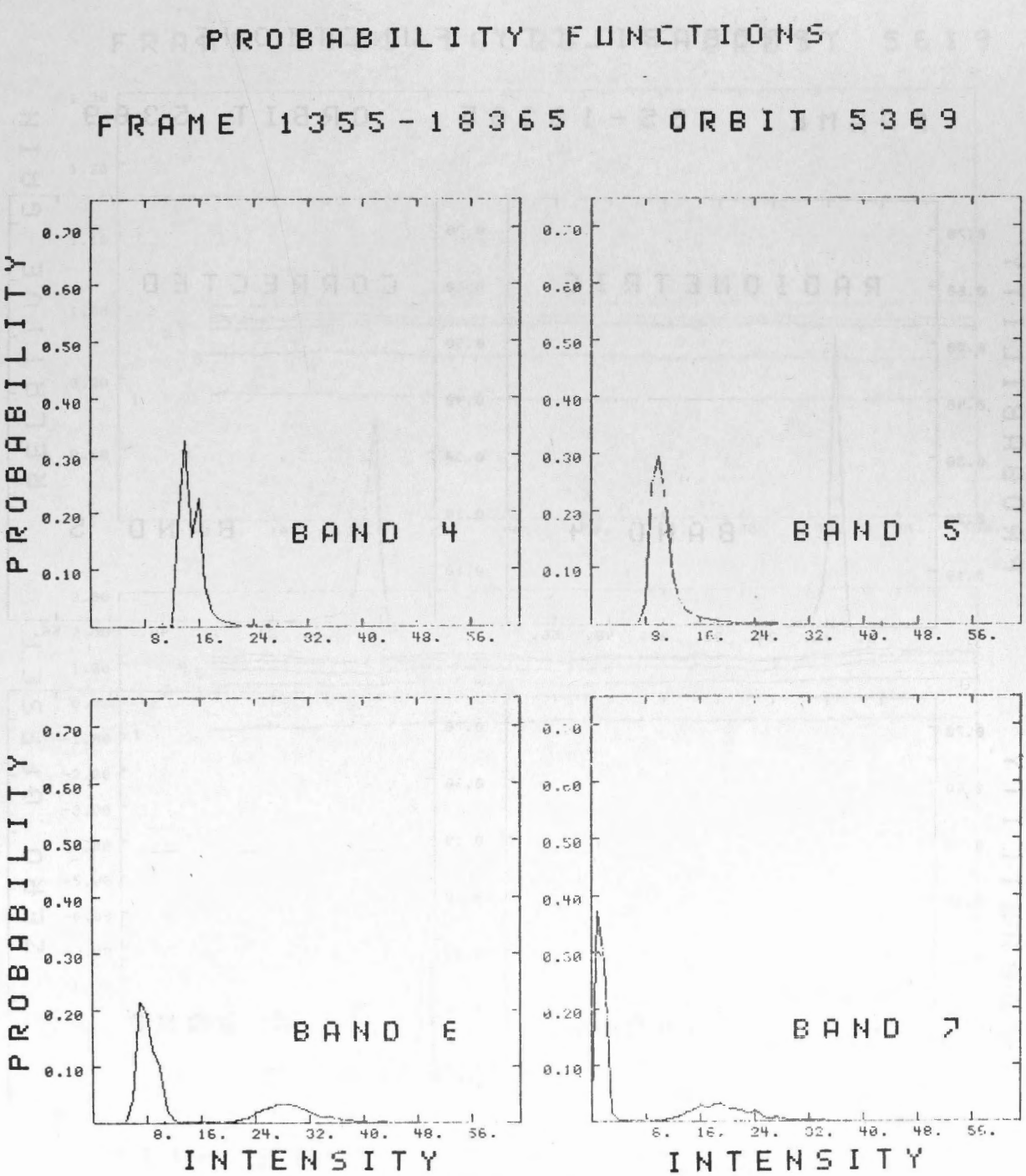

Figure 5. Marginal discrete intensity probability functions for the four MSS bands. No radiometric corrections incorporated.

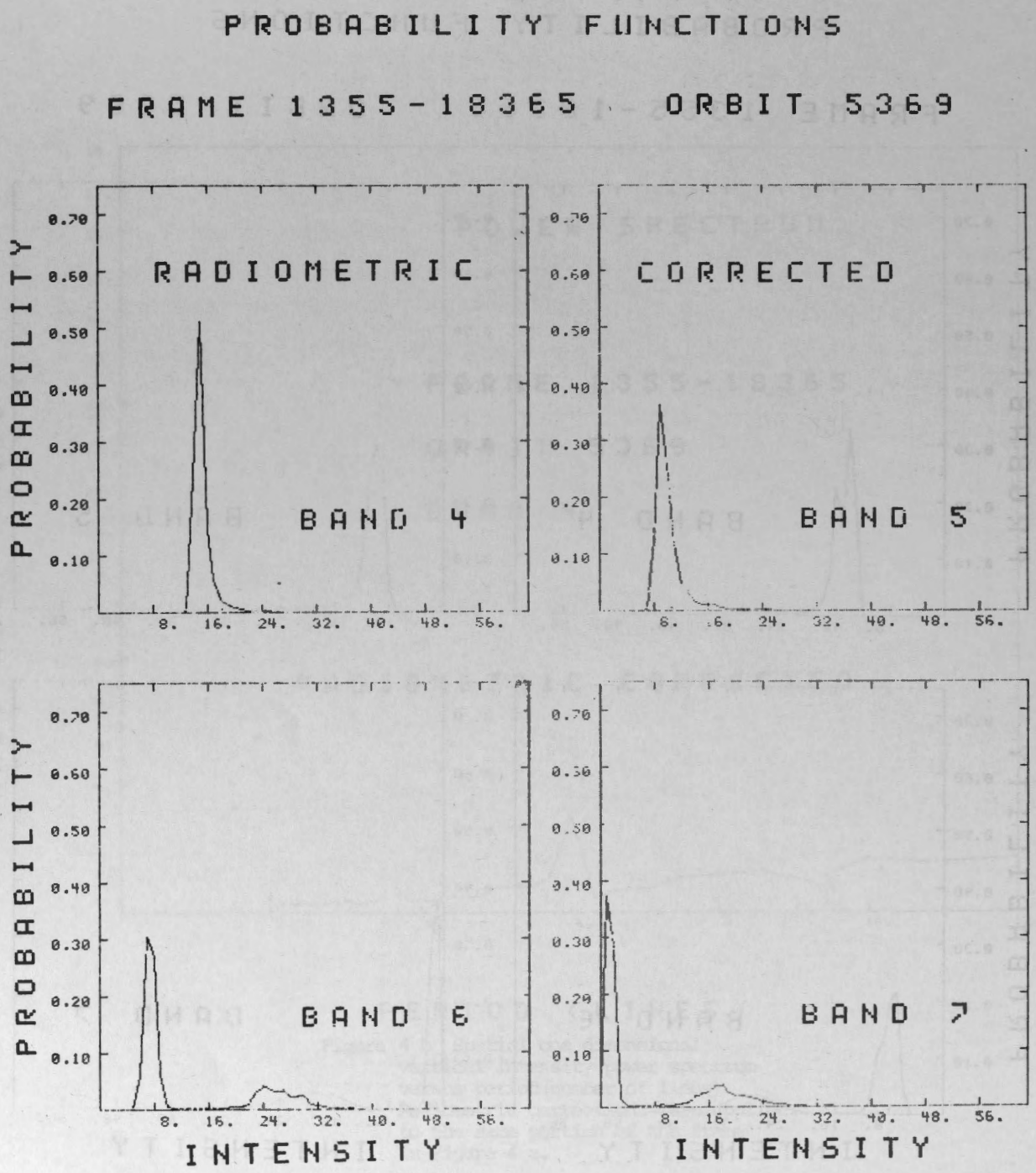

Figure 6. Martinal discrete intensity probability functions for the four MSS bands. Radiometric corrections incorporated.

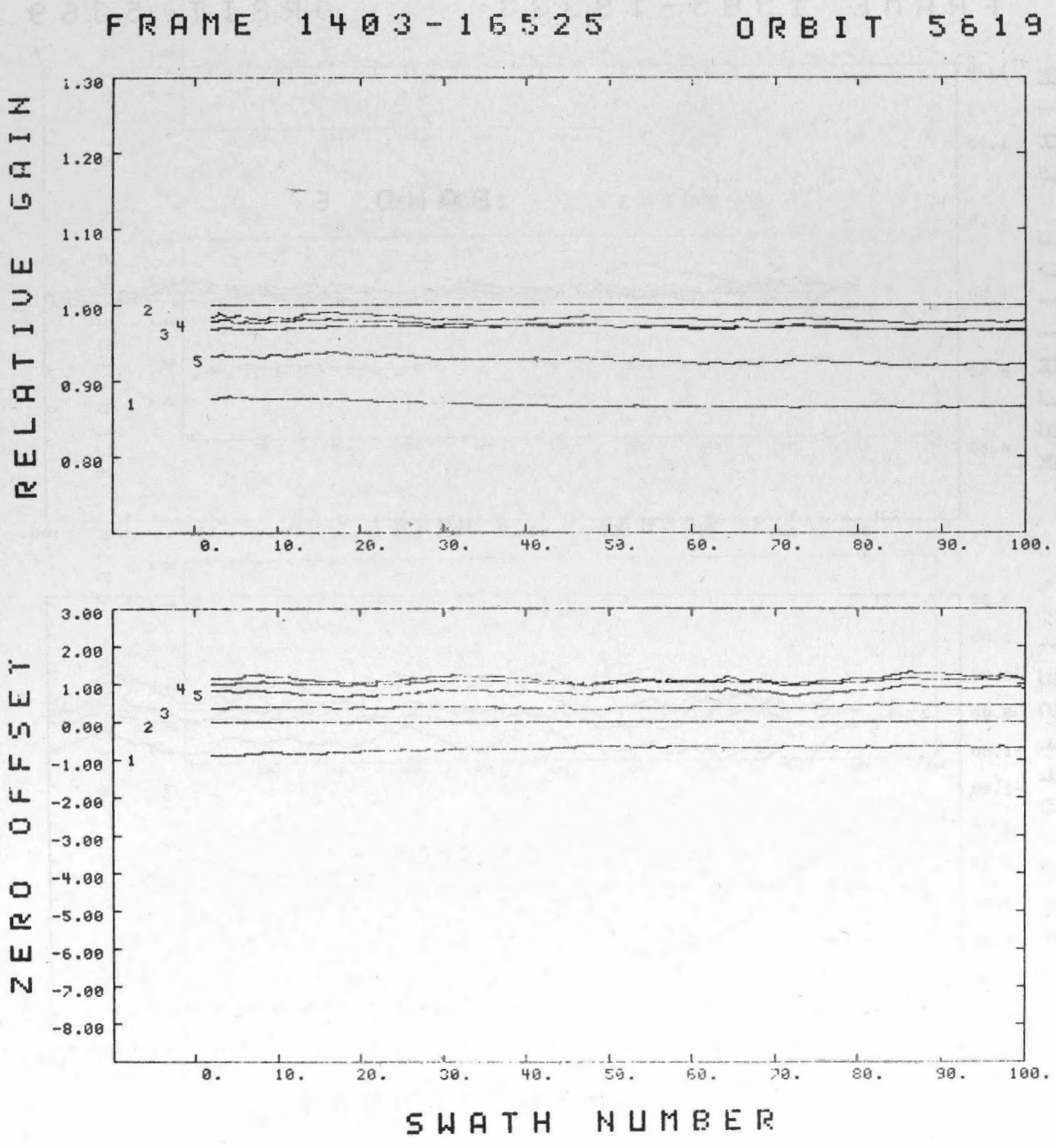

Figure 7. Top: relative gain of the sensors in band 6 versus swath number. Lower: zero offset of the sensors in band 6 versus swath number. A 10 swath moving average was used to compute these parameters from the scenic data.

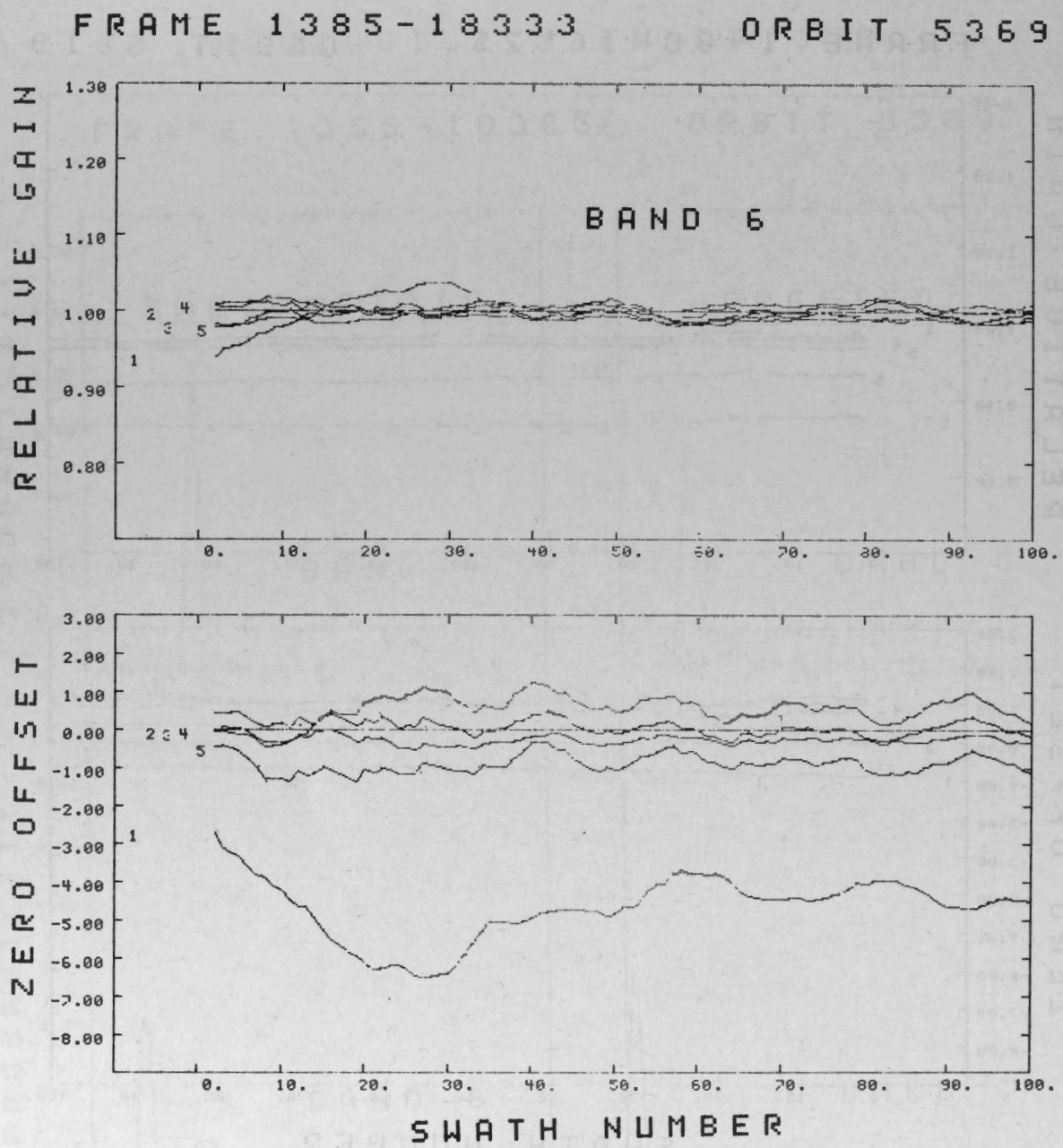

Figure 8. Top: relative gain of the sensors in band 6 versus swath number. Lower: zero offset of the sensors in band 6 versus swath number. A 5 swath moving average was used to compute these parameters from the scenic data.

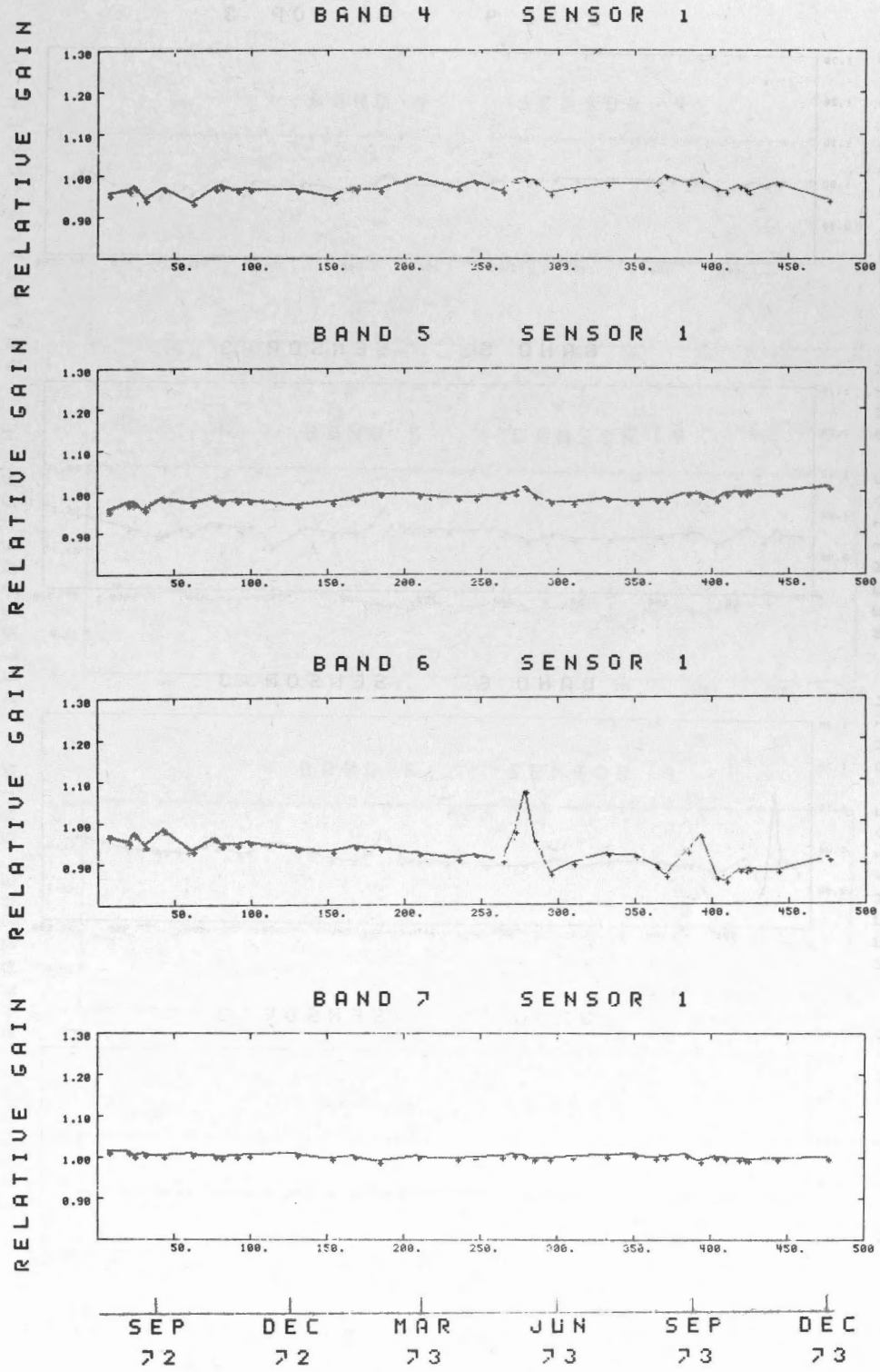

Figure 9. Gain of sensor 2 relative to the other sensors as a function of number of days from launch of ERTS-A. The '+' indicate the actual values which were determined from the first 100 swaths of the image. Some extreme data points were omitted for cosmetic reasons.

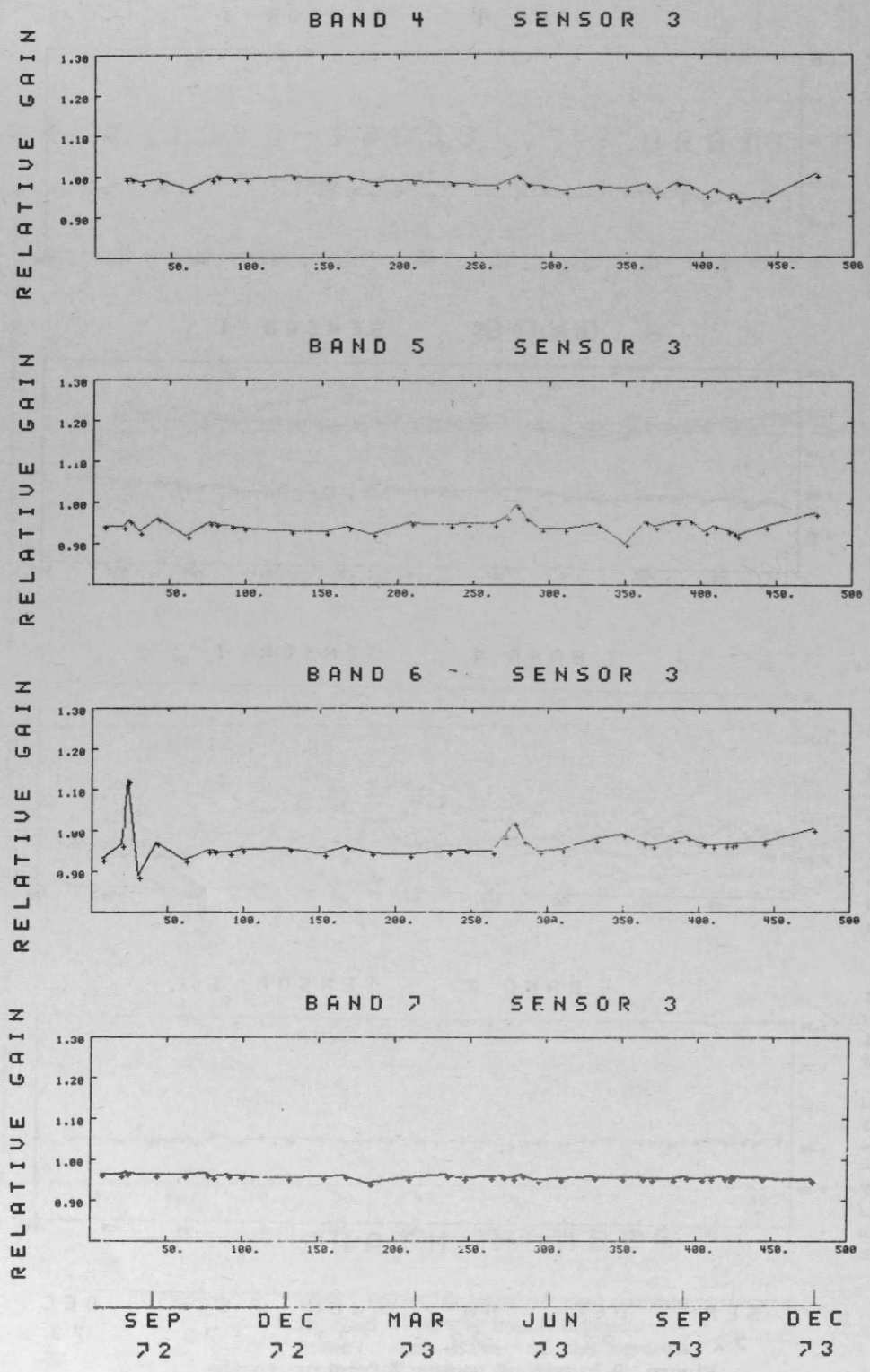

Figure 10. See Figure caption 9.

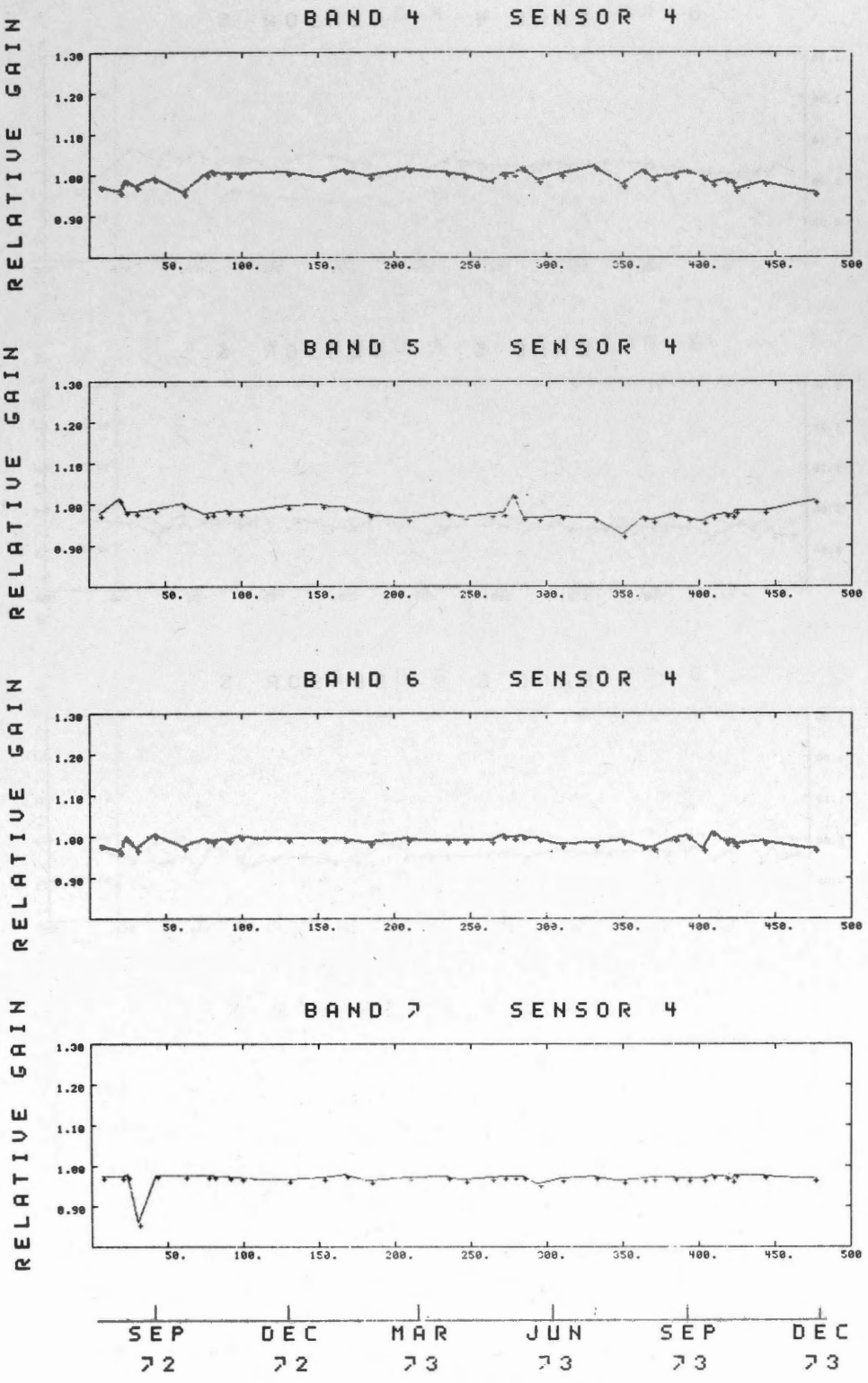

Figure 11. See Figure caption 9.

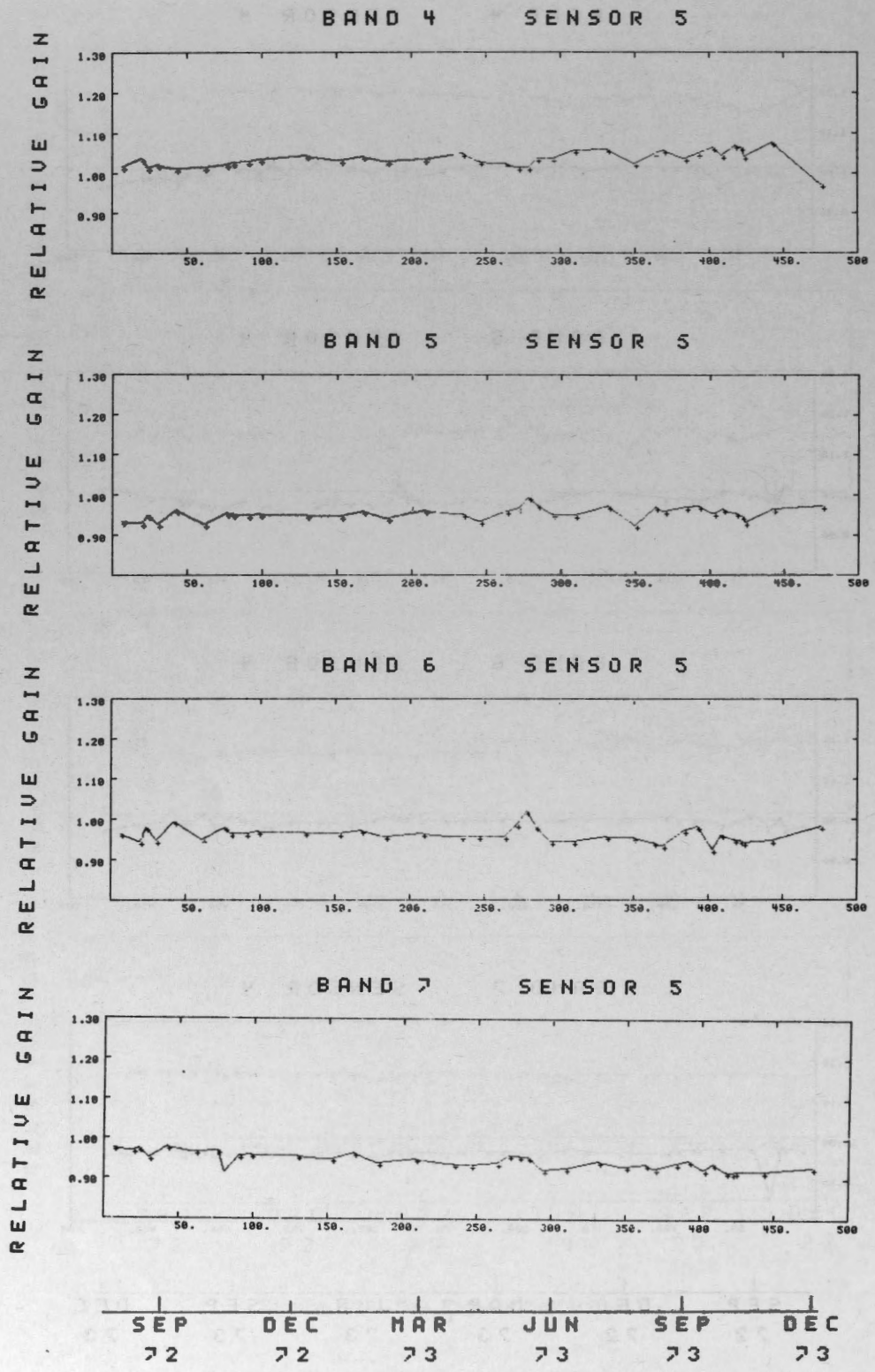

Figure 12. See Figure caption 9.

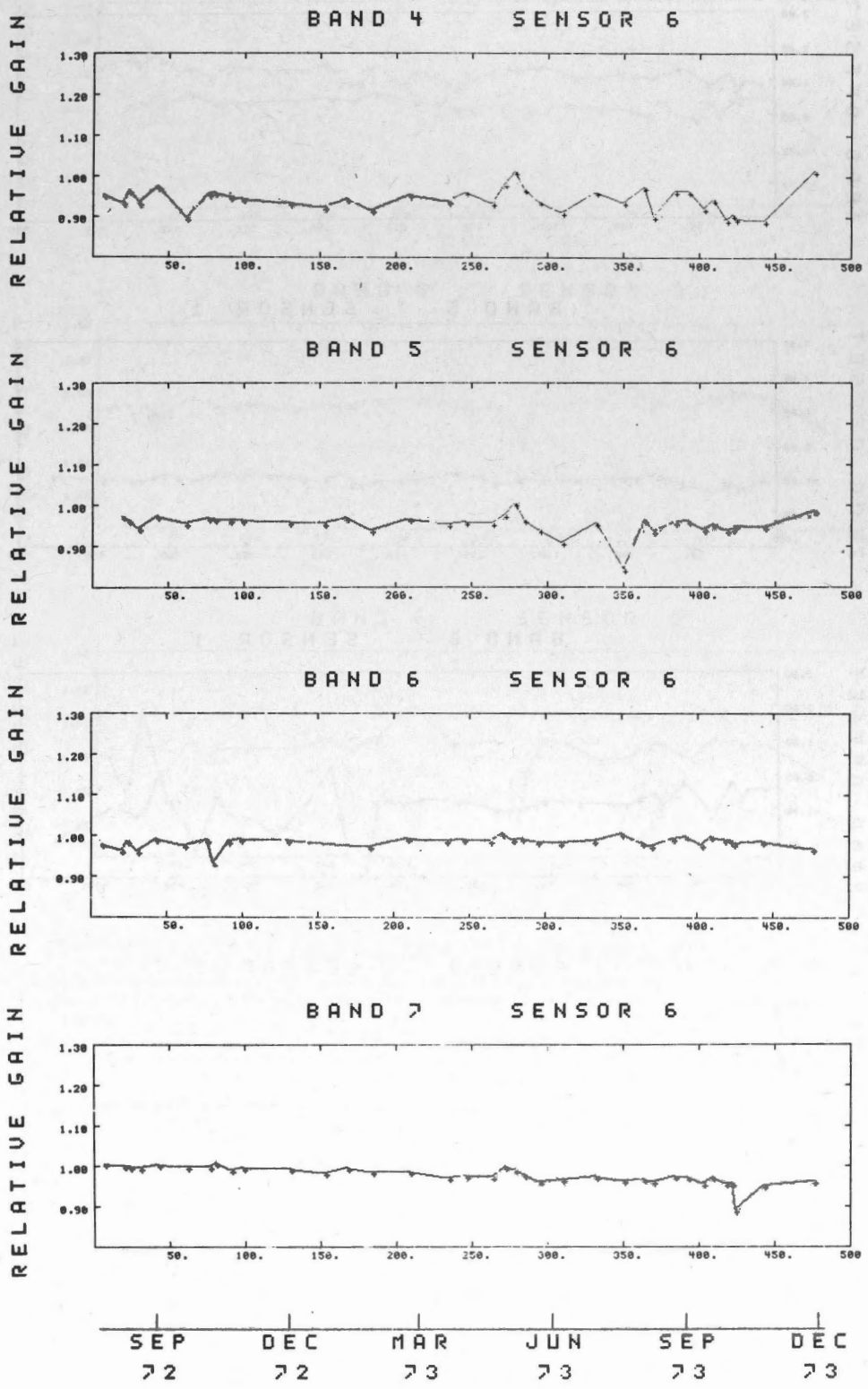

Figure 13. See Figure caption 9.

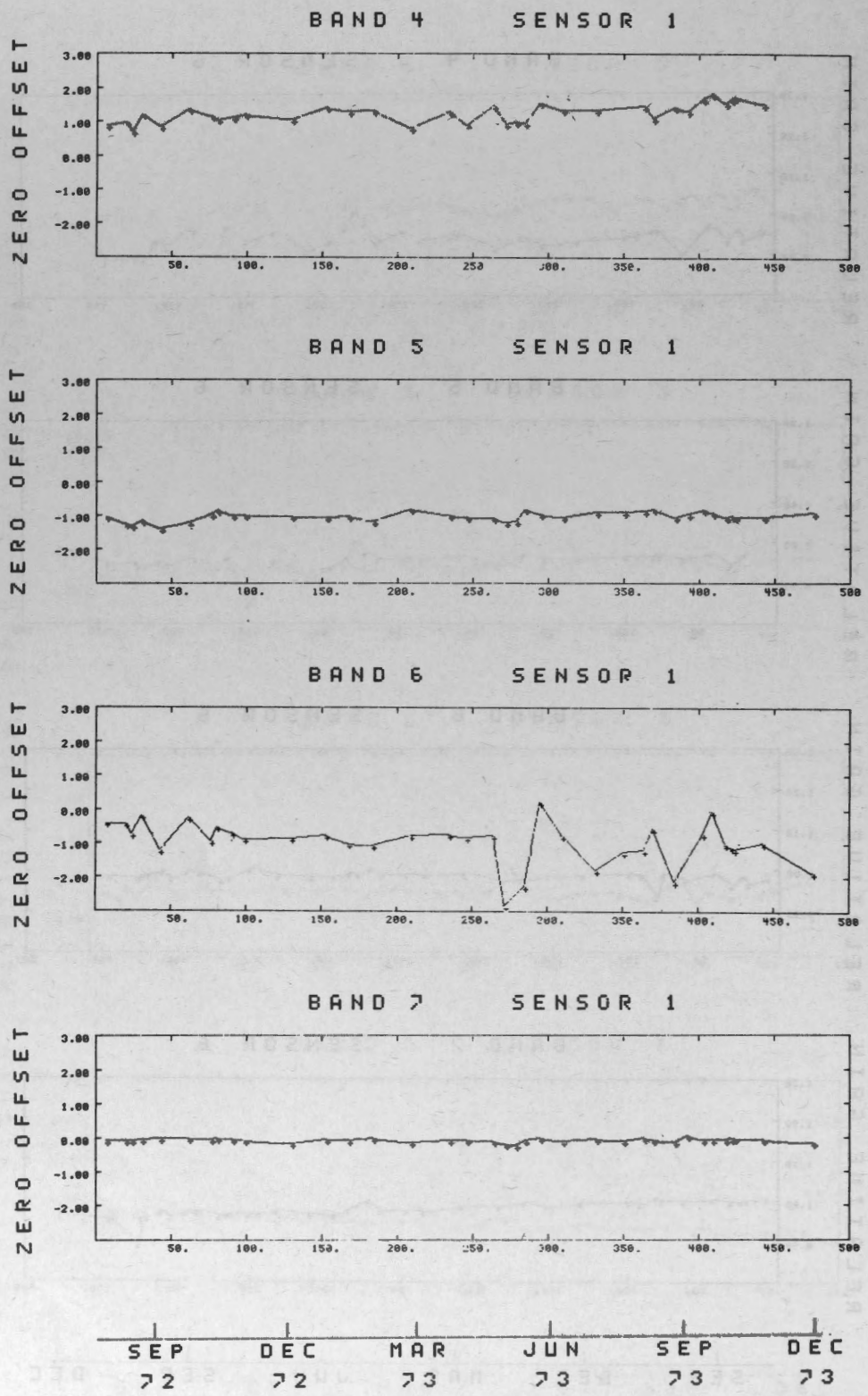

Figure 14. Zero offset of sensor 2 relative to the other sensors as a function of number of days from launch of ERTS-A. The '+' indicate the actual values which were determined from the first 100 swaths of the image. Some extreme data points were omitted for cosmetic reasons.

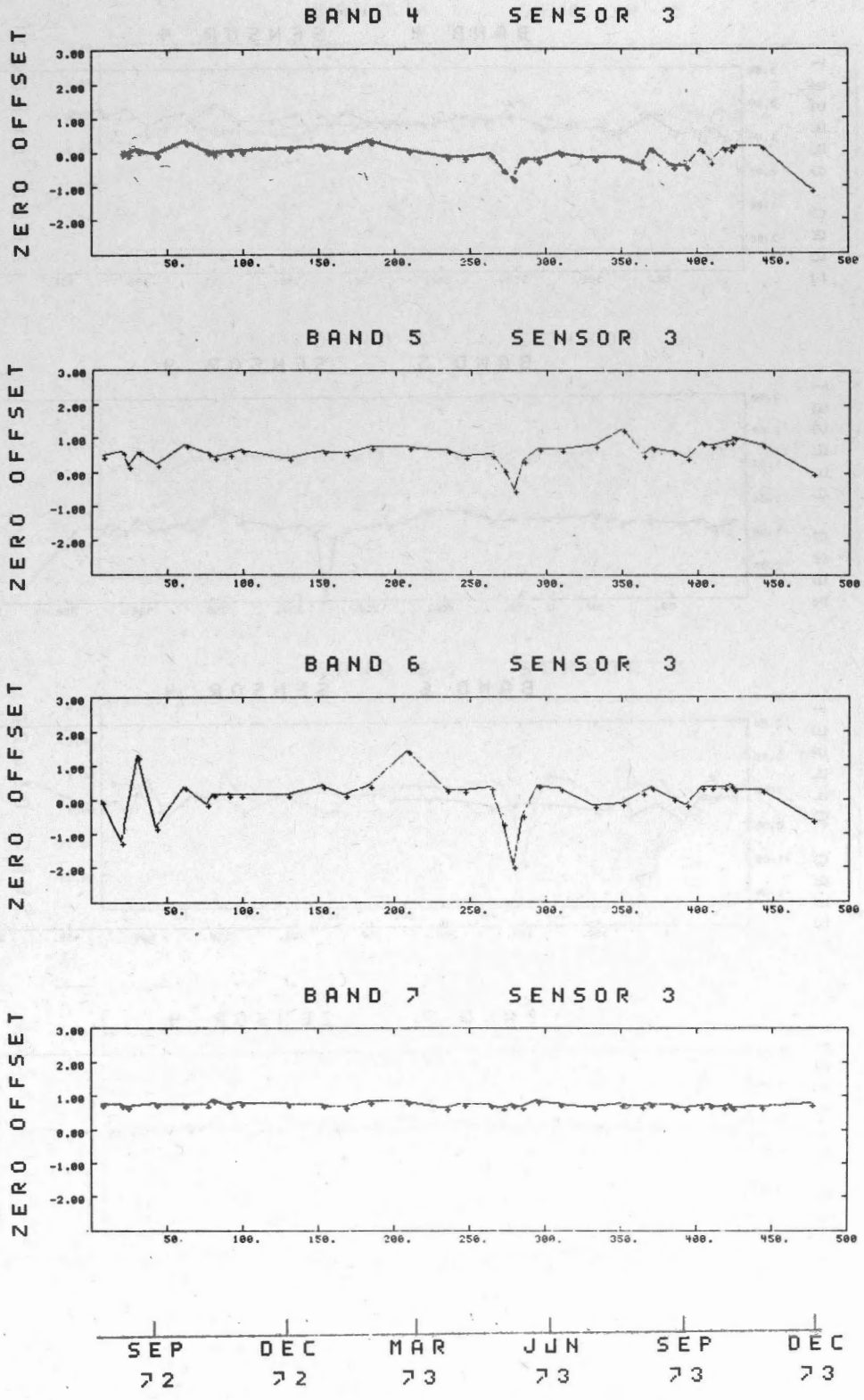

Figure 15. See Figure caption 14.

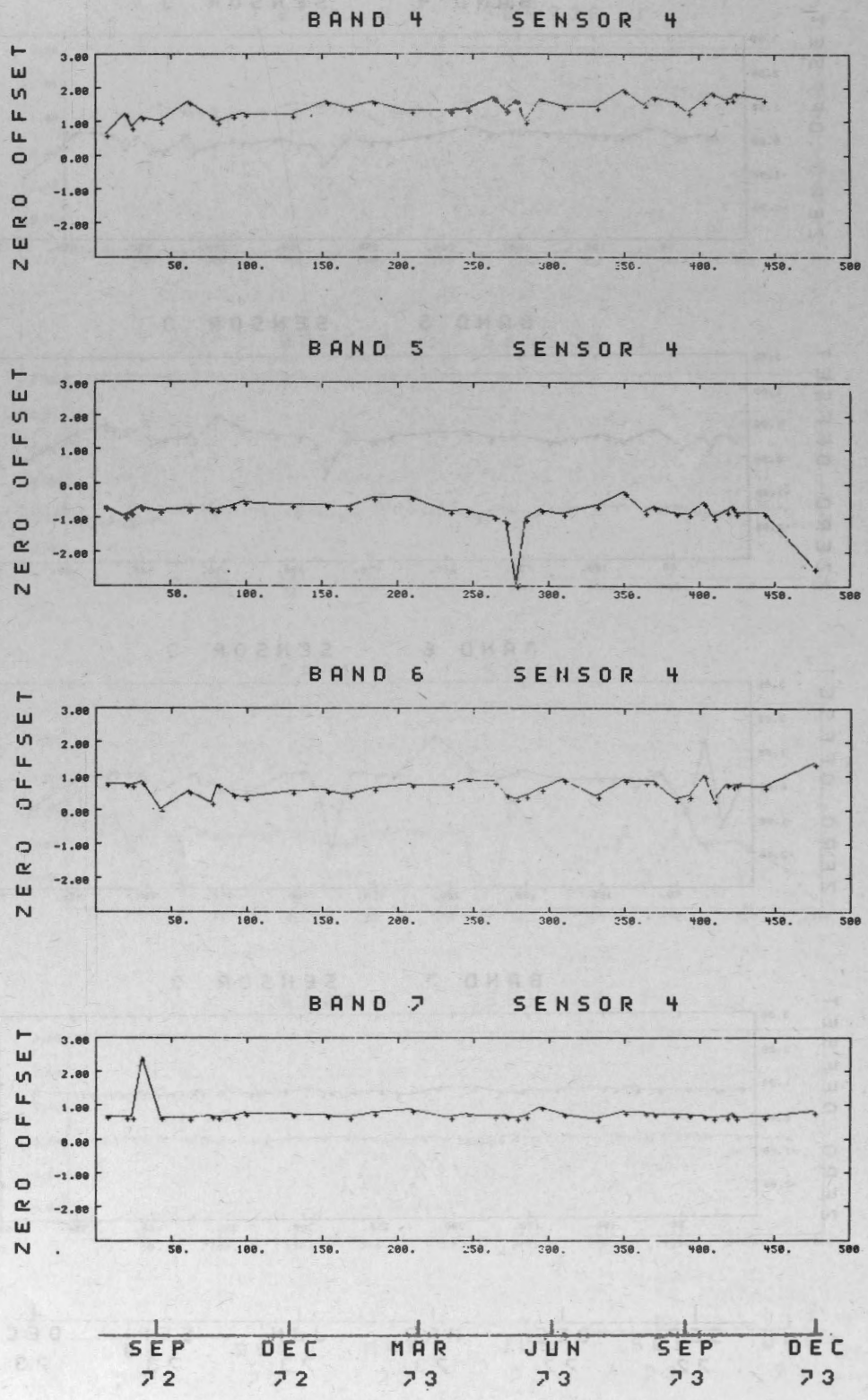

Figure 16. See Figure caption 14.

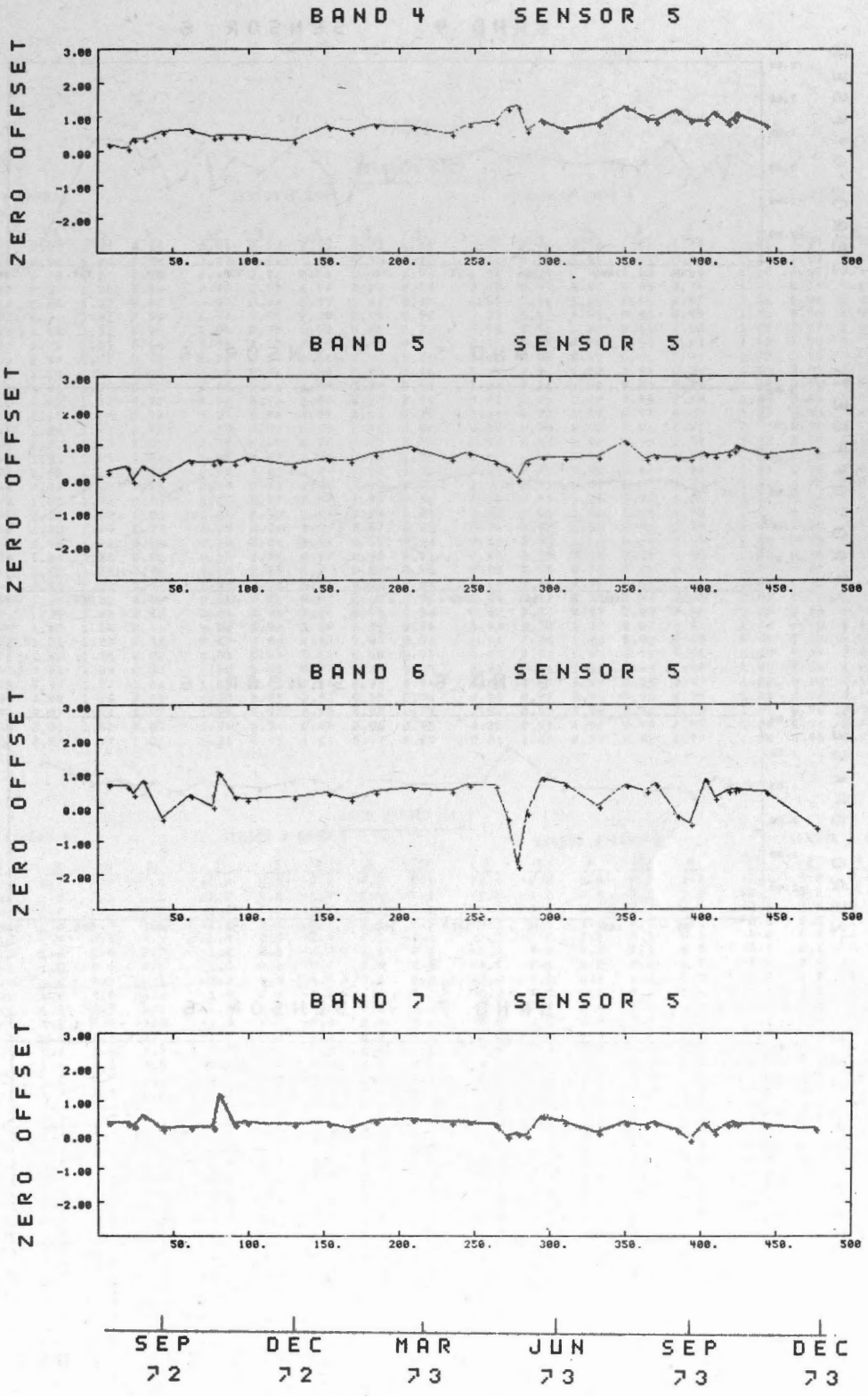

Figure 17. See Figure caption 14.

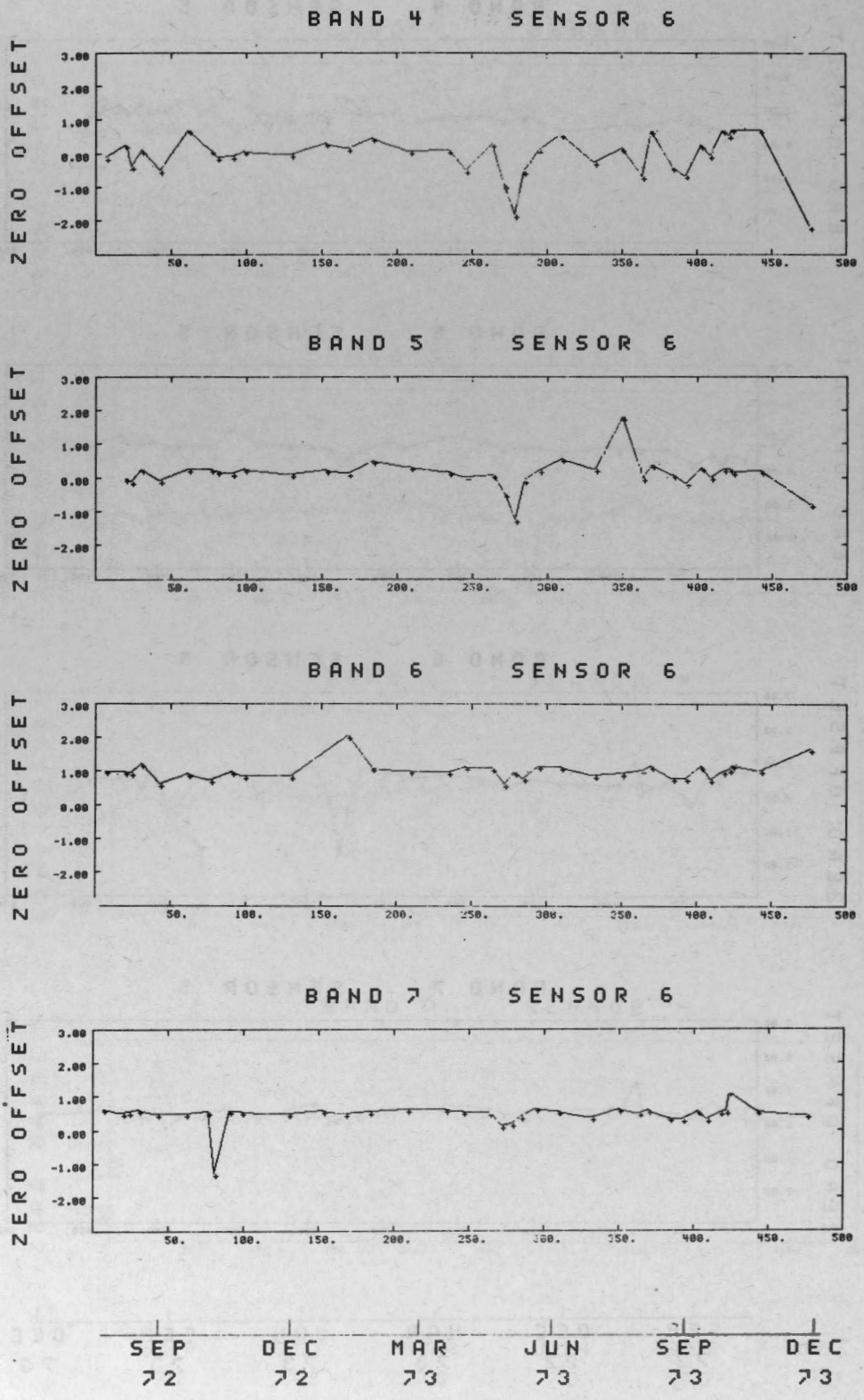

Figure 18. See Figure caption 14.

TABLE 1

RELATIVE GAIN (b_m)

Frame #	SENSOR # BAND 4					SENSOR # BAND 5					SENSOR # BAND 6					SENSOR # BAND 7				
	1	3	4	5	6	1	3	4	5	6	1	3	4	5	6	1	3	4	5	6
1007	0.96		0.97	1.02	0.95	0.96	0.94	0.98	0.93	0.58	0.97	0.93	0.98	0.96	0.98	1.01	0.97	0.97	0.98	1.01
1020	0.97	1.00	0.96	1.04	0.93	0.97	0.94	1.01	0.93	0.97	0.96	0.97	0.97	0.94	0.96	1.01	0.96	0.97	0.97	1.00
1024	0.97	1.00	0.99	1.01	0.96	0.98	0.96	0.98	0.95	0.96	0.98	1.12	1.00	0.98	0.99	1.00	0.97	0.98	0.97	1.00
1031	0.94	0.99	0.97	1.02	0.93	0.96	0.93	0.98	0.93	0.94	0.95	0.89	0.97	0.95	0.96	1.01	0.64	0.86	0.95	1.00
1043	0.97	0.99	0.99	1.01	0.97	0.99	0.96	0.99	0.96	0.97	0.99	0.97	1.01	0.99	0.99	1.00	0.96	0.98	0.98	1.00
1062	0.94	0.97	0.96	1.01	0.98	0.97	0.92	1.00	0.93	0.96	0.93	0.93	0.98	0.95	0.98	1.01	0.96	0.98	0.97	1.00
1077	0.97	0.99	1.00	1.02	0.96	0.99	0.95	0.98	0.95	0.97	0.96	0.95	1.00	0.98	0.99	1.00	0.97	0.98	0.97	1.00
1081	0.98	1.00	1.01	1.03	0.96	0.98	0.95	0.98	0.95	0.97	0.95	0.95	0.99	0.96	0.93	1.00	0.96	0.98	0.91	1.01
1091	0.97	1.00	1.00	1.03	0.95	0.98	0.94	0.98	0.95	0.96	0.95	0.95	0.99	0.96	0.99	1.00	0.96	0.97	0.96	0.99
1099	0.97	0.99	1.00	1.03	0.94	0.98	0.94	0.98	0.95	0.96	0.95	0.95	1.00	0.97	0.99	1.01	0.96	0.97	0.96	1.00
1133	0.97	1.00	1.01	1.04	0.93	0.97	0.93	1.00	0.95	0.96	0.94	0.96	1.00	0.97	0.99	1.01	0.96	0.97	0.96	0.99
1153	0.95	1.00	1.00	1.03	0.92	0.98	0.93	1.00	0.95	0.96	0.93	0.94	1.00	0.96	0.46	1.00	0.96	0.97	0.95	0.98
1168	0.97	1.00	1.01	1.04	0.94	0.99	0.94	0.99	0.96	0.97	0.94	0.96	1.00	0.97	0.77	1.00	0.96	0.98	0.96	1.00
1184	0.97	0.98	1.00	1.03	0.92	1.00	0.92	0.98	0.94	0.94	0.94	0.95	0.99	0.96	0.97	0.99	0.94	0.96	0.94	0.99
1209	1.00	0.99	1.02	1.03	0.95	0.99	0.95	0.97	0.96	0.97	0.93	0.94	1.00	0.96	0.99	1.00	0.96	0.97	0.95	0.99
1235	0.97	0.98	1.01	1.05	0.94	0.99	0.95	0.98	0.95	0.95	0.91	0.95	0.99	0.96	0.99	1.00	0.96	0.97	0.94	0.97
1246	0.99	0.98	1.00	1.03	0.96	0.99	0.95	0.97	0.93	0.96	0.92	0.95	0.99	0.96	0.99	1.00	0.96	0.97	0.93	0.98
1264	0.96	0.98	0.98	1.02	0.93	0.99	0.95	0.98	0.96	0.96	0.91	0.95	0.99	0.96	0.99	1.00	0.96	0.97	0.94	0.97
1272	0.99	0.99	1.00	1.01	0.98	1.00	0.97	0.98	0.97	0.98	0.98	0.99	1.00	0.99	1.01	1.01	0.96	0.97	0.96	1.00
1279	0.99	1.00	1.00	1.01	1.01	1.01	0.99	1.02	0.99	1.00	1.00	1.02	1.00	1.02	0.99	1.01	0.96	0.97	0.96	0.99
1285	0.99	0.98	1.02	1.04	0.97	0.99	0.96	0.97	0.97	0.96	0.96	0.98	1.00	0.98	0.99	1.00	0.96	0.97	0.95	0.98
1295	0.96	0.98	0.99	1.04	0.94	0.98	0.94	0.97	0.95	0.94	0.88	0.95	1.00	0.94	0.99	1.00	0.95	0.96	0.92	0.96
1310	0.97	0.96	1.00	1.06	0.91	0.97	0.94	0.97	0.95	0.91	0.90	0.95	0.98	0.94	0.98	1.00	0.95	0.97	0.93	0.97
1332	0.98	0.98	1.02	1.06	0.96	0.98	0.95	0.97	0.97	0.96	0.92	0.98	0.98	0.96	0.99	1.01	0.96	0.97	0.94	0.97
1350	0.58	0.97	0.98	1.02	0.94	0.98	0.90	0.93	0.92	0.84	0.92	0.99	0.99	0.95	1.01	1.01	0.96	0.96	0.93	0.96
1364	0.98	0.98	1.01	1.05	0.97	0.98	0.96	0.97	0.97	0.96	0.89	0.97	0.98	0.94	0.98	1.00	0.96	0.97	0.94	0.97
1378	1.00	0.95	0.99	1.06	0.98	0.98	0.94	0.96	0.96	0.94	0.87	0.96	0.97	0.93	0.98	1.00	0.95	0.97	0.93	0.96
1384	0.98	0.98	1.00	1.04	0.96	1.00	0.96	0.98	0.97	0.96	0.93	0.98	1.00	0.97	0.99	1.01	0.95	0.97	0.94	0.97
1393	0.99	0.98	1.01	1.05	0.96	0.99	0.96	0.97	0.97	0.96	0.97	0.98	1.00	0.98	1.00	0.99	0.96	0.97	0.95	0.97
1403	0.97	0.95	1.00	1.06	0.92	0.98	0.93	0.96	0.95	0.94	0.87	0.97	0.97	0.92	0.98	1.00	0.95	0.97	0.92	0.96
1409	0.96	0.97	0.98	1.04	0.94	1.00	0.95	0.97	0.96	0.95	0.86	0.96	1.01	0.96	1.00	1.00	0.96	0.98	0.94	0.97
1418	0.98	0.95	0.99	1.07	0.89	1.00	0.93	0.98	0.95	0.94	0.88	0.97	0.99	0.95	0.99	1.00	0.96	0.97	0.92	0.96
1422	0.97	0.95	0.99	1.06	0.91	1.00	0.93	0.97	0.95	0.94	0.88	0.97	0.99	0.95	0.99	1.00	0.95	0.97	0.92	0.96
1424	0.96	0.94	0.97	1.04	0.98	1.00	0.92	0.98	0.93	0.95	0.89	0.97	0.98	0.94	0.98	1.00	0.96	0.98	0.92	0.89
1443	0.98	0.94	0.98	1.08	0.89	1.00	0.94	0.98	0.96	0.95	0.88	0.97	0.99	0.95	0.99	1.00	0.96	0.98	0.92	0.95
1476	0.94	1.00	0.96	0.97	1.01	1.01	0.98	1.01	0.97	0.99	0.91	1.00	0.97	0.98	0.97	1.00	0.95	0.97	0.93	0.96

ZERO OFFSET (a_m)

Frame #	SENSOR # BAND 4					SENSOR # BAND 5					SENSOR # BAND 6					SENSOR # BAND 7				
	1	3	4	5	6	1	3	4	5	6	1	3	4	5	6	1	3	4	5	6
1007	0.9		0.7	0.2	-0.1	-1.0	0.5	-2.7	0.2	5.1	-0.4	-0.0	0.8	0.7	1.0	-0.1	0.8	0.7	0.4	0.6
1020	1.0	0.0	1.2	0.1	0.3	-1.2	0.6	-1.0	0.4	-0.0	-0.4	-1.2	0.8	0.6	1.0	-0.1	0.8	0.7	0.4	0.5
1024	0.7	0.2	0.8	0.4	-0.4	-1.3	0.2	-0.9	-0.0	-0.1	-0.7	-3.6	0.7	0.4	0.9	-0.1	0.7	0.7	0.3	0.6
1031	1.2	0.1	1.2	0.4	0.1	-1.1	0.6	-0.7	0.4	0.2	-0.2	1.3	0.8	0.8	1.2	-0.0	5.5	2.4	0.6	0.6
1043	0.9	-0.3	1.0	0.6	-3.5	-1.4	0.3	-0.8	0.1	-0.1	-1.2	-0.8	0.0	-0.3	0.6	-0.0	0.8	0.7	0.2	0.5
1062	1.4	0.3	1.6	0.6	0.7	-1.2	0.8	-0.7	0.6	0.2	-0.3	0.4	0.6	0.4	0.9	-0.0	0.8	0.6	0.3	0.5
1077	1.2	0.1	1.2	0.4	0.1	-1.0	0.6	-0.7	0.5	0.3	-0.9	-0.1	0.2	0.0	0.7	-0.1	0.8	0.7	0.3	0.6
1081	1.0	0.0	1.0	0.5	-0.1	-0.9	0.5	-0.8	0.6	0.2	-0.5	0.2	0.8	1.0	9.5	-0.0	0.9	0.7	1.2	-1.3
1091	1.1	0.0	1.2	0.5	-0.1	-1.0	0.5	-0.6	0.5	0.1	-0.7	0.2	0.5	0.4	1.0	-0.0	0.8	0.7	0.4	0.6
1099	1.2	0.1	1.3	0.5	0.1	-1.0	0.7	-0.5	0.6	0.3	-0.9	0.2	0.4	0.2	0.8	-0.1	0.8	0.8	0.4	0.6
1130	1.1	0.1	1.2	0.3	-0.0	-1.0	0.4	-0.6	0.4	0.1	-0.8	0.2	0.5	0.3	0.8	-0.2	0.8	0.8	0.3	0.5
1153	1.4	0.2	1.6	0.7	0.3	-1.1	0.7	-0.6	0.6	0.2	-0.8	0.4	0.6	0.4	6.6	-0.1	0.8	0.7	0.4	0.6
1168	1.3	0.1	1.4	0.6	0.2	-1.0	0.6	-0.7	0.6	0.1	-1.0	0.2	0.5	0.2	2.1	-0.1	0.7	0.7	0.2	0.5
1184	1.3	0.3	1.6	0.8	0.5	-1.2	0.8	-0.4	0.8	0.5	-1.1	0.4	0.6	0.5	1.1	-0.0	0.9	0.8	0.4	0.6
1209	0.8	0.1	1.3	0.7	0.1	-0.8	0.8	-0.4	1.0	0.3	-0.8	1.5	0.8	0.6	1.0	-0.1	0.9	0.9	0.5	0.6
1235	1.3	-0.1	1.3	0.5	0.1	-1.0	0.7	-0.8	0.6	0.2	-0.7	0.3	0.7	0.5	1.0	-0.1	0.7	0.7	0.4	0.6
1246	0.9	-0.1	1.4	0.8	-0.5	-1.1	0.5	-0.8	0.8	0.0	-0.8	0.3	0.9	0.7	1.1	-0.1	0.8	0.8	0.4	0.6
1264	1.5	-0.0	1.7	0.9	0.3	-1.1	0.5	-1.0	0.5	0.1	-0.8	0.4	0.9	0.6	1.1	-0.1	0.8	0.7	0.3	0.5
1272	1.0	-0.5	1.4	1.3	-0.9	-1.2	0.1	-1.1	0.3	-0.5	-2.8	-0.7	0.5	-0.3	0.6	-0.2	0.7	0.7	-0.0	0.1
1279	1.0	-0.8	1.6	1.3	-1.8	-1.2	-0.5	-3.0	0.0	-1.2	-7.0	-1.9	0.4	-1.7	1.0	-0.2	0.8	0.6	0.1	0.2
1285	1.0	-0.2	1.0	0.6	-0.5	-0.8	0.4	-1.0	0.5	-0.1	-2.3	-0.4	0.4	-0.2	0.8	-0.1	0.7	0.7	0.0	0.4
1295	1.6	-0.2	1.7	0.9	0.1	-1.0	0.7	-0.7	0.7	0.2	0.2	0.4	0.6	0.9	1.1	-0.0	0.9	1.0	0.6	0.6
1310	1.4	-0.0	1.5	0.7	0.6	-1.1	0.7	-0.8	0.7	0.6	-0.8	0.3	0.9	0.7	1.1	-0.1	0.8	0.8	0.4	0.5
1332	1.4	-0.2	1.4	0.8	-0.2	-0.9	0.8	-0.6	0.7	0.3	-1.8	-0.2	0.4	0.0	0.9	-0.1	0.7	0.6	0.1	0.4
1350	0.9	-0.2	2.0	1.3	0.2	-0.9	1.3	-0.2	1.1	1.8	-1.2	-0.1	3.9	0.7	1.0	-0.1	0.8	0.8	0.4	0.6
1364	1.5	-0.4	1.5	1.0	-0.7	-0.9	0.6	-0.8	0.6	-0.0	-1.2	0.2	0.9	0.5	1.0	-0.0	0.7	0.8	0.3	0.5
1378	1.1	0.1	1.8	0.9	0.7	-0.8	0.8	-0.6	0.7	0.4	-0.6	0.4	0.9	0.7	1.2	-0.1	0.8	0.8	0.4	0.6
1384	1.5	-0.4	1.6	1.2	-0.4	-1.1	0.6	-0.8	0.6	0.1	-2.1	0.0	0.3	-0.2	0.8	-0.1	0.8	0.7	0.2	0.3
1393	1.3	-0.4	1.3	1.0	-0.6	-1.0	0.5	-0.8	0.6	-0.2	-3.6	-0.1	0.4	-0.5	0.8	0.1	0.7	0.7	-0.1	0.3
1403	1.7	0.1	1.6	0.9	0.3	-0.9	0.9	-0.5	0.8	0.3	-0.7	0.4	1.0	0.8	1.2	-0.1	0.7	0.7	0.4	0.5
1409	1.9	-0.3	1.9	1.2	-0.1	-0.9	0.8	-0.9	0.7	0.0	-0.8	0.4	0.3	0.3	0.8	-0.1	0.8	0.6	0.1	0.3
1418	1.6	0.1	1.7	0.9	0.7	-1.1	0.9	-0.8	0.8	0.3	-1.0	0.4	0.8	0.5	1.0	-0.1	0.7	0.7	0.4	0.5
1422	1.7	0.1	1.7	1.0	0.6	-1.0	1.0	-0.7	0.9	0.3	-1.1	0.4	0.7	0.5	1.1	-0.1	0.8	0.8	0.4	0.6
1424	1.7	0.2	1.9	1.1	0.7	-1.1	1.1	-0.8	1.0	0.2	-1.1	0.3	0.8	0.6	1.2	-0.0	0.7	0.6	0.4	1.1
1443	1.5	0.2	1.7	0.8	0.7	-1.1	0.8	-0.8	0.7	0.2	-1.0	0.3	0.7	0.5	1.0	-0.1	0.7	0.7	0.4	0.6
1476	3.3	-1.1	3.3	3.9	-2.2	-0.9	0.0	-2.4	0.9	-3.8	-1.9	-2.6	1.4	-0.6	1.7	-0.2	0.8	0.8	0.2	0.4

INTERPRETATION OF FOREST PATTERNS ON COMPUTER COMPATIBLE TAPES

By

L. SAYN-WITTGENSTEIN
Z. KALENSKY

This paper presented at the Second Canadian Symposium on Remote Sensing, University of Guelph, Guelph, Ontario, April 29 - May 1, 1974.

INTERPRETATION OF FOREST PATTERNS ON COMPUTER COMPATIBLE TAPES

L. SAYN-WITTGENSTEIN AND Z. KALENSKY

CANADIAN FORESTRY SERVICE, OTTAWA

SUMMARY

The identification of spatial patterns should receive more emphasis in the interpretation of ERTS imagery. Spatial patterns can be recognized by involving such concepts and techniques as serial correlation, central tendency, periodicity and spectral analysis. The best results are obtained by using computer compatible tapes, rather than photographic images.

RESUME

L'analyse des données de l'ERTS/MSS par ordinateur permet une corrélation et une interprétation provisoire rapides d'informations spectrales, spatiales et temporelles. Ceci augmentera l'efficacité de l'interprétation en permettant de concentrer sur les données expérimentées et choisies d'avance.

Les auteurs utilisèrent deux produits de l'ERTS/MSS, les rubans magnétiques (CCT) et les films transparents de 70 mm. Les CCT furent traités de façon à fournir un modèle reconstruit de radiance spectrale du sol. Les cartes imprimées de l'ordinateur sont des matrices pinels radiométriquement calibrées. Les auteurs calculèrent à partir de ces matrices différentes statistiques identifiant des classes choisies d'objets. Le succès de l'interprétation repose sur les bonnes spécifications à propos de ces statistiques d'identification.

Les auteurs abordèrent de la même manière les données numériques obtenues d'images de l'ERTS auparavant regardées avec un microdensitomètre.

Ces CCT procurent de meilleures informations que tous les films produits de l'ERTS vu que l'on évite la principale source de dégradation des images: le développement des photos. Cependant, si les cibles au sol s'avèrent bien au-dessus de la limite de résolution du système de traiter l'ERTS/MSS (par exemple: grandes aires brûlées ou inondées, exploitation intensive de la forêt), les images photographiques peuvent être utilisées avantageusement vu qu'elles amènent plus de flexibilité dans le traitement et un choix plus aisé des régions intéressantes.

INTRODUCTION

Two basic types of object signatures are encoded in every ERTS image: spatial and spectral. While spectral signatures are used extensively for ERTS image interpretation, few users have paid attention to spatial signatures. There are several reasons for this: ERTS was designed as an experiment in multi-spectral sensing; the concept of spectral signatures is more readily understood than mathematical approaches to the definition of such terms as "irregular", "smooth" or "wavy" on which the concept of spatial signatures is based; multispectral analysis can be done on a one pixel basis while spatial analysis requires several tens or even hundreds of suitably distributed pixels in every class to obtain statistically significant spatial patterns; analysis of these patterns requires the use of computers while there are several optical and photographic methods for multispectral image analysis; finally, image interpretation based on spectral signatures only does yield very promising results although our initial results (Kalensky and Sayn-Wittgenstein, 1974) did not yield accuracies of land classification that were useful beyond the reconnaissance level.

For many applications, however, all the image information content will have to be utilised to obtain the required accuracy. Furthermore, some object classes cannot be identified at all on the ERTS images using spectral signatures only, because of their low contrast or overlapping responses in MSS (or RBV) spectral bands. Finally, some object classes exhibit a distinct spatial pattern superior for their identification to spectral signatures (e.g. strip and checkerboard logging patterns).

Experience and common sense tell us that spectral characteristics form only part of the information for our visual perception. In a typical landscape an average person can distinguish only about 20 grey tones while the number of distinguishable colors is between 4,500 and 5,000*. Then why do some interpreters still use black and white photography? The reason is that requirements can often be satisfied by identification based on shape, size and texture. A white pine is recognized not by its colour but by its branching habit; a river delta, an orchard or a network of roads are best recognized by their shape and not by their spectral signatures. Shape and form are also the most reliable and most consistent identifying characteristics: a child will recognize an elephant by its shape and it would not matter if the beast is observed in broad daylight, as a silhouette against the sky or under the coloured lights of a circus; a record of its typical spectral signatures would not be particularly useful. There is good reason to expect that similar principles apply to the interpretation of ERTS imagery. We cannot afford to neglect the spatial image characteristics.

Furthermore, interpretation based on spectral information only has some severe limitations. Ground measurements of spectral reflectance which were carried out for the Forest Management Institute in 1973 have emphasized how unpredictable can be the factors which influence spectral signatures and, at the same time have emphasized the low reliability of spectral measurements as interpretation criteria. For example, the spectral signature of a white pine in the Larose Forest near Ottawa was found to be practically identical with that of a white spruce from the same area, but was very different from that of a white pine in Gatineau Park, not far away (Figure 1). The causes could have been many: different state of phenological development, health or age of trees, sun angle, site and weather conditions. For data recorded by satellite, we would have to add all the variables that lead to a degradation and alteration of spectral information during the receiving, transmission, recording and processing stages. Whatever the cause, additional information will have to be found to improve accuracy. One possible source of such information is in the analysis of sequential imagery, in the search for identifying features among the changes from one ERTS pass to the next. Another is the extraction of significant spatial features.

ANALYSIS OF SPATIAL IMAGE PATTERNS

The crucial stage in pattern recognition using spatial characteristics will be to find the key features that identify the required object classes. This search should be systematic and must involve theoretical consideration of spatial variation in forests and other populations. It should begin with concepts of biometrics, ecology and statistics which show that the basic elements of natural populations, such as the trees of a forest or the plants in the field, follow distributions that can be described by mathematical models. The parameters of these models vary with the population and, therefore, the populations can be identified by estimates of these parameters.

Relevant information can be found in a large body of literature. We have begun our search for characteristics of spatial patterns in ERTS data by following some of the concepts reviewed by Sayn-Wittgenstein (1970). These include the following:

1. Populations on forest and agricultural lands are influenced by gradual trends and common influences that impose a certain similarity on adjacent elements in a population. Among the many causes are fertility gradients, common climatic influences, effects of exposure to wind, or a common history of disease or management practices. The resulting population is sometimes well described by fitting the smooth surface of a polynomial to the values observed. Such polynomial trends have been found to be good models for undisturbed forests, e.g. for some mature coniferous stands in the Boreal Forest Region.

---

*These estimates are from Kalensky (1967): "The Quantitative Soil Moisture Interpretation from 35 mm Aerial Colour Photographs". Unpublished M.Sc. thesis, University of New Brunswick. A great range of widely different estimates is reported in literature.

2. Smooth trends however are often not satisfactory, because over short distances the dominating forces governing spatial distribution are the interactions between neighbouring trees. The most important of these is the effect of competition between trees which gives rise to the correlograms described in the important work of Matérn (1960).

The following sections will discuss a number of the resulting mathematical models and patterns of spatial variation in more detail.

Serial Correlation

A number of correlograms have been calculated for ERTS data using both digital records from computer compatible tapes (Figure 2) and digitized microdensity values of 70 mm ERTS film transparencies. Microdensities were measured by an ANSCO Automatic Recording Microdensitometer Model 4 at the National Research Council, Ottawa (Figure 3). Most data were from the Larose Forest near Ottawa (Figure 4).

The correlograms, such as those of Figure 5, have led to the following conclusions:

A. For land covered with vegetation, correlation is positive and correlograms are exponentially decaying and concave upward. This agrees with the model of "topographic variation" postulated by Matérn (1960).

B. Correlograms differ with land class, but the reliability of such differences has yet to be determined.

C. Significant serial correlation usually persists over only short distances, such as 100 metres. This confirms earlier conclusions reached by the analysis of forest survey data.

D. There is a major difference between correlograms calculated from ERTS tapes and those derived from photographic images using a microdensitometer with an aperture corresponding approximately to the sampling interval of the Multispectral Scanner. Apparent serial correlation is generally higher on photographic images (Figure 5). This largely attributed to the degradation of spatial information in the photographic process, mainly due to the smoothing effect of film granularity.

E. High positive serial correlations were occasionally observed. In the absence of other explanations, a characteristic of the scanner or of the processing system must be the suspected causes.

Spectral Analysis of Spatial Information

A related approach is to regard the ERTS scanner data in the same way as electronic signals changing with time and to submit them to spectral analysis to establish component frequencies. Differences between power spectra for different land classes have been observed but so far we have been unable to detect any systematic pattern which could be uniquely correlated with a land class and thus used for its identification.

Spectral analysis is an excellent way to discover periodicities existing in data sets as well as any unusual influences due to the scanner or image processing. It has also been shown how degraded and suppressed high frequency detail is in photographic images compared to data from computer compatible tapes (Figure 6).

Measures of Central Tendency

Various measures of central tendency, including range and standard deviation of sub-sets of pixel values, are an easy way of expressing texture. It is an approach that has already received some attention (eg. Akça, 1971, Haefner and Maurer, 1973) and valuable guidelines are available. Preliminary investigations with ERTS data (Table 1) show the differences in arithmetic mean, deviation and in standard deviation expressed as percentage of arithmetic mean, calculated for eight land classes. For example, pure stands and stands with a very thorough mixture of species can be expected to have lower spatial variations about the mean than vegetation types involving a patchy distribution of species.

The problem now is to use this information effectively in the identification of land classes and in establishing where the boundaries between classes lie. The current approach is to calculate the standard deviation for each possible 3 X 3 pixel block and to enter this value at the location of the central pixel of each block. Standard procedures could then be applied to obtain a

picture of "standard deviation of 3 X 3 pixel blocks" and to combine this information with other spectral or spatial data.

Differences between successive pixel values are another possible approach to indicate texture and to show where the boundaries between land classes lie. There is great scope for experimenting with several levels of smoothing, with differences of various orders and raised to different powers.

Periodicity

One may always expect to encounter some periodic cycles. But with ERTS data obtained over land, one can almost invariably discount any periodic pattern that persists over great distances as due to some characteristic of the scanner or as a purely numerical phenomenon. It is usually possible to find periodicity in any finite series and even, as has been demonstrated, in series of random normal deviates.

A book could be written about the many arguments on periodicity found in statistical literature. However, for natural populations distributed over land, all evidence supports the conclusion of Milne (1959): periodicity does not occur except as a result of human activity. ERTS data reveal many examples of periodicities caused by man; eg. land use patterns influenced by the prevailing land survey system are common (ERTS frame 1192-15395-5 shows a good example). But such periodicities are not unsuspected and there seems to be no purpose in searching for them.

The Effect of Scale and Resolution on Pattern

Patterns can be expected to be very sensitive to scale or, putting it another way, to pixel size or aperture of densitometer. The larger aperture or pixel, the less relative variation between pixels, the smoother the texture. The coefficient of serial correlation is also extremely sensitive to changes in the size of the elements in the series. This is readily illustrated:

Using 1:2,000 aerial photography of an open white spruce stand we outlined a square block which was further divided into square cells. The first order serial correlation (r_1) coefficient was compiled between each cell and all its neighbours. For different cell sizes the results were as follows:

Length of cell side	r_1
1 m	-.6
2 m	-.3
3 m	0.0
4 m	+.2
5 m	+.3
6 m	+.3
7 m	+.5

Such resolution is of course beyond the capability of ERTS, but the principle is illustrated. The degree and rate of change of pattern characteristics with changes in scale or resolution may indeed be of some value in identification.

CONCLUSION

Spatial characteristics should receive more attention in the interpretation of ERTS data. This approach is not in competition with, but complementary to analysis of spectral characteristics. The best approach to identify the essential features of spatial patterns on ERTS imagery is to apply basic concepts of spatial variation discovered by statisticians, ecologists and biologists.

Various mathematical models based on polynomial trends and serial correlation which have been studied in other fields, are relevant to the analysis of ERTS data. The correlograms calculated from digital ERTS data, for example, show the same essential characteristics as those from data collected on the ground. The question of periodicity is just as relevant in the analysis of scanner data, as it is in discussions of systematic sampling.

The first practical results in pattern recognition based on spatial features will come from the use of measures of central tendency as expressions of pattern. But the other approaches referred to, including spectral analysis, are also valuable, because they give insight into the fundamental nature of ERTS data.

Digital data on computer compatible tapes are superior to photographic images for the identification of spatial patterns.

REFERENCES

Akça, A., 1971. Identification of land use classes and forest types by means of microdensitometer and discriminant analysis. In IUFRO, Section 25, Application of Remote Sensors in Forestry, pp. 147-164 (Rombach & Co., Freiburg).

Haefner, H. and H. Maurer, 1973. Digital image processing for land use interpretation. Proceedings, IUFRO Remote Sensing Symposium Freiburg, September 1973. (In press)

Kalensky, Z. and L. Sayn-Wittgenstein, 1974. Thematic map of Larose Forest from ERTS-1/MSS digital data. The Canadian Surveyor, Vol. 28, No. 2. (In press)

Matérn, B., 1960. Spatial variation. Reports of the Swedish Research Institute. Vol. 49, Nr. 5, 144 p.

Milne, A., 1959. The centric systematic area-sample treated as a random sample. Biometrics, Vol. 15, No. 2.

Sayn-Wittgenstein, L., 1970. Patterns of spatial variation in forests and other natural populations. Pattern Recognition. Vol. 2, pp. 245-253.

Table 1 ERTS image statistics of the Larose Forest area.

ERTS-1/MSS Computer Compatible Tapes
Multiband and Multidate Comparisons

A. Frame no. 1044-15170 of Sept. 5, 1972
B. Frame no. 1062-15170 of Sept. 23, 1972
C. Frame no. 1440-15154 of Oct. 6, 1973

OBJECT CLASS	FRAME	BAND 4			BAND 5			BAND 6			BAND 7		
		$\bar{X}$	σ	$100\sigma/\bar{X}$	$\bar{X}$	σ	$100\sigma/\bar{X}$	$\bar{X}$	σ	$100\sigma/\bar{X}$	$\bar{X}$	σ	$100\sigma/\bar{X}$
		counts	counts	%	counts	counts	%	counts	counts	%	counts	counts	%
Mostly Coniferous Forest	A	14.2	0.9	6.3	10.8	1.1	10.2	25.8	2.5	9.7	18.4	4.3	23.4
	B	13.9	0.8	5.8	10.9	1.5	13.8	25.8	2.4	9.3	17.4	2.7	15.5
	C	15.4	1.1	7.1	12.4	2.4	19.3	26.5	1.9	7.2	16.0	1.7	10.6
Mostly Deciduous Forest	A	14.7	0.7	4.8	10.9	0.7	6.4	31.0	1.6	5.2	25.3	2.2	8.7
	B	14.2	0.7	4.9	11.7	1.3	11.1	30.4	1.9	6.2	22.9	2.3	10.0
	C	16.7	4.1	24.5	16.7	4.1	24.5	29.9	5.4	18.1	17.5	4.2	24.0
Mixed Forest	A	14.4	0.6	4.2	10.9	0.7	6.4	29.0	2.4	8.3	22.8	3.3	14.5
	B	14.1	0.6	4.2	11.2	1.2	10.7	28.5	2.3	8.1	20.8	3.0	14.4
	C	16.2	1.0	6.2	14.6	2.1	14.4	27.2	3.0	11.0	16.2	4.0	24.7
Farm Land	A	17.3	0.8	4.6	16.1	1.2	7.4	29.6	1.9	6.4	22.0	2.4	10.9
	B	17.2	0.9	5.2	16.6	1.5	9.0	29.5	1.9	6.4	21.3	2.4	11.3
	C	18.6	1.1	5.9	17.9	1.4	7.8	30.4	3.1	10.2	18.9	3.5	18.5
Silted South Nation River	A	20.3	2.1	10.3	20.3	3.1	15.3	27.6	1.2	4.3	16.7	2.2	13.2
	B	20.8	2.3	11.0	21.1	3.1	14.7	27.6	1.2	4.3	16.4	1.8	11.0
	C	19.4	1.5	7.7	18.7	1.7	9.1	25.4	2.4	9.4	12.4	3.5	28.2
Ottawa River	A	13.0	0.6	4.6	9.8	0.7	7.1	9.0	2.5	27.8	1.9	1.7	89.5
	B	13.2	0.7	5.3	10.1	1.0	9.9	8.8	3.8	43.2	2.1	2.8	133.3
	C	16.6	2.2	13.2	13.9	3.2	23.0	11.1	5.4	48.6	3.1	4.0	129.0
Highway 417 (under construction)	A	22.1	2.6	11.8	23.8	3.6	15.1	32.3	3.6	11.1	22.6	3.7	16.4
	B	21.7	3.4	15.7	23.1	5.0	21.6	32.6	5.7	17.5	21.6	4.7	21.7
	C	18.8	1.4	7.4	17.2	2.3	13.4	30.0	4.0	13.3	18.0	4.3	23.9
Mudslide	A	18.5	1.0	5.4	17.7	1.5	8.5	26.2	1.1	4.2	16.2	1.4	8.6
	B	18.7	1.2	6.4	18.7	1.6	8.5	26.7	1.2	4.5	16.6	1.4	8.4
	C	18.3	0.9	4.9	17.8	0.8	4.5	26.0	1.5	5.8	13.8	1.3	9.4

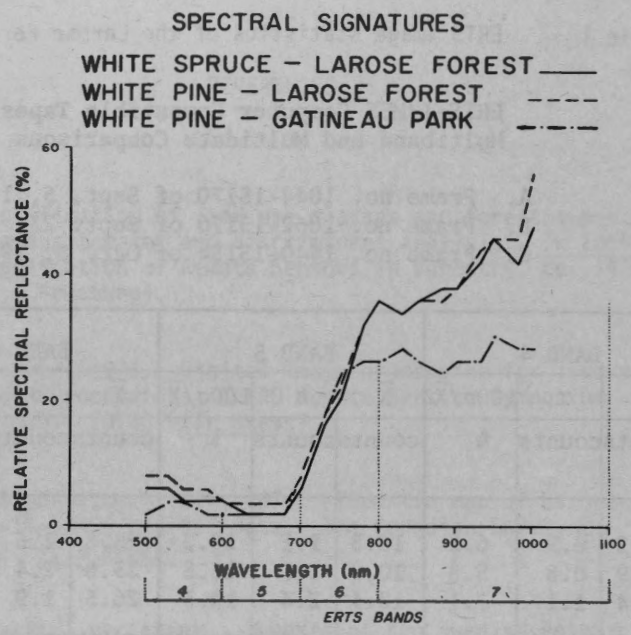

Figure 1. Spectral signatures of three conifers.

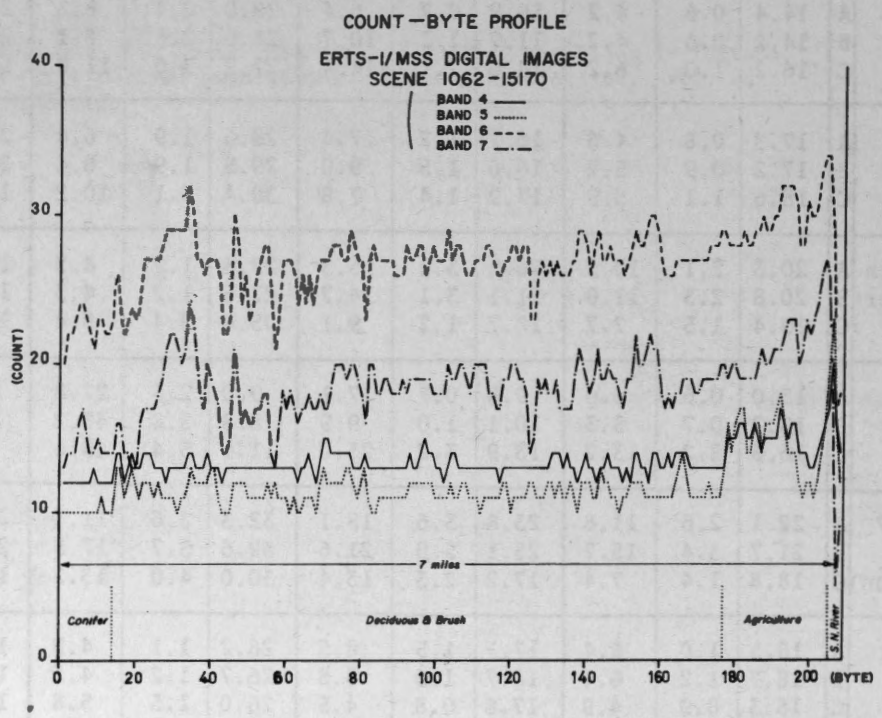

Figure 2. The radiance profiles derived from CCT.

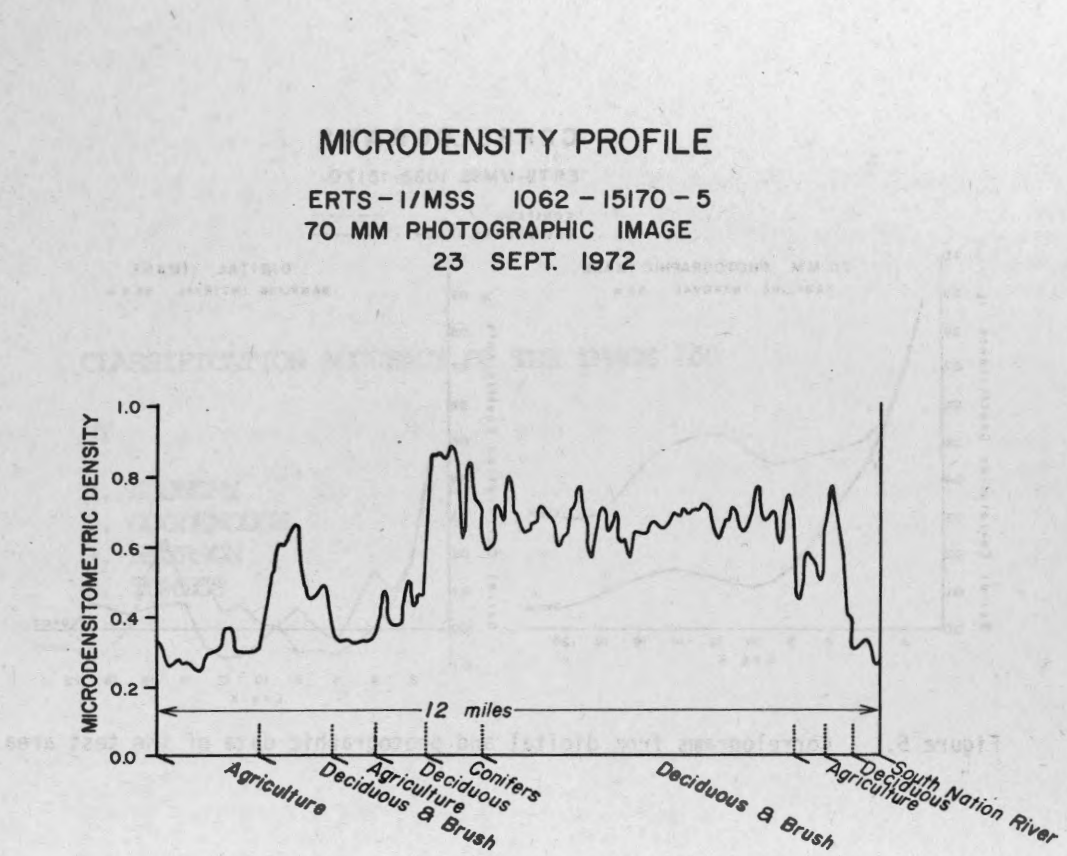

Figure 3. The microdensity profile derived from 70 mm film image.

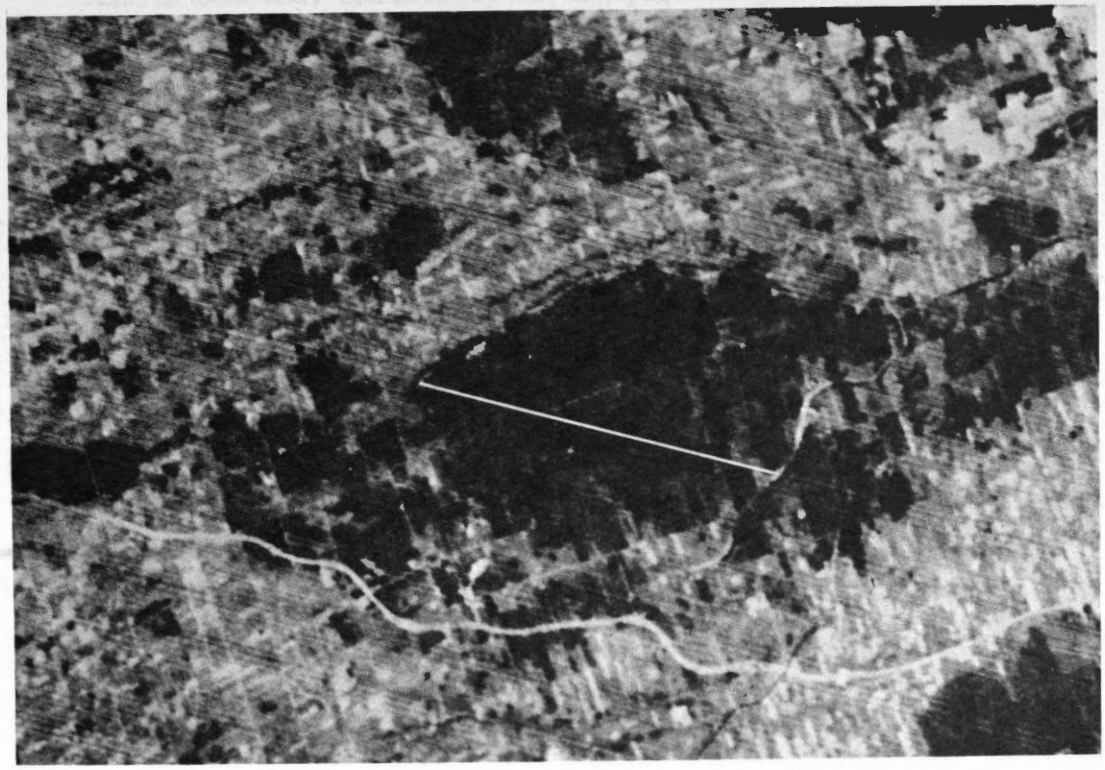

Figure 4. Portion of ERTS image covering the test area.

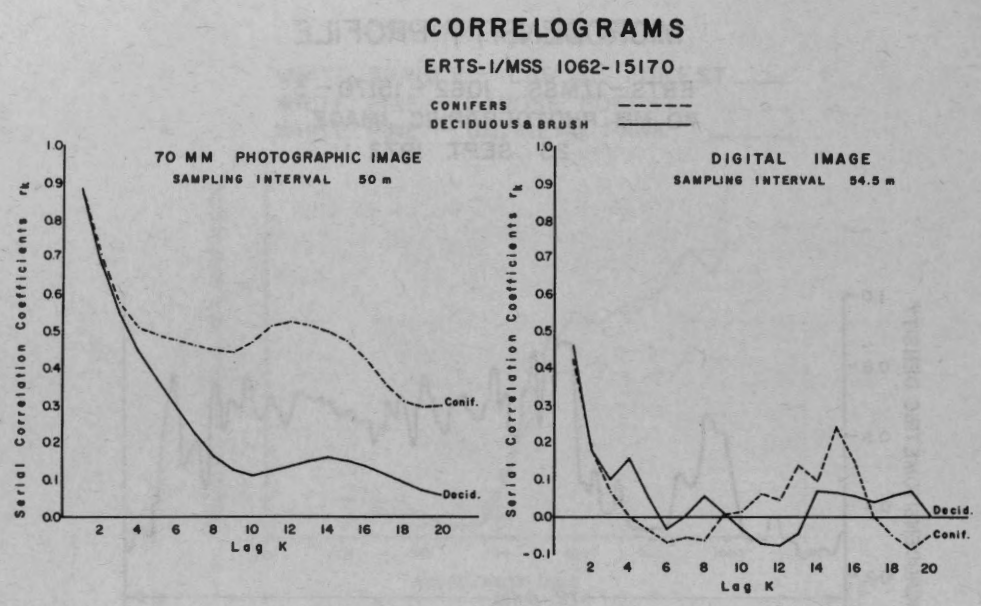

Figure 5. Correlograms from digital and photographic data of the test area.

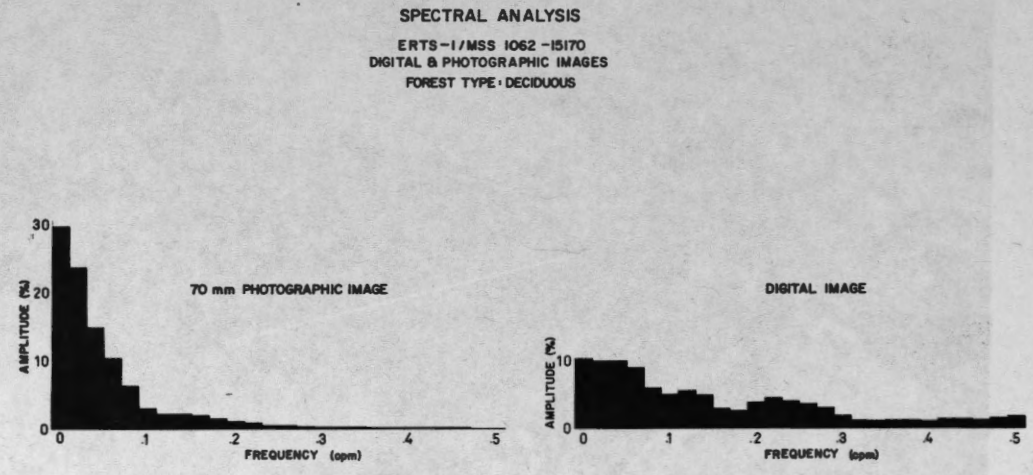

Figure 6. Examples of power spectra calculated from ERTS data.

CLASSIFICATION ACCURACY OF THE IMAGE 100

By

R. ECONOMY
D. GOODENOUGH
R. RYERSON
R. TOWLES

This paper presented at the Second Canadian Symposium on Remote Sensing, University of Guelph, Guelph, Ontario, April 29 - May 1, 1974.

CLASSIFICATION ACCURACY OF THE IMAGE 100

R. Economy*, D. Goodenough**,
R. Ryerson**, R. Towles*.

*Space Division,
General Electric Company,
Daytona Beach, Florida, U.S.A.

**Applications Division,
Canada Centre for Remote Sensing,
Ottawa, Ontario.

ABSTRACT

Recent developments in classification methodology have led to the production of a hardware classification system by General Electric called the IMAGE 100. This device is an interactive multispectral analyzer which enables the user to quickly classify from digital ERTS-1 data. Preliminary classification results of an agricultural scene indicated that crop classification accuracies of 80% and higher could be obtained. To test the classification accuracy of the IMAGE 100 further, we chose two ERTS-1 frames containing a range of typically Canadian cover types. In particular, we concentrated on urban, agricultural, and forested areas where detailed ground truth and underflights were available. Examples of the classification procedures and results obtained are presented.

INTRODUCTION

Methods in classification methodology fall into two main categories, unsupervised and supervised classification. In unsupervised classification, a computer program scans digital image data to find well-separated spectral clusters. These clusters may not correspond to the land-uses of importance to society. This fact and the difficulty of human interaction with most clustering programs led to increased utilization of supervised classification methods.

Supervised classification programs are fed statistical parameters of land-use classes selected by the investigator. The programs then use the parameters to determine such quantities as the areal distributions of the selected land-use classes in a particular scene. Based on the results of these supervised classifications the investigator modifies the statistical parameters to produce the most accurate classifications. The selection of the classes and the modification of their statistical distributions necessitates the development of interactive and rapid multispectral image analysis systems.

Research by Dr. D. Goodenough at the Canada Centre for Remote Sensing (CCRS) on methods for speedy analysis of the data from the Earth Resources Technology Satellite (ERTS-1) showed the need for a hardware classifier to provide interactive, thematic, information extraction from ERTS data. Convergent research by Dr. R. Economy of the Space Division, General Electric Corporation, had led to the development of a hardware classifier embodying some of the necessary properties. Further research and development by General Electric (GE) under contract to CCRS has resulted in delivery to CCRS of the first GE hardware classifier, called the Image 100.

The Image 100 system, shown in Figure 1, is an interactive, supervised classification system. The CCRS Image 100 has digital ERTS tape input to a solid state memory unit. The output from the Image 100 may take the form of direct photographs, printer maps, or digital tapes for image production on a CCRS electron beam image recorder. The procedure one would normally execute in classifying an ERTS scene is as follows. One begins by inputting from a digital tape that portion of the scene, magnified or reduced, that the operator wishes to investigate. After the four or five video channels have been read into the storage device, one selects a preprocessing function for further analysis. The available preprocessing functions include: raw

data mode, ratioing, normalization, and the difference between two channels divided by their sum. The investigator, using a movable cursor, then proceeds to select, based on detailed ground truth information, a training area representative of the particular land-use being studied. Extraction of the four-dimensional spectral distribution and classification of the total scene (256,000 pixels) occurs in less than 4 seconds. By comparison with ground truth information, the operator may now evaluate the classification results.

In terms of four-dimensional feature space the initial acquisition of the spectral signature results in the creation of a four-dimensional, rectangular parallelepiped, the sides of which correspond to the signature limits of the training area in each channel, taken one channel-at-a-time. This initial signature acquisition is called "one-dimensional signature acquisition" of the Image 100. Examination of the classified scene may lead the operator to modify the parallelepiped limits interactively to produce a rectangular parallelepiped which give a more accurate classification. Further improvements in classification accuracy may be achieved by modifying the four-dimensional spectral cluster by means of the "n-dimensional signature acquisition mode". In this mode the actual spectral distribution of the training area is represented by the distribution of four-dimensional cells of unit volume. Each cell contains the number of picture elements (pixels) with intensities corresponding to the coordinates of the cell. These cell counts are thus measures of the probability distribution for the cluster. By raising or lowering the threshold on the cell counts, one can vary the size and four-dimensional probability distribution of the spectral cluster by deleting or adding cells with counts greater than a variable threshold. The effects of this n-dimensional signature manipulation on the classification are quickly displayed, so that the operator may optimize his procedure in terms of classification accuracy. For this paper we utilize the one-dimensional and n-dimensional signature acquisition modes with the raw data mode preprocessing function.

The versatility of the Image 100 enables one to not only perform supervised classification, but also allows one to incorporate clustering or unsupervised methods, the maximum likelihood decision rule, and any desired feature space rotation (e.g. the Hadamard transformation) for feature reduction. The acquisition by CCRS of the Image 100 will allow Canadian research to move ahead very rapidly in pattern recognition as applied to satellite imagery.

ACCURACY OF CLASSIFICATION

Before examining the results of our classifications, we shall discuss our methods of measuring classification accuracy. A common procedure in classification is to select for class training one or two fields for example, in a fifty field test site. The percentage of pixels correctly identified in the training fields yields a reasonable estimate of classification accuracy if the classification method incorporates the maximum likelihood decision rule or other statistical discriminant functions. For this analysis the maximum likelihood decision was not applied. It was, therefore, necessary for us to examine the number of fields or pixels correctly identified for each class in a number of different test sites.

Within each test site the Image 100 classification of each field was checked against the available ground truth. All results were tabulated in the form of confusion matrices in which, for each theme, the percentage of the test sites or fields identified were tabulated as functions of all classes. For the Los Angeles area we also compared misclassifications for one theme against the land-use map areas for the other classed in order to estimate the effect of these errors for land-use planning. The classification accuracy of the Image 100 is dependent not only on the methodology of spectral signature recognition, but also on the quality and veracity of the ground truth information used by the investigator. For one of the frames, Thunder Bay, Ontario, we relied on high and low altitude aircraft imagery combined with the most recently published land-use maps. For the southwestern Manitoba scene, we used the published ground truth results of Woo

(1973), which in turn were based on high altitude aircraft imagery combined with winter examinations of selected fields.

Let us now examine the results of classifications for an agricultural region, a mixed vegetation-urban area, and a major urban centre. For the two Canadian scenes all ERTS data were in raw form. Radiometrically corrected data were used for analysis of the Los Angeles region.

CLASSIFICATION RESULTS

A. Agricultural Area (Sperling, Manitoba)

The ERTS digital data (E-1007-16531) showing southwestern Manitoba was recorded at the Prince Albert Satellite Station on July 30, 1973. Approximately one hundred fields in test areas twenty miles apart and in disparate soil types were selected for the evaluation of the Image 100's classification accuracy for five classes in an agricultural area. In Figure 2 we present the visual results of the classification as displayed on the CCRS Image 100 for rapeseed fields. The figure shows an area of approximately 900 km^2, with a four times magnified window at the bottom of the picture giving detailed examples of the classifications. Accuracies were determined by counting the number of fields correctly identified. A field was said to be correctly identified if more than 75% of the pixels were alarmed. The data listed in Table Ia give average classification accuracy of 80 ± 12 (s.e.)%. The "grain" class included a diverse population of fields. After this classification the ground truth was re-examined. A number of discrepancies between the appearance of some grain fields on airborne imagery and their ground truth classification indicated that errors in ground truth data were contributing to the less accurate classification of the "grain" fields.

B. Thunder Bay, Ontario

Our second experiment was carried out in a region centred on Thunder Bay, Ontario, having a very diverse land-use pattern. Low and high altitude airborne imagery were combined with published land-use maps to produce a very detailed ground-truth map which was accurate for the time of the satellite pass. The ERTS-1 frame (E-1037-16192) used for this classification study was imaged on August 29, 1972. The classes separated on the CCRS Image 100 were: (1) B-Urban-Quarry; (2) H-hardwoods and mixed forests; (3) S-softwood forests; (4) O-agriculture and open space; (5) W-all water; (6) D-clear and deep water; (7) P-sedimented water; (8) R-river and shallow water.

Classification accuracy was based on 69 test sites randomly distributed over the Thunder Bay image. These 69 test sites comprised a total area of 1,500 acres. For each test site and theme, a comparison was made between the pixels identified as belonging to a theme and the pixels actually belonging to that theme as indicated by our ground-truth data.

Figure 3 is a photograph of the "urban-quarry" classification (blue) for an area of 1200 km^2 centred on Thunder Bay. The window insert in the lower right shows the urban theme in and around a heavily industrialized region. One hundred per cent classification accuracy was achieved for this theme. Accuracies of 71% and 100% for "hardwood-mixed" forests and "softwood" forests, respectively, resulted from the classification shown in Figure 4. The "agriculture and open space" theme shown in Figure 5 was 81% accurate with 19% misclassification with the "urban-quarry" theme.

The confusion matrix for the Thunder Bay classification is listed in Table 2. The confusion between the "river-R" theme and the themes "hardwood-H" and "softwoods-S" occurred because of the presence of trees on the Dog River's bank being incorporated into some of the 4-pixel regions used to train the Image 100. Installation of single-pixel training area selectability on the CCRS Image 100 will soon allow the precise addition or deletion of individual pixels from a training area. Confusion between the water classes, "D" and "P", is a result of banding in the raw ERTS data and can be eliminated by the use of radiometrically corrected ERTS tapes. (Shlien and Goodenough, 1974)

Incorporation of the maximum likelihood decision rule will help to reduce, but will not eliminate, the confusion between the themes "hardwoods and mixed hardwoods-softwoods" and "softwoods" (Goodenough and Shlien, 1974). The overall classification accuracy for five themes (B, H, S, O, W- Table II) was 88±12(s.e.)%.

C. Los Angeles, California

Our final experiment was to determine land-use mapping accuracy in a complex urban area in Los Angeles, California. The ERTS frame (E-1144-18015) used was imaged on December 14, 1972, and supplied to us by the National Aeronautics and Space Administration of the United States. Ground-truth information was based on a 1969 Los Angeles land-use map. High altitude airborne imagery, Economy and Willoughby (1973), was used for training and initial evaluations. All classifications were performed on the laboratory model of the Image 100 located at General Electric's Space Division in Daytona Beach, Florida. The laboratory Image 100 and the CCRS Image 100 were used in an identical fashion for classification accuracy determination.

The Los Angeles area is shown in Figure 6. The white border represents the boundary of the Los Angeles County. Seven categories of urban land use were investigated: (1) single-family (high density) residential; (2) heavy industrial areas; (3) heavy commercial regions; (4) parks and open spaces; (5) public land use; (6) services; (7) recreation. The "high density residential" theme is shown in Figure 7.

During the classifications with the Image 100, it appeared that we were achieving considerable accuracy based on comparison with high altitude airborne imagery. We, therefore, decided to follow the procedure that most land-use planners use when evaluating remote-sensing land use classifications; namely, to compare the Image 100 classification with the latest available land-use map drawn up by urban planners. The most recent available urban land use map of Los Angeles was published in 1969. The class coding on this map followed the United States Standard Land-Use Classification System. We note that Anderson, Hardy, and Roach (1972) have pointed out that remote sensing cannot provide accurate urban classification of classes distinguishable solely on the basis of their human uses, such as the recreation class. A second factor which tends to reduce classification accuracy is the limited ground resolution (90 meters) of the ERTS-1 multispectral scanner. Thirdly, errors in ground-truth data limit the attainable classification accuracy by remote sensing. For the Los Angeles scene a comparison of aircraft imagery, obtained at the same time as the satellite overflight in October 1973, with the 1969 land-use map revealed significant changes in the land-use in Los Angeles.

We examined every pixel in a 1241 acre test site and compared the Image 100 classification with the 1969 land-use map. In the first column of TABLE 3 are listed the acreages of each class as derived from the 1969 land-use maps. The percentages of the total test site area (1241 acres) are given in brackets. The second column lists the acreages (in brackets) obtained for each class for the single-family residential Image 100 theme (SFR alarm). The total Image 100 SFR theme area was 810 acres. The percentages in the second column are the percentages of the SFR alarm area. For example, 645 acres or 79.6% of the 810 acres of the SFR alarm, actually belong to the single-family residential class. These 645 acres represent 70% of the single-family residential class area in the test site, as we have tabulated in the third column of Table 3. We are thus separating out omissions in SFR classification for analysis. In our two earlier experiments classification omissions were grouped under the identifier 'no-class' in Table 1a and 2. In the Los Angeles area the Image 100 missed 30% of the SFR class present in the test site.

The remaining items in the third column of Table 3 indicate the effect of a misclassification of the SFR theme as commercial class, for example. The 1.6% error is confusing the SFR class with commercial corresponds to an error in acreage of 13 acres. However, there are only 30.1 acres of commercial land in the test area, so that this misclassification represents an error of 42% from a planner's point of view. Incorporation of the maximum likelihood

decision rule or other statistical decision function would result in increased classification accuracy, but we are fundamentally limited by the spatial resolution of the data (Puckett, 1972).

We, therefore, conclude that given the three limiting factors here of satellite resolution, classification system, and ground-truth data, the 70±12(s.e.)% classification accuracy achieved in the Los Angeles area is as good a value as can be obtained from ERTS-1 scanner data.

CONCLUSIONS

1. An average classification accuracy of 80±12(s.e.)% was achieved for an agricultural area in south-western Manitoba.

2. For an area of diverse land-use centred on Thunder Bay, Ontario, an average accuracy of 88±12(s.e.)% for five themes was achieved.

3. A detailed urban classification of a Los Angeles test site yielded an accuracy of 70±12(s.e.)%. Factors which limited classification accuracy were spatial resolution of the ERTS-1 scanner, the land-use classification system, and inaccuracies in the ground truth.

REFERENCES

Anderson, J. R. Hardy, E. E. and Roach, J. T., 1972, "A Land-Use Classification System for Use with Remote Sensor Data", U. S. Geological Survey Circular 671.

Economy, R. and Willoughby, J. 1973, private communication.

Goodenough, D. and S. Shlien, 1974, "Results of Cover-Type Classification by Maximum Likelihood and Parallelepiped Methods", Second Canadian Symposium on Remote Sensing, Guelph, Ontario.

Puckett, A. E. 1972, "Comments on the Earth Resources Sensing and Data Acquisition Program", Remote Sensing of Earth Resources, p.25, U. S. Gov't Printing Office.

Shlien, S. and Goodenough, D., 1974, "Quantitative Methods for Determining the Information Content of ERTS Imagery for Terrain Classification", Second Canadian Symposium on Remote Sensing, Guelph, Ontario.

Woo, V. 1973, "Red River Crop Study", Technical Report, Manitoba Remote Sensing Office.

TABLE I

WINNIPEG, MANITOBA

(E-1007-16531)

Ia CONFUSION MATRIX

Chosen Class / True Class	Fallow	Wheat	Grain	Pasture Hay	Rapeseed
Fallow	100	0	0	0	0
Wheat	0	83	8	0	0
Grain	0	17	67	11	0
Pasture/Hay	0	0	0	78	0
Rapeseed	0	0	4	0	86
Other or Not Identified	0	0	21	11	14

Ib FIELD DATA

Class	Total Number of Fields*	Number Used for Training
Fallow	23	2
Wheat	14	3
Grain	44	5
Pasture/Hay	9	2
Rapeseed	7	2

* Sample drawn from two areas 20 miles apart and in disparate soil types.

TABLE 2

THUNDER BAY, ONTARIO

(E-1037-16192)

CONFUSION MATRIX

Chosen Class / True Class	B	H	S	O	W	D	P	R
B	100	0	0	19	0	0	0	0
H	0	71	0	0	6	0	0	20
S	0	29	100	0	6	0	0	20
O	0	0	0	81	0	0	0	0
W	0	0	0	0	88	0	0	0
D	0	0	0	0	0	75	25	0
P	0	0	0	0	0	25	75	0
R	0	0	0	0	0	0	0	60
No Class	0	0	0	0	0	0	0	0

LEGEND: (1) B - Urban - Quarry; (2) H - Hardwoods and Mixed;

(3) S - Softwoods; (4) O - Agriculture and Open Space;

(5) W - All water; (6) D - Clear and Deep Water;

(7) P - Sedimented Water; (8) R - River and Shallow Water.

Sixty-nine cells, comprising an area of 1500 acres, and randomly distributed, were used to evaluate classification accuracy. Overall classification accuracy (five classes) was 90%.

TABLE 3

SINGLE-FAMILY RESIDENTIAL CLASSIFICATION

(SFR ALARM)

	Land Use Class Area Acres	Area and % of SFR Alarm By Class	Area Alarmed As % of Land-Use Class Area
Single-Family Residential	907.9 (73.2%	79.6%(645)	70.4%
Multi-Family Residential	1.8 (0.1%)	0%(0)	0%
Commercial	30.1 (2.4%)	1.6%(13)	42.4%
Public	190.7 (15.4%)	12.3%(100)	51.7%
Services	49.3 (4.0%)	5.0%(40)	81.5%
Recreation	54.7 (4.4%)	1.1%(8.9)	16.7%
Open Space	6.4 (0.5%)	0.3%(2.4)	42.9%
TOTAL AREA	1241.0	100% (810)	

SFR THEME AREA = 810 ACRES = 65.3% of 1241 ACRES.

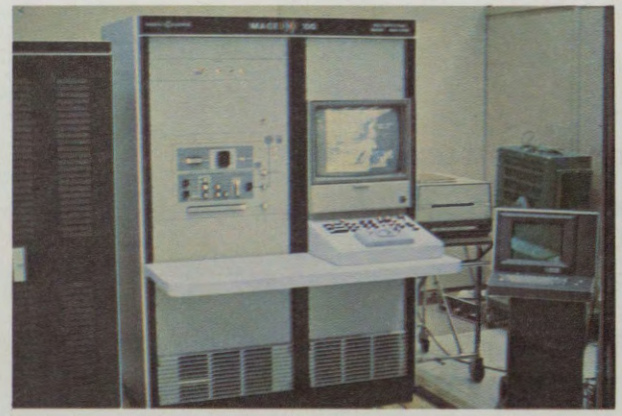

Figure 1

This photograph shows the Image 100 developed by the Canadian General Electric Company under contract to the Canada Centre for Remote Sensing. From left to right the units are: Intel solid-state memory with over ten million bits storage in five channels; high speed digital processing logic unit; colour CRT display with cursor controls; Tektronix display for user interaction with probability density histograms and software generated commands. The process controller, a Digital Equipment Corporation PDP-11/40, is not shown here.

Figure 2

Classification results for the class "Rapeseed-Mustard" are shown in yellow superimposed on the background image of a 900 km^2 area located near Sperling, Manitoba. The black line across the scene is a result of noise occurring during the ERTS-1 transmission of this frame, E-1007-16531, to the Prince Albert Satellite Station. The window inserted in the lower, right-hand corner of the scene shows a four times magnified view of some of the classified fields. An accuracy of 86% was achieved in the classification of this crop.

Figure 3

An area of 1200 km^2 centred on Thunder Bay, Ontario is shown here. The blue theme represents the class "Urban - Quarry", shown in more detail in the magnified window of an industrialized region near the Dog River.

Figure 4

Classification results for two classes, "Softwoods" (green) and "Hardwoods - Mixed" (pink), are presented for the same Thunder Bay area shown in Figure 3. Window inserts, marked "1" and "2" in the picture, enable one to examine in detail the thematic distributions produced by the Image 100. Classification accuracies were measured to be 100% for "softwood" forests and 71% for "hardwood - mixed" forests.

Figure 5

The "agriculture - open space" theme for the Thunder Bay, Ontario region is shown in purple against the background image, E-1037-16192. A classification accuracy of 81% was estimated based on 69 randomly distributed test sites.

Figure 6

The Los Angeles County is delineated by a white line in this photograph of ERTS-1 frame E-1144-18015. The full frame covers an area of 185 km by 185 km. Land-use classification was carried out for seven urban categories, one of which is shown in Figure 7.

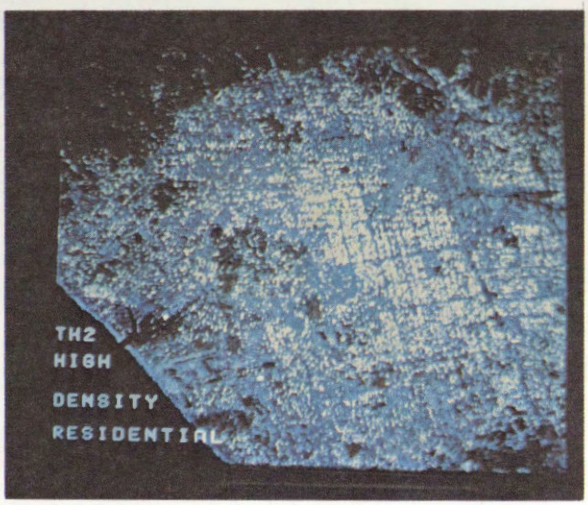

Figure 7

The "single-family" or "high density residential" theme is shown in white superimposed onto a northern portion (blue) of the city of Los Angeles. A 1241 acre test site was examined pixel-by-pixel in order to evaluate the thematic accuracy achieved. Over 70% of the single-family residential class was correctly identified.

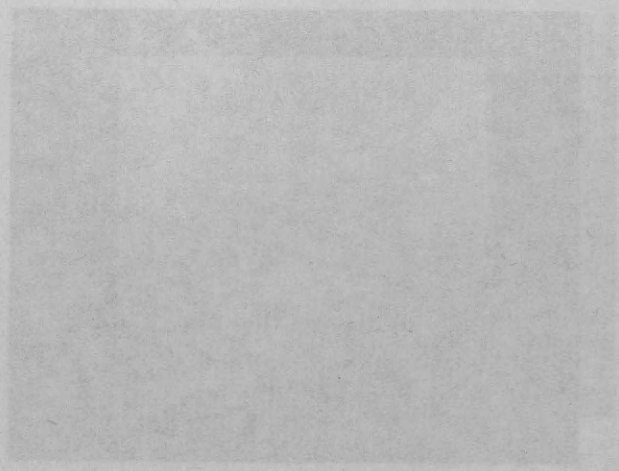

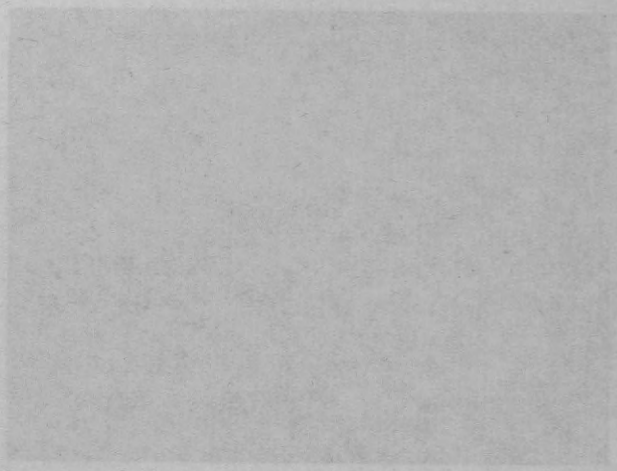

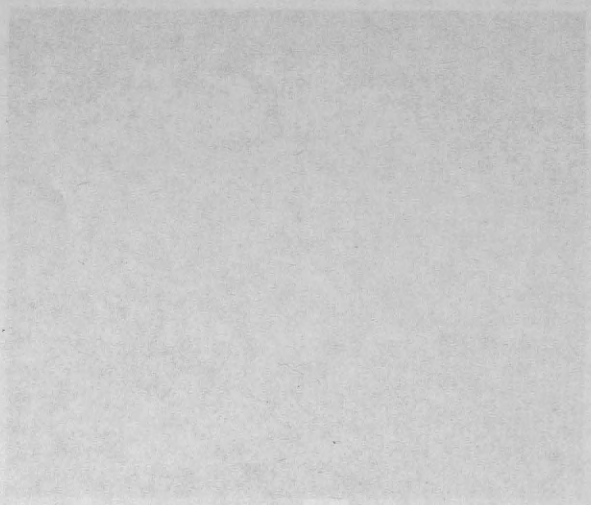

USING DIAZO COLOUR COMPOSITES TO EXTRACT INFORMATION FROM ERTS - 1 MULTISPECTRAL DATA

By

P. WARRINGTON
R. RYERSON

This paper presented at the Second Canadian Symposium on Remote Sensing, University of Guelph, Guelph, Ontario, April 29 - May 1, 1974.

USING DIAZO COLOUR COMPOSITES TO EXTRACT INFORMATION FROM ERTS - 1 MULTISPECTRAL DATA

P. Warrington
B. C. Remote Sensing Centre
Department of Lands, Forests and Water Resources
Province of British Columbia
Victoria, British Columbia

R. Ryerson
Applications Division
Canada Centre for Remote Sensing
Department of Energy, Mines and Resources
Ottawa, Ontario

ABSTRACT

The Diazo process is discussed briefly and various levels of equipment sophistication are described.

Researchers have used Diazo to create colour composites of multiband ERTS-1 imagery. A number of colours may be assigned to both positives and negatives in various combinations so as to highlight features of interest. The limitations and advantages of the Diazo procedure are outlined. A brief indication of the ways in which this process can be employed is included.

RESUME

L'auteur décrit brièvement le procédé Diazo et fait état des divers niveaux de complexité de l'équipement.

Les chercheurs ont utilisé le procédé Diazo pour créer des composés de couleurs à l'aide des images des bandes multispectrales de l'ERTS-1. Il est possible de donner diverses couleurs et combinaisons de couleurs aux positifs ainsi qu'aux négatifs de façon à faire ressortir certaines caractéristiques. L'auteur décrit les advantages et les limites du procédé Diazo et il indique brièvement les diverses façons dont il peut etre utilise.

INTRODUCTION

There is a great deal of information available on the computer compatible tapes from ERTS-1. A major concern of those using this data is how to present or display the material so that the particular information required can be most readily extracted. There are essentially two display methods, digital and photographic; only photographic methods are dealt with in this paper.

Since man can distinguish only about 200 shades of gray on a continuous scale but can recognize approximately 350,000 continuous[1] colour variations, colour displays would seem likely to be the most useful for interpretation, and coloured photographs the most useful for "storing" information. The normal method of colour representation of multispectral imagery is to assign a different colour to each spectral band. The resulting colours on the composite relate to similarities and differences between the spectral bands used. In addition to colour variations, one may also use spatial relationships of the coloured features as an interpretation aid.

Two standard colour photographic composites (of a possible twenty-four using three colours and three out of four bands) are produced by the National Air Photo Library.

These composites are but one of a number of methods that may be used to provide composite colour displays for interpretation. Alternatives are colour additive viewers and diazo overlay sandwiches. The latter is discussed here.

THE DIAZO PROCESS

Diazo is an additive process as compared to the subtractive photographic process where negatives are used to produce positives. The film is coated with a diazo compound which decomposes when exposed to ultraviolet light. Hence the process must be carried out away from windows (sun), or other sources of light which give off U.V.

radiation. Standard incandescent bulbs can be used without exposing the ultraviolet sensitive layer. The rate of decomposition of the diazo emulsion is controlled in part by the transparency being copied, which is in contact with the diazo film and which is situated between the diazo film and the light source. For best resolution the emulsion side of the transparency should be in contact with the emulsion side of the diazo film. Where the transparency is darker the light will act more slowly in decomposing the diazo compound. The exposure process is stabilized by ammonia vapour. An exposed diazo could be kept unfixed for some time without harm, providing it is not again exposed to ultraviolet light. Fixing time (beyond a certain minimum) does not appear to be an important factor with respect to output quality on the less expensive systems.

Diazo film is commercially available at many office supply outlets at a per sheet cost of about forty cents. Each 9"x9" composite would cost $1.20 for diazo film exclusive of capital costs, salaries, mounts, tape, and original imagery. All 24 composites can be made for $4.80; however, since each colour separate is used for several composites, usually only three colours (either red-blue-green or cyan-magenta-yellow) are used. Given both positives and negatives a very large number of three-band composites can be made. Some guidelines on composite design are presented below.

EQUIPMENT

The level of sophistication and hence the cost of equipment varies greatly. At one extreme sunlight could be used for exposure and, for development, ammonia on a sponge in a closed container. Total cost for a composite would be under $2.00. At the other extreme one could use a machine with fine exposure time controls and constant illumination; the capital cost could then exceed $5,000.

The ideal, of course, would be somewhere between. Adequate "off the shelf" systems can be purchased for between $400 and $2,000. "Home made" ultraviolet light sources and simplistic development procedures can be used with very little loss of information but with substantial losses in reproducability.

DESIGNING COLOUR COMPOSITES[2]

It has been noted that both positive and negative transparencies of different bands are suggested for use in making diazo colour composites. The reasons for increased usefulness of positive - negative composites have not previously been stated except for the fact that a wider range of colours is available and one may manipulate figure-ground[3] relations. The reasons for the success of such composites are quite simple and may assist the user in designing task specific composites from the hundreds which are available.

Figure 1

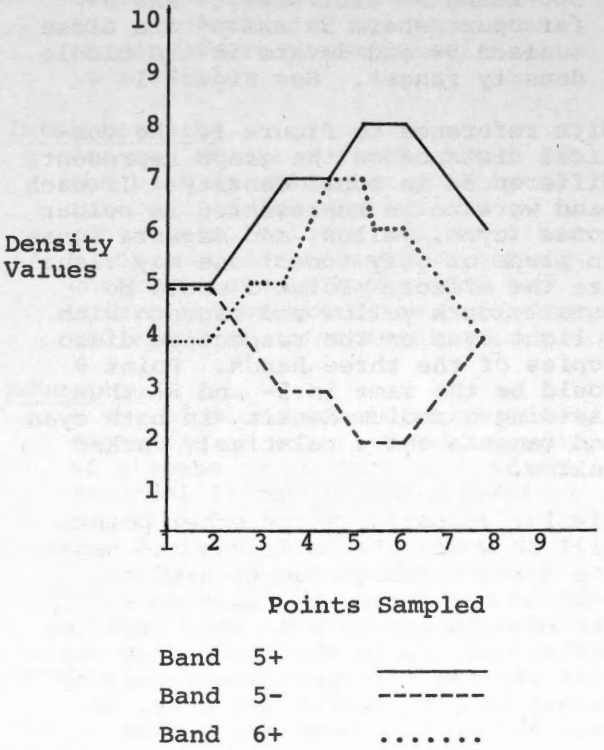

From Ryerson and Warrington

Consider Figure 1 which represents hypothetical density traces across both the positive and negative of band 5 and corresponding points on band 6. Bands 5 and 6 are generally held to be correlated, i.e. increase in density in band 5 is usually accompanied by a related increase in band 6.

The differences are a function of differences in reflected radiation recorded by each band.

The value of positive/negative combinations for correlated bands may be directly attributable to the following:

The use of band 5+ in one colour (say yellow) and 6+ in another colour (say magenta) will emphasize differences between them, (areas of overlap will appear in shades of purple and differences in the respective original colours). See Figure 1.

The use of band 5- in one colour (say cyan) and 6+ in another will emphasize similarities between the two bands. Since 5- mirrors density values on 5+, using 5- will show 6+ and 5- far apart where 5+ and 6+ are close (unless 5+ and 6+ are in the middle density range). See Figure 1.

With reference to Figure 1, the vertical distance on the graph represents differences in tonal density. If each band were to be represented in colour tones (cyan, yellow, and magenta tones in place of gray tones) one may visualize the effect. Point 5 would be equally dark yellow and magenta with a light cyan on the respective diazo copies of the three bands. Point 9 would be the same in 5- and 6+ thus yielding a medium density in both cyan and magenta and a relatively darker yellow.

Similar comparisons for other points will show how the positives and negative taken together can be used not only to emphasize similarities and differences but also to show relative variations. With this knowledge the user may use the approximate density values (light, medium and dark, for example) on each band for ground truthed areas to decide which combination provides maximum discrimination for the features of interest.

When the band selection has been carried out, the second task is to assign colours to various bands to achieve the best figure ground relationships. The following is an example of how this should be done.

To commence the separation of some phenomenon, consider the following: the objective of the researcher is to separate built-up urban areas, cropland, water, and two forest types at a scale of 1:1,000,000. One knows that on a band 7+ water appears dark and urban core usually shows as a dark smudge. Gravel quarries appear light on bands 4+ and 5+. Cropland will be lighter in band 6+, growing darker as the year progresses.
Pasture and hay land will probably become lighter in bands 4+ and 5+ as the season advances. Road pattern and tone allow easy separation of pasture-hay from forested areas. In all cases where light in 4+ appears, one could reverse this to 'dark in 4-' by using negatives. By remembering that lighter areas of the transparency receive little colour and dark areas receive the most colour in the diazo process, one can begin to visualize which colours to combine to achieve certain effects.

Both water and urban areas are of prime concern in the example and should be the dark 'figures.' Forested areas are spatially dominant in the scene used and should form the lighter background. To achieve this figure-ground situation one requires a negative of band 4 to produce dark urban areas and a positive of band seven to bring out the water as dark. Producing a dark colour requires cyan or magenta. Rivers could be brought out from band 7+ by using magenta, leaving cyan for urban areas on band 4-. To give a light background of yellow, 4+ could be used as yellow. The resulting composite is quite attractive.

Using a basic knowledge of colour and tonal signatures, even without a density trace, it is a relatively simple matter to predetermine the end results in the manner presented above.

LIMITATIONS OF THE DIAZO PROCESS

Many of these limitations are not specific to diazo but also apply to other forms of data displays, such as the standard ERTS-1 colour composites.

The resolution limits and amount of detail that can be seen is less than that available on the computer compatible tapes.

The separate spectral bands used must be perfectly registered with one another.

Spectral boundaries do not always coincide with the boundaries of the user's interest.

Diazo does not produce a true white light composite and some information may therefore be lost.

Reproducibility is difficult without expensive and sophisticated equipment. One must have access to, or construct, the necessary equipment.

Transparencies for the area of interest must be obtained. Contrast and tonal range may vary from orbit to orbit for these transparencies.

Each composite used must be constructed by hand.

Where more than one person is doing interpretation, apparent separation of hues on the composites will vary for each interpreter and either careful control must be used (e.g. a "hue" chart for spectral signatures of different features), or one must clearly separate each interpreter's duties and have someone in overall control. Of course, only two of many suitable approaches to this problem have been suggested here.

ADVANTAGES OF THE DIAZO PROCESS

Cost

A set of 12 colour transparency separates costs about $5.00 for diazo materials. This set makes 24 different 3 colour/3 band colour composites in transparency form.

Flexibility

A colour composite transparency made by the diazo process is not a permanent set but can be taken apart and the separates recombined into other composites as dictated by different interpretation needs. If for any reason one wishes to work with a particular colour combination, it is possible to do so. People with various forms of colour blindness can make colour composites which have maximum contrast between object and background to suit the peculiar spectral response discrimination of their eyes.

Variability

One can readily make all 3 colour/3 band positive-negative composites possible, whereas NAPL can produce only three different composites.

Variety

Many types of non-standard colour composites may be made. Composites can be made from positive or negative transparencies or various combinations of the two. Exposure times for each colour may be varied independently to yield a large array of colours.

Universality

The technique is not restricted to ERTS-1 images but may be used for coincident, multispectral imagery where perfect registration is possible.

Interpretation

One may select a given colour for the band in which the objects of interest are to appear, and contrasting colours for the other bands in order to achieve maximum contrast between background and object for greater ease, accuracy, and speed of interpretation.

Education

A set of diazo colour transparency separates of multispectral imagery of a scene is an excellent teaching tool to convey the concept of colour film formation, false-colour film, colour additive concepts, and data acquisition and display from non-visual portions of the electromagnetic spectrum.

APPLICATIONS

The usefulness of diazo for land use mapping has been demonstrated in the United States by Dr. E. Hardy (1973).

The flexibility of diazo is best illustrated in areas where various types of land use with differing spectral responses occur. Tailor-made composites can be made and where one composite is unable to resolve all the use types simultaneously then several composites in succession can

be used.

The process is also useful in theme extraction mapping where snow cover, cloud cover, water bodies, forest land, crop land, or urban areas can be separated from the rest of the available information on the image.

A third use is in presenting results of Agfacontour density slicing. The features separated by each successive slice may be assigned a colour. In this way, a colour image may be built up from the collection of density slices.

The list presented above is not intended to be exhaustive. Other uses have been identified; however, these are essentially variations of the more general uses noted.

SUMMARY

If one has some knowledge of reflectivity of objects in the various ERTS-1 multispectral scanner (MSS) bands and wishes to extract some of this data, diazo may be of great potential use. Unique colour composites may be produced quickly and easily for both display and production purposes using diazo.

Although there are a number of advantages to be gained by using diazo, there are also a number of complications. At first certain tested procedures should be methodically followed until one gains experience and learns what kind of output results from each input.

With sufficient care, practice, and realistic goals and expectations, diazo colour composites will probably prove useful in many areas of study in Canada.

FOOTNOTES

1. The number of Just Noticeable Differences stated assumes that one is working with a continuous scale of colour or gray. In this sense one could see 200 JND's along a gray scale, although only a fraction of this number could be identified as distinct tones when mixed together in a photographic image. (See Hochberg, 22.)

2. Much of this section is drawn from Ryerson and Warrington.

3. Figure-ground is a term drawn from psychology. One may regard the concept, in lay terms, as a perceptual description of foreground - background.

BIBLIOGRAPHY

Alfoldi, T. T., and Ryerson, R. A., 1974. ERTS Imagery Interpretation Package: Suggestions for Laboratory Design. C.C.R.S., Tech. Note Series (in preparation) Ottawa, Ontario, Canada.

Hardy, E. E., 1973. ERTS Evaluation for Land Use Inventory, N.A.S.A., Department of Natural Resources, Cornell University, Ithaca, New York.

Hochberg, J. E., Perception, Prentice Hall Inc., Englewood Cliffs, New Jersey, 1964.

Ryerson, R. A., 1974. Diazo Composites: An Inexpensive Tool for ERTS Imagery Analysis. C.C.R.S., Tech. Note Series (in preparation) Ottawa, Canada

Ryerson, R. A., and Warrington, P. D., 1974. Making Colour Composites of ERTS-1 Imagery by the Diazo Process. C. C. R. S., Tech. Note Series (in preparation, Ottawa, Canada

Warrington, P., 1973. Preparing 'False Colour Composites of ERTS-1 Imagery with Diazo Colour Transparencies. IN: B. C. ERTS Users Handbook, B. C. Remote Sensing Centre, Victoria, British columbia

Warrington, P. D., 1973. Colour Composition of ERTS-1 Images. Report to Marine Sciences Directorate, Department of the Environment, Victoria, British Columbia

Warrington, P.D., 1974. The Diazo Process as a means of extracting information from ERTS-1 Multispectral Data. B.C. ERTS Users Handbook, Second Edition, B. C. Remote Sensing Centre, Victoria, British Columbia, (In Press)

PRINCIPAL COMPONENTS COLOUR DISPLAY OF ERTS IMAGERY

By

M.M. TAYLOR

This paper presented at the Second Canadian Symposium on Remote Sensing, University of Guelph, Guelph, Ontario, April 29 - May 1, 1974.

PRINCIPAL COMPONENTS COLOUR DISPLAY OF ERTS IMAGERY

M.M. Taylor, Defence and Civil Institute of Environmental Medicine*,
1133 Sheppard Avenue West, P.O. Box 2000,
Downsview, Ontario. M3M 3B9

Abstract

Combinations of data from the four ERTS bands into colour images are usually made by selecting three bands and displaying each in a different primary colour (red, green, and blue). Because the data from the different bands are correlated, there is a tendency for the derived pictures to occupy only a small portion of the available colour space. In the most common combination, MSS bands 1 and 2, which are highly correlated, are displayed as blue and green respectively, and band 3 as red. This results in a picture which for most regions might as well have been printed in red and blue-green.

In the technique to be presented, colours are not derived from single bands, but rather from independent linear combinations of the bands. Using a simple model of the processing done by the visual system, three informationally independent linear combinations of the four ERTS bands are mapped onto the three visual colour dimensions of "brightness", "redness-greenness" and "blueness-yellowness". The technique permits user-specific transformations which enhance particular features, but this is not usually needed, since a single transformation provides a picture which conveys much of the information implicit in the ERTS data. Examples of experimental vector images with matched individual band images are shown.

Introduction

The four bands of the ERTS multispectral scanner system provide correlated images. The level of a given picture element (pixel) on one band can to some extent be predicted from the level of that same pixel on another band. The object of this note is to describe a technique of colour display which takes advantage of these correlations to present in a single colour picture essentially all the information sensed by the satellite.

The standard general-purpose colour display of ERTS imagery simulates infrared colour film. Three of the four sensor bands are selected and each presented as a different primary colour to provide a full-colour picture. Band 4 (green) is displayed in blue, band 5 (red) in green, and band 6 or 7 (infrared) in red. This ordinarily results in a picture in which vegetation is represented as shades of red and brown, rock as grey, and water as bluish green. Few other colours appear to any great extent. In particular, few ERTS frames contain both a strong blue and a strong green region. The reason for this is that the data from bands 4 and 5 are highly correlated. If they were perfectly correlated, there would be no point in printing them in different colours. A single image in the mixture colour, blue-green, would have the same effect. The small differences that do exist between bands 4 and 5 show up as minor variations from bluer to greener blue-green.

The present paper describes a quite different approach to the colour display of multispectral imagery. It is not restricted to ERTS data or to four-band imagery, but can be extended to airborne multi-band sensor systems. Rather than attempting to combine pictorially the information from the different bands, the information contained in the various bands is extracted in terms of several statistically uncorrelated images. These extracted images are then used as the basis of a colour display. The human visual system encodes spectral data into a three-dimensional structure, the dimensions being crudely described as "brightness", "red/green" and "blue/yellow". Three of the four independent images derived from the multi-spectral sensor data may be mapped onto these three visual dimensions to provide a colour picture which takes maximal advantage of the colour processing done by the eye.

There are four main stages in the construction of a colour picture by this technique. Firstly, the sensor data are calibrated and transformed to logarithmic values. Secondly,

the eigenvectors and eigenvalues of an inter-sensor covariance matrix based on appropriate scenes are derived. Thirdly, a linear transformation to a basis derived from the scaled eigenvectors is applied to the data. At this stage a further linear transformation may optionally be applied to bring out different features of the data, but this extra transformation should not ordinarily be required. Fourthly, three of the four dimensions of the transformed space are mapped onto the three dimensions of colour vision and an algorithm applied to determine the appropriate values for the primary colours (red, green, and blue) of which any display must be composed. Not all aspects of the system have yet been implemented in final form, and the examples to be shown result from early experimental versions.

Methods

Simplified model of the visual system - The discussion which follows is based largely on Jameson (1973) and Vos and Walraven (1972).

The eye has three types of cone receptor, in addition to the rod receptors which are responsible for vision at low light levels. Rods participate very little in the perception of colour at higher light levels and will be ignored in the following. Each of the three types of cone has a fairly broad spectral response. While we may, for convenience, label these types as "blue", "green" and "red" respectively, these labels do not correctly indicate the peaks of their absorption characteristics or the fact that they are quite broadband absorbers. The 3-dB band for the "blue" receptor is approximately 400-490 nm, for the "green" 470-580 nm, and for the "red" 500-630 nm. The "green" and "red" absorption curves have an overlap of approximately 80%. The images given by those two types of cone therefore must usually be very similar, since the cones will be responding largely to the same spectral range.

The cone outputs are probably not linearly proportional to the energies they absorb. For one thing, the cones adapt to the prevailing light level, so that a particular output may correspond to very different energies depending on the recent history of that cone and of its neighbours. More particularly, though, at any particular state of adaptation, the output after initial processing is probably more nearly proportional to the logarithm of the energy impinging on the receptor, and this logarithmic output is the basic data for further processing operations.

A simplified model of the subsequent processing is shown in Figure 1. The "red" and "green" outputs are summed and differenced, and their sum is summed and differenced with the "blue" output. The red-green sum is the major component of the overall brightness signal. There are relatively few blue receptors, possibly as few as 2% of the total, and their contribution to perceived brightness is commensurately small. The red-green difference determines the balance of long as opposed to medium wavelengths in the spectrum, since these are the wavelengths where the responses of the red receptors and the green receptors differ most strongly. When the red-green difference is zero, the signal is "yellow" and the percept is a colour between yellow and blue. This "yellow" signal must then be balanced against the signal from the blue receptors to determine the overall long vs. short wavelength balance. The blue signal, scaled appropriately, balances the "yellow" signal if the light is white. The result is that there are three essentially independent data channels, one indicating overall brightness, one indicating the red-green balance, and one indicating the blue-yellow balance. Because they are based on logarithms, these balance indicators are affected by the ratios of the energies in the different spectral bands, and hence do not respond to changes in overall illumination level. The three channels, "brightness", "red-green", and "blue-yellow" contain all the information available to the human perceiver about the colour of the world, and are essentially independent.

There have been many attempts to put a Euclidean or other metric onto these three basic colour dimensions. None have been entirely successful, but there are several useful approximations in the literature. If one is to use the three dimensional structure of colour vision effectively, one must be able to specify locations within some Euclidean approximation to the colour space in terms of the primary colours available. No satisfactory algorithm for the full three-dimensional Euclidean colour space as related to both the available primaries and the ERTS statistics has yet been produced, but one based on the space of MacAdam (1971) is being studied.

ERTS data processing - The four ERTS bands produce correlated imagery, just as do the three spectral bands of human vision. If the information contained in the four ERTS images could be conveyed in a space of three dimensions, it could be displayed in a single colour picture, without loss. The standard

colour composite procedure, shown in Figure 2, does not do this. The procedure we follow is (1) Compute the covariance matrix that relates the logarithms of the sensor outputs; (2) Find the eigenvectors of the covariance matrix and use them as a basis set for a new description of the data. In this basis, the data are uncorrelated in the four new dimensions, and the amount of data variance contributed by each dimension is given by the associated eigenvalue; (3) Scale the basis by dividing each dimension by the square root of the associated eigenvalue. This forces the variance on each dimension to be unity, and permits arbitrary rotation of the space without introducing covariance between the rotated basis dimensions; (4) Rotate the space in any arbitrary way, to suit particular needs; (5) Choose three dimensions of the resulting four-space for display and map them onto the three dimensions of colour space. This procedure is diagrammed in Figure 3.

1. Computation of the covariance matrix presents an element of choice. The data that enter into this calculation determine the entire subsequent course of the procedure. They are not the same data as must later be displayed, and should be chosen with certain criteria in mind. In particular, it is desirable that the selection of pixels should be representative of the object types which must be discriminated in the final display. In a completely general purpose system, pixels should be selected at random from everything that the satellite sees. This would result in very good discrimination of clouds and ocean, since most of the earth's surface is covered by one or the other. Very little attention would be paid to urban areas. A slightly more special purpose system would be to sample randomly from frames which are largely cloud-free land. The system used here is still more specialized. Pixels are sampled randomly from frames that other users have requested because they were interested in something in the frame. This weighting technique is still quite general purpose, but what specialization there is follows the interests of the ERTS users. It would be quite feasible to start with the proposition that a display is to be made for foresters or for prairie farmers or for glaciologists, and select the data pixels from scenes of interest to the selected users. Different basis vectors would be derived from different choices. The current technique aims to provide a generally useful display.

A different kind of choice is involved in the decision to base the computation on the logarithms of the sensor values. The intent here is to go some way to removing the effect of changes in illumination on the relative spectral values. One alternative possibility would have been to scale all the values within a pixel so that the sum of the four sensor elements was the same for each pixel. This approach would indeed remove the effects of changing illumination from the differences in the sensor values. It would also enforce a particular primary direction onto the derived space. While such a basic direction (brightness) might be useful, it is probably preferable to be able to leave the choice to a later stage of processing. Flexibility should be retained where possible. Hence the idea of removing the brightness component for separate processing is rejected, and the logarithmic data values are used.

The use of the logarithms of the data values poses a severe restriction on the allowable calibration error. If there is a small relative sensor offset, say 1 unit, it will make a large difference to the ratio between two sensors which read, say, 4 units. Such a small offset will not make much difference to the ratio if the sensors are reading 40 units. Hence the derived colours will change with overall level if there is an appreciable sensor offset. On the other hand, gain variation between sensors will result after logarithmic transformation in a simple additive constant which will not change with the overall level.

2. The eigenvectors of the covariance matrix form a basis for a description space within which the covariance matrix is diagonal, having values which are the eigenvalues of the original covariance matrix. In other words, when the eigenvectors are used to describe the data, the resulting values are uncorrelated. This transformation is shown schematically in Figure 4a-b in a two-dimensional reduction. Each transformed dimension may subsequently be treated independently of the others, and the information it carries is independent of the information carried by the others. Assuming that any noise or uncertainty in the measurement is distributed evenly and in an uncorrelated manner over the four sensors, then the information conveyed by a transformed dimension is proportional to the log of the data variance on that dimension. The eigenvalues of the covariance matrix are these variances, and indicate the relative importance of the new basis dimensions.

3. When the eigenvector basis is scaled (Figure 4b-c) by dividing each coordinate by the square root of the respective eigenvalue, the distribution that results has unit variance

on each dimension. However, the noise distributions are no longer hyperspherical, but are ellipsoidal with axes proportional to the inverses of the associated eigenvalues. This may or may not be relevant for later processing. In either case, the data distribution no longer has any preferred direction, except that some directions are noisier than others.

4. The data distribution in the scaled eigenvector space may be rotated freely by an orthonormal transformation (Figure 4c-d).

5. The last stage, and probably the most difficult to perform optimally, is the mapping of three of the derived dimensions onto the colour space. There is no clear agreement on the metric of colour space. A symposium volume devoted to the topic (Vos, Friele & Walraven, 1972) indicates the current lack of consensus. It is clear, however, that for any selection of primary colours there is only a finite and well defined set of attainable colours. The colour space is some kind of a skew three-faced pyramid. The data distribution, on the other hand, is a more or less Gaussian sphere, which will not fit conveniently into the colour pyramid. Either outlying points will be plotted in an unattainable region of "colour" space, or most of the data distribution will be clustered into a very small range of colours. Either the clear primary colours (including black) will be effectively unused or many pixels will be represented by supersaturated, impossible colours. Accordingly, the data distribution must be distorted before it is fitted into the colour space. This must be done in such a way that the orthogonal relationships among the dimensions are disturbed as little as possible.

The present approach (April 1974) is to compress the tails of the data distribution in each of the second and third dimensions so that the data more nearly equally fill a finite rectangle in (x, y). This rectangle is then transformed into the CIE coordinate space, using a "bipolar" transformation (Figure 5) with properties very close to those of a nearly rectangular colour space proposed by MacAdam (1971). The resulting space (Figure 6) yields roughly constant ease of discrimination for shifts of a given amount in any direction at any point. After the (x, y) position of the colour within CIE space has been fixed, the brightness is determined by multiplication by an amount depending on both the colour and the primary data dimension. The function maintains a fixed perceived brightness for a given value of the first dimension, regardless of the actual colour. The eye sees a given intensity of yellow more brightly than the same intensity of blue, but the calculation compensates for this effect.

Results

Covariance data were obtained from 14 frames, largely of summer scenes in southern Canada, which had been requested by other users for their own purposes. Eigenvectors and eigenvalues were determined from the total data sample. Approximately 10,000 pixels were used in each frame. The scaled eigenvector matrix derived from the averaged data was then used to describe the data from three frames, one a scene of almost bare rock and an ice-filled fjord on Ellesmere Island (78° W, 80°N approximately) very different from most of the scenes used to generate the covariance matrix; one a prairie scene centred on the city of Winnipeg, Manitoba, and one scene centred on Vancouver, B.C., which had not been included in the averaged data and which contained the silt-laden water of the Fraser River. The first two scenes were imaged in August 1973, the third in September 1972.

Initial processing of the data in each case was done by correcting the sensor data according to tables constructed by Vishnubhatla (Strome and Vishnubhatla, 1973) for mid-August 1973. The output of the tables was the logarithm of the calibrated sensor values, scaled so that as the data ranged from 0-63 so also did the table output. The calibration is not exact for very low readings and sensor drift between September 1972 and August 1973 rendered the calibration poorer for the Vancouver scene than for the other two.

Scattergrams of the data taken pairs of bands at a time from the Winnipeg scene are shown in Figure 7 and from the Ellesmere scene in Figure 8. The Winnipeg scene shows high correlation between bands 4 and 5, and between bands 6 and 7, but when one of the visible bands is considered together with one of the infrared bands, the data assume a fan shape. The four-dimensional shape is of a fan thin in two dimensions and fat in the other two -- a conical fan, so as to speak. Such a shape is probably typical of other prairie and farming scenes, though scattergrams have not been made to test this assertion.

The Ellesmere scene shows an entirely different pattern of inter-sensor correlation (Figure 8). The data in any pair of comparisons fall into well defined branches, converging at the very bright end of the data range. The upper

branch in each panel represents the rock and what sparse vegetation may have been included in the sample. The lower branch represents the ice and snow, much of which was probably melting in the summer sun. Melting snow has very low reflectance in the longer wavelengths, but remains bright in the shorter wavelengths.

Scattergrams were not obtained for the Vancouver scene, but one may assume that they would be not much different from those for the Winnipeg scene with the exception that the large amount of water in the scene would emphasize the lower ranges for the infrared bands. Samples would occur which had higher values in band 4 and low values in bands 6 and 7. Such points would plot along the bases of the three left panels in Figures 7 and 8.

Portions of the three scenes are shown in Figures 9, 10 and 11, in the conventional 4-band picture. Like the other pictures in this report, these figures were taken directly from the screen of the Bendix Multispectral Analyser Display (MAD) at the Canada Centre for Remote Sensing (CCRS), in Ottawa. In Figures 9, 10, and 11, the left strip is band 4, the right band 7. In each case, but particularly in the Ellesmere scene, it is evident that much of the variation is progressive from one band to the next. Vegetation, of course, shows up lighter in bands 6 and 7. The horizontal bars on the Winnipeg scene represent data errors.

The three scenes were transformed according to the eigenvectors of the same averaged covariance matrix. Scattergrams of the resulting distributions are shown for the Winnipeg and the Ellesmere scenes in Figures 12 and 13. If all the data that entered the averaging had been transformed into distributions such as these, each panel for the combined data would have shown a circular distribution of unit standard deviation. But since neither of these scenes is representative of the totality of the data, their resulting distributions are not perfect unit circles. The Winnipeg scene shows fairly strong correlation between the second and third dimension in the vector space, and the original fan shape shows up (as it must in at least one projection) in the scattergrams both of the first against the second and of the first against the third dimension (upper left two panels).

The Ellesmere scene involves data which do not even overlap those of the Winnipeg scene, and its bifurcated distribution could never be transformed into a unit hypersphere by any linear transformation. Nevertheless, the averaged data provide vectors which do a fairly good job of rationalizing the strange distribution. Most of the bifurcation appears in the projection of the distribution on the first versus second dimension. (In a space based on the covariance distribution of this particular scene alone, all the bifurcation appears in the single panel of vector 1 vs vector 2, the other panels showing fairly good unit circular distributions). As with the Winnipeg scene, the second and third dimensions are correlated, but this time the correlation is negative. In the colour pictures derived from this eigenspace, the Ellesmere scene is totally in the orange and red area, whereas the Winnipeg scene tends from purple to green.

Images derived from the four vectors of a rotated eigenspace for each of the three scenes are shown in Figures 14, 15 and 16. These images were obtained by applying individually to each vector an offset to avoid negative numbers, and a scale change, and then treating the data thus transformed as grey scale values. While the resulting vector images look superficially like the individual sensor images shown in Figures 7 and 8, they are devoid of obvious correlations among themselves. For example, consider the land, the ice at the edge of the fjord, and the large floe at the upper left of the Ellesmere scene. In the sensor images of Figure 8, this sloe gets darker from band 4 to band 7, while the edge stays bright and the land remains mid-grey. In the vector images, no such trends can be seen.

Figure 16 shows enlarged rotated vector images of a portion of the Winnipeg scene SW of the city. Note that separations are clearly visible in vector 2 between some fields that merge into a single area in vector 3, and vice versa. Neither vector suffices to show all the inter-field discriminations. Vector 1 and 4 show the effects of poor low-level calibration. Both are heavily weighted by bands 6 and 7 in this particular rotation of the eigenspace (vector 1 actually corresponds to a direction in 4-space near the original vector 3), and these bands seem in this image to have the worst low-level calibration correction. Despite the noise in vectors 1 and 4, they may be used to make some discriminations not possible using the other two vectors. In general, each vector makes an independent contribution to the interpretation of the scene.

Let us now consider the amount of information potentially available in each dimension. Since, overall, the data in the

various dimensions are uncorrelated, we can treat each separately. The noise which limits the precision of observation includes quantization noise; the signal can vary ±0.5 units without altering the reported datum. After logarithmic transformation, the size of the quantum depends on the signal level, being large for small signals but small for large signals. On average, it probably is near 1 unit, since the log scale is stretched to cover the same range, 0-63 units, as the original sensor data. On this assumption, the equivalent noise is 0.08 unit^2. At lower signal levels if the quantum is about 3 1/2 units, the noise may go as high as 1 unit^2. Such levels are found in water regions and shadows. To ease further discussion, let us settle on an estimated quantization and calibration noise of about 0.1 unit^2, probably an optimistic estimate for most scenes.

The effect of quantization and calibration errors at low levels can be seen as striping in the rotated vector images for Winnipeg and Vancouver, particularly in rotated vectors 1 and 4. Strong weighting of these vectors on the low level band 7 is responsible. Such effects do not show on the Ellesmere scene, since most of the sensor data were at high levels where quantization effects are minimal

The eigenvalues of the covariance matrix determine the variance due to that dimension. When each of the 14 scenes which were averaged is treated individually to obtain a set of eigenvectors and eigenvalues, the first dimension accounts for, on average, 96% of the total variance, the second for 79% of the rest, and the third for 74% of the remainder. What is left for the fourth vector has a variance of .37 unit^2, barely above the estimate of the quantization variance. Compared to the quantization variance estimate, the signal-to-noise ratio of the four dimensions is about 31 dB, 17 dB, 10 dB and 6 dB respectively.

These figures are obtained when each scene is viewed in its own optimum vector space. When the gross average data are viewed as a group, two things happen. Firstly, there is more overall variance because of the differences among scenes. Secondly, the scenes differ in various ways, so that the overall dimensionality becomes larger. In terms of the last paragraph, the first dimension in the overall data now accounts for only 84% of the variance, the second for 84% of what is left, and the third for 77% of the remainder. The signal-to-noise ratios are 32 dB, 23 dB, 15 dB and 9 dB. These figures show that whereas three dimensions probably give an acceptably complete description of the information available if a scene is described in terms of its own eigenvector space, the fourth dimension may supply some useful information when the scene is described in a space derived from the entire data set. This fact supplies the rationale for rotating the four-dimensional space in various ways to permit different three-dimensional projections which can be viewed in colour space.

In practice, we cannot allow the presentation of each scene in its own eigenspace, since this would present the interpreter with intolerable variation in the relation of colour with ground truth. However, one could admit a small set of rotations for special purposes; one rotation, for example, which would optimally display forests, another which would give best discrimination in agricultural lands, and another for glaciologists. Each interpreter within a discipline would then have to deal with only a single transformation, whose three-dimensional structure would contain essentially all the information relevant to his purposes. Investigation of possible specialized display spaces is intended as an early stage of the continuing investigation. It should be noted that Haralick (1960) found that a three-dimensional space represented well the data from a small forested and mountainous region in Yellowstone Park scanned by a 12-band system operating from the near ultra-violet across the part of the spectrum covered by ERTS. It therefore seems reasonable that three dimensions will adequately deal with most problems of ERTS data display. For those cases where three dimensions are inadequate, either a grey-scale display of the fourth vector or a colour display made up of the second, third and fourth dimensions should supplement the primary colour display.

Summary

The correlated data from the ERTS sensors has been transformed into a space in which the four dimensions are uncorrelated and of equal variance. This was accomplished by determining the eigenvectors of the covariance matrix, and dividing the data projections on the eigenvectors by the square roots of the associated eigenvalues. Data thus transformed may be treated in a variety of ways, primarily by rotating the space. Space rotation in this scaled eigenvector space may be performed freely without introducing correlation among the rotated dimensions. In the rotated space, three dimensions are

chosen for display as the dimensions of colour space. The resulting colour pictures show discriminations rather better than do displays based on band selection. The amount of information carried by the first dimension is considerably greater than by the second, which is in its turn much more informative than the third. The information carried by the fourth dimension is ordinarily very small, but could be important in particular applications. In such cases a display including the fourth dimension could supplement a standard display. For particular applications special displays may well be made either from a specially derived eigenvector set or from a rotation of the basic eigenvector space to emphasis discriminations of interest for the particular application.

Footnotes

*This is DCIEM Research Paper 73-RP-987A. An earlier version of this paper has appeared in the Proceedings of the Third ERTS Users Symposium, Washington, D.C., November 1973.

**Much of this work was done using the display systems at the Canada Centre for Remote Sensing, Ottawa, as a cooperative project between The Defence and Civil Institute of Environmental Medicine and the Canada Centre for Remote Sensing. I thank particularly Mr. Gordon Wayne for the long hours of programming he has spent on the project, and Drs. S.S. Vishnubhatla and S. Schlien for their assistance in providing routines and tables for matrix manipulations and for their stimulating discussions of the principles involved in the work.

References

Haralick, R.M. Multi-image pattern recognition: ideas and results. CRES Tech. Rep. 133-11. University of Kansas, Center for Research Inc. 1969.

Jameson, D. Theoretical issues of color vision. In *Handbook of Sensory Physiology*, Vol. VII/4, Visual Psychophysics. (Eds. Jameson, D. and Hurvich, L.M.) Berlin: Springer-Verlag, 1972.

MacAdam, D.L. Color-difference evaluation. Advances in Chemistry Series, 107, "Industrial Color Technology". American Chemical Society, 1971.

Strome, W.M. and Vishnubhatla, S.S. A system for improving the radiometric corrections for ERTS-1 MSS data. Presented at the XXIV Astronautical Congress, Baku, USSR. October 1973.

Vos, J.J., Friele, L.F.C., and Walraven, P.L. (Eds.) Color Metrics, Soesterberg: AIC/Holland, 1972.

Vos, J.J., and Walraven, P.L. A Zone-fluctuation line element describing colour discrimination. In Vos, Friele and Walraven, 1972.

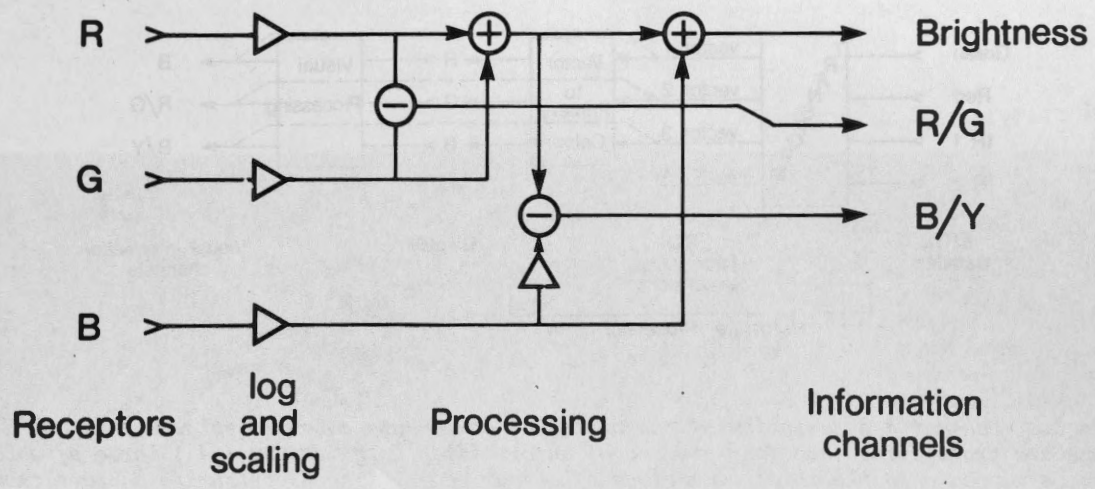

Figure 1. Simplified flow diagram of colour processing in the visual system.

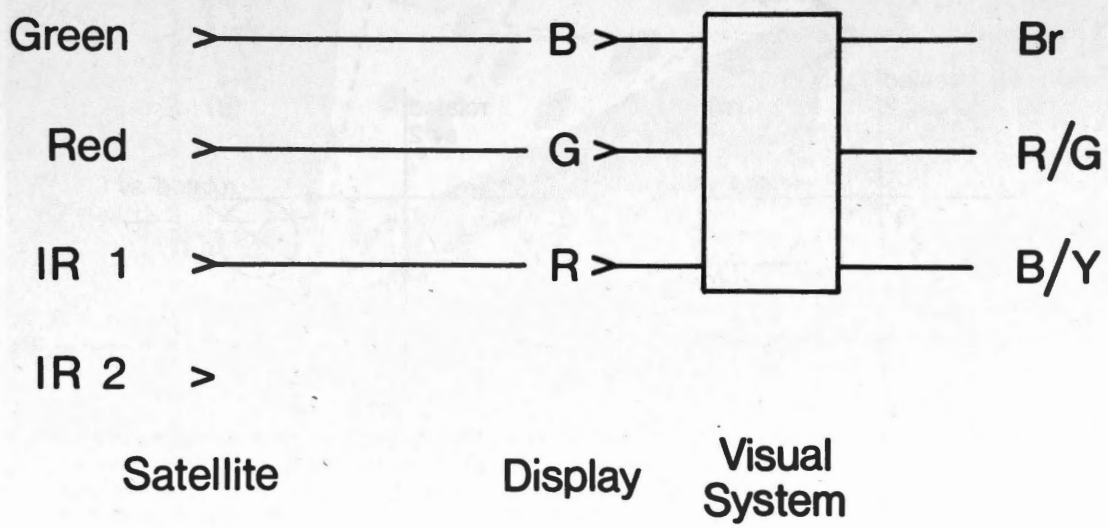

Figure 2. ERTS colour display simulating infrared colour film. Three bands are presented individually in three different primary colours, which the visual system then converts to three dimensions of colour space.

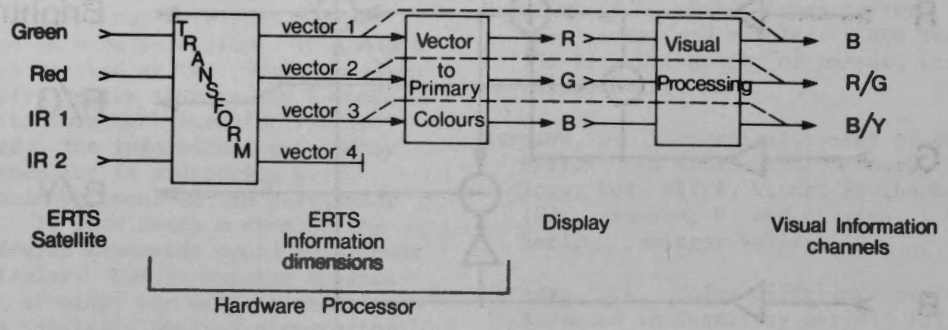

Figure 3. Schematic description of the principal components colour display. The four data streams are transformed into four streams of uncorrelated data (vector 1-4), three of which are to be mapped onto the three dimensions of colour space. The algorithm to convert from the vector representation to colour primaries is supposed to be the inverse of the processing applied by the visual system to produce the three dimensions from the sensed primaries of the display.

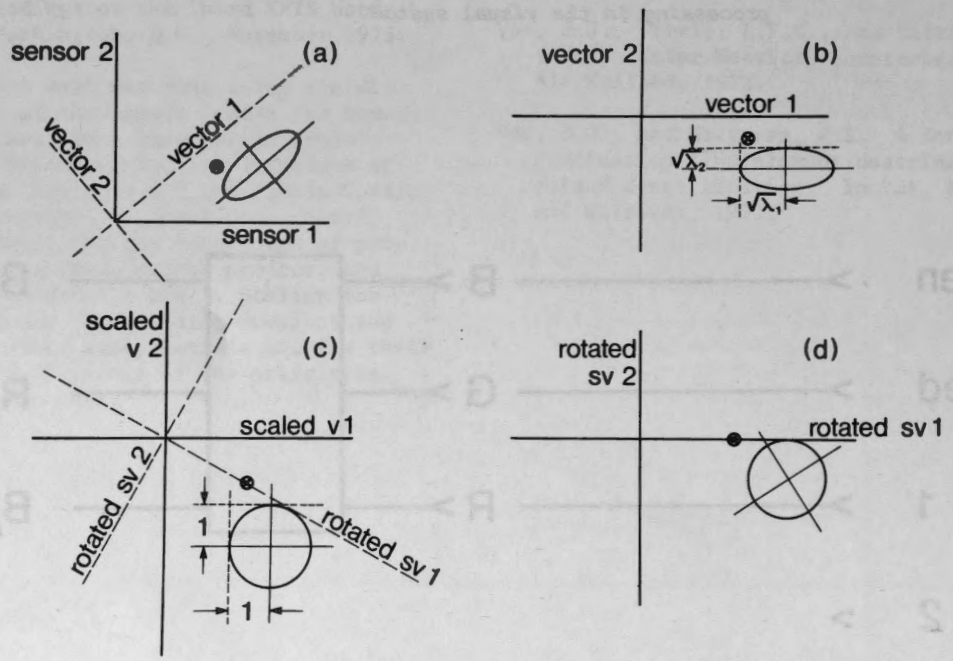

Figure 4. Stages in the construction of the linear transformation from sensor data to independent vector form. (a) The data from two sensors is correlated, and therefore is distributed in a roughly elliptical form with the main axes diagonal. A single isolated data point is also shown. The eigenvector solution of the covariance matrix determines vectors parallel to the main axes of the ellipse. (b) The data distribution rotated into the eigenvector representation. The description in this space is not correlated, as is shown by the fact that the axes of the ellipse are parallel to the coordinate axes. The standard deviations are unequal, being the square roots of the eigenvalues. (c) Each dimension is scaled by the square root of the eigenvalues, so that the standard deviation of the distribution is now unity in every direction. There are no longer any main axes to the data distribution, and the space can be rotated freely without introducing correlation into the description. (d) An arbitrary rotation which places the isolated data point along an axis. It representation in this space is now (k, 0).

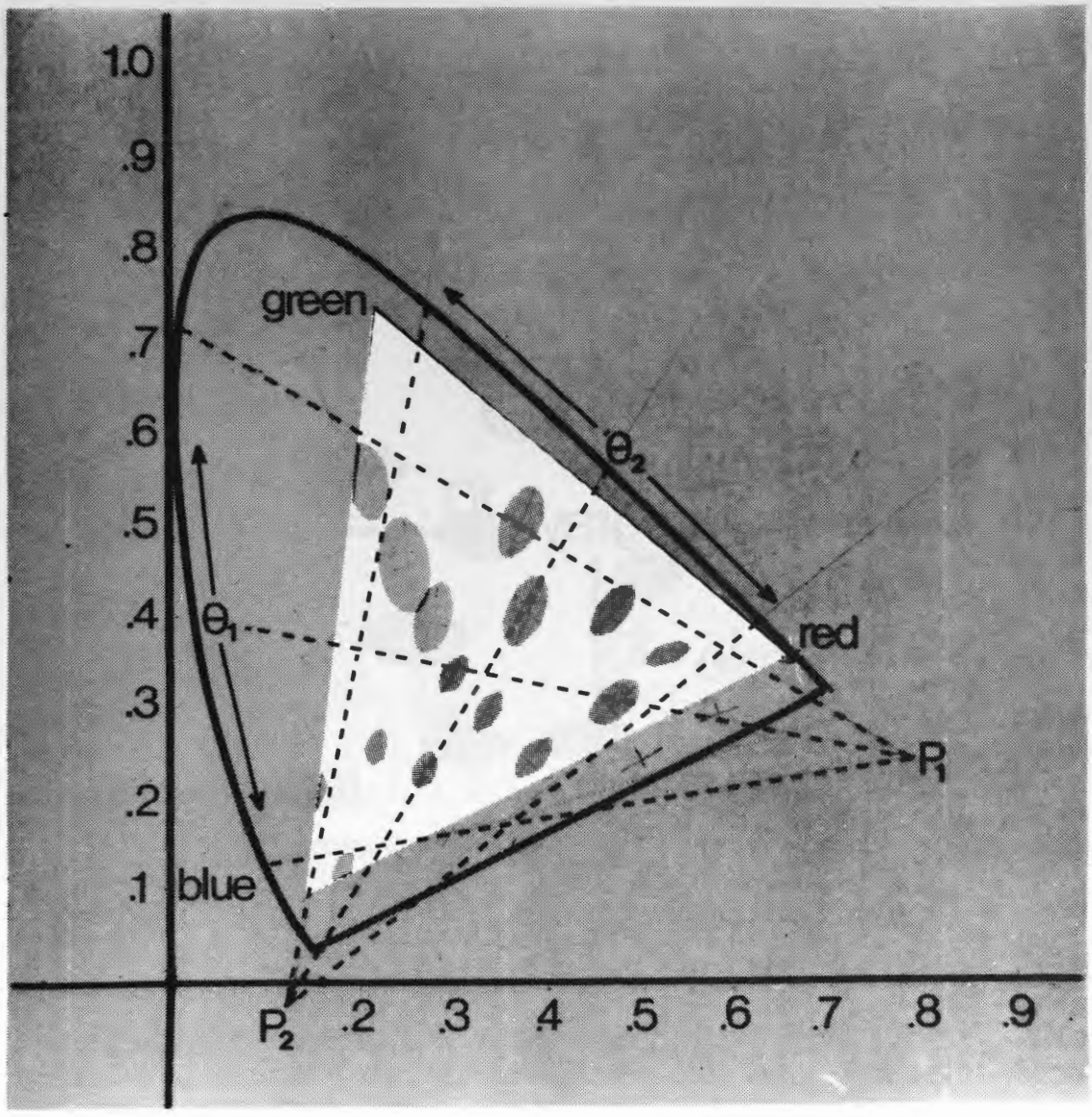

Figure 5. The CIE colour space, showing equal discriminability ellipses and the "bipolar" coordinate system. The equal discriminability ellipses represent colours equally discriminable from the colour at the centre of the ellipse. They vary in size at different places in the colour space.

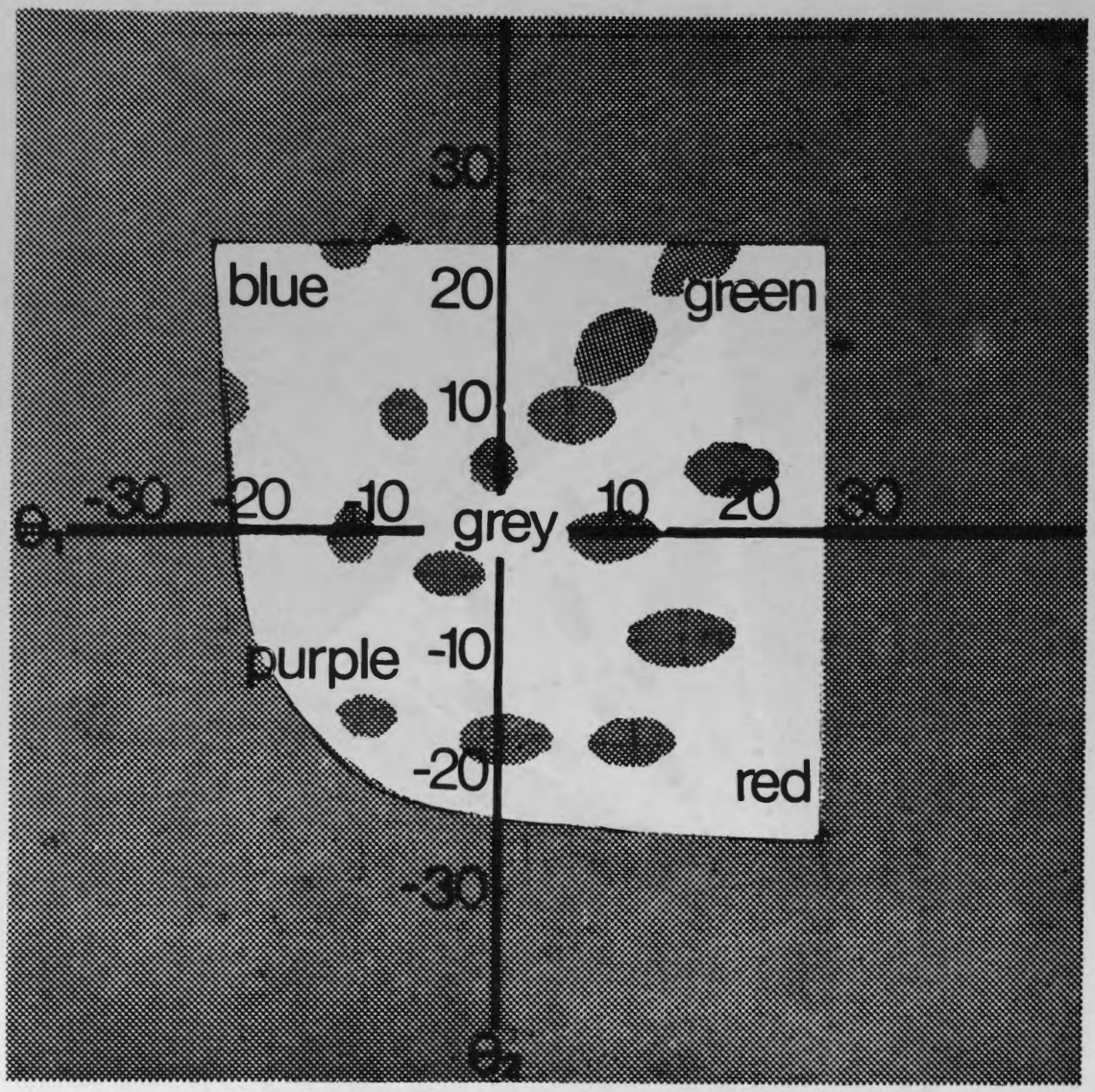

Figure 6. The bipolar colour space, showing equal discriminability ellipses. The ellipses are more nearly equal in size in this co-ordinate system.

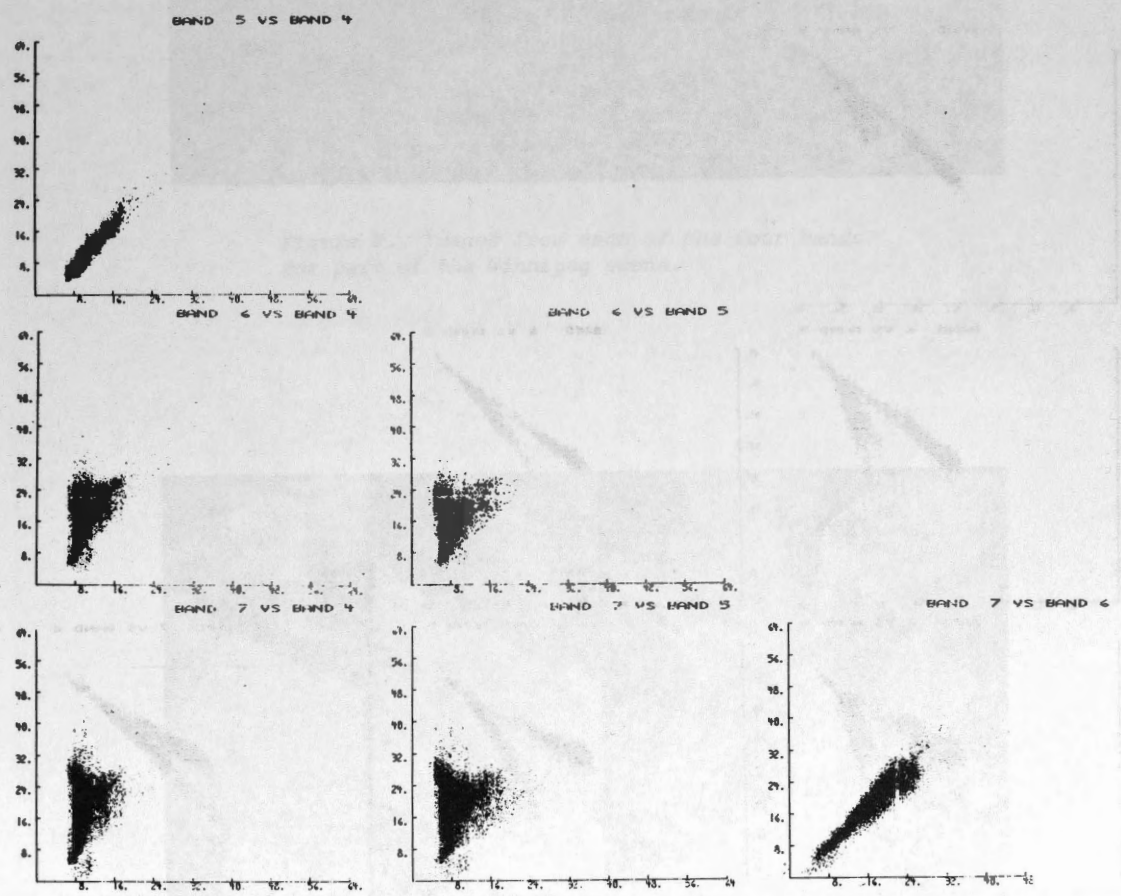

Figure 7. Inter-band correlograms for a scene including the city of Winnipeg. Note the high correlation between bands 4 and 5, and between bands 6 and 7.

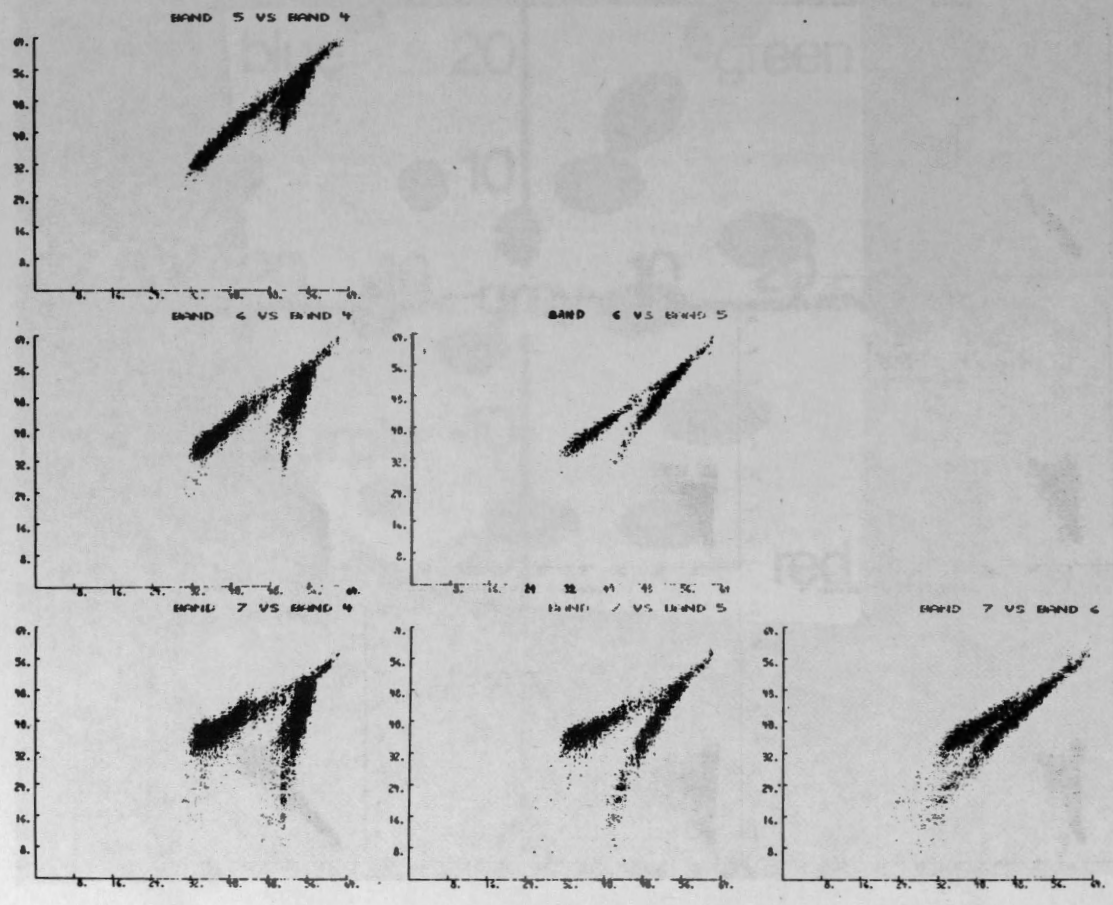

Figure 8. Inter-band correlograms for a scene of an ice-locked fjord and almost bare rock on Ellesmere Island (approx. 80°N). The upper spur in each panel represents the rock, the lower spur the ice.

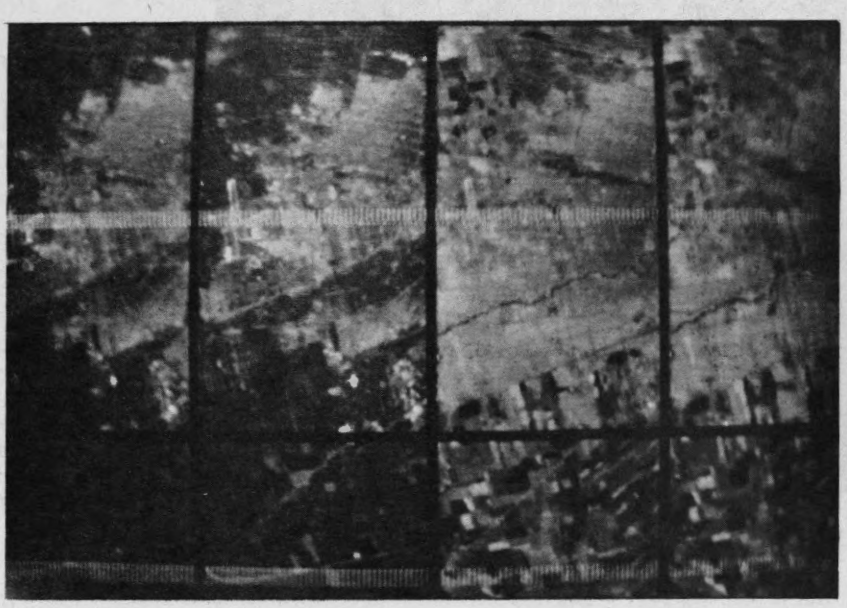

Figure 9. Images from each of the four bands for part of the Winnipeg scene.

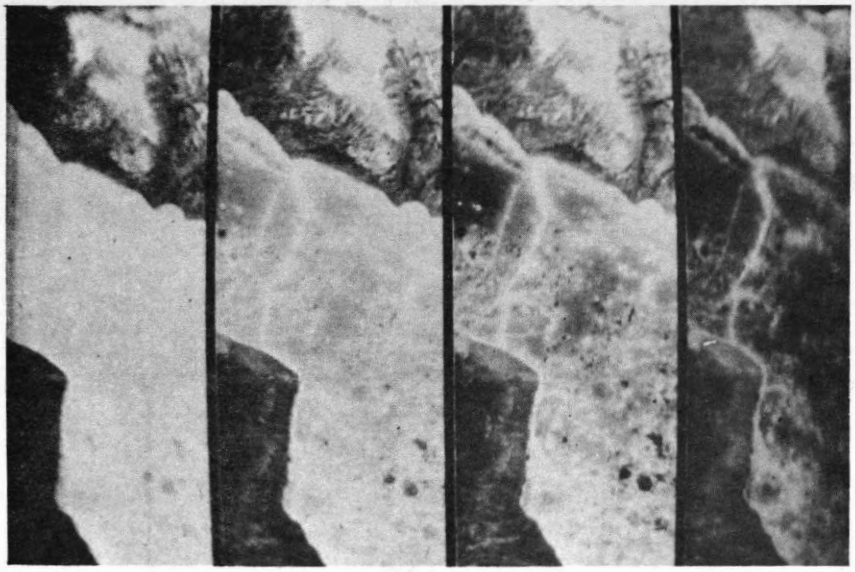

Figure 10. Images from each of the four bands for part of the Ellesmere Island scene.

Figure 11. Images from each of the four bands for a scene including Vancouver city and the mouth of the Fraser River.

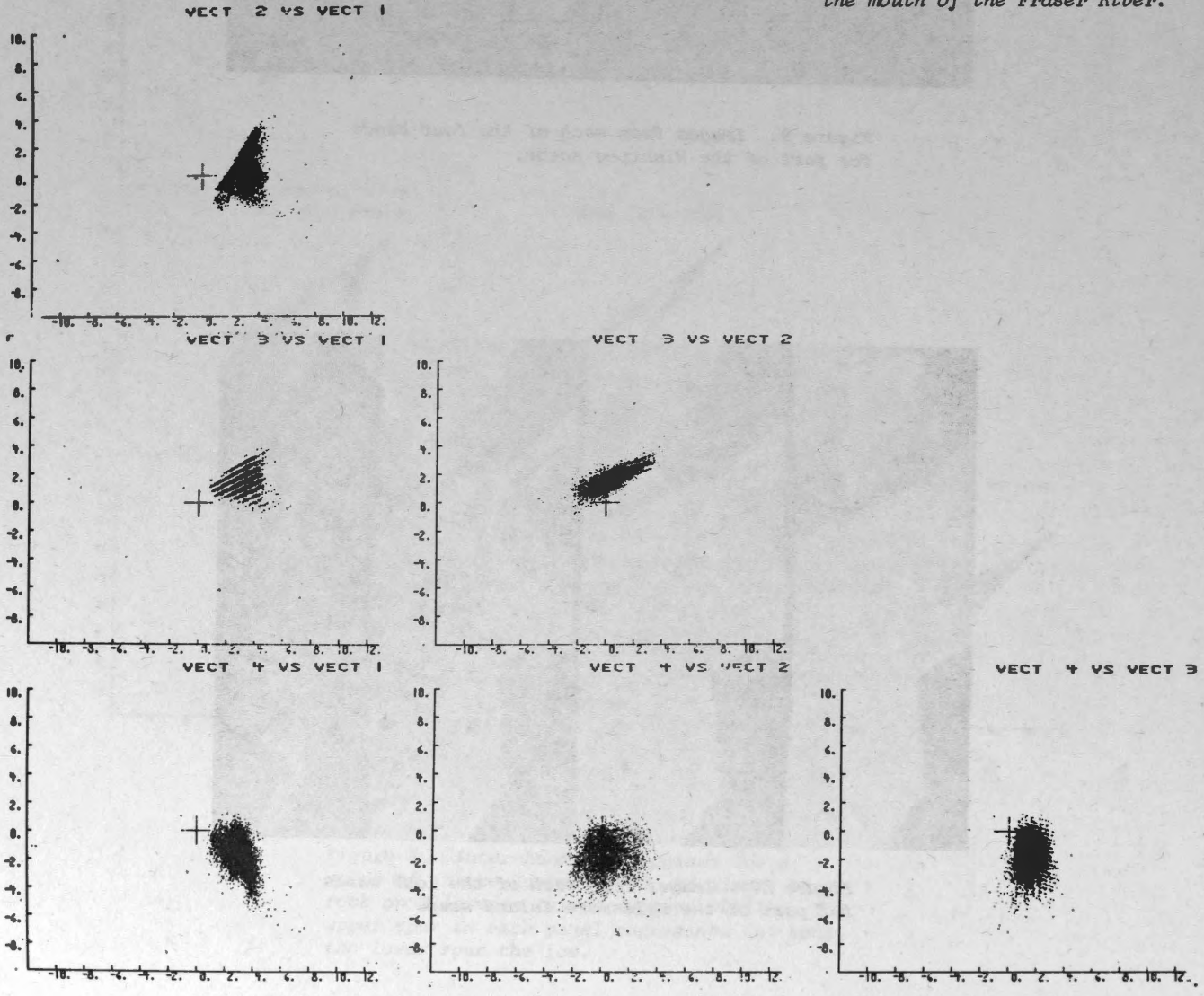

Figure 12. Correlograms of the relations between the scaled eigenvectors for the Winnipeg scene. The data is the same as in Fig. 7. The eigenvector space was determined from a covariance matrix based on 14 different scenes.

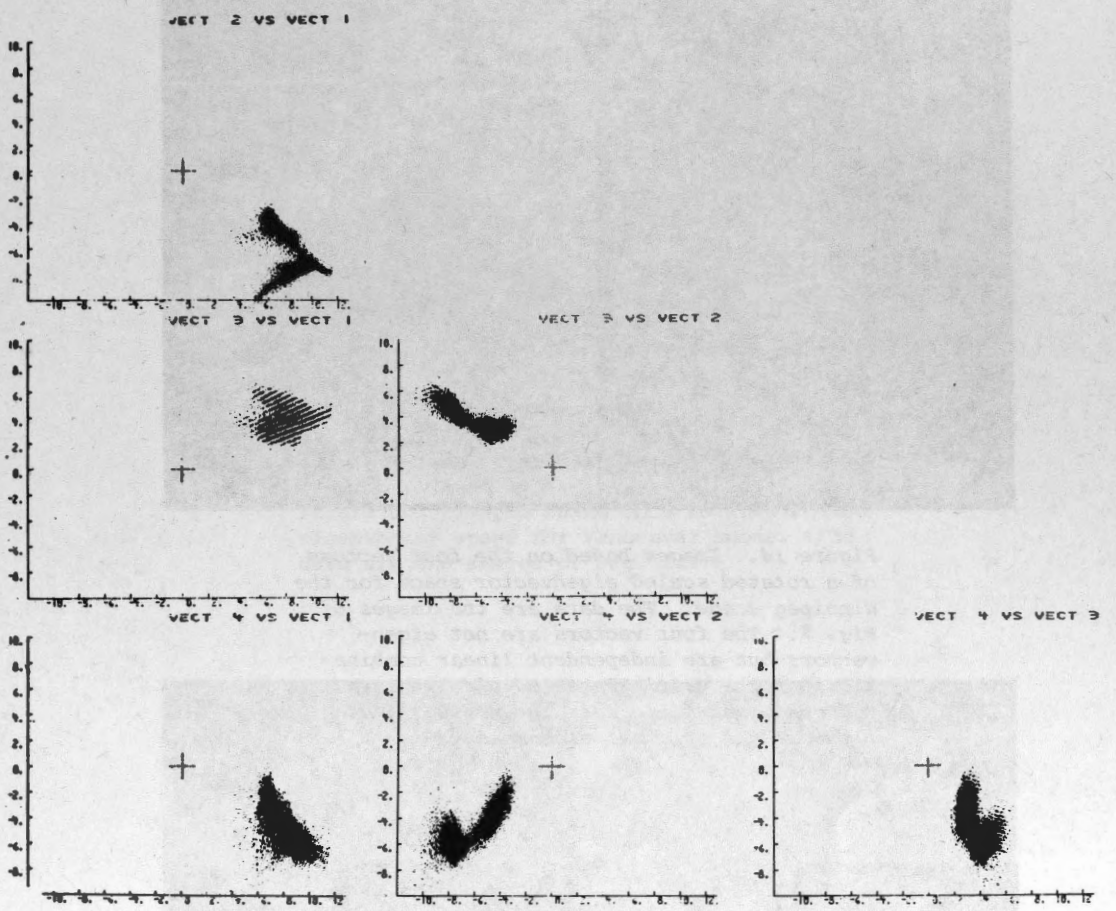

Figure 13. Correlogram of the relations between the eigenvectors for the Ellesmere Island scene. The data are the same as in Fig. 8, and the eigenvector space the same as in Fig. 12. Notice that the double spur shows up most strongly in the relation between vector 1 and vector 2.

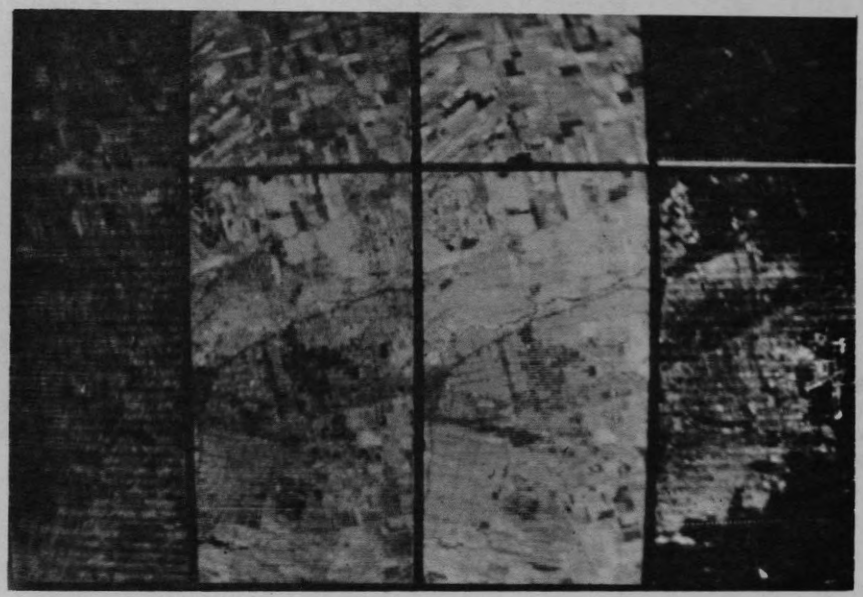

Figure 14. Images based on the four vectors of a rotated scaled eigenvector space for the Winnipeg scene. The data are the images of Fig. 9. The four vectors are not eigenvectors but are independent linear combinations of the original scaled eigenvectors. Vectors 1 and 4 lie near the noisy (3, 4) plane of the original eigenspace.

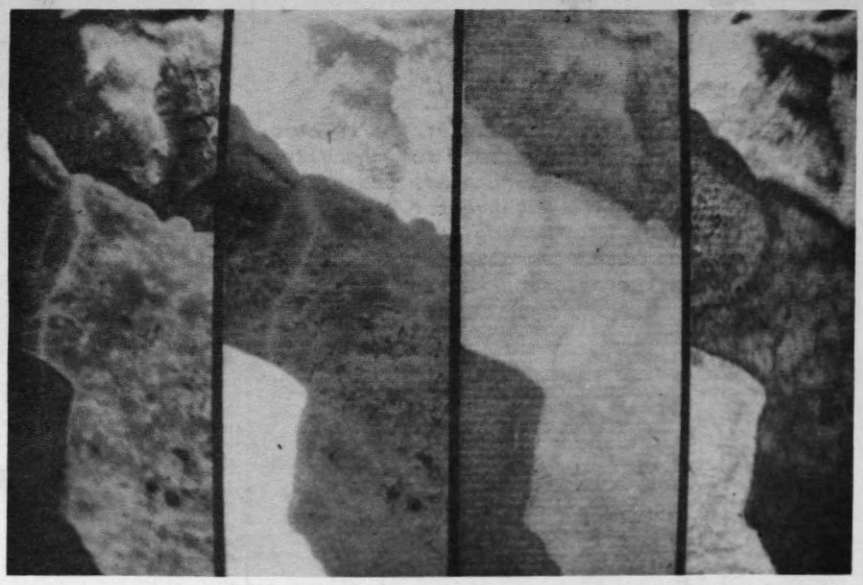

Figure 15. Images based on the four vectors of a rotated scaled eigenvector space for the Ellesmere Island scene. The data are the images of Fig. 10.

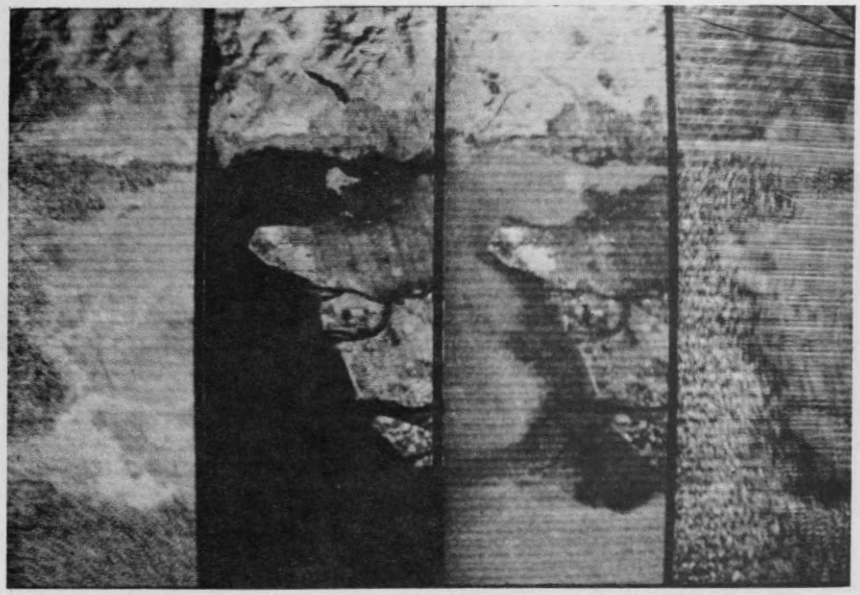

Figure 16. Images based on a rotated scaled eigenvector space for Vancouver scene. The data are the images of Fig. 11.

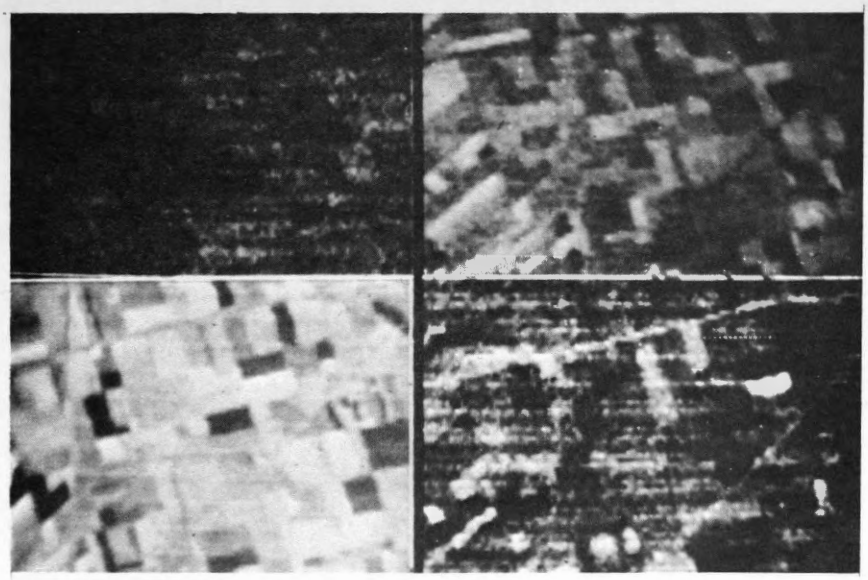

Figure 17. A magnified section of the vector images from Fig. 14, showing fields Southwest of Winnipeg. Vectors 2 and 3 each show discriminations not visible in the other image. Note that these vectors are not eigenvectors, but are derived from a scaled rotated eigenvector space. Vectors 1 and 4 are noisy, due to high loadings on low-level bands (see text). They are both near the (3, 4) plane of the original eigenvector space.

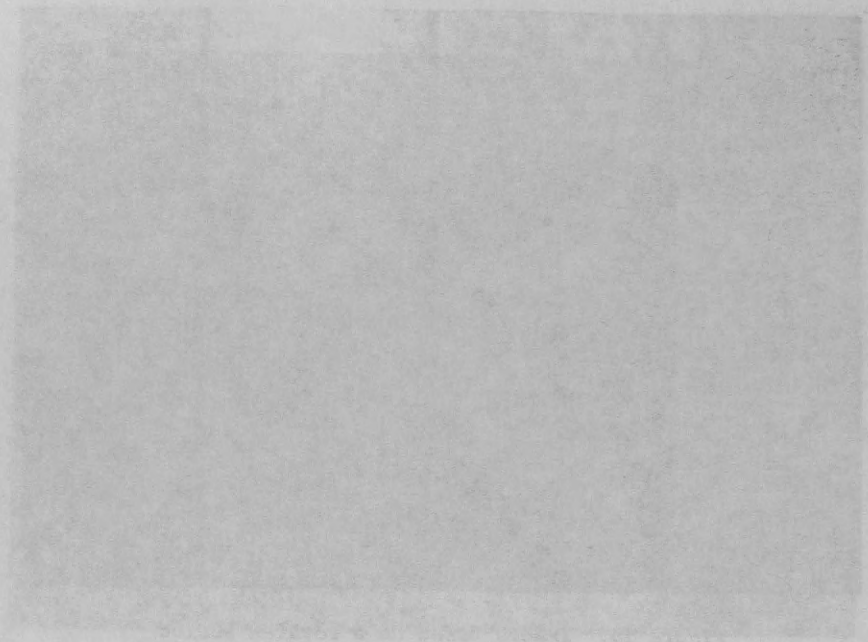

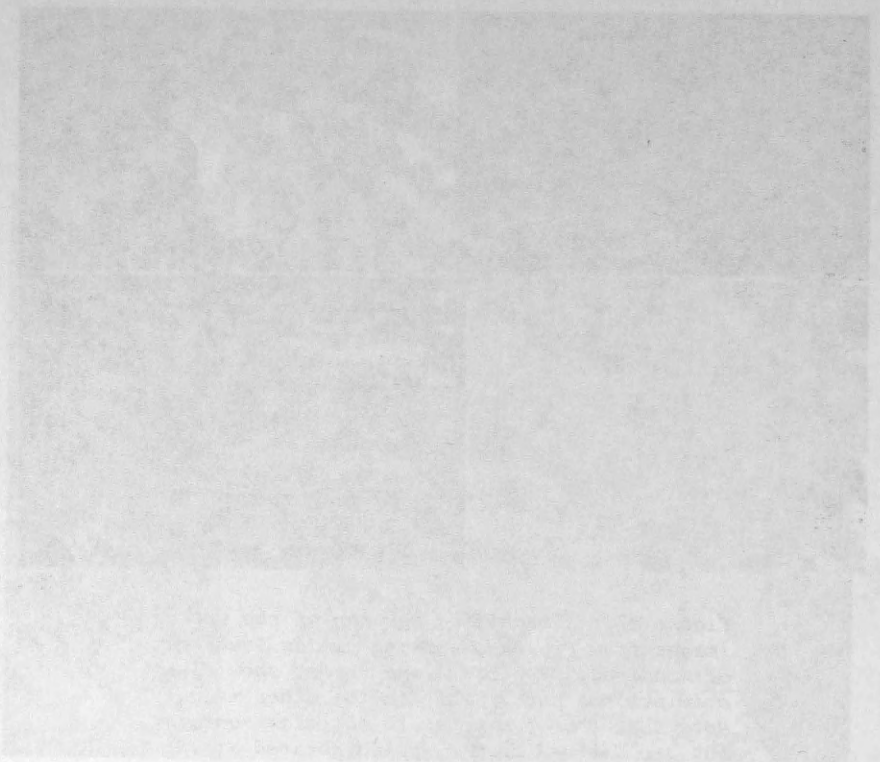

MULTISPECTRAL DATA ANALYSIS FOR RESOURCE MANAGERS IN UTAH

By

EARLE NELSON
DUAN LINKER

This paper presented at the Second Canadian Symposium on Remote Sensing, University of Guelph, Guelph, Ontario, April 29 - May 1, 1974.

MULTISPECTRAL DATA ANALYSIS FOR RESOURCE MANAGERS IN UTAH

Earle Nelson and Duan Linker
Earth Information Services
McDonnell Douglas Astronautics Company
Huntington Beach, California

ABSTRACT

McDonnell Douglas Earth Information Services (EIS) is conducting a thematic mapping project in the Salt Lake City area of Utah in cooperation with the State of Utah, the U. S. Forest Service, the Intermountain Forest and Range Experiment Station, the Soil Conservation Service, and the University of Utah. A widely varied ecological test site of approximately 735 square miles was covered in mid-July 1973 with a 5-channel multispectral scanner, color, and color infrared film. The organizations in Utah have organized in study groups for Land Use, Water Resources, Vegetation-Soils, Geology-Geomorphology, and Imagery. In cooperation with these study groups, EIS is investigating the generation of thematic map overlays for such problems as urban encroachment, agriculture inventory, recreation impact, water pollution, forest inventory, soil classification, geologic hazards, and natural resource location. Both interactive computer processing and manual interpretation of the data have been performed with the classification results overlayed to base maps for final evaluation by the resource managers in Utah.

INTRODUCTION

McDonnell Douglas Earth Information Services (EIS) is participating in a cooperative program with resource managers in the State of Utah. The goal of this program is to develop improved techniques for generating map overlays containing the type of thematic information valuable to resource managers. At the present time, accurate information of this type is difficult and sometimes economically infeasible to obtain. Therefore, this program is attempting to show that using multispectral data with a multistage sampling and computer processing approach can generate useful map overlays on a production basis.

As a proving ground for this approach, an environmentally important and varied use test site located in the vicinity of Salt Lake City, Utah was chosen by a group of land use planners and resource managers as having all the ingredients needed for a comprehensive ecological resource inventory. By starting from this test area, and using both satellite and aircraft multispectral data, this program is evaluating a multisensor approach and automatic computer classification to develop the techniques for performing resource management for both large and small areas.

The reason for evaluating the computer analysis of multispectral data is that resource managers have found they can not afford to collect the required detailed type of information by ground surveys of the areas under their responsibility. Therefore this program was designed to sample the test site with a low-flying aircraft, a high-flying aircraft, and the ERTS satellite. This approach was conceived because only satellites can cover the large areas often required, but in some areas they may not be able to supply the kind of detailed information required by land use planners. So this program was designed to sample the test site at different spatial resolutions and then actual users of the information could determine at what resolution level they should operate for their particular task. With this type of information, these users can specify the most economical sampling technique to collect their data.

The most important aspect of the program is in terms of Utah user utility. The following questions regarding the utility of computer processed multispectral data must be answered: (1) Can the major land use and land cover categories be determined with sufficient accuracy to be beneficial? (2) How many categories can be accurately determined from multispectral data, and do these form a viable set? and (3) Are the boundaries determined with sufficient accuracy to yield a useful product? This evaluation will be made by the user groups in Utah, using the thematic maps developed, plus the evaluations of accuracy determined during the computer analysis.

OBJECTIVES

The broad objectives for this program were originally defined to fulfill the requirements of

an ERTS project and capitalize on McDonnell Douglas' capability in aircraft multispectral sensing and analysis. The first objective was to employ modern technology in remote sensing collection and computer processing to develop new tools for resource management that can be used to monitor and record environmental and natural resource data. The second objective was to develop communication techniques and procedures to integrate user requirements into thematic mapping projects. Another goal was to demonstrate that multispectral analysis techniques could be developed to classify land use, resource, and pollution data. Finally, the development of map overlays that portray information required for land use planning was specified as a primary objective.

COOPERATORS IN UTAH

To meet the objectives of this program, EIS has entered into a cooperative effort with five organizations in Utah concerned with resource management within the State. These organizations are the State of Utah, the Intermountain Region of the U. S. Forest Service, the Intermountain Forest and Range Experiment Station, the Soil Conservation Service, and the University of Utah. These groups provide the wide background needed to develop new tools for resource managers. McDonnell Douglas is conducting the computer analysis of the multispectral data, the Geography Department at the University of Utah is supplying a broad technical and research oriented base in the immediate geographic area of the study, and the Forest Service, State of Utah, and the Soil Conservation Service are relating this information to their resource management objectives and determining its potential for land use planning. The Forest Service also supplies expertise and guidance in mapping requirements and techniques.

STUDY GROUPS AND PROGRAM DEFINITION

Many of the planning details of this study were resolved at a series of meetings held in Salt Lake City. The first meeting, called the Wasatch Front Thematic Workshop, was held on March 19, 1973; the second was a two-day series of meetings with the Thematic Mapping Study Groups held on May 15-16, 1973. One of the major accomplishments at the first meeting was to define the study groups and determine a representative set of members. These groups are Land Use, Water Resources, Vegetation-Soils, Geology-Geomorphology, and Imagery. The members of the groups are shown in Table I, along with the members of the Advisory Board who provided valuable leadership in organizing and conducting the program.

One of the first tasks for the cooperators was to define the boundaries of a test site to include all the ingredients required for a study of land use and environmental impact information. The final test site area is shown in Figure I. The test site includes such varied land uses as the urban area of Salt Lake City, the agricultural land to the south, the intervening area of urban encroachment, the rangeland and forest land in the Wasatch and Uinta National Forests, and the various lakes, streams, and reservoirs in the area.

As a result of the meetings in Salt Lake City, each group defined its problems of immediate concern, and since manpower resources are limited, also established its priorities. The Land Use Group divided its area of interest into three functional categories—agriculture, recreation, and urbanization. Under the agriculture category, the main items are correlating the results of this study with the sample area classifications used by the Soil Conservation Service, and the identification of regions where use has been curtailed by erosion or pollution. For recreation, the important problems are the general impact on the canyons of erosion, water pollution, backpacking, etc., and road and trail identification. The item of first importance under urbanization is to obtain a map of the impervious surfaces; second is to study the structural status to correlate with and amend existing data. The geographic areas that the Land Use Group defined for intensive study and the priorities are shown in Table 2. This group recommended and all the other groups agreed, that the land use classification system proposed by the U. S. Geological Survey (Anderson, et al., 1972) should form the basis for categorization in Utah.

The two main categories of concern defined by the Water Resources Group are water supply and water quality. The group members are interested in monitoring the input/output relationships in the Salt Lake City watershed. They hope to gain some information about springs and seeps, snow melt runoff, stream flow, flood plain aquifiers, and water loss in irrigation, although these features are difficult to monitor by remote sensing. The more easily identified water quality factors, such as industrial pollution, feedlot pollution, and thermal change in the water, are also of great interest to this group. The geographic areas that the Water Resources Group defined for intensive study and the priorities are listed in Table 2.

The Vegetation-Soils Group has defined the classification of various soil information and vegetative cover and the subsequent correlation with existing inventories as the tasks of primary importance. The Soil Conservation Service and the Forest Service both have substantial exist-

ing samples to compare with the computer classification of the remotely-sensed data. Both organizations also are interested in evaluating these techniques for updating their inventory of range and forest lands. The Soil Conservation Service places equal emphasis on surveys of the agricultural crops in the area. The geographic areas the Vegetation-Soils Group specified for intensive study and the list of priorities are shown in Table 2.

Monitoring natural geologic hazards and evaluating the potential for mineral development are the major interests of the Geology-Geomorphology Group. The geologic hazards consist of landslides, floods, fault zones (potential earthquake hazards) and snow avalanches. Also of importance is the search for minerals of economic importance, water-bearing fracture zones, and sand and gravel deposits. The geographic areas defined for intensive study by the Geology-Geomorphology Group and the priority listing are in Table 2.

REMOTE SENSORS

At the workshop in Salt Lake City in March 1973, the Imagery Group and EIS decided to collect aircraft data with a multispectral scanner and two cameras as one of the first steps in fulfilling the objectives of this study.

The multispectral scanner selected was designed by Actron Industries of McDonnell Douglas for data collection anywhere within the 0.3 to 15 micrometer spectral region. For this particular flight, the spectral channels assigned to ERTS-B were used, but other channelizations are possible.

A number of unique features have been incorporated in this sensor. Of first importance is that all spectral bands are in spatial coincidence as the spectral band separations are accomplished after a single field stop. Another unique feature of this scanner is the nadir centered conical scan with the nadir angle fixed at 30 degrees. This type of scan gives constant atmospheric path length, constant ground resolution, and constant target viewing angle. Further, because both fore and aft scans are available, two looks at the target are obtained so stereo coverage is thereby provided, and either fore or aft scan may be used for analysis.

An optical shaft encoder is mechanically linked to the scan mirror. This encoder generates a line start pulse and synchronization pulses such that the exact position of the scan mirror can be determined to a fraction of a pixel at any point in the scan cycle. This, along with recorded line count information, establishes a coordinate reference system that defines the location of every resolution element. A V/H sensor is used to control the scan rate of the mirror to keep the scan lines contiguous regardless of changing altitude or plane velocity. Overlaps of 1.1X, 2X, and 4X are also provided.

Out of each scan circle, 120 degrees is used for the fore scan, 120 degrees is used for the aft scan, and the two 60-degree segments between the scans are used for calibration. Every channel looks at a calibration source on every scan from which absolute radiometric values can be obtained. A summary of the system characteristics is given in Table 3.

The KA-74A camera is a general purpose framing camera that was used on this project with 200 foot rolls of thin base AEROCOLOR Negative Film 2445. This was developed in response to a general need for a reliable day/night camera that produces high resolution negatives from which black and white or color prints may be made. A six-inch, f/2.8 lens is used to cover the 4.5- by 4.5-inch format. The relatively small size and simplicity of this camera makes it suitable for installation in low profile aircraft and pods.

The HP-307 camera is a lightweight, high-resolution, multipurpose, sequential frame 70 mm panoramic camera system in which 400 foot lengths of AEROCHROME Infrared Film 3443 were used for this flight. The rotating lens sweeps an image across the film to produce a scan angle of 130 degrees. The film is held concentric with the optical scan axis by semicircular edge guides. Exposure is provided by a unidirectional, continually moving focal plane shutter which is synchronized with the lens rotation. The 80 mm focal length lens is adjustable from f/2.8 to f/22. Inflight resolution using high definition panchromatic film is 150 lines/mm. Film capacity is 70 mm by 400 feet of thin base (2.5 mil.). A picture format of 2.25 by 7.2 inches is provided. An internal intervalometer enables selection of cycling rates of 1, 2, 4, 8, 16 or 32 sec/cycle.

INTERACTIVE IMAGE ANALYSIS SYSTEM

The McDonnell Douglas Interactive Analysis System used for the computer data analysis during this program is built around an XDS-930 computer facility. This is a medium scale, high speed, general purpose computer dedicated to pattern recognition technology.

Input facilities have been developed to convert both analog magnetic tape and photographic data to digital form for analyses by the interactive system. The main feature for analog tape conversion is a 12-bit analog-to-digital converter with a 16 channel multiplexer. An image dissector tube is used for accessing

data from film. This device scans either prints or transparencies under computer control, converts the pixel information at 6-bit accuracy, and sends the digital data to the computer. In addition, any digital magnetic tape data, such as ERTS digital tapes, can be handled on the IBM compatible tape transports.

Once the data has been read into the computer, the interactive system (Nelson, 1974) permits display, control, and generation of image analysis functions. The software provides a variety of methods to enhance image features and identify categories of interest. The hardware consists of image monitors to display the processed results for evaluation of the analysis options and the XDS-930 computer with interactive operator controls for performing the selected options.

A key element in the operation of this system is an alphanumeric console that permits communication between the analyst and the computer. At each stage in the data analysis, the complete choice of processing or analysis options is presented as a list on a CRT and the operator merely indicates his choice on the keyboard.

Since the display of an image only uses one-fourth of the black and white TV monitor, it is possible for one image to be shown in one subsection and then other data to be displayed in the remaining three quadrants. This permits viewing of multispectral images, images and base maps, and the effect of preprocessing and classification algorithms. The display capability also includes a DICOMED Model 30 with true 1024 line resolution, 64 gray levels, and a completely stable image for photographic purposes. In addition, a color TV is interfaced with an I^2S Digicol Processor that can be used for processing and display of gray scale to color transformations and calculations of the image area occupied by the various colors.

GROUND TRUTH

Ground and water temperature measurements were monitored at flight time. In addition, radiometer readings in the same spectral bands as ERTS were collected at selected test sites from a low level helicopter flight. All geodetic control points were panelled.

In order to fulfill the objectives of this project, it was decided to initiate the work by assembling the types of ground truth information that did not have to be collected at the time of the aircraft flight. Examples of this were (1) geologic maps, (2) flood plain hazard maps, (3) landslide maps, (4) soil maps, (5) timber maps, and (6) vegetative cover maps. Agriculture crop maps were also collected, although these were surveyed again during the flight to check for harvesting and irrigation.

AIRBORNE DATA COLLECTION

The aircraft selected for the data collection flights was a B-25 leased from Tallmantz Aviation. The flights were scheduled for the period July 13-16, 1973. This period was selected because mid-July was historically the best flying weather around Salt Lake City, and July 15 coincided with an overflight by ERTS-I so that comparison with spacecraft data would be possible. Thirty flight lines were planned to cover the test area. Of these 14 were in the valley, 14 in the mountains, and two were low altitude runs down Big Cottonwood Canyon and Little Cottonwood Canyon. With the exception of the canyon runs, the flights were made north and south at an average 8,000 feet above the terrain. The canyons were flown at 6,000 feet in a descending mode.

The weather during the flight program was very poor. Flights were cancelled on Friday the 13th because of clouds. Four lines were flown on Saturday, but equipment problems and the weather prevented more data collection. On Sunday clouds and rain were encountered again, and although Monday was not ideal, 12 lines were flown. Because of the weather, the program in Salt Lake City was extended an extra day, and on Tuesday the 17th, the remaining 14 flight lines were covered. Clouds obscured some portions of the test area, and air currents caused excessive movement of the hardmounted scanner in some sections. Nevertheless, data were collected from most of the areas of intensive study.

Approximately 1,100 feet of Color Aero Neg Film, 800 feet of Color Infrared Film, and eight 9200 foot rolls of 1-inch analog magnetic tape of MSS data were collected during the flights. The first step in the data processing was to process the film and print out one band of the MSS to check both data quality and flight coverage. The U.S. Forest Service and the ASCS have printed one set of B&W contact prints from the Aero Neg film and assembled a photomosaic that shows the flight coverage of the test site. Except for cloud obstructions, the quality of the color and color IR film is excellent. The data signals from the MSS are also excellent, however data shifts caused by the pitch and roll of the aircraft increases the difficulty in extracting useful information in some areas.

In addition ERTS imagery and digital magnetic tape data are available, and color and color infrared film in 9 x 18 inch format were collected by NASA on a high altitude U-2 overflight of the test area.

COMPUTER CLASSIFICATION OF PLANT TYPES

An example of interactive computer processing for resource management was the design of an automatic classification system for plant types using the 5-channel multispectral scanner data. Figure 2 displays the most important steps in this process. The initial step was the identification of ground truth information concerning the categories to be classified from a plant type map of the area of interest provided by the Forest Service (Robinson, 1962). The next step was to display spectral data on the TV monitor so data subsets could be selected to design the computer classification system. The thermal band that was correlated with the ground truth data for design set selection shows the road running through the image with aspen above the road and conifers below it. Then the analyst positioned a series of cross hairs on the image to outline and select design data to define the spectral characteristics of the plant type categories - aspen, conifers, grass, and nonvegetation.

All five channels of the scanner were used to design a maximum likelihood classification equation for plant types, and then the entire area shown in the classification map of Figure 2 was separated into four categories and displayed in gray scale coded form on the TV monitor. The 12 sections comprising the test area were classified on an off-line night run of the computer, and the 12 256 x 256 subsection results were displayed on the TV monitor, photographed, the mosaic in Figure 2 constructed, and then cropped to create the test area display. The individual subsections are curved to recreate a geometrically correct classification map for the conical multispectral scanner.

Although the computer classification map is a relative map of the area, resource managers require the information displayed on a standard map base. To illustrate this product, the computer classification results were overlayed, with the aid of a Zoom Transfer Scope, to a U. S. Geological Survey map at a scale of 1:24,000 as shown in Figure 3. The importance of generating map overlays of this type for use by resource managers and land use planners can not be overemphasized. They are accustomed to using maps of their area and so the computer classification must be displayed at an appropriate scale and related to the map coordinates to apply to their work. In addition, the very important information concerning the acreage occupied by the various categories can be computed automatically after the data transformation to a base map.

The two map overlays of plant types contain a similar classification of general areas but a difference in the boundary placement between categories. Some of these differences have been analyzed with the aid of color aerial photographs and others have been checked on the ground by Forest Service and McDonnell Douglas personnel. On the basis of this favorable comparison, this combination of aircraft multispectral scanning and computer classification shows great promise for the automation of the classification aspect of standard forest inventories.

COMPUTERIZED SOIL SURVEY

Another example of multispectral analysis for resource management information was related to a soil survey. The Soil Conservation Service (SCS) office in Salt Lake City provided data from a recent study in the mountain area of Little Cottonwood Canyon. For the computer analysis, the SCS regrouped their original soil survey information into seven broad categories related to the suitability of the land for different types of development.

The use of ground truth information and the selection of design sets was conducted on the interactive system in the same manner as discussed for plant types. Three maximum likelihood classification systems were designed and tested on different areas and the results combined on the Zoom Transfer Scope to make the thematic overlay shown in Figure 4 along with the SCS classification.

This computerized soil survey is presently under evaluation by the SCS in Utah. It is apparent that the general areas of classification are the same as the original data, but the boundaries are different. A recheck of the soil sample locations and the aerial photographs used in the boundary placement by the SCS cannot resolve the question of which boundary placement is more accurate. This will require another ground check of the area when the snow melts at the test site this Spring.

AUTOMATIC IDENTIFICATION OF IMPERVIOUS SURFACES

Another important application of multispectral data analysis was the identification of impervious surfaces for hydrologic resource management. A test site was selected on a canyon flood plain area undergoing expanding residential development because of its scenic beauty. This information on surfaces with high water runoff was required to specify water drainage channels and to help determine if more man-made impervious surfaces could be permitted.

For the computer analysis illustrated in Figure 5, design sets were selected for impervious

surfaces from the buildings and parking lots of the Olympus Hills Shopping Center and for pervious surfaces from the grass playground behind the Oakridge School. A computer classification system was designed on the interactive system using all five spectral bands from these data sets, and then the entire flight strip was classified. This strip was classified in 12 256 x 256 pixel sections, with the results for each subsection ranging from 2% impervious in the mountain area to 25% impervious in the residential area. A field check of this computer classification map revealed excellent correlation with the ground features. The identification of roads and buildings in the residential area was obvious, while the mountain areas classified as impervious surfaces correlated with natural rock outcroppings.

OUTFALL DETECTION

One form of image preprocessing performed on the Interactive Image Analysis System was a combination of selective gray scale enhancement and contouring to highlight potential water pollution. Figure 6 shows a split screen display of two spectral bands of ERTS multispectral scanner, computer compatible tape data and two processed images. The upper right quadrant displays a 256 x 256 subsection of the 0.6-0.7 μm spectral band and the lower right quadrant contains the 0.8-1.1 μm band. The TV images show the sewage canal from Salt Lake City flowing into the Great Salt Lake.

In this enhancement demonstration, cross hairs were positioned on the image, and then the operator displayed the gray scale values of the selected pixels on the alphanumeric terminal. Knowing the gray scale level of key points within the scene, the operator selected the appropriate threshold levels to construct gray scale contours as shown in the two left quadrants. The cross hair in the lower right of the images next to the shore line locates the point the canal empties into the lake. It appears from the contours that no outfall from the sewage canal into the lake can be detected on the ERTS data.

In addition to computer processing for outfall detection, a manual photo interpretation task has been completed to pinpoint potential pollution outfalls along the Jordon River. Both the color and the color IR film were used for this detection problem, and the location of outfalls and potential outfalls were mapped onto transparent overlays to a series of 1:24,000 scale maps. Photographic documentation of the outfalls was copied from the original photos on a Richards Light Table using a Nikkon 35mm camera. An example of such an overlay is shown in Figure 7.

CONCLUSIONS

One important conclusion from this study is that a great deal of organization and coordination must be done to assemble the required team of resource managers. This must be achieved since many agencies and groups within local, regional, and national government are working in any given area with overlapping requirements and objectives, without coordination. This coordination is required to efficiently satisfy these requirements and to economically schedule data collection flights. Scheduling is vital since some resource problems that can be solved by remote sensing techniques are not economical unless combined with other objectives. A completely unified, coordinated approach was achieved on this program.

It has been shown that the computer analysis of multispectral data shows great promise for solving resource management problems. In addition, this project demonstrates that resource managers at the working level are very receptive to new techniques and will expend great effort to further technique development. Although a final determination of the number of categories that can be classified or the accuracy of boundary placement has not been made, it is clear that the traditional techniques for generating this type of information will undergo significant change in the next few years.

Finally, it was found that most of the objectives of concern to the resource managers cooperating on this program could not be solved with the spatial resolution of the ERTS multispectral scanner. Although ERTS is invaluable for resource management of large areas at the national level, it is clear that resource project planning at the regional level requires high altitude flights while the local areas will require low level aircraft flights to collect the required data.

ACKNOWLEDGEMENTS

The authors wish to thank V. W. Goldsworthy for his important contribution in computer programming and data analysis. A special thanks to all the cooperating personnel in Utah with a warm appreciation to Fleet Stanton of the U. S. Forest Service for his valuable support.

REFERENCES

1. Anderson, J. R., Hardy, E. E., and Roach, J. T., A Land-Use Classification System for Use With Remote-Sensor Data, Geological Survey Circular 671, 1972.
2. Nelson, E. E., Interactive Computer Processing for Land Use Planning, presented at

Ninth International Symposium on Remote Sensing of Environment, Ann Arbor, Michigan, April 16, 1974.

3. Robinson, E. B., Birds of Brighton and Parley's Park Wasatch Mountains, Utah, M. S. Thesis, University of Utah, 1962.

Table 1
UTAH PERSONNEL IN WASATCH FRONT PROJECT

● ADVISORY BOARD	
FLEET STANTON	U.S. FOREST SERVICE
MERRILL RIDD	UNIV. OF UTAH
LEE KAPALOSKI	UTAH STATE PLANNING OFFICE
DALE CARPENTER (REPLACED KAPALOSKI, FALL '73)	UTAH STATE DEPT. OF NATURAL RESOURCES
● LAND USE GROUP	
CARPENTER, DALE, GROUP LEADER	DEPT. OF NATURAL RESOURCES
BARNES, JEROLD H.	SALT LAKE COUNTY PLANNING
ELMER, STAN	UTAH DEPT OF NATURAL RESOURCES
KEATING, J. BRUCE	UNIV. OF UTAH, GEOGRAPHY
LEE, CHUNG-MYUN	UNIV. OF UTAH, GEOGRAPHY
MC GILL, NEIL F.	U.S. FOREST INTERMOUNTAIN EXP STATION
METCALF, JOHN W.	SOIL CONSERVATION SERVICE
OSTERGAARD, CLARK	WASATCH NATIONAL FOREST
PRICE, TERRY	WASATCH NATIONAL FOREST
RIDD, MERRILL	UNIV. OF UTAH, GEOGRAPHY
SUHR, JIM	U.S. FOREST SERVICE
THOMPSON, BILL	WASATCH NATIONAL FOREST
● WATER RESOURCES GROUP	
MC COY, ROGER M., GROUP LEADER	UNIV. OF UTAH, GEOGRAPHY
BARTOS, LOUIE	U.S. FOREST SERVICE
CHRISTENSEN, BOYD J.	U.S. FOREST SERVICE
DONALDSON, HAROLD D.	DIV. OF WATER RIGHTS – STATE OF UTAH
DOWNS, DE WANE	SOIL CONSERVATION SERVICE
MCGILL, NEIL F.	U.S. FOREST INTERMOUNTAIN EXP STATION
NEILSON, JOHN W.	U.S. FOREST SERVICE
● VEGETATION – SOILS GROUP	
HUTCHINGS, T. B., GROUP LEADER	SOIL CONSERVATION SERVICE
BARTOS, LOUIE	U.S. FOREST SERVICE
BARNES, JEROLD H.	SALT LAKE COUNTY PLANNING
CHRISTENSEN, BOYD J.	U.S. FOREST SERVICE
COLBY, GORDON	U.S. FOREST SERVICE
KIMBAL, JIM	U.S. FOREST SERVICE
MC GILL, NEIL F.	U.S. FOREST INTERMOUNTAIN EXP STATION
PETERSON, GARY E.	U.S. FOREST SERVICE
PROCTOR, DON	U.S. FOREST SERVICE
RAPIN, DALE	U.S. FOREST SERVICE
SCHLATTERER, ED	U.S. FOREST SERVICE
● GEOLOGY-GEOMORPHOLOGY GROUP	
CURREY, DONALD, GROUP LEADER	UNIV. OF UTAH, GEOGRAPHY
BAILEY, BOB	U.S. FOREST SERVICE
COCHRANE, JIM	WASATCH NATIONAL FOREST
KLASON, DICK	UTAH STATE FORESTER'S OFFICE
OLSON, EARL P.	WASATCH NATIONAL FOREST
SUHR, JIM	U.S. FOREST SERVICE
● IMAGERY GROUP	
KEATING, BRUCE, GROUP LEADER	UNIV. OF UTAH, GEOGRAPHY
MC GILL, NEIL F.	INTERMOUNTAIN EXPERIMENT STATION
IVERSON, JOHN	U.S. DEPT OF AGRICULTURE, ASCS
JENSEN, RAY	U.S. FOREST SERVICE
WIESE, LYNN	U.S. FOREST SERVICE

Table 2
PRIORITY LISTING OF STUDY AREAS

LAND USE

1. MAP OF IMPERVIOUS SURFACES SOUTH OF MILL CREEK CANYON
2. RECREATION IMPACT IN ALTA-SNOWBIRD AREA
3. CROP CLASSIFICATION SOUTH OF SALT LAKE CITY
4. RECREATION USE OF EAST CANYON RESERVOIR
5. EROSION DAMAGE NORTH OF CITY CREEK CANYON
6. POLLUTION SOURCES IN JORDON RIVER
7. RECREATION IMPACT ON BIG COTTONWOOD CANYON
8. RECREATION IMPACT ON AMERICAN FORK CANYON
9. RECREATION IMPACT ON CITY CREEK CANYON
10. EFFECTS OF SHEEP GRAZING ON RANGELAND NORTH OF BIG COTTONWOOD CANYON

WATER RESOURCES

1. INDUSTRIAL POLLUTION MONITORING ALONG JORDON RIVER
2. FEEDLOT POLLUTION MONITORING ALONG JORDON RIVER

VEGETATION

1. FOREST AND RANGE INVENTORY IN BIG COTTONWOOD CANYON
2. FOREST AND RANGE INVENTORY IN FORT DOUGLAS PRISTINE AREA
3. FOREST AND RANGE INVENTORY IN MILL CREEK CANYON. COMPARE WITH PRISTINE AREA
4. RANGELAND CLASSIFICATION AT MOUTH OF EMIGRATION CANYON
5. PHREATOPHYTE CLASSIFICATION NORTH OF SALT LAKE CITY
6. CHECK REGROWTH OF RECENT BURNED AREA AT STEEP MOUNTAIN

SOILS

1. SOILS MAP AROUND ALTA
2. SOILS MAP WEST OF SOUTH JORDON
3. SOILS MAP NORTH OF SALT LAKE CITY AIRPORT
4. SOILS MAP SOUTH OF ALTA
5. SOILS MAP NORTH OF DRAPER

GEOLOGY – GEOMORPHOLOGY

1. FLOOD PLAIN MAPPING SOUTH OF MILL CREEK CANYON
2. FAULT LOCATION SOUTH OF LITTLE COTTONWOOD CANYON
3. FLOOD PLAIN MAPPING WEST OF ROPER YARDS
4. SNOW AVALANCHE MAPPING IN LITTLE COTTONWOOD CANYON
5. LANDSLIDE MAPPING NEAR MILL CREEK CANYON
6. SAND AND GRAVEL LOCATION SOUTHEAST OF DRAPER
7. MINERAL AND FRACTURE ZONE IDENTIFICATION IN LITTLE COTTONWOOD CANYON

Table 3

SPECIFICATIONS FOR ACTRON HMS 564 MULTISPECTRAL POINT SCANNER

Spectral Channel	Spectral Range (micrometers)	NEΔR (Noise Level)	Dynamic Range
1	0.5 - 0.6	0.1%	1000/1
2	0.6 - 0.7	0.1%	1000/1
3	0.7 - 0.8	0.1%	1000/1
4	0.8 - 1.1	0.1%	1000/1
5	10.2 - 12.6	0.2K	(-20)-(+70)°C (Range may be shifted)

IFOV	2.0 milliradians (normal to optical axis)
V/H max	0.1 radian/sec
Scan Type	Conical, nadir centered, 30° nadir angle
Cross Track Swath Width	53°
Spectral Purity	Less than 10% contribution to adjacent channels
Calibration Sources	Once per scan, 4 levels per visual spectral channel and 1 for thermal
Synchronization Pulses	1.6 pulses/2 milliradians
Video Bandwidth	29 KHz/channel max
Video Signal	0 - 10 VDC
Load Impedance	1 kilohm min
Power Requirement	28 VDC, 10A Average, 20A Surge
Weight	175 lbs. + mounting provisions

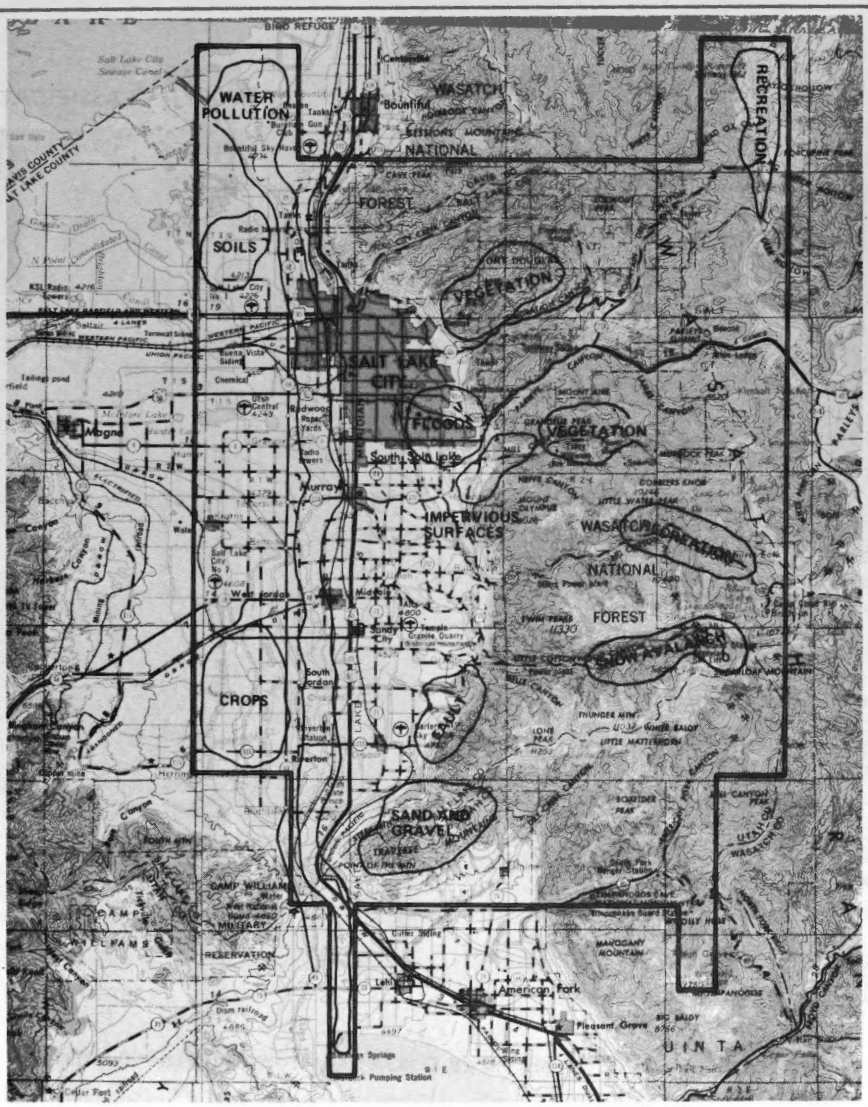

Figure 1. Utah Test Site

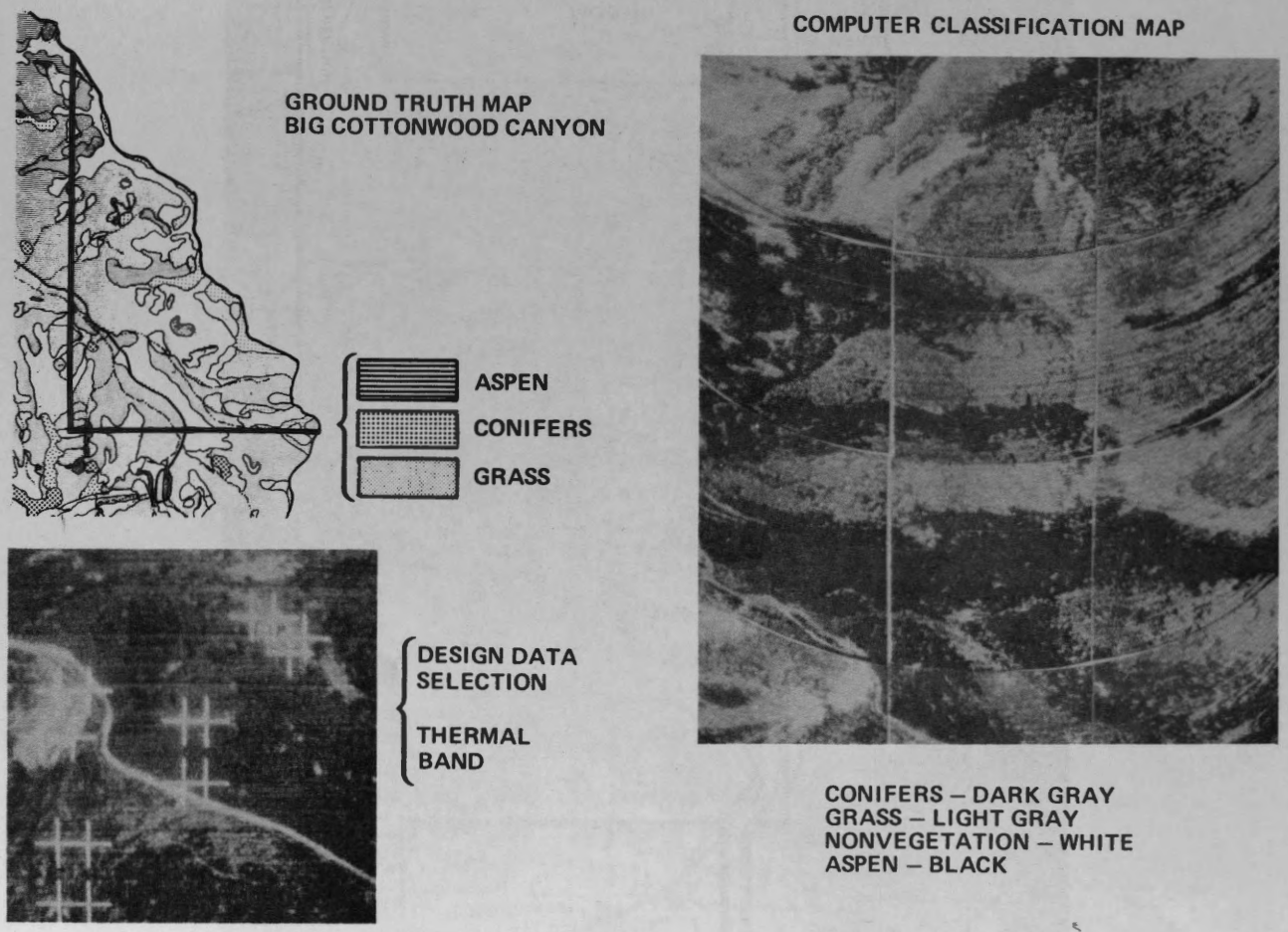

Figure 2. Computer Classification of Plant Types

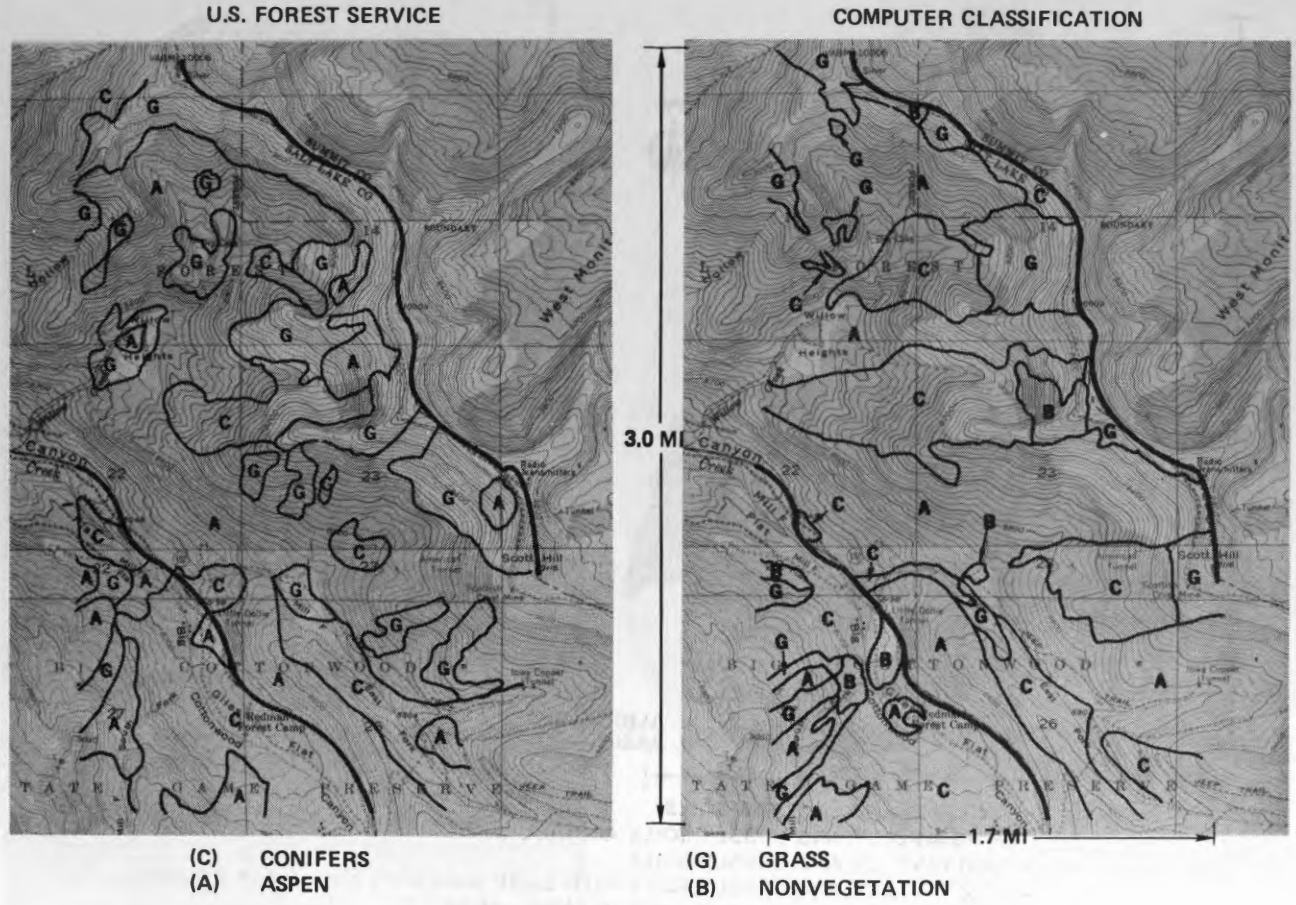

Figure 3. Map Overlays for Plant Types

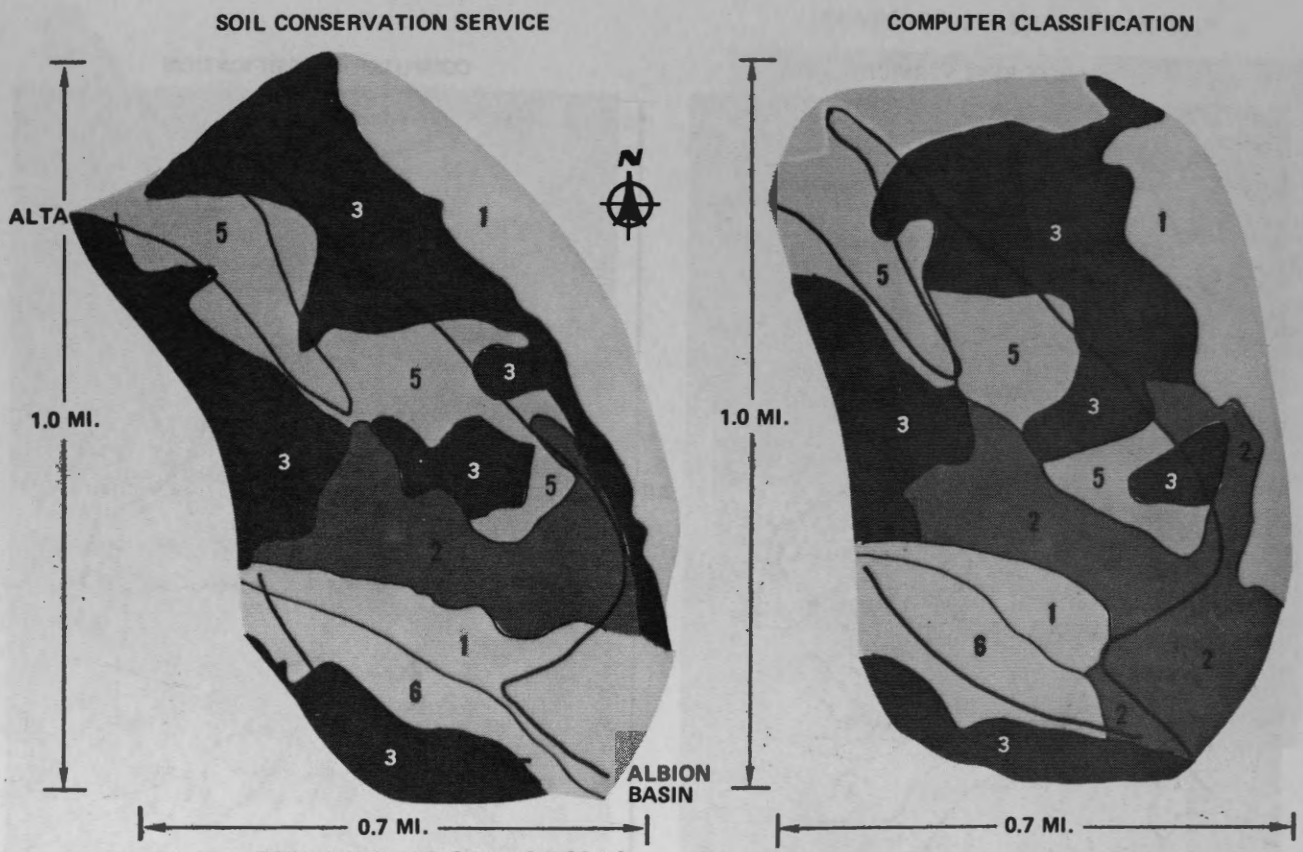

Figure 4. Soil Survey Map

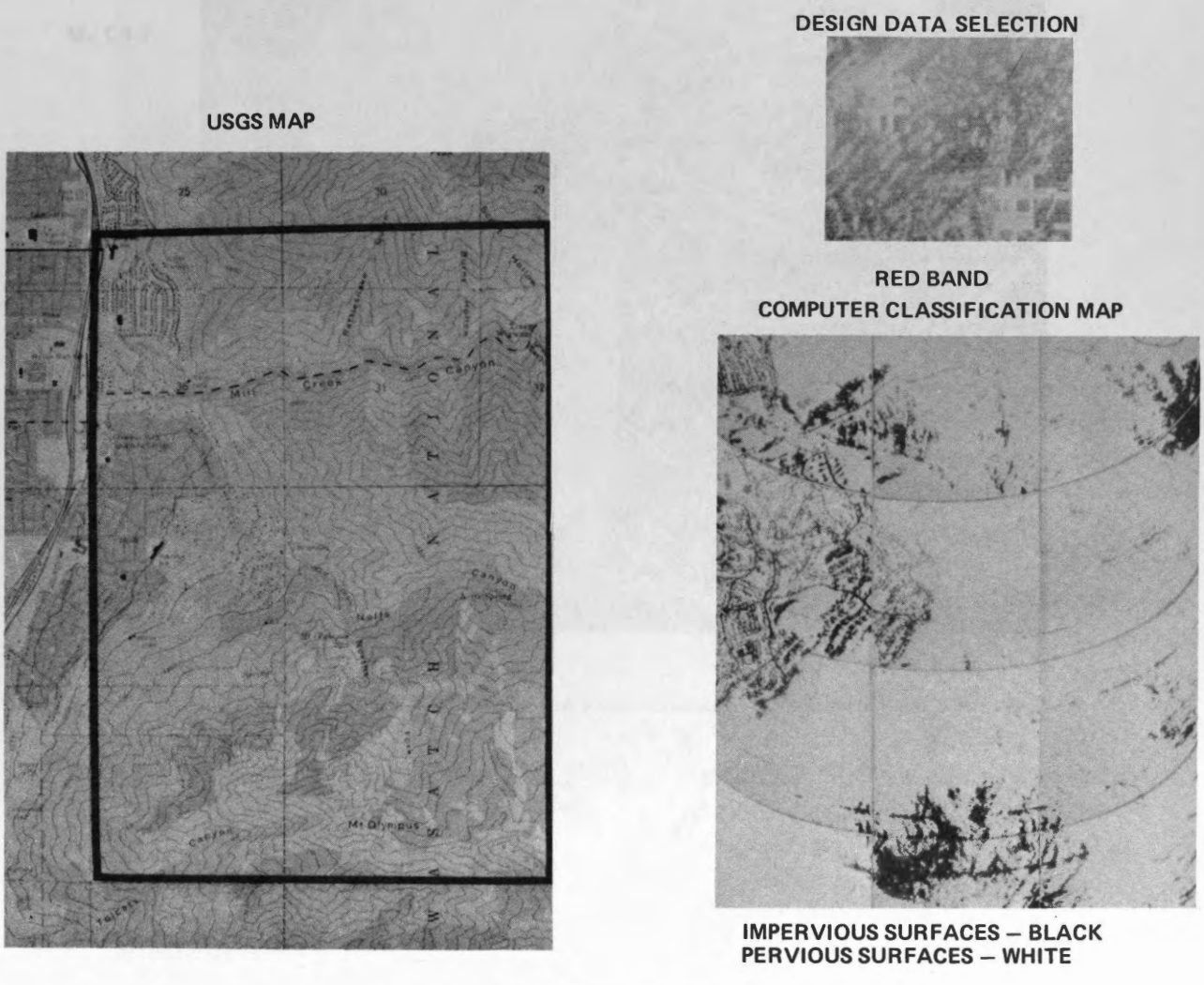

Figure 5. Computer Classification of Impervious Surfaces

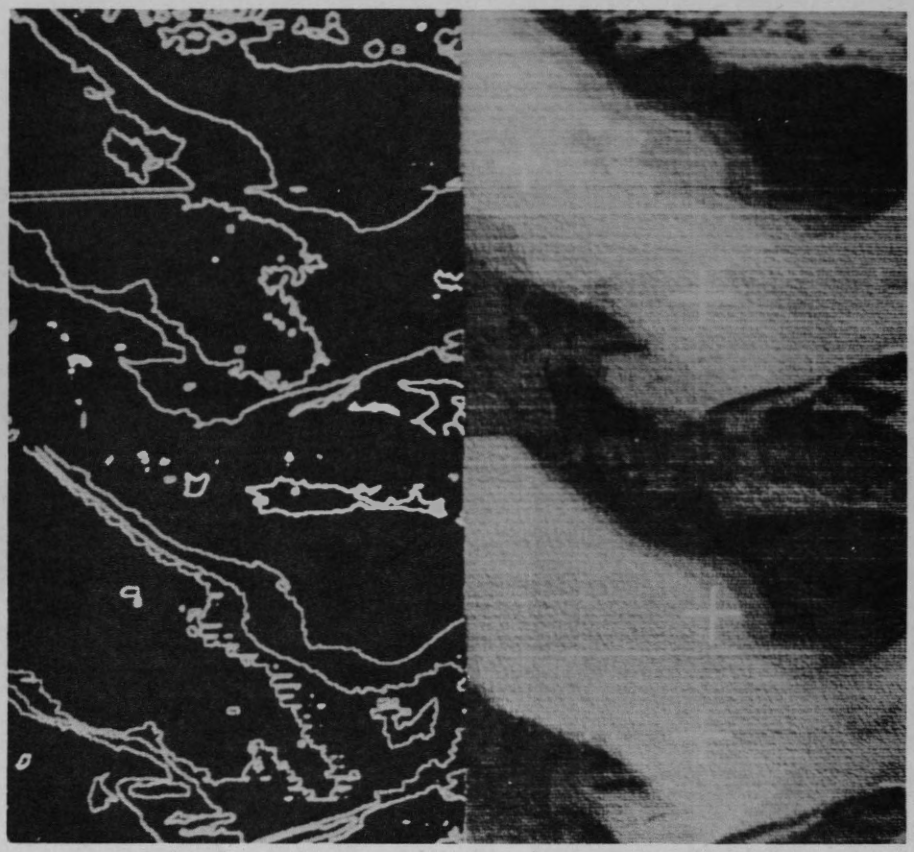

Figure 6. Gray Scale Enhancement and Contouring - Great Salt Lake

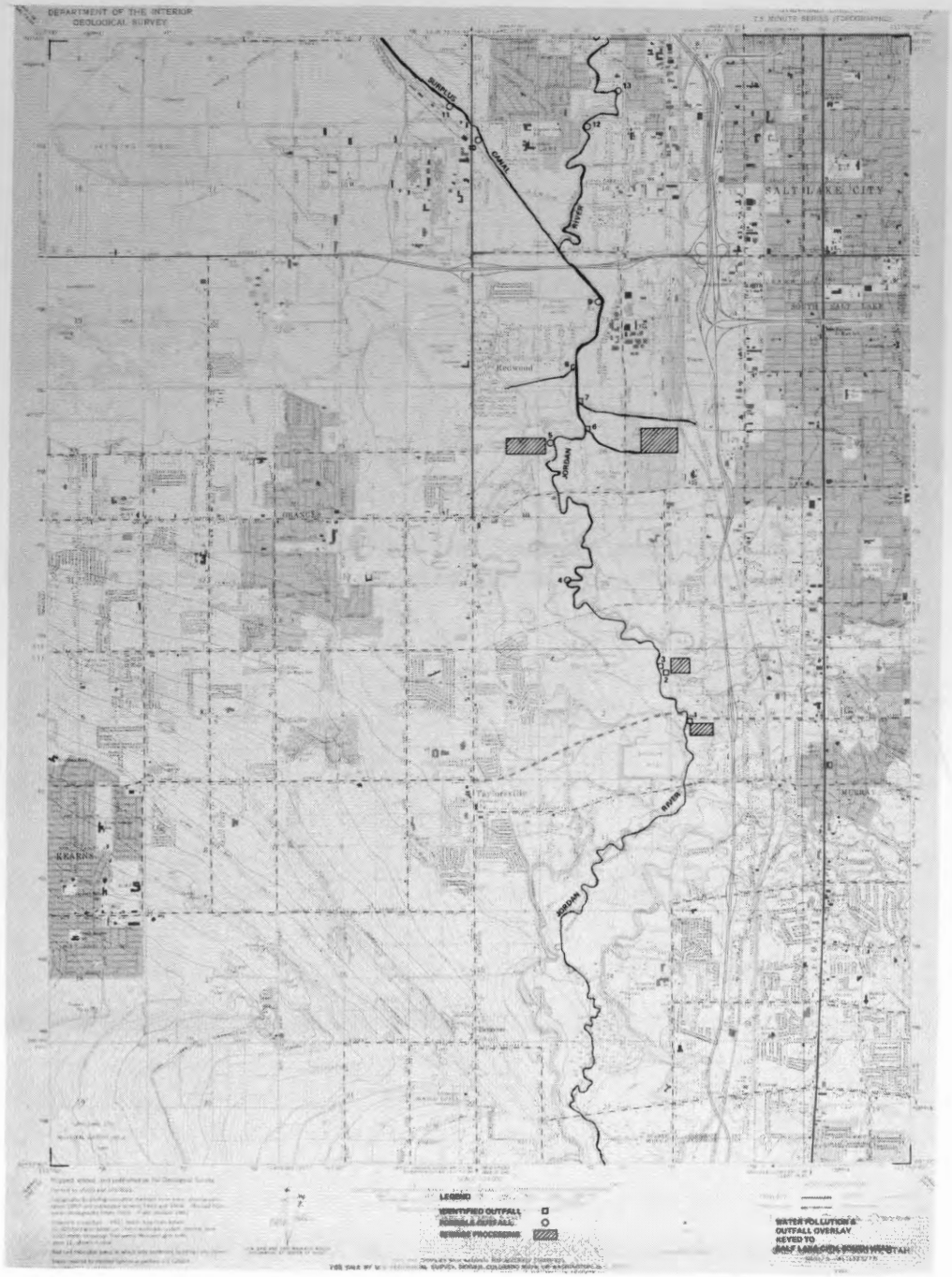

Figure 7. Water Pollution and Outfall Overlay

REMOTE SENSING AS A TOOL IN APPRAISING RIGHT OF WAY DAMAGES

By

D.L. HOOVER

This paper presented at the Second Canadian Symposium on Remote Sensing, University of Guelph, Guelph, Ontario, April 29 - May 1, 1974.

REMOTE SENSING AS A TOOL IN APPRAISING RIGHT OF WAY DAMAGES

D.L. Hoover, A.A.C.I., P.Ag., Vice-President,
The Sibbald Group, Edmonton, Alberta

ABSTRACT

Detailed damage appraisals were requested by a petroleum company approximately two years after landowners had suffered damage from installation of a gas pipeline in the Buck Lake area of Alberta. Fortunately, the petroleum company had previously taken 1:10,000 color and false color infrared aerial photographs, during and after construction. These were made available to our appraisers. Machair Surveys Ltd., Calgary, Alberta, who had conducted the aerial surveys were able to place the photographs in a stereo-plotter to map the exact width and length of the damage areas relating to each landowner, including areas compacted or crops damaged where company vehicles had driven off the pipeline right of way. The stereoplotter also measured approximate number and height of trees destroyed or damaged by pipeline construction activities along the right of way. Shortly after the submission of our damage appraisal reports, our client was able to successfully negotiate a fair settlement with landowners involved.

INTRODUCTION

When right of way damage claims are filed by landowners, it is often necessary to have an independent valuation of damages, so that reasonable compensation can be paid. Generally, the services of an Accredited Appraiser are utilized. Briefly, an Accredited Appraiser is a person who is professionally trained by the Appraisal Institute of Canada to establish the value of an adequately described parcel of property at a specified date for a specified purpose. Appraisers are finding more and more use for aerial photography in their work.

In the particular case described in this paper, the site of the damage claims was the Minnehik - Buck Lake natural gas gathering system in west central Alberta. One pipeline had been placed in the original right of way and all claims resulting from it had been paid. During the winter of 1970 - 1971, a second parallel pipeline was added partly along the same right of way and partly along an extension of the original right of way. Late in 1972, almost 2 years later, a total of fourteen damage claims resulting from the second pipeline installation still remained unsettled. Landowners on those 14 parcels of land had jointly submitted a claim of $92,870.74 plus a 15% administration fee, for a total damage claim of $106,801.24.

The type of claims filed varied slightly from farmer to farmer. In the main, they concerned loss of trees, loss of crop, cattle and equipment becoming stuck in the pipeline trench during and after construction, and inconvenience caused by the trench getting in the way of farm operations. The landowners, in general, filed a very complete list of claims; many of them were difficult to estimate.

APPRAISAL METHOD

Aerial photographs taken in August 1971 and August 1972 were available from our client. They had been taken as a precautionary measure to assist in documenting potential damage to the environment.

The aerial photographs were taken by Machair Surveys Ltd., Calgary, Alberta. The aircraft was a Cessna 206, mount-

ing an RC8 camera. Overall photo coverage was obtained in false color infrared, film type 2443, in both 1971 and 1972, using a panchromatic 540 filter. Partial coverage in true color, film type SO397, was obtained in 1972 only.

The aerial photographs were first scanned to determine major problem areas. Our appraisers then took the photos out to the damaged area for a ground survey. Later, they contacted each individual landowner and took statements as to the extent and cause of damages claimed.

The photographs were then placed on a Wild A8 stereoplotter where damages on and off the pipeline right of way were measured for each individual parcel of land. An estimate of the heights of trees destroyed was also ascertained.

A final interpretation of the aerial photographs was then undertaken, noting in particular the disturbed areas that had not revegetated properly.

Economic parameters based upon known and projected values for land, crops and livestock were then formulated, and damages were estimated.

DISCUSSION AND CONCLUSIONS

The damages, which had been sustained almost two years previously, could not have been appraised satisfactorily without aerial photographs showing vegetation and soil disturbances. The photographs provided information on the state of the microenvironment, the changes caused by the addition of a second pipeline along the right of way and the early restoration of vegetation. In addition, some continuing problems created by the second pipeline were assessed, e.g., areas of improper replacement of topsoil by the construction crew, which were evident in the photographs. As the operations of various utility companies expand across Canada, resistance from landowners will harden. Aerial photographs are valuable tools in the hands of agricultural appraisal firms who are staffed and equipped to interpret them properly. Photographs represent "hard" evidence of the situation on the ground at a given time. Both sides to a dispute, the company and the landowner, are more confident concerning the damage settlement when aerial photographs are available. As a consequence, settlements are expedited, and tend to be more equitable.

In the Buck Lake pipeline appraisals, valid grievances for each landowner were determined and damages were estimated. A summary of the final outcome follows. Note that the petroleum company was able to achieve a good settlement while landowners received almost twice the amount of the appraised damages, and the cost of aerial photography was very reasonable.

1. Buck Lake landowners' original claim for damages $106,801.24

2. The Sibbald Group estimate of damages . $ 16,712.27

3. The settlement finally reached between the landowners and the petroleum company . . . . . $ 32,550.00

4. Total costs incurred by the petroleum company:

Settlement	$32,550.00	
Aerial photography	$ 1,500.00	
Appraisal services	$ 5,733.00	
TOTAL		$ 39,783.00

5. Total costs incurred by the petroleum company, as a percent of original landowners' claims 37.2%

ANALYSIS OF ERTS-1 IMAGERY FOR WIND DAMAGE TO FORESTS

By

W.C. MOORE

This paper presented at the Second Canadian Symposium on Remote Sensing, University of Guelph, Guelph, Ontario, April 29 - May 1, 1974.

ANALYSIS OF ERTS-1 IMAGERY FOR WIND DAMAGE TO FORESTS

W.C. Moore
Forest Management Institute
Canadian Forestry Service
Ottawa, Ontario, K1A OW2

ABSTRACT

Interpretation of ERTS-1 imagery was used to determine that a linear anomaly, visible on images from bands 4 and 5 in the summer season, was caused by a tornado near Sudbury, Ontario in August 1970. The reasons for its clear imaging in those bands are discussed. In another example, a diazo-overlay interpretation technique was applied to uneven film densities arising from the spectral variations caused by severe forest damage in a widespread "blow-down" near Dryden, Ontario in July 1973. The advantages and disadvantages of the technique are discussed. With further development of techniques, ERTS-1 imagery should be suitable for primary reconnaissance of certain types of forest damage caused by high winds.

RESUME

L'auteur en interprétant l'imagerie ERTS-1 détermina qu'une anomalie linéaire, visible sur les images des bandes 4 et 5 prises en été, découlait d'une tornade en août 1970 près de Sudbury, Ontario. Il discute les raisons pourquoi ces images sont claires sur ces bandes. Dans un autre exemple, il se servit d'une technique d'interprétation par diazo-superposition pour étudier les densités inégales du film résultant de variations spectrales causées par d'importants dommages aux forêts en juillet 1973 lors de grandes tempêtes de vent près de Dryden, Ontario. Il discute des avantages et des désavantages de cette technique. Avec les progrès de la technique, l'imagerie ERTS-1 pourra servir à la reconnaissance primaire de certains types de dommages causés aux forêts par les grands vents.

INTRODUCTION

Severe wind damage to forests in more remote areas remains unnoticed until it is either encounted on the ground, spotted from the air, or the concentrations of windfallen trees start to burn. Simple interpretation techniques can be used with ERTS-1 imagery to detect, locate and generally assess the extent of such forest damage. There is a requirement for this type of preliminary survey. For example, staff from the Dryden Administrative District of the Ontario Ministry of Natural Resources were looking for a simple method of classifying the blown-down forest areas after a storm in July 1973. The requirement was immediate because the results were to be used to plan and to monitor salvage operations (pers. comm. E.P. Herrington, November 1973). ERTS-1 imagery, using an interpretation technique based on multispectral and multidate (sequential) imagery can be used to identify and delineate forest damage caused by high winds.

The purpose of this paper is to demonstrate the usefulness of ERTS-1 imagery for analyses of wind damage to forests, and to identify the future potential, and limitations, of ERTS-1 for wind-damage reconnaissance.

TEST AREAS AND AVAILABLE IMAGERY

Forested areas near Sudbury and near Dryden in Ontario were selected as test areas.

The Sudbury test area was a 2- by 86-kilometre swath of forest damaged by a tornado on 20 August, 1970. It occurred in a variety of forest types and land-use patterns. The ERTS-1 image used to examine the damage was frame E-1337-15461 band 4, taken 25 June, 1973.[1] In addition, frame E-1265-15465, taken 14 April, 1973, was examined to determine how the tornado damage was imaged by ERTS-1 outside the growing season.

The second test area was a much more heavily forested area between Kenora and Dryden in Ontario where several thousand acres of timber were blown-down in July, 1973. The ERTS-1 imagery used to examine the damage consisted of images E-1310-16370 band 5, taken 29 May, 1973, and E-1364-16361 band 5, taken 22 July, 1973, to provide sequential coverage of the area from before and after the storm. In

[1] The band 5 image was not available when reordered.

addition, ERTS-1 frame E-1401-16412 colour composite 1, taken 28 August 1973, showed the damage much more clearly, but such imagery only becomes available months after a storm and thus might have limited reconnaissance value.

METHODS

The Sudbury test area was used to examine characteristic ERTS-1 spectral-band responses to severe forest damage caused by high winds. The tornado damage was investigated with an ERTS/map/air-photo/low-altitude observation technique that entailed the examination of successively smaller areas in greater detail. The age of the damage, and subsequent new growth, could be a factor affecting spectral signatures, but areal contrasts in the imagery, between damaged and undamaged forest cover, should be more important. The characteristic image contrasts of severe forest damage should only vary in degree with the age of the damage at the ultra-small-scales of ERTS-1 imagery. The spectral contrasts evident in the Sudbury test area, therefore, were used as a basis for investigating the extent of more recent forest damage in the Dryden test area.

The Dryden area was used to test the effectiveness of an ERTS-1 sequential interpretation technique to detect, delineate and monitor the extent of a blow-down immediately following a severe wind storm. Colour-coding of sequential ERTS-1 transparencies was attempted, so that one can be superimposed on the other, to highlight abnormal spectral changes over time. Such an application of the diazo-colouring process has been described for the high, uniform and sharply delineated contrasts between flooded and non-flooded land (Moore, 1974). The differences, advantages and disadvantages of applying this technique to a reconnaissance of severe forest damage were investigated.

RESULTS

The severe forest damage caused by the Sudbury tornado was evident in the June, 1973 ERTS-1 image (Figure 1). The ragged, uneven film densities along the edges of the spectral anomaly are similar to wind-associated air-pollution damage as described by Murtha (1973). The tornado also appeared to vary in intensity at ground level along its path. The tornado damage becomes obscured at the western end of its path because of cloud, and the linear anomaly in the ERTS-1 image disappears in the vicinity of Sudbury. That anomaly was not evident in the April, 1973 ERTS-1 image taken before the vegetation in that area had leafed-out.

The linear spectral anomaly was transferred to a topographic map (Figure 2) to locate the damage relative to other landscape features in a common location reference system and at a standard scale. The evidence of forest damage disappears as the tornado's path approaches Lively, Ontario because the whole vicinity of Sudbury is mostly devoid of forest cover (pers. comm. D.E. McKale, Sudbury District Forester for Timber, 1971). The lack of sharp edges along the anomaly distinguishes the tornado's path from cultural features such as highways and power lines. Small-scale air photos would contain clearer evidence of these characteristics, but such post-storm photography was not available for the whole length of the tornado's path.

The eastern end of the linear spectral anomaly could be studied in greater detail by examining the small-scale air-photo mosaic (Figure 3). The anomaly is evident in this 1971 photography, but it is not as clearly apparent as it was in the 1973 ERTS-1 imagery. Cultural features on the ground can also be examined in greater detail in Figure 3 than was possible with the even smaller-scaled map in Figure 2. The tornado apparently did not dissipate before it reached the community of Lively but, because of a lack of continuous forest cover in that locality, evidence of its passage is lacking on ERTS-1 imagery.

The oblique, low-altitude air-photos (Figure 4) were used to confirm the interpretation of the smaller-scaled imagery and photographs. The "tangled mess" of dead tree stems is conclusive evidence that severe wind-caused damage and mortality was the origin of the spectral anomaly in the June ERTS-1 imagery. The spectral characteristics of severe forest damage evident in the Sudbury test area should, with some differences, also be evident in the Dryden test area.

Band 5 ERTS-1 images from before and after the 6 July, 1973 blow-down near Dryden, Ontario were differently coloured through the diazo process, superimposed and displayed in Figure 5. The more pinkish tones in forested areas depict the locations of extensive forest damage. This diazo overlay technique did not work as well as had been expected in this instance, but the problems are not entirely insurmountable and the technique should be considered further in future applications. Varying water levels (i.e. spring/summer), satellite orientation/altitude, cloud cover and sequential-image registration problems are limiting factors, but it would be difficult to find a simpler method of showing the extent of severe forest damage caused by high winds.

This would be particularly true for detecting and delineating, for reconnaissance purposes, the subtle spectral changes evident immediately following a storm.

DISCUSSION OF RESULTS

The forest canopy is clearly evident in ERTS-1 bands 4 and 5 (0.5 to 0.6 and 0.6 to 0.7 microns respectively) because of its low reflectance relative to other terrain features in those spectral regions (Figure 6). The highest reflectance of dead foliage and tree bark are in the 0.61- to 0.69-micron spectral region (Steiner and Gutermann, 1966). Consequently, dead, windfallen trees present the highest contrasts with the surrounding forest canopy in ERTS-1 band 5 images. These image contrasts are important for sequential ERTS-1 imagery interpretation techniques.

The relative spectral reflectance of the forest canopy in band 5 images from the Dryden area would more or less maintain consistent areal-image contrasts in spite of seasonal alterations in the total reflectances. The topography/forest canopy of the area, however, does not represent a smooth surface of uniform spectral reflectance. Misregistration of sequential ERTS-1 images was also a serious problem. The two weeks between the storm and the ERTS-1 passage might have resulted in lower contrasts between undisturbed and damaged reflectance than were evident in the nearly-three-years-old Subdury tornado damage. Nor is severe forest damage likely to be evident in ERTS-1 before leaf-out or after leaf-fall. Nevertheless, extensively severe forest damage is evident in Figure 5, and the earliest possible images after a storm would have the most value for preliminary surveys. Rapidly available contrast-stretched or thematically mapped imagery from ERTS-1 (Aldred, 1974), therefore, would be required for effective wind-damage reconnaissance. Simple diazo-coloured overlays from black-and-white transparencies might be the most timely and economic means of accurately assessing such reprocessed ERTS-1 imagery.

CONCLUSIONS

Tornado damage to forests was imaged as a ragged, light-toned line across a darker-toned forest canopy in ERTS-1 bands 4 and 5 images. The high spectral contrasts between the live-forest canopy and dead leaves and tree bark explain why ERTS-1 band 5 images are best suited for ERTS-1 reconnaissance of the extent of severe forest damage. More general, but still severe, wind damage had similar reflectance characteristics in ERTS-1 imagery. The age of the wind-caused mortality affects band 5 image contrasts, but even recent severely damaged areas could be highlighted by overlaying differently coloured band 5 transparencies from before and after the storm. Additional information is required for detailed examinations of the damage.

The following factors are plausible explanations of why the severe forest damage stood out so clearly in ERTS-1 imagery:

1. There was high tree mortality and the damage was nearly three years old when imaged by ERTS-1 after the Sudbury tornado;
2. Linear features in particular tend to stand out from their surroundings;
3. ERTS-1 bands 4 and 5 have relatively narrow spectral sensitivities; and,
4. The remnants of dead vegetation have a distinctive spectral reflectance that contrasts sharply with the undisturbed forest canopy in ERTS-1 band 5 transparencies in particular.

Difficulties with image-contrast enhancement and sequential-image registration must be alleviated for reliable forest-damage reconnaissance with ERTS-1 imagery interpretation. More digital ERTS-1 data reprocessing and interpretation development appear to be required for generally accurate classifications of forest damage caused by high winds with ERTS-1 imagery. For such reconnaissance, the prompt delivery of custom-reprocessed imagery to investigators is also important.

ACKNOWLEDGEMENTS

The cooperation of D.E. McKale (Sudbury) and E.P. Harrington (Dryden), Ontario Ministry of Natural Resources, in acquiring ground documentation and background information respectively, and the assistance of B.F. Findlay (Atmosphere Environment Service) and B.J. Stocks (Great Lakes Forest Research Centre) are acknowledged.

REFERENCES

Aldred, A.H. 1974. Design of an experiment to compare several methods of using ERTS-1 imagery for forest interpretation. The Canadian Surveyor, June 1974, *(In Press)*.

Moore, W.C. 1974. Detection and delineation of natural disasters: landslides and floods. The Canadian Surveyor, June 1974, *(In Press)*.

Murtha, P.A. 1973. ERTS records SO_2 fume damage to forests, Wawa, Ontario. For. Chron. 49(6): 251-252.

Steiner, Dieter and Thomas Gutermann. 1966. Russian data on spectral reflectance of vegetation, soil and rock type. Dep. Geogr., Univ. Zurich, Zurich, Switz. 232 p.

Figure 1. ERTS Band 4 image containing August 1970 tornado damage. The spectral signature of forest disturbances in this band (500-600 nm) is similar to that of human activity and rock outcrops. Additional evidence is required to positively identify the spectral anomaly as forest damage.

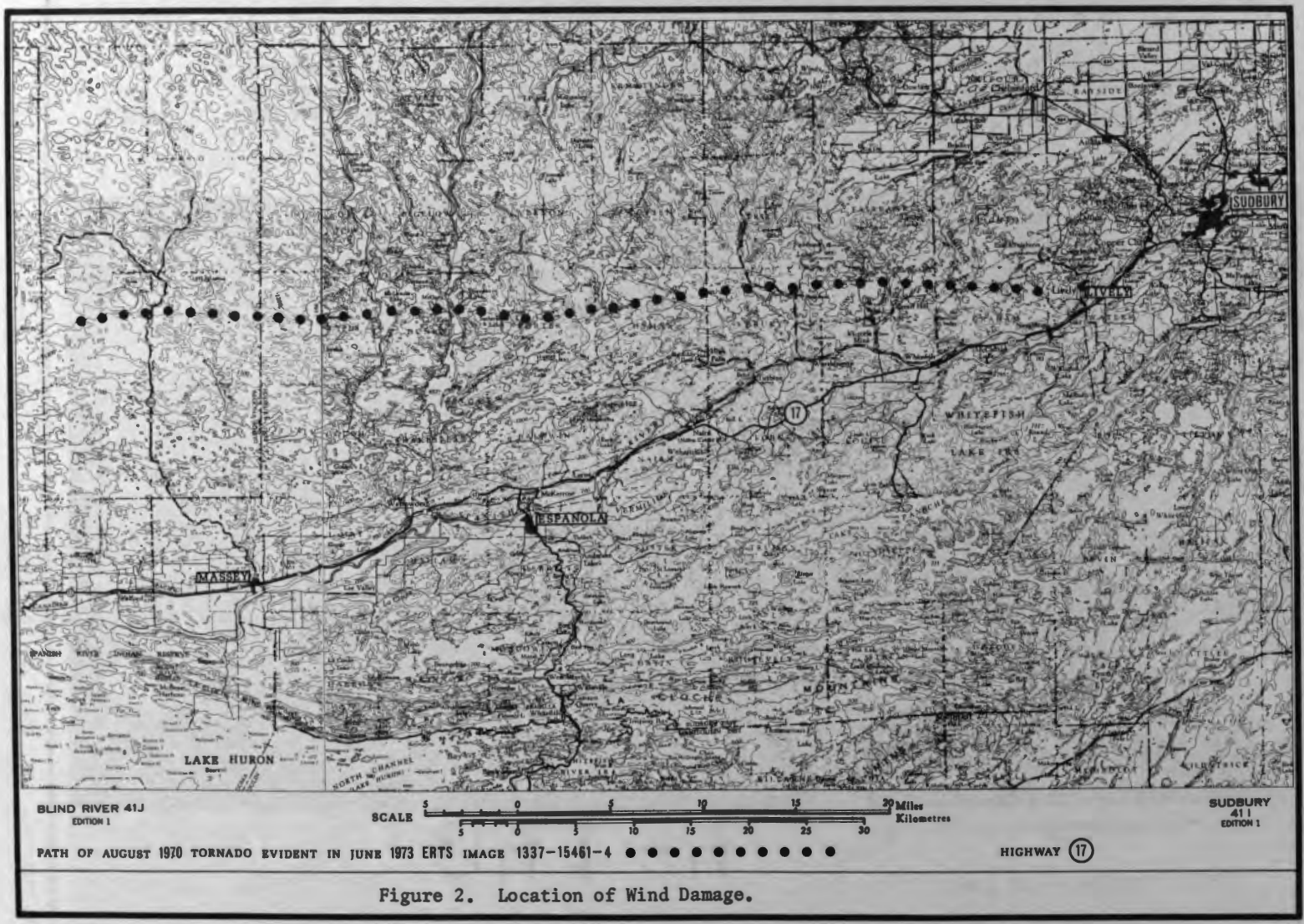

Figure 2. Location of Wind Damage.

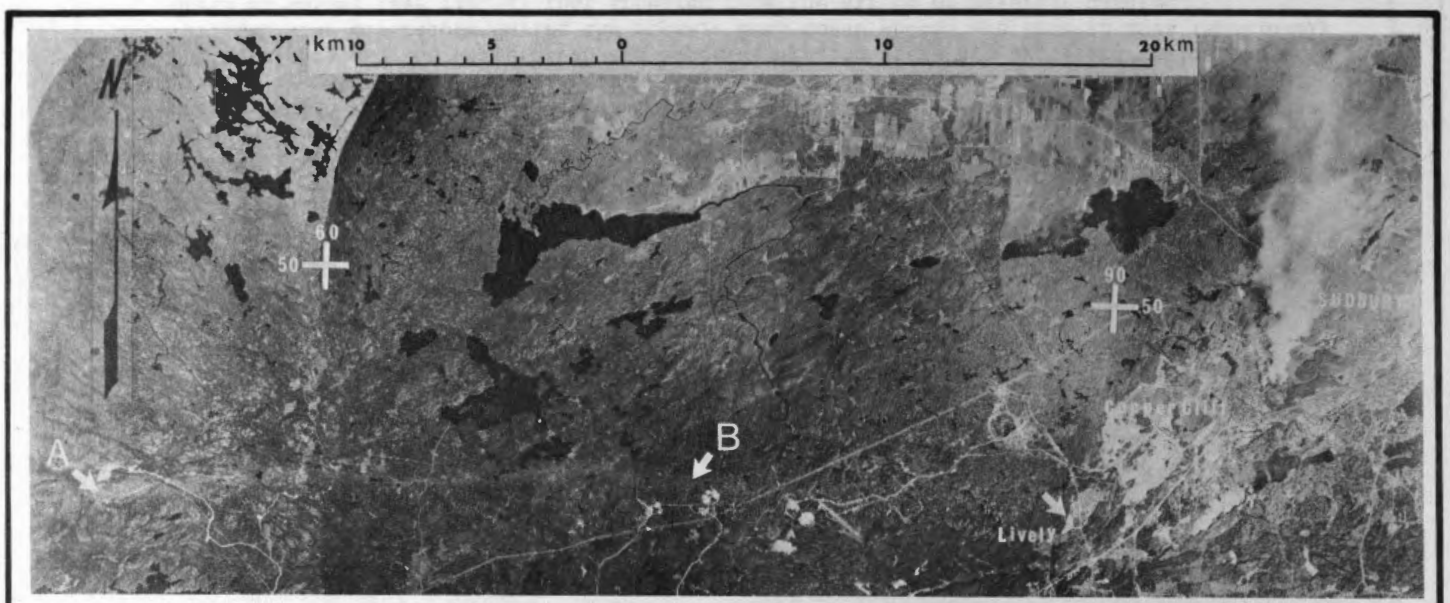

Figure 3. August 1971 small-scale air photos (A30362-44 to -47). (UTM location reference from Canadian N.T.S. 41 I/5 and 41 I/6). The spectral anomaly between "A" and "B" exists because of wind-fallen trees and the remnants of other forest disturbances caused by the tornado winds. The line of forest damage between "A" and "B" disappears east of "B" into an area of vegetation extensively damaged from other causes.

Figure 4. August 1970 tornado damage photographed from a light aircraft in October, 1972. The high oblique photo (left) provides a general overview of some of the more severe forest damage evident from the air. A smaller area can be examined in greater detail with the low oblique photo (right) and the white birch and aspen windfallen stems are excellent indicators of variable wind directions during the storm. Both these photos are from an area immediately north of Massey (*see* Fig. 2) that appeared from the air to be severely damaged.

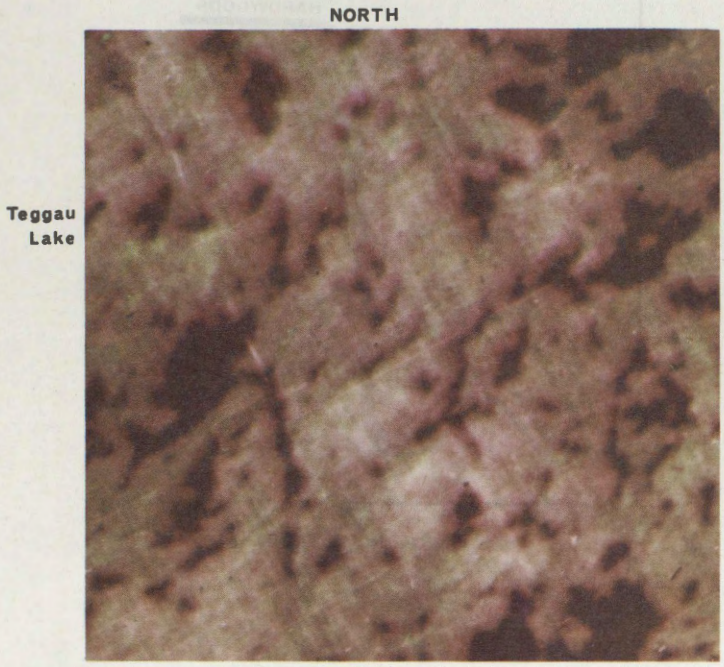

Figure 5. Diazo-coloured overlays for severe forest damage west of Dryden, Ontario. A green-coloured 22 July, 1973 ERTS-1 band 5 transparency was superimposed on a magenta-coloured 29 May, 1973 ERTS-1 band 5 transparency. With accurate registration, the resultant image is a range of greenish-brown tones, except where the relative reflectances have been abnormally altered between the two dates. The more pinkish tones in the forested areas represent the areal extent of severe forest damage.

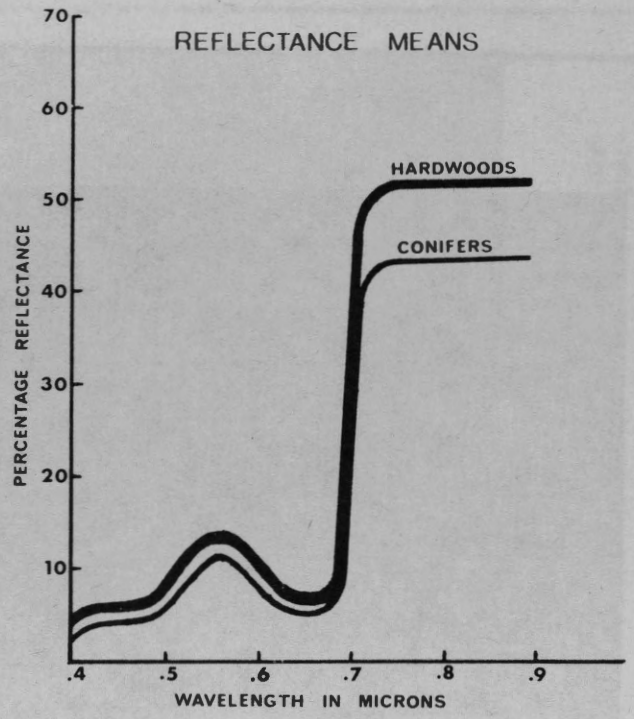

Figure 6. Generalized reflectance means (*adapted from* Steiner and Gutermann, 1966).

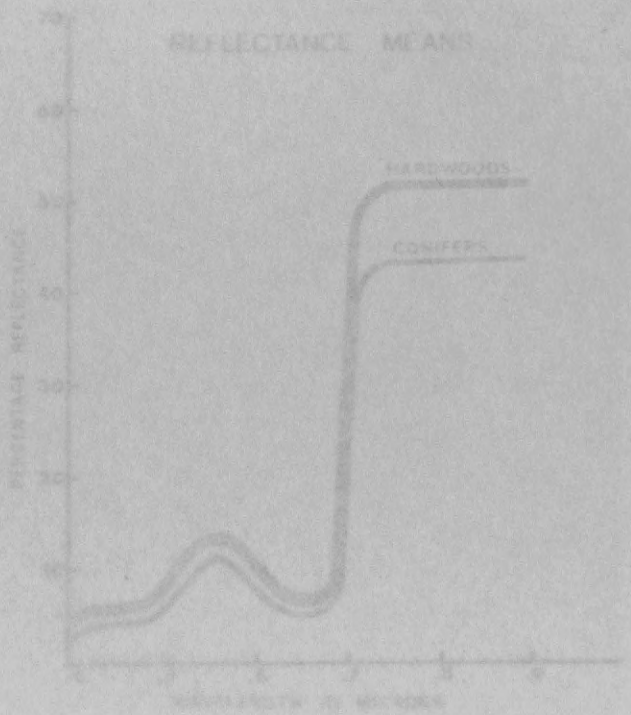
REFLECTANCE MEANS
HARDWOODS
CONIFERS